

PURSUIT OF THE TRIDECAPEPTIDE FEGLYMYCIN
AND THE MANZAMINE ALKALOID KAULUAMINE

By

Amanda Blane Doody

Dissertation

Submitted to the Faculty of the
Graduate School of Vanderbilt University
in partial fulfillment of the requirements

for the degree of

DOCTOR OF PHILOSOPHY

in

CHEMISTRY

May, 2014

Nashville, TN

Approved:

Dr. Jeffrey N. Johnston

Dr. Brian O. Bachmann

Dr. Ned A. Porter

Dr. Gary A. Sulikowski

To my family and Joel for their love and support.

ACKNOWLEDGEMENTS

There have been a number of individuals throughout my academic tenure who have helped and encouraged me in significant ways. Without these folks, the following document may not have been realized. Prof. Jeffrey N. Johnston, my advisor and mentor, was the reason I chose to pursue my graduate studies at Vanderbilt. From the moment I met him, I could tell that he was a great teacher, and since I wanted to be such a teacher, I knew I wanted to learn from him. Over the last several years, his guidance, patience, and support have led me to the completion of this work. He has both taught and granted me intellectual freedom in my studies, and while sometimes it is easier just to have someone tell you how to think, being mentored and taught to interpret things for myself has had significant impacts both on my graduate studies and my personal life. Jeff has been a great resource, from bouncing back and forth ideas to helping me get the wording of things just right.

The inspiration for the pursuit of this degree came from my professors at Wofford College, who created a learning and community environment that both nurtured and encouraged myself, my studies, and my relationships with others and the world. Specifically, Prof. Charles G. “Bassman” Bass, whose entertaining lectures in organic chemistry made me think, “this is what I want.” Bassman is also a wonderful human, and I am certain that everyone who meets him can agree.

My labmates have been great sources of intellectual discussion and comic relief. Dr. Hubert Muchalski, my graduate student mentor and great friend, taught me just about everything I know about performing chemical reactions and how to fix my computers. Also, he lets me knit gifts for his two natural products. Dr. Sergey V. Tsukanov and Dr. Dawn M. Makley have worked with me on feglymycin, and their hands, help, and discussions have been tremendous. Dr. Aroop Chandra and Dr. Priya A. Mathew have taught me persistence in total synthesis and have been great sounding boards. Dr. Mark C. Dobish, who is an excellent troubleshooter, has bestowed the “just do it” skill upon me, whether I need to call up a supplier and order something or figure out how to fix the HPLC.

As newbies were arriving at the beginning of my second year of graduate school, I heard rumors of a new student with tons of awards, an NSF fellowship, and a desire to join our group. I was intimidated. However, upon meeting Ms. Jessica Shackelford Flinn, the two of us became instant friends, with me standing up as one of her bridesmaids less than a year later. Jessica has been a wonderful friend and supporter who is never more than a text or phone call away, whether I am excited about something, need to grumble, or just need to chat. To her I owe a great deal of thanks.

My mom and dad taught me to pursue my dreams and instilled upon me a love of learning and crafting. From the first day of kindergarten, I knew I would go to college when I finished high school. It was never a question of if or when, but of where. My mom practiced spelling words with me in the mornings, and when I was bad at times tables, she forced me to practice taking timed tests during the summer. I didn't like it at the time, but I went on to be very good at math, even completing a minor in the subject in college. The encouragement, love, and support that I have received from my parents over the last 27 years or so have been invaluable. I am forever grateful to them. My sisters, Cynthia, Catherine, Abigail, and Bridgett, are my friends and companions, and I hope that this work will inspire them to do whatever they want, as long as it makes them happy, and not to do something to make someone else happy at the expense of their own happiness.

Finally, Joel L. Stephens. Words cannot describe how much his love, encouragement, support, and inspiration have helped me. When we met, he asked how long I had until I finished my degree, and I responded with, as is typical for a graduate student nearing the end of their graduate career, “about a year.” In fact, I defended this work two weeks before the anniversary of our meeting, and I will move to Atlanta, GA to start my career one year and one day after our meeting. Joel showed me the benefits of being in the world outside of graduate school, and he held me to my declaration and helped me make it real. I look forward to a life of love and happiness with him.

TABLE OF CONTENTS

| | Page |
|---|------|
| DEDICATION | ii |
| ACKNOWLEDGEMENTS | iii |
| LIST OF SCHEMES | v |
| LIST OF TABLES | x |
| LIST OF FIGURES | xi |
| Chapter | |
| PROGRESS TOWARDS THE TOTAL SYNTHESIS OF A FEGLYMYCIN ANALOG | 1 |
| 1.1 Introduction & Background | 1 |
| 1.1.1 Umpolung Amide Synthesis | 3 |
| 1.1.2 Enantioselective Aryl Glycine Synthesis | 4 |
| Direct Approaches to Aryl Glycines | 5 |
| Enantioselective Aza-Henry Reactions | 7 |
| 1.1.3 Feglymycin | 8 |
| Isolation and Key Structural Features | 8 |
| Biological Activity of Feglymycin | 9 |
| Previous Synthesis of Feglymycin | 10 |
| Biological Studies of Feglymycin Analogs | 14 |
| 1.1.4 Feglymycin Retrosynthetic Analysis | 16 |
| 1.1.5 Previous Work | 17 |
| Building Block Synthesis | 17 |
| Preparation and Elaboration of Dipeptide 42 | 18 |
| 1.2 Synthetic Efforts Towards Feglymycin | 19 |
| Fmoc-Dipeptide 54 Deprotection Reoptimization | 19 |
| 1.2.1 Fragment A | 21 |
| Hydrogenolysis of Boc-Triptide A 56 and Completion of Fragment A (39) | 21 |
| 1.2.2 Fragment B | 22 |
| Preparation of Fmoc-Triptide B 55 | 22 |
| Deprotection of Fmoc-Triptide B 55 | 23 |
| An Alternate Route to Triptide Amine 59 | 24 |
| Attempts to Prepare Fmoc-Tetrapeptide B 61 | 24 |
| Accessing Tetrapeptide Analog 72 | 28 |

| | |
|---|-----------|
| Synthesis of Pentapeptide Amine B Analog 75 | 29 |
| Attempts to Prepare Fmoc-Hexapeptide Analog 77 | 30 |
| Hydrogenolysis of Hexapeptide Analog 78 | 31 |
| 1.2.3 Fragment C..... | 31 |
| 1.2.4 Coupling Fragments B & C | 33 |
| 1.3 Conclusions and Future Work | 34 |
| STUDIES TOWARDS THE TOTAL SYNTHESIS OF KAULUAMINE | 36 |
| 2.1 Kauluamine and the Manzamine Family of Natural Products..... | 36 |
| 2.1.1 Isolation and Key Structural Features..... | 36 |
| 2.1.2 Manzamine Biosynthesis | 37 |
| 2.1.3 Manzamine Syntheses and Synthetic Efforts..... | 39 |
| Total Syntheses of Manzamine A..... | 40 |
| Efforts Towards the Total Synthesis of Manzamine B..... | 42 |
| 2.2 Kauluamine Model Studies..... | 43 |
| 2.2.1 Background & Model Retrosynthetic Analysis | 43 |
| Aminohydroxylation Reactions | 43 |
| Stereochemical Models for Cyclization..... | 44 |
| 2.2.2 Construction of the Azide Subunit..... | 45 |
| 2.2.3 Aminohydroxylation | 49 |
| 2.2.4 Cyclization to the Piperidine Core | 50 |
| 2.2.5 Structural Elucidation of the Piperidine Core | 51 |
| 2.2.6 Model Study Conclusions | 58 |
| 2.3 Studies Towards the Synthesis of Kauluamine..... | 58 |
| 2.3.1 Kauluamine Retrosynthetic Analysis..... | 58 |
| Key Disconnections | 58 |
| Stereochemical Models for Ipso-Substitution..... | 60 |
| Stereochemical Models for Piperidine Cyclization | 61 |
| Azide and Acryloyl Imide Design | 62 |
| 2.3.2 β -Carboline Construction and Triflate-Formation Challenges | 64 |
| 2.3.3 Construction of the δ -Azido γ -Lactone..... | 65 |
| Attempted Elaboration of Azido Vinyl Bromide 197 | 70 |
| [3+2] Cycloaddition with Azide 197 | 71 |
| 2.3.4 Preparation of the Acryloyl Imide | 72 |
| 2.3.5 Brønsted Acid-Catalyzed Aminohydroxylation Studies..... | 73 |
| [3+2] Cycloaddition Optimization..... | 75 |
| Attempted [3+2] Cycloaddition with Cyclic Imide 176 | 76 |

| | |
|--|-----|
| Structural Identification of 234 | 76 |
| Attempted [3+2] Cycloadditions with Imide 186 | 78 |
| 2.4 Conclusions and Future Work | 78 |
| EXPERIMENTAL SECTION | 80 |
| SUPPLEMENTAL INFORMATION | 102 |

LIST OF SCHEMES

| | |
|---|----|
| Scheme 1. Dehydrative Coupling to form Amide Bonds | 1 |
| Scheme 2. Recent Approaches to Amide Synthesis | 1 |
| Scheme 3. Epimerization Pathways in Active Ester Amide Bond Formations | 2 |
| Scheme 4. Conventional vs. Umpolung Amide Synthesis | 3 |
| Scheme 5. Umpolung Amide Synthesis Mechanism..... | 3 |
| Scheme 6. Representative Umpolung Amide Synthesis Reaction..... | 4 |
| Scheme 7. Evans' Chiral Auxiliary-Based Approach to Aryl Glycines | 5 |
| Scheme 8. Nicolau's Use of Sharpless' Asymmetric Dihydroxylation for the Synthesis of Aryl Glycines..... | 5 |
| Scheme 9. Sharpless Asymmetric Aminohydroxylation for the Synthesis of Arylglycinols | 6 |
| Scheme 10. Recent Developments in Enantioselective Aryl Glycine Synthesis..... | 6 |
| Scheme 11. Incorporation of Aryl Glycine Residues via Aza-Henry & Umpolung Amide Synthesis | 7 |
| Scheme 12. Süßmuth's Retrosynthesis of Feglymycin | 11 |
| Scheme 13. Synthesis of D-Dpg via Sharpless Asymmetric Aminohydroxylation | 12 |
| Scheme 14. Süßmuth's Preparation of Dipeptides 21 , 23 , and 32 | 12 |
| Scheme 15. Süßmuth's Preparation of Tripeptide 20 | 13 |
| Scheme 16. Süßmuth's Preparation of Hexapeptide 19 | 13 |
| Scheme 17. Süßmuth's Synthesis of Heptapeptide 18 and Completion of Feglymycin (17) | 14 |
| Scheme 18. Partial Feglymycin Retrosynthesis..... | 16 |
| Scheme 19. Retrosynthesis of Fragments A (39), B (40), and C (41) From Six Building Blocks | 17 |
| Scheme 20. Preparation of Hpg and Dpg α -Bromonitroalkane Donor..... | 18 |
| Scheme 21. Preparation of Boc-Hpg α -Bromonitroalkane Donors | 18 |
| Scheme 22. Synthesis of Dipeptide 42 | 19 |
| Scheme 23. Initial Preparation of Fmoc-Tripeptide B 55 | 19 |
| Scheme 24. Optimized Fmoc-Dipeptide 54 Deprotection and Purification Conditions..... | 20 |
| Scheme 25. Preparation of Boc-Tripeptide A 56 | 21 |

| | |
|--|----|
| Scheme 26. Completion of Fragment A (39) Via Hydrogenolysis of 56 | 22 |
| Scheme 27. Model Reaction for Hydrogenolysis Conditions..... | 22 |
| Scheme 28. Optimized Conditions for Preparation of Tripeptide B 55 | 23 |
| Scheme 29. Optimized Deprotection of 55 | 24 |
| Scheme 30. Alternate Preparation of Tripeptide B Amine 59 | 24 |
| Scheme 31. Attempted Umpolung Amide Synthesis Reaction to Form Tetrapeptide B 61 | 25 |
| Scheme 32. Successful UmAS Coupling of 59 to Surrogate α -Bromonitroalkane Donor 62 | 25 |
| Scheme 33. Preparation of ⁱ Pr-Dpg 66 | 26 |
| Scheme 34. Preparation of MeO-Dpg 69 | 27 |
| Scheme 35. UmAS Coupling Between 66 and 59 | 27 |
| Scheme 36. Preparation and Deprotection of Tetrapeptide Analog 72 | 28 |
| Scheme 37. Alternate Two-Step Sequence to Prepare Tetrapeptide 72 from Boc-Tripeptide 60 | 29 |
| Scheme 38. Preparation and Deprotection of Fmoc-Pentapeptide Analog 74 | 29 |
| Scheme 39. Attempted Installation of Fmoc-Dpg Residue to Prepare Hexapeptide 77 | 30 |
| Scheme 40. Synthesis of Protected Fragment B Hexapeptide Analog 78 | 31 |
| Scheme 41. Successful Hydrogenolysis of Hexapeptide 78 | 31 |
| Scheme 42. Synthesis and Deprotection of Dipeptide C 80 | 32 |
| Scheme 43. Synthesis of Tripeptide Amine C 82 | 32 |
| Scheme 44. Synthesis of Tetrapeptide Amine C Analog 84 | 33 |
| Scheme 45. Coupling of Fragments B & C Surrogates 79 & 84 | 33 |
| Scheme 46. Model System For Amide Coupling Optimization | 34 |
| Scheme 47. Anticipated Completion of Feglymycin Analog 88 | 34 |
| Scheme 48. Proposed Biosynthesis of Manzamine C..... | 37 |
| Scheme 49. Proposed Biosynthesis of Manzamine Family of Alkaloids | 38 |
| Scheme 50. Synthesis of Keramaphidin B..... | 39 |
| Scheme 51. Proposed Dimerization Pathway for Kauluamine..... | 39 |

| | |
|---|----|
| Scheme 52. Winkler's Approach to Manzamine A..... | 40 |
| Scheme 53. Martin's Stille/Diels-Alder Cascade | 41 |
| Scheme 54. Martin's Solution to Undesired Ring-Closing Metathesis..... | 41 |
| Scheme 55. Fukuyama's Approach to Manzamine A..... | 42 |
| Scheme 56. Nishida's Preparation of the Tricyclic Core of Manzamine B | 42 |
| Scheme 57. Aminohydroxylation Reactions..... | 43 |
| Scheme 58. Mechanism of Brønsted Acid-Catalyzed Aminohydroxylation Reaction..... | 43 |
| Scheme 59. Tandem O→N Acyl Transfer/Aminohydroxylation | 44 |
| Scheme 60. Kauluamine Core Retrosynthesis | 44 |
| Scheme 61. Azido Ester Retrosynthesis | 45 |
| Scheme 62. Palladium(II) Coupling of Diazoacetates with Allyl Bromide (Wang) | 46 |
| Scheme 63. Preparation of Allylic Alcohol 67 and Attempted Dehydration | 46 |
| Scheme 64. Preparation of Diene 151 | 47 |
| Scheme 65. Sharpless Asymmetric Dihydroxylation | 47 |
| Scheme 66. Mitsunobu Gives Undesired Regioselectivity..... | 48 |
| Scheme 67. Mitsunobu to Install Ester | 48 |
| Scheme 68. Preparation of Azido Ester 149 | 49 |
| Scheme 69. Tandem Aminohydroxylation-Acyl Transfer..... | 49 |
| Scheme 70. Expected and Observed Treatment with SmI ₂ | 50 |
| Scheme 71. Aminohydroxylation and Attempted Acyl Transfer | 50 |
| Scheme 72. Aminohydroxylation with Azido Alcohol 157 | 50 |
| Scheme 73. Cyclization to Piperidine Core | 51 |
| Scheme 74. Preparation of Model Piperidine Core of Kauluamine..... | 58 |
| Scheme 75. Ipso-Substitution Stereochemical Model | 60 |
| Scheme 76. Alternate Ipso-Substitution with Nitrilium | 61 |
| Scheme 77. Predicted Elimination to Z-Enamine..... | 61 |

| | |
|---|----|
| Scheme 78. Stereochemical Model for Cyclization..... | 62 |
| Scheme 79. Azide 87 Retrosynthesis..... | 63 |
| Scheme 80. Route to Acryloyl Imide 176 | 63 |
| Scheme 81. Bracher's Route to Acetyl β -Carboline 192 | 64 |
| Scheme 82. Alternate Preparation of Acetyl β -Carboline 192 | 64 |
| Scheme 83. Attempted Formation of Vinyl Triflate 184 | 65 |
| Scheme 84. Attempted Triflate Formation with 193 | 65 |
| Scheme 85. Route to Azide Via γ -Lactone..... | 65 |
| Scheme 86. Jacobsen's Conversion of Terminal Epoxides to γ -Butanolides..... | 66 |
| Scheme 87. Epiazidohydrin as a Substrate | 66 |
| Scheme 88. Epichlorohydrin and Epibromohydrin as Substrates..... | 67 |
| Scheme 89. Optimized Conditions for Epiazidohydrin | 69 |
| Scheme 90. Elimination to Azido Vinyl Bromide 197 | 70 |
| Scheme 91. Attempted Sonagashira Coupling with 197 | 70 |
| Scheme 92. Attempted Stille Coupling with 197 | 70 |
| Scheme 93. Attempted Diiodination..... | 71 |
| Scheme 94. Installation of C11-15 After BACC | 71 |
| Scheme 95. Aminohydroxylation with Azido Vinyl Bromide 197 | 71 |
| Scheme 96. Synthesis of Imide 186 | 72 |
| Scheme 97. Preparation of Alternate Imide 222 | 72 |
| Scheme 98. Formation of Cyclic Imide 176 Via RCM | 73 |
| Scheme 99. Competition Experiment Between α - and β -Substituted Imides (KBH)..... | 73 |
| Scheme 100. Acid-Promoted Aza-Schmidt Azide Rearrangement | 74 |
| Scheme 101. Aminohydroxylation with α -Substituted Imides..... | 74 |
| Scheme 102. Reactivity Control Experiments for 197 and 176 | 74 |
| Scheme 103. Iminoacetoxylation of Imide 176 | 76 |

| | |
|---|----|
| Scheme 104. Attempted [3+2] Cyclization with Imide 186 | 78 |
| Scheme 105. Aminohydroxylation & Tandem Acyl Transfer/Piperidine Cyclization..... | 79 |
| Scheme 106. Brønsted Acid-Catalyzed [3+2] Cycloaddition Pathway | 79 |

LIST OF TABLES

| | |
|---|----|
| Table 1. Elimination to 151 Temperature Screen | 47 |
| Table 2. Initial Temperature Screen..... | 68 |
| Table 3. Second Temperature Screen | 69 |
| Table 4. [3+2] Cycloaddition Acid Screen | 75 |
| Table 5. [3+2] Cycloaddition Temperature Screen | 76 |

LIST OF FIGURES

| | |
|---|----|
| Figure 1. Common Coupling Reagents..... | 2 |
| Figure 2. Aryl Glycine Containing Natural Products | 4 |
| Figure 3. (<i>R,R</i>)-PBAM and (<i>S,S</i>)-PBAM..... | 7 |
| Figure 4. Structure of Feglymycin | 8 |
| Figure 5. Crystal Structure of Feglymycin | 9 |
| Figure 6. Feglymycin Residue Numbering System for Alanine Scan | 14 |
| Figure 7. Residues Important for Antibacterial Activity Against <i>S. Aureus</i> Strains | 15 |
| Figure 8. Residues Important for Enzyme MurA Inhibitory Activity | 15 |
| Figure 9. Preparation and Deprotection of Boc-Pentapeptide Analog 76 | 30 |
| Figure 10. Manzamines A (89), B (90), and C (91) and Kauluamine (92)..... | 36 |
| Figure 11. Similarities Between Proposed Biosynthetic Intermediates and Natural Products | 38 |
| Figure 12. Nakadomarin A, Papuamine, and Manzamine C | 40 |
| Figure 13. Chair Transition States for Cyclization | 45 |
| Figure 14. Stereochemical Model for Intramolecular Michael Addition | 45 |
| Figure 15. HMBC Structural Elucidation | 52 |
| Figure 16. New Connectivity and Precursor..... | 53 |
| Figure 17. Expanded Spin Systems and Precursor | 53 |
| Figure 18. HMBC Correlations to Suggest Cyclization and Precursor | 53 |
| Figure 19. Piperidine Skeleton and Precursor..... | 54 |
| Figure 20. Expanded Skeleton and Precursor | 54 |
| Figure 21. Possible Structures..... | 55 |
| Figure 22. Labeling for NOESY Discussion | 55 |
| Figure 23. NOESY Correlations (168): β , γ anti | 55 |
| Figure 24. NOESY Correlations (168): β , γ syn..... | 56 |
| Figure 25. NOESY Correlations (169): β , γ syn, α anti..... | 56 |

| | |
|--|-----|
| Figure 26. NOESY Correlations (169): α , β , γ syn..... | 56 |
| Figure 27. NOESY Correlations (169): α , γ anti | 57 |
| Figure 28. Final Structure | 57 |
| Figure 29. NOESY Confirmed: Newman Projections (β , δ in Front)..... | 57 |
| Figure 30. NOESY Confirmed: Newman Projections (δ , CH ₂ in Front)..... | 57 |
| Figure 31. Kauluamine Retrosynthesis | 59 |
| Figure 32. Kauluamine Retrosynthesis Cont'd | 59 |
| Figure 33. Ipso-Substitution Transition States..... | 60 |
| Figure 34. Chair Transition States for Cyclization | 62 |
| Figure 35. Azide 175 and Kauluamine Unit A Triflate 170 | 62 |
| Figure 36. Acryloyl Imide 176 and Kauluamine Unit A Triflate 170 | 63 |
| Figure 37. Proposed Reaction Pathways..... | 67 |
| Figure 38. Shifts of Aromatic Protons in 231 and 234 | 77 |
| Figure 39. TOCSY Spin-System & COSY Correlations | 77 |
| Figure 40. ¹ H NMR (DMSO- <i>d</i> ₆) of 39 | 103 |
| Figure 41. ¹³ C NMR (DMSO- <i>d</i> ₆) of 39 | 104 |
| Figure 42. ¹ H NMR (DMSO- <i>d</i> ₆) of 55 | 105 |
| Figure 43. ¹³ C NMR (DMSO- <i>d</i> ₆) of 55 | 106 |
| Figure 44. ¹ H NMR (DMSO- <i>d</i> ₆) of 56 | 107 |
| Figure 45. ¹³ C NMR (DMSO- <i>d</i> ₆) of 56 | 108 |
| Figure 46. ¹ H NMR (DMSO- <i>d</i> ₆) of TFA· 59 | 109 |
| Figure 47. ¹³ C NMR (DMSO- <i>d</i> ₆) of TFA· 59 | 110 |
| Figure 48. ¹⁹ F NMR (DMSO- <i>d</i> ₆) of TFA· 59 | 111 |
| Figure 49. ¹ H NMR (DMSO- <i>d</i> ₆) of 63 | 112 |
| Figure 50. ¹³ C NMR (DMSO- <i>d</i> ₆) of 63 | 113 |
| Figure 51. ¹ H NMR (CDCl ₃) of 65 | 114 |

| | |
|---|-----|
| Figure 52. ^1H NMR (DMSO- d_6) of 66 | 115 |
| Figure 53. ^{13}C NMR (DMSO- d_6) of 66 | 116 |
| Figure 54. ^1H NMR (CDCl_3) of 68 | 117 |
| Figure 55. ^1H NMR (DMSO- d_6) of 69 | 118 |
| Figure 56. ^{13}C NMR (DMSO- d_6) of 69 | 119 |
| Figure 57. ^1H NMR (DMSO- d_6) of 72 | 120 |
| Figure 58. ^{13}C NMR (DMSO- d_6) of 72 | 121 |
| Figure 59. ^{19}F NMR (DMSO- d_6) of 72 | 122 |
| Figure 60. ^1H NMR (DMSO- d_6) of HCl· 73 | 123 |
| Figure 61. ^{13}C NMR (DMSO- d_6) of HCl· 73 | 124 |
| Figure 62. ^{19}F NMR (DMSO- d_6) of HCl· 73 | 125 |
| Figure 63. ^1H NMR (DMSO- d_6) of 74 | 126 |
| Figure 64. ^{13}C NMR (DMSO- d_6) of 74 | 127 |
| Figure 65. ^{19}F NMR (DMSO- d_6) of 74 | 128 |
| Figure 66. ^1H NMR (DMSO- d_6) of TFA· 75 | 129 |
| Figure 67. ^{13}C NMR (DMSO- d_6) of TFA· 75 | 130 |
| Figure 68. ^{19}F NMR (DMSO- d_6) of TFA· 75 | 131 |
| Figure 69. ^1H NMR (DMSO- d_6) of 76 | 132 |
| Figure 70. ^{13}C NMR (DMSO- d_6) of 76 | 133 |
| Figure 71. ^{19}F NMR (DMSO- d_6) of 76 | 134 |
| Figure 72. ^1H NMR (DMSO- d_6) of 78 | 135 |
| Figure 73. ^{13}C NMR (DMSO- d_6) of 78 | 136 |
| Figure 74. ^{19}F NMR (DMSO- d_6) of 78 | 137 |
| Figure 75. ^{13}H NMR (DMSO- d_6) of 79 | 138 |
| Figure 76. ^{13}C NMR (DMSO- d_6) of 79 | 139 |
| Figure 77. ^{19}F NMR (DMSO- d_6) of 79 | 140 |

| | |
|---|-----|
| Figure 78. ^1H NMR (DMSO- d_6) of 86 | 141 |
| Figure 79. ^{13}C NMR (DMSO- d_6) of 86 | 142 |
| Figure 80. ^{19}F NMR (DMSO- d_6) of 86 | 143 |
| Figure 81. ^1H NMR (CDCl_3) of 149 | 144 |
| Figure 82. ^{13}C NMR (CDCl_3) of 149 | 145 |
| Figure 86. ^{13}C NMR (CDCl_3) of 150 | 146 |
| Figure 83. ^1H NMR (CDCl_3) of 150 | 147 |
| Figure 84. ^1H NMR (CDCl_3) of 151 | 148 |
| Figure 85. NOESY (CDCl_3) of 151 | 149 |
| Figure 87. ^1H NMR (CDCl_3) of 155 | 150 |
| Figure 88. ^{13}C NMR (CDCl_3) of 155 | 151 |
| Figure 89. ^1H NMR (CDCl_3) of 156 | 152 |
| Figure 90. ^{13}C NMR (CDCl_3) of 156 | 153 |
| Figure 91. ^1H NMR (CDCl_3) of 157 | 154 |
| Figure 92. ^{13}C NMR (CDCl_3) of 157 | 155 |
| Figure 93. ^1H NMR (CDCl_3) of 159 | 156 |
| Figure 94. ^{13}C NMR (CDCl_3) of 159 | 157 |
| Figure 95. ^1H NMR (CDCl_3) of 160 | 158 |
| Figure 96. ^{13}C NMR (CDCl_3) of 160 | 159 |
| Figure 97. ^1H NMR (CDCl_3) of 161 | 160 |
| Figure 98. ^{13}C NMR (CDCl_3) of 161 | 161 |
| Figure 99. ^1H NMR (CDCl_3) of 163 | 162 |
| Figure 100. ^{13}C NMR (CDCl_3) of 163 | 163 |
| Figure 101. ^1H NMR (CDCl_3) of 164 | 164 |
| Figure 102. ^{13}C NMR (CDCl_3) of 164 | 165 |
| Figure 103. ^1H NMR (CDCl_3) of 167 | 166 |

| | |
|--|-----|
| Figure 104. ^{13}C NMR (CDCl_3) of 167 | 167 |
| Figure 105. COSY (CDCl_3) of 167 | 168 |
| Figure 106. HSQC (CDCl_3) of 167 | 169 |
| Figure 107. HMBC (CDCl_3) of 167 | 170 |
| Figure 108. NOESY (CDCl_3) of 167 | 171 |
| Figure 109. ^1H NMR (CDCl_3) of 176 | 172 |
| Figure 110. ^{13}C NMR (CDCl_3) of 176 | 173 |
| Figure 111. HSQC (CDCl_3) of 176 | 174 |
| Figure 112. NOESY (CDCl_3) of 176 | 175 |
| Figure 113. ^1H NMR (CDCl_3) of 186 | 176 |
| Figure 114. ^{13}C NMR (CDCl_3) of 186 | 177 |
| Figure 115. ^1H NMR (CDCl_3) of 197 | 178 |
| Figure 116. ^{13}C NMR (CDCl_3) of 197 | 179 |
| Figure 117. ^1H NMR (CDCl_3) of 204 | 180 |
| Figure 118. ^{13}C NMR (CDCl_3) of 204 | 181 |
| Figure 119. ^1H NMR (CDCl_3) of 205 | 182 |
| Figure 120. ^{13}C NMR (CDCl_3) of 205 | 183 |
| Figure 121. ^1H NMR (CDCl_3) of 206 | 184 |
| Figure 122. ^{13}C NMR (CDCl_3) of 206 | 185 |
| Figure 123. ^1H NMR (CDCl_3) of 212 | 186 |
| Figure 124. ^{13}C NMR (CDCl_3) of 212 | 187 |
| Figure 125. ^1H NMR (CDCl_3) of 214 | 188 |
| Figure 126. ^{13}C NMR (CDCl_3) of 214 | 189 |
| Figure 127. ^1H NMR (CDCl_3) of 216-d1 | 190 |
| Figure 128. ^{13}C NMR (CDCl_3) of 216-d1 | 191 |
| Figure 129. ^1H NMR (CDCl_3) of 216-d2 | 192 |

| | |
|--|-----|
| Figure 130. ^{13}C NMR (CDCl_3) of 216-d2 | 193 |
| Figure 131. ^1H NMR (CDCl_3) of 220 | 194 |
| Figure 132. ^{13}C NMR (CDCl_3) of 220 | 195 |
| Figure 133. ^1H NMR (CDCl_3) of 221 | 196 |
| Figure 134. ^{13}C NMR (CDCl_3) of 221 | 197 |
| Figure 135. ^1H NMR (CDCl_3) of 222 | 198 |
| Figure 136. ^{13}C NMR (CDCl_3) of 222 | 199 |
| Figure 137. ^1H NMR (CDCl_3) of 223 | 200 |
| Figure 138. ^{13}C NMR (CDCl_3) of 223 | 201 |
| Figure 139. ^1H NMR (CDCl_3) of 231 | 202 |
| Figure 140. ^{13}C NMR (CDCl_3) of 231 | 203 |
| Figure 141. ^1H NMR (CDCl_3) of 234 | 204 |
| Figure 142. ^{13}C NMR (CDCl_3) of 234 | 205 |
| Figure 143. COSY (CDCl_3) of 234 | 206 |
| Figure 144. TOCSY (CDCl_3) of 234 | 207 |
| Figure 145. HSQC (CDCl_3) of 234 | 208 |

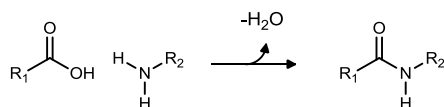
CHAPTER I

PROGRESS TOWARDS THE TOTAL SYNTHESIS OF A FEGLYMYCIN ANALOG

1.1 Introduction & Background

The earliest discoveries of amino acids, widely considered to be the building blocks of life, were reported at the beginning of the nineteenth century.¹ It was not until almost a hundred years later that Emil Fischer and Franz Hofmeister proposed that the linkage between amino acids, the amide or peptide bond (Scheme 1), is what allowed for the formation of long chains of amino acids, called proteins. The construction

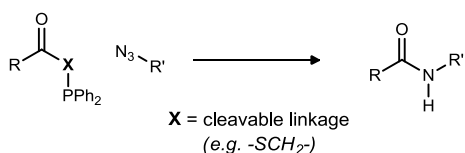
Scheme 1. Dehydrative Coupling to form Amide Bonds



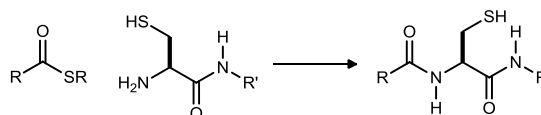
of these proteins proceeds smoothly and is facile for nature's rather elegant machinery, formally condensing an amine with a carboxylic acid to lose a molecule of water, but the formation of amide bonds in the laboratory is a challenge that still receives considerable attention today. From Staudinger's peptide ligation² to solid phase synthesis³ to the more recent ketoacid-hydroxylamine ligation,⁴ studies of the use and formation of amide bonds have a rich and innovative history.⁵ Some of the more successful methods (Scheme 2) also include native chemical ligation,⁶ hydrative amide synthesis through alkyne-azide coupling,⁷ and oxidative amidation of

Scheme 2. Recent Approaches to Amide Synthesis

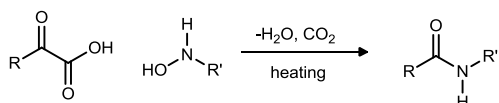
Staudinger ligation:



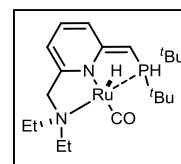
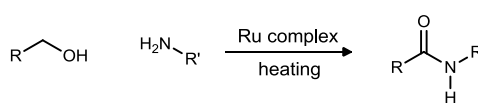
Native chemical ligation:



Ketoacid-hydroxylamine ligation:



Direct amide synthesis from alcohols and amines:



alcohols,⁸ aldehydes,⁹ or alkynes,¹⁰ among others.

¹ Vickery, H. B.; Schmidt, C. L. A. *Chem. Rev.* **1981**, *9*, 169.

² a) Saxon, E.; Armstrong, J. I.; Bertozzi, C. R. *Org. Lett.* **2000**, *2*, 2141. b) Saxon, E.; Bertozzi, C. R. *Science*, **2000**, *287*, 2007. c) Saxon, E. *et al. J. Am. Chem. Soc.* **2002**, *124*, 14893. d) Nilsson, B. L.; Kiessling, L. L.; Raines, R. T. *Org. Lett.* **2000**, *2*, 1939. e) Kohn, M.; Breinbauer, R. *Angew. Chem. Int. Ed.* **2004**, *43*, 3106.

³ a) Merrifield, R. B. *J. Am. Chem. Soc.* **1963**, *85*, 2149. b) Merrifield, R. B. *J. Am. Chem. Soc.* **1964**, *86*, 304.

⁴ Bode, J. W.; Fox, R. M.; Baucom, K. D. *Angew. Chem. Int. Ed.* **2006**, *45*, 1248.

⁵ Bode, J. W. *Curr. Opin. Drug Disc. Dev.* **2006**, *9*, 765.

⁶ Dawson, P. E.; Muir, T. W.; Clarklewis, I.; Kent, S. B. H. *Science* **1994**, *266*, 776.

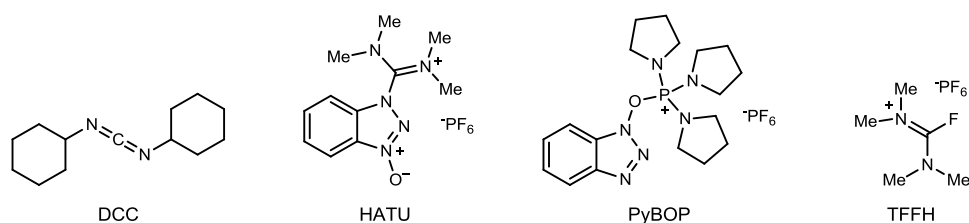
⁷ a) Cho, S. H.; Yoo, E. J.; Bae, L.; Chang, C. *J. Am. Chem. Soc.* **2005**, *127*, 16046. b) Cassidy, M. P.; Raushel, J.; Fokin, V. V. *Angew. Chem. Int. Ed.* **2006**, *45*, 3154.

⁸ a) Gunanathan, C.; Ben-David, Y.; Milstein, D. *Science* **2007**, *317*, 790. b) Nordstrom, L. U.; Vogt, H.; Madsen, R. *J. Am. Chem.*

Amide bonds are widely found in compounds on the market today, particularly in pharmaceuticals. Of the top 200 drugs sold in the U.S. in 2012, more than 20% were proteins, including the number six drug Humira, an antirheumatic, and another 25% contained amide bonds, including the immunosuppressant Restasis, which ranked seventy-first in retail sales.¹¹ Thus, with almost half of the top drugs sold in 2012 containing amide bonds, it is unsurprising that new methods for the construction of amide bonds are continually appearing in the scientific literature. With the success of these pharmacologically active compounds and the potential benefits of undiscovered amides and other functional group-containing compounds, the search for and synthesis of even more useful compounds continues.

Perhaps the most commonly used dehydrative method to form amide bonds is the active ester method, in which the carboxylic acid is activated through the use of electrophilic coupling reagents (Figure 1) such as carbodiimides,¹² uronium salts, and phosphonium salts towards attack by the nucleophilic amine.¹³

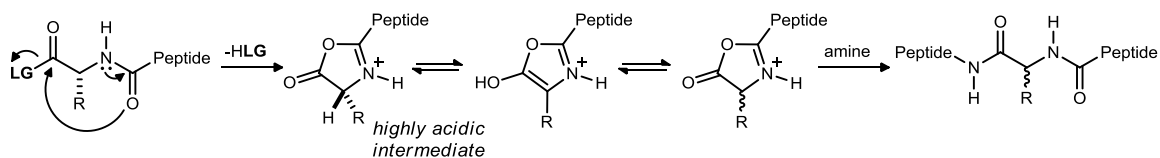
Figure 1. Common Coupling Reagents



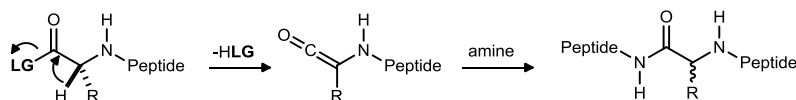
Unfortunately, in the case of α -substituted carboxylic acids, the α -proton becomes more acidic following formation of the active ester, which can lead to epimerization of the α -stereocenter via ketene or azlactone formation (Scheme 3). In order to avoid these pathways, great excesses of high molecular weight racemization suppressants such as hydroxybenzotriazole (HOBt) are commonly used. This event becomes particularly problematic when attempting to incorporate amino acids such as aryl glycines, which possess an inherently lower pK_a at the α -position, and peptidic carboxylic acids, which contain nucleophilic moieties that may lead to intramolecular cyclization and subsequently epimerization.

Scheme 3. Epimerization Pathways in Active Ester Amide Bond Formations

azlactone formation:



ketene formation:



LG = leaving group

Soc. **2008**, *130*, 17672.

⁹ a) Yoo, W. J.; Li, C. J. *J. Am. Chem. Soc.* **2006**, *128*, 13064. b) Gao, J.; Wang, G.-W. *J. Org. Chem.* **2008**, *73*, 2955.

¹⁰ Chan, W. K.; Ho, C. M.; Wong, M. K.; Che, C. M. *J. Am. Chem. Soc.* **2006**, *128*, 14796.

¹¹ McGrath, N. A.; Brichacek, M.; Njardarson, J. T. *J. Chem. Ed.* **2010**, *87*, 1348-1439.; http://cbc.arizona.edu/njardarson/group/sites/default/files/Top200%20Pharmaceutical%20Products%20by%20US%20Retail%20Sales%20in%202012_0.pdf

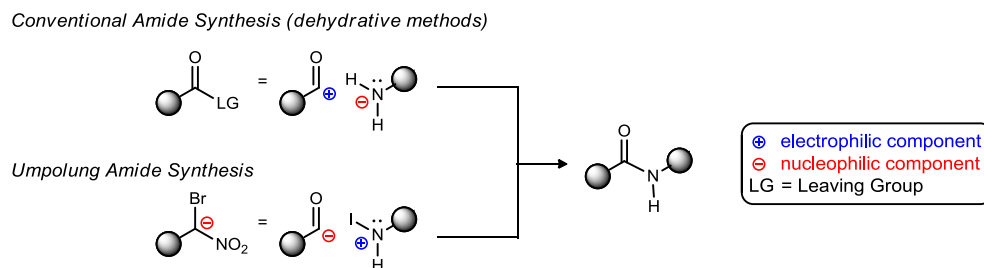
¹² Sheehan, J. C. Hess, G. P. *J. Am. Chem. Soc.* **1955**, *77*, 1067.

¹³ For recent reviews, see: a) Han, S. Y.; Kim, Y. A. *Tetrahedron* **2004**, *60*, 2447. b) Montalbetti, C. A. G. N.; Falque, V. *Tetrahedron* **2005**, *61*, 10827. c) Valeur, E.; Bradley, M. *Chem. Soc. Rev.* **2009**, *38*, 606.

1.1.1 Umpolung Amide Synthesis

A recent report¹⁴ by our group reveals a novel amide bond-forming reaction that mechanistically disallows racemization of the α -stereocenter and alleviates reliance upon commercially available carboxylic acids. The method, called Umpolung Amide Synthesis (UmAS), effectively reverses the polarities (German, *umpolung*) of the carbon and nitrogen in the key C-N bond-forming step by using an α -bromonitro alkane as a nucleophilic carboxylic acid surrogate and an electrophilic *N*-halo amine in place of the more conventional electrophilically active ester and nucleophilic amine (Scheme 4). More recently, a mechanistic study of the

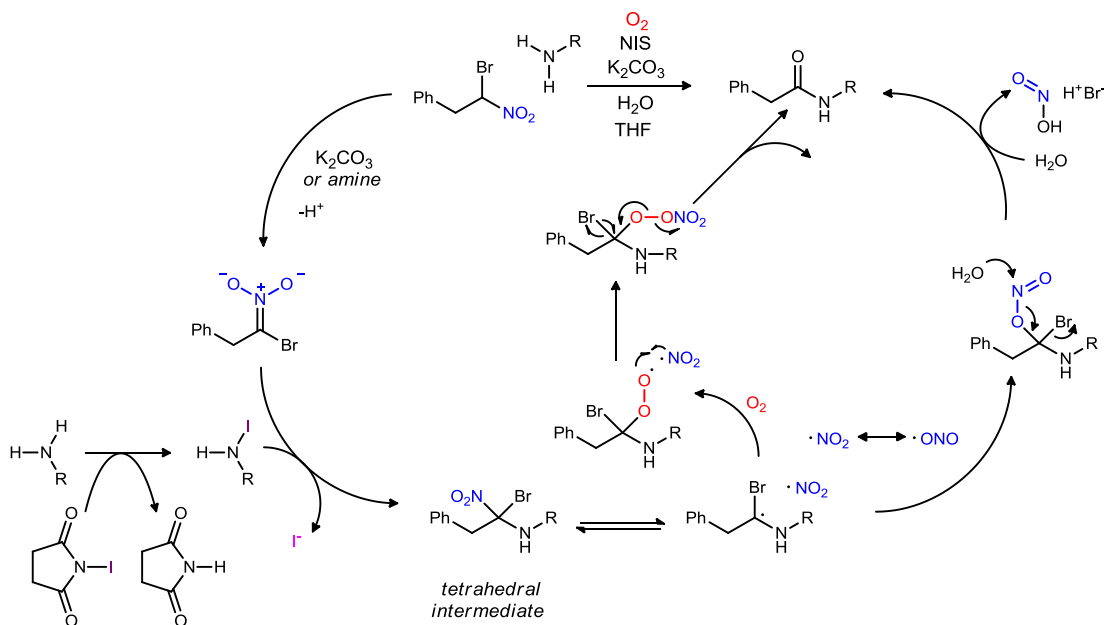
Scheme 4. Conventional vs. Umpolung Amide Synthesis



reaction led to the discovery of the ability to site-selectively incorporate ¹⁸O labels into the amide functional groups,¹⁵ and we have also demonstrated the utility of the reaction through the synthesis of α -oxy amides.¹⁶

The proposed reaction mechanism is shown in Scheme 5. The method utilizes *N*-iodosuccinimide to electrophilically activate a monosubstituted amine, forming *N*-iodo amine *in situ*. The α -bromonitro donor is deprotonated under basic conditions to form the nitronate, which nucleophilically attacks the *N*-iodo amine, forming a putative tetrahedral intermediate. Collapse of the tetrahedral intermediate under either aerobic or anaerobic conditions then leads to amide formation. Through reaction development, we have found that the reaction proceeds best in ethereal solvents and with a small amount of water to solubilize an inorganic base,

Scheme 5. Umpolung Amide Synthesis Mechanism



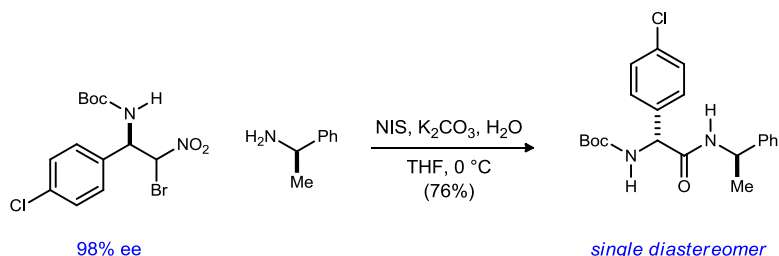
¹⁴ Shen, B.; Makley, D. M.; Johnston, J. N. *Nature* **2010**, 465, 1027.

¹⁵ Shackleford, J. P.; Shen, B.; Johnston, J. N. *Proc. Natl. Acad. Sci.* **2012**, 109, 44.

¹⁶ Leighty, M.; Shen, B.; Johnston, J. N. *J. Am. Chem. Soc.* **2012**, 134, 15233.

typically potassium carbonate. Representative conditions for the umpolung amide synthesis reaction are given in Scheme 6. Because formation of an active ester intermediate is avoided and racemization is mechanistically

Scheme 6. Representative Umpolung Amide Synthesis Reaction

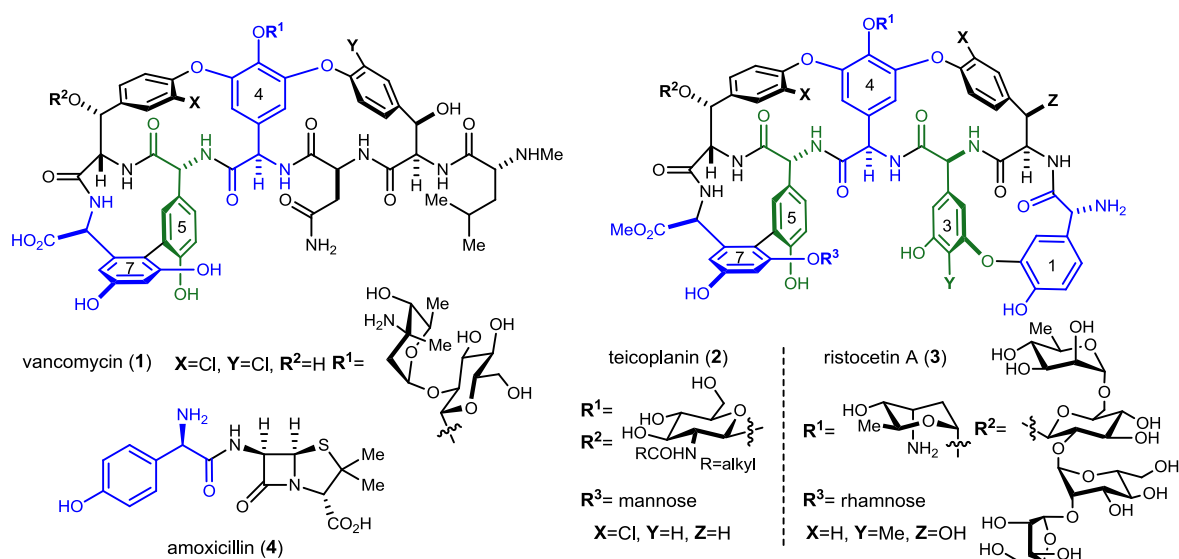


avoided, this method is ideal for the incorporation of aryl glycine residues into peptides, and we observe no racemization at the α -position. We have also had success incorporating all twenty canonical amino acids when they are used as the amine acceptors.¹⁴

1.1.2 Enantioselective Aryl Glycine Synthesis

While not as ubiquitous as the twenty canonical amino acids, aryl glycines represent an important class of nonproteinogenic amino acids. Aryl glycine residues appear in many biologically important natural products that have been isolated and studied in the last sixty years. Perhaps the most well-known example of these is the glycopeptide antibiotic vancomycin (Figure 2, **1**).¹⁷ Vancomycin is a heptapeptide containing three aryl glycine

Figure 2. Aryl Glycine Containing Natural Products



residues and is used as the last line of defense against drug-resistant strains of bacteria.¹⁸ The compound has received much attention over recent years, and vancomycin and its aglycon form have been the subject of many synthetic manuscripts.¹⁹ Other notable aryl glycine-containing compounds include teicoplanin (**2**), ristocetin A (**3**), and amoxycillin (**4**), all of which are used medicinally.²⁰

¹⁷ McCormick, M.H.; Stark, W.M.; Pittenger, G.E.; Pittenger, R.C.; McGuire, G.M. *Antibiot. Annu.* **1955**, 606.

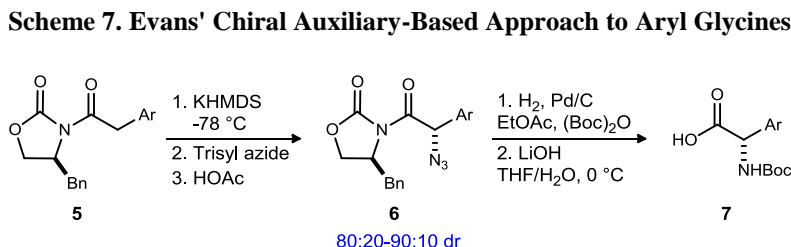
¹⁸ Williams, D. H.; Rajananda, D.; Williamson, M. P.; Bojeson, G. *Top. Antibiot. Chem.* **1980**, 5, 119.

¹⁹ a) Evans, D. A.; Wood, M. R.; Trotter, B. W.; Richardson, T. I.; Barrow, J. C.; Katz, J. L. *Angew. Chem. Int. Ed.* **1998**, 37, 2700. b) Evans, D. A.; Dinsmore, C. J.; Watson, P. S.; Wood, M. R.; Richardson, T. I.; Trotter, B. W.; Katz, J. L. *Angew. Chem. Int. Ed.* **1998**, 37, 2704. c) Nicolaou, K. C.; Natarajan, S.; Li, H.; Jain, N. F.; Hughes, R.; Solomon, M. E.; Ramanujulu, J. M.; Boddy, C. N. C.;

Direct Approaches to Aryl Glycines

With compounds that contain aryl glycine residues exhibiting significant antibacterial properties, it is unsurprising that synthesis of the functionality has been the focus of much research. The synthesis of these moieties in racemic form was achieved more than a century ago, and Strecker's method to prepare aryl glycines via a nitrile intermediate is still the most commonly used method for preparing aryl glycines.²⁰ As mentioned previously, aryl glycines are more acidic at the α -position than other α -amino acids due to the electron-withdrawing nature of the aromatic ring, making the enantioselective synthesis of these functional groups challenging.

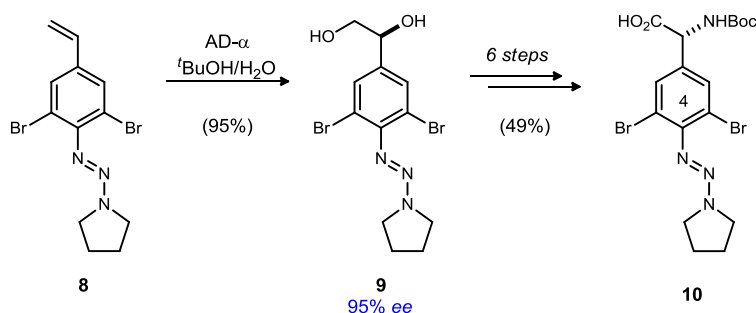
The last fifteen years has proven quite beneficial to the enantioselective synthesis of aryl glycine residues. The Evans group developed a chiral auxiliary-based approach to constructing aryl glycines (Scheme 7), utilizing a chiral auxiliary to direct an asymmetric enolate azidation reaction.²¹ Treatment of **5** with KHMDS



to form an enolate, followed by azidation on the least hindered face, gives **6** in moderate diastereomeric ratio (dr). Facile separation of the diastereomers, followed by hydrogenation and saponification, results in aryl glycine **7** in high enantiomeric excess (ee). Evans successfully used this method in his synthesis of aryl glycine residues for vancomycin.

An alternate approach to enantioselective aryl glycine synthesis is Nicolau's use of the Sharpless asymmetric dihydroxylation of styrenes (Scheme 8) in his synthesis of vancomycin.²² The dihydroxylation of styrene **8** gave diol **9** in high enantiomeric excess and yield. Diol **9** was then transformed, in six steps that included a Mitsunobu azide substitution²³ and subsequent Staudinger reduction,²⁴ to aryl glycine **10** in 49% yield. This rather lengthy approach to the asymmetric synthesis of aryl glycines was quickly supplanted by use

Scheme 8. Nicolau's Use of Sharpless' Asymmetric Dihydroxylation for the Synthesis of Aryl Glycines



Takayanagi, M. *Angew. Chem. Int. Ed.* **1998**, *37*, 2708. d) Nicolaou, K. C.; Jain, N. F.; Natarajan, S.; Hughes, R.; Solomon, M. E.; Li, H.; Ramanjulu, J. M.; Takayanagi, M.; Koumbis, A. E.; Bando, T. *Angew. Chem. Int. Ed.* **1998**, *37*, 2714. e) Nicolaou, K. C.; Takayanagi, M.; Jain, N. F.; Natarajan, S.; Koumbis, A. E.; Bando, T.; Ramanjulu, J. M. *Angew. Chem. Int. Ed.* **1998**, *37*, 2717. f) Boger, D. L.; Miyazaki, S.; Kim, S. H.; Wu, J. H.; Castle, S. L.; Loiseleur, O.; Jin, Q. *J. Am. Chem. Soc.* **1999**, *121*, 10004.

²⁰ Williams, R. M.; Hendrix, J. A. *Chem. Rev.* **1992**, *92*, 889.

²¹ a) Evans, D. A.; Evrard, D. A.; Rychnovsky, S. D.; Fruh, T.; Wittingham, W. G.; DeVries, K. M. *Tet. Lett.* **1992**, *33*, 1189. b) Evans, D. A.; Britton, T. C.; Ellman, J. A.; Dorow, R. L. *J. Am. Chem. Soc.* **1990**, *112*, 4011. c) Evans, D. A.; Weber, A. E. *J. Am. Chem. Soc.* **1987**, *109*, 7151.

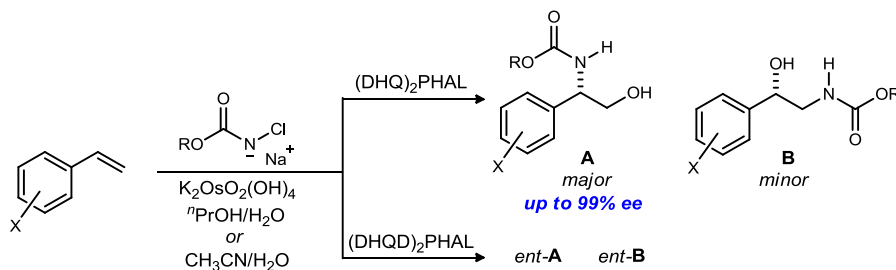
²² Kolb, H. C.; VanNieuwenhze, M. S.; Sharpless, K. B. *Chem. Rev.* **1994**, *94*, 2484.

²³ Lal, B.; Pramanik, B.; Manha, M. S.; Bose, A. K. *Tet. Lett.* **1977**, 1977.

²⁴ Staudinger, H.; Meyer, J. *Hel. Chem. Acta.* **1919**, *2*, 635.

of the Sharpless asymmetric aminohydroxylation reaction, published in the same year as Evans's and Nicolau's routes. Sharpless reported the asymmetric aminohydroxylation of styrenes,²⁵ which resulted in the *N*-carbamate protected arylglycinols in high enantiomeric excess (Scheme 9). A single oxidation step could then lead to the

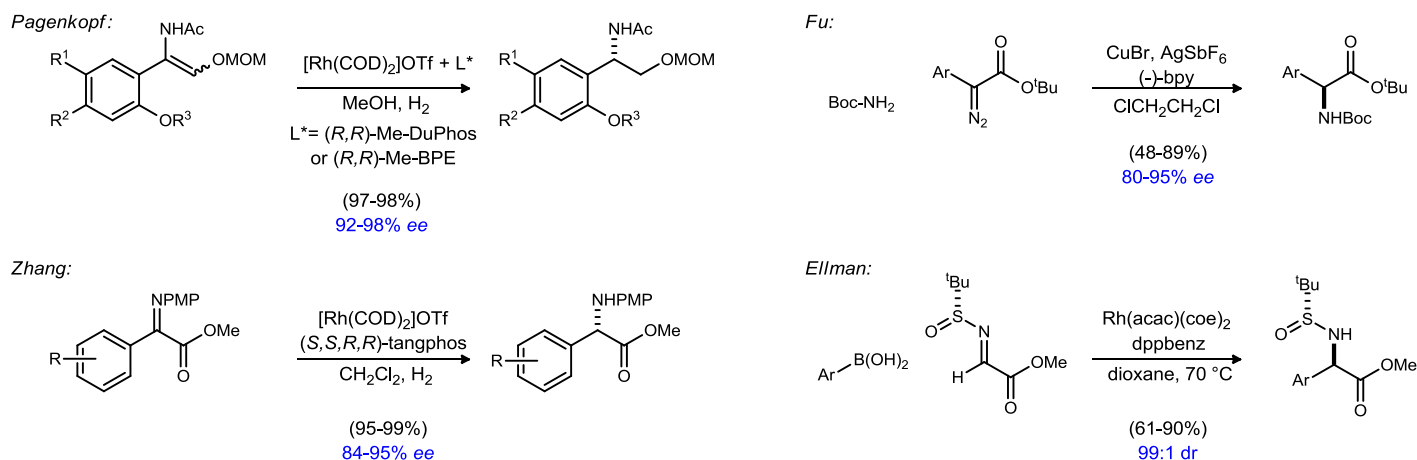
Scheme 9. Sharpless Asymmetric Aminohydroxylation for the Synthesis of Arylglycinols



elusive aryl glycines. Unfortunately, the reaction suffered from less than perfect regioselectivity, with some of the undesired regioisomer (**B**) always observed. Despite the regioselectivity issues, however, the Sharpless asymmetric aminohydroxylation became the method of choice for the asymmetric construction of aryl glycine residues for the purpose of natural product total synthesis.²⁶

More recent approaches to the enantioselective synthesis of aryl glycine residues include the hydrogenation of aryl enamides²⁷ and imino esters,²⁸ diazo insertion into N-H bonds,²⁹ and the addition of arylboronic acids to imino esters.³⁰ General reaction schemes for these approaches are shown in Scheme 10.

Scheme 10. Recent Developments in Enantioselective Aryl Glycine Synthesis



²⁵ Reddy, K. L.; Sharpless, K. B. *J. Am. Chem. Soc.* **1998**, *120*, 1207.

²⁶ *Vancomycin*: a) Crowley, B. M.; Boger, D. L. *J. Am. Chem. Soc.* **2006**, *128*, 2885. *Teicoplanin*: b) Evans, D. A.; Katz, J. L.; Peterson, G. S. *J. Am. Chem. Soc.* **2001**, *123*, 12411. *Ristocetin*: c) Crowley, B. M.; Mori, Y.; McComas, C. C.; Tang, D.; Boger, D. L. *J. Am. Chem. Soc.* **2004**, *126*, 4310. d) McComas, C. C.; Crowley, B. M.; Hwang, I.; Boger, D. L. *Bioorg. Med. Chem. Lett.* **2003**, *13*, 2933. *Chloropeptin/Complestatin*: e) Elder, A. M.; Rich, D. H. *Org. Lett.* **1999**, *1*, 1443. *Feglymycin*: f) Dettner, F.; Hanchen, A.; Schols, D.; Toti, L.; Nuber, A.; Sussmuth, R. D. *Angew. Chem. Int. Ed.* **2009**, *48*, 1856.

²⁷ Pagenkopf, B. L.; Le, J. C. D. *J. Org. Chem.* **2004**, *69*, 4177.

²⁸ Shang, G.; Yang, Q.; Zhang, X. *Angew. Chem. Int. Ed.* **2006**, *45*, 6360.

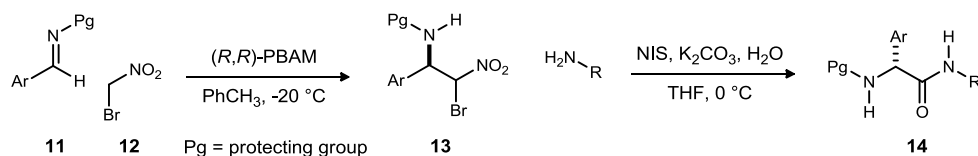
²⁹ Lee, E. C.; Fu, G. C. *J. Am. Chem. Soc.* **2007**, *129*, 12067.

³⁰ Beenen, M. A.; Weix, D. J.; Ellman, J. A. *J. Am. Chem. Soc.* **2006**, *128*, 6304.

Enantioselective Aza-Henry Reactions

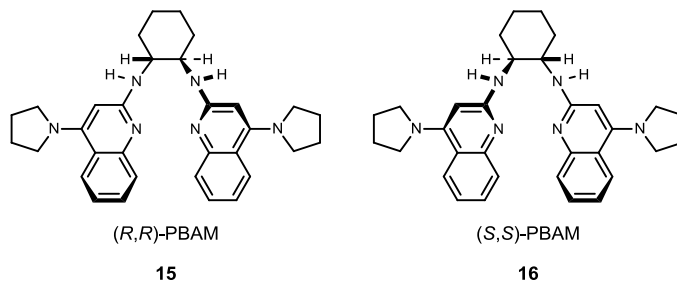
Recent advances in the area of asymmetric Henry reactions,³¹ aza-Henry reactions, and Michael additions to nitroalkenes³² have resulted in a diverse population of chiral, enantioenriched nitroalkanes.³³ Our approach to aryl glycine synthesis is via the enantioselective aza-Henry reaction developed in our lab.³⁴ While we do not directly prepare the individual aryl glycine residues, the aza-Henry addition of bromonitromethane (**12**) into protected imines (**11**) leads to the formation of β -amino, α -bromonitroalkanes (**13**), which, when subjected to umpolung amide synthesis, results in the incorporation of aryl glycine residues into peptides (**14**), as shown in Scheme 11.

Scheme 11. Incorporation of Aryl Glycine Residues via Aza-Henry & Umpolung Amide Synthesis



Extensive studies by the Johnston group with regards to the types of aromatic imines that can be used as well as the imine protecting group (Pg) have resulted in the availability of a variety of aryl glycine donors. The PBAM-catalyzed addition of bromonitromethane (BNM, **12**) into imines was originally developed with the *tert*-butylcarbamate protecting group in mind, and high yields (81-99%) and enantioselectivity (85-99% ee) have been achieved in the synthesis of these substrates.¹⁴ The development of a novel enantioselective aza-Henry addition of bromonitromethane into trimethylsilyl-protected imines followed by quenching with a variety of acyl halides³⁵ has led to the incorporation of a wide variety of protecting groups with relevance to peptide synthesis, including acetate (Ac), phenyl acetate (PhAc), azidoacetate (N₃Ac), benzoyl (Bz), pivaloyl (Piv), methoxy carbonyl (Moc), carbobenzyloxy (Cbz), fluorenylmethyloxy carbonyl (Fmoc), trichloroethyloxy carbonyl (Troc) and allyloxy carbonyl (Alloc), all in good yields (67-85%) and enantioselectivities (91-95% ee). Additionally, the use of either (*R,R*)-PBAM (**15**) or (*S,S*)-PBAM³⁶ (**16**) has allowed for access to both the (*R*-

Figure 3. (*R,R*)-PBAM and (*S,S*)-PBAM



³¹ For recent reviews, see: a) Palomo, C.; Oiarbide, M.; Mielgo, A. *Angew. Chem. Int. Ed.* **2004**, *43*, 5442. b) Boruwa, J.; Gogoi, N.; Saikia, P. P.; Barua, N. C. *Tetrahedron: Asymmetry* **2006**, *17*, 3315. c) Palomo, C.; Oiarbide, M.; Laso, A. *Eur. J. Org. Chem.* **2007**, 2516.

³² For recent reviews, see: a) Krause, N.; Hoffmann-Roder, A. *Synthesis* **2001**, 171. b) Berner, O. M.; Tedeschi, L.; Enders, D. *Eur. J. Org. Chem.* **2002**, 1877. c) Chistoffers, J.; Koripelly, G.; Rosiak, A.; Rossle, M. *Synthesis* **2007**, 1279. d) Tsogoeva, S. B. *Eur. J. Org. Chem.* **2007**, 1701.

³³ Ono, N. *The Nitro Group in Organic Synthesis*. Wiley-VCB: New York, New York, 2001.

³⁴ a) Nugent, B. M.; Yoder, R. A.; Johnston, J. N. *J. Am. Chem. Soc.* **2004**, *126*, 3418. b) Sing, A.; Yoder, R. A.; Shen, B.; Johnston, J. N. *J. Am. Chem. Soc.* **2007**, *129*, 3466. c) Singh, A.; Johnston, J. N. *J. Am. Chem. Soc.* **2008**, *130*, 5866. d) Wilt, J. C.; Pink, M.; Johnston, J. N. *Chem. Commun.* **2008**, *35*, 4177. e) Shen, B.; Johnston, J. N. *Org. Lett.* **2008**, *10*, 4397. f) Davis, T. A.; Wilt, J. C.; Johnston, J. N. *J. Am. Chem. Soc.* **2010**, *132*, 2880. g) Leighty, M. W.; Shen, B.; Johnston, J. N. *J. Am. Chem. Soc.* **2012**, *134*, 15233.

³⁵ Makley, D. M.; Johnston, J. N. Ph.D. Dissertation **2012**, Department of Chemistry, Vanderbilt University.

³⁶ Davis, T. A.; Dobish, M. C.; Schwieter, K. E.; Chun, A. C.; Johnston, J. N. *Org. Synth.* **2012**, *89*, 380.

and (*S*)- configured aryl glycine donors. While the aza-Henry addition results in a one to one mixture of diastereomers, the subsequent umpolung amide synthesis step results in a single diastereomer of product when a chiral amine acceptor is used.

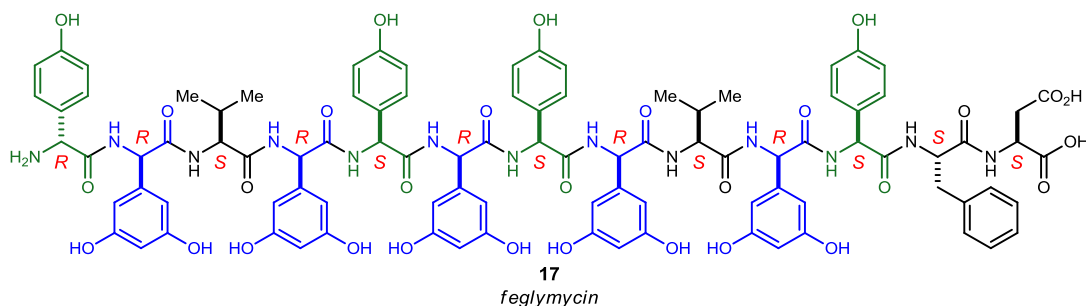
1.1.3 Feglymycin

When combined, umpolung amide synthesis and our enantioselective aryl glycine synthesis methods provide a powerful tool for preparing peptides that contain aryl glycines. To demonstrate the utility of these methods, the total synthesis of a peptidic natural product featuring aryl glycine residues whose biological activity is both interesting and desirable is being pursued.

Isolation and Key Structural Features

First reported in 1999, feglymycin (Figure 4, **17**) was isolated from a culture of *Streptomyces* sp. DSM

Figure 4. Structure of Feglymycin



11171.³⁷ Following fermentation and incubation of the cultures, the compound was isolated via solid phase extraction, size exclusion chromatography, and reverse-phase chromatography. Feglymycin was detected during reverse-phase high pressure liquid chromatography (RP-HPLC) by monitoring at 210 nm and was eluted from the C18 column with a retention time of 12.9 minutes when a 25% acetonitrile in water mobile phase that was doped with 0.1% trifluoroacetic acid (TFA) at a flow rate of 1.0 mL/min was used. Following acidic hydrolysis of feglymycin at 105 °C, the canonical amino acids L-valine (two), L-phenyl alanine, and L-aspartic acid were identified as components of the compound. The compound's structure was determined using ¹H (proton) and ¹³C (carbon) nuclear magnetic resonance (NMR) experiments, as well as the two-dimensional experiments COSY, TOCSY, NOESY, HSQC, and HMBC. The compound was found to have an [M+H]⁺ *m/z* at 1900.6 and an [M+2H]²⁺ *m/z* at 950.9. The monoisotopic molecular weight was thus determined to be 1899.6, which would indicate an odd number of nitrogens and a molecular formula of C₉₅H₉₇N₁₃O₃₀. Analysis of the MS-MS results confirmed the amino acid sequence of feglymycin, and it was found to feature several of the rare amino acids 4-hydroxyphenylglycine (Hpg) and 3,5-dihydroxyphenylglycine (Dpg).

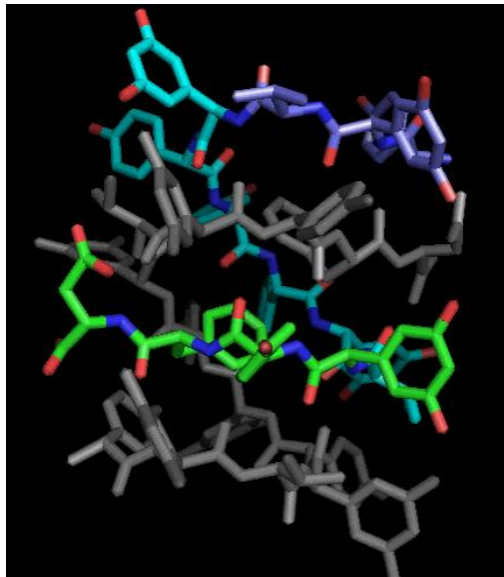
While the sequence of amino acids was determined using a combination of NMR and MS-MS, the relative stereochemistries of the Hpg and Dpg residues were not identified until 2005, when the crystal structure (Figure 5) of the molecule was reported.³⁸ It was found that the amino acid residues of this 13-membered peptide alternated in the *D,L*-configurations, except at the two termini. The crystal structure of feglymycin, as determined by analysis of its X-ray diffraction pattern, exhibited perfect merohedral twinning, and the single crystal grown from an aqueous solution contained six dimers of the molecule. With 1033 non-hydrogen atoms, the structure was the largest equal-atom structure to be solved using direct ab initio methods. The feglymycin dimers were found to be wide, antiparallel, double-stranded β helices, with a helical pitch of 9.0 residues per turn; the dimer is stabilized through intermolecular hydrogen bonding between phenolic OH groups. The channel formed by the helical dimer of feglymycin is occupied by the phenyl alanine side chains (Figure 5),

³⁷ Vértesy, L.; Aretz, W.; Knauf, M.; Markus, A.; Vogel, M.; Wink, J. J. *Antibiotics* **1999**, *52*, 374.

³⁸ Bunkóczi, G.; Vértesy, L.; Sheldrick, G. M. *Angew. Chem. Int. Ed.* **2005**, *44*, 1340.

which gives some insight to the possible mode of action for feglymycin's biological activity, which is discussed in the next section.

Figure 5. Crystal Structure of Feglymycin³⁹



Biological Activity of Feglymycin

Initial reports of feglymycin's antibacterial activity indicated that it had only weak antibacterial activity against Gram positive bacteria, with IC_{50} values between 32 and 64 μM against several strains of *Staphylococcus aureus*.³⁷ Following their synthesis of feglymycin, Süssmuth and coworkers found that feglymycin was also active against methicillin-resistant *S. aureus* strains, prompting further studies into the natural product's mechanism of action. Based on the compound's size and structure, it was hypothesized to have a similar mode of action to those of such aryl glycine-containing peptides as vancomycin and ramoplanin. These compounds are known to inhibit the late stages of peptidoglycan synthesis, which results in their interference with cell wall biosynthesis. However, studies of feglymycin's activity indicated that it did not have an effect on these late stages. Instead, feglymycin was found to inhibit earlier stages of peptidoglycan biosynthesis. The enzymes MurA-F are known to catalyze the first six steps of peptidoglycan synthesis, so feglymycin was tested against these enzymes. Süssmuth and coworkers reported that feglymycin had the most significant impact on the enzymes MurA and MurC, noncompetitively inhibiting them and making feglymycin the first known natural inhibitor of these enzymes. With such a unique mechanism of action, feglymycin may prove to be useful against antibiotic-resistant bacterial strains.⁴⁰

In the report of the isolation of feglymycin, the compound was also found to strongly inhibit the formation of human immunodeficiency virus (HIV) syncytia *in vitro* ($IC_{50} = 5 \mu M$).³⁷ Syncytia are formed when two or more mononucleate cells merge together, resulting in a multinucleate cell.⁴¹ Syncytia formed when multiple CD^{4+} T-cells are joined have thus become a hallmark of HIV infection. HIV entry into healthy cells begins with binding of the heavy glycosylated envelope protein gp120 to the cellular CD4 receptor, which results in conformational changes inside the viral envelope, allowing for interactions with the chemokine receptors CCR5 and/or CXCR4. Interaction of gp120 with these receptors results in insertion of gp41 into the target membrane.⁴² The membrane fusion protein gp41, a subunit of the envelope protein complex of the HIV retrovirus, is responsible for the second step of HIV entry into white blood cells. Following binding of HIV to

³⁹ Image created using the PyMOL Molecular Graphics System, Version 1.3 Schrödinger, LLC.

⁴⁰ Rausch, S.; Hänchen, A.; Denisiuk, A.; Lohken, M.; Schneider, T.; Süssmuth, R. D. *Chem. Bio. Chem.* **2011**, *12*, 1171.

⁴¹ Daubenmire, R. F. *Science* **1936**, *84*, 533.

⁴² Tilton, J. C.; Doms, R. W. *Antiviral Res.* **2010**, *85*, 91.

CD⁴⁺ T-cells, gp41 acts by fusing HIV to the T-cell's cell membrane, allowing it to enter the cell.⁴³ Once HIV has entered a healthy CD⁴⁺ T-cell, it causes the cell to produce viral proteins, including the membrane fusion protein gp41, which is then displayed on the cell membrane, allowing the infected cell to fuse to nearby healthy CD⁴⁺ T-cells via the same mechanism by which HIV initially enters the cell, resulting in non-functional syncytia.⁴⁴ Because syncytia formation is used to determine the efficacy of drug candidates at inhibiting the membrane fusion protein gp41, a compound that is found to inhibit syncytia formation will also likely inhibit gp41, thereby inhibiting HIV infection.

A recent study by Schols and coworkers further explored the anti-HIV activity and mode of action of feglymycin.⁴⁵ Feglymycin was determined to have half maximal effective concentration (EC₅₀) values in the low μ M range for several HIV strains, including some HIV-1 virus strains that are known to be entry inhibitor resistant. Through a series of time-of-drug addition (TOA) experiments, the group found that feglymycin inhibits HIV entry into cells, as hypothesized due to its inhibition of HIV syncytia formation, by acting as an early viral binding/adsorption inhibitor. As mentioned previously, the first step of HIV entry into cells is the binding of gp120 to the CD4 receptor. Through a series of experiments, including an sCD4/HIV-1 ELISA and a flow cytometric cellular virus binding assay, feglymycin was found to significantly inhibit the binding of HIV-1 NL4.3 to CD4-coated plates. The researchers thus concluded that feglymycin interferes with the CD4/gp120 binding process, thereby preventing HIV cell uptake. The interactions of feglymycin with HIV were also investigated using surface plasmon resonance (SPR) technology. Feglymycin was found to interact potently with gp120 of multiple HIV strains, and in addition to inhibiting uptake of cell-free virus, feglymycin was found to prevent cell-to-cell virus transmission between HIV-infected and non-infected CD⁴⁺ T-cells.⁴⁵

While crystal structures of feglymycin binding to those substrates it helps to inhibit HIV cell uptake or bacterial growth have not been reported, the crystal structure of feglymycin itself may suggest a mode of function. Although similar helical peptides⁴⁶ can function as membrane transport proteins, the feglymycin helix is not long enough to span a cell membrane, and as mentioned previously, the phenyl alanine side chains block the helix channel, suggesting that feglymycin is unlikely to function in this manner. Instead, Vértesy³⁷ and Sheldrick³⁸ suggest that feglymycin could act as an ion carrier.

Previous Synthesis of Feglymycin

The first total synthesis of feglymycin was completed by Süssmuth and coworkers in 2009.⁴⁷ When determining their synthetic strategy, the group recognized that the primary difficulty in preparing feglymycin would be in avoiding racemization of the Dpg,⁴⁸ due to the increased acidity of the α -position during active ester amide couplings. This was particularly troubling since they found that as the peptide grew, the diastereomers that were formed due to racemization pathways were inseparable by standard chromatography. They concluded, then, that their synthesis must not be entirely iterative.

⁴³ Kim P. S.; Malashkevich V. N.; Chan D. C.; Chutkowski C. T. *Proc. Natl. Acad. Sci. U.S.A.* **1998**, *95*, 9134.

⁴⁴ Huerta, L.; López-Balderas, N.; Rivera-Toledo, E.; Sandoval, G.; Gřmez-Icazbalceta, G.; Villarreal, C.; Lamoyi, E.; Larralde, C. *The Scientific World Journal* **2009**, *9*, 746.

⁴⁵ Fćrir, G.; Hānchen, A.; Franois, K. O.; Hoorelbeke, B.; Huskens, D.; Dettner, F.; Süssmuth, R. D.; Schols, D. *Virology* **2012**, *433*, 308.

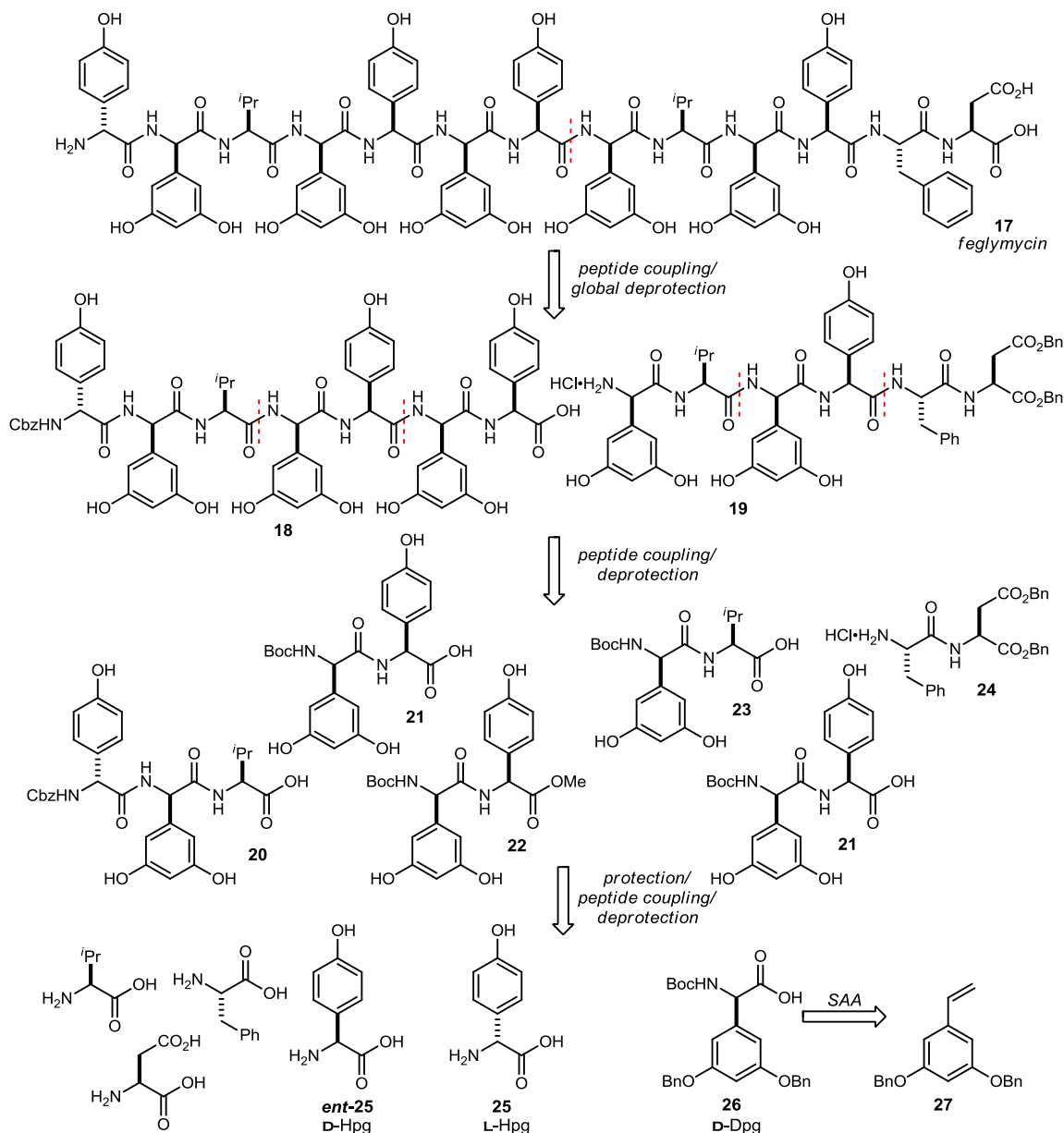
⁴⁶ Langs, D. A. *Science*, **1988**, *241*, 188.

⁴⁷ Dettner, F.; Hānchen, A.; Schols, D.; Toti, L.; Nuer, A.; Süssmuth, R. D. *Angew. Chem. Int. Ed.* **2009**, *48*, 1856.

⁴⁸ While both are aryl glycines, racemization when Hpg was coupled was not as facile as when Dpg was coupled.

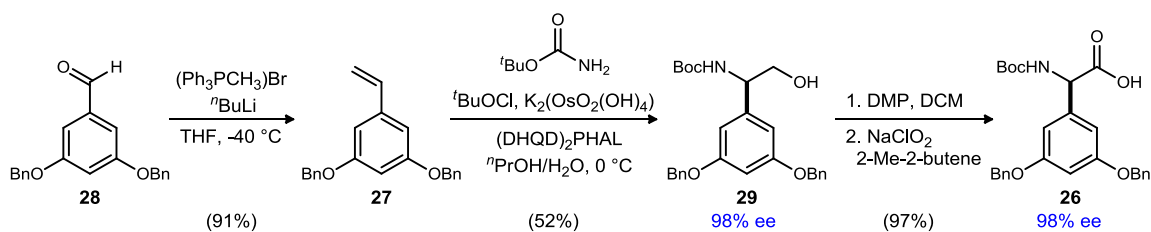
Retrosynthetically, dividing the 13-peptide chain of feglymycin (**17**) into a heptapeptide (**18**) and hexapeptide (**19**), then further dividing these portions into a series of dipeptides (**21**, **22**, and **23**) and a tripeptide (**20**), they planned to prepare feglymycin in a convergent manner, while avoiding late-stage coupling with a Dpg free acid. Dipeptides **21**, **22**, and **23** and tripeptide **20** would be prepared from couplings of the commercially available amino acids valine, phenyl alanine, aspartic acid, D-Hpg *ent*-**25** (\$1/g from Sigma Aldrich), and L-Hpg **25** (\$10/g from Sigma Aldrich).

Scheme 12. Süßmuth's Retrosynthesis of Feglymycin



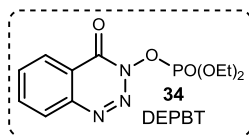
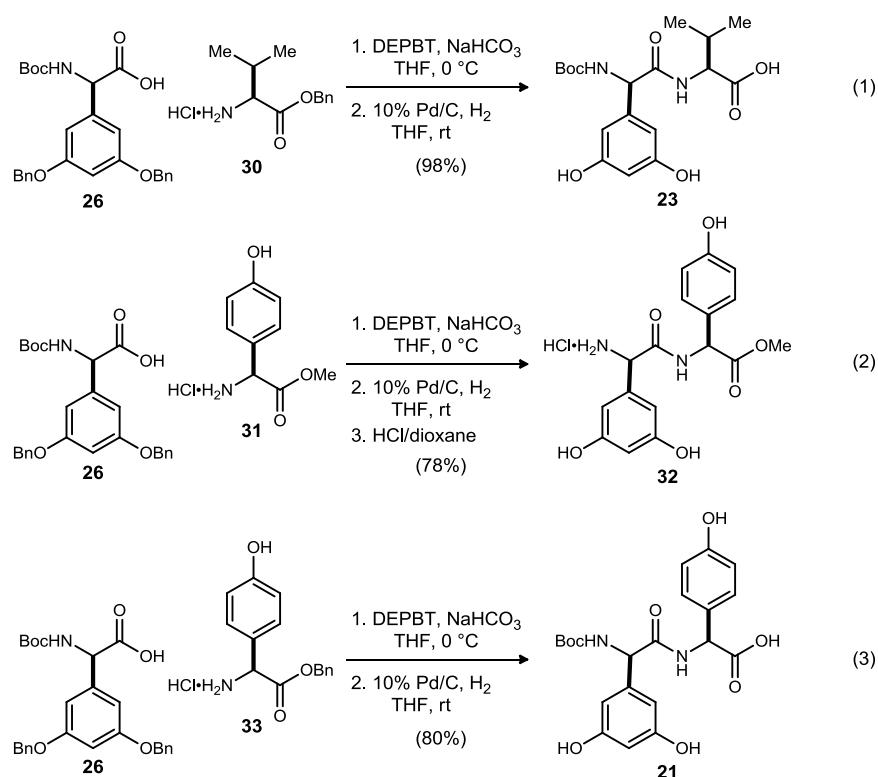
To synthesize the only non-commercially available residue, D-Dpg **26**, they began with commercially available 3,5-dibenzyloxybenzaldehyde (**28**, \$80/g from Sigma Aldrich) and performed a Wittig reaction with methyltriphenylphosphonium bromide to prepare the corresponding styrene (**27**) in 91% yield (Scheme 13). A Sharpless asymmetric aminohydroxylation reaction with *tert*-butyl carbamate as the amine donor and (DHQD)₂PHAL as the chiral ligand resulted in protected aminoalcohol **29** in 52% yield and 98% ee. The material was oxidized to its corresponding alcohol using Dess-Martin periodinane (DMP), and then further oxidized to give the D-Dpg acid (**26**) in 97% yield.

Scheme 13. Synthesis of **D**-Dpg via Sharpless Asymmetric Aminohydroxylation



With **26** in hand, the group then proceeded to assemble the dipeptides **21**, **22**, and **23** (Scheme 14). They found that the acid activating reagent 3-(diethoxyphosphoryloxy)-1,2,3-benzotriazin-4(3*H*)-one (DEPBT, **34**) resulted in the most success and the least amount of epimerization of the Dpg and Hpg groups. Subjection of **26** and benzyl-protected valine **30** to DEPBT coupling conditions followed by hydrogenolysis resulted in dipeptide **23**. While protection of the Dpg **26** phenols as benzyl ethers was necessary to minimize epimerization of the

Scheme 14. Süßmuth's Preparation of Dipeptides **21**, **23**, and **32**

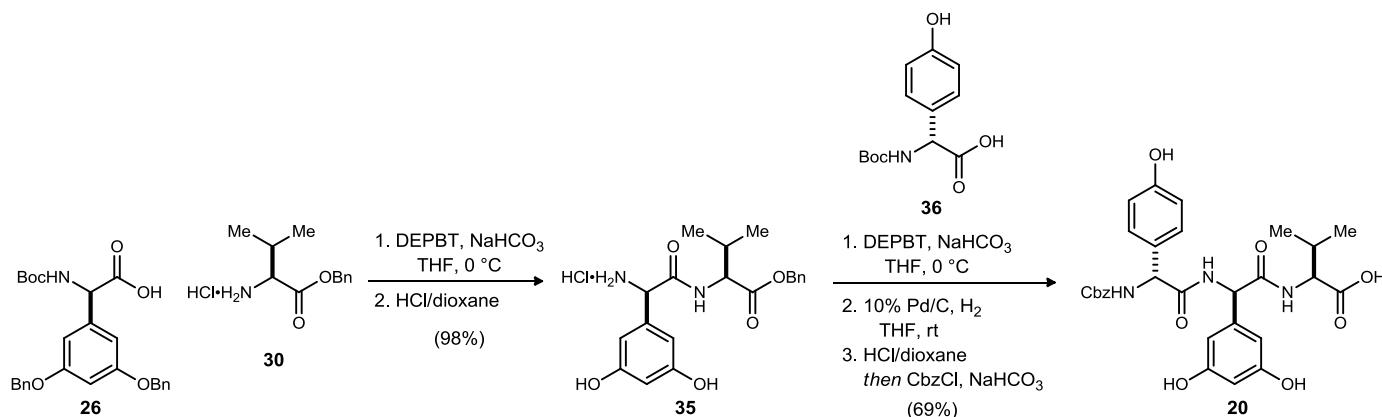


Dpg during amide bond coupling, the group found it necessary to remove the benzyl protecting groups at the dipeptide stage; if these protected dipeptides were used in subsequent couplings, the result was peptide fragments that had poor solubility in both aqueous and organic solvents. Thus, the final two dipeptides were prepared in a similar fashion, with a condensation reaction of **26** and the methyl ester Hpg **31**, followed by hydrogenolysis and Boc-deprotection, resulting in dipeptide **32**. Finally, dipeptide **21** was prepared via the benzyl ester Hpg **33**, with hydrogenolysis revealing the C-terminus for subsequent coupling.

Tripeptide **20** was prepared using an intermediate on the way to dipeptide **23** (Scheme 15). Instead of a benzyl deprotection, however, the N-terminus was first liberated via hydrochloric acid deprotection to give

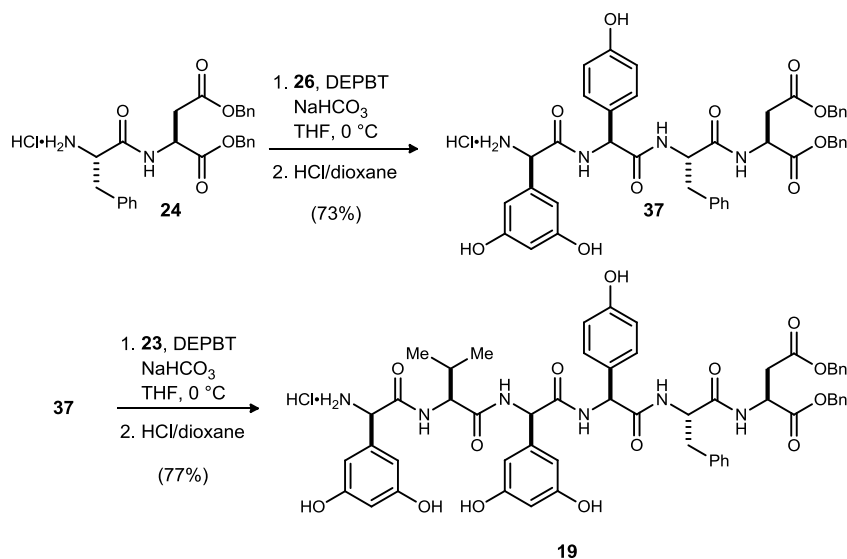
dipeptide **35**. This free amine was then coupled to the Boc-protected Hpg **36**. The resulting tripeptide was subjected to hydrogenolysis conditions to unmask the carboxylic acid and the phenols, followed by a deprotection/reprotection sequence performed on the N-terminus to give tripeptide **20**.

Scheme 15. Süßmuth's Preparation of Tripeptide 20



With the di- and tripeptide fragments thus assembled, the group was poised to prepare the two larger peptide fragments, **18** and **19**. A DEPBT-mediated coupling between **26** and dipeptide **24**, which was prepared via an EDT coupling of phenyl alanine and the benzyl ester of aspartic acid, followed by a Boc-deprotection, resulted in tetramer **37**. Tetramer **37** was then coupled to dipeptide **23** to give the eastern half of feglymycin, **19**, in good yield.

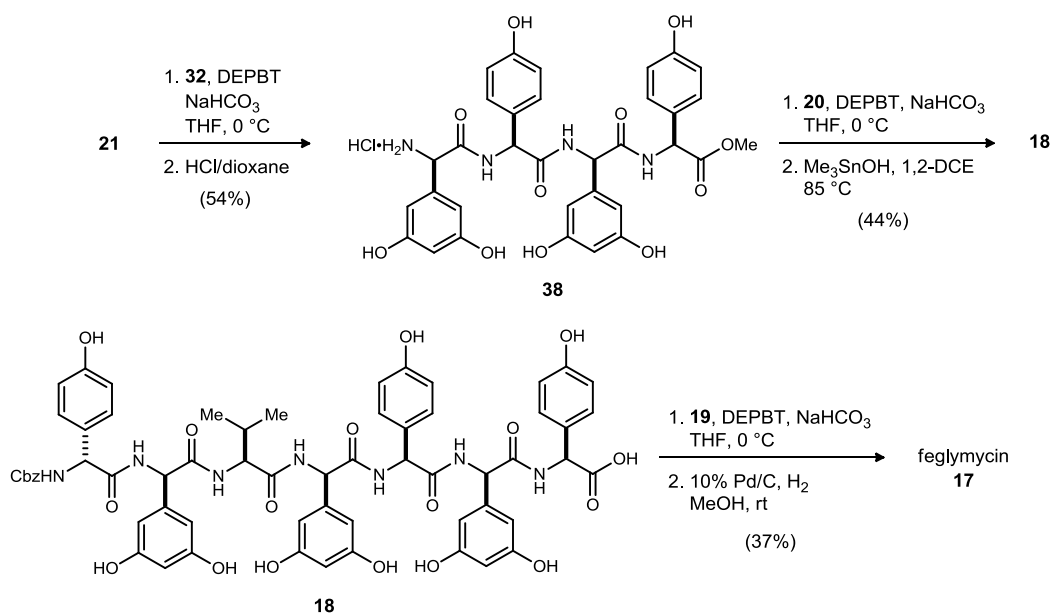
Scheme 16. Süßmuth's Preparation of Hexapeptide 19



Similar methods were used to prepare heptapeptide **18** (Scheme 17). A DEPBT-mediated coupling of dipeptide fragments **21** and **32**, followed by Boc-deprotection, gave tetrapeptide **38**. Coupling of this fragment with tripeptide **20** gave a heptapeptide, which was deprotected at the C-terminus using trimethyltin hydroxide saponification conditions to give **18**.

Finally, a DEPBT-mediated condensation of heptapeptide acid **18** and hexapeptide amine **19** gave the thirteen-membered peptide in 37% yield (Scheme 17). Hydrogenolysis of the Cbz and Bn protecting groups thus resulted in the first total synthesis of feglymycin (**17**). Thus, through use of the specialized coupling reagent DEPBT and a convergent approach, Süßmuth and coworkers achieved the total synthesis of feglymycin (**17**) in 34 total steps, with 14 steps in the longest linear sequence and an overall yield of 4% while minimizing epimerization of the sensitive Hpg and Dpg amino acid residues.

Scheme 17. Süßmuth's Synthesis of Heptapeptide 18 and Completion of Feglymycin (17)



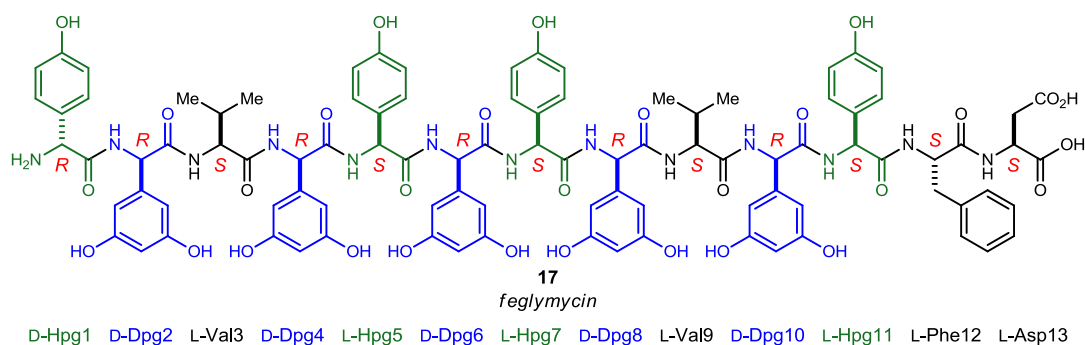
Biological Studies of Feglymycin Analogs

With a complete and convergent synthesis of feglymycin completed, Süßmuth and coworkers set out to analyze the thirteen amino acid residues contained in feglymycin for their importance to the natural product's bioactivity. As previously mentioned, the compound has been found to exhibit antibacterial activity towards *Staphylococcus aureus* strains and to inhibit the peptidoglycan biosynthesis enzymes MurA and MurC.

The researchers performed an alanine scan of feglymycin for the purposes of their study. Essentially, they synthesized thirteen analogs of feglymycin, with each analog containing one of the natural product residues replaced with an alanine residue. To achieve this, the group first prepared alanine-containing analogs of the three dipeptides and the tripeptide used in the synthesis of feglymycin, where replacing a single residue with alanine at a time resulted in three tripeptides and seven dipeptides in addition to those used in the natural product synthesis. The analog peptides were then coupled to the appropriate natural product fragments using the same convergent method as in their synthesis of feglymycin, resulting in seven heptapeptides and six hexapeptides, which in turn led to the thirteen tridecapeptides necessary to complete the alanine scan studies.

To determine whether the replacement of an original residue with alanine affected the secondary structure of the corresponding tridecapeptides, the group recorded circular dichroic (CD) spectra of the compounds. With the exception of [L-Ala13]-feglymycin (where the C-terminal L-Asp has been replaced with alanine, see Figure 6), all analogs showed comparable CD spectra to that of the natural product, suggesting that they assemble similarly to feglymycin, that is, in antiparallel β -helical dimers. Incidentally, mutation of the

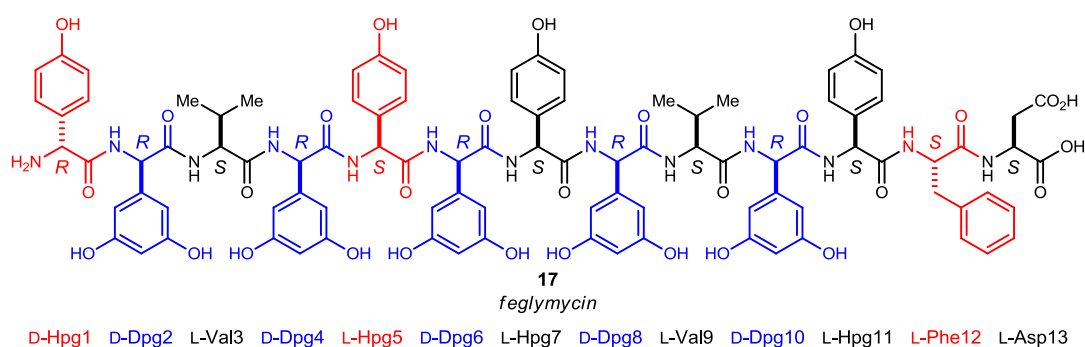
Figure 6. Feglymycin Residue Numbering System for Alanine Scan



other terminus to give [D-Ala1]-feglymycin, was the only analog to have solubility properties different from those of feglymycin, showing diminished solubility in water and methanol (MeOH).

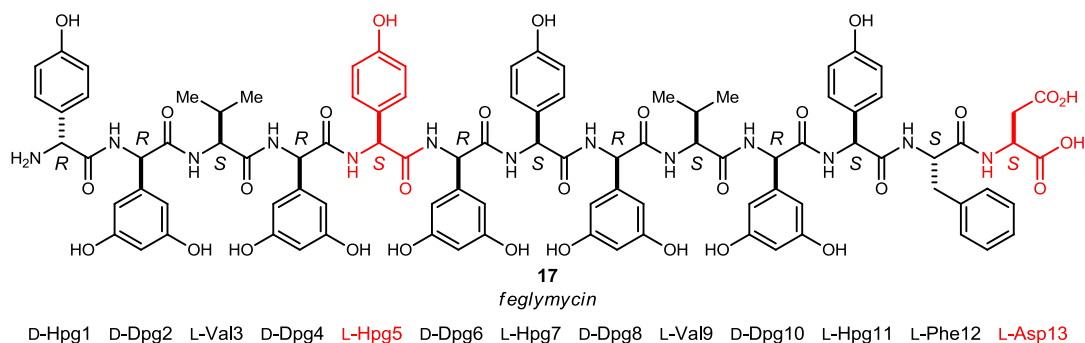
The group tested for antibacterial activity against three strains of *S. aureus*, using MRSA ATCC33592, which is resistant to the antibacterial compounds gentamicin and methicillin, and MSSA ATCC29213 and MSSA ATCC13709, which are both sensitive to methicillin and oxacillin. They assessed the influence of the alanine exchanges on inhibition of bacterial growth by recording minimum inhibitory concentration (MIC) values for each compound. Mutations of Val3, Hpg7, Val9, Hpg11, and Asp13 had similar MIC values to feglymycin (0.25-0.5 μM), indicating that they were not necessary for antibacterial activity against these strains. Substitution of any Dpg residue resulted in decreased activity, giving increased MIC values by a factor of 4-16. The most pronounced effects were observed for [D-Ala1]-feglymycin (MIC = 8 μM), [L-Ala5]-feglymycin (MIC > 32 μM), and [L-Ala12]-feglymycin (MIC > 32 μM), indicating that residues D-Hpg1, L-Hpg5, and L-Phe12 are important for retention of antibacterial activity. These are highlighted in red in Figure 7. Residues of medium importance (4-16-fold decrease of activity) are highlighted in blue.

Figure 7. Residues Important for Antibacterial Activity Against *S. Aureus* Strains



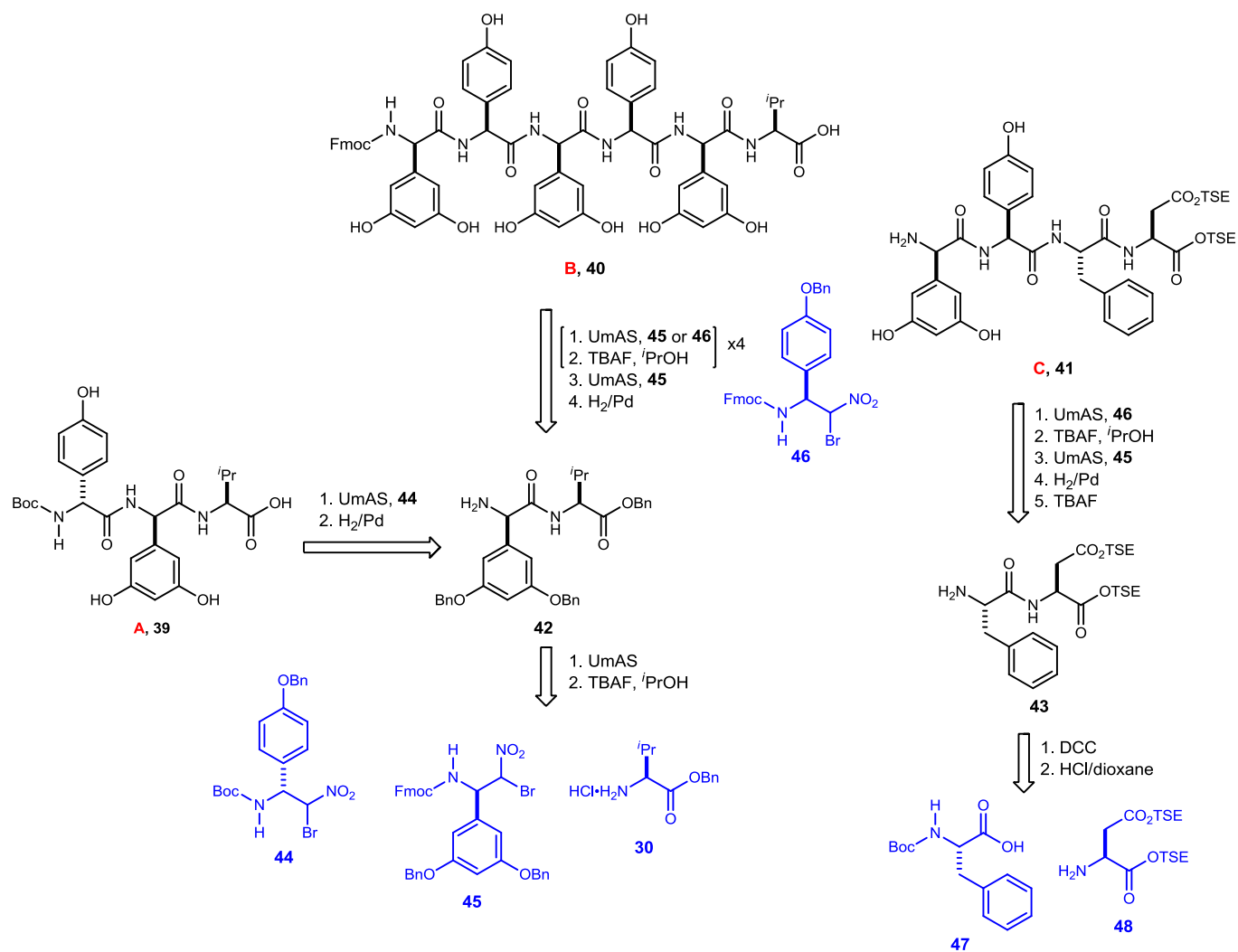
The thirteen tridecapeptides were then tested for their inhibition of peptidoglycan biosynthesis enzymes MurA and MurC. The half maximal inhibitory concentration (IC_{50}) values were determined for these compounds using the same protocols that were established for determining wild-type feglymycin's activity against these enzymes. Feglymycin (**17**) had an IC_{50} value of 0.3 μM against MurC and an IC_{50} value of 2.5 μM against MurA. With the exception of [L-Ala5]-feglymycin (IC_{50} = 11.2 μM) and [L-Ala13]-feglymycin (IC_{50} = 16.9 μM), all mutants exhibited similar IC_{50} values against MurA to that of feglymycin, indicating that L-Hpg5 and L-Asp13 are the most important residues for MurA inhibition (highlighted in red, Figure 8). The only substitution to negatively impact MurC inhibition was that of L-Asp13 (IC_{50} = 3.4 μM).

Figure 8. Residues Important for Enzyme MurA Inhibitory Activity



A later study of the importance of feglymycin's residues for its anti-HIV activity revealed that only substitution of L-Asp13 negatively affected the biological activity, with a 6.5-fold decrease in activity compared to wild-type feglymycin.⁴⁵ Thus, replacement of L-Hpg5 had the most negative impact for all antibacterial activity of feglymycin, and substitution of L-Asp13 had a negative impact on both the antibacterial and anti-HIV activity of feglymycin. Recall that this mutant also was found to disrupt the secondary structure of feglymycin,

Scheme 19. Retrosynthesis of Fragments A (39), B (40), and C (41) From Six Building Blocks



enantioselective aza-Henry methods to ensure high enantioselection and, vis á vis, single diastereomers along the way. Thus, feglymycin will be synthesized from only six amino acids or amino acid surrogates.

1.1.5 Previous Work

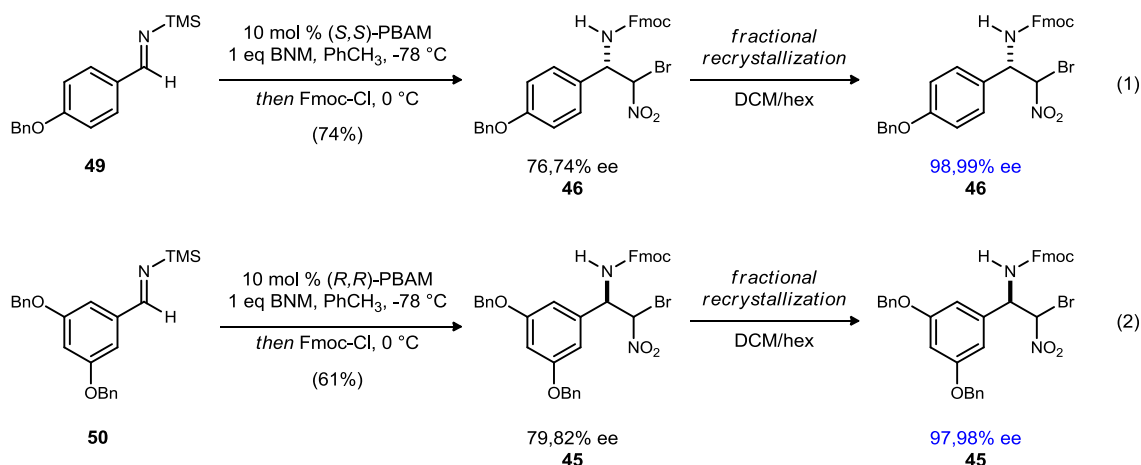
Our pursuit of feglymycin has undergone several revisions since its initial experiments by Bo Shen. Dawn M. Makley laid much of the groundwork for feglymycin, including working out much of our protecting group strategy and retrosynthesis, and the most recent iterations of Makley's work and discoveries are recounted here, as they formed the basis for my contributions to the project, which have been in concert with Dr. Sergey V. Tsukanov.

Building Block Synthesis

As mentioned in the previous section, feglymycin would be built from six building blocks. While three of these are derivatives of canonical amino acids, the remaining three were prepared utilizing aza-Henry chemistry. Dpg **45** and Hpg **46**, both of which require Fmoc protecting groups, were prepared via the TMS imine, as shown in Scheme 21.³⁵ The TMS imines were prepared according to a modified procedure by Collet and coworkers⁴⁹ from the corresponding aldehydes via condensation with lithium hexamethyldisilazide and

⁴⁹ Vidal, J.; Damestoy, S.; Guy, L.; Hannachi, J. C.; Aubry, A.; Collet, A. *Chem. Eur. J.* **1997**, *3*, 1691.

Scheme 21. Preparation of Hpg and Dpg α -Bromonitroalkane Donors

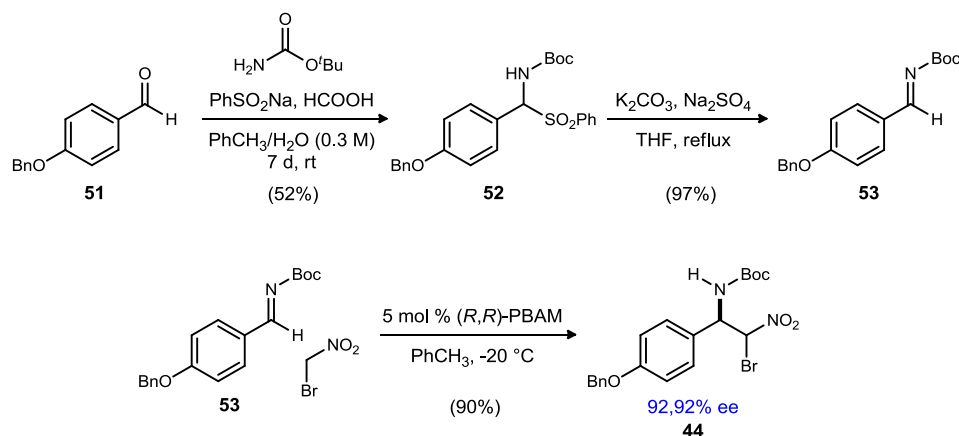


quenching with chlorotrimethylsilane. Treatment of the TMS-imines (**49** and **50**) with PBAM and bromonitromethane, which was added in 0.2 equivalent portions over a period of 10 hours at -78 °C, followed by quenching with Fmoc-Cl resulted in the desired α -bromonitroalkanes (**46** and **45**) in good yield and enantioselection. As feglymycin would be prepared as a single diastereomer, it was necessary to perform a fractional recrystallization on this material, and the desired adducts were obtained in essentially enantiopure form.

Synthesis of the Boc-protected α -bromonitroalkane **44** was slightly more straight-forward (Scheme 20). The Boc-protected imine (**53**) was prepared from the corresponding commercially-available aldehyde **51** using a modification of known procedures.⁵⁰ In order to obtain good yields for this electron-rich substrate, it was necessary to prepare the α -amidosulfone (**52**) in a mixture of toluene (PhCH₃) and water, rather than the usual tetrahydrofuran (THF).³⁵ As quite a bit of this material and its enantiomer are used in this synthesis of feglymycin and it represents a good substrate for umpolung amide synthesis, a scale-up of the preparation of this material for publication in *Organic Syntheses* is currently being prepared with an undergraduate researcher, Victoria T. Lim.

Preparation and Elaboration of Dipeptide **42**

Scheme 20. Preparation of Boc-Hpg α -Bromonitroalkane Donor

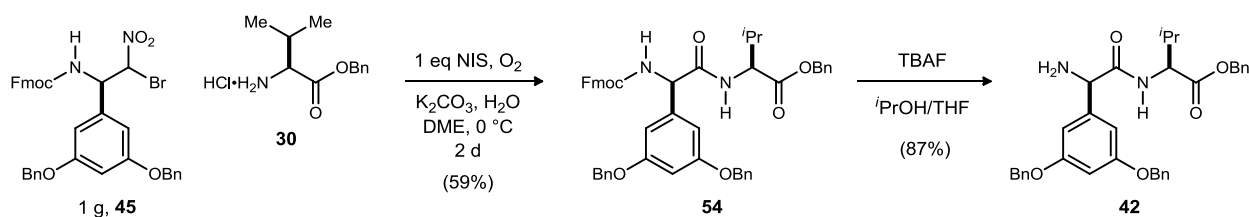


⁵⁰ Kanazawa, A. M.; Denis, J.; Greene, A. E. *J. Org. Chem.* **1994**, *59*, 1238.

A common intermediate for both fragments A and B (**39** and **40**, respectively), dipeptide **54** was prepared via an umpolung amide synthesis coupling between Dpg α -bromonitroalkane donor **45** and the benzyl ester of valine (**30**). Makley optimized this reaction for a one gram scale (Scheme 22), obtaining the product in 59% yield, and with specialized glassware and use of an overhead mechanical stirrer, the scale of the reaction has since been tripled, and flash column chromatographic purification has been replaced with trituration to obtain the product in comparable yield. As will be discussed later, proper purification of this compound is necessary for good yields in subsequent steps.

Deprotection of dipeptide **54** to its free amine **42** was achieved using tetrabutylammonium fluoride in a

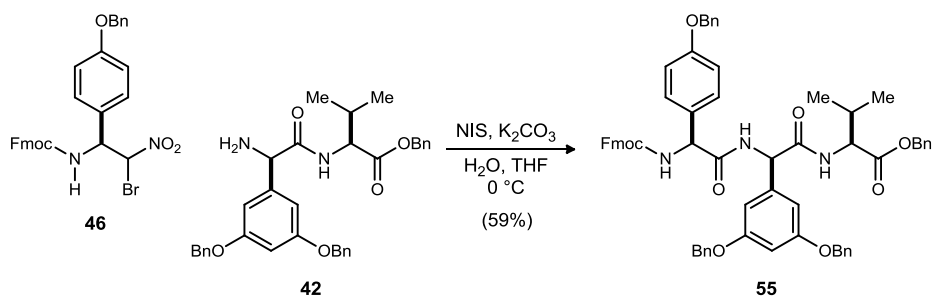
Scheme 22. Synthesis of Dipeptide 42



mixture of isopropanol and tetrahydrofuran (Scheme 22). A flash column chromatographic method which converts the free amine to its acetone imine on the column by elution with 30% acetone in hexanes led to the isolation of the desired product **42** in 87% yield on small scale.³⁵

Dipeptide amine **42** was further elaborated using an umpolung amide synthesis coupling reaction on the path to the synthesis of fragment B. Amine **42** was treated with Fmoc-protected Hpg α -bromonitroalkane donor **46** under umpolung amide synthesis conditions to obtain tripeptide B (**55**) in 59% yield on small scale (Scheme 23).³⁵

Scheme 23. Initial Preparation of Fmoc-Tripeptide B 55



1.2 Synthetic Efforts Towards Feglymycin

Fmoc-Dipeptide 54 Deprotection Reoptimization

While the deprotection of dipeptide **54** on small scale had previously been optimized to a yield of 87% as described above, it was found that scale-up and new batches of dipeptide **54** rendered the deprotection step irreproducible, resulting in yields of only 31-59%, occasionally with TBAF salt contaminants from the flash column chromatographic purification. Analysis of the crude ¹H NMR spectrum of this deprotection step following an aqueous sodium bicarbonate and dichloromethane work-up indicated that the reaction cleanly converted to the desired amine **42**. Other materials observed in this crude spectrum were limited to the fulvene side product resulting from Fmoc deprotection and some tetrabutylammonium salts. In order to avoid a purification sequence that resulted in poor product recovery, the crude material was used in the subsequent umpolung amide synthesis step to prepare Fmoc-tripeptide B **55**. Unfortunately, this resulted in poor yields for product formation.

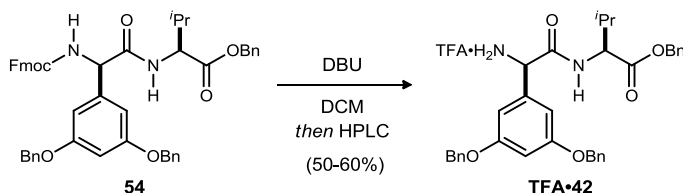
Having thus concluded that purification at the amine **42** stage was necessary prior to subsequent couplings, alternate work-up procedures for the Fmoc-dipeptide **54** deprotection step were considered. In some cases, an aqueous ammonium chloride solution workup with ethyl acetate as the organic solvent for extraction was successfully used in place of the previous method. After this new work-up procedure, the product was successfully isolated reproducibly in 72% yield via trituration with ethyl acetate and hexanes, without column chromatography. This procedure resulted in very clean product which behaved well in subsequent umpolung amide synthesis couplings.

Unfortunately, difficulty reproducing the results of this deprotection work-up procedure was eventually encountered as well. Attempts to identify the cause of irreproducibility included the changing of solvent and TBAF sources, as well as reducing the amount of TBAF and isopropanol used in the reaction, but to no avail. It was determined that the most likely cause for irreproducibility of the deprotection results was due to a change in batches of Fmoc-dipeptide **54**. Even when using recrystallized **54** that was free of organic impurities, only a small amount of product could be isolated via trituration, and preparatory reverse-phase HPLC, which could reproducibly give clean material in 66% yield, was used instead.

At this point, an alternate, more reliable Fmoc-deprotection procedure was sought. Fmoc-dipeptide **54** was treated with a variety of reagents, including DBU, cesium fluoride (CsF), and diethyl amine/DBU, following up with the ammonium chloride work-up and trituration protocol. While CsF did not result in deprotection, DBU and the diethyl amine/DBU mixture both gave the desired product as a solid, though in poor yields (11% and 31%, respectively). Going back to the earlier purification procedure via column chromatography, the yield of the DBU-promoted deprotection was successfully increased to 35%. Unfortunately, not all of the crude material from this reaction was soluble in dichloromethane, which was used to load the sample onto the flash column, so the material was instead purified via prep-RP-HPLC. This method allowed for the isolation of another 31% of the material, resulting in a total 66% yield.

In order to streamline the purification of this material, all of the crude material following deprotection with DBU and an aqueous ammonium chloride work-up was loaded onto the reversed-phase preparatory HPLC instrument. An Agilent Technologies 1260 Infinity preparatory HPLC system set up with a Waters XBridgeTM Prep C18 5 μm OBDTM column measuring 19x150 mm was used with a flow rate of 20 mL/min, and the method for elution was 50% acetonitrile (CH₃CN) in water (H₂O), doped with 0.1% TFA⁵¹ for two minutes, followed by an eight minute gradient from 50% CH₃CN/H₂O to 95% CH₃CN/H₂O. After holding at 95% for 1.5 minutes, a thirty second gradient from 95% to 50% CH₃CN/H₂O, followed by a thirty second hold at 50% CH₃CN/H₂O returned the column to its initial conditions. The desired peak eluted cleanly between 5.0 and 6.5 minutes, with DBU eluting earlier ($t_r = 2.25$ min) and the fulvene side product eluting later ($t_r = 8.50$ min). The DMSO used to load the column eluted at $t_r = 1.33$ min. The clean amine TFA·**42** was consistently isolated in 47-52% yields using this method. This purification process could be further streamlined by omitting the aqueous work-up and directly loading the crude material onto the reversed-phase preparatory HPLC using DMSO as the loading solvent, allowing for the consistent isolation of the material in 50-60% yields. It was

Scheme 24. Optimized Fmoc-Dipeptide **54** Deprotection and Purification Conditions



found that later batches of dipeptide **54** occasionally resulted in yields up to 99% of the amine following preparatory HPLC purification, but only 50-60% yield of the desired product could be relied on consistently. This procedure is limited to 900 μL injections onto the preparatory HPLC, with smaller injections (500 μL)

⁵¹ All solvent systems for the reversed-phase preparatory HPLC were prepared with a 0.1% TFA additive.

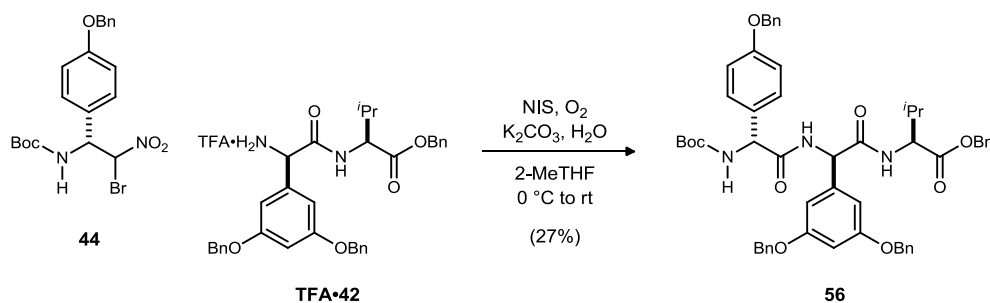
yielding better results since it does not risk column overload. For a typical 100 mg-scale deprotection, this requires up to five injections of 500 μ L onto the preparatory HPLC.

Recently, it has been found that upon scale-up to a half-gram deprotection, the product can be purified in a shorter period of time using a C18 column and reversed-phase conditions on a Combiflash instrument.⁵² Yields of the desired product are slightly lower, but can be obtained more quickly.

1.2.1 Fragment A

Now able to reproducibly prepare amine dipeptide **42**, we moved on to constructing fragment A (**39**) of feglymycin (**17**). As shown in the retrosynthesis (Scheme 19), only an umpolung amide synthesis coupling with Boc-Hpg **44** and a hydrogenolysis reaction were needed to prepare the fragment for coupling. Under the standard umpolung amide synthesis conditions (1.0 eq NIS, 1.2 eq K_2CO_3 , 5 eq H_2O in THF), 23% of the desired Boc-tripeptide A **56** could be isolated on a 13 mg scale, following purification by flash column chromatography. Unfortunately, increasing to a 70 mg scale resulted in a drop in yield to 12%. Changing the solvent to 2-MeTHF, which does not undergo NIS-mediated oxidation as readily as THF, resulted in an increase in yield to 27% (Scheme 25). Despite attempts to optimize this reaction further, we have not met with success in

Scheme 25. Preparation of Boc-Tripeptide A **56**



further increasing the reaction output. As will be discussed later, this reaction works well for constructing the diastereomer of the product (where *ent*-**44** is used in place of **44**), so it was hypothesized that the configuration at the Hpg center is preventing an increase in yield.

Hydrogenolysis of Boc-Tripeptide A **56** and Completion of Fragment A (**39**)

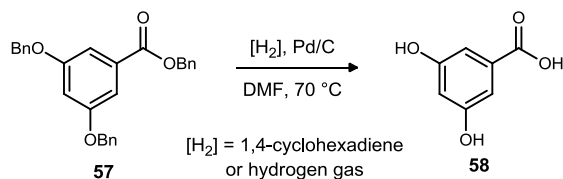
Conditions for the hydrogenolysis of Boc-tripeptide A (**56**) to arrive at fragment A (**39**) were next explored. We first attempted to cleave the benzyl ethers of **57** using a catalytic transfer hydrogenation protocol developed by Felix et al.⁵³ specifically for peptidic compounds. The method was utilized by Evans¹⁹ in the late stages of the synthesis of vancomycin. The key component of the reaction is 1,4-cyclohexadiene, which is used as a hydrogen source. The protocol was appealing due to its mild conditions, solvent versatility, and quick conversions; reactions were typically complete in two hours. The standard reaction conditions called for the use of absolute ethanol as a solvent. While substrate **56** was not soluble in ethanol, the reaction could be performed in *N,N*-dimethylformamide (DMF).

The hydrogenolysis study was begun by using benzyl ester **57**, an early intermediate in the route to prepare imine **50**. Unfortunately, even after an overnight reaction using ten equivalents of 1,4-cyclohexadiene and 10% palladium on carbon, no conversion was observed. Another 40 equivalents of the hydrogen surrogate were added, and after heating to 70 °C, full conversion was observed after two hours. The reaction was filtered over Celite and eluted with DMF. Upon concentration via rotary evaporation, full conversion to 3,5-dihydroxybenzoic acid (**58**) was observed by 1H NMR (Scheme 27). We reasoned that if the substrate was reactive towards the transfer hydrogenolysis reagent 1,4-cyclohexadiene and Pd/C, it should also be reactive

⁵² Tsukanov, S. V.; Johnston, J. N. *unpublished results*.

⁵³ Felix, A. M.; Heimer, E. P.; Lambros, T. J.; Tzougraki, C.; Meienhofer, J. *J. Org. Chem.* **1978**, *43*, 4194.

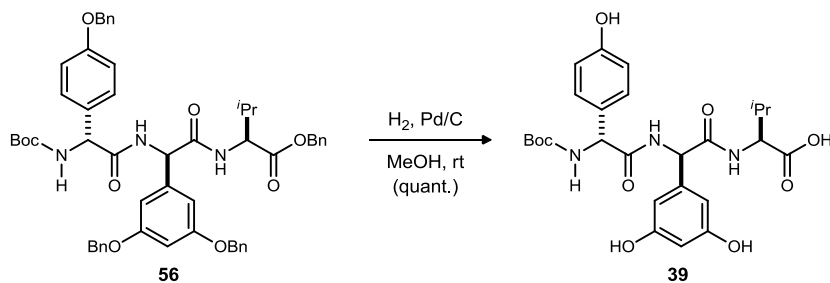
Scheme 27. Model Reaction for Hydrogenolysis Conditions



towards hydrogen gas and Pd/C. The reaction was attempted using DMF as solvent and heating to 70 °C. Complete, clean conversion to the desired product was observed by 1H NMR in less than 20 minutes.

Having found success with this model substrate, **56** was subjected to similar conditions. Monitoring of the reaction by thin layer chromatography showed that consumption of the starting material was rapid, and the reaction was again complete within 20 minutes. Unfortunately, following filtration through Celite and rotary evaporation, only a few peaks in the aromatic region of a 1H NMR taken in $CDCl_3$ were observed. There were no signs of either the product or starting material present. Based on consideration that the use of a high boiling solvent may be problematic, the reaction was reattempted at room temperature using methanol as the solvent. Again, the reaction proceeded to full conversion in only 30 minutes as judged by thin layer chromatography. However, upon filtration and concentration, the 1H NMR spectrum was the same as it had been when DMF was used. Puzzled by the apparent disappearance of material, we re-evaluated the experimental procedure and noticed that a thin residue remained in the evaporation flask following preparation of the NMR sample in $CDCl_3$. We were pleased to find that a 1H NMR of the residue taken in $DMSO-d_6$ looked promising, with peaks that appeared to correspond to the desired product. The LCMS of this residue matched the predicted spectrum for the desired deprotected Boc-tripeptide **A 39**.

Scheme 26. Completion of Fragment A (39) Via Hydrogenolysis of 56



Thus fragment A (**39**) for feglymycin was successfully prepared in two steps from the dipeptide amine (**42**). Because the hydrogenolysis reaction resulted in a quantitative yield, fragment A (**39**) was prepared in 27% yield over two steps from **42**.

1.2.2 Fragment B

As shown in the retrosynthetic analysis (Scheme 19), the planned approach for fragment B (**40**) involved five iterative umpolung amide synthesis steps to incorporate the five aryl glycine residues. The aryl glycine residues on fragment B alternate between Dpg and Hpg, so α -bromonitroalkane donors **45** and **46** were prepared as described in section 1.1.5. Fragment B comes from the same dipeptide amine (**42**) as fragment A, so we began building upon that piece.

Preparation of Fmoc-Tripeptide B 55

The initial coupling of dipeptide amine **42** with Dpg α -bromonitroalkane donor **45** had previously been achieved in 59% yield.³⁵ The protocol for the isolation and purification of **55** called for removal of the reaction solvent and flash column chromatography, which was successful on small scale, but as the reaction was scaled up, Fmoc-tripeptide B (**55**) became increasingly insoluble in organic solvents, exhibiting poor solubility in

dichloromethane and even worse solubility in ethyl acetate and hexanes, making it quite difficult to isolate significant quantities of the material via column chromatography. Yields for this procedure were abysmal, coming in at <10%.

It was not until a full aqueous work-up using hydrochloric acid (1 N) to quench the potassium carbonate and a sodium thiosulfate wash to remove remaining *N*-iodo species was utilized that **55** could be reproducibly prepared in workable yields. Furthermore, addition of a final wash with brine resulted in the cleanest isolated material, and rather than having to purify the material via column chromatography, this aqueous work-up procedure allowed for isolation of the material via trituration with ethyl acetate and hexanes. It is notable that while **55** had poor solubility in dichloromethane, DCM could be used as the extracting solvent when the reaction was not concentrated fully prior to work-up.

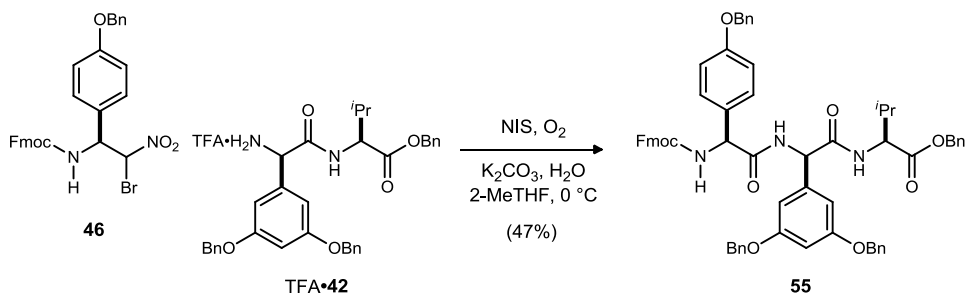
Thus, subjecting dipeptide amine **42** to umpolung amide synthesis conditions in dimethoxyethane (DME), Fmoc-tripeptide B **55** could be isolated in 23% yield. Changing the base from potassium carbonate to potassium hydroxide did not affect the reaction outcome (23%), and using *tert*-butyl methyl ether as the solvent did not increase the yield significantly (26%). A quick solvent screen revealed that 2-MeTHF was optimal for this substrate, giving the product in 37% yield, while using THF resulted in product isolation in a median 33% yield. Extending the reaction time to four days rather than two days also improved the yield (57% in 2-MeTHF and 50% in DME). Further extending the reaction time to eight days, however, resulted in a drop in yield (43%).

Following these optimizations, a new batch of Fmoc-dipeptide **54**, which is used to prepare starting material **42** for this reaction, was brought through, causing a minor setback in the production of Fmoc-tripeptide B **55**. Attempts to use amine **42** that had been isolated via trituration or column chromatography did not result in product formation. However, when material that had been purified by prep-HPLC was used, isolation of desired product **55** from this umpolung amide synthesis could again be achieved.

In order to again reoptimize this reaction, HPLC-purified TFA·**42** was subjected to umpolung amide synthesis conditions in 2-MeTHF for two days. This resulted in a 28% yield of **55**. Increasing the reaction temperature to 55 °C in an attempt to increase homogeneity of the reaction mixture did not affect the yield (24%). Increasing the amount of water from 5 equivalents to 50 equivalents resulted in an increase in yield to 47%. Adding an extra equivalent of potassium carbonate (2.5 equivalents rather than 1.2 equivalents) to account for the TFA salt had a detrimental effect, dropping the yield to 33%. Considering that the increase in potassium carbonate might not take full effect due to insolubility, the amount of water in the reaction was also doubled, but this only resulted in 28% isolation of product. Dilution of the reaction from 0.1 M to 0.05 M led to a slight drop in yield (37%). Finally, adding trifluoroethanol as a cosolvent (1:9 with 2-MeTHF) did not improve the yield of the reaction (26%).

Through this reoptimization sequence, it was determined that treatment of amine TFA·**42** with 1.2 equivalents of Hpg α -bromonitroalkane donor **46**, 1.2 equivalents of K₂CO₃, and 50 equivalents of H₂O in 0.1 M 2-MeTHF resulted in the best yields (47%) and were reproducible.

Scheme 28. Optimized Conditions for Preparation of Tripeptide B 55



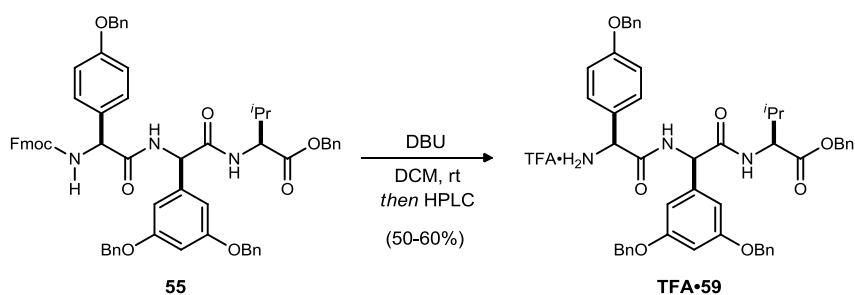
Deprotection of Fmoc-Tripeptide B 55

With Fmoc-tripeptide B **55** in hand, the removal of the Fmoc group could be optimized. Deprotection using the same TBAF/isopropanol system that had previously worked when deprotecting **54** was first attempted.

Unfortunately, no conversion was observed. Treatment of **55** with DBU in dichloromethane, however, resulted in full conversion in less than an hour. The starting material **55** was not fully soluble in DCM, but as the reaction progressed, it became more homogenous. The material was concentrated without an aqueous work-up, and the crude ^1H NMR showed no starting material **55** remaining. The residue was purified via column chromatography as previously described for the deprotection of **54**, but the acetone imine of **59**, which forms on the column, proved to be robust, preventing hydrolysis back to the amine.

With the subjection of crude **59** to umpolung amide synthesis conditions leading to poor yields, it was necessary to purify the material prior to subsequent reactions. Conditions were developed for purification of tripeptide amine B **59** via preparatory reversed-phase HPLC. Using the same method as for purification of **42**, it was found that TFA·**59** has a retention time of 7.5-8.5 minutes, eluting just before the fulvene side product. This purification procedure proved to be the best option, giving reproducible yields of TFA·**59** in the range of 50-60%. These yields are optimal when no aqueous work-up is performed and the crude reaction is instead concentrated and the residue dissolved in DMSO and directly loaded onto the prep-HPLC column.

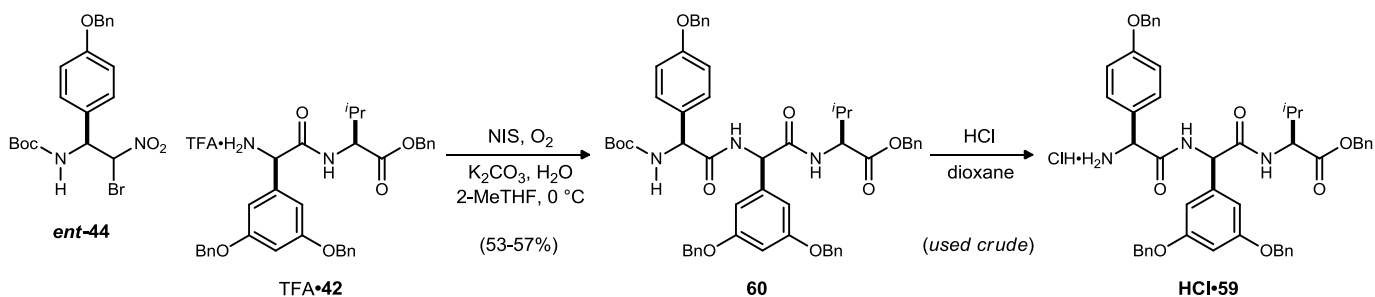
Scheme 29. Optimized Deprotection of 55



An Alternate Route to Tripeptide Amine 59

As mentioned previously, the preparatory HPLC purification sequence can be cumbersome and time-consuming. Upon scale-up of the deprotection reaction, these problems can amplify. Use a Boc-protected Hpg α -bromonitroalkane (*ent*-**44**) instead of the Fmoc-protected **46** resulted in yields of 53-57% on a 400 mg scale. Deprotection of the Boc-tripeptide **60** with HCl/dioxanes did not require purification prior to use in the next umpolung amide synthesis coupling reaction, but as will be discussed later, it resulted in slightly lower yields for subsequent reactions.⁵²

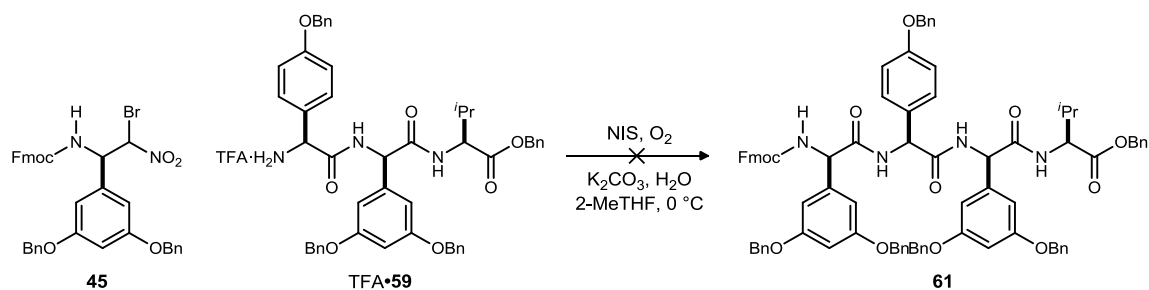
Scheme 30. Alternate Preparation of Tripeptide B Amine 59



Attempts to Prepare Fmoc-Tetrapeptide B 61

With tripeptide amine TFA·**59** in hand, the next umpolung amide synthesis coupling to install the fourth residue, a Dpg, was explored. Using the best conditions for the preparation of **55**, TFA·**59** was subjected to umpolung amide synthesis conditions with **45** as the Dpg α -bromonitroalkane donor. Unfortunately, following the now-standard work-up procedure, a lower-than usual crude mass was isolated and presence of the desired product could not be detected by either ^1H NMR or LCMS.

Scheme 31. Attempted Umpolung Amide Synthesis Reaction to Form Tetrapeptide B 61

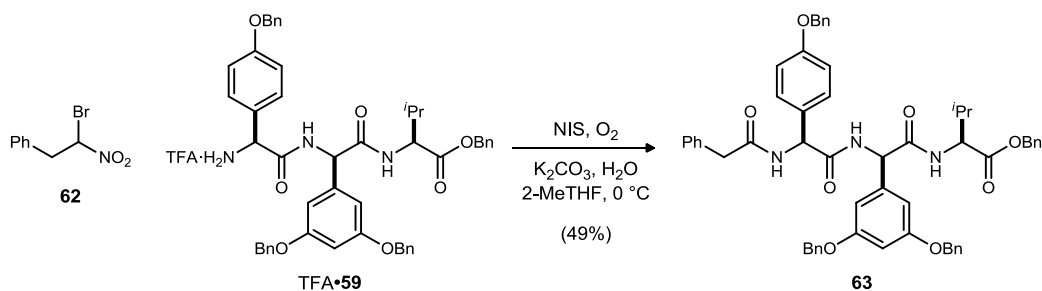


Detection of the desired product might be complicated by solubility and poor ionization factors, so the crude mixture of this reaction was subjected to deprotection conditions, allowing that the free tetrapeptide amine **B** might fare better on the C18 column. Unfortunately, the desired mass was not detected in the LCMS trace, and prep-HPLC purification of the resulting mixture did not yield any desired product.

Considering that the problem might lie in the aqueous work-up procedure, the material was concentrated directly from the crude reaction without an aqueous work-up. This yielded an appropriate crude mass, but again no desired product could be detected, even after passage of the material through a silica gel plug.

At this point, it was hypothesized that the desired reaction might not be occurring due to either the bulkiness of Fmoc-Dpg α -bromonitroalkane **45** or the lowered reactivity of the amine of **59**. The availability of the amine was first tested by treating TFA·**59** with simple α -bromonitroalkane **62** under umpolung amide synthesis conditions. While isolation of the product (**63**) in 49% yield confirmed that the amino group of TFA·**59** could undergo electrophilic activation and nucleophilic substitution via an umpolung amide synthesis pathway, it also confirmed that Dpg **45** was unsuitable for coupling with TFA·**59**.

Scheme 32. Successful UmAS Coupling of 59 to Surrogate α -Bromonitroalkane Donor 62

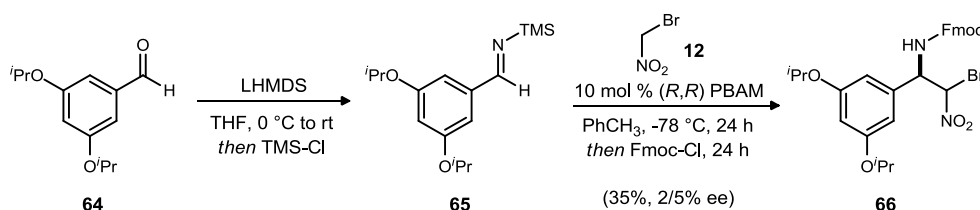


Thus, the problem was not specifically with Dpg α -bromonitroalkane **45** since it was used in a previous step or with tripeptide amine **59**, but with the combination of the two. The use of alternate protecting groups for the phenols of the Dpg α -bromonitroalkane was considered. Isopropyl and methyl ethers were attractive because we expected them to have similar electronics to the benzyl ether, and both protecting groups have been removed in late stages of the total syntheses of aryl glycine-containing natural products.⁵⁴ The isopropyl ether was more attractive due to the ability of the isopropyl group to pack in order to form crystalline solids. A crystalline solid is desirable so that the enantiomeric excess obtained in the aza-Henry reaction can be enhanced through recrystallization.

⁵⁴ The isopropyl ether can be removed using BCl₃, as demonstrated by Shaw in the synthesis of viriditoxin: *Angew. Chem. Int. Ed.*, **2011**, *50*, 3730. The methyl ether can be removed using AlBr₃ and EtSH, as demonstrated by Evans in the synthesis of the vancomycin aglycon: *Angew. Chem. Int. Ed.* **1998**, *37*, 2700.

In order to test the effect of alternate protecting groups, 3,5-diisopropoxybenzaldehyde⁵⁵ (**64**) was prepared from commercially-available 3,5-dihydroxybenzoic acid. Aldehyde **64** was then converted to the TMS imine necessary for our enantioselective aza-Henry protocol. The reaction proceeded cleanly as expected. Unfortunately, TMS imine **65** proved to be unstable for long periods of time, with decomposition occurring in less than 2.5 hours, whereas the corresponding benzyl protected TMS imine (**50**) was stable indefinitely at -78 °C and was stable at least overnight at room temperature. Despite the fragility of **65**, the crude material was subjected to aza-Henry conditions. Unfortunately, no significant enantioselection for was observed, with standard conditions providing the desired α -bromonitroalkane **66** in only 2/5% ee.

Scheme 33. Preparation of *i*-Pr-Dpg **66**



While more electron-rich TMS imines typically give reduced enantioselectivity⁵⁶ in the aza-Henry addition, the electronics of the isopropyl ether were expected to be very similar to that of the benzyl ether. Because this substitution pattern would not allow for electron donation via resonance, substitution at the 3- and 5- positions of the aromatic ring would instead result in inductive electron-withdrawal and a slightly electron-poor imine compared with a standard unsubstituted benzaldehyde. Although, as mentioned, a difference in reactivity towards the aza-Henry addition between isopropyl ether-substituted benzaldimine **65** and benzyl ether-substituted benzaldimine **50** was not expected, a rather significant difference was indeed observed.

A possible explanation for the drop in enantioselection is that **65** is too good an electrophile, resulting in a significant background reaction for the aza-Henry reaction. In other words, BNM could add to **65** without the need for catalyst, resulting in no enantioselectivity. Because the reaction is carried out at -78 °C, there is not much that could be done to attenuate this reactivity. Another explanation would be that a contaminant remaining from the imine formation could be catalyzing the nonselective pathway. This was considered unlikely since **50** could be prepared and used without the need for distillation while maintaining high enantioselectivity. However, this hypothesis could not be completely dismissed before testing it. Because imine **65** is unusually unstable, a distillation attempt was not expected to be successful. Instead, to minimize the number of byproducts carried over with the crude imine, the imine was prepared using solid, commercially available LHMDS instead of generating it *in situ* from *n*-butyl lithium and HMDS. Gratifyingly, this resulted in an increase in enantioselection to 18/27%.

Another possible source of side products during imine formation is the use of a stoichiometric amount of chlorotrimethylsilane. Mechanistically, the chlorotrimethylsilane is not necessary for TMS imine formation. Rather, the TMS-Cl silylates the byproduct silanol and forms lithium chloride, which is precipitated with the addition of hexanes and removed via Schlenk filtration. To minimize any complications from using a full equivalent of TMS-Cl, the imine preparation was attempted using only a catalytic (10 mol %) amount of TMS-Cl. Gratifyingly, this resulted in a cleaner crude spectrum for **65**.

Finally, the drop in enantioselection could also be attributed to *lower* reactivity for **65**. In other words, **65** could be not as good an electrophile as **50**, making the reaction too slow at -78 °C. In this case, the first 24-hour period would result in no reaction, while the aza-Henry addition and subsequent acylation would occur during the second 24-hour period, when the reaction is warmed to 0 °C. It was reasoned that if this was the case, then the enantioselection at 0 °C must be 18/27%. To test this hypothesis, the aza-Henry reaction was performed at -20 °C, in hopes that this would result in enough energy for the reaction to proceed. Unfortunately, only a 22/22% ee was observed for this reaction. To rule out a time limitation for the reaction, the aza-Henry

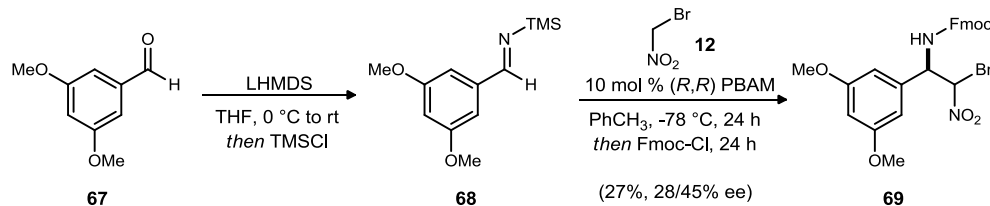
⁵⁵ Fei, Z.; McDonald, F. E. *Org. Lett.* **2007**, *9*, 3547.

⁵⁶ DMM Thesis:³⁵ para MeO gave 62/62% ee, where para Cl gave 91/91% ee and phenyl gave 65/66% ee.

addition was allowed to proceed for a full 48 hours at $-20\text{ }^{\circ}\text{C}$ before proceeding to the acylation step. Unfortunately, the longer reaction time resulted in only 17/18% ee. While these experiments do not rule out the possibility that the reaction is still too slow at $-20\text{ }^{\circ}\text{C}$, it appears that the maximum ee resulting from this substrate is around 20%, which, unfortunately, is too low for use in the synthesis of feglymycin.

In the hopes of finding a suitable protecting group that would result in higher enantioselection, the methyl ether-protected benzaldimine **68** was prepared from commercially available **67**. Fortunately, this imine

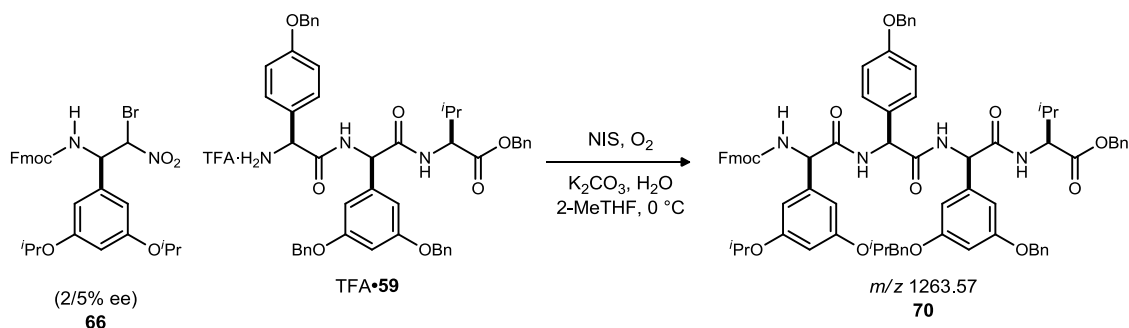
Scheme 34. Preparation of MeO-Dpg **69**



appeared to be more robust than **65**, with only a small amount of decomposition occurring when the crude imine was stored at $-78\text{ }^{\circ}\text{C}$ overnight. Regardless, to minimize potential problems, the imine was prepared and used immediately. This substrate, however, proved difficult to work with. It was found that vigorous stirring of the reaction was essential; without it, the reaction formed a thick gel-like substance and appeared to polymerize. The reaction could be rendered homogenous with a spatula, but the enantioselectivity was compromised since the reaction was warmed in an effort to break up the gel. Although the compound was allowed to react for 24 hours at $-78\text{ }^{\circ}\text{C}$ following achievement of homogeneity, the enantioselection was poor, giving only 5/26% ee. This experiment, however, proved to be instructive in that this problem could be avoided in future attempts with **68**. When **68** was subjected to aza-Henry conditions at $-78\text{ }^{\circ}\text{C}$ over a period of 48 hours then acylated at $0\text{ }^{\circ}\text{C}$ over a period of 24 hours with vigorous stirring so as to avoid the apparent polymerization, the enantioselectivity proved better, giving 28/45% ee. While this was a move in the right direction, the ideal substrate was still required to be formed in better enantioselection.

Although the enantiomeric excess was poor for the preparation of the isopropyl ether-protected aza-Henry adduct **66**, it remained to be determined if the alternate protecting group would solve the problem presented by the benzyl ether. Namely, determination of whether an alternate substrate would lead to preparation of a tetrapeptide using umpolung amide synthesis was essential. To this end, TFA·**59** was treated with Dpg **66** (2/5% ee) under optimized umpolung amide synthesis conditions for 48 hours. At the end of this period, the crude reaction mixture was concentrated, and a sample was immediately subjected to LCMS analysis. To our delight, a mass corresponding to desired product **70** was observed at $1263.57\text{ }m/z$. The exact mass calculated for $\text{C}_{78}\text{H}_{79}\text{N}_4\text{O}_{12}$ $[\text{M}+\text{H}]^+$ was 1263.57. The remainder of the crude reaction mixture was then immediately purified using preparatory reversed-phase HPLC, and the compound whose mass corresponded to the desired molecule was isolated. Although the reaction output was too small for full characterization, the ^1H NMR contained signals consistent with the desired tetrapeptide **70** and appeared to represent a single

Scheme 35. UmAS Coupling Between **66** and **59**



diastereomer. This experiment confirmed that preparation of the desired tetrapeptide was possible using umpolung amide synthesis conditions. Unfortunately, it was necessary to use enantioenriched material for the umpolung amide synthesis couplings in order to avoid inseparable diastereomers in subsequent steps.

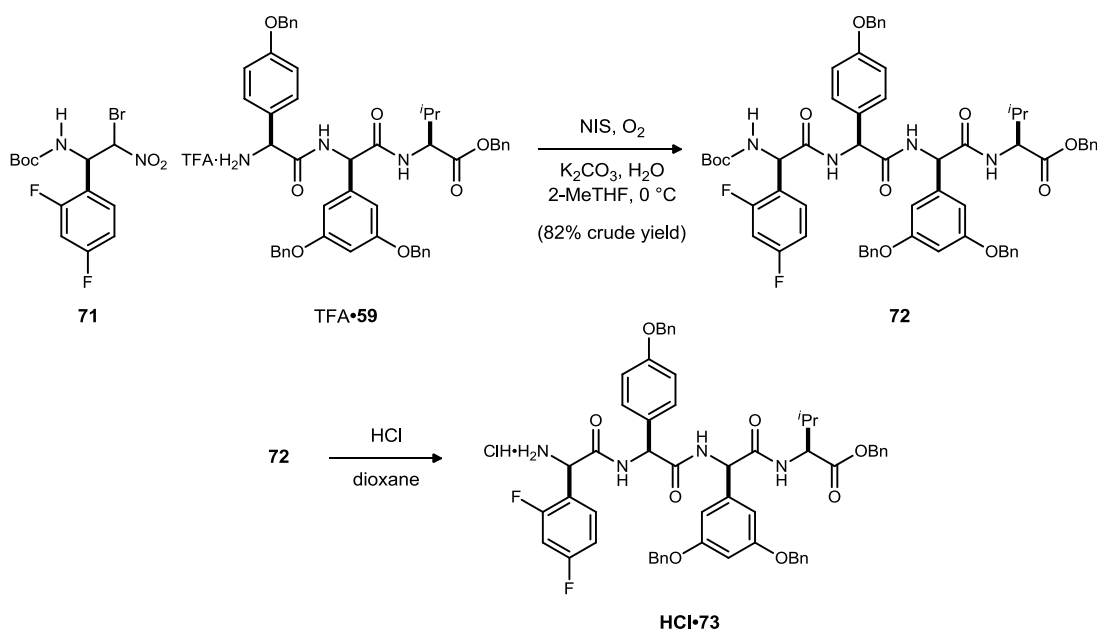
Accessing Tetrapeptide Analog **72**

Attempts to construct desired the tetrapeptide **61** for fragment B of feglymycin were thus far met with failure or non-workable yields. Attempts to couple the desired 3,5-benzyloxy substituted residue in the fourth position of fragment B (**40**) have been unsuccessful. While some coupling of 3,5-isopropoxy residue **66** into the fourth position was detected, the product was not produced in workable or characterizable quantities, and sufficient quantities of pure material to use effectively in the synthesis could not be obtained.

A possible explanation for the marginal failure of fourth residue incorporation is that the second (3,5-dibenzyloxy substituted) residue significantly hinders or prevents this incorporation due to its size. Unfortunately, an exploration of smaller protecting groups was not fruitful, as the α -bromonitroalkane donor is required to be produced with good to excellent enantioselection in the aza-Henry addition to TMS-protected imines. An alternate approach to evaluate the above hypothesis involves the incorporation of a small residue at the fourth position. In doing this, a small residue would presumably alternate steric interactions with the second (3,5-dibenzyloxy) residue. Likewise, having a small residue at the fourth position would allow for incorporation of the fifth and sixth residues and for evaluation of the proposed late-stage chemistry, leading to an analog of the natural product.

To this end, the tripeptide amine TFA·**59** was treated with Boc-protected 2,4-difluoroaryl α -bromonitroalkane⁵⁷ **71** under optimal reaction conditions. Delightfully, the corresponding tetrapeptide (**72**) was produced in 82% crude yield. Production of this tetrapeptide **72** occurred cleanly, and deprotection of the Boc-protected tetrapeptide analog **72** could be achieved by stirring overnight with 4 M HCl in dioxanes (Scheme

Scheme 36. Preparation and Deprotection of Tetrapeptide Analog **72**

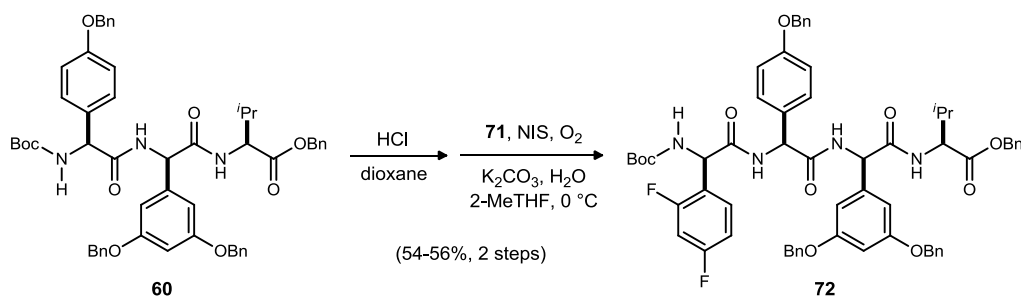


36). Again, this crude material was produced cleanly, and further purification of tetrapeptide amine **73** proved unnecessary, although a trituration sequence with ethyl acetate and hexanes was always performed on tetrapeptide **72** to remove any remaining **71**. Up to 99% yield has been achieved for this umpolung amide synthesis coupling reaction, which corresponds to a 50-60% yield over two steps, from Fmoc-tripeptide **55** to tetrapeptide **72**.

⁵⁷ Dobish, M. C.; Johnston, J. N. Ph.D. Dissertation **2012**, Department of Chemistry, Vanderbilt University.

In later iterations of the synthesis, Fmoc-Hpg **46** has been replaced with Boc-Hpg *ent*-**44**, as mentioned previously. The resulting Boc-tripeptide **60** is deprotected with HCl/dioxanes and carried on crude to the umpolung amide synthesis coupling reaction to prepare tetrapeptide **72**.⁵² The two-step yield for this sequence is comparable to that of the Fmoc-sequence, coming in at 54-56% yield on 200-300 mg scale following purification by trituration. As mentioned previously, this route is beneficial because it avoids the necessity for HPLC purification following deprotection of the tripeptide.

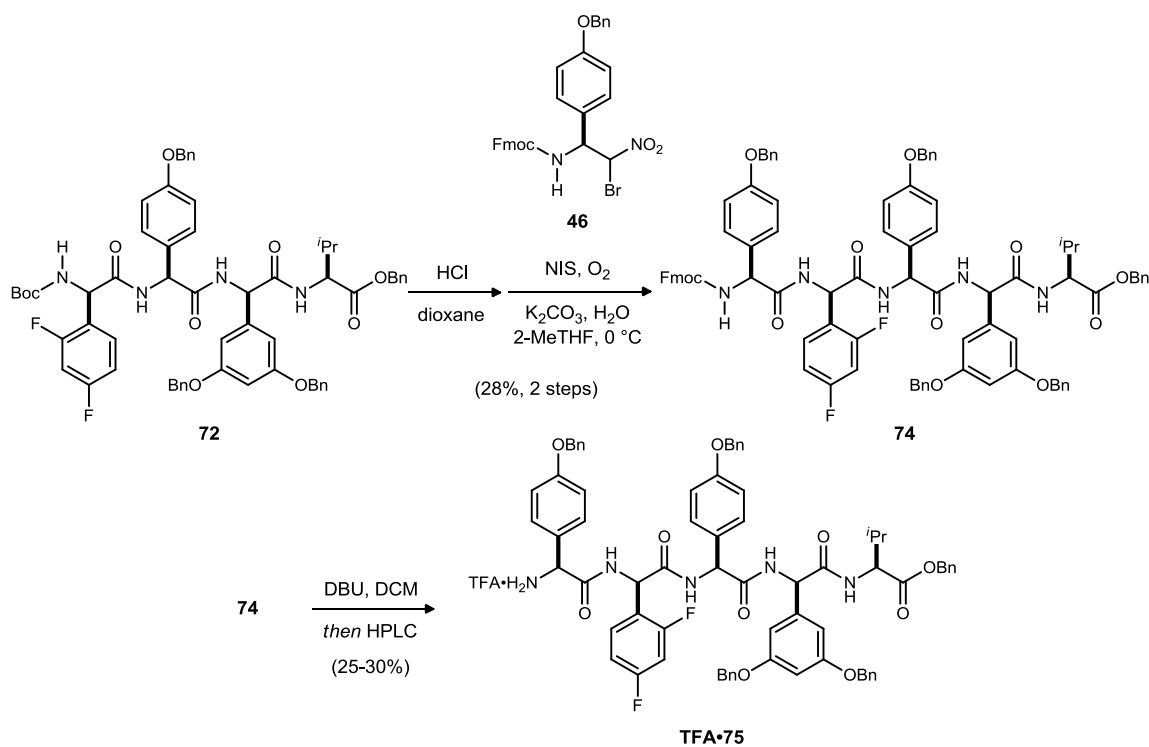
Scheme 37. Alternate Two-Step Sequence to Prepare Tetrapeptide 72 from Boc-Tripeptide 60



Synthesis of Pentapeptide Amine B Analog 75

With the synthesis of a tetrapeptide analog (**72**) for fragment B thus achieved, the studies to determine the efficacy of planned late-stage synthetic manipulations were continued. Deprotection of tetrapeptide **72** was facile under HCl/dioxanes conditions, not requiring purification prior to subsequent steps, although an analytical sample could be obtained via reversed-phase preparatory HPLC purification. An initial experiment to prepare the pentapeptide utilized Fmoc-Hpg **46**, and an umpolung amide synthesis coupling to prepare **74** was achieved in 19% yield over two steps from **72**. As the sequence was scaled up, it was found that the yields for these two reactions could be improved, and on a 100-200 mg scale, the pentapeptide was isolated in 28% yield over two steps (Scheme 38). Deprotection of **74** proceeded smoothly using conditions that had previously been worked out, and the resulting pentapeptide amine **75** was purified via the reversed-phase preparatory HPLC method that had been developed for the other peptidic amines, eluting at 9.0-9.5 minutes. Unfortunately, the

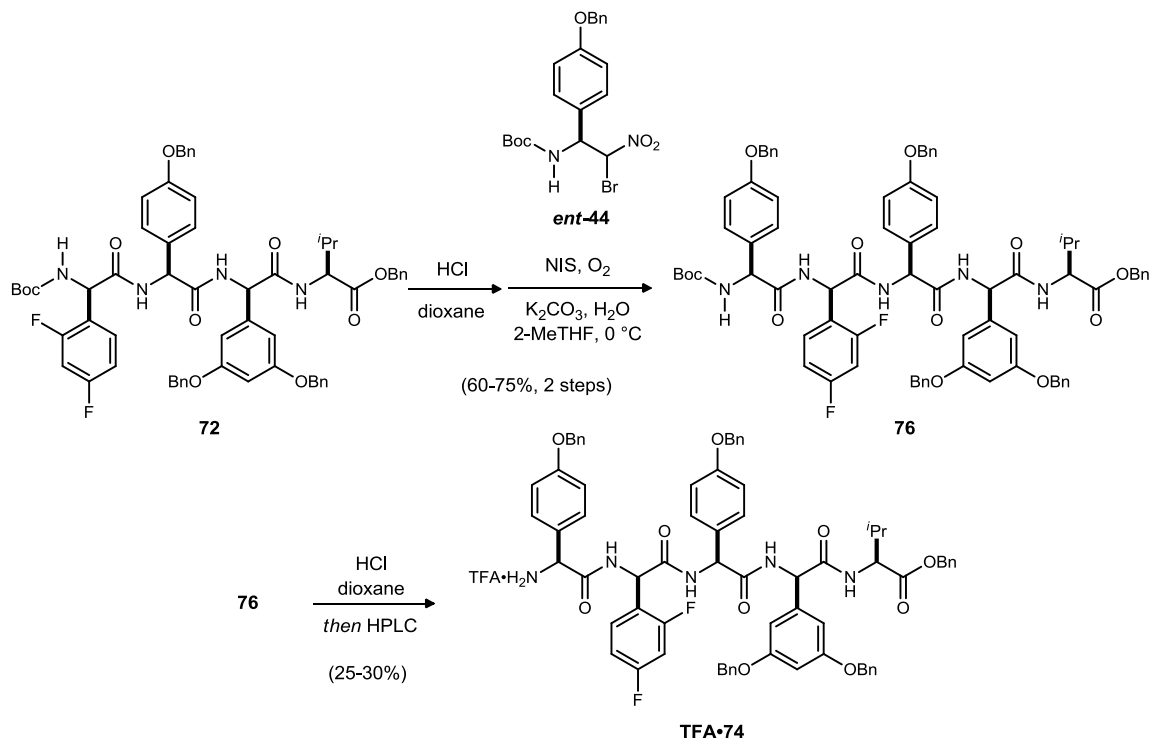
Scheme 38. Preparation and Deprotection of Fmoc-Pentapeptide Analog 74



yield of this deprotection proved to be poorer (25-30%).

It was hypothesized that deprotection of the corresponding Boc-pentapeptide **76** might be met with more success, so it was prepared from **72** using the Boc-Hpg α -bromonitroalkane donor *ent*-**44**. This resulted in a better yield for the umpolung amide synthesis coupling reaction (60-75%), but the deprotection yields for **76** continued to hover around (25-30%). While the crude ^1H NMRs for appear to be free of organic impurities, the

Figure 9. Preparation and Deprotection of Boc-Pentapeptide Analog 76

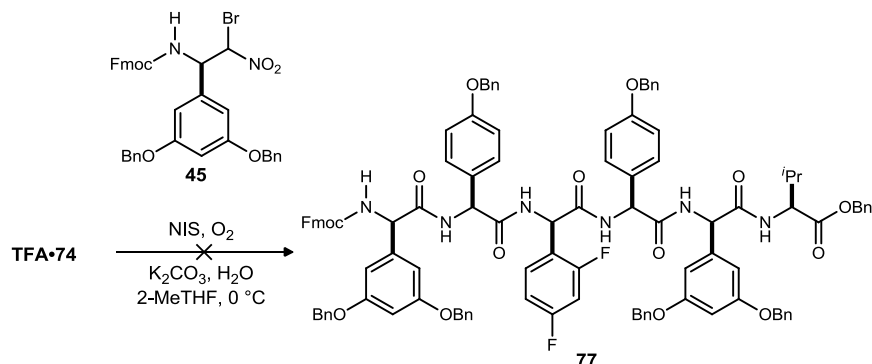


yields suggest that the crude material may contain inorganic impurities. Although subsequent couplings with the crude material produce product, the purification of later products proves to be challenging, necessitating the production of analytically pure material at this step.

Attempts to Prepare Fmoc-Hexapeptide Analog 77

As mentioned previously, it had been hypothesized that by altering the sterics in preparing the hexapeptide, the benzyl ether-protected Fmoc-Dpg α -bromonitroalkane donor **45** might be successfully installed at the sixth position of fragment B. Thus, with analytically pure pentapeptide amine TFA-**74** in hand, an attempt was made to append the sixth residue via umpolung amide synthesis. Unfortunately, this reaction proved problematic, and as with the attempt to install this residue at the fourth position, no desired product (**77**) could

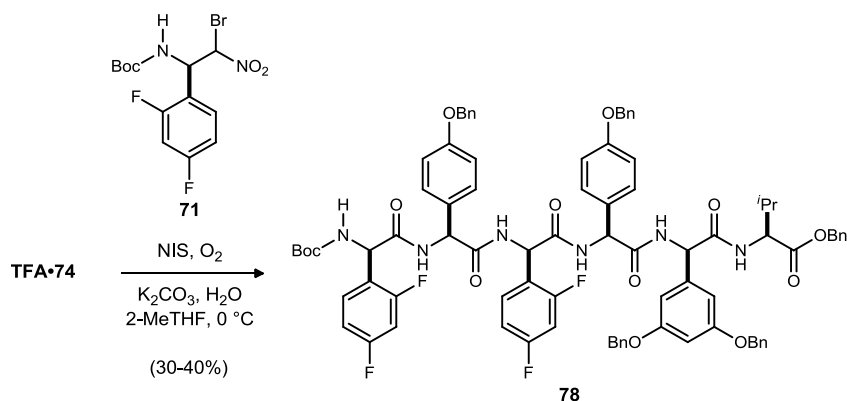
Scheme 39. Attempted Installation of Fmoc-Dpg Residue to Prepare Hexapeptide 77



be detected either by ^1H NMR or by LCMS. As with the attempt to prepare the tetrapeptide **61**, it was concluded that the benzyl ether-protected Fmoc-Dpg α -bromonitroalkane donor **45** was just too bulky.

However, in order to confirm that the problem lay with the α -bromonitroalkane donor rather than with pentapeptide amine TFA-**74**, the amine was treated with 2,4-difluoroaryl glycine surrogate **71** under umpolung amide synthesis conditions. Delightfully, this reaction proceeded to full conversion, producing the desired hexapeptide **78** in good yield. While this material appeared to be free of organic impurities by ^1H NMR, we continued to triturate the residue with ethyl acetate and hexanes to obtain the desired product **78** in 30-40% yield on average (Scheme 40). If left unpurified, subsequent byproducts were inseparable from subsequent desired products.

Scheme 40. Synthesis of Protected Fragment B Hexapeptide Analog 78

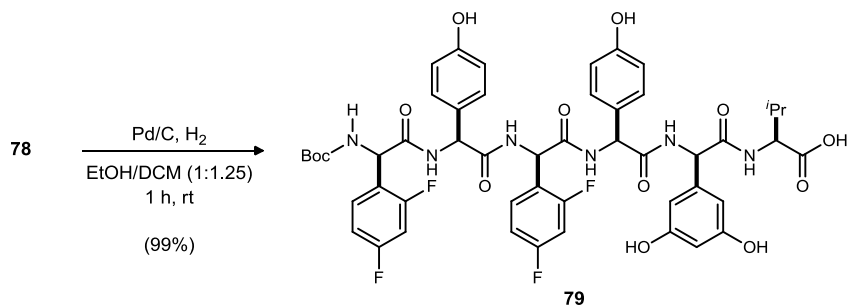


Hydrogenolysis of Hexapeptide Analog 78

With hexapeptide **78** in hand, only one step remained in the synthesis of a fragment B analog. Application of the conditions that had been optimized for the hydrogenolysis of fragment A (**56**) was not successful in this case. Unsurprisingly, hexapeptide **78** proved to be insoluble in methanol (MeOH), ethanol (EtOH), mixtures of EtOH and ethyl acetate (EtOAc), mixtures of MeOH and EtOAc, and hot MeOH. An attempt to hydrogenolyze **78** in DMF was unsuccessful.

Success was finally realized when hexapeptide **78** was dissolved in a very dilute (0.005 M) 1:1.25 mixture of EtOH/DCM. Thus, following treatment of **78** with hydrogen gas and palladium on carbon in ethanol and dichloromethane at room temperature for one hour, fragment B analog **79** was obtained in nearly quantitative yield. The product was confirmed both by ^1H NMR and positive and negative ion modes of LCMS, with an $[\text{M}-\text{Boc}+\text{H}]^+$ ion observed in the positive mode and an $[\text{M}-\text{H}]^-$ ion observed in the negative mode.

Scheme 41. Successful Hydrogenolysis of Hexapeptide 78

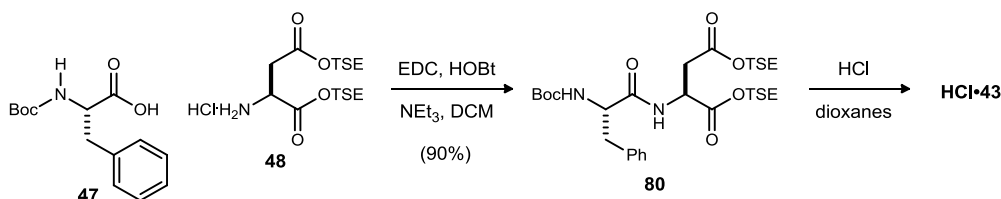


1.2.3 Fragment C

As described in section 1.1.4, fragment C (**41**) would be prepared from protected aspartic acid **48** and *N*-protected phenyl alanine **47**. A simple EDC-mediated amide coupling reaction between **48** and **47** provided dipeptide C **80** in 90% yield. HOBT was added to the reaction to minimize racemization, and the material was

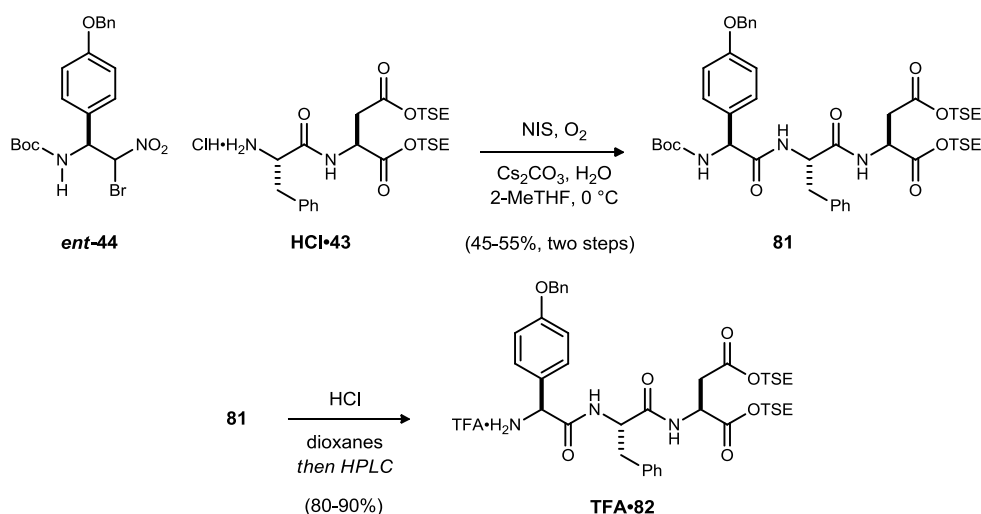
sufficiently pure so as to be used in the next step without purification. Removal of the Boc-group proceeded cleanly in HCl/dioxanes to give the desired amine hydrochloride salt (HCl·**43**), which could also be used without purification.⁵²

Scheme 42. Synthesis and Deprotection of Dipeptide C 80



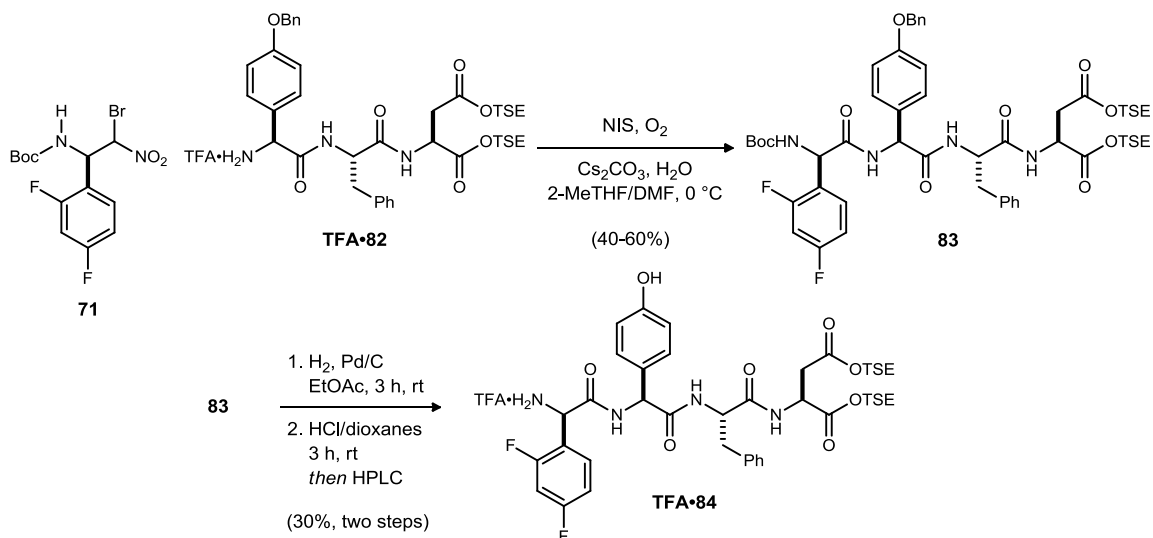
An umpolung amide synthesis reaction between HCl·**43** and α -bromonitroalkane donor *ent*-**44** proceeded smoothly, forming tripeptide C **81** in 45-55% yield over two steps. Cesium carbonate (Cs_2CO_3) was found to be optimal for this reaction. To prepare for the final umpolung amide synthesis coupling to fragment C, **81** was deprotected using HCl/dioxanes. It was determined that reversed-phase preparatory HPLC was necessary to sufficiently purify **82** prior to subsequent steps, and TFA·**82** was isolated in 80-90% yield following this purification, as shown in Scheme 43.⁵²

Scheme 43. Synthesis of Tripeptide Amine C 82



Synthesis of tetrapeptide C **41** was achieved via an umpolung amide synthesis coupling between TFA·**85** and Fmoc-Dpg α -bromonitroalkane donor **45**, but the reaction unfortunately suffered from poor yields. In order to produce quantities of material sufficient for studying the late stages of the synthesis, TFA·**82** was instead coupled to 2,4-difluoroaryl glycine surrogate **71** via an umpolung amide synthesis reaction to give tetrapeptide C analog **83** in 40-60% yield (Scheme 44). It was necessary to use DMF as a cosolvent in this reaction so as to fully solubilize the starting materials. Finally, **83** was deprotected first via hydrogenolysis, then using HCl/dioxanes. Following a reversed-phase preparatory HPLC purification, TFA·**84** could be isolated in 30% yield over two steps, providing a substrate for use in determining the optimal conditions for late-stage synthetic transformations.⁵²

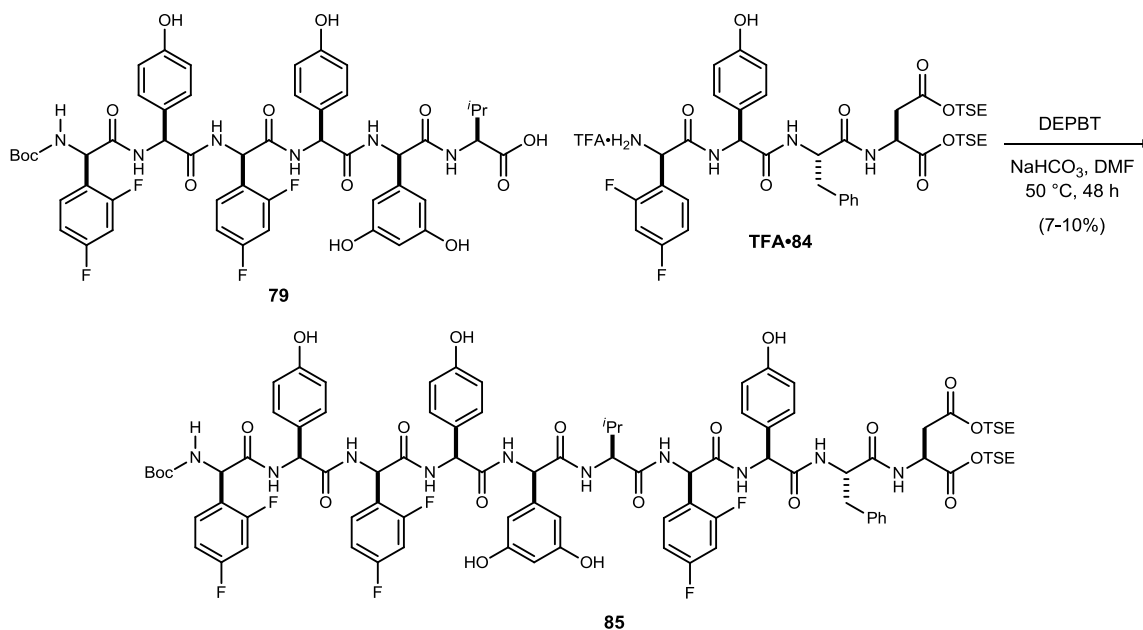
Scheme 44. Synthesis of Tetrapeptide Amine C Analog 84



1.2.4 Coupling Fragments B & C

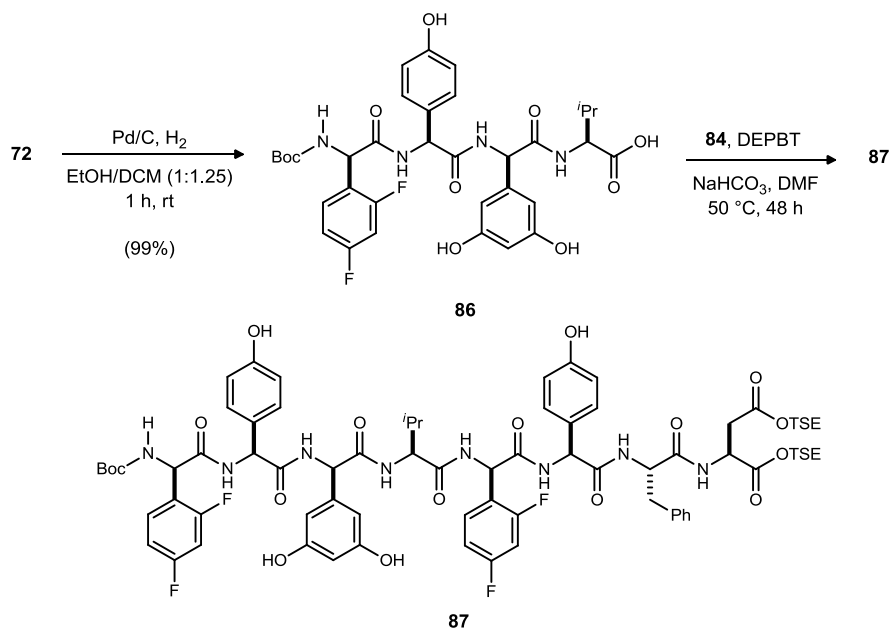
With analogs of fragments B and C in hand, studies for the synthesis of feglymycin continued. Initial attempts to couple carboxylic acid **79** with amine TFA•**84** using traditional amide coupling reagents EDC and PyBOP were unsuccessful. Utilizing the same reagent used by Sussmuth and coworkers, DEPBT, the decapeptide **85** could be isolated in small amounts via reversed-phase preparatory HPLC and identified via HRMS (Scheme 45). Unfortunately, the yield was low (7-10%). The coupling reaction is currently being

Scheme 45. Coupling of Fragments B & C Surrogates 79 & 84



optimized using a surrogate carboxylic acid, **86**, which is obtained via the hydrogenolysis of tetrapeptide analog **72** (Scheme 46). Thus far, DEPBT has proven to be the best coupling reagent for this reaction (Scheme 46), as alternate coupling reagents such as PyBrOP, PyCIU, and TFFH resulted in no octapeptide **87**.

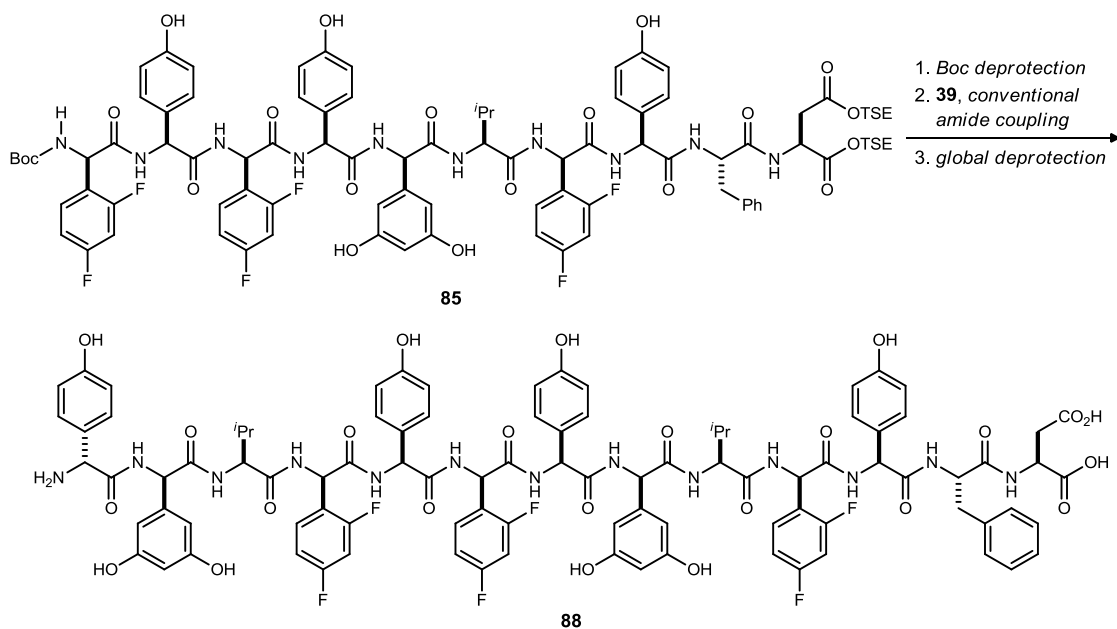
Scheme 46. Model System For Amide Coupling Optimization



1.3 Conclusions and Future Work

Thus far, the synthesis of fragment A (**39**) and syntheses of analogs of fragment B (**79**) and fragment C (**84**) have been completed. The C-terminal deprotection and phenol deprotection of fragment B analogs **79** and **72** have both been achieved via hydrogenolysis. The N-terminal deprotection and phenol deprotection of fragment C analog **83** has been achieved, and the conventional amide bond formation between fragment B analog **79** and fragment C analog **84** has been achieved using the specialized coupling reagent DEPBT to produce decapeptide **85**, albeit in low yields. Following optimization of this coupling reaction, the resulting fragment BC analog **85** will be deprotected at the N-terminus, and a conventional amide bond forming reaction between **85** and **39** will complete the installation of all thirteen residues into the tridecapeptide of feglymycin analog. Finally, deprotection of both the N- and C-termini using TFA will result in the synthesis of a single diastereomer of **88**. The synthesis will be achieved using only 16 steps in the longest linear sequence from

Scheme 47. Anticipated Completion of Feglymycin Analog **88**



commercially available starting materials and 34 total synthetic manipulations.

The synthesis highlights the utility of Umpolung Amide Synthesis (UmAS) and the enantioselective aza-Henry addition of α -bromonitromethane into both TMS- and Boc-protected imines, which allow for the diversification of aryl glycine protecting groups. Following the completion of the synthesis of feglymycin analog **88**, these optimized conditions will be applied to a route incorporating the Dpg residue at positions 4, 6, and 10, either via direct methods with a suitably protected Dpg α -bromonitroalkane donor or via indirect methods with a surrogate that can later be transformed to the desired 3,5-dihydroxy residues. Installation of the Dpg residues will allow for the total synthesis of the anti-HIV and anti-bacterial natural product feglymycin (**17**). Biological studies of analog **88** are anticipated.

STUDIES TOWARDS THE TOTAL SYNTHESIS OF KAULUAMINE

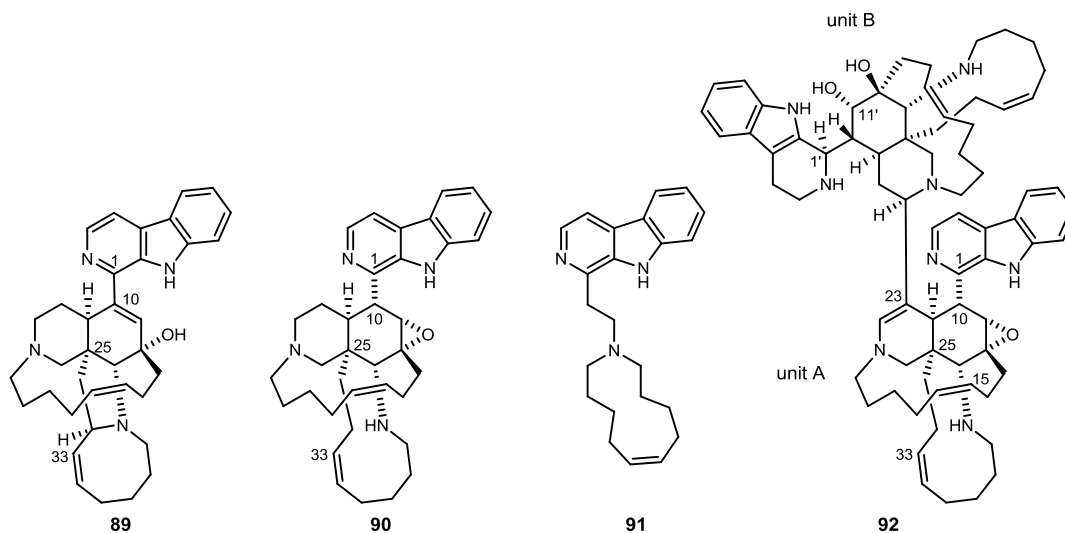
2.1 Kauluamine and the Manzamine Family of Natural Products

2.1.1 Isolation and Key Structural Features

The manzamine class of alkaloids is generally characterized by a fused tetra- or pentacyclic ring system and typically has a β -carboline group. Manzamine A (**89**, Figure 10), the first compound of this class to be described, was isolated as its hydrochloride salt in 1986 by Higa from a marine sponge off the coast of Okinawa.⁵⁸ Its structure was primarily determined via X-ray crystallography and was found to have a fused piperidine, cyclohexene, and pyrrolidine core, as well as an unusually rigid 13-membered macrocycle, an eight-membered ring, and a β -carboline moiety.

Since the isolation of manzamine A, more than 80 related alkaloids have been reported.⁵⁹ The natural

Figure 10. Manzamines A (**89**), B (**90**), and C (**91**) and Kauluamine (**92**)



products have been isolated from sponges from a variety of genus, including *Haliclona*, *Ircinia*, *Amphimedon*, *Xestospongia*, and *Acanthostrongylophora*.⁶⁰ Manzamines B (**90**) and C (**91**), like manzamine A, were first isolated from marine sponges of the genus *Haliclona*.⁶¹ Manzamine B differs from manzamine A in that it has an 11-membered ring rather than the fused pyrrolidine and eight-membered rings. Manzamine B also lacks the unsaturation at C10-C11 and instead has an epoxide at C11-C12. Manzamine C lacks the tetra- or pentacyclic core of manzamines B or A and instead is comprised of a β -carboline unit and a 12-membered macrocycle.

Reported in 1995, kauluamine (**92**) was the first manzamine dimer to be described.⁶² Kauluamine was isolated by Scheuer from a marine sponge originally classified as *Prianos*⁶³ that was collected in Manado Bay,

⁵⁸ Sakai, R.; Higa, T. *J. Am. Chem. Soc.* **1986**, *108*, 6404.

⁵⁹ Peng, J.; Rao, K. V.; Choo, Y.; Hamann, M. T. *Manzamine Alkaloids*. In *Modern Alkaloids: Structure, Isolation, Synthesis, and Biology*; Fattorusso, E.; Taglialetela-Scafati, O., Eds.; Wiley-VCH: Weinheim, 2008; pp 189-232.

⁶⁰ Hu, J.; Hamann, M. T.; Hill, R.; Kelly, M. *The Manzamine Alkaloids*. In *The Alkaloids: Chemistry and Biology*; Cordell, G. A., Ed.; Elsevier, 2003; Vol. 60, pp 207-285.

⁶¹ Sakai, R.; Kohmoto, S.; Higa, T.; Jefford, C. W.; Bernardinelli, G. *Tetrahedron Lett.* **1987**, *45*, 5493.

⁶² Ohtani, I. I.; Ichiba, T.; Isobe, M.; Kelly-Borges, M.; Scheuer, P. J. *J. Am. Chem. Soc.* **1995**, *117*, 10743.

⁶³ The sponge was originally classified as belonging to the genus *Prianos*, but has since been reclassified as *Acanthostrongylophora* by Hu.⁶⁰

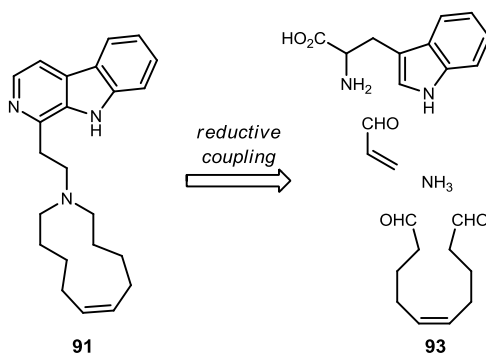
Indonesia. *Kaulua* is the Hawaiian word for a double-hulled voyaging canoe, and the name kauluamine was chosen to reflect the compound's dimeric nature. Kauluamine (**92**) is structurally most closely related to manzamine B (**90**). The natural product is comprised of two only slightly varying units, each of which contains the tetracyclic core, 13-membered bridge, and β -carboline moiety similar to the core of manzamine B. Both the 11- and 13-membered rings feature *Z*-olefins. Unit A of kauluamine differs from manzamine B only in its degree of unsaturation at C22-C23, where it is linked to unit B via a carbon-carbon bond at C23-C22'. In unit B of kauluamine, the C11'-12' epoxide has been opened at the C12' position with a molecule of water, and C1'-N2' and C3'-C4' of the β -carboline moiety have been reduced. Kauluamine (**92**), like manzamine B (**90**), contains six contiguous stereocenters in the cyclohexane ring (C10-12, C24-26), including one all-carbon stereocenter (C25). Unlike in manzamine B, these stereocenters are contained in each unit of the kauluamine dimer, and in unit B, the stereochemistry at C12' is reversed due to the epoxide ring-opening. The differences in oxidation state at C22-C23 and the connection to C22' distinguish kauluamine from its manzamine relatives and make it a synthetically interesting target.

The manzamines have been generally reported to show a variety of biological activity, including cytotoxicity,⁵⁸ antimalarial,^{64a} and inhibitory^{64b} activity, among others.⁵⁹ Kauluamine was found to be only moderately active, showing some immunosuppressive activity (MLR IC₅₀ 1.57 μ g/mL, LcV IC₅₀ >25.0 μ g/mL, LcV/MLR >16) in the mixed lymphoma reaction. The compound was inactive in cytotoxicity and antiviral assays.⁶² There have been no further reports of kauluamine's bioactivity.⁶⁵

2.1.2 Manzamine Biosynthesis

Baldwin and Whitehead proposed a biosynthesis of the manzamine class of molecules in 1992 (Scheme 48 and Scheme 49).⁶⁶ In analyzing the structures of manzamines A, B, and C, they broke the compounds into four main components: tryptophan, acrolein, the symmetric ten-carbon unit (*Z*-dec-5-enedial (**93**), and ammonia. They noted that a reductive coupling of these four components would lead to manzamine C (Scheme 48).

Scheme 48. Proposed Biosynthesis of Manzamine C



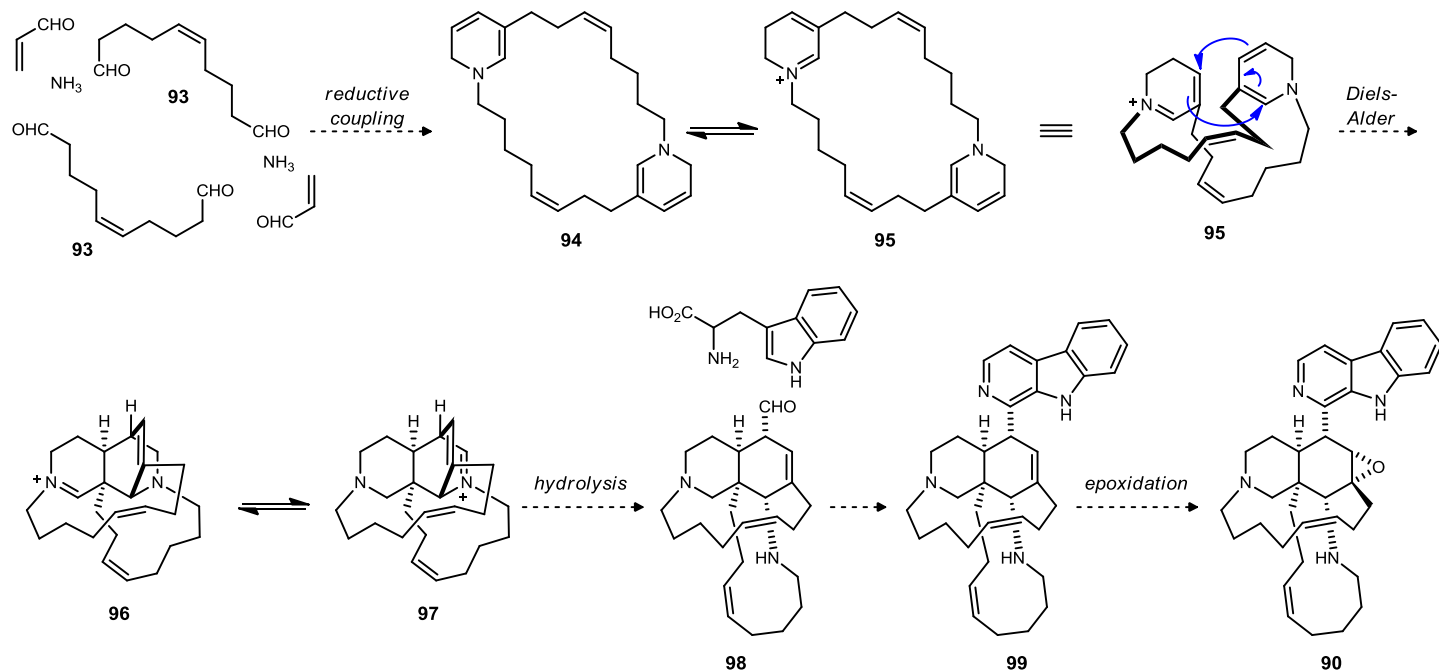
The connectivity and stereochemistry of manzamines A and B can be explained by an intramolecular *endo* Diels-Alder cycloaddition of **95**, which arises from the reductive coupling of two units of acrolein, **93**, and ammonia (Scheme 49). A redox exchange between the two piperidine rings gives **97**, and subsequent hydrolysis of the iminium results in the core structure (**98**) of the manzamines. Finally, condensation with tryptophan is proposed to form **99**. Epoxidation of the C11-C12 bond leads to manzamine B (**90**), and epoxide ring opening with water and elimination to the allylic alcohol gives manzamine A (**89**).

⁶⁴ a) El Sayed, K. A.; Kelly, M.; Kara, U. A. K.; Ang, K. K. H.; Katsuyama, I.; Dunbar, D. C.; Kahn, A. A.; Hamann, M. T. *J. Am. Chem. Soc.* **2001**, *123* 1804. b) Rao, K. V.; Hamann, M. T., et al. *J. Nat. Prod.* **2006**, *69*, 1034.

⁶⁵ This absence of publication on the bioactivity of kauluamine may be due to its instability; the compound was isolated as an unstable solid and could not be crystallized as a salt due to decomposition in acid.⁶²

⁶⁶ Baldwin, J. E.; Whitehead, R. C. *Tetrahedron Lett.* **1992**, *33*, 2059.

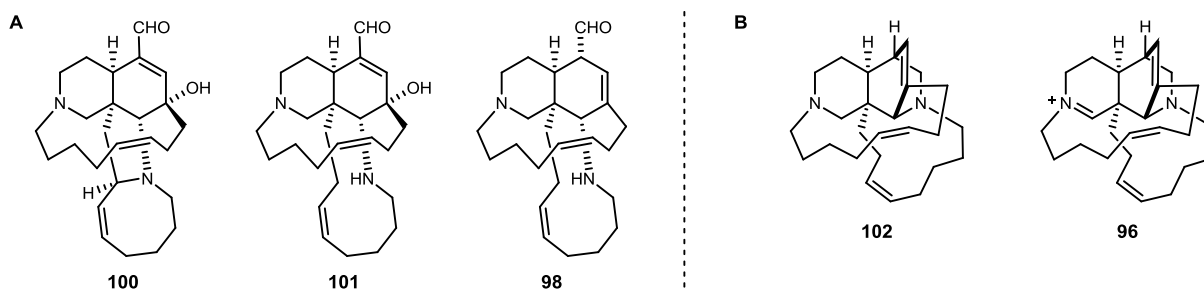
Scheme 49. Proposed Biosynthesis of Manzamine Family of Alkaloids



Several natural products similar to the manzamines were later reported. Some of these natural products appear to closely resemble intermediates along the proposed biosynthetic pathway. For example, ircinal A and B⁶⁷ (**100** and **101**, respectively) lack the β -carboline unit of manzamines A and B and resemble proposed intermediate **98** (Figure 11A). Kobayashi's isolation and structural elucidation of keramaphidin B⁶⁸ (**102**) two years after Baldwin's proposal seemed to further support the proposed biosynthesis due to its similarity to Diels-Alder adduct **86**. Keramaphidin B (**102**) is simply the reduced form of the proposed intermediate **96** (Figure 11B).^{68,69e}

Synthetic studies to support the proposed biosynthetic pathway have been undertaken by the groups of Baldwin and Marazano.⁶⁹ Among those studies is Baldwin's biomimetic synthesis of keramaphidin B (**102**).^{69f}

Figure 11. Similarities Between Proposed Biosynthetic Intermediates and Natural Products



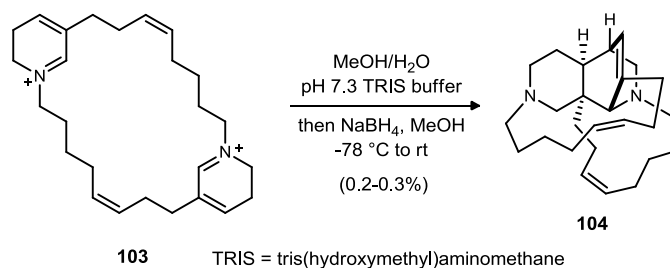
⁶⁷ Kondo, K.; Shigemori, H.; Kikuchi, Y.; Ishibashi, M.; Sasaki, T.; Kobayashi, J. *J. Org. Chem.* **1992**, *57*, 2480.

⁶⁸ Kobayashi, J.; Tsuda, M.; Kawasaki, N.; Matsumoto, K.; Adachi, T. *Tetrahedron Lett.* **1994**, *35*, 4383.

⁶⁹ For synthetic studies, see: a) Baldwin, J. E.; Claridge, T. D. W.; Heupel, F. A.; Whitehead, R. C. *Tetrahedron Lett.* **1994**, *35*, 7829. b) Gil, L.; Gateau-Olesker, A.; Marazano, C.; Das, B. C. *Tetrahedron Lett.* **1995**, *36*, 707. c) Gil, L.; Gateau-Olesker, A.; Wong, Y.; Chernatova, L.; Marazano, C.; Das, B. C. *Tetrahedron Lett.* **1995**, *36*, 2059. d) Gil, L.; Baucherel, X.; Martin, M.; Marazano, C.; Das, B. C. *Tetrahedron Lett.* **1995**, *35*, 6231. e) Baldwin, J. E.; Bischoff, L.; Claridge, T. D. W.; Heupel, F. A.; Spring, D. R.; Whitehead, R. C. *Tetrahedron* **1997**, *53*, 2271. f) Baldwin, J. E.; Claridge, T. D. W.; Culshaw, A. J.; Heupel, F. A.; Lee, V.; Spring, D. R.; Whitehead, R. C.; Boughtflower, R. J.; Mutton, I. M.; Upton, R. J. *Angew. Chem. Int. Ed.* **1998**, *37*, 2661.

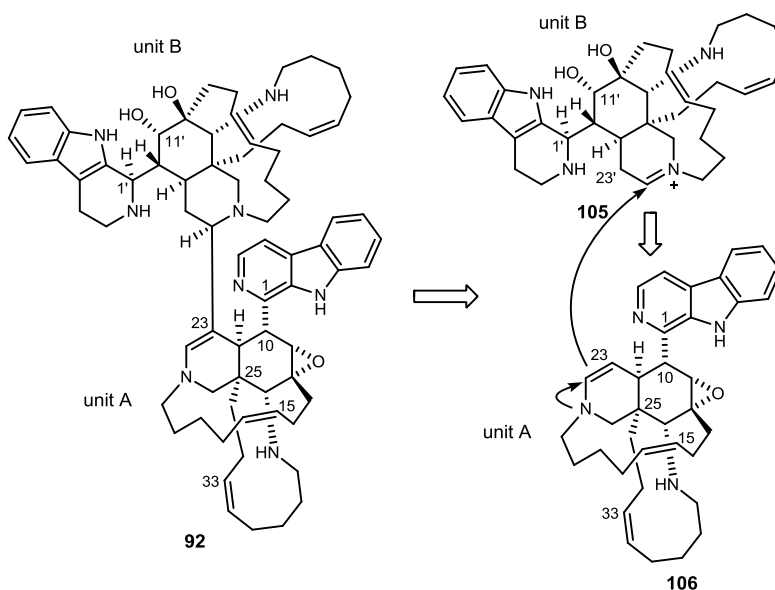
Treatment of *bis*-dihydropyridine⁷⁰ **103** with an aqueous methanol buffer, followed by a sodium borohydride quench, resulted in the formation of keramaphidin B (**102**) in 0.2-0.3% yield (Scheme 50). While this yield is low, it presumably forms via an intramolecular Diels-Alder reaction and illustrates the plausibility of **95** as an intermediate in the biosynthetic pathway.

Scheme 50. Synthesis of Keramaphidin B



The kauluamine dimer is proposed to form from two molecules of unit A (Scheme 51).⁶² Unit B is formed from one molecule of unit A (**106**), where the epoxide (C11'-12') is opened at the C12' position with a molecule of water, reversing the stereochemistry at that center. Reduction of the β -carboline at C1'-N2' and C3'-C4' and tautomerization of the enamine to its iminium form gives unit B (**105**). Finally, the enamine addition of **106** into the iminium of **105** and tautomerization of the resulting iminium completes the dimerization of kauluamine (**92**).

Scheme 51. Proposed Dimerization Pathway for Kauluamine



2.1.3 Manzamine Syntheses and Synthetic Efforts

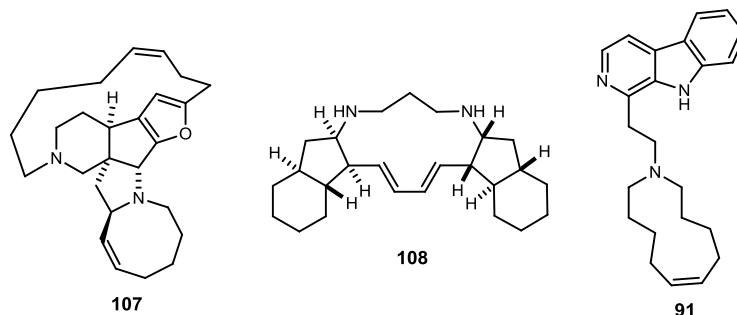
Because of their complex structures and interesting bioactivity, the manzamine class of alkaloids has been a target for natural product total syntheses.⁷¹ To date, manzamine A has been synthesized only three times,

⁷⁰ Baldwin, J. E.; Claridge, T. D. W.; Culshaw, A. J.; Heupel, F. A.; Smrcková, S.; Whitehead, R. C. *Tetrahedron Lett.* **1996**, *38*, 6919.

⁷¹ Reviews: a) Nishida, A.; Nagata, T.; Nakagawa, M. Strategies for the Synthesis of Manzamine Alkaloids. In *Topics in Heterocyclic Chemistry: Marine Natural Products*; Kiyota, H., Ed.; Springer: Berlin/Heidelberg, 2006; Vol. 5, pp 255-280. b) Magnier, E.; Langlois, Y. *Tetrahedron* **1998**, *54*, 6201-6258.

first by Winkler⁷² in 1998 and the following year by Martin.⁷³ Fukuyama reported the total synthesis of manzamine A in 2010.⁷⁴ Manzamine B, which contains an 11-membered azacycle and six consecutive stereocenters, has never been synthesized, though attempts have been made.⁷⁵ Some other members of this class have been synthesized, including nakadomarin A⁷⁶ (**107**), papuamine (**108**), and manzamine C (**91**).⁷¹ These compounds (Figure 12) do not contain the *cis*-decalin core of manzamines A and B and kauluamine.

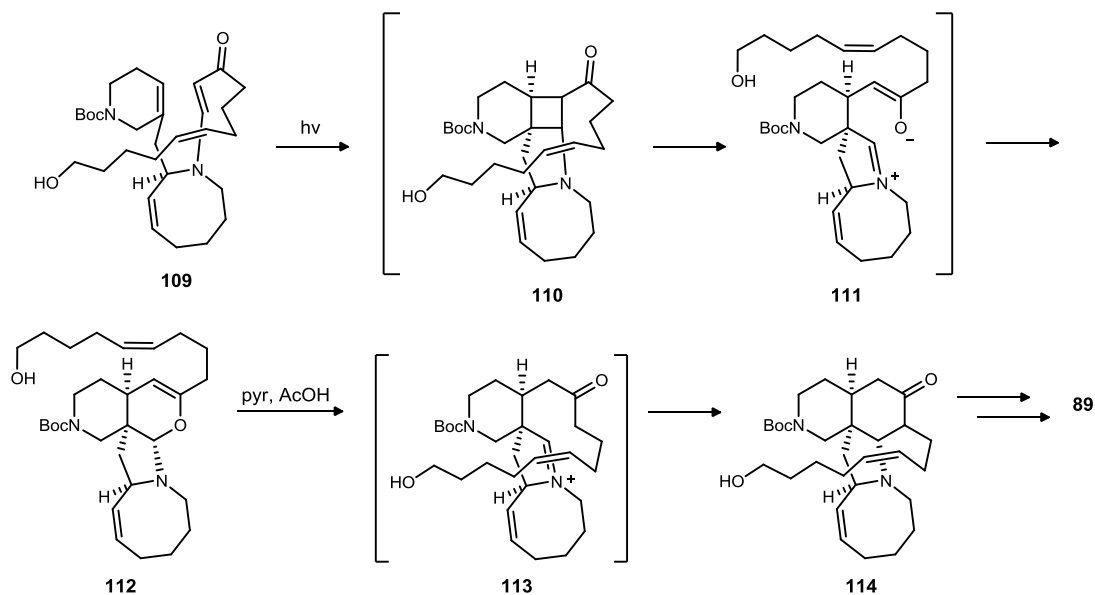
Figure 12. Nakadomarin A, Papuamine, and Manzamine C



Total Syntheses of Manzamine A

The first total synthesis of manzamine A⁷² was completed by Winkler and co-workers in 31 steps from pyridine-3-methanol. The approach utilizes a unique intramolecular vinylogous amide photoaddition/fragmentation/Mannich sequence (Scheme 52) to form the fused tetracyclic core of manzamine A and proceeds through ircinal A (**100**) as a synthetic intermediate.

Scheme 52. Winkler's Approach to Manzamine A



⁷² Winkler, J. D.; Axten, J. M. *J. Am. Chem. Soc.* **1998**, *120*, 6425. b) Winkler, J. D.; Axten, J. M.; Hammach, A.; Kwak, Y.; Lucero, M.; Houk, K. N. *Tetrahedron* **1998**, *54*, 7045.

⁷³ a) Martin, S. F.; Humphrey, J. M.; Ali, A.; Hiller, M. C. *J. Am. Chem. Soc.* **1999**, *121*, 866. b) Humphrey, J. M.; Liao, Y.; Ali, A.; Rein, T.; Wong, Y.; Chen, H.; Courtney, A. K.; Martin, S. F. *J. Am. Chem. Soc.* **2002**, *124*, 8584.

⁷⁴ Toma, T.; Kita, Y.; Fukuyama, T. *J. Am. Chem. Soc.* **2010**, *132*, 10233.

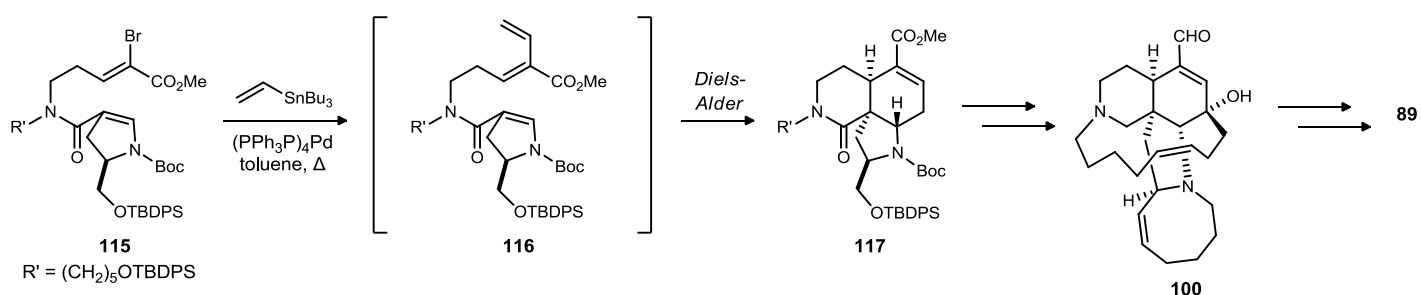
⁷⁵ a) Matsumura, T.; Akiba, M.; Arai, S.; Nakagawa, M.; Nishida, A. *Tetrahedron Lett.* **2007**, *48*, 1265. b) Torisawa, Y.; Ali, M. A.; Tavet, F.; Kageyama, A.; Aikawa, M.; Fukui, N.; Hino, T.; Nakagawa, M. *Heterocycles* **1996**, *42*, 677.

⁷⁶ a) Nilson, M. G.; Funk, R. L. *Org. Lett.* **2010**, *12*, 4912. b) Inagaki, F.; Kinebuchi, M.; Miyakoshi, N.; Mukai, C. *Org. Lett.* **2010**, *12*, 1800. c) Jakubec, P.; Cockfield, D. M.; Dixon, D. J. *J. Am. Chem. Soc.* **2009**, *131*, 16632. d) Martin, D. B. C.; Vanderwal, C. D. *Angew. Chem. Int. Ed.* **2010**, *49*, 2830. (Review includes syntheses prior to 2010.)

The key step of the synthesis proceeds from vinylogous amide **109**, which was prepared in 17 steps from pyridine-3-methanol.^{72b} The vinylogous amide (**109**) undergoes photoaddition to form cyclobutane intermediate **110**. A retro-Mannich fragmentation of **110** led to iminium **111**, which underwent ring closure to give aminal **112**. This compound (**112**) underwent isomerization to give the manzamine tetracycle (**114**) as a single stereoisomer upon treatment with pyridinium acetate. Transformation of **114** to icrinal A (**100**) was achieved in 15 steps. Icrinal A was converted to manzamine A (**89**) according to Kobayashi's protocol.⁶⁷

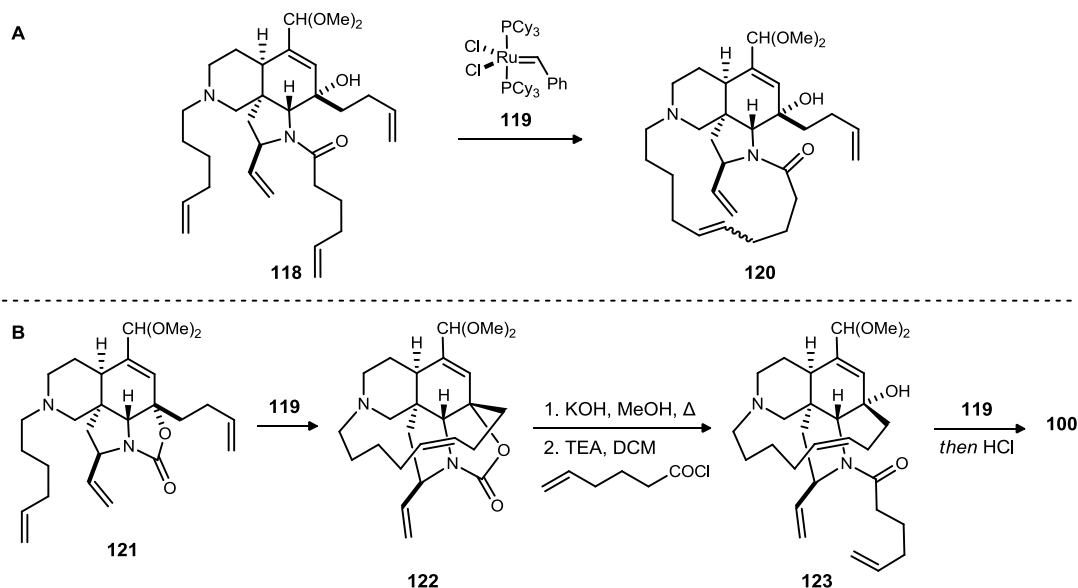
The total synthesis of manzamine A⁷³ by Martin, et al. also proceeded through icrinal A (**100**) as a synthetic intermediate. The approach used a novel Stille/Diels-Alder cascade (Scheme 53) to prepare the tricyclic core (**117**) of manzamine A. Vinyl bromide (**115**) was prepared in nine linear steps from 5-aminopentan-1-ol. A Stille coupling of **115** with vinyl tributylstannane was used to form intermediate **116**. This intermediate (**116**) underwent a spontaneous Diels-Alder cycloaddition to form **117**. Conversion of the tricyclic core (**117**) to icrinal A (**100**) was accomplished in 12 steps. Icrinal A was then transformed to manzamine A according to Kobayashi's protocol (Scheme 53).⁶⁷

Scheme 53. Martin's Stille/Diels-Alder Cascade



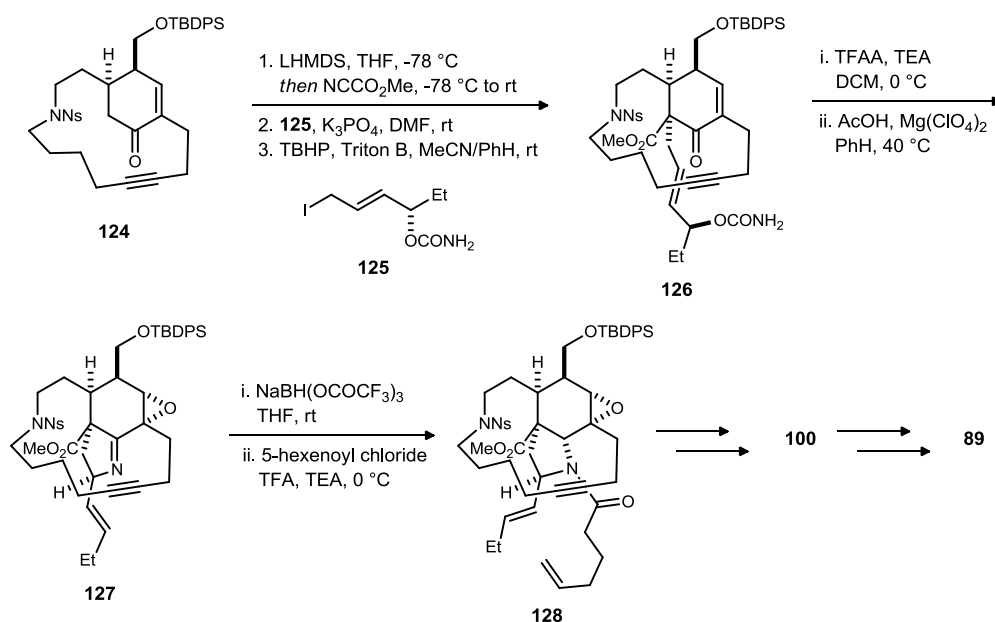
Martin's synthetic efforts also served to highlight the difficulty in performing a selective ring-closing metathesis on a compound (**118**) containing four terminal olefins.^{73b} Rather than forming the desired 13-membered and 8-membered macrocycles, tetraene **118** was converted to a 15-membered bridged macrocycle (**120**, Scheme 54A). To circumvent this undesired pathway, triene **121** was prepared. Upon treatment with Grubbs I catalyst (**119**), the desired 13-membered azacycle was formed. Following decarboxylation of carbamate **122** and acylation to prepare **123**, a second ring-closing metathesis was performed using Grubbs I catalyst (Scheme 54B) to form the desired 8-membered ring of icrinal A (**100**).

Scheme 54. Martin's Solution to Undesired Ring-Closing Metathesis



Fukuyama's synthesis of manzamine A uses a bridged 15-membered azacycle (**124**) to introduce stereochemistry to the cyclohexene ring of manzamine A (**89**). The C26-N27 bond was formed via a [3,3] sigmatropic rearrangement (Scheme 55). Key intermediate **124** was prepared in 16 steps from a known alkyl bromide. Ketone **124** was converted to its β -ketoester using Mander's reagent. The intermediate β -ketoester was selectively alkylated from the α -face of the molecule and then epoxidized, again from the α -face, to give **126**. Facial selectivity was attributed to conformational restraints induced by the bridged 15-membered macrocycle. Dehydration of intermediate **126** led to the [3,3] sigmatropic rearrangement that formed an intermediate isocyanate, which was converted to imine **127** in the same pot due to stability issues. Imine **127** was then reduced and acylated to give **128**, concluding the formation of manzamine A's stereocenters. Intermediate **128** was converted to ircinal A (**100**) in six steps, then converted to manzamine A using a modification of Kobayashi's procedure.⁶⁷

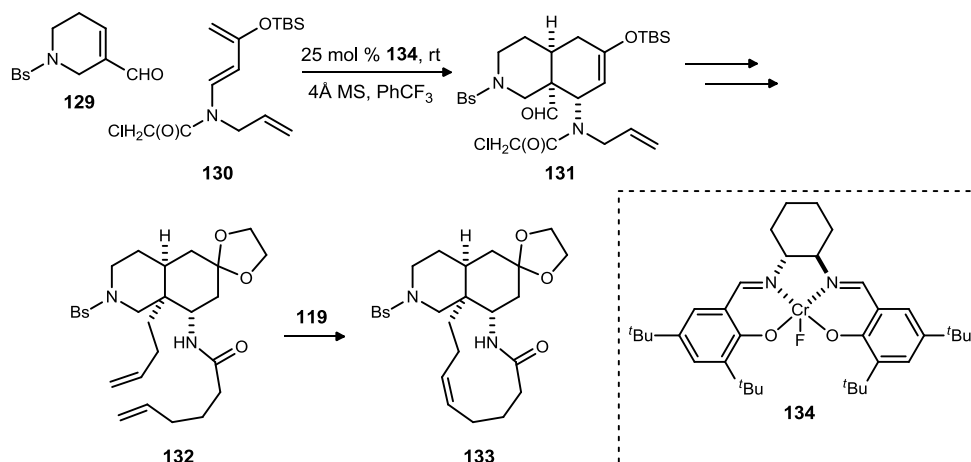
Scheme 55. Fukuyama's Approach to Manzamine A



Efforts Towards the Total Synthesis of Manzamine B

Studies towards the synthesis of manzamine B (**90**) and ircinal B (**101**), which share the same tetracyclic core structure have been reported by the groups of Nishida and Nakagawa.⁷⁵ In 2007, Nishida and co-workers reported the synthesis of the tricyclic core (**133**) of manzamine B (**90**), applying Rawal's asymmetric Diels-

Scheme 56. Nishida's Preparation of the Tricyclic Core of Manzamine B



Alder reaction to set the stereochemistry in the cyclohexane ring of the molecule (Scheme 56).^{75a} A chromium-salen complex (**134**) was used to induce asymmetry in the Diels-Alder reaction between dienophile **129** and diene **130**. The final ring-closing metathesis using Grubbs I catalyst (**119**) completed the tricyclic core (**133**) of manzamine B.

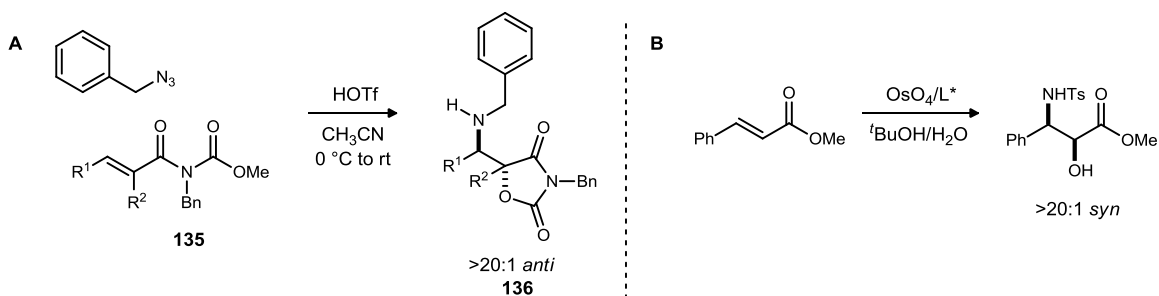
2.2 Kauluamine Model Studies

2.2.1 Background & Model Retrosynthetic Analysis

Aminohydroxylation Reactions

In 2005, Johnston and co-workers reported a Brønsted acid-promoted formal *anti*-aminohydroxylation reaction between electron-rich benzyl azide and a variety of acryloyl imides (**135**).⁷⁷ The triflic acid-catalyzed reaction enjoyed good to excellent yields, and in cases where two diastereomers were possible, excellent diastereoselection (Scheme 57A). This report came as a nice alternative to the Sharpless asymmetric aminohydroxylation reaction, which gives the *syn*-diastereomer (Scheme 57B).⁷⁸ Johnston's method has the

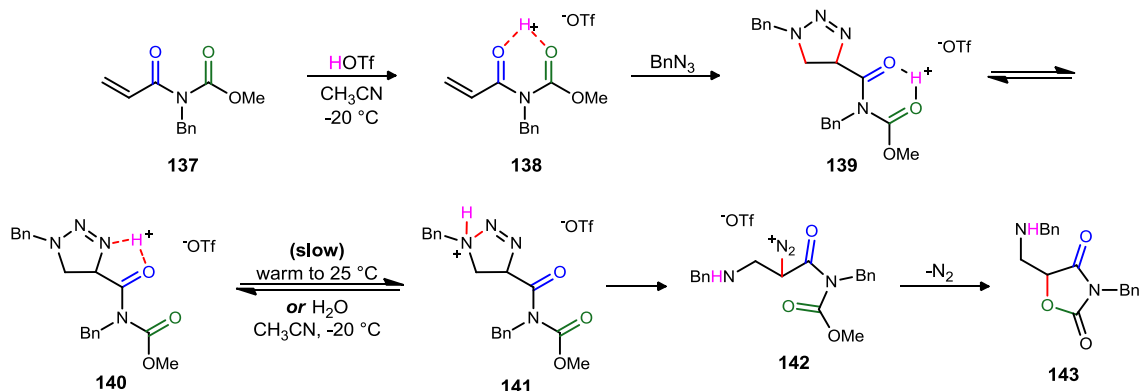
Scheme 57. Aminohydroxylation Reactions



advantage of being metal-free, as opposed to Sharpless's method, which requires the use of toxic osmium tetroxide. Additionally, Johnston's method is oxidant-free; the azide is reduced to dinitrogen, a benign byproduct liberated during the reaction. The Sharpless aminohydroxylation, on the other hand, requires the use of super-stoichiometric amounts of co-oxidant.

Johnston's report was followed by one in which the authors disclosed formation of a key triazoline intermediate from the [3+2] cycloaddition between benzyl azide and the activated olefin.⁷⁹ This triazoline intermediate could be decomposed to the oxazolidine dione/formal aminohydroxylation product upon warming

Scheme 58. Mechanism of Brønsted Acid-Catalyzed Aminohydroxylation Reaction



⁷⁷ Mahoney, J. M.; Smith, C. R.; Johnston, J. N. *J. Am. Chem. Soc.* **2005**, *127*, 1354.

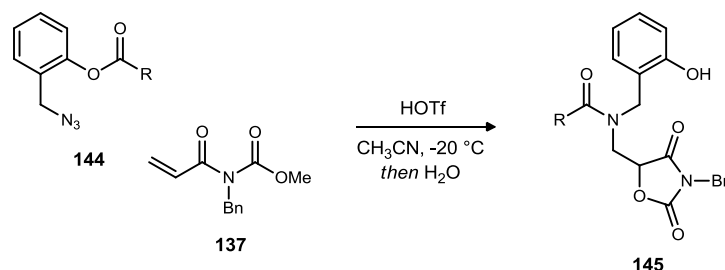
⁷⁸ Li, G.; Chang, H.; Sharpless, K. B. *Angew. Chem. Int. Ed.* **1996**, *35*, 451.

⁷⁹ a) Hong, K. B.; Donahue, M. G.; Johnston, J. N. *J. Am. Chem. Soc.* **2008**, *130*, 2323. b) Donahue, M. G.; Hong, K. B.; Johnston, J. N. *Bioorg. Med. Chem. Lett.* **2009**, *19*, 4971.

or treatment with water. Water was proposed to effectively shuttle the proton from its triazoline-imide carbonyl binding site (**140**) to N1 (**141**), thereby accelerating the rate of triazoline fragmentation and decomposition to the oxazolidine dione.

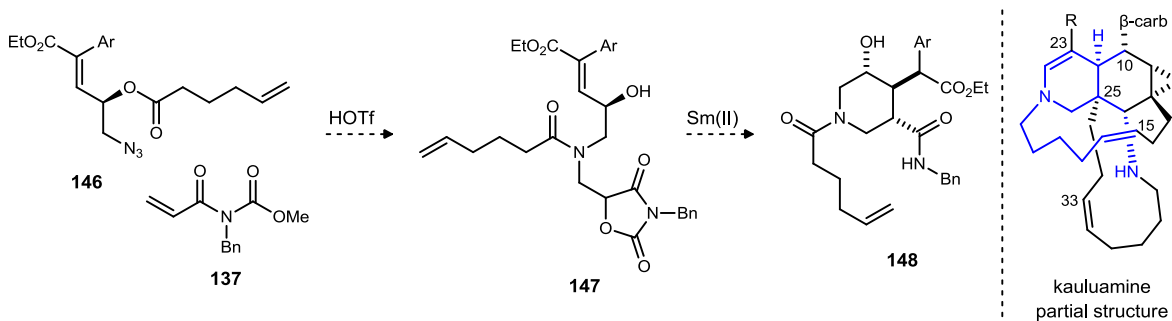
Johnston later showed that the benzyl azide, when bearing an ester group at the *ortho*-position (**144**), could be used as an acyl carrier (Scheme 59).⁸⁰ During the course of the aminohydroxylation reaction, the acyl group was found to transfer O → N, resulting in a tertiary amide (**145**) rather than a disubstituted amine, again in good to excellent yields. It is this finding that we hypothesized could lead to a convergent strategy to synthesize the natural product kauluamine (Scheme 60).

Scheme 59. Tandem O→N Acyl Transfer/Aminohydroxylation



By constructing an azide that bears an ester group outfitted with the C16-20 fragment of kauluamine, we can expect acyl transfer to occur during the tandem aminohydroxylation/acyl transfer reaction to result in amide **147**. The azide starting material (**146**) will also be equipped with a suitable Michael acceptor, and following a samarium(II) iodide-mediated reductive C-O bond cleavage of **147** to the amide enolate, diastereoselective cyclization to the piperidine core of kauluamine is expected to occur.

Scheme 60. Kauluamine Core Retrosynthesis



Stereochemical Models for Cyclization

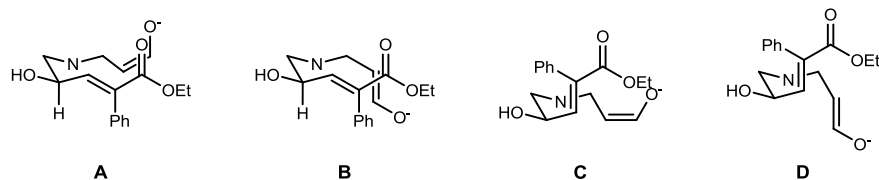
Following samarium(II) iodide reduction of oxazolidinone **147** to its amide enolate, an intramolecular Michael addition of this enolate into the α,β -unsaturated ester is expected to occur. The stereochemistry of this cyclization should be controlled by the C23 hydroxyl group, whose absolute stereochemistry will be set via a Sharpless asymmetric dihydroxylation reaction. Three new stereocenters are formed during this cyclization, so there are eight possible diastereomers. We do not expect to control the final protonation of the enolate that forms following the Michael addition.

Since a six-membered ring is being formed, we expect the cyclization reaction to resemble a chair-like transition state,⁸¹ with the C23 hydroxyl group and the electrophilic double bond expected to be pseudo-equatorially disposed. The four possible chair conformations in which the hydroxyl group is pseudo-equatorial are shown below (Figure 13).

⁸⁰ Donahue, M. G.; Johnston, J. N. *unpublished results*.

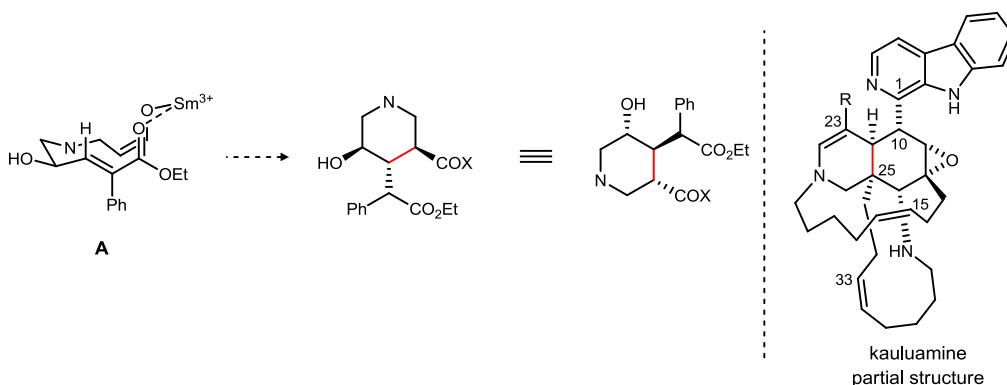
⁸¹ Zimmerman, H. E.; Traxler, M. D. *J. Am. Chem. Soc.* **1957**, *79*, 1920.

Figure 13. Chair Transition States for Cyclization



Of these structures, only conformation A results in pseudo-equatorial positioning of both the enolate and the electrophilic double bond. While conformations A and B both experience $A^{1,3}$ strain between the phenyl group and the γ hydrogen, conformation B also suffers from pseudo-axial positioning of the enolate. Conformations C and D, in addition to the torsional strain⁸² created by pseudo-axial positioning of the reactive centers, suffers from $A^{1,3}$ bisecting strain in which the phenyl group has unfavorable interactions both with the hydroxyl group and the methylene group. Since eclipsing interactions between the phenyl and a hydrogen are less energetic than bisecting interactions between a phenyl and a methylene or hydroxyl group,⁸² conformation A is expected to be the least energetic of all possible conformations, making it favored over the others. As shown in Figure 14, conformation A leads to the desired diastereomers. Conformation A has the added benefit of both the ester carbonyl and the enolate oxygen in positions where they could both coordinate to the Sm^{3+} cation during the proposed reaction.

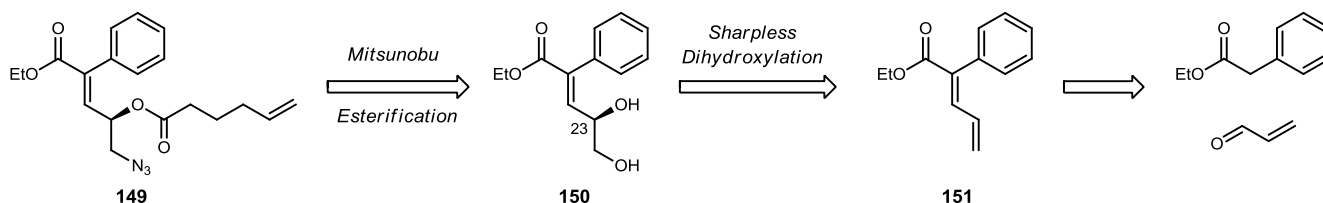
Figure 14. Stereochemical Model for Intramolecular Michael Addition



2.2.2 Construction of the Azide Subunit

For the purpose of this model study, a simple phenyl group will be substituted for the β -carboline ring. We proposed to prepare azide **149** from diene **151** using the Sharpless asymmetric dihydroxylation reaction to introduce stereochemistry at C23, followed by a Mitsunobu reaction to install the azide and esterification to

Scheme 61. Azido Ester Retrosynthesis



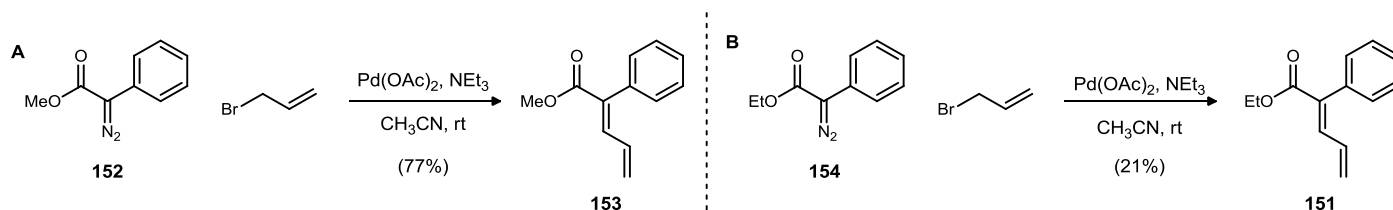
⁸² Hoffmann, R. W. *Chem. Rev.* **1989**, *89*, 1841. In the case of 3-methyl-1-butene, $A^{1,3}$ eclipsing interactions between two hydrogens have a relative energy of 0 kcal/mol, where eclipsing interactions between a hydrogen and a methyl have a relative energy of +0.73 kcal/mol. Bisecting interactions where a hydrogen bisects two methyl groups have a relative energy of +2 kcal/mol.

bring in the side chain (Scheme 61). Diene **151** had previously been prepared by Paulmier⁸³ in 35% yield over three steps via an α -phenylselenenyl ester. We thought a simple aldol condensation might instead be used to access this diene (**151**).

Initial attempts to prepare the desired diene via aldol condensation or Knoevenagel condensation were unsuccessful. Heating ethyl phenylacetate in *N,N*-dimethylformamide in the presence of acrolein and potassium carbonate did not result in formation of **151**. Likewise, the desired diene (**151**) did not form when ethyl phenylacetate and acrolein were heated together in benzene in the presence of ammonium acetate and acetic acid, and zinc(II) acetate dihydrate in dioxane and dimethylsulfoxide⁸⁴ did not promote the condensation of ethyl phenylacetate with acrolein.

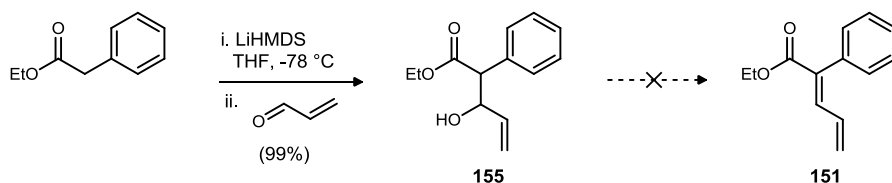
In 2008, Jianbo Wang reported the preparation of the methyl ester of the desired diene (**151**) via a palladium(II) coupling of α -phenyl methyl diazoacetate (**152**) and allyl bromide in 77% yield (Scheme 62A).⁸⁵ An attempt to duplicate the reaction using α -phenyl ethyl diazoacetate (**154**)⁸⁶ resulted only in poor yield (21%) of the desired compound (Scheme 62B). It was later found that diene **151** decomposes upon purification via silica gel, so it is possible that the yield for this reaction might have been higher if purification were not necessary.

Scheme 62. Palladium(II) Coupling of Diazoacetates with Allyl Bromide (Wang)



At this point, we decided that it might be simpler to prepare the desired diene using a two-step aldol condensation, in which we would first prepare the allylic alcohol (**155**) and then effect dehydration to give (**151**). Treatment of ethyl phenylacetate with lithium hexamethyldisilazide followed by freshly distilled acrolein resulted in the desired allylic alcohol (**155**) in 99% yield (Scheme 63), and it was found that the crude product was suitable for use in subsequent reactions without the need for purification.

Scheme 63. Preparation of Allylic Alcohol 67 and Attempted Dehydration



With the allylic alcohol (**155**), we sought to dehydrate the compound using a variety of conditions, including treatment of **155** with triflic anhydride and pyridine, with mesyl chloride or tosyl chloride in the presence of Hünig's base, and with potassium hydrogen sulfate in refluxing toluene. While triflic anhydride and pyridine did lead to some product formation, the yields were scant and required purification via column chromatography to isolate the product.

In a further attempt to dehydrate **155**, we treated the allylic alcohol with thionyl chloride or phosphorous oxychloride. These conditions resulted in S_N2' attack of the reaction intermediate to give allylic chloride **156** as

⁸³ Lebarillier, L.; Outurquin, F.; Paulmier, C. *Tetrahedron* **2000**, *56*, 7483.

⁸⁴ Gol'ding, I. R.; Petrovskii, P. V.; Borbulevych, O. Y.; Shishkin, O. V.; Gruber, W.; Gololobov, Y. G.; Shchegolikhin, A. N. *Russ. Chem. Bull.* **1999**, *48*, 924.

⁸⁵ Chen, S.; Wang, J. *Chem. Commun.* **2008**, 4198.

⁸⁶ Peng, C.; Cheng, J.; Wang, J. *J. Am. Chem. Soc.* **2007**, *129*, 8708.

the major product. We were not discouraged by this result, however, as we recognized that treatment of allylic chloride **156** with a mild base should result in elimination of hydrochloric acid to give the desired diene (**151**). While Hünig's base and pyridine were not strong enough to effect the desired elimination to **151** cleanly, we found that treatment of **156** with 1,8-diazabicycloundec-7-ene (DBU) in dichloromethane at 0 °C resulted in 8:1 formation of the *E:Z* isomers of **151**. The desired *E*-isomer was favored, and a temperature screen revealed that the allylic chloride could be converted to the desired *E*-diene via treatment with DBU at -78 °C in >20:1 *E:Z*.⁸⁷ Results of the temperature screen are shown in Table 1.

Table 1. Elimination to 151 Temperature Screen

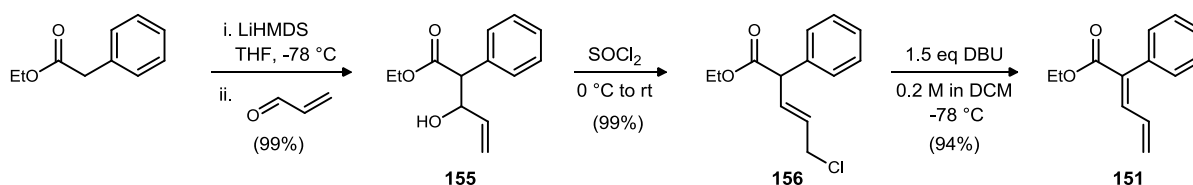


| entry ^a | T (°C) | <i>E:Z</i> ^b |
|--------------------|--------|-------------------------|
| 1 | rt | 7.7:1 |
| 2 | 0 | 8:1 |
| 3 | -20 | 8:1 |
| 4 | -78 | >20:1 |

^aAll reactions proceeded for 20 min (full conversion) then quenched with 1N HCl. ^bBased on crude ¹H NMR.

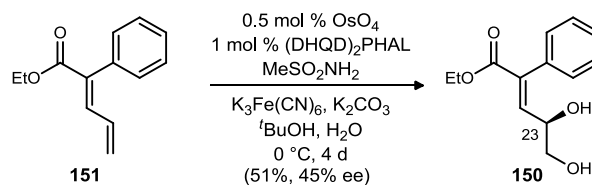
Upon reaction optimization, we were able to prepare allylic chloride **156** in excellent yield (99%) with no need for purification of the product prior to subsequent reactions (Scheme 64). Elimination with DBU to form diene **151** was also achieved in excellent yields (94%) and did not require purification. Thus, we were able to access the desired diene (**151**) in three steps from commercially available starting materials with no purification and nearly quantitative yields.

Scheme 64. Preparation of Diene 151



The Sharpless asymmetric dihydroxylation, using a procedure reported by O'Doherty in his 2005 report⁸⁸ of a remote steric effect on the regioselectivity of the dihydroxylation of $\alpha,\beta,\gamma,\delta$ -unsaturated esters, was utilized to install stereochemistry at C23. Absolute stereochemical assignment was made based on the

Scheme 65. Sharpless Asymmetric Dihydroxylation



⁸⁷ Although **63** had been previously reported, its characterization did not include information on how the *E/Z* geometry was assigned. A NOESY experiment of the diene supported the assignment, with a correlation observed between the γ -proton (δ 6.40) and a phenyl proton (δ 7.23). There was no clear correlation between the β -proton (δ 7.45) and any phenyl protons.

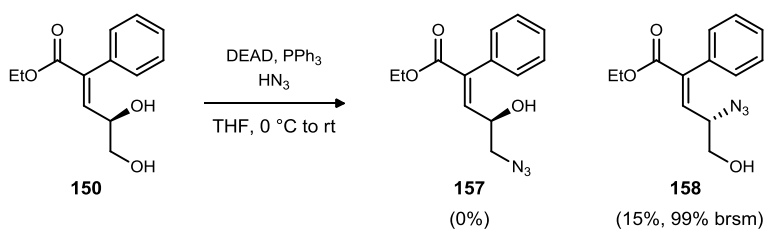
⁸⁸ Zhang, Y.; O'Doherty, G. A. *Tetrahedron* **2005**, *61*, 6337.

mnemonic for the Sharpless asymmetric dihydroxylation.⁸⁹ The reaction resulted in 45-69% enantiomeric excess, with larger scale reactions having lower ee, probably due to a difficulty in controlling the reaction temperature at large scale.

As previously mentioned, we planned to prepare azido alcohol **157** using a Mitsunobu reaction. Although both hydroxyl groups were unprotected, we expected the less-hindered primary alcohol to undergo reaction faster than the secondary allylic alcohol. No reaction was observed upon treatment of the diol (**150**) with diethylazodicarboxylate (DEAD), triphenylphosphine, and diphenylphosphorylazide (DPPA). We hypothesized that DPPA was not a strong enough azide-transfer reagent for this reaction and sought instead to use hydrazoic acid as the acidic nucleophile for the reaction. When trimethylsilylazide and acetic acid were used to generate hydrazoic acid in situ, a mixture of products was observed, including the secondary azide and several silylated products. The desired primary azide was not observed, either silylated or not.

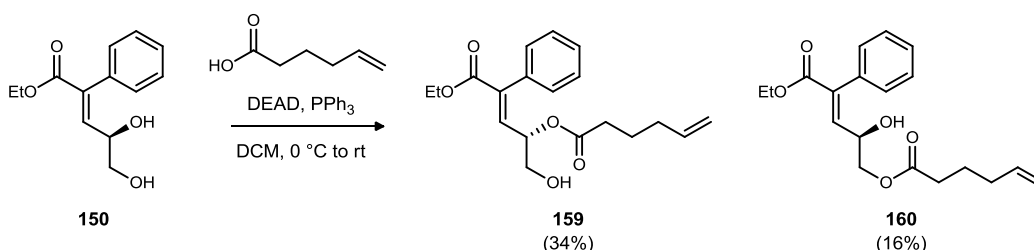
A stock solution of hydrazoic acid in benzene was prepared from sodium azide and sulfuric acid,⁹⁰ and the Mitsunobu reaction was performed using hydrazoic acid as the azide donor (Scheme 66). This reaction resulted in clean formation of the undesired secondary azido alcohol (**158**). While **158** was isolated in poor yield (15%), the starting material was recovered for the balance of the mass, indicating a preference for the Mitsunobu reaction to occur at the secondary allylic alcohol rather than at the primary alcohol.

Scheme 66. Mitsunobu Gives Undesired Regioselectivity



Since Mitsunobu reactions can be used to install esters in place of alcohols, we recognized that we might be able to first install the ester selectively at the secondary allylic position. Unfortunately, the reaction using 5-hexenoic acid was not as selective for the secondary hydroxyl group as the azide reaction had been, with the best conditions used resulting in 59% conversion from the diol (**150**), with 34% yield of the secondary ester (**159**) and 16% yield of the primary ester (**160**).

Scheme 67. Mitsunobu to Install Ester



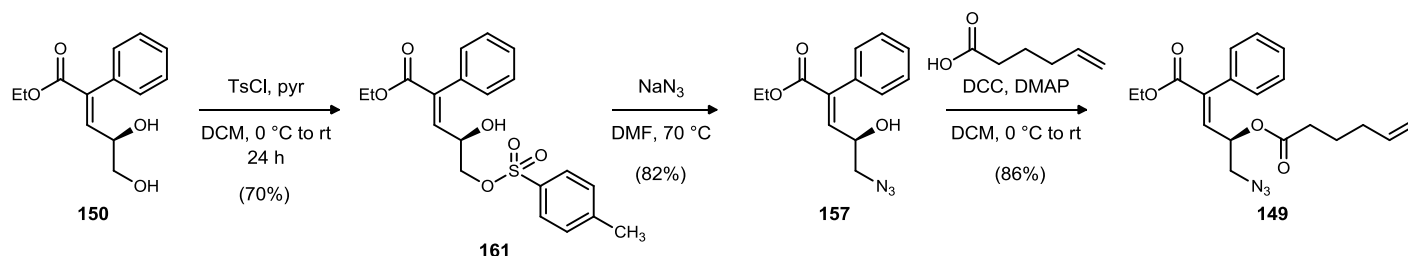
With no luck in installing the azide functionality in one step via the Mitsunobu reaction, we moved on to conversion of the primary alcohol to a good leaving group, followed by S_N2 displacement of the group with an azide nucleophile. While both the primary mesylate and primary tosylate were prepared, use of the tosylate resulted in higher yields for azide formation, and displacement of the tosylate was found to proceed faster (Scheme 68). Thus, the chosen route proceeded via tosylate (**161**) formation by treatment of diol **150** with tosyl chloride and pyridine in dichloromethane at room temperature. Tosylate **161** was then converted to azido alcohol **157** in good yields (82%) by heating in the presence of sodium azide and *N,N*-dimethylformamide.

⁸⁹ Sharpless, K. B.; Amberg, W., et al. *J. Org. Chem.* **1992**, 57, 2768.

⁹⁰ Wolff, H. The Schmidt Reaction. In *Organic Reactions*; Adams, R., Ed.; Wiley: New York, 1946; Vol. III, pp 307-336.

Finally, a dicyclohexylcarbodiimide-mediated coupling of 5-hexenoic acid with azido alcohol **157** resulted in formation of the desired azido ester (**149**) in excellent yield (86%).

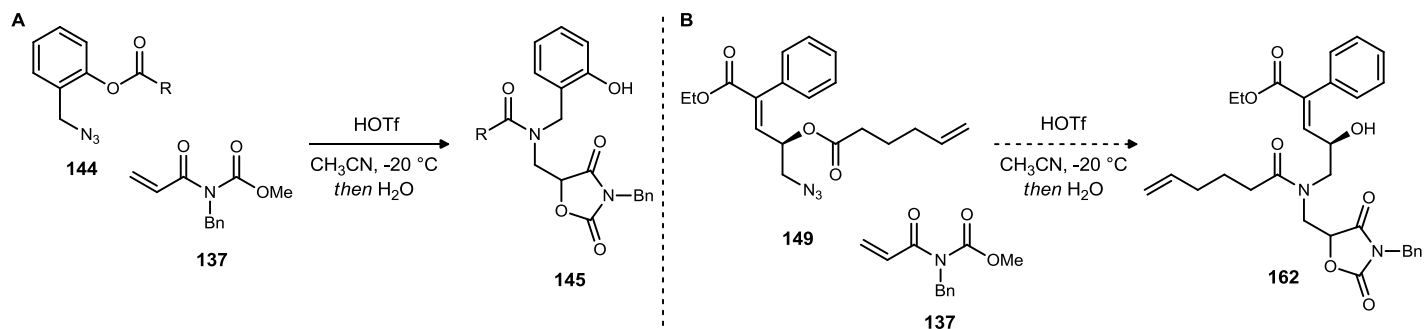
Scheme 68. Preparation of Azido Ester 149



2.2.3 Aminohydroxylation

For the purpose of this model study, acryloyl imide **137** was used as the activated olefin in the aminohydroxylation reaction. Using reaction conditions previously developed in the group, treatment of azido ester **149** and imide **137** with triflic acid, followed by water, was expected to result in triazoline formation and subsequent decomposition to oxazolidine dione **162**. In systems studied by Matt Donahue, the azido esters (**144**) were found to undergo acyl transfer to form the amide (**145**) following triazoline formation and decomposition (Scheme 69A). While the transition state for acyl transfer in those systems was a six-membered ring, this system was expected to undergo acyl transfer via a five-membered transition state to give desired oxazolidine dione amide **162** (Scheme 69B). No diastereoselectivity was expected for this reaction.

Scheme 69. Tandem Aminohydroxylation-Acyl Transfer

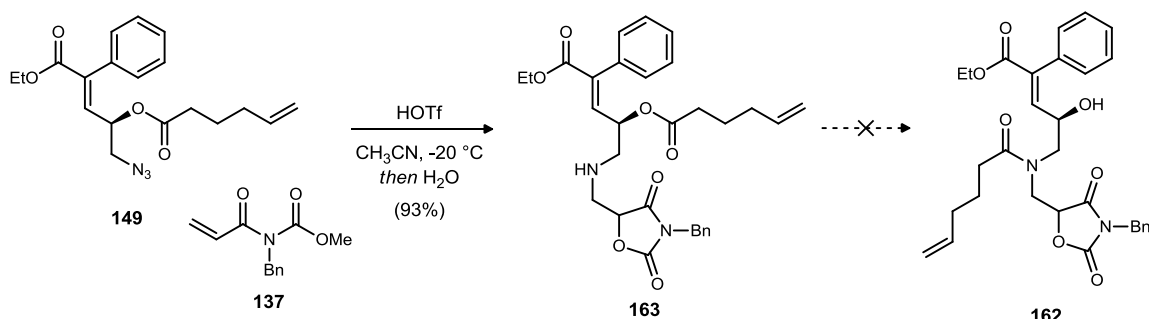


Instead of acyl transfer to give oxazolidine dione amide **162**, the product of this Brønsted acid-catalyzed aminohydroxylation was oxazolidine dione ester **163** (Scheme 71). As expected, no diastereoselectivity was observed for this reaction.

Attempts to effect acyl migration from the ester (**163**) to the amide (**162**) were unsuccessful (Scheme 71). Treatment with strong base (*n*-butyl lithium) and milder base (DBU) did not result in acyl migration. Neither was acyl transfer observed when the amine base used to quench the aminohydroxylation reaction was varied (TEA, pyr, DBU). Conditions for an intermolecular O→N acyl transfer reaction developed by Birman that uses triazole and DBU to form an active ester in situ⁹¹ were found to be ineffective in promoting the desired intramolecular acyl transfer.

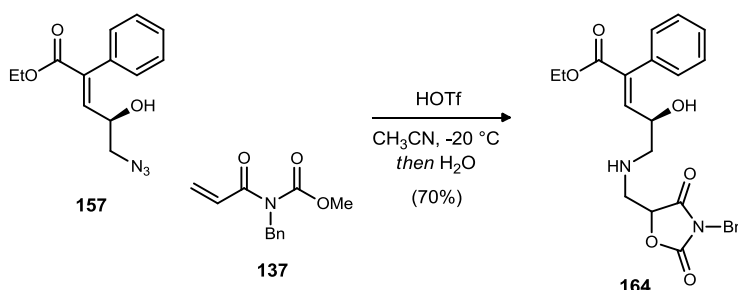
⁹¹ Yang, X.; Birman, V. B. *Org. Lett.* **2009**, *11*, 1499.

Scheme 71. Aminohydroxylation and Attempted Acyl Transfer



With the thought that the acyl group could be installed on the secondary amine at a later stage, azido alcohol **157** was converted under aminohydroxylation reaction conditions to the oxazolidinone dione alcohol (**164**) in good yields (70%). Isolation of this free-OH/NH oxazolidinone dione (**164**) proved to be tricky, and the reaction had to be filtered through neutral alumina and purified using a deactivated silica column.

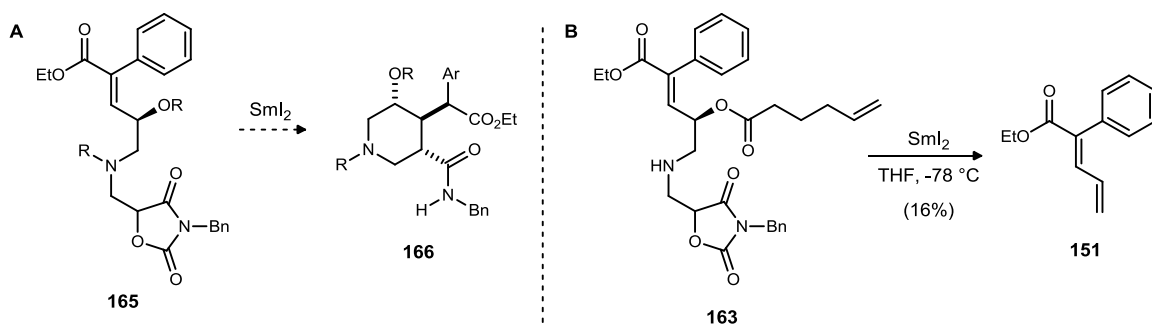
Scheme 72. Aminohydroxylation with Azido Alcohol 157



2.2.4 Cyclization to the Piperidine Core

As described in the retrosynthetic analysis, treatment of the oxazolidinone dione (**165**) with samarium(II) iodide was expected to result in reduction of the oxazolidinone dione to the amide enolate and deoxygenation of the oxazolidinone dione α -carbon, followed by cyclization and Michael addition of the amide enolate to the α,β -unsaturated ester (Scheme 70A). Unfortunately, no reaction was observed when the oxazolidinone dione alcohol (**164**) was treated with four equivalents of samarium(II) iodide. When the oxazolidinone dione ester (**163**) was treated with four equivalents of samarium(II) iodide, diene **151** was isolated in 16% yield (Scheme 70B). Addition of HMPA to the reaction with **163** resulted neither in diene formation nor in desired product formation.

Scheme 70. Expected and Observed Treatment with SmI₂

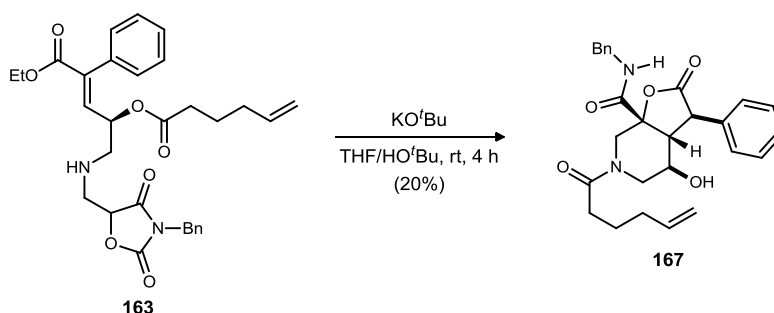


Finding no success in reducing the oxazolidinone functional group using samarium(II) iodide, we moved on to attempting to effect cyclization of the oxazolidinone dione alcohol (**164**) via deprotonation at the α -

position of the oxazolidine dione. These attempts were largely unsuccessful. Treatment with base (K_2CO_3 , LiHMDS, tBuLi) did not result in desired product formation. Treatment of the oxazolidine dione alcohol (**164**) with trimethylsilyl triflate in the presence of di-*tert*-butylpyridine, as well as treatment with dibutylboryl triflate in the presence of Hünig's base, also did not result in cyclization. Attempts to trap the amide enolate with a trimethylsilyl group, followed by treatment with Lewis acids ($BF_3 \cdot OEt_2$, $SnCl_4$, $TiCl_4$) to activate the α,β -unsaturated ester for Michael addition only returned the starting oxazolidine dione alcohol (**164**). A deuterium labeling experiment in which we deprotonated the α -position of the oxazolidine dione alcohol (**164**) with lithium diisopropylamide and quenched with deuterium oxide resulted in 50% incorporation of deuterium at the α -position, confirming that we were, in fact, able to form the amide enolate.

In a return to attempts to induce acyl migration from the ester to the amide, we found that treatment of oxazolidine dione ester **163** with potassium *tert*-butoxide in *tert*-butanol resulted in formation of a cyclization product (**167**). While the reaction was temperamental, the best yields (7-20%) were observed when the oxazolidine dione ester (**163**) was treated with *tert*-butoxide in a 1:1 mixture of tetrahydrofuran and *tert*-butanol. No other cyclization products were isolated from the reaction. A detailed structural elucidation is included below.

Scheme 73. Cyclization to Piperidine Core



2.2.5 Structural Elucidation of the Piperidine Core

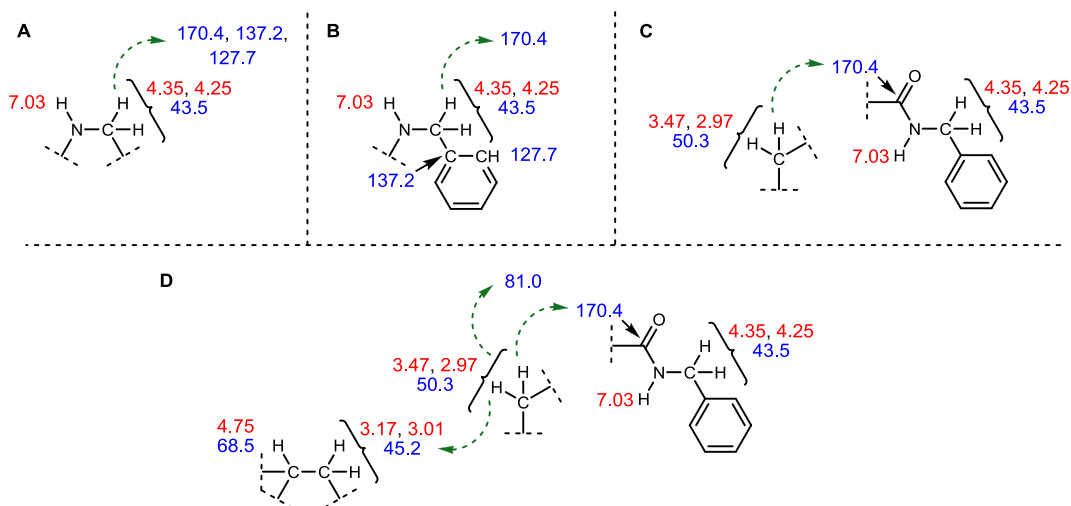
A single compound was isolated from the treatment of oxazolidine dione ester **163** with potassium *tert*-butoxide. An initial analysis of the compound's proton NMR spectrum revealed that the isolated compound might be of interest. The ethyl ester's methylene group, which typically appeared at approximately δ 4.20, was conspicuously absent, possibly indicating some type of hydrolysis or acyl substitution of the ethyl ester. In addition, the benzyl methylene protons were split into two doublets of doublets, suggesting that the oxazolidine dione ring had been opened. Finally, the vinyl proton, which appeared as two doublets at δ 6.75 in the oxazolidine dione ester (**163**) due to the presence of two diastereomers, was absent; a proton that appeared at δ 6.84 as a doublet of doublets was originally assigned as the vinyl proton in question; however, upon addition of d_6 -DMSO to the NMR sample, that proton shifted to δ 7.03, suggesting its attachment to a heteroatom. With this data in mind, it was concluded that the oxazolidine dione ester had indeed undergone some type of cyclization upon treatment with potassium *tert*-butoxide.

Further analysis of the compound by 1H NMR, ^{13}C NMR, mass spectrometry, COSY, HSQC, and HMBC experiments led to the identification of the compound's structure, and the results of a NOESY experiment were used to determine the compound's relative configuration. The absolute configuration was assigned by the mnemonic for Sharpless dihydroxylation,⁸⁹ which was used to establish C23.

Beginning with the proton (δ 7.03) attached to a heteroatom, the cyclization product's structure was elucidated as follows: the broad doublet of doublets at δ 7.03 ($J = 5.5, 5.5$ Hz) integrated to one proton and did not correlate to any carbons in the HSQC experiment. The signal coupled to a pair of doublets of doublets at δ 4.35 ($J = 14.7, 5.8$ Hz) and 4.25 ($J = 14.7, 5.6$ Hz), each of which also had a relative integration of one; the COSY experiment indicated that these two protons coupled only to one another and to the signal at δ 7.03, and the HSQC experiment revealed a correlation between the two protons and a methylene carbon at 43.5 ppm. In the compound's precursor, the benzyl methylene appeared at 43.7 ppm. Thus, based on the chemical shifts of these protons and their carbon, as well as their splitting patterns, they were determined to be the *N*-benzyl

protons, formerly of the oxazolidinone ring system, and their coupling partner was concluded to be the corresponding NH. This isolated spin system is shown in Figure 15A.

Figure 15. HMBC Structural Elucidation



An HMBC experiment revealed that the benzyl methylene protons (δ 4.35 and 4.25) exhibited long-range coupling correlations to carbons at 170.4, 137.2, and 127.7 ppm. The carbons at 137.2 and 127.7 ppm also exhibited HMBC correlations with aromatic protons (δ 7.38-7.27 (m, 6H) and 7.15 (d, J = 6.8 Hz)), and DEPT experiments indicated that the carbon at 127.7 ppm was a methine, while the carbon at 137.2 ppm had no attached protons. This data supports assignment of the benzylic position to the previously mentioned methylene protons, as shown in Figure 15B.

Based on its chemical shift and the connectivity of **75**, it is reasonable to infer that the remaining carbon (170.4 ppm) to which the benzylic protons exhibited correlations via HMBC is that of an amide carbonyl, formerly of the oxazolidinone ring system (Figure 15C).

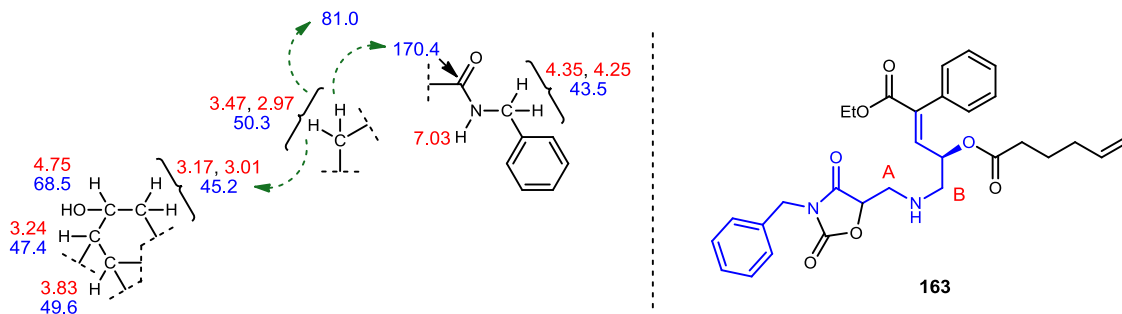
Protons at δ 3.47 (d, J = 14.3 Hz, 1H) and 2.97 (d, J = 14.4 Hz, 1H), which were confirmed to be coupled only to one another by COSY and which shared a methylene carbon at 50.3 ppm by HSQC, also exhibited correlations with the amide carbonyl carbon (170.4 ppm). The two spin systems are shown together in Figure 15C.

The isolated methylene protons (δ 3.47 and 2.97) also correlate to carbons at 81.0 and 45.2 ppm via HMBC. The carbon at 45.2 ppm is a methylene by HSQC; its protons are both doublets of doublets at δ 3.17 (J = 14.3, 3.4 Hz, 1H) and 3.01 (J = 14.3, 4.9 Hz, 1H), and they reciprocate with an HMBC correlation to the isolated methylene carbon (50.3 ppm). The COSY experiment confirms that these protons (δ 3.17, 3.01) couple to one another and to a proton at δ 4.75 (br ddd, J = 4.1, 4.1, 4.1 Hz, 1H), whose carbon appears at 68.5 ppm and is a methine by DEPT and HSQC. The expanded spin systems are displayed in Figure 15D.

Given the broadness of the proton signal (δ 4.75), as well as its downfield positioning and that of its carbon (68.5 ppm) signal, it is likely that this carbon bears the hydroxyl group, which was formerly esterified. The proton is also coupled to the doublet of doublets at δ 3.24 (J = 8.9, 4.6 Hz), whose methine carbon appears at 47.4 ppm. In turn, the δ 3.24 proton is coupled to a doublet at δ 3.83 (J = 8.9 Hz), whose methine carbon appears at 49.6 ppm. The new spin system is shown in conjunction with the previous systems in Figure 17. The unknown compound's precursor, **163**, is shown for comparison, with the portions currently being discussed highlighted in blue.

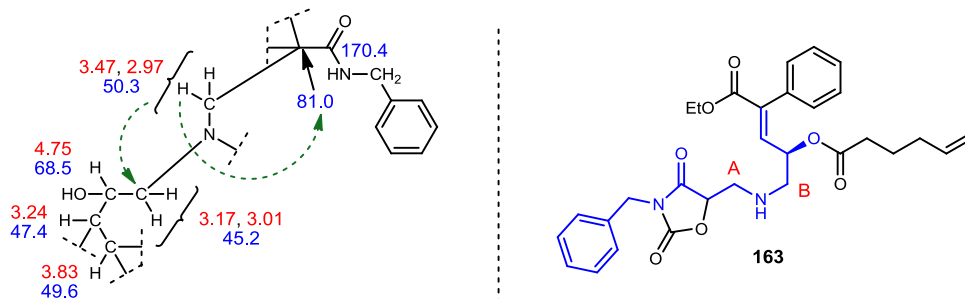
Consider the connectivity of the unknown's precursor (**163**). Only two methylenes are present in the main chain of the structure, one on each side of the free disubstituted amine. One of these methylenes, labeled 'A,' is β to the oxazolidinone ring system and exhibits the appropriate coupling. The other methylene, labeled 'B,' is adjacent to the ester-bearing asymmetric methine. Taken together, these data suggest that the carbon at 45.2 ppm corresponds to what was formerly methylene B, since it is adjacent to the now hydroxyl-bearing methine, and that the isolated methylene (50.3 ppm) is nearer the former oxazolidinone ring system,

Figure 17. Expanded Spin Systems and Precursor



which is supported by the HMBC correlation to the amide carbonyl (170.4 ppm). The α -carbon of the oxazolidinone dione ring system must then be accounted for, and, indeed, the lone methylene protons (δ 3.47, 2.97) give an HMBC correlation to a quaternary carbon at 81.0 ppm. The proposed connectivity is shown in Figure 16 and includes the disubstituted amine and the quaternary carbon, formerly α of the oxazolidinone dione ring.

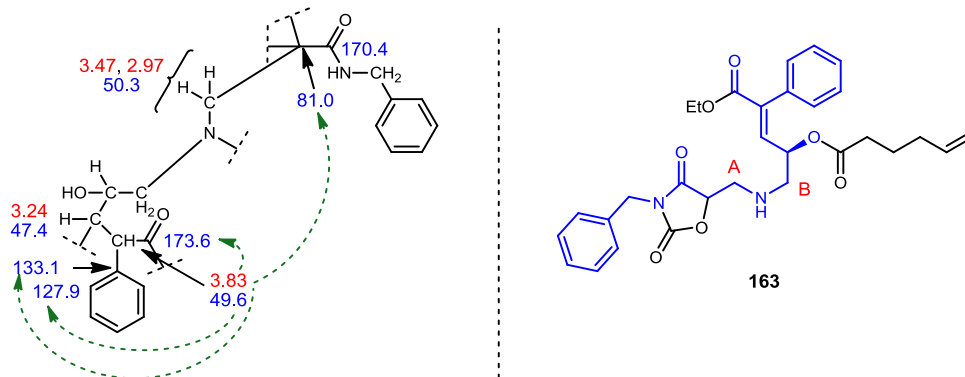
Figure 16. New Connectivity and Precursor



That the methine (47.4 ppm) adjacent to the hydroxyl-bearing methine and its neighboring methine (49.6 ppm) are no longer in the sp^2 region of the carbon spectrum suggests that the olefin underwent Michael addition as desired. Furthermore, since the α -carbon of the oxazolidinone dione ring system is no longer a methine and now appears as a quaternary carbon (81.0 ppm), it is possible that the oxazolidinone dione α -carbon acted as the nucleophile for Michael addition into the α,β -unsaturated ester.

The proton at δ 3.83, which connects to the 49.6 ppm methine, gives HMBC correlations to carbons at 173.6, 133.1, 127.9, and 81.0 ppm. The carbons at 133.1 and 127.9 ppm have zero and one protons, respectively, by HSQC and DEPT, and their shifts and HMBC correlations are further support of the hypothesis of a Michael addition into the α,β -unsaturated ester, since they must be part of the phenyl ring attached to the α -

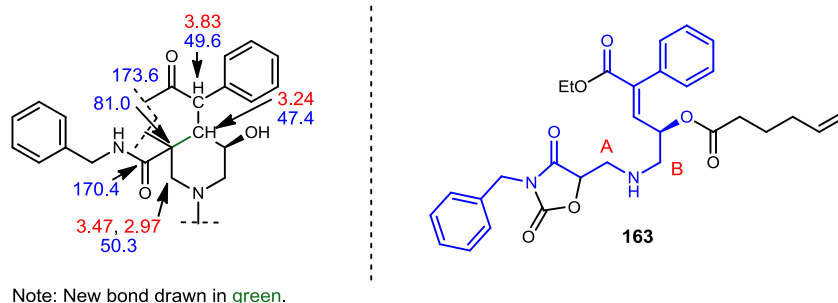
Figure 18. HMBC Correlations to Suggest Cyclization and Precursor



position of the former α,β -unsaturated ester. The carbon at 173.6 ppm is likely the carbonyl of the former α,β -unsaturated ester.

Since the carbon at 49.6 ppm has no more room for substituents (see Figure 18), the HMBC correlation to the 81.0 ppm carbon must arise from a three-bond connection through the carbon at 47.4 ppm, formerly the β -carbon of the α,β -unsaturated ester. The alternative would be a three-bond connection through the former ester carbonyl, but 173.6 ppm is too far upfield in the carbon spectrum to correspond to a ketone carbon. Thus, the desired Michael addition must have occurred. The resulting piperidine skeleton is shown in Figure 19.

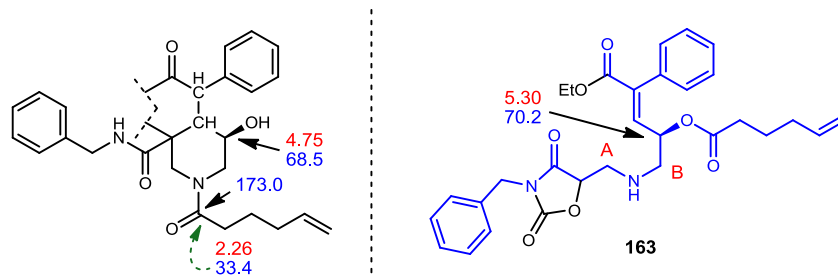
Figure 19. Piperidine Skeleton and Precursor



Proton NMR, COSY, and HSQC experiments indicated that the side chain spin system was still intact, and relative integration supports the hypothesis that the side chain was indeed part of the unknown molecule. Its proton and carbon shifts are as follows: δ 5.73 (dddd, $J = 17.0, 10.2, 6.7, 6.7$ Hz, 1H; ^{13}C ppm 137.4, CH), 4.99 (dddd, $J = 17.1, 1.6, 1.6, 1.6$ Hz, 1H; ^{13}C ppm 115.5, CH_2), 4.95 (br d, $J = 10.2$ Hz, 1H; ^{13}C ppm 115.5, CH_2), 2.26 (ddd, $J = 7.6, 7.6, 1.6$ Hz, 2H; ^{13}C ppm 33.4, CH_2), 2.03 (br ddd, $J = 7.2, 7.2, 7.2$ Hz, 2H; ^{13}C ppm 32.9, CH_2), 1.68 (dddd, $J = 7.5, 7.5, 7.5, 7.5$ Hz, 2H; ^{13}C 23.7, CH_2). The methylenes at δ 2.26 and 1.68 both gave HMBC correlations to a carbon at 173.0 ppm.

While no supportive HMBC correlations were present, the absence of a signal does not preclude the attachment of the side chain to the molecule, and the side chain was proposed to have undergone the desired ester to amide acyl-transfer. The carbonyl shift (173.0 ppm) is consistent with both an ester and a tertiary aliphatic amide,⁹² so no conclusions can be drawn from that datum. Support for the proposed acyl transfer, however, includes the absence of coupling and no broadening of the four methylene protons (δ 3.47, 2.97 and δ 3.17, 3.01) adjacent to the nitrogen, as well as the upfield positioning of the hydroxyl methine (δ 4.75, 68.5 ppm) relative to its corresponding position on the oxazolidinone ester/precursor molecule (**163**) (δ 5.30, 70.2 ppm). The skeleton can then be expanded, as shown in Figure 20.

Figure 20. Expanded Skeleton and Precursor

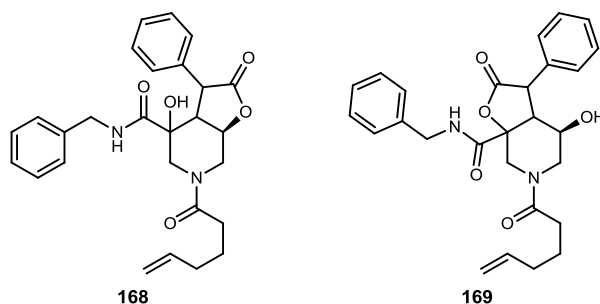


As previously mentioned, the ethyl group that would correspond to an ethyl ester was absent from the unknown's proton NMR spectrum. We hypothesized that the ester underwent hydrolysis to give the corresponding carboxylic acid. However, HRMS was not consistent with the carboxylic acid mass ($\text{C}_{27}\text{H}_{32}\text{N}_2\text{O}_6$,

⁹² Pretsch, E.; Buhlmann, P.; Affolter, C. *Structure Determination of Organic Compounds*; Springer: Berlin, 2000; pp 138.

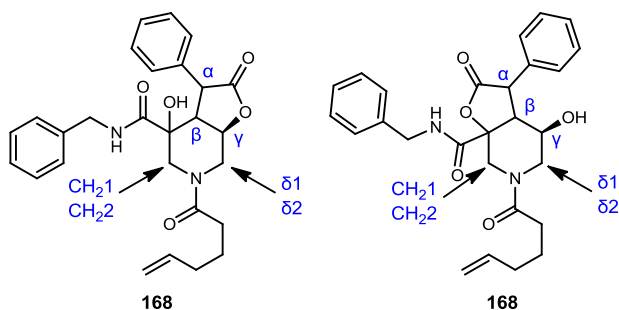
MW = 480.55; observed peak: 463.11), but instead $[M+H]^+$ corresponding to a lactone structure, where one of the hydroxyl groups condensed with the ethyl ester. The lactone proposed is consistent with HRMS (ESI): Exact mass calcd for $C_{27}H_{31}N_2O_5$ $[M+H]^+$ 483.2233, found 463.2233. These results lead to the possibility of two structures, shown in Figure 21.

Figure 21. Possible Structures



A NOESY experiment on the unknown compound provided access to further data that aided in the compound's structural elucidation. In order to better discuss the correlations, the protons have been labeled (Figure 22) starting from the α -proton of the lactone, where α is the proton at δ 3.83, β is at δ 3.24, γ is at δ 4.75, and $\delta 1$ and $\delta 2$ are at δ 3.17 and 3.01, respectively. The methylene protons between the piperidine nitrogen and the quaternary carbon, δ 3.47 and 2.97, are labeled as $CH_2 1$ and $CH_2 2$, respectively.

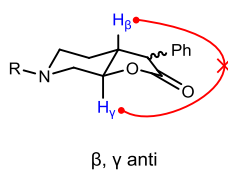
Figure 22. Labeling for NOESY Discussion



Key NOESY correlations appear between α and γ , α and β , β and γ , β and NH, α and $\delta 1$, and α and $CH_2 2$. Because NOESY correlations appear when two protons are near each other in space and not through coupling, it is important to consider the conformation of the molecule during the experiment. Additionally, there are three new stereocenters in each of the proposed structures, leading to the possibility of eight diastereomers for each, so sixteen possible compounds are considered for the following connectivity and diastereomeric structural elucidations.

First, consider the less-hindered lactone, where the former oxazolidinone oxygen is the free hydroxyl group, as in structure **168**. Because the stereochemistry at the γ -carbon (C23) was established using the Sharpless asymmetric dihydroxylation, the γ -proton is known to be down. If the β -proton is up, or *anti* to the γ -proton, there is a *trans*-fused [4.3.0] ring system (Figure 23). In this case, it would not be possible for a NOESY correlation to be observed between the β and γ -protons because the fused-ring system is rigid. Furthermore,

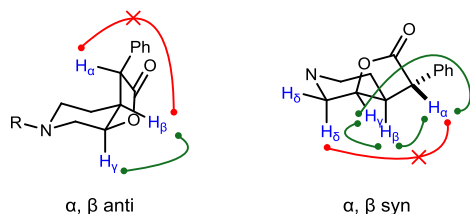
Figure 23. NOESY Correlations (168): β , γ anti



with α up, a NOESY correlation with γ would not be possible, while with α down, correlations with $\delta 1$ and $\text{CH}_2 2$ would be unlikely. Thus, β cannot be *anti* to γ (Figure 23).

For this lactone, then, β must be *syn* to γ , or down. Now consider the α -proton. If α is up, or *anti* to β , a NOESY correlation between α and γ would not be possible (see Figure 24). However, if α is down, or *syn* to β , then $\delta 1$ and $\text{CH}_2 2$ would be too far from α , and NOESY correlations would not be possible (see Figure 24). Therefore, α can be neither *anti* nor *syn* to β , so β cannot be *syn* to γ . Having already determined that β cannot be *anti* to γ , it stands to reason that the less-hindered lactone must be ruled out as a possibility.

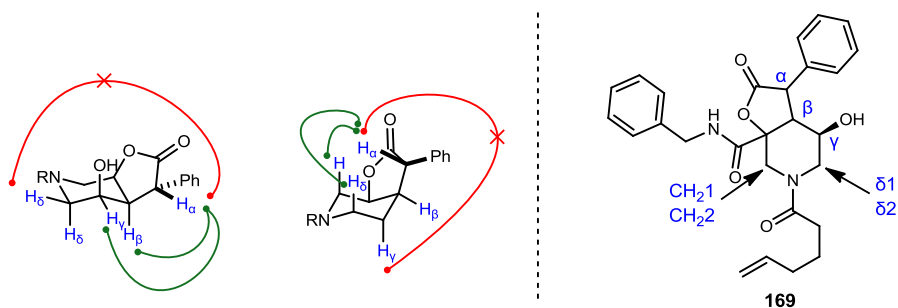
Figure 24. NOESY Correlations (168): β , γ syn



Consider the more hindered lactone, where the lactone is cyclized onto the former oxazolidine dione oxygen (**169**). The NOESY correlation between β and NH requires the benzyl amide to be *syn* to β , and so the former oxazolidine dione oxygen, now part of the lactone, must be *anti* to β . For clarity, the benzyl amide is not shown in the conformation structures.

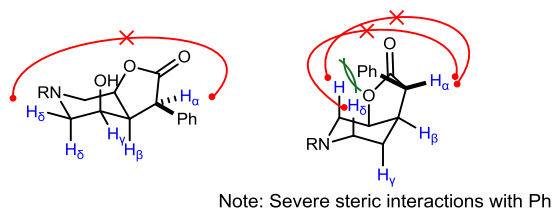
Beginning with β down, or *syn* to γ , consider the relative configuration of α . If α is up, or *anti* to β and γ , it is not possible for NOESY correlations to exist between α and γ and α and $\delta 1$ and $\text{CH}_2 2$ at the same time, or in the same conformation (Figure 25). Thus, if β is *syn* to γ , α must also be *syn* to β and γ , or down.

Figure 25. NOESY Correlations (169): β , γ syn, α anti



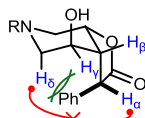
However, if γ , β , and α are all down or *syn*, it is not possible for α to exhibit NOESY correlations with either $\delta 1$ or $\text{CH}_2 2$ in any conformation (Figure 26). Then, when β is down relative to γ , α can be neither up nor down. Thus, it can be ruled out that β is down, and β must be up relative to γ , or *anti*.

Figure 26. NOESY Correlations (169): α , β , γ syn



Thus, γ is set as down, and β must be up relative to γ . Now, consider α as being up, or *anti* to γ . In this case, it is not possible for α to exhibit NOESY correlations to either $\delta 1$ or $\text{CH}_2 2$ (Figure 27). Thus, α must be down, or *syn*, relative to γ .

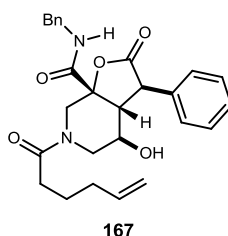
Figure 27. NOESY Correlations (169): α , γ anti



Note: Severe steric interactions with Ph

Given that the stereochemistry at the γ -carbon was established using the Sharpless asymmetric dihydroxylation reaction, the absolute stereochemistry of the cyclization product is known. Above, it was determined that the β -proton must be *anti* relative to γ , and that the α -proton must be *syn* relative to γ and *anti* relative to β . Also, due to observed NOESY correlations between β and the benzyl amide NH, the benzyl amide must be *syn* relative to β . Thus, the compound was found to be (3*R*,3*aR*, 4*R*, 7*aR*)-*N*-benzyl-6-hex-5-enoyl-4-hydroxy-2-oxo-3-phenyloctahydrofuro[2,3-*c*]pyridine-7*a*-carboxamide (**167**), where configuration at the α -position is *R*, configuration at the β -position is *R*, configuration at the γ -position is *R*, and configuration at the

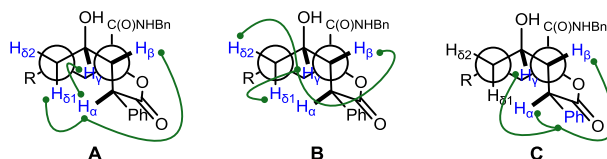
Figure 28. Final Structure



quaternary center is *R*.

All observed NOESY correlations can be confirmed by a single conformation of the structure. By looking at a Newman projection of the piperidine ring, where the δ -carbon and the β -carbon are in the front, key NOESY correlations are consistent between γ and α , α and β , and α and $\delta 1$, as in A of Figure 29. Also, correlations between γ and $\delta 1$ and $\delta 2$, as well as between γ and β , are confirmed, as shown in Figure 29B.

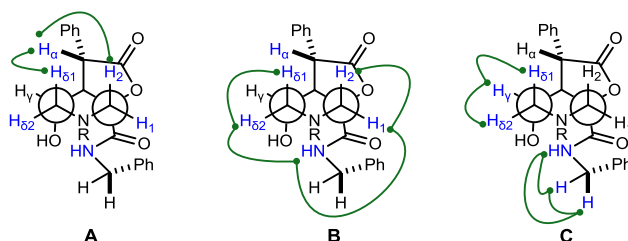
Figure 29. NOESY Confirmed: Newman Projections (β , δ in Front)



Projection C shows the observed NOESY correlations between γ and Ar-H, β and Ar-H, and α and Ar-H.

By looking at the Newman projection where the δ -carbon and the methylene carbon between the nitrogen and quaternary center are the front carbons, the remaining NOESY correlations can be confirmed. The

Figure 30. NOESY Confirmed: Newman Projections (δ , CH₂ in Front)



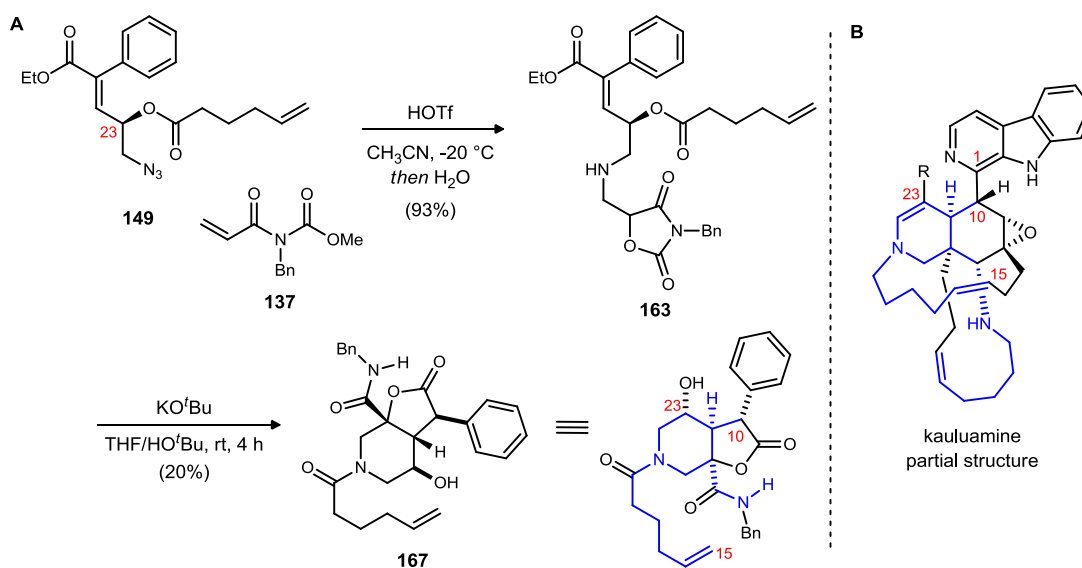
structure on the left (Figure 30A) shows the NOESY correlations between α and $\delta 1$ and between α and $\text{CH}_2 2$. The structure in the center (B) shows the correlations between $\delta 1$ and $\delta 2$, between $\text{CH}_2 1$ and $\text{CH}_2 2$, between $\delta 2$ and NH, and between NH and $\text{CH}_2 1$. Finally, C (Figure 30) illustrates NOESY correlations between $\delta 1$ and γ , between $\delta 2$ and γ , and between the NH and both benzyl protons, as well as between the two benzyl protons. Thus, all observed NOESY correlations are confirmed and illustrated.

2.2.6 Model Study Conclusions

Following preparation of azido ester **149** in seven steps, we utilized a Brønsted-acid catalyzed azide-olefin addition reaction to combine **149** with acryloyl imide **137**. The resulting oxazolidine dione ester (**163**) was subjected to potassium *tert*-butoxide to effect cyclization to a highly functionalized piperidine model core of kauluamine.

We originally hypothesized that the hydroxyl group at the γ -position could be used to control the stereochemistry of the piperidine. While we were not able to deoxygenate the oxazolidine dione, we were able to confirm the expected stereocontrol and found that by setting a single stereocenter at the γ -position (C23), cyclization to form the desired piperidine could be achieved. To our surprise and delight, in the obtained product of the cyclization reaction, the stereocenter at the α -position was set in addition to the two intended stereocenters at the β -position and at the C25 position (**167**, Scheme 74). The stereocenter at the α -position resulted from protonation of the intermediate enolate that resulted from Michael addition to the α, β -unsaturated ester. The compound was isolated as a single diastereomer. This unique cyclization reaction also resulted in acyl transfer to give the desired *N*-acyl piperidine, and the conditions also effectively opened the oxazolidine dione moiety and resulted in transesterification of the ethyl ester to form a [4.3.0] ring system containing fused piperidine and lactone rings.

Scheme 74. Preparation of Model Piperidine Core of Kauluamine



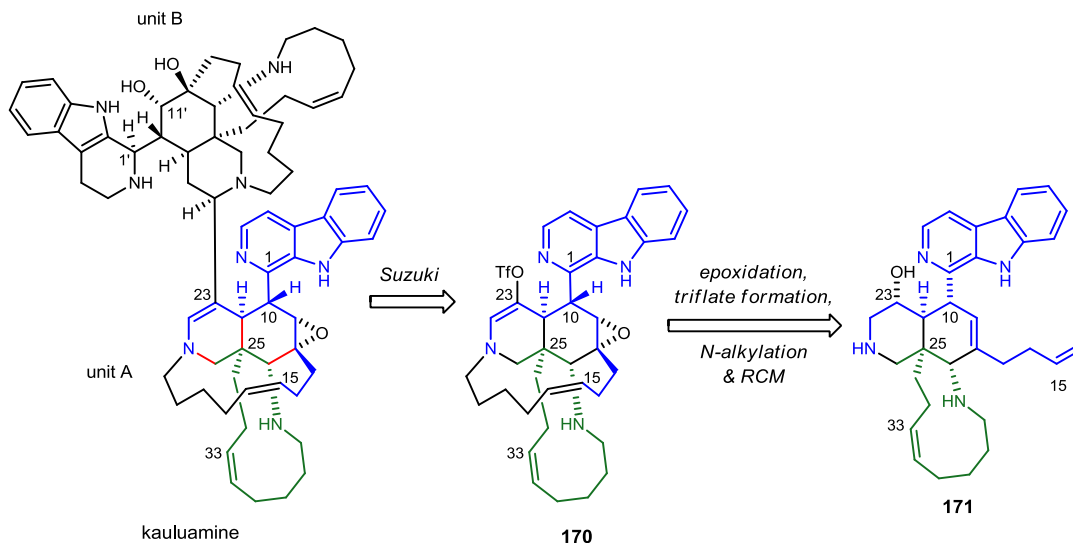
2.3 Studies Towards the Synthesis of Kauluamine

2.3.1 Kauluamine Retrosynthetic Analysis

Key Disconnections

The principal goal of the model study was to establish the viability of a series of steps to convergently and stereoselectively construct the substituted piperidine core of kauluamine. We envision four chief disconnections when analyzing kauluamine (Figure 31, key bonds shown in red). First, the C23-C22' bond that connects the two halves of the dimer would be formed via a *B*-alkyl Suzuki-Miyaura cross-coupling between the triflate of unit A and the alkyl borane of unit B. Each unit would be formed along similar lines, with only a

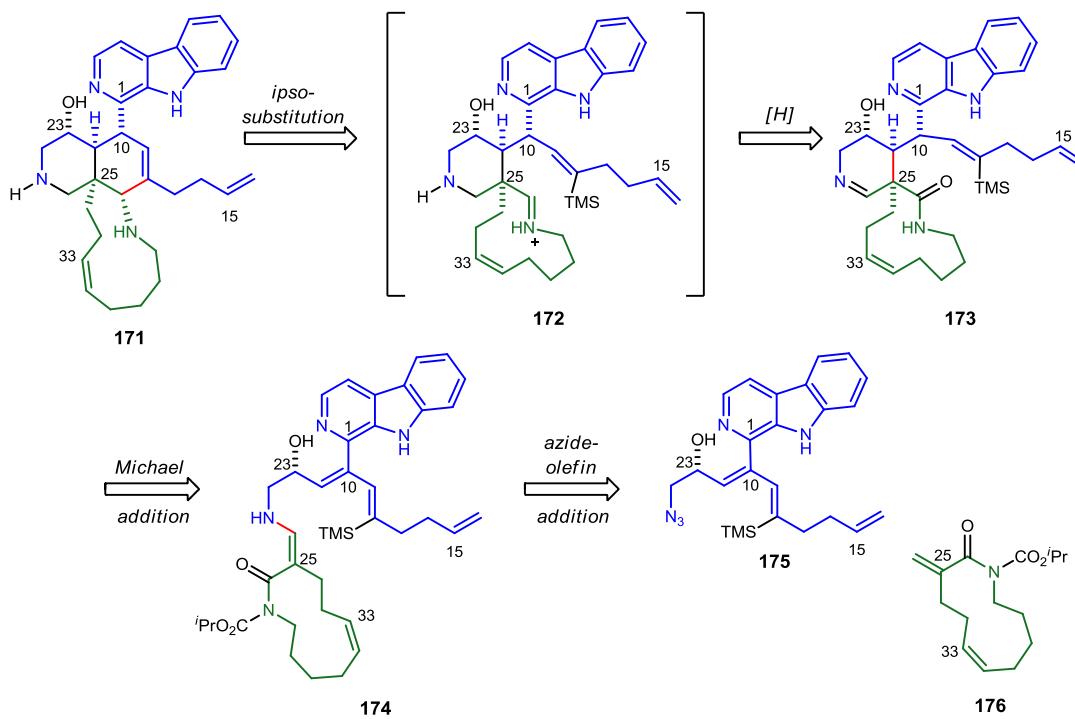
Figure 31. Kauluamine Retrosynthesis



few modifications to diverge to unit A or unit B. Triflate **170** (unit A) would be formed from **171** via oxidation of the alcohol (C23) to a ketone and conversion to the triflate. Epoxidation of the C11-C12 bond, followed by an *N*-alkylation to install C16-C20⁹³ and a ring closing metathesis⁹⁴ would form the 13-membered ring.

For the construction of unit A, we propose to form the key N21-C36 bond via a Brønsted acid-catalyzed azide-olefin addition (Figure 32). Based on the results of our model study in which we encountered difficulty in effecting deoxygenation at C25, we plan to avoid the necessity for deoxygenation by constructing our acryloyl imide (**175**) such that triazolone decomposition will lead to enamine formation rather than to oxazolidine dione

Figure 32. Kauluamine Retrosynthesis Cont'd



⁹³ While two disubstituted amines are present in the molecule, N27 is expected to be more sterically hindered than N21 due to its positioning in the 11-membered azacycle and *syn* to the β -carboline unit.

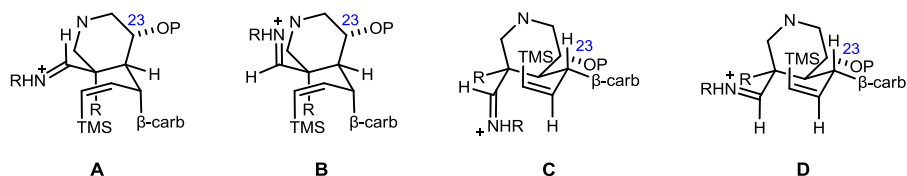
⁹⁴ As mentioned in section 2.1.3, Martin used a *Z*-selective ring closing metathesis to form this 13-membered D ring of manzamine A.

formation. This enamine (**174**) will then be used to forge the C24-C25 bond, acting as a nucleophile to add in a Michael fashion to the α,β -unsaturation at the C10-C24 double bond. We expect the β -carboline to stabilize the intermediate during the Michael addition. The final key bond, C12-C26, would be formed via an *ipso*-substitution between the necessary vinyl silane (C11-12) and the iminium at C26-N27 (**172**) that we would prepare from reduction of the C26-N27 amide (**173**).⁹⁵ All carbons for unit A bar C16-C20, which would be introduced post-cyclization to the piperidine, would thus be present in the molecule following the azide-olefin addition.

Stereochemical Models for *Ips*o-Substitution

In 1984, Overman reported the importance of the *Z*-geometry of vinyl silanes for σ - π stabilization in the transition state of exocyclic vinyl silane additions to iminium ions.⁹⁶ In our models of the proposed cyclization, there are four possible chair transition states. Given that the C12-Si bond needs to line up parallel to the developing cation *p*-orbital, the only point of difference is the conformation that the iminium takes. The iminium can take on pseudo-equatorial positions in which it is either down or up, or it can take on pseudo-axial

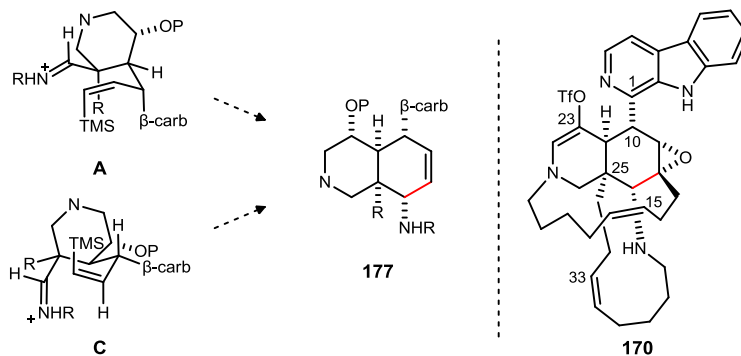
Figure 33. *Ips*o-Substitution Transition States



positions in which it is either down or up, as shown in Figure 33. For clarity, the 11-membered ring is shown simply as "R" groups attached to the iminium and to the bridgehead carbon. The C13-15 alkyl chain is also not shown; it is connected to the same carbon as the silyl group. There is quite a bit of steric strain in each possible transition state. Of the transition states in which the silyl group and β -carbonyl experience 1,3-diaxial interactions (A and B), we would expect the conformation in which the iminium is down and equatorial (A) to be favored due to tethering of the 11-membered ring. With the use of a large protecting group on the C23 hydroxyl, we may be able to force this conformation.

Alternatively, between the conformations in which the β -carbonyl ring and the alkyl chain (C13-15) are pseudo-equatorial (C and D), we expect the 11-membered ring to force the conformation in which the iminium is pseudo-axial (C) to be favored. Either conformation A or C will lead to the desired stereochemistry, as shown in Scheme 75.

Scheme 75. *Ips*o-Substitution Stereochemical Model

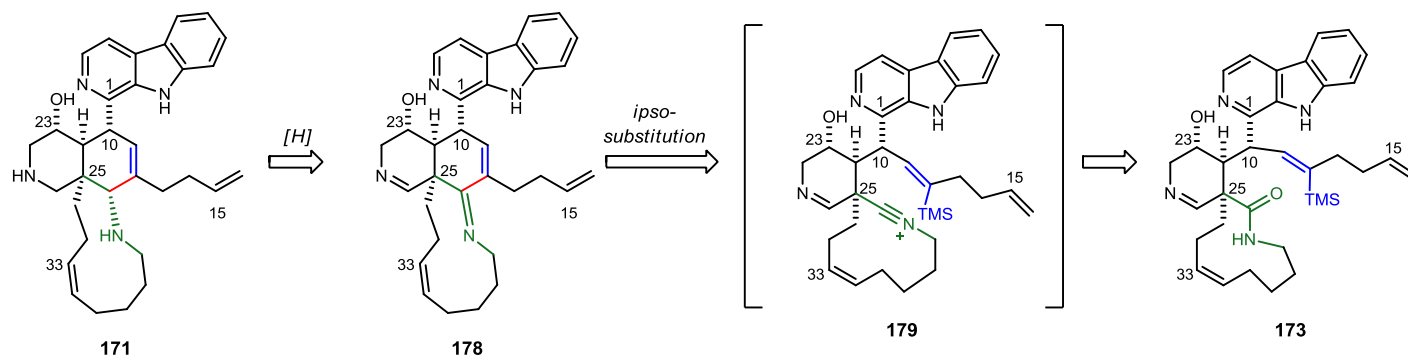


⁹⁵ For a mild reduction of amides to imines, see: Pelletier, G.; Bechara, W. S.; Charette, A. B. *J. Am. Chem. Soc.* **2010**, *132*, 12817. For the reduction of *N*-acyl iminium ions to amines, see: Rudolph, A. C.; Machauer, R.; Martin, S. F. *Tetrahedron Lett.* **2004**, *45*, 4895.

⁹⁶ Overman, L. E.; Burk, R. M. *Tetrahedron Lett.* **1984**, *25*, 5739.

In the event that we cannot achieve either of these desired chair transition states for the *ipso*-substitution, we plan to convert the amide to its corresponding nitrilium ion⁹⁷ (see Scheme 76) and perform the *ipso*-substitution with that moiety. Since the nitrilium ion would be sp hybridized and the resulting imine sp^2 hybridized, the transition state would be inconsequential to the resulting stereochemistry, since there is none. The imine (**178**) would then be diastereoselectively reduced to the desired amine (**171**). We expect reduction from the β -face to be favored over reduction from the α -face.

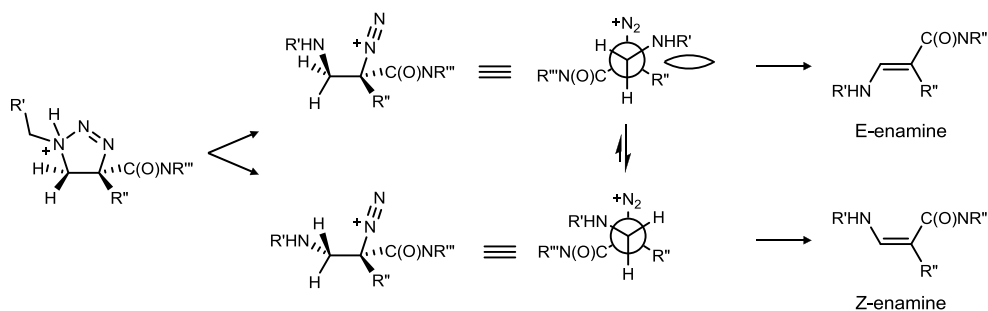
Scheme 76. Alternate *Ips*-Substitution with Nitrilium



Stereochemical Models for Piperidine Cyclization

We expect decomposition of the triazolone to result in the *Z*-enamine. Following Brønsted acid-catalyzed opening of the aziridine to form the intermediate diazonium, we expect proton elimination to liberate dinitrogen. In order for this elimination to occur, the leaving proton must be antiperiplanar to the leaving diazonium ion. There are two conformations in which this can occur, one of which leads to the *E*-enamine, and the other of which leads to the *Z*-enamine. By comparing Newman projections of the two conformations, it appears that hydrogen-bonding, as well as the absence of steric strain, will favor elimination to the *Z*-enamine. Facial selectivity is not an issue in this case; if the azide adds from the bottom face of the acryloyl imide, the same transition states would apply.

Scheme 77. Predicted Elimination to *Z*-Enamine

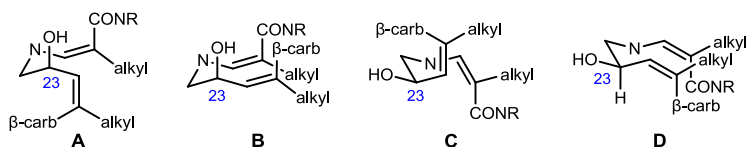


Having established that the enamine formed would be the *Z*-enamine, we next had to determine the stereochemistry required for the C23 hydroxyl group. Based on the following analysis of the possible chair transition states (Figure 34), we determined that an *R*-configuration at C23 will result in the desired enantiomer. We plan to set the α,β -unsaturation as the *Z*-double bond as well. For the cyclization, there are four possible chair transition states (Figure 34). In conformations A and B, the C23 hydroxyl group is pseudo-equatorial. Conformation A suffers from $A^{1,3}$ bisecting interactions between the β -carboline ring and the methylene, while conformation B results in $A^{1,3}$ eclipsing interactions between the hydroxyl group and the β -carboline. For conformations C and D, the hydroxyl group is pseudo-equatorial. In addition to the strain created by the pseudo-

⁹⁷ Gawley, R. E.; Chemburkar, S. *Tetrahedron Lett.* **1986**, 27, 2071.

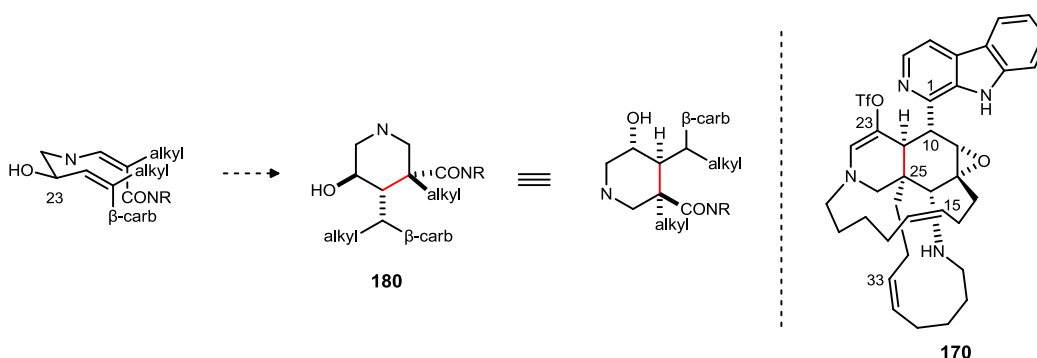
axial positioning of the α,β -unsaturated reactive center, conformation C also would experience $A^{1,3}$ bisecting strain in which the β -carboline group has unfavorable interactions both with the hydroxyl group and the methylene group. Finally, while conformation D would experience $A^{1,3}$ strain from interactions between the hydrogen and the β -carboline, this conformation is expected to be the least energetic of those possible. The strain created by the steric bulk of the alkyl groups should not be discounted, but it is expected in all conformations. A Lewis acid to bind to the amide and the pyridine nitrogen of the β -carboline could be used to encourage the formation of transition state D.

Figure 34. Chair Transition States for Cyclization



If transition state D (Figure 34) is indeed the best of those available, it would lead to the formation of piperidine **180**, which corresponds with the desired stereochemistry (Scheme 78). The hydroxyl group should be α relative to the β -carboline, or in an *R*-configuration.

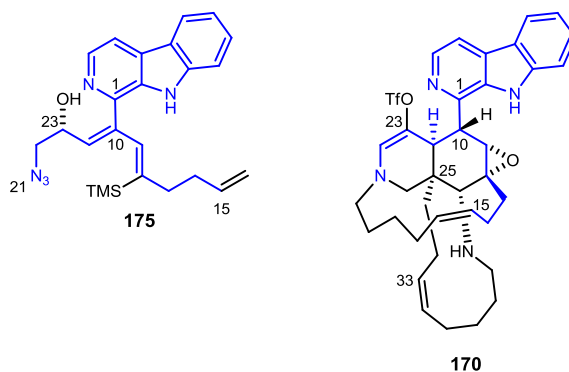
Scheme 78. Stereochemical Model for Cyclization



Azide and Acryloyl Imide Design

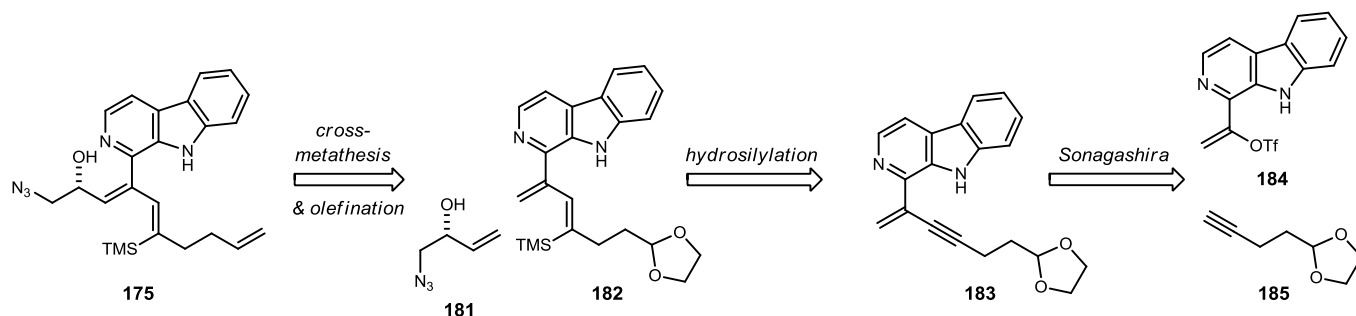
As required by our stereochemical models for both the piperidine cyclization and the *ipso*-substitution, our azide should have the *Z*-configuration at C10-C24, the stereochemistry at C23 should be *R*, and the vinyl silane should have a *Z*-geometry. For comparison, the azide (**175**) is shown in Figure 35 with the numbering that corresponds to kauluamine's numbering system. The azide portion will contain just over half (58%) of the carbon/nitrogen count for unit A of kauluamine (**170**) and will be comprised of C1-15, C22-24, and N2, N9, and N21.

Figure 35. Azide 175 and Kauluamine Unit A Triflate 170



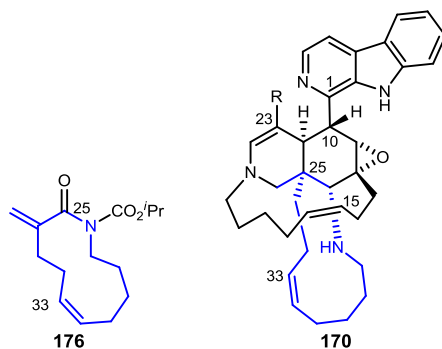
The Z-vinyl silane will be installed via hydrosilylation⁹⁸ of the corresponding alkyne (**183**, Scheme 79), which will in turn be prepared from a Sonagashira coupling of terminal alkyne **185**⁹⁹ and vinyl triflate **184**. So as to avoid the undesired cross-metathesis when bringing in the azido alcohol subunit (**181**),¹⁰⁰ the terminal olefin that will be used in a ring-closing metathesis to form the 13-membered ring late in the synthesis will be masked as the acetal; it will be converted to the olefin using a Wittig or Tebbe olefination prior to the Brønsted acid-catalyzed azide-olefin addition.

Scheme 79. Azide **87** Retrosynthesis



The acryloyl imide (**176**, Figure 36) necessary for the azide-olefin addition will have the 11-membered ring in tact prior to that addition. The imide will contain 30% of the carbon/nitrogen count for unit A of

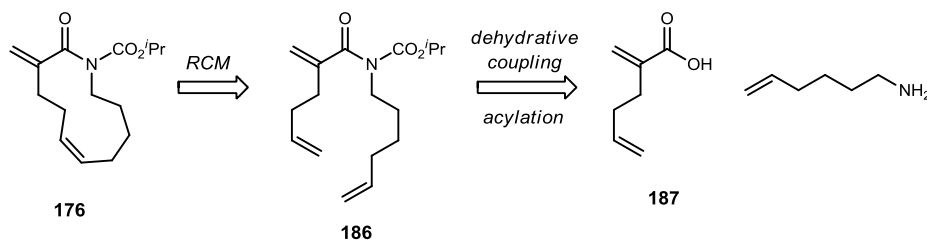
Figure 36. Acryloyl Imide **176** and Kauluamine Unit A Triflate **170**



kauluamine (**170**) and will be comprised of C25-36 and N27.

The acryloyl imide (**176**) could be prepared via a ring-closing metathesis of the corresponding isopropyl carbamate (**186**, Scheme 80). The isopropyl carbamate is required to achieve Brønsted acid activation of the

Scheme 80. Route to Acryloyl Imide **176**



⁹⁸ Trost, B. M.; Ball, Z. T. *J. Am. Chem. Soc.* **2001**, *123*, 12726.

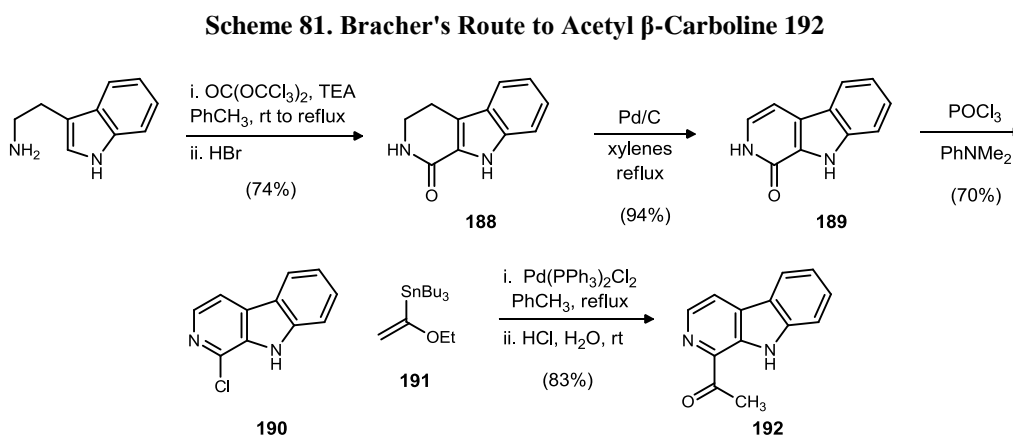
⁹⁹ Ahmar, M.; Duyck, C.; Fleming, I. *J. Chem. Soc., Perkin Trans. 1* **1998**, 2721.

¹⁰⁰ Azido alcohol **93** will be prepared via an azide displacement of the corresponding tosylate, which is commercially available.

olefin for the cycloaddition.^{77,79} Due to steric hindrance of the α -position, as well as the tethering of the 11-membered lactam, the aminohydroxylation product would not be expected. Imide **186** would be prepared via acylation of the amide formed from the simple dehydrative coupling of acrylic acid **187**¹⁰¹ and 5-hexenamine,¹⁰² as outlined in Scheme 80.

2.3.2 β -Carboline Construction and Triflate-Formation Challenges

Acetyl β -carboline **192** was prepared via a modified route developed by Bracher (Scheme 81).¹⁰³ The original route called for an acylation/cyclization reaction with phosgene to form lactam **188**, followed by dehydrogenation using palladium(0)/carbon to oxidize to pyridone **189**. Treatment with phosphorous oxychloride led to chloro- β -carboline **190**. Finally, a Stille coupling with (1-ethoxyethenyl)tri-*n*-butylstannane

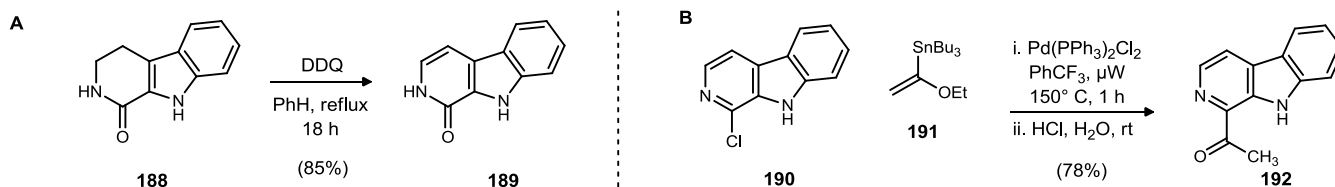


(**191**)¹⁰⁴ and acid hydrolysis would yield the desired β -carboline (**192**, Scheme 81).

However, despite using several different sources of palladium(0), as well as an oxygen atmosphere, we were unable to reproduce the dehydrogenation. Instead, we found that oxidation of the dihydropyridone (**188**) with 2,3-dichloro-5,6-dicyano-1,4-benzoquinone (DDQ) led to formation of the desired pyridone (**189**) in 85% yield (Scheme 82A).

The Stille coupling also presented a problem in that comparable yields could not be achieved, and we isolated the desired acetyl β -carboline (**192**) only in poor yields (<10%) when the chloro β -carboline (**190**), stannane **191**, and PdCl₂(PPh₃)₂ were heated to reflux in benzene overnight at atmospheric pressure, according to the procedure. However, we were able to achieve the desired coupling by instead using microwave conditions. Our optimized conditions of 150 °C for 1 hour in trifluorotoluene, followed by acid hydrolysis as

Scheme 82. Alternate Preparation of Acetyl β -Carboline **192**



described, led to isolation of the desired acetyl β -carboline (**192**) in 78% yield (Scheme 82B).

With acetyl β -carboline **192** in hand, we then attempted to convert to the vinyl triflate for use in a Sonagashira reaction with alkyne **185**. Treatment of **192** with triflic anhydride and pyridine resulted in full

¹⁰¹ Yip, K.; Zhu, N.; Yang, D. *Org. Lett.* **2009**, *11*, 1911.

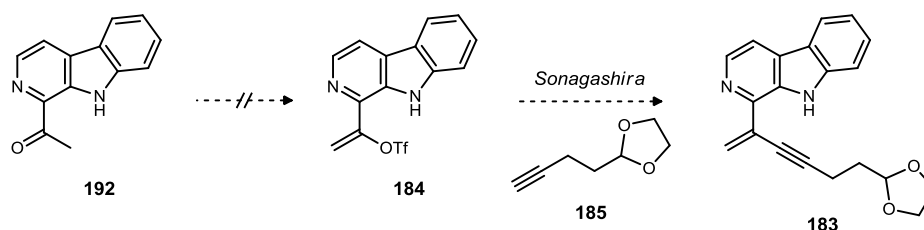
¹⁰² Smith, B. J.; Sulikowski, G. A. *Angew. Chem. Int. Ed.* **2010**, *49*, 1599.

¹⁰³ a) Bracher, F.; Hildebrand, D. *Liebigs Ann. Chem.* **1993**, *8*, 837. b) Bracher, F.; Hildebrand, D. *Liebigs Ann. Chem.* **1992**, *7*, 1315.

¹⁰⁴ Gadwood, R. C.; Rubino, M. R.; Nagarajan, S. C.; Michel, S. T. *J. Org. Chem.* **1985**, *50*, 3255.

conversion of the starting material, but an aqueous workup only yielded the original starting material (Scheme 83). Use of a stronger base (LDA) or other triflating reagents (PhNTf₂) led to the same result. A labeling experiment in which we treated the acetyl β -carboline (**192**) with lithium diisopropylamide and quenched with deuterium oxide resulted in deuterium incorporation only at the indole nitrogen. Increased equivalents of base,

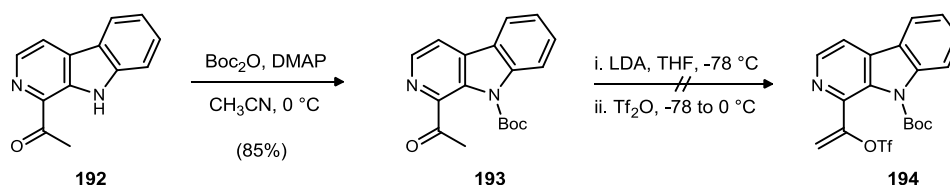
Scheme 83. Attempted Formation of Vinyl Triflate 184



however, did not lead to the desired triflate.

Hypothesizing that the difficulty might lie in forming the dianion, since the indole would be deprotonated first, we converted to the Boc-protected acetyl β -carboline (**193**), but treatment of **193** with LDA

Scheme 84. Attempted Triflate Formation with 193



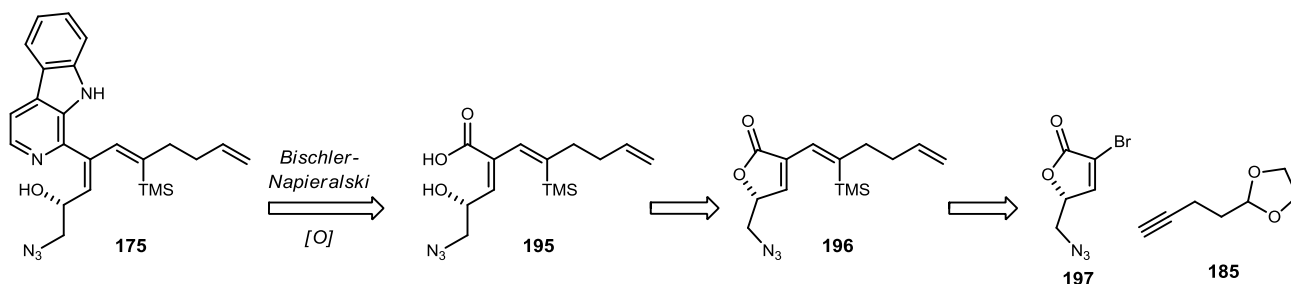
and triflic anhydride resulted only in the recovery of starting material (Scheme 84).

Having ruled out the indole nitrogen as the hindrance to triflate formation, we concluded that the pyridine nitrogen was causing this problem. Being unable to protect this nitrogen, we decided to pursue another route to azide **175** and to install the β -carboline at a later point in the synthesis.

2.3.3 Construction of the δ -Azido γ -Lactone

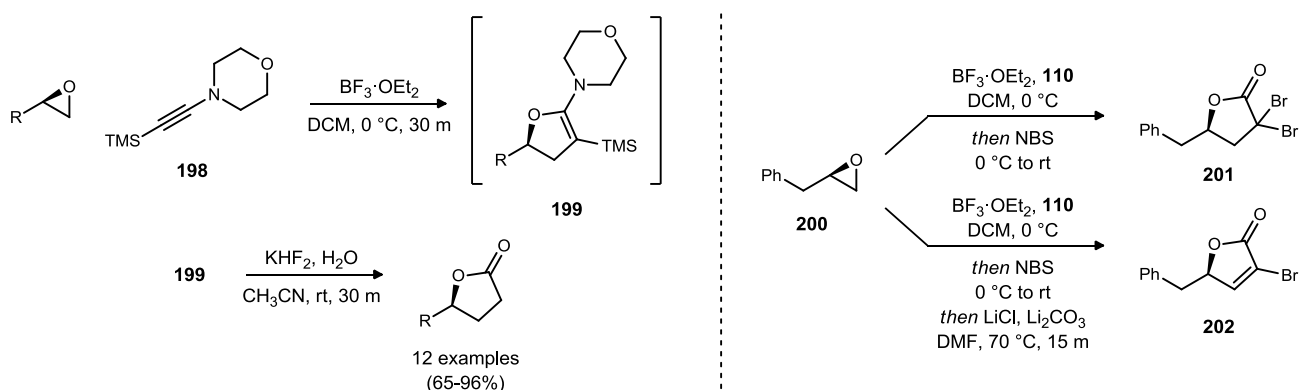
The challenges thus presented by the pyridine nitrogen of the β -carboline unit could be avoided by bringing in the β -carboline unit at a later stage via a Bischler-Napieralski reaction between tryptamine and the necessary carboxylic acid (**195**, Scheme 85), followed by oxidation to the desired β -carboline (**195**). With the placement of the hydroxyl group at the γ -position relative to the carboxylic acid, we recognized that a γ -lactone (**196**) might be used to prepare the desired azide. This γ -lactone would carry the added benefit of forcing the *Z*-geometry that is expected to aid in the control of the diastereoselection of cyclization to the piperidine core of kauluamine. We hoped to arrive at azide **196** using the same hydrosilylation sequence we had planned for the β -carboline, utilizing a Sonagashira coupling between alkyne **185** and vinyl bromide **197**.

Scheme 85. Route to Azide Via γ -Lactone



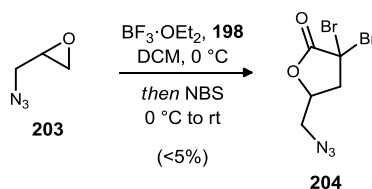
To prepare vinyl bromide **197**, we took advantage of Jacobsen's methodology to convert terminal epoxides to γ -butanolides in excellent yields (Scheme 86).¹⁰⁵ The reaction proceeds via a cyclic silyl keteneaminal (**199**), which, in terms of its reactivity with electrophiles, is equivalent to the α,α -dianion of a γ -lactone. It is noteworthy that when enantiopure epoxides were used in the reaction, the product was also enantiopure, and no epimerization was observed. The method is primarily concerned with preparing the dihydrofuranones using potassium bifluoride as the electrophile; however, they also demonstrate that, in the case of (*R*)-1-epoxy-3-phenyl-propane (**200**), the electrophile scope could be extended to the use of *N*-bromosuccinimide in order to access the corresponding α,α -dibromo- γ -butanolide (**201**). When immediately followed by treatment with base, this α,α -dibromide could be converted to a vinyl bromide (**202**) similar to **197**. Jacobsen's method was especially appealing since our attempts to α,α -dihalogenate 5-(azidomethyl)dihydrofuran-2(3H)-one,¹⁰⁶ which could be prepared in enantiopure form from the non-natural enantiomer of glutamic acid,¹⁰⁷ resulted in only poor yields.

Scheme 86. Jacobsen's Conversion of Terminal Epoxides to γ -Butanolides



While Jacobsen's substrate scope, in terms of substituted epoxides, is extensive and demonstrative that the methodology is highly functional group tolerant, epiazidohydrin (**203**),¹⁰⁸ with which we hoped to access **197**, was absent from the scope, suggesting that the reaction might not tolerate the azide functional group. Indeed, our initial attempt to apply this chemistry to epiazidohydrin resulted in less than 5% yield of the δ -azido- α,α -dibromo lactone (**204**).

Scheme 87. Epiazidohydrin as a Substrate



We were not discouraged, however, since Jacobsen's substrate scope for preparation of the dihydrofuranones included both epichlorohydrin and epibromohydrin. We hypothesized that these starting materials could be used to prepare the α,α -dibromo- δ -chloro lactone (**205**) and the α,α,δ -tribromo lactone (**206**),¹⁰⁹ respectively, which could subsequently be used to access desired azide **204** via an S_N2 displacement of

¹⁰⁵ Movassaghi, M.; Jacobsen, E. N. *J. Am. Chem. Soc.* **2002**, *124*, 2456.

¹⁰⁶ For monobromination, see: Appleton, D.; Duguid, A. B.; Lee, S.; Ha, Y.; Ha, H.; Leeper, F. J. *J. Chem. Soc., Perkin Trans. 1: Org. and Bio-Org. Chem.* **1998**, *1*, 89.

¹⁰⁷ a) Ravid, U.; Silverstein, R. M.; Smith, L. R. *Tetrahedron* **1978**, *34*, 1449. b) Olsen, R. K.; Bhat, K. L.; Wardle, R. B.; Hennen, W. J.; Kini, G. D. *J. Org. Chem.* **1985**, *50*, 896.

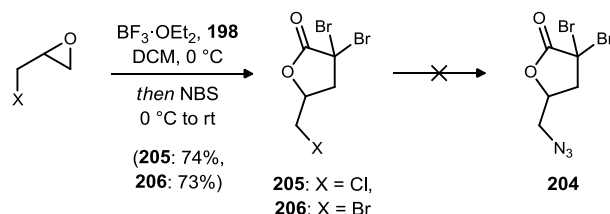
¹⁰⁸ Lutje Spelberg, J. H.; Tang, L.; Kellogg, R. M.; Janssen, D. B. *Tetrahedron: Asymmetry* **2004**, *15*, 1095.

¹⁰⁹ Leuchs, H.; Spletstosser, O. *Ber. der Deut. Chem. Gesellschaft* **1907**, *40*, 301.

either the δ -chloride or δ -bromide. Indeed, treatment of epichlorohydrin and epibromohydrin with silyl ynamine **110** under standard conditions gave the desired compounds **205** and **206** in good yields (74% and 73%, respectively). Unfortunately, treatment of **205** with sodium azide in DMF at reflux or with sodium azide and sodium iodide under Finkelstein conditions did not result in formation of **204**. Similarly, treatment of tribromide **206** with sodium azide under a variety of conditions did not lead to formation of the desired azide (**204**).

At this point, we reconsidered epiazidohydrin as a substrate for this reaction since its production was

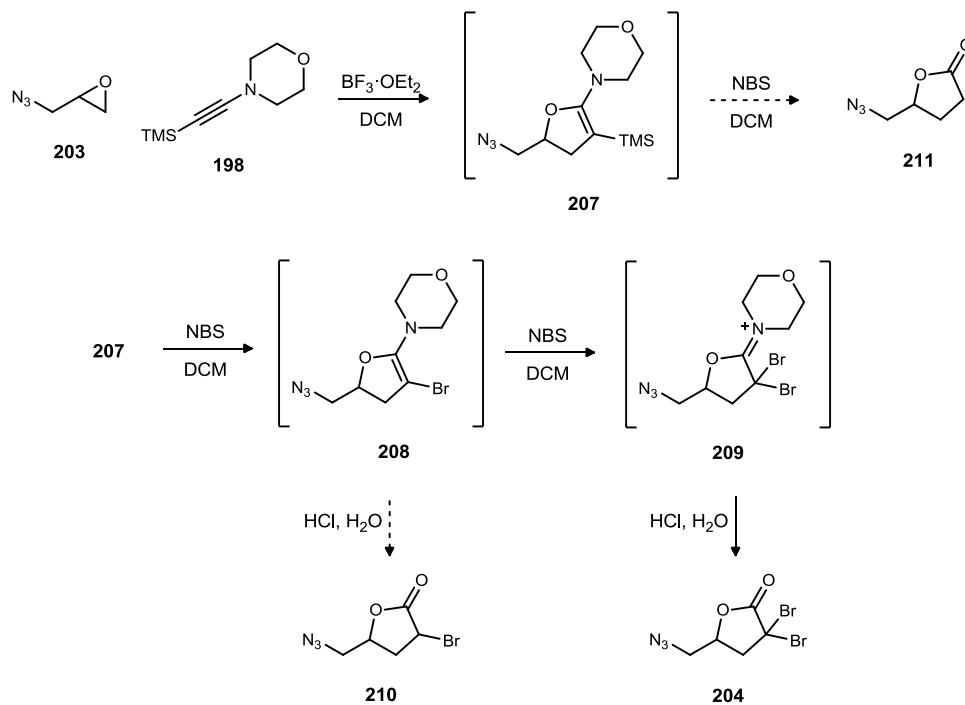
Scheme 88. Epichlorohydrin and Epibromohydrin as Substrates



noted, if even at low levels (<5%). We hypothesized that there might be a competing reaction between the azide and the ynamine (**198**). If this undesired pathway was thermodynamically favored, we might be able to avoid it, or at least suppress it, by varying the temperature of the reaction. The reaction proceeds in three stages, as shown in Figure 37¹¹⁰; in stage one (S1), the epoxide reacts with silyl ynamine **198** to form cyclic silyl keteneaminal **207**, and in stage two (S2), the cyclic silyl keteneaminal acts as a nucleophile to displace succinimide. Following elimination of the silyl group, the keteneaminal moiety is reformed (**208**), and a second equivalent of bromonium is introduced. The third stage (S3) involves hydrolysis of the resulting iminium ion (**209**) to form the desired α,α -dibromo γ -lactone (**204**).

These three stages are important to consider when thinking about optimizing the reaction for use of

Figure 37. Proposed Reaction Pathways



¹¹⁰ Presumed reaction pathway based on Movassaghi, M.; Jacobsen, E. N. *J. Am. Chem. Soc.* **2002**, *124*, 2456. Evidence of intermediate **111/119** is reported therein.

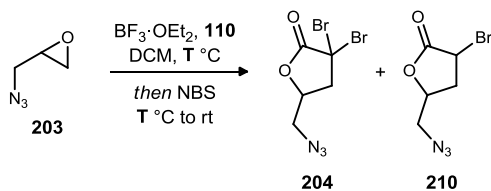
epiazidohydrin; in a temperature screen, we would expect the reaction, whether via the desired or undesired pathway, to proceed more slowly at lower temperatures and more quickly at higher temperatures, thus reaction time must be considered as well. Finally, since our initial concern is formation of cyclic silyl keteneaminal **207**, we can consider formation of the desired α,α -dibromide (**204**), the α -monobromide (**210**), or the dihydrofuranone (**211**) a success in avoiding the decomposition pathway; **210** and **211** would be observed when not enough time is allowed in S2 for bromination.

Thus, the initial temperature screen would seek only to determine if the desired pathway can be favored over the decomposition pathway. To this end, the time of each stage was not changed, and only the temperature of S1 and the beginning of S2 were changed; the second half of S2 proceeds at room temperature in all cases. For the analysis of the temperature screen, crude ^1H NMR was used as a semi-quantitative means to determine the relative amount of formation of the desired product versus the competing pathway. As previously mentioned, for this screen, formation of **204**, **210**, or **211** would be considered a sign of formation of intermediate **207**, and the combined integrations of these products were compared to the integration of the alternate pathway products, which appear between δ 4.38 and 3.33 in the ^1H NMR spectrum.¹¹¹ While this relative integration cannot be used to accurately determine yields, it does give an idea of whether the reaction is proceeding down the desired pathway or the decomposition pathway.

Standard reaction conditions allow for 30 m at 0 °C for formation of cyclic silyl keteneaminal **207** (S1), 20 m at 0 °C, followed by warming to room temperature (30 m) for introduction of both bromonium ions (S2), and finally acid hydrolysis for 30 m at room temperature (S3). When the reaction was performed under these standard conditions for S1, both **204** and **210** were observed (1:1), and the relative integration of the decomposition region, accounting for product signals that appear in this area, to that of the products was 61:1; the non-brominated product **211** was never observed (Table 2, entry 2). When performed at room temperature, the reaction bubbled vigorously upon the addition of epiazidohydrin, suggesting dinitrogen evolution and that the decomposition pathway is the major pathway at this temperature. Although no α,α -dibromo product (**204**) was observed at this temperature, some α -monobromo product (**210**) was observed, and the relative integration of the decomposition region to that of **210** was 190:1 (Table 2, entry 3). We were pleased to find that when S1 was performed at -20 °C, the relative integration of the decomposition region to that of the **204** and **210** (1:4) decreased to 12:1 (Table 2, entry 1). Thus, as we hypothesized, the undesired decomposition pathway can at least be lowered at lower reaction temperatures.

While the experiment in which S1 was performed at room temperature gave none of the desired product (**204**), we found it fortunate to have observed nitrogen evolution upon addition of epiazidohydrin to the reaction

Table 2. Initial Temperature Screen



| entry ^a | T (°C) ^b | Dec : Prods ^c | 204 : 210 ^d |
|--------------------|---------------------|--------------------------|--------------------------------------|
| 1 | -20 | 11.8 : 1.0 | 1.0 : 3.7 |
| 2 | 0 | 61.1 : 1.0 | 1.0 : 1.0 |
| 3 | rt | 190 : 1.0 | 0 : 1.0 |

^aFor all reactions, S1 proceeded for 30 m, and S2 proceeded for 20 m at designated T, followed by 30 m at rt. ^bTemperature for S1. ^cBased on crude ^1H NMR; ratio of decomposition region to desired products **204** and **210**; signals for **204** and **210** that appear in this region were taken into account. ^dBased on crude ^1H NMR.

¹¹¹ Although the identity of the alternate pathway products could not be determined, signals other than for the β and δ protons are absent from this area of the spectrum in crude spectra when epichlorohydrin and epibromohydrin are used; thus, signals in this region that do not correspond to either the β or δ protons must derive from a side reaction with the azido functional group.

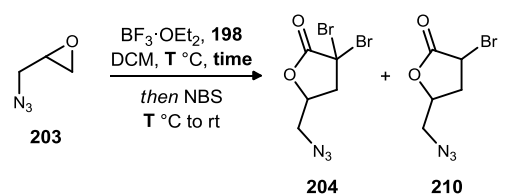
mixture. Since the reaction could not be followed via thin layer chromatography, this bubbling at room temperature could be used to monitor the progress of S1, or formation of the cyclic silyl keteneaminal (**207**); bubbling in a capillary tube, then, would indicate that epiazidohydrin was still present in the reaction and that S1 was not complete.

Our second temperature screen took into account the progress of S1. Since results had improved upon cooling the reaction to $-20\text{ }^{\circ}\text{C}$, they might improve further with more cooling. We were concerned, however, that these even lower temperatures might further slow the desired reaction, and if S1 was not complete, epiazidohydrin would remain in the reaction upon warming during S2, and the undesired decomposition would occur.

We found that for reactions at $-20\text{ }^{\circ}\text{C}$, S1 was complete in 1 h to 1.25 h, while cooling further to $-40\text{ }^{\circ}\text{C}$ required 2.5 h for completion of S2. The reaction did not proceed at $-78\text{ }^{\circ}\text{C}$. Due to the presence of **210** in our previous run at $-20\text{ }^{\circ}\text{C}$, S2 was extended to 25 m at the S1 temperature and 2 h at room temperature in order to allow for further bromination. We found, then, that at $-40\text{ }^{\circ}\text{C}$, the integration of the decomposition region relative to desired products **204** and **210** was 11:1, while at $-20\text{ }^{\circ}\text{C}$, that integration was 12:1. Thus a decrease in temperature to $-40\text{ }^{\circ}\text{C}$ did not offer significant improvement over results achieved at $-20\text{ }^{\circ}\text{C}$; it only served in extending overall reaction time.

Further changes to reaction times did not result in any improvement, and keeping the reaction at $-20\text{ }^{\circ}\text{C}$ for the duration of S2 for an extended period of time (20 h) only resulted in formation of the α -monobromo

Table 3. Second Temperature Screen

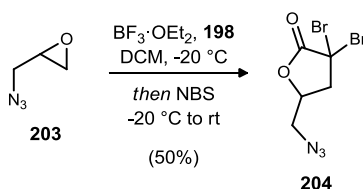


| entry ^a | T ($^{\circ}\text{C}$) | Time (m) ^b | Dec : Prods ^c | 204 : 210 ^d |
|--------------------|--------------------------|-----------------------|--------------------------|--------------------------------------|
| 1 | -78 | 150 | -- | -- |
| 2 | -40 | 150 | 10.5 : 1.0 | 1.0 : 2.4 |
| 3 | -20 | 60 | 11.5 : 1.0 | 2.3 : 1.0 |

^aFor all reactions, S2 proceeded for 25 m at designated T, followed by 2 h at rt. ^bTime for S1; reaction proceeded until no nitrogen evolution was observed at rt. ^cBased on crude ^1H NMR; ratio of decomposition region to desired products **204** and **210**; signals for **204** and **210** that appear in this region were taken into account. ^dBased on crude ^1H NMR.

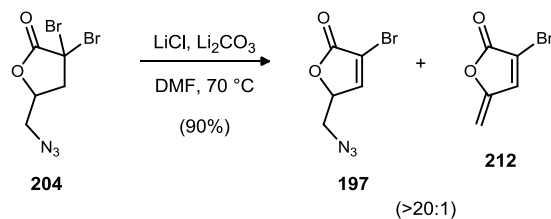
product (**210**). We concluded, then, that warming S2 to room temperature was necessary for the second bromination. Thus, by cooling the reaction to $-20\text{ }^{\circ}\text{C}$ and allowing S1 to proceed to completion, followed by extension of the S2 period at room temperature to 2 h, we could partially suppress the decomposition pathway and achieve isolation of the desired α,α -dibromide (**204**) in 50% yield, which is a 10-fold improvement over our initial results.

Scheme 89. Optimized Conditions for Epiazidohydrin



With **204** thus available in good yields, we could proceed to elimination to the desired azido vinyl bromide (**197**). With careful adjustment of reaction times to avoid double elimination to **212**,¹¹² we found that the reaction proceeded smoothly to the desired product when **204** was heated to 70 °C in DMF for 20 minutes in the presence of lithium chloride and lithium carbonate. In cases where double elimination was avoided, the product could be used without purification.

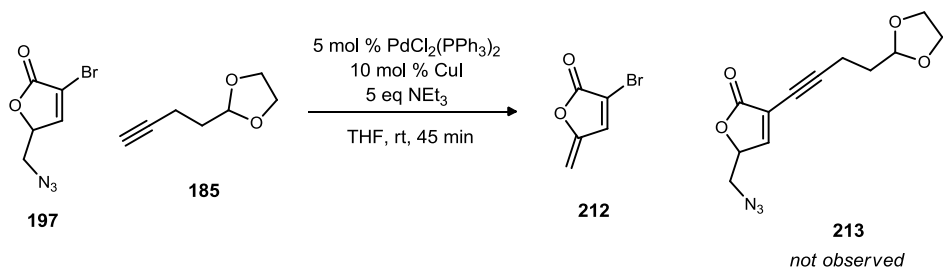
Scheme 90. Elimination to Azido Vinyl Bromide **197**



Attempted Elaboration of Azido Vinyl Bromide **197**

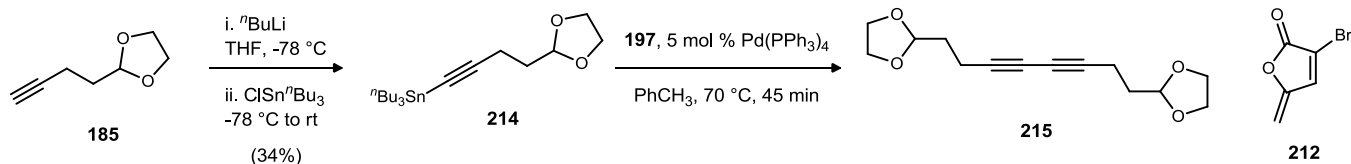
As mentioned previously, coupling of azido vinyl bromide **197** to alkyne **185** via a Sonagashira reaction would be used to install C11-C15. However, treatment of **197** and **185** with $\text{PdCl}_2(\text{PPh}_3)_2$, CuI , and triethylamine led only to formation of elimination product **212**. Variation of the base and palladium source did not result in formation of the desired product (**213**).

Scheme 91. Attempted Sonagashira Coupling with **197**



We hypothesized that the presence of base in the coupling reaction was leading to formation of elimination product **212**, so we sought coupling methods that did not require base to install the C11-C15 chain. Alkyne **185** was converted to the corresponding alkynyl stannane (**214**, Scheme 92) for use in a Stille coupling reaction. Treatment of azido vinyl bromide **197** with $\text{Pd}(\text{PPh}_3)_4$ and alkynyl stannane **214**, however, led primarily to the elimination product (**212**). A small amount of the alkyne homodimer (**215**) was isolated, confirming that oxidative addition of the alkynyl stannane was occurring.

Scheme 92. Attempted Stille Coupling with **197**

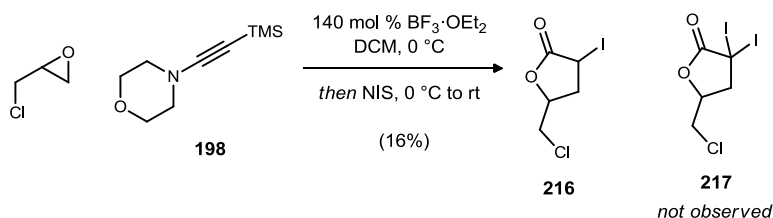


We thought to improve oxidative addition of the azido vinyl bromide (**197**) by instead using the corresponding azido vinyl iodide. In order to determine whether we would be able to install the two iodines on the lactone made from epiazidohydrin, we first attempted to install them using epichlorohydrin as the substrate,

¹¹² Ochoa de Echagüen, C.; Ortuño, R. M. *Tetrahedron* **1994**, *50*, 12457.

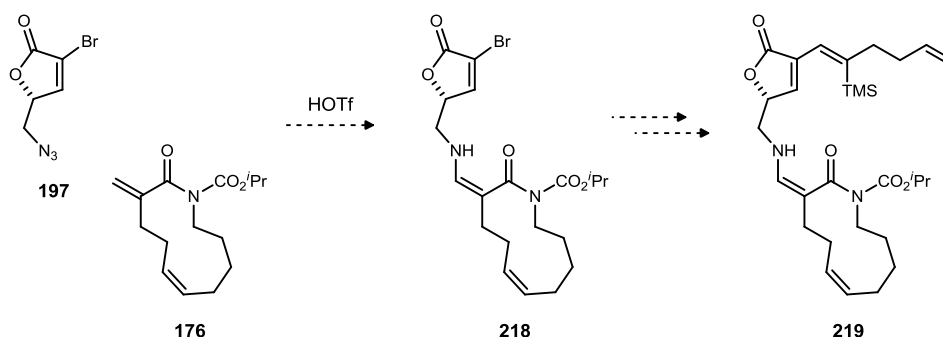
since epichlorohydrin does not present the same difficulties as does epiazidohydrin. Unfortunately, using Jacobsen's method and either NIS or I₂, we were only able to install a single iodide, leading to **216**.

Scheme 93. Attempted Diiodination



While elimination of the azido group to **212** prevents palladium-catalyzed cross coupling with the azido vinyl bromide (**197**), this coupling might be realized at a later point in the synthesis. A debrominated product was never observed in the attempted couplings, which suggests that elimination of the azido group is occurring prior to oxidative addition. To avoid this elimination, we propose to render the azido group less susceptible to elimination by subjecting azido vinyl bromide **197** and acryloyl imide **176** to Brønsted acid-catalyzed [3+2] conditions prior to installing C11-15 (Scheme 94). The resulting enamine (**218**) is not expected to eliminate with the same facility as the azido group.

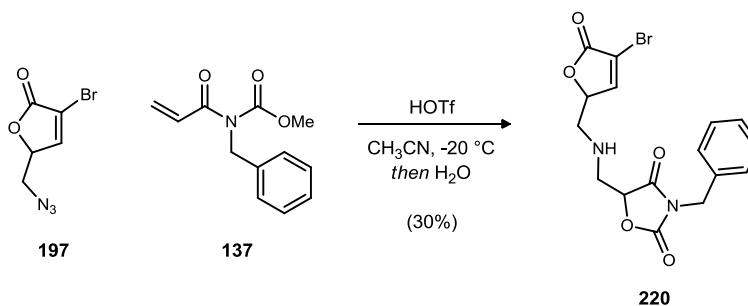
Scheme 94. Installation of C11-15 After BACC



[3+2] Cycloaddition with Azide **197**

To confirm that azido vinyl bromide **197** would survive the Brønsted acid conditions, it was subjected to aminohydroxylation reaction conditions with imide **137**. As expected, oxazolidine dione **220** was isolated in 30% unoptimized yield. Thus, electron-rich azide **197** was confirmed to be a competent donor for the [3+2] cycloaddition and aminohydroxylation reaction, at least with simple imide substrates.

Scheme 95. Aminohydroxylation with Azido Vinyl Bromide **197**

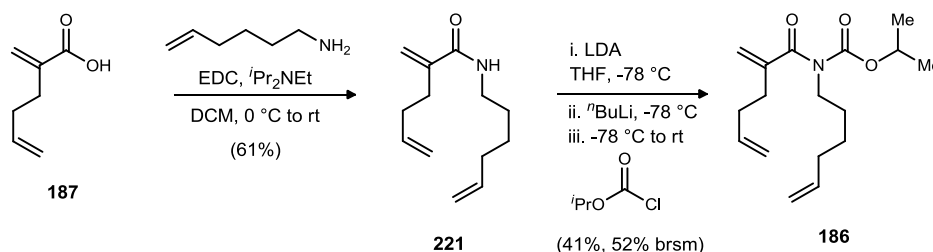


2.3.4 Preparation of the Acryloyl Imide

Amide **221** was prepared via a dehydrative coupling from acrylic acid **187** and 5-hexenamine using EDC as the coupling reagent in 61% yield (Scheme 96). Attempts to prepare the amide through acyl substitution of the corresponding acyl chloride resulted in poor yields, as did the use of other coupling reagents to effect amide formation.

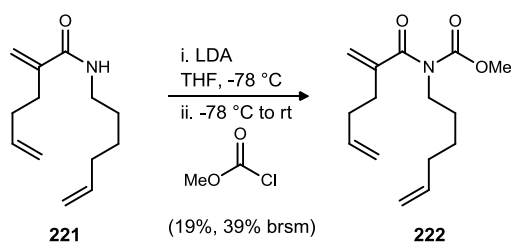
Early attempts to prepare the desired imide via acylation of amide **221** with isopropyl chloroformate resulted in poor yields. LiHMDS was not found to be a suitable base for deprotonation of the amide; yield of the desired product when this base was used was less than 10%. Use of LDA as the base resulted in isolation of the desired imide in 32% yield (49% brsm), with the ^1H NMR of the unpurified reaction mixture showing approximately 60% conversion from the amide to the imide. Addition of triethylamine (5 eq) resulted in less than 10% conversion. Variation in the concentration of the reaction from the standard 0.3 M also resulted in poorer conversion, with dilute conditions (0.15 M) and more concentrated conditions (0.6 M) resulting in 25% and 28% conversion, respectively. Use of two equivalents of LDA also did not improve the reaction (18%, 35% brsm, 35% conversion). Addition of an equivalent of *n*-butyl lithium following deprotonation of the amide¹¹³ resulted in greater conversion (76%) as well as isolation of the product (41%, 52% brsm) (Scheme 96). Warming the reaction to 0 °C for 5 min following addition of the *n*-butyl lithium gave similar results (33%, 68% brsm, 62% conversion). Use of 2.4 equivalents of isopropyl chloroformate instead of the standard 1.2 equivalents also did not improve the reaction (30% yield).

Scheme 96. Synthesis of Imide **186**



With the thought that isopropyl chloroformate might be too hindered, methyl chloroformate was used as the acylating reagent. This reaction resulted in 19% yield (39% brsm), which was lower than the corresponding reaction with isopropyl chloroformate (Scheme 97).

Scheme 97. Preparation of Alternate Imide **222**

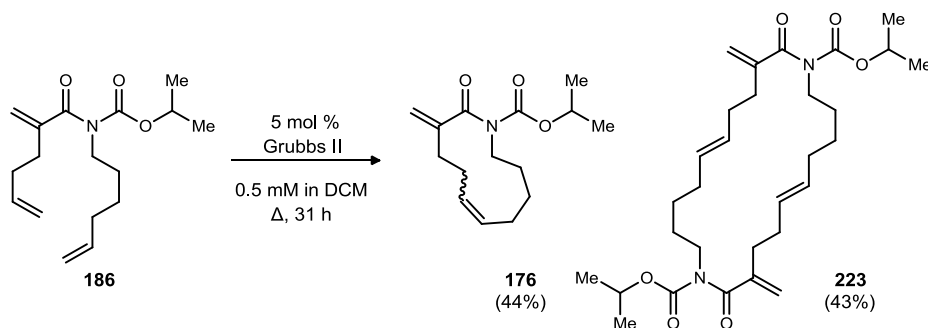


With acryloyl imide **186** in hand, we then proceeded to convert it to the 11-membered ring that is present in kauluamine. Imide **186** was found to be unreactive towards Grubbs 1st Generation Catalyst, but upon treatment with 15 mol % Grubbs 2nd Generation Catalyst, imide **186** was converted to cyclic imide **176** and cyclic dimer **223** in 5 h. A lower catalyst loading (5 mol %) required a longer reaction time, but the reaction did not proceed to completion, even after 6 days and additional catalyst. The best conversion to time ratio was achieved upon treatment of the imide with 5 mol % Grubbs II catalyst for 31 h, with an additional 5 mol %

¹¹³ For a discussion of the aggregation of lithium enolates: Seebach, D.; Amstutz, R.; Dunitz, J. D. *Helv. Chim. Act.* **1981**, *64*.

catalyst added after 25 h, in refluxing dichloromethane; these conditions resulted in 87% conversion. The monomer and dimer were formed in equal amounts, and starting material was recovered for the balance of the mass.

Scheme 98. Formation of Cyclic Imide **176** Via RCM

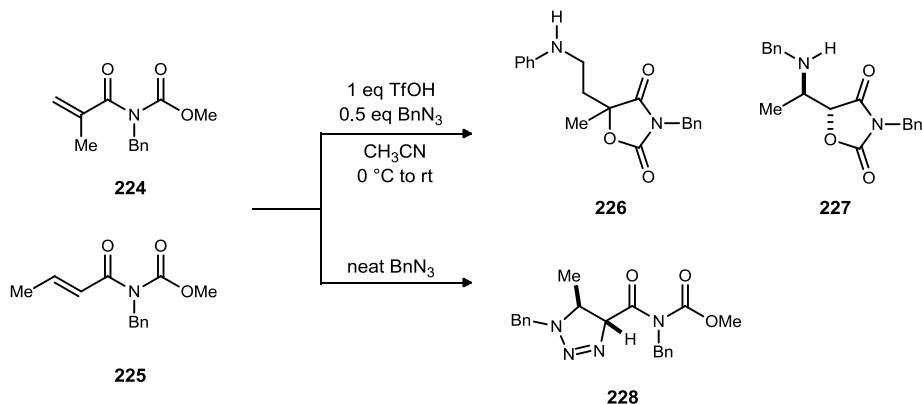


The geometry of the formed disubstituted bond could not be determined due to overlap of the vinyl protons in the ^1H NMR, even with extensive NMR studies, including ^1H - ^{13}C coupled ^{13}C NMR. This reaction may be improved by slow addition of the catalyst or even more dilute conditions, since the dimer must be a result of too little solvent. Use of a more hindered catalyst might also disfavor dimerization. Analysis of later intermediates revealed that we had formed the undesired *E*-isomer of **176**. We may be able to control the selectivity of this double bond formation using recent methods developed by Schreiber¹¹⁴ and Furstner,¹¹⁵ in which the selectivity is controlled by a removable vinyl silyl group, or by use of a different catalyst.

2.3.5 Brønsted Acid-Catalyzed Aminohydroxylation Studies

As discussed in section 2.3.1, we planned to use an aminohydroxylation reaction to bring together azido lactone **197** and acryloyl imide **176**. During some previous work in our group, Ki Bum Hong found that α -substituted imides (**224**) were less reactive than unsubstituted or β -substituted imides (**225**) towards Brønsted acid-catalyzed [3+2] cycloadditions with benzyl azide and that at higher temperatures, α -substituted imides reacted via an aza-Schmidt pathway (Scheme 99).¹¹⁶ Recall that the imide (**137**) that was utilized in the kauluamine model studies was unsubstituted at the α -position. Because of the electron rich nature of both azide and imide coupling partners, a decrease in reactivity was expected for both of these relative to benzyl azide and the imides discussed in section 2.2.1.

Scheme 99. Competition Experiment Between α - and β -Substituted Imides (KBH)



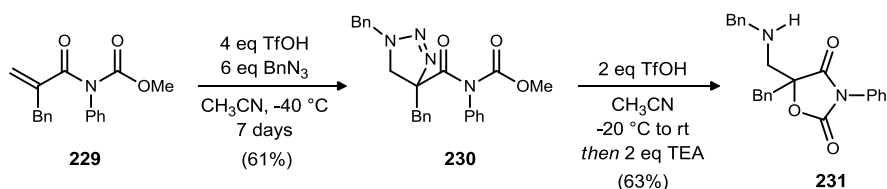
¹¹⁴ Wang, Y.; Jiminez, M.; Hansen, A. S.; Raiber, E.; Schreiber, S. L.; Young, D. W. *J. Am. Chem. Soc.* **2011**, *133*, 9196.

¹¹⁵ Gallenkamp, D.; Furstner, A. *J. Am. Chem. Soc.* **2011**, *133*, 9232.

¹¹⁶ Hong, K. B.; Johnston, J. N. *unpublished results*.

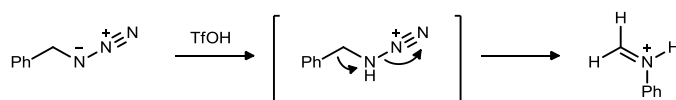
During optimization of the aminohydroxylation reaction for α -substituted imides, it was found that the least reactive of the screened substrates, α -benzyl *N*-phenyl imide **229**, underwent triflic acid-catalyzed cycloaddition at $-40\text{ }^\circ\text{C}$ in 61% yield (Scheme 101). The reaction was found to be slow and took seven days and a large excess of the azide coupling partner to proceed to completion. When the reactions were performed at

Scheme 101. Aminohydroxylation with α -Substituted Imides



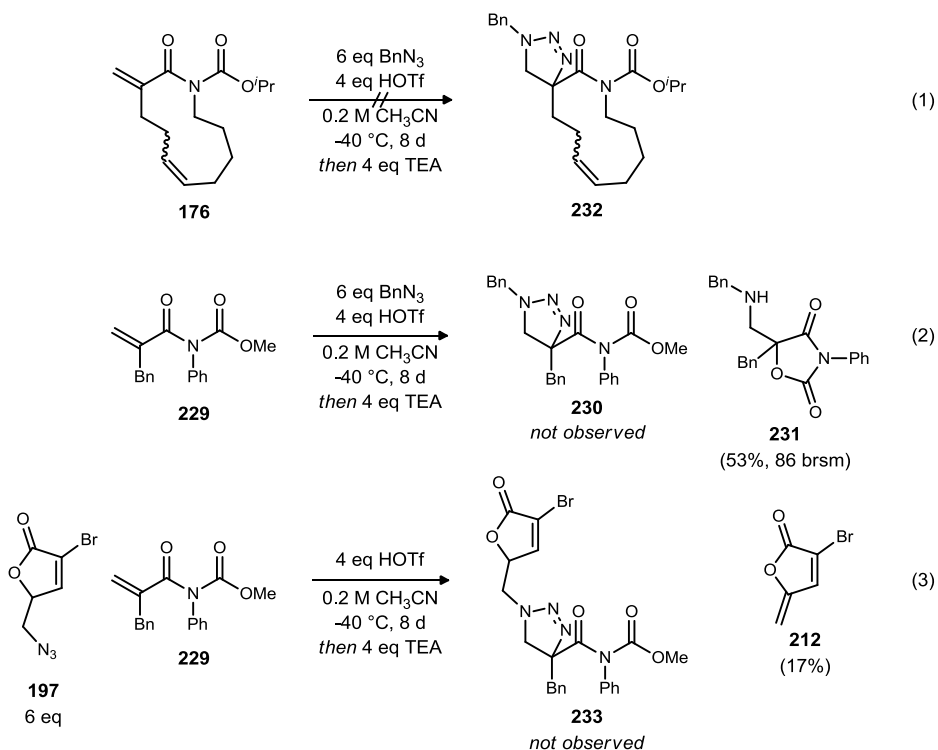
higher temperatures, the undesired aza-Schmidt pathway predominated, whereby benzyl azide decomposed to the *N*-phenyl formimine (Scheme 100), and this substrate underwent nucleophilic attack from the α -substituted imide.

Scheme 100. Acid-Promoted Aza-Schmidt Azide Rearrangement



Thus, the relatively unreactive α -benzyl *N*-phenyl imide **229** and benzyl azide were used to gauge the reactivities of cyclic imide **176** and azido lactone **197**. No reaction was observed when cyclic imide **176** was treated with six equivalents of benzyl azide and four equivalents of triflic acid at $-40\text{ }^\circ\text{C}$ for 8 days (Scheme 102, eq 1). Likewise, no reaction was observed between azido lactone **197** and α -benzyl *N*-phenyl imide **229**. Upon quenching this reaction with four equivalents of triethylamine, approximately 17% decomposition of the azide to the elimination product (**212**) was observed (Scheme 102, eq 3). Significant decomposition of the azide

Scheme 102. Reactivity Control Experiments for 197 and 176



in this reaction had previously been seen when quenching with excess triethylamine, so it was important to carefully manage the amount of base used to quench the reaction when our base-sensitive azido lactone (**197**) was used as a substrate.

As a control reaction, α -benzyl *N*-phenyl imide (**229**) was also treated with benzyl azide and triflic acid at -40 °C for 8 days (Scheme 102, eq 2). While expected intermediate triazoline compound **230** was not observed, the aminohydroxylation product (**231**) was isolated in 53% yield.¹¹⁷ Ki Bum Hong found that decomposition of the triazoline to the aminohydroxylation product is facile, and it is likely that under these conditions the triazoline intermediate proceeds to the aminohydroxylation product prior to quenching.

Thus, cyclic imide **176** and azido lactone **197** were confirmed to be significantly less reactive than α -benzyl *N*-phenyl imide **229** and benzyl azide, respectively, towards triflic acid-promoted [3+2] cycloaddition. We also found that the cyclic imide (**176**), as well as the α -benzyl *N*-phenyl imide (**229**), is unreactive towards the electron-rich azidotrimethylsilane.

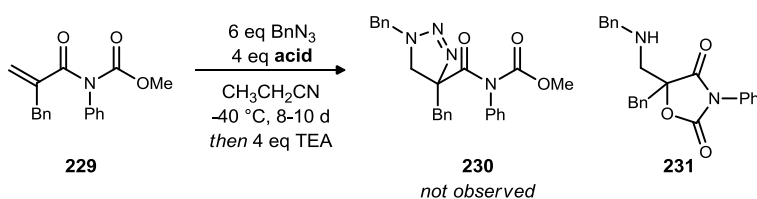
[3+2] Cycloaddition Optimization

Because the desired substrates were unreactive under triflic acid-promoted [3+2] cycloaddition conditions, a series of acids were screened in the reaction of α -benzyl *N*-phenyl imide **229** with benzyl azide. If we were able to find an acid that catalyzed the reaction better than triflic acid for α -benzyl *N*-phenyl imide **229** and benzyl azide, we anticipated the increased reactivity would extend to cyclic imide **176** and azido lactone **197**. The results of this acid screen are shown below, in Table 4.

Non-triflated reagents did not seem to promote the reaction at all. The Lewis acid boron trifluoride etherate (Table 4, entry 7), as well as the Brønsted acid methanesulfonic acid (Table 4, entry 5), failed to promote the desired cycloaddition. The Lewis acid trimethylsilyltriflate (Table 4, entry 6) was found to perform better than the standard triflic acid (Table 4, entry 1) in the reaction. Although this reagent was not distilled prior to the reaction, it is reasonable to conclude that the reaction was at least largely promoted by the Lewis acid rather than any residual triflic acid since it performed better than the triflic acid alone.

Triflimide was found to promote the desired cycloaddition faster than triflic acid under the same conditions (Table 4, entry 2). In addition to a 50% increase in isolated yield, the balance of the starting material was recovered, indicating little to no decomposition under reaction conditions. Bistriflyl methane, which is the carbon acid equivalent to triflimide and triflic acid, failed to promote the desired reaction; decomposition of the starting materials was not observed with this acid (Table 4, entry 3). The tethered, cyclic sulfonimide, 1,1,2,2,3,3-hexafluoropropane-1,3-disulfonimide, which would be less hindered than triflimide and more acidic, performed about as well as triflic acid but did not offer an improvement (Table 4, entry 4).

Table 4. [3+2] Cycloaddition Acid Screen



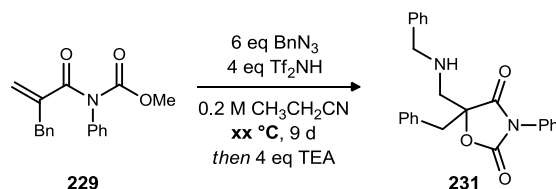
| entry ^a | acid | result |
|--------------------|----------------------------------|----------------------------|
| 1 ^b | HOTf | 231, 53% |
| 2 | Tf₂NH | 231, 77%, 96% brsm |
| 3 | Tf ₂ CH ₂ | no reaction |
| 4 | cyclic | 231 , 54%, 69% brsm |
| 5 | MsOH | no reaction |
| 6 | TMSOTf | 231 , 61%, 76% brsm |
| 7 | BF ₃ OEt ₂ | no reaction |

^aAll reactions were performed 0.2 M in CH₃CH₂CN over a period of 8-10 days. ^bIn CH₃CN.

¹¹⁷ Identification of this product required reassignment of the compound isolated by KBH as the product of triazoline decomposition.

Triflimide was chosen for further studies. Since we had such good recovery of the starting material and did not see any decomposition of the benzyl azide, we performed a temperature screen with this acid. The results are shown below, in Table 5. While decomposition of benzyl azide via the aza-Schmidt pathway was not observed in any case, the isolated yield of the reaction did decrease as the temperature was increased. It was disappointing that the yield for this reaction did not increase with temperature; however, it provides a point for the potential increase in reactivity for the desired cyclic substrate. That is, if cyclic imide **176** is not reactive at -40 °C with triflimide, an increase in reaction temperature may not be detrimental to the reaction.

Table 5. [3+2] Cycloaddition Temperature Screen



| entry | T (°C) | result |
|-------|--------|---------------|
| 1 | -40 | 77%, 96% brsm |
| 2 | -20 | 59%, 61% brsm |
| 3 | 0 | 37%, 51% brsm |

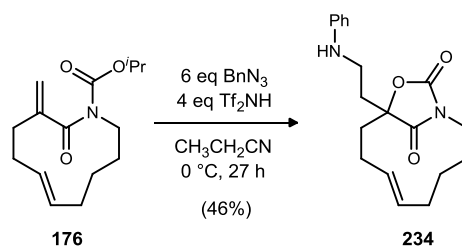
^aNote: aza-Schmidt and rearrangement products were not observed at any temperature.

Attempted [3+2] Cycloaddition with Cyclic Imide **176**

With a seemingly more suitable acid in hand, these conditions were applied to a reaction between cyclic imide **176** and benzyl azide. While none of the desired triazoline (**232**) or the possible aminohydroxylation product were observed, triflimide promoted the formation of iminoacetoxylation product **234**. At -40 °C, the reaction had progressed to only partial conversion after 8 days, with an isolated yield of 38% (71% brsm), although purification was incomplete at this point. This reaction appeared to be clean by ¹H NMR, with little to no conversion to other products. When the reaction was performed at 0 °C, full conversion of the starting material was observed after only 27 h, though the isolated yield only increased to 46%, with no starting material or other identifiable products isolated.

While iminoacetoxylation was not the desired result, Brønsted acid-activation of cyclic imide **176** had been achieved in some form. This result also served to disprove our hypothesis that cyclization to the oxazolidine dione would be prevented by the 11-membered macrocycle, at least in the case of the *E*-olefin. Furthermore, identification of the product allowed us to confirm that the cyclic imide (**176**) formed via ring-closing metathesis catalyzed by Grubbs II did have the *E*-geometry, which is the undesired isomer, thus necessitating a revision of the chosen cyclization method.

Scheme 103. Iminoacetoxylation of Imide **176**

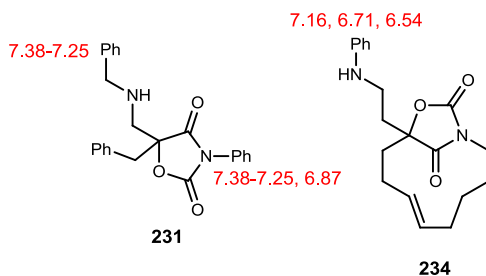


Structural Identification of **234**

The product of the triflimide-catalyzed reaction between benzyl azide and cyclic imide **176** was assigned as that of the iminoacetoxylation pathway (**234**). Analysis of the compound's ¹H NMR revealed aromatic protons (δ 7.16, 6.71, and 6.54) that were further upfield than would be expected for a benzyl amine (δ 7.38-

7.25) similar to the aminohydroxylation product that we obtained when α -Bn *N*-Ph imide **229** was used instead (Figure 38). This shift upfield indicated a possible rearrangement to an aniline-type substrate.

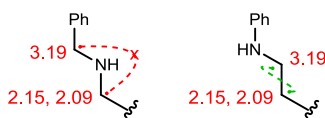
Figure 38. Shifts of Aromatic Protons in 231 and 234



A further indication that we had not formed the desired triazoline was the absence of signals corresponding to an isopropyl group, suggesting that the reaction had resulted in cyclization of the carbamate to an oxazolidine dione. The presence of four quaternary carbons, including two carbonyls (176.4 and 155.8 ppm), which would correspond to the amide and carbamate carbonyls of the oxazolidine dione moiety, respectively, one aromatic carbon (147.3 ppm), and one sp^3 carbon (86.0 ppm), which would correspond to the α -carbon of the oxazolidine dione, supported structural assignment as that of either the aminohydroxylation or iminoacetoxylation product.

A 2D-TOCSY experiment revealed a spin system containing protons at δ 3.19 (ddd, $J = 7.2, 7.2, 1.8$ Hz, 2H), 2.15 (ddd, $J = 14.6, 7.3, 7.3$ Hz, 1H), and 2.09 (ddd, $J = 14.6, 6.4, 6.4$ Hz, 1H) (Figure 39). These resonances also had weak correlations to a water peak in the sample, indicating the possibility of an exchangeable proton within the spin system. While a spin system containing two sets of geminal protons and an exchangeable *NH* proton would be consistent with both the aminohydroxylation and iminoacetoxylation products, distinct correlations between the δ 3.19 signal and both δ 2.15 and 2.09 protons in a 2D-COSY experiment, as well as coupling constants, indicated direct coupling between the two sets of protons, suggesting that their carbons (37.9 and 37.7 ppm, respectively), as determined by HSQC, shared a bond. Only the protons at δ 3.19 had a coupling constant (1.8 Hz) that would correspond to coupling with a fifth proton in the spin system, presumably the *NH*.

Figure 39. TOCSY Spin-System & COSY Correlations



While an *NH* proton was not observed by ^1H NMR, an IR stretch at 3398 cm^{-1} indicated the presence of an O-H or N-H in the molecule. Thus, taken with the upfield shifts of the aromatic protons, the system was assigned as a Ph-NH-CH₂-CH₂ system rather than a Ph-CH₂-NH-CH₂ system. The 2D-TOCSY experiment indicated that these protons did not overlap with any of the other spin systems in the molecule. Thus, with all other requisite protons and carbons accounted for, the compound was assigned as that of iminoacetoxylation product **234**.

Coupling between the vinyl protons of the 11-membered ring, which appear at δ 5.47 (dddd, $J = 15.2, 10.4, 4.8, 1.5$ Hz, 1H) and 5.25 (dddd, $J = 14.9, 11.2, 3.8, 1.4$ Hz, 1H), allow for assignment of the olefin as having an *E*-geometry.¹¹⁸ This assignment, in turn, indicated that the cyclic imide precursor (**176**) also contains that geometry, although its vinyl protons overlapped, and coupling constants were not elucidated.

¹¹⁸ Pretsch, E.; Buhlmann, P.; Affolter, C. *Structure Determination of Organic Compounds*; Springer: Berlin, 2000; pp 168. Typical ranges for coupling constants between vinyl protons are 4 to 12 Hz for *cis* and 14 to 19 Hz for *trans*.

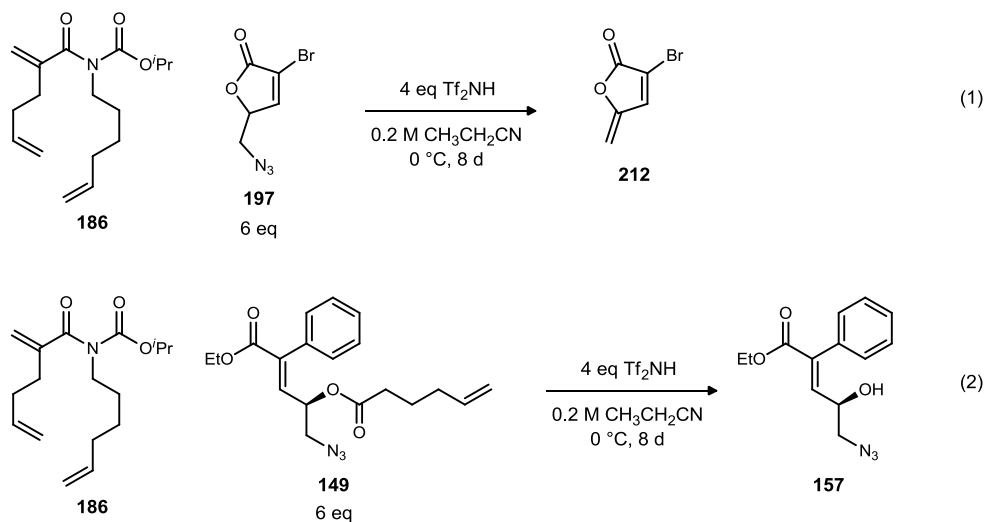
Attempted [3+2] Cycloadditions with Imide **186**

Having established that Grubbs II-catalyzed ring-closing metathesis led to the undesired olefin geometry, the [3+2] cycloaddition studies with uncyclized imide **186**. We hoped to establish reaction conditions that would lead to activation of this α -substituted imide towards [3+2] cycloaddition with azide **197**.

Subjection of imide **186** and azide **197** to triflimide in propionitrile at 0 °C for several days, which corresponded to the best conditions for aminohydroxylation, as established in Table 5, led only to decomposition of azide **197** via an elimination pathway (Scheme 104, eq 1). We were unable to detect any products that would indicate the substrates underwent a [3+2] cycloaddition reaction.

To further establish the unreactivity of imide **186** towards electron-rich azides, **186** was treated with azide **149**, which had been used in the model study and which was less prone to elimination. Unfortunately, this reaction again suffered from poor conversion, and the only products observed corresponded to deprotection of the C23 alcohol (Scheme 104, eq 2). Warming the reaction to room temperature did not increase reactivity. Again, only poor conversion and some deprotection of the C23 alcohol were observed. Further attempts to treat imide **186** with either model azide **149** or azido lactone **197** under the original [3+2] cycloaddition conditions, specifically triflic acid at 0 °C, led only to recovered imide and some azide decomposition in both cases.

Scheme 104. Attempted [3+2] Cyclization with Imide **186**



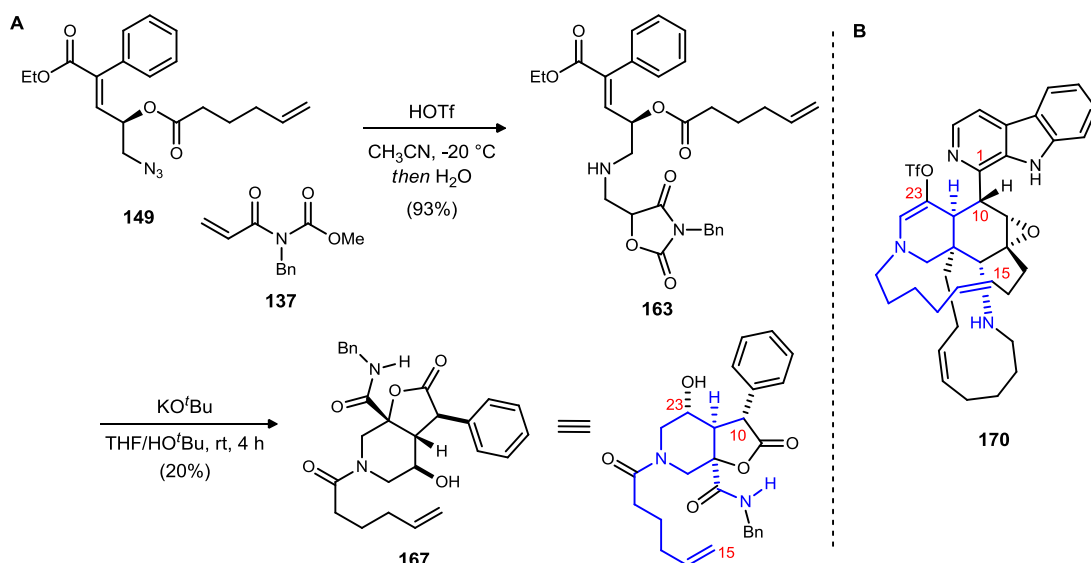
Following this series of reactions, it was concluded that imide **186** was too unreactive under Brønsted-acid catalyzed [3+2] cycloaddition conditions to effectively react with the electron-rich azides, which are unlikely to undergo an aza-Schmidt type rearrangement, before they underwent decomposition. This unreactivity can be attributed to a combination of the α -substitution of the imide and to the electron-rich alkyl group on the imide nitrogen.

2.4 Conclusions and Future Work

Following the preparation of azido ester **149** and Brønsted-acid catalyzed aminohydroxylation with imide **137**, tandem O \rightarrow N acyl transfer and base-promoted cyclization of **163** to the highly functionalized piperidine core (**167**) of kauluamine (Scheme 105) were achieved. The absolute stereochemistry of piperidine **167** was assigned based on NOESY experiments and the mnemonic for Sharpless asymmetric dihydroxylation, with which we established the configuration at C23. The piperidine stereochemistry was used to confirm our models for cyclization, and a retrosynthesis based on these cyclization models was developed for the natural product kauluamine.

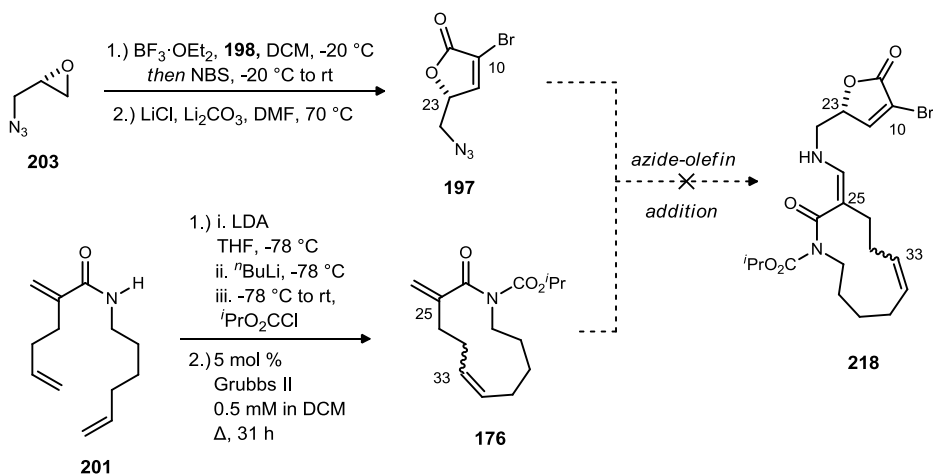
Azide **175** and imide **176** were then prepared as the starting points for a total synthesis of kauluamine. While acetyl β -carboline **192** could not be converted to its enol triflate (**184**), azido lactone **197** could instead be prepared via a modification of known methods. Azido lactone **197** comprises the N21-C24 and C1/C10 unit of kauluamine and is set up with a vinyl bromide moiety for a Sonagashira or other palladium-catalyzed coupling

Scheme 105. Aminohydroxylation & Tandem Acyl Transfer/Piperidine Cyclization



reaction to install C11-C15 following the Brønsted acid-catalyzed azide-olefin addition to form enamine **218** (Scheme 106). Based on an optimization study of the Brønsted acid-catalyzed [3+2] cycloaddition reaction using a model system that would emulate the diminished reactivity of electron-rich azides and α -substituted imides, it was determined that triflimide was the best catalyst for these reactions. Unfortunately, through a series of reactions with cyclic imide **176**, imide **212**, and azides **197** and **149**, the Brønsted acid-catalyzed [3+2] cycloaddition reaction pathway was found to be unsuitable for the convergent construction of kauluamine from our desired starting materials. It may be possible to append the C25 alkyl group at a later time via enolate alkylation.

Scheme 106. Brønsted Acid-Catalyzed [3+2] Cycloaddition Pathway



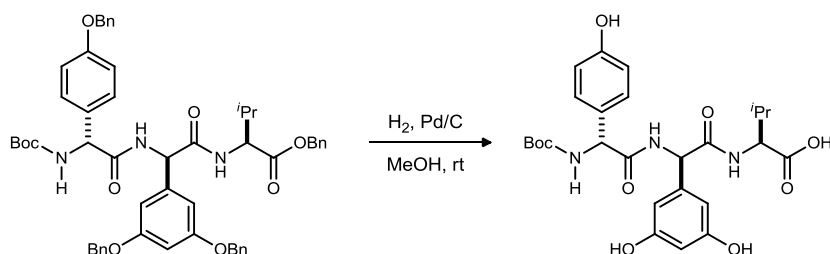
CHAPTER III

EXPERIMENTAL SECTION

Flame-dried (under vacuum) or oven-dried glassware and an inert atmosphere (argon) were used for all non-aqueous reactions. All reagents and solvents were commercial grade and purified prior to use when necessary. Tetrahydrofuran (THF), acetonitrile (CH₃CN), and dichloromethane (CH₂Cl₂), were dried by passage through a column of activated alumina as described by Grubbs.¹¹⁹

For small-scale reactions, tetrahydrofuran (THF) was distilled from sodium/benzophenone. For reactions involving an aqueous work-up, the final organic solutions were dried over magnesium sulfate (MgSO₄) unless otherwise noted.

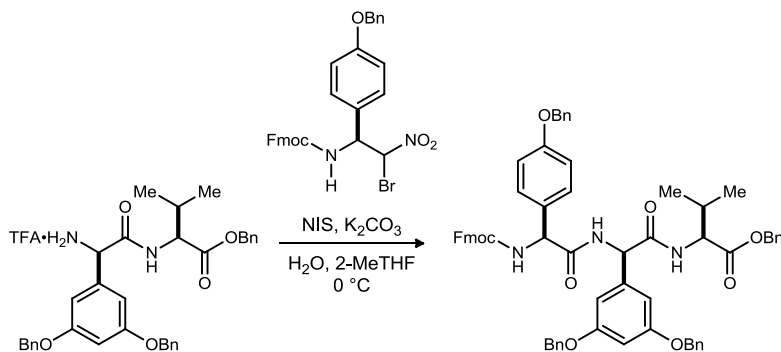
Thin layer chromatography (TLC) was performed using glass-backed silica gel (250 μm) plates, and flash chromatography utilized 230-400 mesh silica gel from Scientific Adsorbents. Products were visualized by UV light. Nuclear magnetic resonance spectra (NMR) were acquired on a Bruker DRX-600 (600 MHz), Bruker DRX-500 (500 MHz), or Bruker DRX-400 (400 MHz) instrument. Chemical shifts are measured relative to residual solvent peaks as an internal standard set to 7.26 for CDCl₃.



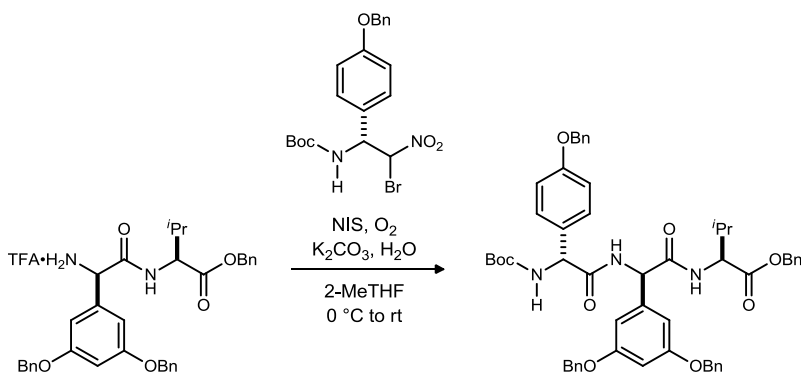
(6*R*,9*R*,12*S*)-9-(3,5-Dihydroxyphenyl)-6-(4-hydroxyphenyl)-12-isopropyl-2,2-dimethyl-4,7,10-trioxo-3-oxa-5,8,11-triazatridecan-13-oic acid (39). Boc-tripeptide A (20 mg, 22 μmol) was suspended in methanol (1.2 mL) with stirring, and 10% palladium on carbon (80 mg) was added in one portion. The reaction atmosphere was replaced with hydrogen gas. After 1 h, no starting material remained by TLC, and the crude mixture was filtered through Celite, eluting with methanol and dichloromethane. The solution was concentrated to give a purplish film, which was triturated with ethyl acetate and hexanes and filtered using fluted filter paper. After air drying for 10 min, the purplish crystals that had been collected were dissolved in methanol, passed through the filter paper, and collected in a tared round-bottomed flask. The solution was concentrated via rotary evaporation and dried under vacuum to give the clean product as a purplish film (12.4 mg, quantitative). $R_f = 0.00$ (5% MeOH/DCM); IR (film) 3359, 2969, 1661, 1597, 1514, 1396 cm⁻¹; ¹H NMR (600 MHz, DMSO-*d*₆) δ 9.47 (br s, 3H), 8.42 (d, $J = 7.6$ Hz, 1H), 7.27 (d, $J = 8.3$ Hz, 1H), 7.22 (d, $J = 9.4$ Hz, 1H), 7.17 (d, $J = 8.5$ Hz, 2H), 6.66 (d, $J = 8.5$ Hz, 2H), 6.30 (d, $J = 2.1$ Hz, 2H), 6.10 (t, $J = 2.1$ Hz, H), 5.24 (d, $J = 7.6$ Hz, 1H), 5.19 (d, $J = 8.5$ Hz, 1H), 3.75 (dd, $J = 8.3, 4.2$ Hz, 1H), 1.93 (tt, $J = 6.8, 6.8, 4.3$ Hz, 1H), 1.37 (br s, 9H), 0.61 (d, $J = 7.0$ Hz, 3H), 0.59 (d, $J = 7.0$ Hz, 3H); ¹³C NMR (150 MHz, DMSO-*d*₆) ppm 173.5, 170.1, 168.6, 158.7, 157.5, 155.1, 141.6, 129.4, 128.7, 115.4, 105.8, 101.1, 78.7, 59.6, 57.4, 57.2, 31.6, 28.6, 20.1, 18.4; $[\alpha]_D^{20}$ 0.0¹²⁰ (c 0.00, CHCl₃); HRMS (ESI): Exact mass calcd for C₂₆H₃₃N₃NaO₉ [M+Na]⁺ 554.2114, found 554.2126.

¹¹⁹ Pangborn, A. B.; Giardello, M. A.; Grubbs, R. H.; Rosen, R. K.; Timmers, F. J. *Organometallics* **1996**, *15*, 1518.

¹²⁰ An optical rotation could not be obtained for this compound due to a “low energy” reading, even after several attempts in MeOH, DMSO, and CHCl₃ at various concentrations.

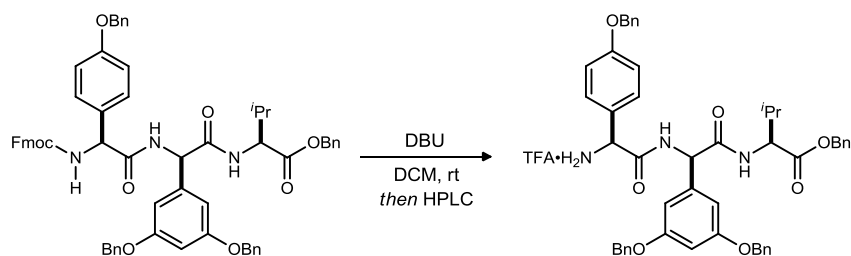


(5*S*,8*R*,11*S*)-Benzyl 5-(4-(benzyloxy)phenyl)-8-(3,5-bis(benzyloxy)phenyl)-1-(9*H*-fluoren-9-yl)-11-isopropyl-3,6,9-trioxo-2-oxa-4,7,10-triazadodecan-12-oate (55). The dipeptide amine (41.6 mg, 75.3 μmol , purified via prep-HPLC) was dissolved in 2-methyltetrahydrofuran (750 μL) with stirring, and the solution was cooled to 0 $^{\circ}\text{C}$. Water (68.0 μL , 3.80 mmol), *N*-iodosuccinimide (16.9 mg, 75.3 μmol), potassium carbonate (12.5 mg, 90.3 μmol), and the α -bromonitro alkane (51.8 mg, 90.3 μmol) were added. The reaction flask was fitted with a rubber septum and an oxygen inlet needle, and the reaction was allowed to slowly warm to room temperature and stirred for 48 h. The crude reaction mixture was transferred to a separatory funnel containing 1 N HCl with dichloromethane. The layers were separated, and the aqueous layer was extracted one time with DCM. The combined organic layers were washed with satd. aqueous $\text{Na}_2\text{S}_2\text{O}_3$ and brine, then dried (MgSO_4), filtered, and concentrated to give a pale yellow solid. The solid was rinsed with ethyl acetate and hexanes then filtered to give the product (35.5 mg, 47%) as a pale yellow solid. Mp = 196-198 $^{\circ}\text{C}$; R_f = 0.84 (5% MeOH/DCM); IR (film) 3296, 3034, 2965, 1729, 1689, 1641, 1605, 1514, 1450 cm^{-1} ; ^1H NMR (600 MHz, DMSO-d_6) δ 8.91 (d, J = 82. Hz, 1H), 8.76 (d, J = 8.3 Hz, 1H), 8.09 (d, J = 8.5 Hz, 1H), 7.88 (d, J = 7.2 Hz, 2H), 7.75 (dd, J = 8.1, 8.1 Hz, 2H), 7.41-7.27 (m, 24H), 6.93 (d, J = 8.5 Hz, 2H), 6.65 (s, 2H), 6.49 (s, 1H), 5.68 (d, J = 8.2 Hz, 1H), 5.54 (d, J = 8.5 Hz, 1H), 5.18 (d, J = 12.4 Hz, 1H), 5.14 (d, J = 12.2 Hz, 1H), 4.96 (s, 2H), 4.93 (d, J = 11.8 Hz, 2H), 4.88 (d, J = 11.8 Hz, 2H), 4.24-4.20 (m, 4H), 2.06-2.02 (m, 1H), 0.79 (d, J = 6.7 Hz, 3H), 0.73 (d, J = 6.5 Hz, 3H); ^{13}C NMR (150 MHz, DMSO-d_6) ppm 171.7, 170.3, 170.1, 159.7, 158.2, 156.1, 144.3, 144.2, 141.6, 141.1, 137.4, 137.2, 136.2, 131.2, 129.1, 128.9, 128.84, 128.80, 128.52, 128.47, 128.3, 128.2, 128.12, 128.09, 128.05, 128.0, 127.5, 125.9, 125.8, 120.5, 114.8, 106.0, 101.3, 69.7, 69.5, 66.5, 66.4, 57.9, 57.5, 55.9, 47.0, 30.6, 19.2, 18.3; $[\alpha]_D^{20}$ -16.3 (c 1.04, DMSO); HRMS (APCI): Exact mass calcd for $\text{C}_{64}\text{H}_{60}\text{N}_3\text{O}_9$ $[\text{M}+\text{H}]^+$ 1014.4330, found 1014.4378.

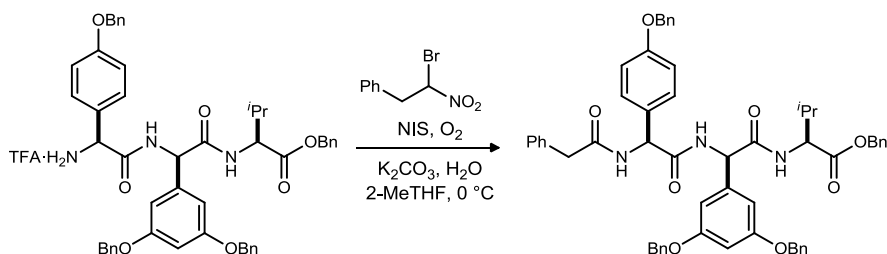


(6*R*,9*R*,12*S*)-Benzyl 6-(4-(benzyloxy)phenyl)-9-(3,5-bis(benzyloxy)phenyl)-12-isopropyl-2,2-dimethyl-4,7,10-trioxo-3-oxa-5,8,11-triazatridecan-13-oate (56). The dipeptide amine (46.5 mg, 84.1 μmol) was dissolved in 2-methyltetrahydrofuran (840 μL) with stirring and cooled to 0 $^{\circ}\text{C}$. Water (7.6 μL , 420 μmol), *N*-iodosuccinimide (18.9 mg, 84.1 μmol), potassium carbonate (14.0 mg, 101 μmol), and α -bromonitro alkane (46.0 mg, 101 μmol) were added. The reaction flask was fitted with a rubber septum with an oxygen inlet needle, and the reaction was allowed to slowly warm to room temperature and was stirred for 60 h. The crude mixture was transferred to a separatory funnel containing 1 N HCl with dichloromethane. The layers were separated, and the aqueous layer was extracted once with dichloromethane. The combined organic layers were

washed with satd. aqueous Na₂S₂O₃ and brine, then dried (MgSO₄), filtered, and concentrated to give the crude mixture as a pale yellow oil. The oil was rinsed with ethyl acetate and hexanes then filtered to provide the desired product as a white solid (20 mg, 27%). (Note: when concentrated from other solvents, the material is a yellow oil.) *R*_f = 0.19 (30% EtOAc/hexanes); IR (film) 3294, 3065, 2969, 1713, 1639, 1604, 1509, 1453 cm⁻¹; ¹H NMR (600 MHz, DMSO-*d*₆) δ 8.64 (d, *J* = 8.4 Hz, 1H), 8.62 (d, *J* = 8.2 Hz, 1H), 7.50-7.32 (m, 22 H), 6.92 (d, *J* = 8.46, 2H), 6.82 (d, *J* = 1.9 Hz, 2H), 6.56 (br s, 1H), 5.64 (d, *J* = 8.2 Hz, 1H), 5.30 (d, *J* = 9.0 Hz, 1H), 5.13 (br s, 2H), 5.05 (d, *J* = 11.8 Hz, 3H), 5.02 (d, *J* = 10.1 Hz, 3H), 4.18 (dd, *J* = 8.3, 6.4 Hz, 1H), 2.00 (dq, *J* = 6.6, 6.6, 6.6 Hz, 1H), 1.36 (br s, 9H), 0.74 (d, *J* = 6.6 Hz, 3H), 0.69 (d, *J* = 6.4 Hz, 3H); ¹³C NMR (150 MHz, DMSO-*d*₆) ppm 171.5, 170.3, 170.1, 159.8, 158.2, 155.3, 141.8, 137.4, 137.3, 136.2, 131.2, 128.99, 128.85, 128.83, 128.5, 128.44, 128.37, 128.3, 128.2, 128.1, 128.0, 114.8, 106.4, 101.2, 78.9, 69.8, 69.6, 66.4, 57.7, 56.0, 30.7, 28.6, 19.2, 18.2; [α]_D²⁰ -64.8 (*c* 0.48, CHCl₃); HRMS (APCI): Exact mass calcd for C₅₄H₅₈N₃O₉ [M+H]⁺ 892.4173, found 892.4184.

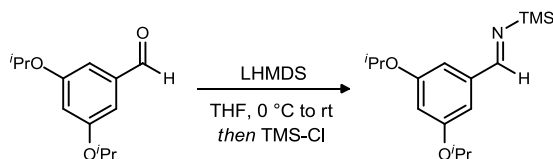


(S)-Benzyl 2-((R)-2-((S)-2-amino-2-(4-(benzyloxy)phenyl)acetamido)-2-(3,5-bis(benzyloxy)phenyl)acetamido)-3-methylbutanoate (59). The Fmoc-tripeptide (29.7 mg, 29.3 μmol) was suspended in dichloromethane (0.9 mL) with stirring, and the reaction atmosphere was replaced with argon. 1,8-Diazabicyclo[5.4.0]undec-7-ene (4.4 μL, 29.3 μmol) was added, and the reaction was allowed to stir until the solution became homogenous. At this point, TLC indicated consumption of starting material, and the reaction was concentrated via rotary evaporation. A crude ¹H NMR was taken in CDCl₃, and the solution was once again concentrated by rotary evaporation. The residue was dissolved in DMSO (approx. 2 mL) and loaded onto the preparatory HPLC in 500 μL portions for purification. The product was isolated as a yellow film (13.4 mg, 58%). HPLC Method: Waters XBridge™ Prep C18 5 μm OBD™ column, 19x150 mm, flow rate = 20 mL/min gradient from 50% CH₃CN/H₂O to 95% CH₃CN/H₂O, *t*_r = 7.5-8.5 minutes. *R*_f = 0.37 (5% MeOH/DCM); IR (film) 3293, 3045, 2963, 2929, 1669, 1601, 1540, 1514, 1453 cm⁻¹; ¹H NMR (600 MHz, DMSO-*d*₆) δ 9.29 (d, *J* = 8.1 Hz, 1H), 8.91 (d, *J* = 8.4 Hz, 1H), 8.63-8.53 (m, 3H), 7.49 (d, *J* = 8.8 Hz, 2H), 7.42-7.31 (m, 20H), 7.04 (d, *J* = 8.7 Hz, 2H), 6.52 (d, *J* = 2.1 Hz, 2H), 6.49 (t, *J* = 2.2 Hz, 1H), 5.77 (d, *J* = 8.2 Hz, 1H), 5.19 (d, *J* = 12.3 Hz, 1H), 5.17-5.16 (m, 1H), 5.16 (d, *J* = 12.3 Hz, 1H), 4.95 (s, 2H), 4.90 (d, *J* = 11.8 Hz, 2H), 4.81 (d, *J* = 11.8 Hz, 2H), 4.22 (dd, *J* = 8.3, 6.2 Hz, 1H), 2.06 (qqd, *J* = 6.6, 6.6, 6.6 Hz, 1H), 0.80 (d, *J* = 6.8 Hz, 3H), 0.74 (d, *J* = 6.8 Hz, 3H); ¹³C NMR (150 MHz, DMSO-*d*₆) ppm 171.7, 169.7, 167.6, 159.7, 159.3, 158.2 (q, ²*J*_{CF} = 32.3 Hz, 1C), 141.2, 137.10, 137.07, 136.2, 129.7, 128.93, 128.89, 128.85, 128.80, 128.7, 128.6, 128.4, 128.2, 128.1, 127.9, 126.4, 115.3, 105.6, 101.4, 69.6, 69.5, 66.6, 57.8, 55.7, 54.9, 30.7, 19.2, 18.2 [CF₃ not observed]; ¹⁹F NMR (282 MHz, DMSO-*d*₆) δ -71.97 (s, 3F); [α]_D²⁰ -2.0 (*c* 1.34, CHCl₃); HRMS (APCI): Exact mass calcd for C₄₉H₅₀N₃O₇ [M+H]⁺ 792.3649, found 792.3688.

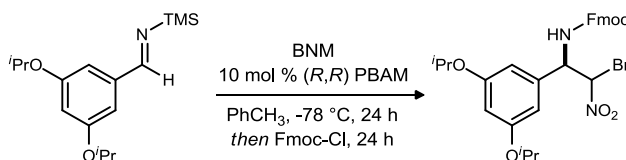


(S)-Benzyl 2-((R)-2-((S)-2-(4-(benzyloxy)phenyl)-2-(2-phenylacetamido)acetamido)-2-(3,5-bis(benzyloxy)phenyl)acetamido)-3-methylbutanoate (63). The amine (12 mg, 13 μmol) was dissolved in 2-

methyltetrahydrofuran (130 μL) and cooled to 0 $^{\circ}\text{C}$ using an ice/water bath. The α -bromonitroalkane (3.7 mg, 16 μmol), potassium carbonate (2.2 mg, 16 μmol), water (12 μL , 66 μmol), and *N*-iodosuccinimide (3.0 mg, 13 μmol) were added, and the reaction was placed under an oxygen atmosphere. The reaction was allowed to warm slowly to room temperature and was stirred for two days. The solvent was removed *in vacuo*, and the material was dissolved in DMSO and purified via reversed-phase preparatory HPLC (60-95% acetonitrile/water, eluted at 9.776 min) to provide the product as a white film (5.9 mg, 49%). $R_f = 0.89$ (5% MeOH/DCM); IR (film) 3291, 3064, 3033, 2961, 2926, 1733, 1633, 1604, 1512, 1451, 1379 cm^{-1} ; ^1H NMR (600 MHz, DMSO- d_6) δ 8.99 (d, $J = 8.3$ Hz, 1H), 8.73 (d, $J = 8.5$ Hz, 1H), 8.72 (d, $J = 8.3$ Hz, 1H), 7.43-7.25 (m, 27H), 6.91 (d, $J = 8.8$ Hz, 2H), 6.65 (d, $J = 2.0$ Hz, 2H), 6.49 (dd, $J = 2.1, 2.1$ Hz, 1H), 5.74 (d, $J = 8.0$ Hz, 1H), 5.66 (d, $J = 8.3$ Hz, 1H), 5.18 (d, $J = 12.4$ Hz, 1H), 5.15 (d, $J = 12.4$ Hz, 1H), 4.95 (d, $J = 11.9$ Hz, 1H), 4.94 (d, $J = 11.8$ Hz, 2H), 4.93 (d, $J = 12.1$ Hz, 1H), 4.88 (d, $J = 11.8$ Hz, 2H), 4.20 (dd, $J = 8.3, 6.3$ Hz, 1H), 3.58 (d, $J = 14.0$ Hz, 1H), 3.53 (d, $J = 14.0$ Hz, 1H), 2.03 (dt, $J = 6.7, 6.7, 6.7$ Hz, 1H), 0.78 (d, $J = 6.8$ Hz, 3H), 0.73 (d, $J = 6.8$ Hz, 3H); ^{13}C NMR (150 MHz, DMSO- d_6) ppm 171.7, 170.2, 170.13, 170.09, 159.7, 158.2, 141.6, 137.4, 137.2, 136.8, 136.2, 129.5, 128.90, 128.88, 128.84, 128.79, 128.6, 128.53, 128.48, 128.3, 128.2, 128.1, 128.0, 126.7, 114.8, 106.0, 101.3, 69.7, 69.5, 66.5, 57.9, 55.9, 55.5, 42.2, 30.6, 19.2, 18.3; $[\alpha]_D^{20} -2.9$ (c 0.59, DMSO); HRMS (ESI): Exact mass calcd for $\text{C}_{57}\text{H}_{55}\text{N}_3\text{NaO}_8$ $[\text{M}+\text{Na}]^+$ 932.3887, found 932.3896.



(*E*)-*N*-(3,5-Diisopropoxybenzylidene)-1,1,1-trimethylsilanamine (65). Lithium hexamethyldisilylamide (376 mg, 2.25 mmol) was loaded into a flame-dried 25-mL round-bottomed flask containing a magnetic stir bar under argon atmosphere and cooled to 0 $^{\circ}\text{C}$. Freshly distilled tetrahydrofuran (0.75 mL) was added via syringe. The aldehyde (500 mg, 2.25 mmol) was added via μ syringe, and the reaction was stirred for 5 minutes at 0 $^{\circ}\text{C}$. The ice/water bath was removed, and the reaction was allowed to warm to room temperature. After one hour, freshly distilled chlorotrimethylsilane (28.0 μL , 225 μmol) was added via μ syringe, and the reaction was stirred at room temperature for one hour, after which time hexanes (7.5 mL, dried over molecular sieves for at least two hours under argon atmosphere) was added via syringe. The reaction mixture was transferred via cannula to a Schlenk filter and was filtered over sodium sulfate under argon atmosphere and collected in a two-neck 100-mL round-bottomed flask. The reaction flask was rinsed with hexanes (2.0 mL), and the rinse was filtered and collected. The filtered solution was transferred via cannula to a flame-dried 25-mL round-bottomed flask under argon atmosphere, then concentrated via rotary evaporation. Care was taken to minimize exposure to air. Following concentration, the imine was placed under high vacuum for ten minutes, and a crude ^1H NMR showed clean material. The imine was used crude for the next reaction. (Note: This imine is not stable for extended periods of time and must be used immediately. Decomposition occurs in less than 2.5 h.) ^1H NMR (400 MHz, CDCl_3) δ 8.86 (s, 1H), 6.94 (d, $J = 2.2$ Hz, 2H), 6.55 (t, $J = 2.2$ Hz, 1H), 4.62 (septet, $J = 6.1$ Hz, 2H), 1.36 (d, $J = 6.0$ Hz, 12 H), 0.26 (s, 9H).

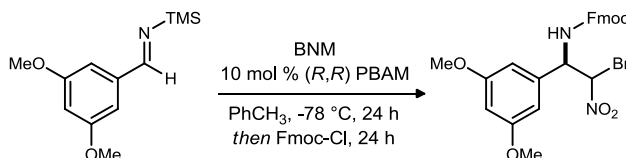


(9H-Fluoren-9-yl)methyl ((1*R*)-2-bromo-1-(3,5-diisopropoxyphenyl)-2-nitroethyl)carbamate (66). The crude imine (2.25 mmol) was dissolved in toluene (7.5 mL) and cooled to -20 $^{\circ}\text{C}$. (*R,R*)-PBAM (114 mg, 225 μmol) was added in one portion, and bromonitromethane (175 μL , 2.25 mmol) was added in five portions over ten hours. The reaction was allowed to stir at -20 $^{\circ}\text{C}$ for 48 h, then Fmoc-Cl (582 mg, 2.25 mmol) was added in one portion, and the reaction was allowed to warm to 0 $^{\circ}\text{C}$. The reaction was stirred for 24 h at this temperature, then the solvent was removed *in vacuo*, and the crude residue was purified via flash column chromatography

(10% ethyl acetate/hexanes) to give the desired product as a white solid (335 mg, 26%, 17/18% ee). The compound was characterized as a 1.5:1 mixture of diastereomers. $R_f = 0.37$ (20% EtOAc/hexanes); IR (film) 3332, 2978, 2936, 1698, 1597, 1567, 1529, 1453 cm^{-1} ; ^1H NMR (600 MHz, DMSO- d_6) δ 8.42 (d, $J = 9.8$ Hz, 1H_{D1}), 8.26 (d, $J = 10.0$ Hz, 1H_{D2}), 7.89 (dd, $J = 7.1, 7.1$ Hz, 2H_{D1} & 2H_{D2}), 7.72 (d, $J = 7.6$ Hz, 1H_{D2}), 7.69 (d, $J = 7.5$ Hz, 1H_{D2}), 7.64 (d, $J = 7.3$ Hz, 1H_{D1}), 7.63 (d, $J = 7.1$ Hz, 1H_{D1}), 7.43-7.39 (m, 2H_{D1} & 2H_{D2}), 7.34-7.24 (m, 2H_{D1} & 2H_{D2}), 6.73 (d, $J = 7.8$ Hz, 1H_{D2}), 6.64 (d, $J = 8.5$ Hz, 1H_{D1}), 6.63 (s, 2H_{D1}), 6.55 (d, $J = 1.9$ Hz, 2H_{D2}), 6.39 (dd, $J = 2.1, 2.1$ Hz, 1H_{D1} & 1H_{D2}), 5.36 (dd, $J = 9.7, 8.0$ Hz, 1H_{D2}), 5.27 (dd, $J = 9.6, 9.6$ Hz, 1H_{D1}), 4.61 (qq, $J = 6.0, 6.0$ Hz, 2H_{D1}), 4.58 (qq, $J = 6.1, 6.1$ Hz, 2H_{D2}), 4.47 (dd, $J = 10.5, 6.6$ Hz, 1H_{D2}), 4.36 (dd, $J = 10.3, 6.8$ Hz, 1H_{D1}), 4.31 (dd, $J = 10.5, 7.2$ Hz, 1H_{D2}), 4.27-4.19 (m, 2H_{D1} & 1H_{D2}), 1.27-1.23 (m, 12H_{D1} & 12H_{D2}); ^{13}C NMR (150 MHz, DMSO- d_6) ppm 159.2, 159.1, 156.0, 155.6, 144.12, 144.06, 144.0, 143.9, 141.2, 141.1, 138.39, 138.35, 128.09, 128.06, 127.51, 127.48, 127.42, 127.41, 125.7, 125.6, 125.5, 120.6, 107.6, 107.1, 103.6, 103.5, 83.9, 81.1, 69.7, 69.6, 66.5, 66.4, 59.5, 59.0, 47.0, 46.9, 22.3, 22.20, 22.15; HRMS (ESI): Exact mass calcd for $\text{C}_{29}\text{H}_{32}\text{N}_2\text{O}_6$ $[\text{M}+\text{H}]^+$ 583.1444, found 583.1440.

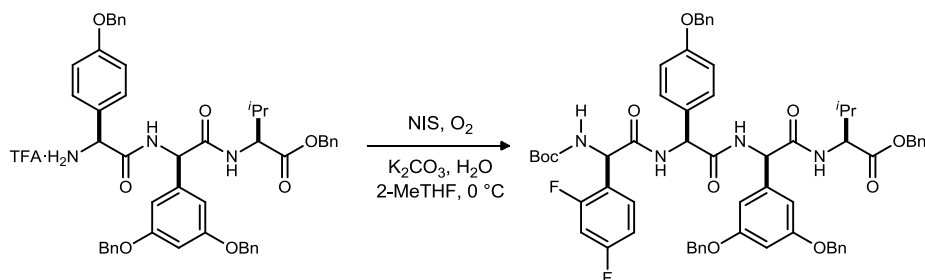


(E)-N-(3,5-Dimethoxybenzylidene)-1,1,1-trimethylsilanimine (68). Lithium hexamethyldisilylamide (378 mg, 2.26 mmol) was loaded into a flame-dried 25-mL round-bottomed flask containing a magnetic stir bar under argon atmosphere and cooled to 0 °C. In a separate flame-dried flask under argon, the aldehyde (375 mg, 2.26 mmol) was dissolved in freshly distilled tetrahydrofuran (0.75 mL). The solution was transferred via cannula to the reaction flask, and the reaction was stirred for 5 minutes at 0 °C. The ice/water bath was removed, and the reaction was allowed to warm to room temperature. After one hour, freshly distilled chlorotrimethylsilane (28.4 μL , 226 μmol) was added via $\mu\text{syringe}$, and the reaction was stirred at room temperature for one hour, after which time hexanes (7.5 mL, dried over molecular sieves for at least two hours under argon atmosphere) was added via syringe. The reaction mixture was transferred via cannula to a Schlenk filter and was filtered over sodium sulfate under argon atmosphere and collected in a two-neck 100-mL round-bottomed flask. The reaction flask was rinsed with hexanes (2.0 mL), and the rinse was filtered and collected. The filtered solution was transferred via cannula to a flame-dried 25-mL round-bottomed flask under argon atmosphere, then concentrated via rotary evaporation. Care was taken to minimize exposure to air. Following concentration, the imine was placed under high vacuum for ten minutes, and a crude ^1H NMR showed clean material. The imine was used crude for the next reaction. ^1H NMR (400 MHz, CDCl_3) δ 8.90 (s, 1H), 6.98 (d, $J = 2.4$ Hz, 2H), 6.58 (t, $J = 2.3$ Hz, 1H), 3.87 (s, 6H), 0.28 (s, 9H).

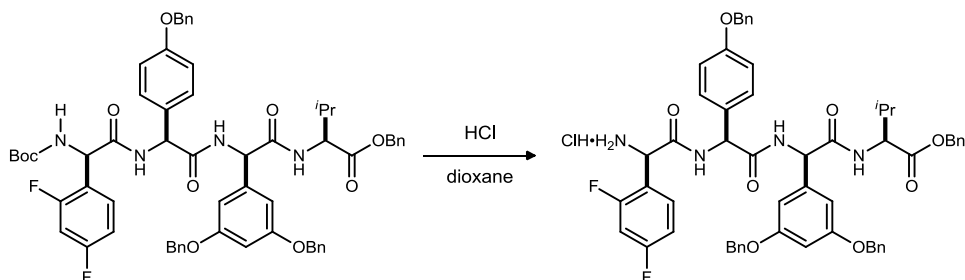


(9H-Fluoren-9-yl)methyl ((1R)-2-bromo-1-(3,5-dimethoxyphenyl)-2-nitroethyl)carbamate (69). The crude imine (2.26 mmol) was dissolved in toluene (7.5 mL) and cooled to -78 °C. (*R,R*)-PBAM (115 mg, 226 μmol) was added in one portion, and bromonitromethane (175 μL , 2.26 mmol) was added in five portions over ten hours. The reaction was allowed to stir vigorously at -78 °C for 48 h, then Fmoc-Cl (584 mg, 2.26 mmol) was added in one portion, and the reaction was allowed to warm to 0 °C. The reaction was stirred for 24 h at this temperature, then the solvent was removed *in vacuo*, and the crude residue was purified via flash column chromatography (15% ethyl acetate/hexanes) to give the desired product as a white solid (326 mg, 27%, 28/45% ee). The compound was characterized as a 1.5:1 mixture of diastereomers. $R_f = 0.21$ (20% EtOAc/hexanes); IR (film) 3325, 3012, 2959, 1701, 1601, 1565, 1520, 1454 cm^{-1} ; ^1H NMR (600 MHz, DMSO- d_6) δ 8.44 (d, $J = 9.8$ Hz, 1H), 8.29 (d, $J = 9.9$ Hz, 1H), 7.89 (dd, $J = 6.7, 6.7$ Hz, 4H), 7.72 (d, $J = 7.5$ Hz, 1H), 7.70 (d, $J = 7.5$ Hz,

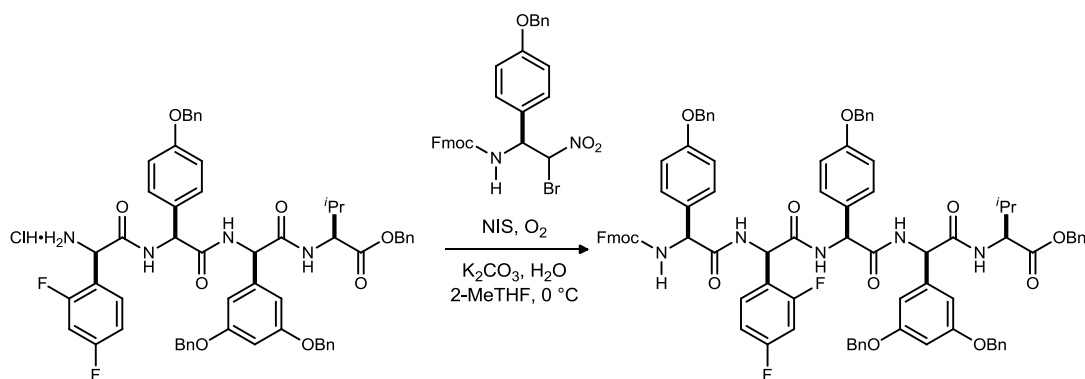
1H), 7.64 (d, $J = 7.3$ Hz, 1H), 7.63 (d, $J = 7.2$ Hz, 1H), 7.43-7.39 (m, 4H), 7.34-7.25 (m, 4H), 6.77 (d, $J = 7.7$ Hz, 1H), 6.70 (d, $J = 1.5$ Hz, 2H), 6.65 (d, $J = 9.7$ Hz, 1H), 6.63 (d, $J = 2.0$ Hz, 2H), 6.49-6.48 (m, 2H), 5.40 (dd, $J = 9.8, 7.9$ Hz, 1H), 5.29 (dd, $J = 9.7, 9.7$ Hz, 1H), 4.48 (dd, $J = 10.6, 6.7$ Hz, 1H), 4.36 (dd, $J = 10.5, 6.9$ Hz, 1H), 4.32 (dd, $J = 10.6, 7.1$ Hz, 1H), 4.27-4.24 (m, 2H), 4.21-4.19 (m, 1H), 3.76 (s, 6H), 3.74 (s, 6H); ^{13}C NMR (150 MHz, DMSO- d_6) ppm 161.0, 160.9, 156.0, 155.5, 144.1, 144.0, 141.2, 141.1, 138.5, 138.4, 128.1, 127.52, 127.49, 127.4, 125.7, 125.55, 125.47, 120.6, 106.7, 106.1, 100.7, 100.6, 83.9, 80.9, 66.44, 66.37, 59.5, 59.0, 55.7, 47.0, 46.9; HRMS (ESI): Exact mass calcd for $\text{C}_{27}\text{H}_{22}\text{BrN}_2\text{O}_6$ $[\text{M}+\text{H}]^+$ 549.0661, found 549.0650.



(6*R*,9*S*,12*R*,15*S*)-Benzyl 9-(4-(benzyloxy)phenyl)-12-(3,5-bis(benzyloxy)phenyl)-6-(2,4-difluorophenyl)-15-isopropyl-2,2-dimethyl-4,7,10,13-tetraoxo-3-oxa-5,8,11,14-tetraazahexadecan-16-oate (72). The amine salt (12.7 mg, 14.0 μmol) was dissolved in 2-methyltetrahydrofuran (200 μL) and cooled to 0 $^\circ\text{C}$. Water (12.6 μL , 700 μmol), potassium carbonate (2.3 mg, 17 μmol), *N*-iodosuccinimide (3.2 mg, 14 μmol), and the Boc-protected α -bromonitroalkane (6.4 mg, 17 μmol) were added. The atmosphere in the reaction vessel was replaced with oxygen, and the reaction was allowed to slowly warm to room temperature and stirred for two days. The reaction mixture was diluted with dichloromethane and washed sequentially with 1 N aq HCl, satd aq $\text{Na}_2\text{S}_2\text{O}_4$, and brine, and then dried (MgSO_4), filtered, and concentrated to give an oil (15 mg). An analytical sample was obtained via reversed-phase preparatory HPLC (70% to 95% $\text{CH}_3\text{CN}/\text{H}_2\text{O}$ gradient over 8 min, C18 column, $t_r = 8.5$ -9.5 min) to give the desired product as a white film (4.4 mg, 30% yield). $R_f = 0.15$ (2% MeOH/DCM); IR (film) 3299, 3065, 3035, 2962, 2927, 2858, 1729, 1679, 1641, 1605, 1509, 1453, 1380 cm^{-1} ; ^1H NMR (600 MHz, DMSO- d_6) δ 9.05 (d, $J = 7.7$ Hz, 1H), 8.76 (d, $J = 8.4$ Hz, 1H), 8.52 (d, $J = 7.8$ Hz, 1H), 7.55 (d, $J = 8.1$ Hz, 1H), 7.43-7.30 (m, 23 H), 7.19 (ddd, $J = 10.1, 10.1, 2.4$ Hz, 1H), 6.97 (ddd, $J = 8.4, 8.4, 2.1$ Hz, 1H), 6.88 (d, $J = 8.6$ Hz, 2H), 6.63 (br s, 2H), 6.48 (dd, $J = 2.1, 2.1$ Hz, 1H), 5.72 (d, $J = 7.2$ Hz, 1H), 5.67 (d, $J = 8.2$ Hz, 1H), 5.51 (d, $J = 8.5$ Hz, 1H), 5.19 (d, $J = 12.3$ Hz, 1H), 5.14 (d, $J = 12.4$ Hz, 1H), 5.06-5.04 (m, 1H), 4.94-4.91 (m, 2H), 4.93 (d, $J = 11.5$ Hz, 2H), 4.87 (d, $J = 11.9$ Hz, 2H), 4.21 (dd, $J = 8.3, 6.4$ Hz, 1H), 2.06-2.00 (m, 1H), 1.38 (s, 9H), 0.78 (d, $J = 6.7$ Hz, 3H), 0.72 (d, $J = 6.8$ Hz, 3H); ^{13}C NMR (150 MHz, DMSO- d_6) ppm 171.7, 170.0, 169.7, 168.9, 160.58 (d, $^1J_{\text{CF}} = 251.0$ Hz), 160.54 (d, $^1J_{\text{CF}} = 242.5$ Hz), 159.7, 158.2, 141.5, 137.3, 137.2, 136.2, 131.1, 130.9 (dd, $^3J_{\text{CF}} = 10.2, 4.4$ Hz), 128.93, 128.88, 128.84, 128.78, 128.7, 128.6, 128.5, 128.4, 128.3, 128.18, 128.15, 128.08, 128.01, 127.95, 122.4 (dd, $^2J_{\text{CF}} = 15.2$ Hz, $^4J_{\text{CF}} = 4.1$ Hz), 114.7, 111.6 (dd, $^2J_{\text{CF}} = 21.9$ Hz, $^4J_{\text{CF}} = 2.9$ Hz), 106.0, 105.2, 104.1 (dd, $^2J_{\text{CF}} = 26.7, 26.7$ Hz), 101.3, 79.1, 69.6, 69.5, 66.5, 57.8, 55.9, 55.6, 52.0, 40.7, 28.5, 19.2, 18.3; ^{19}F NMR (282 MHz, DMSO- d_6) ppm -71.58 (s, 1F) $[\text{F}_3\text{CCOOH}]$, -109.01 (dd, $J = 8.8, 8.8$ Hz, 1F), -110.44 (d, $J = 6.8$ Hz, 1F); $[\alpha]_D^{20} -5.3$ (c 0.32, CHCl_3); HRMS (ESI): Exact mass calcd for $\text{C}_{62}\text{H}_{63}\text{F}_2\text{N}_4\text{O}_{10}$ $[\text{M}+\text{H}]^+$ 1061.4512, found 1061.4508. (Note: The $[\text{M}+\text{NH}_4]^+$ and $[\text{M}+\text{Na}]^+$ ions were also observed.)

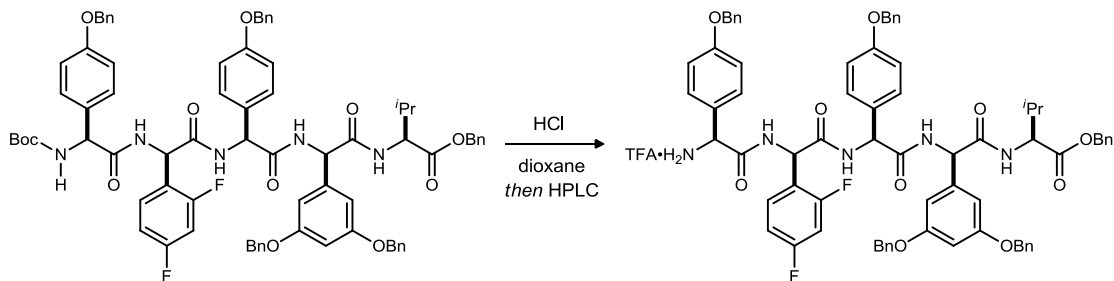


(S)-Benzyl 2-((R)-2-((S)-2-((R)-2-Amino-2-(2,4-difluorophenyl)acetamido)-2-(4-(benzyloxy)phenyl)acetamido)-2-(3,5-bis(benzyloxy)phenyl)acetamido)-3-methylbutanoate hydrochloride (73). To the unpurified Boc-protected tetrapeptide (15.9 mg, 15 μmol) was added HCl (350 μL , 4.0 M in dioxane). The reaction was stirred at room temperature for 18 h, and the solvent and excess HCl were then removed via rotary evaporation and reduced pressure to give the desired compound as its HCl salt. It was used without further purification. $R_f = 0.25$ (2% MeOH/DCM); IR (film) 3301, 3036, 2925, 2855, 1729, 1640, 1605, 1511, 1454 cm^{-1} ; ^1H NMR (600 MHz, DMSO- d_6) δ 9.38 (d, $J = 8.0$ Hz, 1H), 9.23 (d, $J = 8.5$ Hz, 1H), 8.81 (d, $J = 8.3$ Hz, 1H), 8.66 (br s, 3H), 7.45-7.32 (m, 26H), 7.24 (d, $J = 8.7$ Hz, 2H), 7.10 (ddd, $J = 8.5, 8.5, 2.3$ Hz, 1H), 6.85 (d, $J = 8.8$ Hz, 2H), 6.67 (d, $J = 2.2$ Hz, 2H), 6.49 (dd, $J = 2.2, 2.2$ Hz, 1H), 5.91 (d, $J = 8.0$ Hz, 1H), 5.70 (d, $J = 8.5$ Hz, 1H), 5.30 (br s, 1H), 5.20 (d, $J = 12.4$ Hz, 1H), 5.16 (d, $J = 12.4$ Hz, 1H), 4.95 (d, $J = 11.9$ Hz, 2H), 4.92 (d, $J = 15.8$ Hz, 1H), 4.89 (d, $J = 16.0$ Hz, 1H), 4.88 (d, $J = 11.9$ Hz, 2H), 4.22 (dd, $J = 8.3, 6.1$ Hz, 1H), 2.07-2.02 (m, 1H), 0.79 (d, $J = 6.8$ Hz, 3H), 0.72 (d, $J = 6.8$ Hz, 3H); ^{13}C NMR (150 MHz, DMSO- d_6) ppm 171.9, 170.1, 169.3, 166.1, 163.3 (dd, $^1J_{\text{CF}} = 248.9$ Hz, $^3J_{\text{CF}} = 12.3$ Hz), 160.9 (dd, $^1J_{\text{CF}} = 252.1$ Hz, $^3J_{\text{CF}} = 13.3$ Hz), 159.7, 158.3, 141.4, 137.3, 137.2, 136.2, 131.4 (dd, $^3J_{\text{CF}} = 11.2, 4.4$ Hz), 130.7, 128.93, 128.85, 128.79, 128.66, 128.5, 128.3, 128.22, 128.16, 128.07, 127.97, 118.0-117.8 (m), 114.76, 112.3 (dd, $^2J_{\text{CF}} = 19.3$ Hz, $^4J_{\text{CF}} = 2.8$ Hz), 106.0, 104.9 (dd, $^2J_{\text{CF}} = 26.0, 26.0$ Hz), 101.3, 69.7, 69.5, 66.5, 57.8, 55.6, 55.5, 49.0, 30.7, 19.2, 18.2; ^{19}F NMR (282 MHz, DMSO- d_6) ppm -105.69 (s, 1F), -107.38 (s, 1F); $[\alpha]_D^{20}$ -11.0 (c 0.31, CHCl_3); HRMS (ESI): Exact mass calcd for $\text{C}_{57}\text{H}_{55}\text{F}_2\text{N}_4\text{O}_8$ $[\text{M}+\text{H}]^+$ 961.3988, found 961.3976.

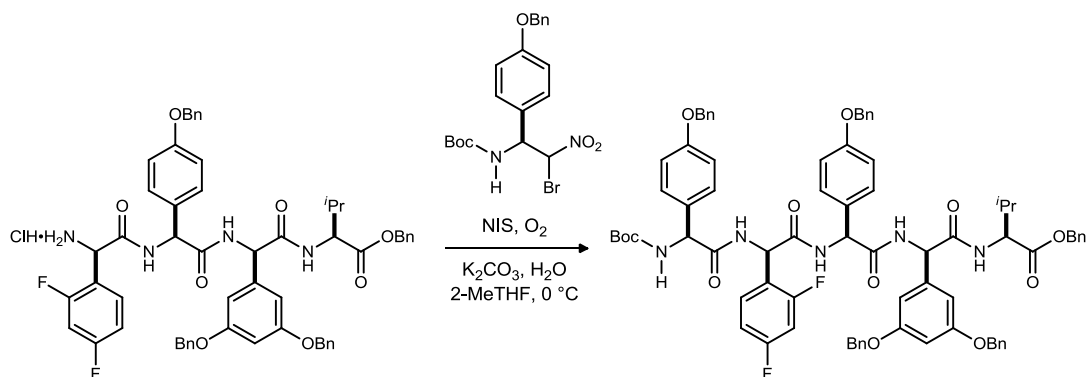


(5S,8R,11S,14R,17S)-Benzyl 5,11-bis(4-(benzyloxy)phenyl)-14-(3,5-bis(benzyloxy)phenyl)-8-(2,4-difluorophenyl)-1-(9H-fluoren-9-yl)-17-isopropyl-3,6,9,12,15-pentaoxo-2-oxa-4,7,10,13,16-pentaazaocetadecan-18-oate (74). The crude amine salt (15.0 μmol) was dissolved in 2-methyl tetrahydrofuran (200 μL) and cooled to 0 $^{\circ}\text{C}$. Water (13.5 μL , 749 μmol), potassium carbonate (5.2 mg, 37 μmol), *N*-iodosuccinimide (3.2 mg, 15 μmol), and the Fmoc-protected α -bromonitroalkane (10.3 mg, 18 μmol) were added. The atmosphere in the reaction vessel was replaced with oxygen, and the reaction was allowed to warm to room temperature overnight and stirred for 48 h. The reaction mixture was diluted with dichloromethane and washed sequentially with 1 N aq HCl, satd aq $\text{Na}_2\text{S}_2\text{O}_4$, and brine, and then dried (MgSO_4), filtered, and concentrated to give a crude oil. Trituration with ethyl acetate and hexanes, followed by filtration, resulted in a pure white solid (4 mg, 19% yield over two steps). $R_f = 0.31$ (2% MeOH/DCM); IR (film) 3289, 3067, 3036, 2963, 2929, 1719, 1639, 1608, 1509, 1453 cm^{-1} ; ^1H NMR (600 MHz, DMSO- d_6) δ 9.09 (d, $J = 8.2$ Hz, 1H), 8.91 (d, $J = 7.8$ Hz, 1H), 8.89 (d, $J = 7.8$ Hz, 1H), 8.78 (d, $J = 8.3$ Hz, 1H), 8.03 (d, $J = 8.5$ Hz, 1H), 7.90-7.87 (m, 2H), 7.74 (dd, $J = 7.2, 7.2$ Hz, 2H), 7.45-7.27 (m, 33H), 7.13-7.07 (m, 2H), 6.94 (d, $J = 8.6$ Hz, 2H), 6.84 (d, $J = 8.7$ Hz, 2H), 6.82-6.80 (m, 1H), 6.63 (d, $J = 1.7$ Hz, 2H), 6.47 (br s, 1H), 5.85 (d, $J = 7.7$ Hz, 1H), 5.78 (d, $J = 7.9$ Hz, 1H), 5.70 (d, $J = 8.3$ Hz, 1H), 5.40 (d, $J = 8.5$ Hz, 1H), 5.17 (d, $J = 12.4$ Hz, 1H), 5.13 (d, $J = 12.6$ Hz, 1H), 5.11-5.08 (m, 3H), 5.03-5.00 (m, 1H), 4.92 (d, $J = 11.8$ Hz, 2H), 4.85 (d, $J = 11.6$ Hz, 2H), 4.25-4.19 (m, 4H), 2.05-2.01 (m, 1H), 0.77 (d, $J = 6.7$ Hz, 3H), 0.71 (d, $J = 6.8$ Hz, 3H); ^{13}C NMR (150 MHz, DMSO- d_6) ppm 171.8, 170.4, 170.1, 169.8, 159.7, 158.2, 156.0, 144.3, 144.1, 141.7, 141.1, 137.5, 137.2, 136.1, 130.9, 129.0, 128.9, 128.83, 128.75, 128.6, 128.5, 128.3, 128.2, 128.1, 128.0, 127.9, 127.5, 125.8, 120.5, 114.8, 114.6, 105.9, 104.2, 101.3, 69.6, 69.53, 69.45, 66.5, 66.4, 57.8, 55.8, 55.6, 50.5, 47.0, 30.7, 19.2, 18.2; $[\alpha]_D^{20}$

+24.3 (*c* 0.40, CHCl₃); HRMS (ESI): Exact mass calcd for C₈₇H₇₈F₂N₅O₁₂ [M+H]⁺ 1422.5615, found 1422.5630.

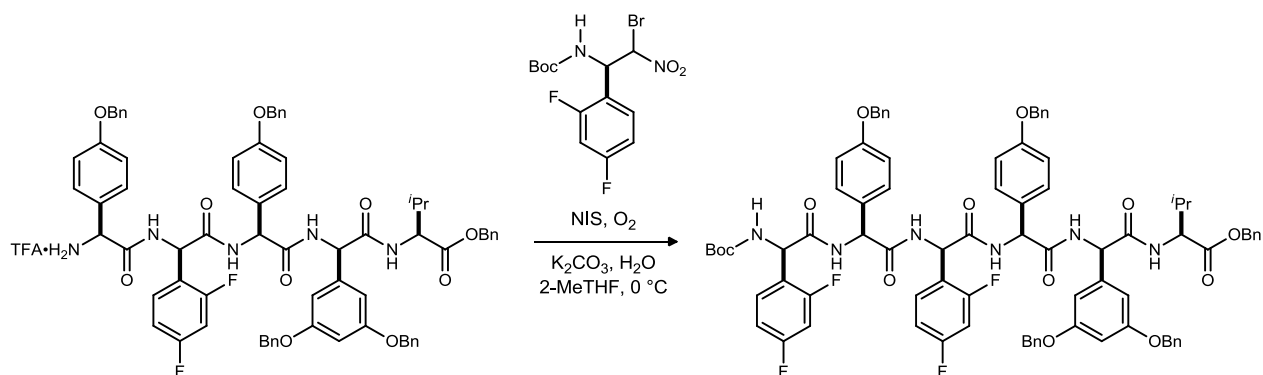


(2*S*,5*R*,8*S*,11*R*,14*S*)-Benzyl 14-amino-8,14-bis(4-(benzyloxy)phenyl)-5-(3,5-bis(benzyloxy)phenyl)-11-(2,4-difluorophenyl)-2-isopropyl-4,7,10,13-tetraoxo-3,6,9,12-tetraazatetradecan-1-oate (75). The pentapeptide (50 mg, 38 μmol) was dissolved in 4.0 M HCl in dioxane (1.0 mL) and allowed to stir for four hours at room temperature. The crude reaction was concentrated via rotary evaporation, then dissolved in DMSO and purified via preparatory HPLC to give the TFA salt as a thin film (13.5 mg, 27%). HPLC Method: Waters XBridgeTM Prep C18 5 μm OBDTM column, 19x150 mm, flow rate = 20 mL/min gradient from 50% CH₃CN/H₂O to 95% CH₃CN/H₂O, *t_r* = 9.0-9.5 minutes. *R_f* = 0.54 (10% MeOH/CH₂Cl₂); IR (film) 3274, 3066, 2963, 2929, 2872, 1724, 1662, 1638, 1607, 1537, 1511, 1454, 1382 cm⁻¹; ¹H NMR (600 MHz, DMSO-*d*₆) δ 9.19 (d, *J* = 8.2 Hz, 1H), 9.15 (d, *J* = 8.2 Hz, 1H), 9.12 (d, *J* = 8.5 Hz, 1H), 9.78 (d, *J* = 8.3 Hz, 1H), 8.56 (br d, *J* = 4.4 Hz, 2H), 7.45-7.30 (m, 25H), 7.11 (ddd, *J* = 9.8, 9.8, 2.4 Hz, 1H), 7.04 (d, *J* = 8.8 Hz, 2H), 7.00 (ddd, *J* = 8.5, 8.5, 6.6 Hz, 1H), 6.86 (d, *J* = 8.8 Hz, 2H), 6.83 (ddd, *J* = 8.5, 8.5, 2.2 Hz, 1H), 6.65 (d, *J* = 2.0 Hz, 2H), 6.49 (dd, *J* = 2.0 Hz, 1H), 6.01 (d, *J* = 8.2 Hz, 1H), 5.82 (d, *J* = 8.2 Hz, 1H), 5.68 (d, *J* = 8.5 Hz, 1H), 5.21 (d, *J* = 12.3 Hz, 1H), 5.17 (d, *J* = 12.3 Hz, 1H), 5.13 (br s, 2H), 5.03-5.00 (br m, 1H), 4.94 (d, *J* = 11.8 Hz, 2H), 4.92 (d, *J* = 12.1 Hz, 1H), 4.89 (d, *J* = 11.8 Hz, 1H), 4.88 (d, *J* = 11.9 Hz, 2H), 4.22 (dd, *J* = 8.2, 6.2 Hz, 1H), 2.05 (qqd, *J* = 6.8, 6.8, 6.2 Hz, 1H), 0.78 (d, *J* = 6.8 Hz, 3H), 0.72 (d, *J* = 6.8 Hz, 3H); ¹³C NMR (150 MHz, DMSO-*d*₆) ppm 171.8, 170.2, 169.7, 167.9, 167.5, 162.2 (dd, ¹*J*_{CF} = 247.2 Hz, ³*J*_{CF} = 11.9 Hz), 160.5 (dd, ¹*J*_{CF} = 251.0 Hz, ³*J*_{CF} = 12.2 Hz), 159.7, 159.2, 158.4 (q, ²*J*_{CF} = 33.2 Hz), 158.2, 141.4, 137.3, 137.23, 137.18, 137.14, 130.9, 130.0 (dd, ³*J*_{CF} = 9.8, 4.6 Hz), 129.6, 128.94, 128.85, 128.78, 128.75, 128.69, 128.58, 128.3, 128.2, 128.1, 128.0, 126.2, 121.8 (dd, ²*J*_{CF} = 15.4 Hz, ⁴*J*_{CF} = 3.3 Hz), 115.3, 114.7, 111.5 (dd, ²*J*_{CF} = 20.8 Hz, ⁴*J*_{CF} = 3.1 Hz), 106.0, 104.4 (dd, ²*J*_{CF} = 25.8, 25.8 Hz), 101.3, 69.7, 69.6, 69.5, 66.6, 57.8, 55.7, 55.4, 55.0, 50.3, 30.7, 19.2, 18.2; ¹⁹F NMR (282 MHz, DMSO-*d*₆) δ -72.24 (s, 3F), -108.57 (d, *J* = 7.6 Hz, 1F), -109.26 (d, *J* = 7.4 Hz, 1F); [α]_D²⁰ -4.9 (*c* 0.68, CHCl₃); HRMS (CI): Exact mass calcd for C₇₄H₆₇F₅N₅O₁₁ [M]⁺ 1296.48, found xx. *Submitted.*



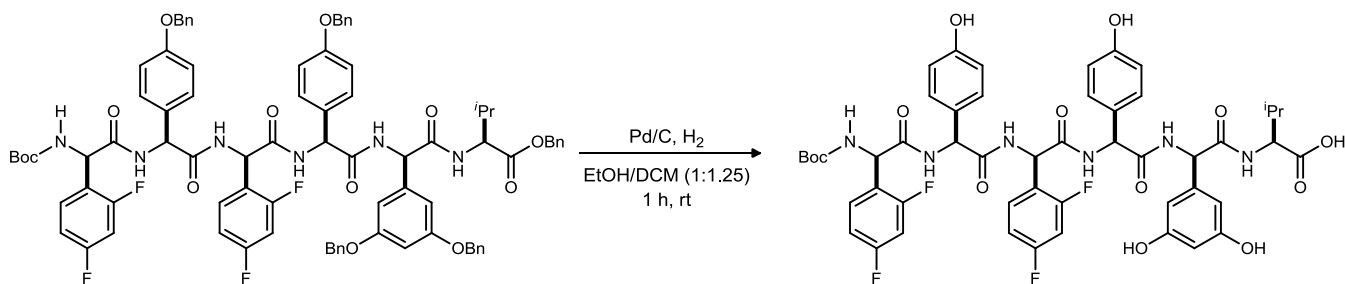
(6*S*,9*R*,12*S*,15*R*,18*S*)-Benzyl 6,12-bis(4-(benzyloxy)phenyl)-15-(3,5-bis(benzyloxy)phenyl)-9-(2,4-difluorophenyl)-18-isopropyl-2,2-dimethyl-4,7,10,13,16-pentaoxo-3-oxa-5,8,11,14,17-pentaazanonadecan-19-oate (76). The crude amine salt (200 μmol) was dissolved in 2-methyl tetrahydrofuran (2.00 mL) and cooled to 0 °C. Water (181 μL, 10.0 mmol), potassium carbonate (69 mg, 500 μmol), *N*-iodosuccinimide (45.0 mg, 200 μmol), and the Boc-protected α-bromonitroalkane (109 mg, 240 μmol) were added. The atmosphere in the reaction vessel was replaced with oxygen, and the reaction was allowed to warm to room temperature overnight

and stirred for 48 h. The solvent was removed *in vacuo*, then the crude residue was diluted with dichloromethane and washed sequentially with 1 N aq HCl, satd aq Na₂S₂O₄, and brine, and then dried (MgSO₄), filtered, and concentrated to give a crude oil. Trituration with ethyl acetate and hexanes, followed by filtration, resulted in a tan solid (171 mg, 66% yield over two steps). An analytical sample was obtained via flash column chromatography (20% to 100% ethyl acetate in hexanes). *R_f* = 0.94 (5% MeOH/DCM); IR (film) 3289, 3034, 2966, 1640, 1603, 1508, 1454, 1378, 1307 cm⁻¹; ¹H NMR (600 MHz, DMSO-*d*₆) δ 9.08 (d, *J* = 8.2 Hz, 1H), 8.86 (d, *J* = 7.4 Hz, 1H), 8.79 (d, *J* = 8.4 Hz, 1H), 8.76 (d, *J* = 7.7 Hz, 1H), 7.45-7.28 (m, 26H), 7.22 (d, *J* = 8.1 Hz, 1H), 7.12 (td, *J* = 10.1, 2.5 Hz, 1H), 6.90 (d, *J* = 8.6 Hz, 2H), 6.87 (d, *J* = 8.8 Hz, 2H), 6.83 (br t, *J* = 7.5 Hz, 1H), 6.63 (br s, 2H), 6.47 (dd, *J* = 2.1, 2.0 Hz, 1H), 5.82 (d, *J* = 7.5 Hz, 1H), 5.77 (d, *J* = 7.8 Hz, 1H), 5.70 (d, *J* = 8.3 Hz, 1H), 5.27 (d, *J* = 8.2 Hz, 1H), 5.19 (d, *J* = 12.3 Hz, 1H), 5.15 (d, *J* = 12.4 Hz, 1H), 5.08 (br s, 2H), 4.93 (d, *J* = 11.8 Hz, 2H), 4.91 (d, *J* = 11.5 Hz, 1H), 4.89 (d, *J* = 12.1 Hz, 1H), 4.86 (d, *J* = 11.8 Hz, 2H), 4.22 (dd, *J* = 8.1, 6.4 Hz, 1H), 2.03 (qqd, *J* = 6.7, 6.7, 6.4 Hz, 1H), 0.78 (d, *J* = 6.7 Hz, 3H), 0.72 (d, *J* = 6.8 Hz, 3H); ¹³C NMR (150 MHz, DMSO-*d*₆) ppm 171.8, 170.5, 170.1, 169.8, 168.4, 162.1 (dd, ¹*J*_{CF} = 246.5 Hz, ³*J*_{CF} = 12.4 Hz), 160.4 (dd, ¹*J*_{CF} = 249.7 Hz, ³*J*_{CF} = 13.3 Hz), 159.7, 158.2, 158.1, 155.2, 141.7, 137.5, 137.3, 137.2, 136.2, 131.1, 130.9, 130.3 (br m), 128.94, 128.89, 128.84, 128.77, 128.63, 128.55, 128.4, 128.3, 128.2, 128.13, 128.07, 128.03, 127.95, 122.3 (d, ³*J*_{CF} = 14.8 Hz), 114.8, 114.7, 111.3 (d, ³*J*_{CF} = 21.0 Hz), 105.9, 104.2 (dd, ²*J*_{CF} = 25.8, 25.7 Hz), 101.3, 78.8, 69.6, 69.52, 69.49, 66.5, 57.8, 57.3, 55.8, 55.6, 50.6, 30.7, 28.5, 19.2, 18.2; ¹⁹F NMR (282 MHz, DMSO-*d*₆) ppm -109.03 (d, *J* = 7.4 Hz, 1F), -109.77 (d, *J* = 6.2 Hz, 1F); [α]_D²⁰ 24.3 (*c* 0.40, CHCl₃); HRMS (CI): Exact mass calcd for C₇₇H₇₅F₂N₅O₁₂ [M]⁺ 1299.54, found xx. *Submitted.*



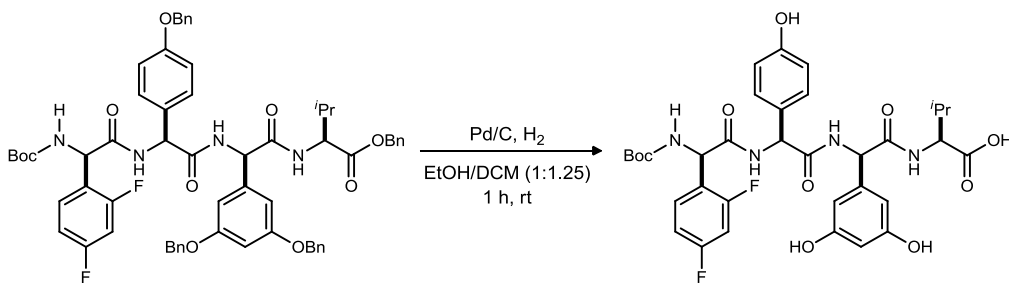
(6R,9S,12R,15S,18R,21S)-benzyl 9,15-bis(4-(benzyloxy)phenyl)-18-(3,5-bis(benzyloxy)phenyl)-6,12-bis(2,4-difluorophenyl)-21-isopropyl-2,2-dimethyl-4,7,10,13,16,19-hexaoxo-3-oxa-5,8,11,14,17,20-hexaazadocosan-22-oate (78). The pure amine salt (39 mg, 30 μmol) was dissolved in 2-methyl tetrahydrofuran (1.0 mL) and cooled to 0 °C. Water (27 μL, 1.5 mmol), potassium carbonate (5.0 mg, 36 μmol), *N*-iodosuccinimide (7.0 mg, 31 μmol), and the Boc-protected α -bromonitroalkane (14 mg, 36 μmol) were added. The atmosphere in the reaction vessel was replaced with oxygen, and the reaction was allowed to warm to room temperature overnight and stirred for 48 h. The solvent was removed *in vacuo*, then the crude residue was diluted with dichloromethane and washed sequentially with 1 N aq HCl, satd aq Na₂S₂O₄, and brine, and then dried (MgSO₄), filtered, and concentrated to give a crude oil. Trituration with ethyl acetate and hexanes, followed by filtration, resulted in a tan solid (15 mg, 34% yield). *R_f* = 0.00 (5% MeOH/DCM); IR (film) 3285, 3068, 3035, 2974, 2932, 1720, 1638, 1608, 1567, 1508, 1455 cm⁻¹; ¹H NMR (600 MHz, DMSO-*d*₆) δ 9.10 (d, *J* = 8.2 Hz, 1H), 9.01 (d, *J* = 7.7 Hz, 1H), 8.93 (d, *J* = 7.3 Hz, 1H), 8.80 (d, *J* = 8.3 Hz, 1H), 8.51 (d, *J* = 7.1 Hz, 1H), 7.48-6.93 (m, 30H), 6.90 (d, *J* = 8.8 Hz, 2H), 6.85 (d, *J* = 8.8 Hz, 2H), 6.82-6.79 (m, 1H), 6.63 (s, 2H), 6.47 (s, 1H), 5.85 (d, *J* = 7.8 Hz, 1H), 5.80 (d, *J* = 7.9 Hz, 1H), 5.69 (d, *J* = 8.3 Hz, 1H), 5.56 (d, *J* = 7.5 Hz, 1H), 5.49 (d, *J* = 8.3 Hz, 1H), 5.19 (d, *J* = 12.4 Hz, 1H), 5.15 (d, *J* = 12.3 Hz, 1H), 5.08 (s, 2H), 4.94-4.84 (m, 6H), 4.22 (dd, *J* = 8.3, 6.2 Hz, 1H), 2.06-2.00 (m, 1H), 1.38 (br s, 9H), 0.77 (d, *J* = 6.8 Hz, 3H), 0.71 (d, *J* = 6.8 Hz, 3H); ¹³C NMR (150 MHz, DMSO-*d*₆) ppm 171.8, 170.1, 169.80, 169.76, 169.0, 168.3, 163.0-159.5 (m, 4C), 159.7, 158.21, 158.18, 155.5, 155.3, 141.6, 137.5, 137.3, 137.2, 136.1, 131.0, 130.6, 130.2, 128.9, 128.84, 128.76, 128.64, 128.57, 128.3, 128.2, 128.12, 128.06, 128.01, 127.98, 127.95, 122.4 (d, ²*J*_{CF} = 16.2 Hz), 122.1 (d, ²*J*_{CF} = 14.4 Hz), 114.8, 114.6, 112.0 (d, ²*J*_{CF} = 20.6 Hz), 111.6 (d, ²*J*_{CF} = 20.9 Hz), 105.9, 104.21 (dd, ²*J*_{CF} =

26.0, 26.0 Hz), 104.16 (d, $^2J_{CF} = 25.5, 25.5$ Hz), 101.3, 79.2, 79.1, 69.6, 69.53, 69.47, 66.5, 60.2, 57.7, 55.84, 55.78, 55.6, 50.8, 50.5, 30.7, 28.55, 28.49, 19.2, 18.2; ^{19}F NMR (282 MHz, DMSO- d_6) ppm -108.64 (d, $J = 6.4$ Hz), -108.85 (d, $J = 7.0$ Hz), -108.98 (d, $J = 6.8$ Hz), -109.69, -110.39, -111.60 (d, $J = 7.0$ Hz); $[\alpha]_D^{20}$ -5.4 (c 0.77, CHCl_3); HRMS (ESI): Exact mass calcd for $\text{C}_{85}\text{H}_{81}\text{F}_4\text{N}_6\text{O}_{13}$ $[\text{M}+\text{H}]^+$ 1469.5798, found 1469.5824.



(6R,9S,12R,15S,18R,21S)-6,12-bis(2,4-difluorophenyl)-18-(3,5-dihydroxyphenyl)-9,15-bis(4-hydroxyphenyl)-21-isopropyl-2,2-dimethyl-4,7,10,13,16,19-hexaoxo-3-oxa-5,8,11,14,17,20-hexaazadocosan-22-oic acid (79).

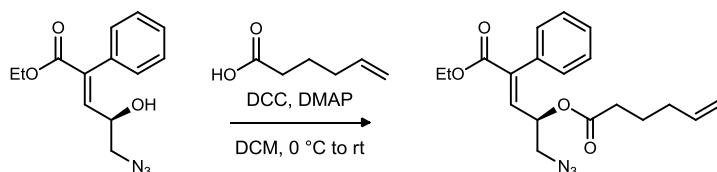
Boc-hexapeptide B (15 mg, 10 μmol) was suspended in ethanol (1.0 mL) and dichloromethane (1.3 mL) with stirring, and 10% palladium on carbon (75 mg) was added in one portion. The reaction atmosphere was replaced with hydrogen gas. After 1 h, the crude mixture was filtered through Celite, and eluted with dichloromethane and methanol. The solution was concentrated via rotary evaporation and dried *in vacuo* to give the desired product as a white film (12 mg, quantitative). $R_f = 0.60$ (5% MeOH/DCM); IR (film) 3400, 2923, 2853, 1660, 1602, 1509, 1462, 1405, 1261 cm^{-1} ; ^1H NMR (600 MHz, DMSO- d_6) δ 9.42 (s, 1H), 9.34 (s, 1H), 9.13 (s, 2H), 8.94 (d, $J = 7.9$ Hz, 1H), 8.81-8.78 (m, 2H), 8.43 (d, $J = 7.3$ Hz, 1H), 8.38 (d, $J = 8.7$ Hz, 1H), 7.51-7.13 (m, 4H), 7.10 (d, $J = 8.6$ Hz, 2H), 7.07 (d, $J = 8.6$ Hz, 2H), 7.03-7.00 (m, 1H), 6.62 (d, $J = 8.6$ Hz, 2H), 6.59 (d, $J = 8.6$ Hz, 2H), 6.23 (br s, 2H), 6.07 (br s, 1H), 5.83 (d, $J = 7.9$ Hz, 1H), 5.67 (d, $J = 8.0$ Hz, 1H), 5.49 (br d, $J = 7.9$ Hz, 1H), 5.47 (d, $J = 6.2$ Hz, 1H), 4.12 (dd, $J = 8.7, 5.9$ Hz, 1H), 2.01-1.95 (m, 1H), 1.38 (br s, 9H), 0.75 (d, $J = 6.8$ Hz, 3H), 0.71 (d, $J = 6.8$ Hz, 3H); ^{13}C NMR (150 MHz, DMSO- d_6) ppm 174.1, 170.3, 169.9, 168.2, 166.9, 162.9-159.4 (m, 4C), 158.3, 158.0, 157.1, 155.4, 141.0, 131.0, 130.5, 129.0, 128.7, 128.5, 127.4, 122.7-122.4 (m, 2C), 115.6, 115.2, 111.8 (d, $^2J_{CF} = 22.2$ Hz), 111.3 (d, $^2J_{CF} = 21.9$ Hz), 106.0, 104.3-103.8 (m, 2C), 102.0, 79.1, 59.9, 57.1, 58.8, 55.6, 52.0, 50.5, 31.4, 28.5, 20.0, 18.6; ^{19}F NMR (282 MHz, DMSO- d_6) ppm -108.97, -109.57, -109.78, -110.88; $[\alpha]_D^{20}$ -6.9 (c 0.84, MeOH); HRMS (ESI): Exact mass calcd for $\text{C}_{50}\text{H}_{50}\text{F}_4\text{N}_6\text{O}_{13}$ $[\text{M}]^+$ 1018.34, found xx. Submitted; matched by LCMS.



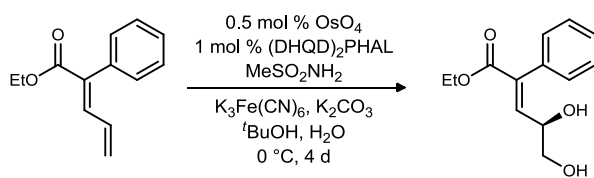
(6R,9S,12R,15S)-6-(2,4-difluorophenyl)-12-(3,5-dihydroxyphenyl)-9-(4-hydroxyphenyl)-15-isopropyl-2,2-dimethyl-4,7,10,13-tetraoxo-3-oxa-5,8,11,14-tetraazahexadecan-16-oic acid (86).

Boc-tetrapeptide B (184 mg, 173 μmol) was suspended in ethanol (7.70 mL) and dichloromethane (9.60 mL) with stirring, and 10% palladium on carbon (736 mg) was added in one portion. The reaction atmosphere was replaced with hydrogen gas. After 1 h, the crude mixture was filtered through Celite, and eluted with dichloromethane and methanol. The solution was concentrated via rotary evaporation and dried *in vacuo* to give the desired product as a white film (120 mg, 99%). $R_f = 0.05$ (5% MeOH/DCM); IR (film) 3257, 2971, 1664, 1603, 1511, 1368 cm^{-1} ; ^1H NMR (400 MHz, DMSO- d_6) δ 9.23 (br s, 2H), 8.73 (d, $J = 8.0$ Hz, 1H), 8.38 (br d, $J = 7.2$ Hz, 1H), 7.84 (br s, 1H), 7.59 (br d, $J = 7.9$ Hz, 1H), 7.37 (ddd, $J = 8.5, 8.5, 6.8$ Hz, 1H), 7.17 (ddd, $J = 9.7, 9.6, 2.1$ Hz, 1H), 7.09 (d, $J =$

8.6 Hz, 2H), 6.98 (ddd, $J = 8.6, 8.6, 2.1$ Hz, 1H), 6.62 (d, $J = 8.5$ Hz, 2H), 6.22 (br d, $J = 1.7$ Hz, 2H), 6.09 (br dd, $J = 2.0, 2.0$ Hz, 1H), 5.56 (d, $J = 7.6$ Hz, 1H), 5.44 (d, $J = 8.0$ Hz, 1H), 5.33 (d, $J = 7.9$ Hz, 1H), 3.98 (dd, $J = 8.3, 5.3$ Hz, 1H), 2.01-1.95 (m, 1H), 1.37 (br s, 9H), 0.69 (d, $J = 6.9$ Hz, 3H), 0.67 (d, $J = 6.8$ Hz, 3H); ^{13}C NMR (150 MHz, DMSO- d_6) ppm 173.6, 169.8, 169.6, 168.8, 162.2 (dd, $^1J_{\text{CF}} = 246.2$, $^3J_{\text{CF}} = 12.0$ Hz), 160.5 (dd, $^1J_{\text{CF}} = 236.5$, $^3J_{\text{CF}} = 12.6$ Hz), 158.4, 157.2, 155.3, 140.8, 131.0 (dd, $^3J_{\text{CF}} = 9.7, 4.8$ Hz), 129.0, 128.4, 122.4 (d, $^2J_{\text{CF}} = 14.8$ Hz), 115.3, 104.1 (dd, $^2J_{\text{CF}} = 26.0, 26.0$ Hz), 102.1, 79.3, 58.6, 56.9, 55.7, 52.0, 31.1, 28.5, 19.7, 18.3; ^{19}F NMR (282 MHz, DMSO- d_6) ppm -108.89, -110.66; $[\alpha]_D^{20}$ -0.0 121 (c 0.00, CHCl_3); HRMS (ESI): Exact mass calcd for $\text{C}_{34}\text{H}_{38}\text{F}_2\text{N}_4\text{O}_{10}$ $[\text{M}+\text{H}]^+$ 700.26, found xx. *Submitted.*



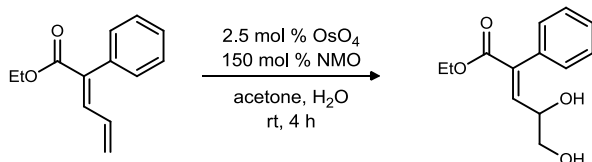
(*R,E*)-1-Azido-5-ethoxy-5-oxo-4-phenylpent-3-en-2-yl hex-5-enoate (149). The azido alcohol (1.0 g, 2.8 mmol) and 4-(*N,N*-dimethylamino)pyridine (70 mg, 0.57 mmol) were dissolved in dichloromethane (7.7 mL) and cooled to 0 °C. 5-Hexenoic acid (0.55 mL, 4.6 mmol) and dicyclohexylcarbodiimide (0.95 g, 4.6 mmol) were added, and the reaction was allowed to slowly warm to room temperature while monitored by TLC. After 4 h, the reaction was filtered through Celite. The filtrate was diluted with dichloromethane, washed with 1 N HCl, satd aq NaHCO_3 , and brine. The solution was dried, filtered, and concentrated. The residue was purified via flash column chromatography (5% ethyl acetate in hexanes) to give the product as a colorless oil (1.2 g, 55%). $R_f = 0.12$ (6% EtOAc/hexanes); IR (film) 3063, 2979, 2928, 2854, 2102, 1742, 1718, 1641, 1444 cm^{-1} ; ^1H NMR (600 MHz, CDCl_3) δ 7.41-7.34 (m, 3H), 7.24-7.22 (m, 2H), 5.82 (d, $J = 8.5$ Hz, 1H), 5.77 (dddd, $J = 16.0, 10.2, 6.7, 6.7$ Hz, 1H), 5.41 (ddd, $J = 8.4, 6.7, 3.9$ Hz, 1H), 5.03 (dddd, $J = 17.1, 1.7, 1.7, 1.7$ Hz, 1H), 4.99 (dddd, $J = 10.2, 2.2, 1.2, 1.2$ Hz, 1H), 4.23 (dq, $J = 10.9, 7.1$ Hz, 1H), 4.21 (dq, $J = 10.9, 7.1$ Hz, 1H), 3.35 (dd, $J = 13.1, 6.7$ Hz, 1H), 3.28 (dd, $J = 13.1, 3.8$ Hz, 1H), 2.34 (ddd, $J = 16.0, 7.5, 7.5$ Hz, 1H), 2.30 (ddd, $J = 16.1, 7.5, 7.5$ Hz, 1H), 2.09 (dddd, $J = 8.0, 6.7, 6.7, 1.4, 1.4$ Hz, 2H), 1.72 (dddd, $J = 7.5, 7.5, 7.5, 7.5$ Hz, 2H), 1.26 (dd, $J = 7.1, 7.1$ Hz, 3H); ^{13}C NMR (150 MHz, CDCl_3) ppm 172.3, 166.1, 137.7, 137.4, 136.9, 133.8, 128.9, 128.3, 128.2, 115.5, 70.6, 61.5, 53.1, 33.3, 32.9, 23.7, 14.1; $[\alpha]_D^{20}$ +11.1 (c 0.99, CHCl_3); HRMS (ESI): Exact mass calcd for $\text{C}_{19}\text{H}_{23}\text{N}_3\text{NaO}_4$ $[\text{M}+\text{Na}]^+$ 380.1586, found 380.1605.



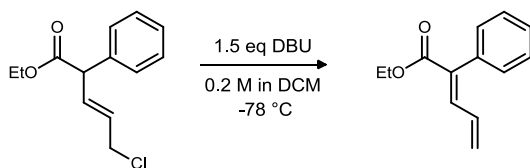
(*R,E*)-Ethyl 4,5-dihydroxy-2-phenylpent-2-enoate (150). Potassium ferricyanide (9.23 g, 28 mmol), potassium carbonate (3.9 g, 28 mmol), methanesulfonamide (0.76 g, 8 mmol), hydroquinidine 1,4-phthalazinediyl diether (62.4 mg, 80 μmol), and potassium osmate dihydrate (14.8 mg, 40 μmol) were combined in a 100-mL round-bottomed flask. The solids were suspended in a mixture of *tert*-butanol (13.3 mL) and water (13.3 mL) and stirred at room temperature for 15 m. The mixture was cooled to 0 °C in an ice/water bath, and the diene (1.6 g, 8.0 mmol) was added. The reaction was stirred 4 d at 0 °C, then quenched with satd aq sodium sulfite and transferred to a separatory funnel containing satd aq sodium sulfite and ethyl acetate. The layers were separated, and the aqueous layer was extracted with ethyl acetate. The combined organic layers were washed with 1 N KOH and brine, then dried, filtered, and concentrated. The residue was purified via column chromatography (30-50% ethyl acetate in hexanes) to give the product as a pale yellow oil (0.96 g,

¹²¹ An optical rotation could not be obtained for this compound due to a “low energy” reading, even after several attempts in MeOH, DMSO, and CHCl_3 at various concentrations.

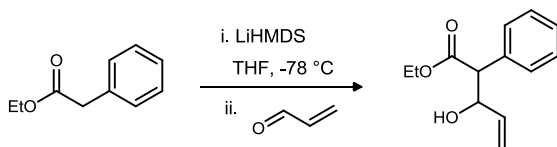
51%, 45% ee). $R_f = 0.10$ (36% EtOAc/hexanes); IR (film) 3405, 3058, 2982, 2935, 1715, 1642, 1601, 1497, 1445 cm^{-1} ; ^1H NMR (600 MHz, CDCl_3) δ 7.39-7.33 (m, 3H), 7.21-7.19 (m, 2H), 6.91 (d, $J = 9.0$ Hz, 1H), 4.28 (ddd, $J = 9.0, 7.4, 3.5$ Hz, 1H), 4.24 (dt, $J = 10.9, 7.1$ Hz, 1H), 4.21 (dt, $J = 10.9, 7.1$ Hz, 1H), 3.64 (d, $J = 11.2, 1\text{H}$), 3.59 (dd, $J = 11.2, 7.3$ Hz, 1H), 2.20 (s, 1H), 1.89 (s, 1H), 1.27 (dd, $J = 7.2, 7.2$ Hz, 3H); ^{13}C NMR (150 MHz, CDCl_3) ppm 166.6, 139.9, 136.8, 134.3, 129.3, 128.2, 128.0, 69.5, 65.5, 61.3, 14.1; $[\alpha]_D^{20} -6.2$ (c 0.29, CHCl_3); HRMS (CI): Exact mass calcd for $\text{C}_{13}\text{H}_{17}\text{O}_4$ $[\text{M}+\text{H}]^+$ 237.1121, found 237.1131.



(E)-Ethyl 4,5-dihydroxy-2-phenylpent-2-enoate (rac-150). *N*-Methylmorpholine-*N*-oxide (21.7 mg, 185 μmol) was dissolved in a mixture of water (25 μL) and acetone (100 μL), then osmium tetroxide (2.5 wt% in *tert*-butanol, 31 μL , 2.4 μmol) was added. The diene (25 mg, 124 μmol), dissolved in acetone (100 μL), was added with stirring. After 4 h, the reaction was complete by TLC, and the reaction mixture was transferred to a separatory funnel containing ethyl acetate and satd aq sodium sulfite. The layers were separated, and the aqueous layer was extracted with ethyl acetate. The combined organic layers were washed with satd aq sodium sulfite and brine, dried, filtered, and concentrated. The residue was purified via flash column chromatography (50% ethyl acetate in hexanes) to give the product as a colorless oil (12.4 mg, 42%). See 62 for analytical details.



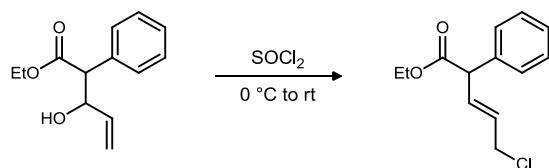
(E)-Ethyl 2-phenylpenta-2,4-dienoate (151).¹²² The unpurified allylic chloride (250 mg, 1.05 mmol) was dissolved in dichloromethane (5.2 mL) and cooled to -78 $^{\circ}\text{C}$. 1,8-Diazabicyclo[5.4.0]undec-7-ene (235 μL , 1.57 mmol) was added via syringe. After 20 min, the reaction was complete by TLC and was transferred to a separatory funnel containing 1 N HCl and dichloromethane. The layers were separated, and the organic layer was washed with 1 N HCl, 0.5 M aq CuSO_4 , and brine. The resulting solution was dried, filtered, and concentrated to give exclusively the *E*-isomer as a light yellow oil (198 mg, 94%), which was used without further purification. The crude product matched previously reported analytical data. The *E*-isomer was confirmed via a NOESY correlation between the γ -proton at δ 6.40 and an ArH at δ 7.23.



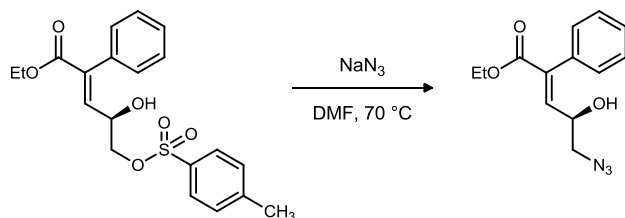
Ethyl 3-hydroxy-2-phenylpent-4-enoate (155). Hexamethyldisilazane (17.0 mL, 81.5 mmol) was dissolved in THF (122 mL) and cooled to -78 $^{\circ}\text{C}$ in a dry ice/acetone bath. *n*-Butyllithium (2.5 M in hexanes, 30.1 mL, 75.3 mmol) was added via syringe over 5 m; the reaction temperature was not allowed to exceed -50 $^{\circ}\text{C}$ during addition. The reaction was allowed to stir for 20 m, then a solution of ethyl phenylacetate (10.0 mL, 62.7 mmol) in THF (47 mL) was added via cannula over 10 m. The reaction was stirred for 1 h, then freshly distilled acrolein (7.0 mL, 94.1 mmol) was added via syringe over 2-3 m. The reaction was stirred for 1.5 h, then quenched with 1 N HCl (100 mL). The ice bath was removed, and the reaction was allowed to come to room

¹²² Lebarillier, L.; Outurquin, F.; Paulmier, C. *Tetrahedron*, **2000**, *56*, 7483.

temperature with stirring. The mixture was transferred to a separatory funnel containing diethyl ether and 1 N HCl. The layers were separated, and the aqueous layer was extracted with diethyl ether. The organic layers were combined and washed with 1 N HCl and brine. The solution was dried, filtered, and concentrated to give a clear, orange/red oil (14.2 g, 99%) that was used without further purification. An analytical sample was obtained by purification via flash column chromatography (12% ethyl acetate in hexanes) to give the product as a colorless oil. The product was characterized as a 1:1 mixture of diastereomers. $R_f = 0.17$ (12% EtOAc/hexanes); IR (film) 3473, 3064, 3031, 2983, 2937, 1730, 1602, 1498, 1455, 1425 cm^{-1} ; $^1\text{H NMR}$ (600 MHz, CDCl_3) δ 7.39-7.29 (m, 10H), 5.85 (ddd, $J = 17.1, 10.6, 6.4$ Hz, 1H), 5.69 (ddd, $J = 17.1, 10.0, 5.7$ Hz, 1H), 5.33 (dt, $J = 17.2, 1.3$ Hz, 1H), 5.20 (dt, $J = 17.2, 1.4$ Hz, 1H), 5.19 (dt, $J = 10.4, 1.2$ Hz, 1H), 5.06 (dt, $J = 10.6, 1.4$ Hz, 1H), 4.71-4.65 (m, 2H), 4.24-4.08 (m, 4H), 3.66 (d, $J = 7.3$ Hz, 1H), 3.62 (d, $J = 8.7$ Hz, 1H), 2.86 (d, $J = 5.2$ Hz, 1H), 2.30 (d, $J = 3.1$ Hz, 1H), 1.21 (dd, $J = 7.1, 7.1$ Hz, 6H); $^{13}\text{C NMR}$ (150 MHz, CDCl_3) ppm 173.1, 172.3, 137.2, 137.2, 135.5, 134.8, 129.1, 128.6, 128.6, 128.5, 127.8, 127.6, 117.1, 116.4, 74.8, 73.8, 61.1, 61.0, 58.1, 57.8, 14.0; HRMS (CI): Exact mass calcd for $\text{C}_{13}\text{H}_{17}\text{O}_3$ $[\text{M}+\text{H}]^+$ 221.1172, found 221.1167.

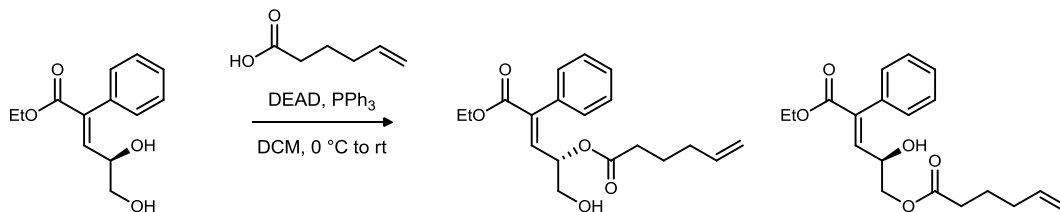


(E)-Ethyl 5-chloro-2-phenylpent-3-enoate (156). The unpurified allylic alcohol (14.2 g, 64.5 mmol) was transferred to a flame-dried 3-neck round-bottomed flask equipped with an overhead mechanical stirrer with a small amount of dichloromethane (<10 mL), and the solution was cooled to 0 °C. Thionyl chloride (8.53 mL, 80.6 mmol) was added via syringe over 5 m, and the reaction was stirred. The reaction flask was connected to a base bath (6 M NaOH) and flushed with positive nitrogen pressure throughout the reaction. The reaction was allowed to slowly warm to room temperature and was monitored by TLC. After 5 h, the mixture was concentrated to give the product as a red oil (14.9 g, 97%), which was used without further purification. An analytical sample was obtained by purification via flash column chromatography (3% ethyl acetate in hexanes) to give the product as a colorless oil. $R_f = 0.24$ (5% EtOAc/hexanes); IR (film) 3063, 3030, 2982, 1731, 1664, 1601, 1496, 1454 cm^{-1} ; $^1\text{H NMR}$ (600 MHz, CDCl_3) δ 7.35-7.26 (m, 5H), 6.18 (ddt, $J = 15.3, 8.2, 1.1$ Hz, 1H), 5.72 (dddd, $J = 15.2, 7.0, 7.0, 1.1$ Hz, 1H), 4.32 (d, $J = 8.2$ Hz, 1H), 4.19 (dq, $J = 10.9, 7.2$ Hz, 1H), 4.14 (dq, $J = 10.9, 7.2$ Hz, 1H), 4.06 (d, $J = 6.9$ Hz, 2H), 1.24 (dd, $J = 7.1, 7.1$ Hz, 3H); $^{13}\text{C NMR}$ (150 MHz, CDCl_3) ppm 171.9, 137.6, 132.3, 128.8, 128.7, 128.6, 127.9, 127.5, 61.2, 54.1, 44.4, 14.0 ppm; HRMS (CI): Exact mass calcd for $\text{C}_{13}\text{H}_{14}\text{ClO}_2$ $[\text{M}-\text{H}]^+$ 237.0677, found 237.0687.



(R,E)-Ethyl 5-azido-4-hydroxy-2-phenylpent-3-enoate (157). Sodium azide (7.8 mg, 50 μmol) was added to a stirring solution of the tosylate (13 mg, 33 μmol) in anhydrous DMF (0.3 mL). The reaction was heated to 70 °C and monitored by TLC. After 3.5 h, the reaction was cooled to room temperature, and the mixture was transferred to a separatory funnel containing water. The aqueous solution was extracted with diethyl ether, and the combined organic layers were washed with water and brine, and dried, filtered, and concentrated. The residue was purified via flash column chromatography (25% ethyl acetate in hexanes) to give the product as a yellow oil (7.1 mg, 82%). An analytical sample was obtained via column chromatography (15% ethyl acetate in hexanes). $R_f = 0.18$ (20% EtOAc/hexanes); IR (film) 3423, 2982, 2924, 2852, 2102, 1715, 1642, 1497, 1444 cm^{-1} ; $^1\text{H NMR}$ (600 MHz, CDCl_3) δ 7.40-7.35 (m, 3H), 7.20-7.18 (m, 2H), 6.90 (d, $J = 8.9$ Hz, 1H), 4.37-3.34 (br m, 1H), 4.24 (dq, $J = 11.0, 7.0$ Hz, 1H), 4.22 (dq, $J = 11.0, 7.0$ Hz, 1H), 3.37 (dd, $J = 12.5, 6.8$ Hz, 1H), 3.33 (dd, $J = 12.5, 4.1$ Hz, 1H), 2.08 (d, $J = 3.1$ Hz, 1H), 1.28 (dd, $J = 7.1, 7.1$ Hz, 3H); $^{13}\text{C NMR}$ (150 MHz, CDCl_3)

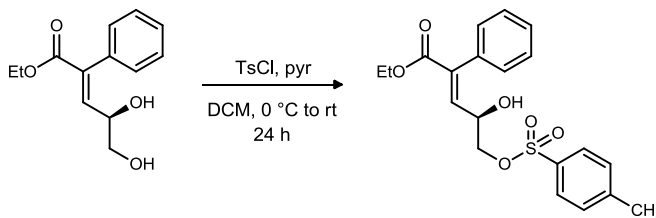
ppm 166.4, 139.7, 137.0, 134.0, 129.2, 128.3, 128.2, 68.2, 61.4, 55.8, 14.1; $[\alpha]_D^{20}$ -13.5 (*c* 0.46, CHCl₃); HRMS (ESI): Exact mass calcd for C₁₃H₁₅N₃NaO₃ [M+Na]⁺ 284.1011, found 284.1003.



(S,E)-5-Ethoxy-1-hydroxy-5-oxo-4-phenylpent-3-en-2-yl hex-5-enoate (159) and **(R,E)-5-Ethoxy-2-hydroxy-5-oxo-4-phenylpent-3-enyl hex-5-enoate (160)**. 5-Hexenoic acid (7.5 μ L, 63 μ mol, 1.5 eq) and triphenylphosphine (22.2 mg, 85 μ mol) were added to a stirring solution of diol (10 mg, 42 μ mol) in dichloromethane (0.17 mL) at 0 °C. Diethylazodicarboxylate (13.3 μ L, 85 μ mol), as a solution in dichloromethane (0.13 mL) was added dropwise. After 5 m, the ice bath was removed, and the reaction was allowed to warm to room temperature. After 26 h, the reaction mixture was transferred to a separatory funnel containing satd aq NaHCO₃ and ethyl acetate. The layers were separated, and the aqueous solution was extracted with ethyl acetate. The combined organic layers were washed with brine, then dried, filtered, and concentrated. The residue was purified via flash column chromatography (20% ethyl acetate in hexanes) to give the desired secondary ester (4.8 mg, 34%) and the primary ester (2.3 mg, 16%) as colorless oils.

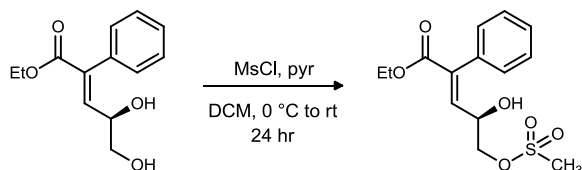
(159). R_f = 0.11 (20% EtOAc/hexanes); IR (film) 3474, 3062, 2925, 2851, 1738, 1717, 1641, 1444, 1417 cm⁻¹; ¹H NMR (600 MHz, CDCl₃) δ 7.40-7.33 (m, 3H), 7.25-7.24 (m, 2H), 6.83 (d, *J* = 8.6 Hz, 1H), 5.76 (dddd, *J* = 17.0, 10.2, 6.7, 6.7 Hz, 1H), 5.33 (ddd, *J* = 8.6, 6.6, 3.9 Hz, 1H), 5.03 (dddd, *J* = 17.2, 1.7, 1.7, 1.7 Hz, 1H), 4.99 (dddd, *J* = 10.2, 1.2, 1.2, 1.2 Hz, 1H), 4.22 (dq, *J* = 10.6, 7.1 Hz, 1H), 4.20 (dq, *J* = 10.4, 7.1 Hz, 1H), 3.70-3.63 (m, 2H), 2.32 (ddd, *J* = 16.0, 7.6, 7.6 Hz, 1H), 2.29 (ddd, *J* = 16.0, 7.5, 7.5 Hz, 1H), 2.08 (br ddd, *J* = 7.2, 7.2, 7.2 Hz, 2H), 1.71 (dddd, *J* = 7.5, 7.5, 7.5, 7.5 Hz, 2H), 1.26 (dd, *J* = 7.1, 7.1 Hz, 3H) [OH not observed]; ¹³C NMR (150 MHz, CDCl₃) ppm 172.9, 166.3, 137.5, 137.4, 137.1, 134.1, 129.1, 128.2, 128.1, 115.5, 72.8, 64.0, 61.4, 33.3, 32.9, 23.8, 14.1 ppm; HRMS (ESI): Exact mass calcd for C₁₉H₂₄NaO₅ [M+Na]⁺ 355.1521, found 355.1537.

(160). R_f = 0.13 (20% EtOAc/hexanes); IR (film) 3456, 2979, 2919, 2850, 1735, 1715, 1640, 1444 cm⁻¹; ¹H NMR (600 MHz, CDCl₃) δ 7.41-7.34 (m, 3H), 7.23-7.21 (m, 2H), 6.89 (d, *J* = 9.1 Hz, 1H), 5.76 (dddd, *J* = 16.9, 10.2, 6.7, 6.7 Hz, 1H), 5.02 (ddd, *J* = 17.1, 3.4, 1.7 Hz, 1H), 4.98 (ddd, *J* = 10.1, 3.1, 1.2 Hz, 1H), 4.40 (dddd, *J* = 8.9, 6.6, 4.4, 4.4 Hz, 1H), 4.24 (dq, *J* = 9.1, 7.1 Hz, 1H), 4.23 (dq, *J* = 9.1, 7.1 Hz, 1H), 4.13 (dd, *J* = 11.6, 3.8 Hz, 1H), 4.10 (dd, *J* = 11.6, 6.6 Hz, 1H), 2.35 (dd, *J* = 7.6, 7.6 Hz, 2H), 2.16 (d, *J* = 4.6 Hz, 1H), 2.08 (ddd, *J* = 7.2, 7.2, 7.2 Hz, 2H), 1.73 (dddd, *J* = 7.3, 7.3, 7.3, 7.3 Hz, 2H), 1.27 (dd, *J* = 7.1, 7.1 Hz, 3H); ¹³C NMR (150 MHz, CDCl₃) ppm 173.5, 166.5, 139.0, 137.5, 137.4, 134.1, 129.2, 128.2, 128.1, 115.5, 67.4, 67.0, 61.3, 33.3, 32.9, 23.9, 14.1; HRMS (ESI): Exact mass calcd for C₁₉H₂₄NaO₅ [M+Na]⁺ 355.1521, found 355.1536.

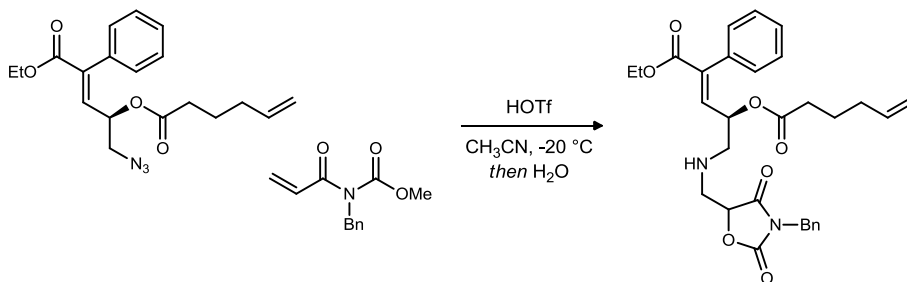


(R,E)-Ethyl 4-hydroxy-2-phenyl-5-(tosyloxy)pent-2-enoate (161). Tosyl chloride (3.2 g, 17 mmol) was added to a stirring solution of diol (2.0 g, 8.5 mmol) in dichloromethane (8.5 mL) at 0 °C. Pyridine (1.0 mL, 13 mmol) was added, and the solution was allowed to slowly warm to room temperature. The reaction was stirred at room temperature for 24 h, and then quenched with 1 N HCl. The aqueous solution was extracted with

dichloromethane, and the organic layers were washed with 0.5 M aq CuSO₄ and brine, and then dried, filtered, and concentrated. The residue was purified via flash column chromatography (20% ethyl acetate in hexanes) to give the product as a pale yellow oil (2.3 g, 70%). $R_f = 0.05$ (20% EtOAc/hexanes); IR (film) 3489, 2924, 2851, 1716, 1643, 1598, 1496, 1445 cm⁻¹; ¹H NMR (600 MHz, CDCl₃) δ 7.74 (d, $J = 8.3$ Hz, 2H), 7.36-7.33 (m, 5H), 7.13-7.11 (m, 2H), 6.78 (d, $J = 8.9$ Hz, 1H), 4.40 (ddd, $J = 9.0, 6.8, 3.6$ Hz, 1H), 4.22 (dq, $J = 10.9, 7.1$ Hz, 1H), 4.20 (dq, $J = 10.9, 7.1$ Hz, 1H), 3.99 (dd, $J = 10.4, 3.7$ Hz, 1H), 3.96 (dd, $J = 10.4, 6.8$ Hz, 1H), 2.46 (s, 3H), 2.25 (br s, 1H), 1.26 (dd, $J = 7.1, 7.1$ Hz, 3H); ¹³C NMR (150 MHz, CDCl₃) ppm 166.2, 145.2, 137.8, 137.6, 133.8, 132.2, 130.0, 129.1, 128.3, 128.2, 128.0, 72.0, 67.0, 61.5, 21.7, 14.1; $[\alpha]_D^{20} -11.2$ (c 1.08, CHCl₃); HRMS (ESI): Exact mass calcd for C₂₀H₂₂NaO₆S [M+Na]⁺ 413.1035, found 413.1026.

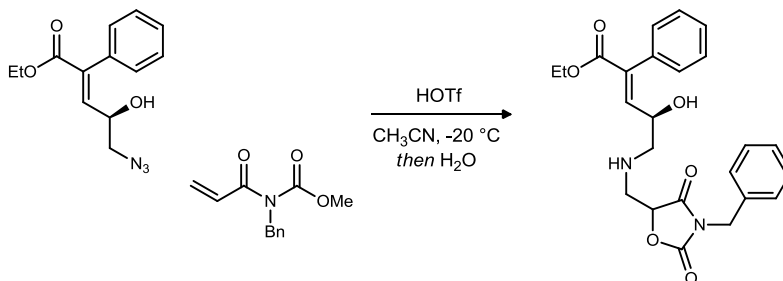


(*R,E*)-Ethyl 4-hydroxy-5-(methylsulfonyloxy)-2-phenylpent-2-enoate. Mesyl chloride (9.8 μ L, 127 μ mol) was added to a stirring solution of diol (25 mg, 106 μ mol) in dichloromethane (1.1 mL) at 0 °C. Pyridine (12.8 μ L, 159 μ mol) was added, and the solution was allowed to slowly warm to room temperature. After 24 h, the reaction was quenched with 1 N HCl. The aqueous solution was extracted with dichloromethane. The organic solution was washed with 0.5 M aq CuSO₄ and brine, and then dried, filtered, and concentrated. The residue was purified via flash column chromatography (35% ethyl acetate in hexanes) to give the product as a pale yellow oil (12.7 mg, 38%) in addition to diol substrate (7.4 mg, 30%). IR (film) 3494, 2983, 2938, 1714, 1643, 1497, 1445 cm⁻¹; ¹H NMR (600 MHz, CDCl₃) δ 7.41-7.37 (m, 3H), 7.21-7.19 (m, 2H), 6.86 (d, $J = 9.0$ Hz, 1H), 4.48 (ddd, $J = 8.9, 6.4, 3.3$ Hz, 1H), 4.23 (dq, $J = 14.1, 7.1$ Hz, 1H), 4.23 (dq, $J = 14.1, 7.1$ Hz, 1H), 4.21 (dd, $J = 10.9, 3.7$ Hz, 1H), 4.18 (dd, $J = 10.8, 6.2$ Hz, 1H), 3.02 (s, 3H), 2.42 (br s, 1H), 1.27 (dd, $J = 7.2, 7.2$ Hz, 3H); ¹³C NMR (150 MHz, CDCl₃) ppm 166.2, 138.0, 137.6, 133.8, 132.6, 129.1, 128.4, 71.7, 67.2, 61.5, 37.6, 14.1; HRMS (ESI): Exact mass calcd for C₁₄H₁₈NaO₆S [M+Na]⁺ 337.0722, found 337.0727.



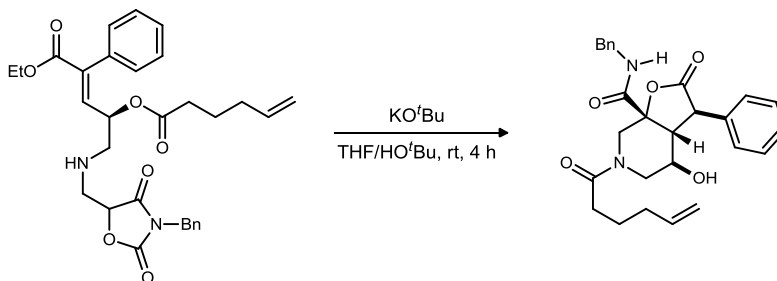
(*2R,E*)-1-((3-benzyl-2,4-dioxoxazolidin-5-yl)methylamino)-5-ethoxy-5-oxo-4-phenylpent-3-en-2-yl hex-5-enoate (163). The azido ester (350 mg, 979 μ mol) and imide (107 mg, 490 μ mol) were dissolved in acetonitrile (1.6 mL) and cooled to -20 °C. Triflic acid (86.7 μ L, 979 μ mol) was added, and the reaction was monitored by TLC. After 1.5 h, no imide remained by TLC, and water (89 μ L, 5.5 M in CH₃CN, 490 μ mol) was added. After 1.5 h, nitrogen evolution had ceased, and the reaction was quenched with triethylamine (136 μ L, 979 μ mol). The reaction mixture was concentrated, and the residue was purified via flash column chromatography (22% ethyl acetate in hexanes) to give the product as a yellow foam (243 mg, 93%). $R_f = 0.09$ (20% EtOAc/hexanes); IR (film) 3356, 3065, 2925, 2853, 1817, 1739, 1642, 1497, 1441, 1414 cm⁻¹; ¹H NMR (400 MHz, CDCl₃) δ 7.41-7.28 (m, 16H), 7.24-7.22 (m, 4H), 6.76 (d, $J = 8.9$ Hz, 1H), 6.74 (d, $J = 8.8$ Hz, 1H), 5.76 (dddd, $J = 17.0, 10.1, 6.7, 6.7$ Hz, 2H), 5.29-5.23 (m, 2H), 5.05-4.98 (m, 4H), 4.70-4.67 (m, 2H), 4.66-4.64 (m, 4H), 4.25-4.17 (m, 4H), 3.06 (dd, $J = 14.0, 3.4$ Hz, 1H), 2.99 (dd, $J = 14.0, 3.8$ Hz, 1H), 2.89 (dd, $J = 14.2, 3.5$ Hz, 1H), 2.83-2.76 (m, 3H), 2.68 (dd, $J = 13.1, 4.4$ Hz, 1H), 2.68 (13.5, 4.0 Hz, 1H), 2.28-2.24 (m, 4H), 2.10-2.04 (m, 4H), 1.69 (dddd, $J = 7.4, 7.4, 7.4, 7.4$ Hz, 4H), 1.25 (dd, $J = 7.1, 7.1$ Hz, 6H); ¹³C NMR (150 MHz, CDCl₃) ppm 172.7, 172.6, 166.2, 155.1, 138.5, 137.5, 134.5, 134.5, 134.1, 134.0, 129.1, 129.1, 128.7, 128.5, 128.3, 128.1,

128.0, 115.4, 79.5, 70.1, 61.3, 52.2, 47.7, 47.5, 43.7, 43.7, 33.3, 32.9, 23.75, 14.1; $[\alpha]_D^{20}$ -3.5 (*c* 0.52, CHCl₃); HRMS (ESI): Exact mass calcd for C₃₀H₃₄N₂NaO₇ [M+Na]⁺ 557.2264, found 557.2255.



(4*R*,*E*)-Ethyl 5-((3-benzyl-2,4-dioxooxazolidin-5-yl)methylamino)-4-hydroxy-2-phenylpent-2-enoate (164).

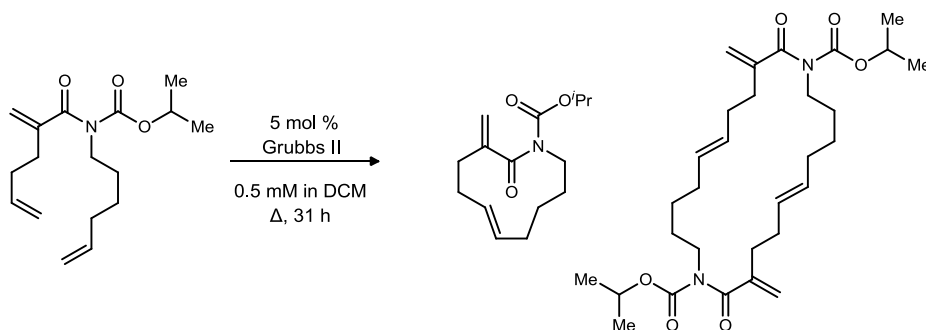
The azido alcohol (0.90 g, 3.4 mmol) and imide (0.38 g, 1.7 mmol) were dissolved in acetonitrile (5.7 mL) and cooled to -20 °C. Triflic acid (0.31 mL, 3.4 mmol) was added, and the reaction was monitored by TLC. After 1.5 h, no imide remained by TLC, and water (0.31 mL, 5.5 M in CH₃CN, 1.7 mmol) was added. After 1 h, nitrogen evolution had ceased, and the reaction was quenched with triethylamine (0.48 mL, 3.4 mmol); bubbling was observed at this point. The reaction mixture was passed through a plug of neutral alumina and concentrated. The residue was purified via flash column chromatography (35% ethyl acetate/2% TEA in hexanes) to give the product as a yellow foam (0.53 g, 70%). The compound was characterized as a 1:1 mixture of diastereomers. *R_f* = 0.22 (50% EtOAc/hexanes); IR (film) 3483, 3363, 2980, 2957, 2925, 2853, 1816, 1740, 1714, 1643, 1497, 1442, 1415 cm⁻¹; ¹H NMR (400 MHz, CDCl₃) δ 7.40-7.27 (m, 16H), 7.19-7.16 (m, 4H), 6.82 (d, *J* = 8.8 Hz, 1H), 6.81 (d, *J* = 8.9 Hz, 1H), 4.78-4.74 (br m, 2H), 4.678 (d, *J* = 14.5 Hz, 1H), 4.676 (d, *J* = 14.5 Hz, 1H), 4.633 (d, *J* = 14.5 Hz, 1H), 4.630 (d, *J* = 14.5 Hz, 1H), 4.27-4.16 (m, 4H), 4.08 (ddd, *J* = 8.9, 7.2, 5.2 Hz, 1H), 4.03 (dd, *J* = 8.9, 3.5 Hz, 1H), 3.16 (dd, *J* = 13.8, 3.5 Hz, 1H), 3.10 (dd, *J* = 13.9, 3.5 Hz, 1H), 3.01 (dd, *J* = 14.0, 4.3 Hz, 1H), 2.97 (dd, *J* = 13.9, 4.2 Hz, 1H), 2.70 (dd, *J* = 12.5, 3.5 Hz, 1H), 2.64-2.55 (m, 3H), 1.26 (dd, *J* = 7.1, 7.1 Hz, 6H) [OH/NH not observed]; ¹³C NMR (100 MHz, CDCl₃) ppm 171.7, 171.6, 166.6, 166.5, 155.1, 141.7, 141.6, 136.1, 136.0, 134.5, 134.4, 134.3, 129.3, 128.8, 128.5, 128.4, 128.1, 127.9, 79.7, 79.6, 67.5, 67.1, 61.2, 54.2, 54.0, 45.3, 47.9, 43.7, 14.1; $[\alpha]_D^{20}$ -26.3 (*c* 0.76, CHCl₃); HRMS (ESI): Exact mass calcd for C₂₄H₂₇N₂O₆ [M+H]⁺ 439.1869, found 439.1849.



(3*R*,3*aR*,4*R*,7*aR*)-*N*-Benzyl-6-hex-5-enoyl-4-hydroxy-2-oxo-3-phenyloctahydrofuro[2,3-*c*]pyridine-7*a*-carboxamide (167).

The oxazolidinone ester (25 mg, 47 μmol) was dissolved in tetrahydrofuran (0.24 mL). *tert*-Butanol (0.24 mL) was added, followed by potassium *tert*-butoxide (13.1 mg, 117 μmol), and the reaction was allowed to stir at room temperature. After 4 h, the solvents were removed via rotary evaporation. The mixture was diluted with dichloromethane, treated with 1 N HCl, and brine was added. The aqueous solution was extracted with dichloromethane, and the combined organic layers were dried, filtered, and concentrated. The residue was purified via flash column chromatography (80%-100% ethyl acetate in hexanes) to give the product as a white film (4.3 mg, 20%): *R_f* = 0.07 (50% EtOAc/hexanes); IR (film) 3347, 3065, 3032, 2925, 2854, 1784, 1738, 1733, 1674, 1606, 1538, 1498, 1455 cm⁻¹; ¹H NMR (600 MHz, CDCl₃/d₆-DMSO, 30:1) δ 7.38-7.27 (m, 6H), 7.15 (d, *J* = 6.8 Hz, 2H), 7.03 (dd, *J* = 5.5, 5.5 Hz, 1H), 5.73 (dddd, *J* = 17.0, 10.2, 6.7, 6.7 Hz, 1H), 4.99 (dddd, *J* = 17.1, 1.6, 1.6, 1.6 Hz, 1H), 4.95 (br d, *J* = 10.2 Hz, 1H), 4.75 (br ddd, *J* = 4.1, 4.1, 4.1 Hz, 1H), 4.35 (dd, *J* = 14.7, 5.8 Hz, 1H), 4.35 (dd, *J* = 14.7, 5.6 Hz, 1H), 3.83 (d, *J* = 8.9 Hz, 1H), 3.47 (d, *J*

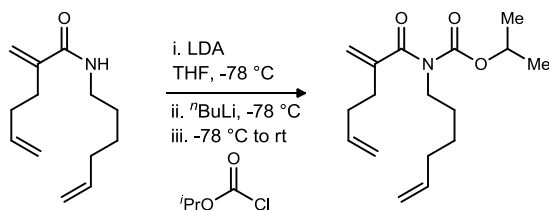
= 14.3 Hz, 1H), 3.24 (dd, $J = 8.9, 4.6$ Hz, 1H), 3.17 (dd, $J = 14.3, 3.4$ Hz, 1H), 3.01 (dd, $J = 14.3, 4.9$ Hz, 1H), 2.97 (d, $J = 14.4$ Hz, 1H), 2.26 (ddd, $J = 7.6, 7.6, 1.6$ Hz, 2H), 2.03 (br ddd, $J = 7.2, 7.2, 7.2$ Hz, 2H), 1.68 (dddd, $J = 7.5, 7.5, 7.5, 7.5$ Hz, 2H); ^{13}C NMR (150 MHz, CDCl_3) ppm 173.6, 173.0, 170.4, 137.4, 137.2, 133.1, 129.1, 128.8, 128.3, 127.9, 127.7, 127.7, 115.5, 81.0, 68.5, 50.3, 49.6, 47.4, 45.2, 43.5, 33.4, 32.9, 23.7; $[\alpha]_D^{20}$ -6.7 (c 0.45, CHCl_3); HRMS (ESI): Exact mass calcd for $\text{C}_{27}\text{H}_{31}\text{N}_2\text{O}_5$ $[\text{M}+\text{H}]^+$ 463.2233, found 463.2233.



(E)-Isopropyl 3-methylene-2-oxoazacycloundec-6-ene-1-carboxylate (176) and **(6E,17E)-diisopropyl 3,14-dimethylene-2,13-dioxo-1,12-diazacyclodocosa-6,17-diene-1,12-dicarboxylate (223)**. Grubbs Second Generation Catalyst (3.0 mg, 3.4 μmol) was dissolved in dichloromethane (140 mL), and the carbamate (21 mg, 71 μmol) was added as a solution in dichloromethane (2.0 mL). A condenser was attached, and the reaction was heated to reflux. After 24.5 h, a second batch of catalyst (3.0 mg, 3.4 μmol) was added, and the reaction was heated for another 6.5 h, then concentrated. The residue was immediately purified via flash column chromatography (0-3% ethyl acetate in hexanes) to give the products as colorless oils (monomer = 8.0 mg, 40%; dimer = 8.0 mg, 40%) in addition to carbamate substrate (4.0 mg, 20%).

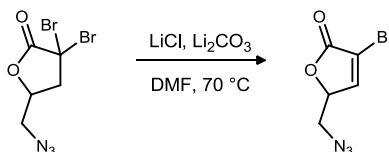
176: $R_f = 0.24$ (7% EtOAc/hexanes); IR (film) 2980, 2930, 2855, 1728, 1676, 1632, 1447 cm^{-1} ; ^1H NMR (400 MHz, CDCl_3) δ 5.40-5.32 (m, 2H), 5.18 (ddd, $J = 1.1, 1.1, 1.1$ Hz, 1H), 5.15 (d, $J = 0.9$ Hz, 1H), 5.03 (qq, $J = 6.4, 6.4$ Hz, 1H), 3.75 (dd, $J = 5.8, 5.8$ Hz, 2H), 2.58-2.56 (m, 2H), 2.24-2.21 (m, 2H), 1.91 (ddd, $J = 5.9, 5.9, 5.9$ Hz, 2H), 1.72-1.68 (m, 2H), 1.55-1.51 (m, 2H), 1.32 (d, $J = 6.3$ Hz, 6H); ^{13}C NMR (150 MHz, CDCl_3) ppm 173.4, 154.2, 147.9, 132.6, 129.6, 116.4, 70.9, 46.1, 34.3, 33.7, 31.8, 26.3, 25.4, 21.8; HRMS (ESI): Exact mass calcd for $\text{C}_{15}\text{H}_{23}\text{NNaO}_3$ $[\text{M}+\text{Na}]^+$ 288.1576, found 288.1562.

223: $R_f = 0.10$ (7% EtOAc/hexanes); IR (film) 2980, 2930, 2856, 1733, 1675, 1632, 1444, 1368 cm^{-1} ; ^1H NMR (600 MHz, CDCl_3) δ 5.41-5.36 (m, 2H), 5.26-5.10 (m, 2H), 5.01-4.97 (m, 1H), 3.75-3.68 (m, 2H), 2.37-2.32 (m, 2H), 2.25-2.14 (m, 2H), 2.08-1.99 (m, 2H), 1.55-1.50 (m, 2H), 1.39-1.31 (m, 2H), 1.28 (d, $J = 6.2$ Hz, 6H); ^{13}C NMR (150 MHz, CDCl_3) ppm 173.5, 154.2, 147.5, 130.6, 129.6, 114.7, 71.1, 44.1, 33.3, 32.0, 30.7, 27.7, 26.0, 21.6; HRMS (ESI): Exact mass calcd for $\text{C}_{30}\text{H}_{46}\text{N}_2\text{NaO}_6$ $[\text{M}+\text{Na}]^+$ 553.3254, found 553.3280.

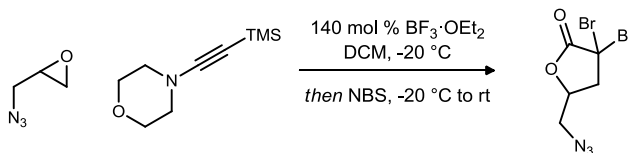


Isopropyl hex-5-enyl(2-methylenehex-5-enoyl)carbamate (186). Diisopropylamine (37.3 μL , 265 μmol) was dissolved in THF (0.8 mL) and cooled to -78 $^\circ\text{C}$ in a dry ice/acetone bath. n -Butyl lithium (2.56 M in hexanes, 99.0 μL , 253 μmol) was added. After 2 m, the reaction was warmed to 0 $^\circ\text{C}$, stirred for 5 m, then cooled back down to -78 $^\circ\text{C}$. The reaction was allowed to stir for 5 m, then the amide (50.0 mg, 241 μmol) was added via microsyringe. The reaction was stirred for 15 m, then a second equivalent of n -butyl lithium (2.56 M in hexanes, 99.0 μL , 253 μmol) was added. After 5 m, the isopropyl chloroformate (1.0 M in toluene, 289 μL , 289 μmol) was added. The reaction was stirred for 20 m at -78 $^\circ\text{C}$, then allowed to warm to room temperature and stirred

for 2.5 h, then quenched with 1 N HCl. The mixture was transferred to a separatory funnel containing diethyl ether and 1 N HCl. The layers were separated, and the aqueous layer was extracted with diethyl ether. The organic layers were combined and washed with satd aq NaHCO₃. The organic solution was dried, filtered, and concentrated, and the residue was purified via flash column chromatography (0-2% ethyl acetate in hexanes) to give the product as a colorless oil (28.9 mg, 41%) in addition to amide substrate (10.7 mg, 21%). $R_f = 0.21$ (5% EtOAc/hexanes); IR (film) 3078, 2981, 2932, 2861, 1735, 1678, 1639, 1443 cm⁻¹; ¹H NMR (400 MHz, CDCl₃) δ 5.84 (ddt, $J = 16.8, 10.2, 6.5$ Hz, 1H), 5.79 (ddt, $J = 16.9, 10.2, 6.6$ Hz, 1H), 5.20 (br s, 1H), 5.16 (br s, 1H), 5.09-4.93 (m, 5H), 3.68 (dd, $J = 7.4, 7.4$ Hz, 2H), 2.44-2.40 (m, 2H), 2.27 (br tt, $J = 7.6, 7.6$ Hz, 2H), 2.07 (br tt, $J = 7.1, 7.1$ Hz, 2H), 1.63-1.55 (m, 2H), 1.45-1.37 (m, 2H), 1.27 (d, $J = 6.3$ Hz, 6H); ¹³C NMR (150 MHz, CDCl₃) ppm 173.8, 154.4, 147.1, 138.4, 137.6, 115.04, 115.02, 114.7, 71.1, 44.8, 33.3, 32.2, 31.7, 28.1, 26.0, 21.6; HRMS (ESI): Exact mass calcd for C₁₇H₂₇NNaO₃ [M+Na]⁺ 316.1889, found 316.1893.

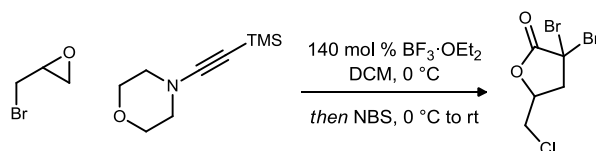


5-(Azidomethyl)-3-bromofuran-2(5H)-one (197). The lactone (25 mg, 84 μ mol), lithium chloride (18 mg, 420 μ mol), and lithium carbonate (6.2 mg, 84 μ mol) were dissolved in DMF (170 μ L) and heated to 70 °C for 20 m. The hot solution was transferred to a separatory funnel containing water, and the aqueous phase was extracted with diethyl ether. The solution was dried, filtered, and concentrated to give a yellow oil (16 mg, 90%), which was used without further purification. An analytical sample was obtained via flash column chromatography (10% ethyl acetate in hexanes). $R_f = 0.12$ (20% EtOAc/hexanes); IR (film) 3095, 2922, 2853, 2104, 1769, 1608, 1440 cm⁻¹; ¹H NMR (600 MHz, CDCl₃) δ 7.49 (d, $J = 1.8$ Hz, 1H), 5.10 (ddd, $J = 5.0, 5.0, 1.8$ Hz, 1H), 3.67 (dd, $J = 13.1, 4.8$ Hz, 1H), 3.61 (dd, $J = 13.2, 5.1$ Hz, 1H); ¹³C NMR (150 MHz, CDCl₃) ppm 167.3, 149.1, 115.3, 80.5, 51.9; HRMS (CI): Exact mass calcd for C₅H₄BrN₁O₂ [M-N₂]⁺ 188.9420, found 188.9412.

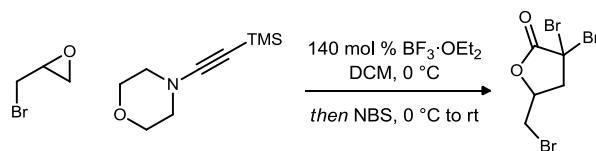


5-(Azidomethyl)-3,3-dibromodihydrofuran-2(3H)-one (204). The ynamine¹²⁴ (324 mg, 1.77 mmol) was dissolved in dichloromethane (7.4 mL), and cooled to -20 °C. Boron trifluoride etherate (223 μ L, 1.77 mmol) was added dropwise, followed by epiazidohydrin¹²³ (125 mg, 1.26 mmol), and the reaction was stirred at -20 °C until an aliquot drawn up in a TLC spotter no longer bubbled at room temperature (1.25 h). *N*-Bromosuccinimide (674 mg, 3.78 mmol) was added, and the reaction was stirred for 25 m at -20 °C, then warmed to room temperature and stirred for an additional 2 h. The reaction was quenched with the addition of dichloromethane (9.0 mL) and 1 N HCl (9.0 mL), followed by 30 m of stirring at room temperature. The mixture was extracted with dichloromethane, and the combined organic layers were washed with brine, dried, filtered, and concentrated. The residue was purified via flash column chromatography (10% ethyl acetate in hexanes) to give a colorless oil (189 mg, 50%). $R_f = 0.36$ (30% EtOAc/hexanes); IR (film) 2924, 2852, 2106, 1790, 1436 cm⁻¹; ¹H NMR (600 MHz, CDCl₃) δ 4.77 (dddd, $J = 9.7, 4.9, 4.9, 3.8$ Hz, 1H), 3.75 (dd, $J = 13.7, 3.9$ Hz, 1H), 3.55 (dd, $J = 13.7, 4.7$ Hz, 1H), 3.23 (dd, $J = 14.5, 5.2$ Hz, 1H), 3.12 (dd, $J = 14.6, 9.5$ Hz, 1H); ¹³C NMR (150 MHz, CDCl₃) ppm 167.8, 76.2, 51.6, 48.6, 46.6; HRMS (CI): Exact mass calcd for C₅H₆⁷⁹Br⁸¹BrN₃O₂ [M+H]⁺ 299.8801, found 299.8813.

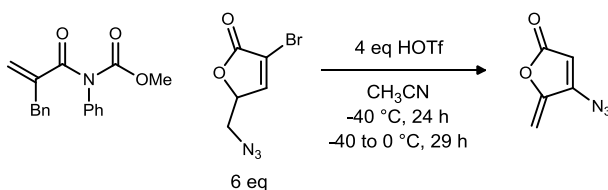
¹²³ Lutje Spelberg, J. H.; Tang, L.; Kellogg, R. M.; Janssen, D.B., *Tetrahedron: Asymmetry*, **2004**, *15*, 1095.



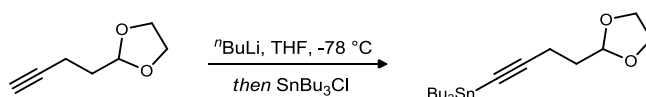
3,3-Dibromo-5-(chloromethyl)dihydrofuran-2(3H)-one (205). The lactone was prepared from epichlorohydrin (58.4 μL , 746 μmol) as described by Jacobsen¹²⁴ and purified via flash column chromatography (15% ethyl acetate in hexanes) to give a colorless oil (161 mg, 74%). R_f = 0.33 (20% EtOAc/hexanes); IR (film) 2922, 1786, 1430 cm^{-1} ; ^1H NMR (600 MHz, CDCl_3) δ 4.86 (dddd, J = 10.0, 5.2, 5.2, 5.2 Hz, 1H), 3.81 (dd, J = 12.1, 5.5 Hz, 1H), 3.78 (dd, J = 12.0, 4.6 Hz, 1H), 3.37 (dd, J = 14.6, 5.2 Hz, 1H), 3.17 (dd, J = 14.7, 9.2 Hz, 1H); ^{13}C NMR (150 MHz, CDCl_3) ppm 167.7, 76.1, 49.6, 46.3, 43.1; HRMS (EI): Exact mass calcd for $\text{C}_4\text{H}_3\text{Br}_2\text{O}_2$ [$\text{M}-\text{CH}_2\text{Cl}$] $^+$ 240.8494, found 240.8495.



3,3-Dibromo-5-(bromomethyl)dihydrofuran-2(3H)-one (206). The lactone¹²⁵ was prepared from epibromohydrin (63.8 μL , 746 μmol) as described by Jacobsen¹²⁴ and purified via flash column chromatography (15% ethyl acetate in hexanes) to give a colorless oil (182 mg, 73%). R_f = 0.35 (20% EtOAc/hexanes); IR (film) 2923, 2858, 1783, 1430 cm^{-1} ; ^1H NMR (600 MHz, CDCl_3) δ 4.83 (dddd, J = 9.4, 6.6, 5.0, 5.0 Hz, 1H), 3.65 (dd, J = 11.1, 4.5 Hz, 1H), 3.59 (dd, J = 11.0, 6.7 Hz, 1H), 3.43 (dd, J = 14.7, 5.1 Hz, 1H), 3.10 (dd, J = 14.6, 9.2 Hz, 1H); ^{13}C NMR (150 MHz, CDCl_3) ppm 167.8, 75.9, 50.9, 46.5, 30.5; HRMS (EI): Exact mass calcd for $\text{C}_4\text{H}_3\text{Br}_2\text{O}_2$ [$\text{M}-\text{CH}_2\text{Br}$] $^+$ 240.8494, found 240.8483.



4-Azido-5-methylenefuran-2(5H)-one (212). The imide (5.3 mg, 18 μmol) was dissolved in acetonitrile (90 μL), and the vinyl bromide (23.3 mg, 107 μmol) was added as a solution in acetonitrile (90 μL). The mixture was cooled to -40 $^\circ\text{C}$, and triflic acid (6.4 μL , 72 μmol) was added. After 24 h, the reaction was slowly warmed to 0 $^\circ\text{C}$ and stirred for another 29 h. The reaction was then cooled to -78 $^\circ\text{C}$ for 18.5 h, then warmed back to 0 $^\circ\text{C}$ and quenched with triethylamine (25 μL , 180 μmol). The reaction was concentrated, and the residue was purified via flash column chromatography (0-3% ethyl acetate in hexanes) to give the product as a brown microcrystalline solid which was only slightly soluble in most organic solvents. R_f = 0.26 (7% EtOAc/hexanes); IR (film) 2921, 2851, 2123, 1750, 1643, 1599 cm^{-1} ; ^1H NMR (600 MHz, CDCl_3) δ 6.63 (s, 1H), 5.19 (d, J = 2.9 Hz, 1H), 4.85 (d, J = 2.8 Hz, 1H); ^{13}C NMR (150 MHz, CDCl_3) ppm 164.3, 151.8, 131.0, 119.9, 97.4.



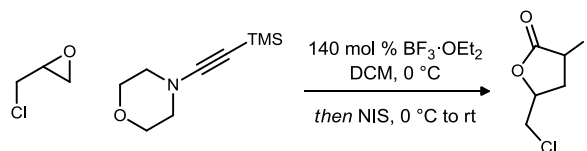
4-(1,3-Dioxolan-2-yl)but-1-ynyltributylstannane (214). *n*-Butyllithium (2.31 M in hexanes, 360 μL , 832 μmol) was added to a stirring solution of the alkyne¹²⁶ (100 mg, 793 μmol) in THF (7.9 mL) at -78 $^\circ\text{C}$. After 30

¹²⁴ Movassaghi, M.; Jacobsen, E. N., *J. Am. Chem. Soc.*, **2002**, 124, 2456.

¹²⁵ Leuchs, H.; Spletstosser, O., *Berichte der Deutschen Chemischen Gesellschaft*, **1907**, 40, 301.

¹²⁶ Ahmar, M.; Duyck, C.; Fleming, I., *J. Chem. Soc., Perkin Trans. 1: Org. and Bio-Org. Chem.*, **1998**, 2721.

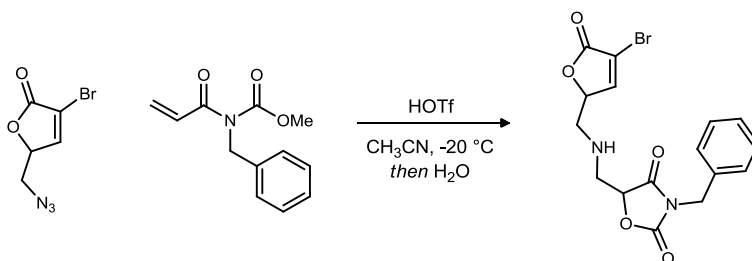
m, tributyltin chloride (258 μL , 951 μmol) was added. The reaction was stirred for 15 m, then the cold bath was removed, and the reaction was allowed to warm to room temperature. After 2 h, the cloudy white mixture was transferred to a separatory funnel containing water, and the aqueous phase was extracted with diethyl ether. The solution was dried, filtered, and concentrated. Purification of the residue via flash column chromatography (4-6% ethyl acetate in hexanes) gave the product as a colorless oil (110.5 mg, 34%). $R_f = 0.61$ (20% EtOAc/hexanes); IR (film) 2957, 2873, 2151, 1461 cm^{-1} ; ^1H NMR (600 MHz, CDCl_3) δ 4.99 (t, $J = 4.8$ Hz, 1H), 3.98-3.83 (m, 4H), 2.38 (t, $J = 7.5$ Hz, 2H), 1.87 (td, $J = 7.5, 4.8$ Hz, 2H), 1.57-1.52 (m, 6H), 1.35-1.31 (m, 6H), 0.96-0.93 (m, 6H), 0.90 (t, $J = 7.3$ Hz, 9H); ^{13}C NMR (150 MHz, CDCl_3) ppm 110.4, 103.3, 82.0, 64.9, 33.5, 28.8, 26.9, 15.1, 13.6, 10.9; HRMS (EI): Exact mass calcd for $\text{C}_{15}\text{H}_{27}\text{O}_2\text{Sn} [\text{M}-\text{C}_4\text{H}_9]^+$ 359.1028, found 359.1020.



5-(Chloromethyl)-3-iododihydrofuran-2(3H)-one (216). The ynamine¹²⁴ (69.3 mg, 378 μmol) was dissolved in dichloromethane (1.6 mL), and cooled to 0 $^\circ\text{C}$. Boron trifluoride etherate (46.7 μL , 378 μmol) was added dropwise, followed by epichlorohydrin (25 mg, 270 μmol), and the reaction was stirred at 0 $^\circ\text{C}$ for 30 m. *N*-Iodosuccinimide (182 mg, 811 μmol) was added, and the reaction was stirred for 20 m at 0 $^\circ\text{C}$, then warmed to room temperature and stirred for an additional 25 m. The reaction was quenched with the addition of dichloromethane (1.8 mL) and 1 N HCl (2.0 mL), followed by 30 m of stirring at room temperature. The mixture was extracted with dichloromethane, and the combined organic layers were dried, filtered, and concentrated. The residue was purified via flash column chromatography (20% ethyl acetate in hexanes) to give each diastereomer as a colorless oil (d_1 : 6.1 mg, 9%; d_2 : 4.8 mg, 7%).

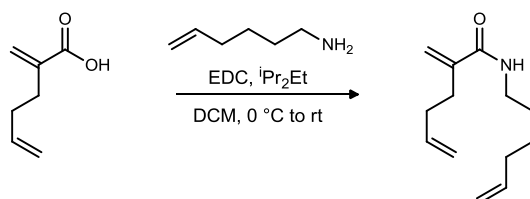
d_1 : $R_f = 0.16$ (40% EtOAc/hexanes); IR (film) 3018, 2962, 1787, 1432 cm^{-1} ; ^1H NMR (400 MHz, CDCl_3) δ 4.99 (dddd, $J = 6.8, 6.8, 4.7, 3.7$ Hz, 1H), 4.58 (dd, $J = 7.7, 4.1$ Hz, 1H), 3.82 (dd, $J = 12.1, 4.8$ Hz, 1H), 3.73 (dd, $J = 12.1, 3.6$ Hz, 1H), 2.72 (ddd, $J = 14.4, 7.6, 6.9$ Hz, 1H), 2.60 (ddd, $J = 14.4, 6.7, 4.1$ Hz, 1H); ^{13}C NMR (126 MHz, CDCl_3) ppm 171.2, 76.5, 50.3, 45.0, 36.1; HRMS (CI): Exact mass calcd for $\text{C}_5\text{H}_7\text{ClIO} [\text{M}+\text{H}]^+$ 260.9174, found 260.9177.

d_2 : $R_f = 0.14$ (40% EtOAc/hexanes); IR (film) 2957, 2921, 2850, 1787, 1648, 1447, 1431 cm^{-1} ; ^1H NMR (400 MHz, CDCl_3) δ 4.70 (dddd, $J = 7.8, 6.3, 6.3, 5.0$ Hz, 1H), 4.56 (dd, $J = 8.8, 8.8$ Hz, 1H), 3.79 (dd, $J = 11.7, 4.9$ Hz, 1H), 3.75 (dd, $J = 11.7, 6.3$ Hz, 1H), 2.99 (ddd, $J = 13.8, 8.7, 6.4$ Hz, 1H), 2.43 (ddd, $J = 13.8, 8.8, 8.0$ Hz, 1H); ^{13}C NMR (126 MHz, CDCl_3) ppm 171.0, 76.1, 50.1, 44.4, 35.9; HRMS (CI): Exact mass calcd for $\text{C}_5\text{H}_7\text{ClIO} [\text{M}+\text{H}]^+$ 260.9174, found 260.9176.

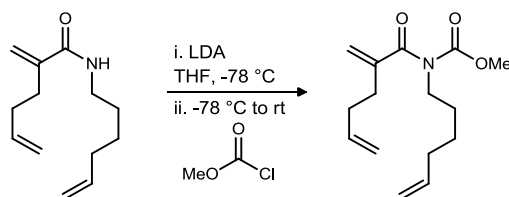


3-Benzyl-5-(((4-bromo-5-oxo-2,5-dihydrofuran-2-yl)methylamino)methyl)oxazolidine-2,4-dione (220). The azido lactone (30 mg, 140 μmol) and imide (15 mg, 69 μmol) were dissolved in acetonitrile (230 μL) and cooled to -20 $^\circ\text{C}$. Triflic acid (12.2 μL , 138 μmol) was added, and the reaction was monitored by TLC. After 1.5 h, no imide remained by TLC, and water (12.5 μL , 5.5 M in CH_3CN , 69 μmol) was added. After 1.7 h, the reaction was quenched with triethylamine (19 μL , 140 μmol). The reaction mixture was concentrated, and the residue was purified via flash column chromatography (15% ethyl acetate in hexanes) to give the product as a

colorless oil (8.3 mg, 30%). The compound was characterized as a 1:1 mixture of diastereomers. R_f = 0.11 (40% EtOAc/hexanes); IR (film) 3355, 3090, 2919, 2849, 1814, 1767, 1736, 1607, 1440, 1414 cm^{-1} ; ^1H NMR (600 MHz, CDCl_3) δ 7.43-7.41 (m, 4H), 7.36-7.30 (m, 6H), 7.26 (d, J = 1.9 Hz, 1H), 7.20 (d, J = 1.7 Hz, 1H), 4.79 (ddd, J = 5.7, 3.0, 3.0 Hz, 2H), 4.76 (ddd, J = 6.6, 5.1, 1.6 Hz, 1H), 4.72, (d, J = 14.6 Hz, 1H), 4.72 (ddd, J = 5.7, 5.7, 1.7 Hz, 1H), 4.69 (s, 2H), 4.67 (d, J = 14.5 Hz, 1H), 3.29 (dd, J = 14.2, 3.2 Hz, 1H), 3.26 (dd, J = 14.3, 3.2 Hz, 1H), 3.20 (dd, J = 14.2, 3.3 Hz, 1H), 3.14 (dd, J = 14.2, 3.1 Hz, 1H), 2.92 (dd, J = 13.2, 5.1 Hz, 1H), 2.92-2.87 (m, 2H), 2.84 (dd, J = 13.3, 6.6 Hz, 1H) [NH not observed]; ^{13}C NMR (126 MHz, CDCl_3) ppm 171.71, 171.66, 167.8, 155.3, 155.2, 150.7, 150.6, 134.6, 134.5, 128.8, 128.7 (3C), 128.5, 128.4, 114.0, 113.9, 82.1, 81.9, 80.0, 79.9, 51.49, 51.47, 48.3, 48.1, 43.8; HRMS (ESI): Exact mass calcd for $\text{C}_{16}\text{H}_{15}\text{BrN}_2\text{O}_5$ [M] $^+$ 394.02, found xx.



***N*-(Hex-5-enyl)-2-methylenehex-5-enamide (221).** The amine¹²⁷ (472 mg, 4.76 mmol) was added to a solution of the carboxylic acid¹²⁸ (500 mg, 3.96 mmol) in dichloromethane (20 mL) at 0 °C. 1-Ethyl-3-(3'-dimethylaminopropyl)carbodiimide hydrochloride (1.06 g, 5.55 mmol) was added as a solid, followed by diisopropylethylamine (967 μL , 5.55 mmol), and the reaction was allowed to slowly warm to room temperature over 20 h. The mixture was washed with 1 N HCl, water, and satd aq sodium bicarbonate, and the resulting organic solution was dried, filtered, and concentrated to give a colorless oil (503 mg, 61%), which was used without further purification. An analytical sample was obtained via flash column chromatography (12% ethyl acetate in hexanes). R_f = 0.27 (20% EtOAc/hexanes); IR (film) 3313, 3076, 2975, 2928, 2858, 1652, 1614, 1536, 1439 cm^{-1} ; ^1H NMR (600 MHz, CDCl_3) δ 5.90 (br s, 1H), 5.78 (ddt, J = 16.9, 10.3, 6.6 Hz, 1H), 5.77 (ddt, J = 16.9, 10.3, 6.7 Hz, 1H), 5.53 (s, 1H), 5.23 (s, 1H), 5.01 (ddt, J = 17.2, 1.7, 1.7 Hz, 1H), 4.99 (ddt, J = 17.1, 1.7, 1.7 Hz, 1H), 4.95 (ddt, J = 10.0, 1.3, 1.3 Hz, 1H), 4.94 (ddt, J = 10.1, 1.3, 1.3 Hz, 1H), 3.28 (td, J = 7.2, 5.8 Hz, 2H), 2.39 (br t, J = 7.7 Hz, 2H), 2.06 (ttdd, J = 7.1, 7.1, 1.3, 1.3 Hz, 2H), 2.20 (ttdd, J = 7.9, 6.4, 1.4, 1.4 Hz, 2H), 1.55-1.50 (m, 2H), 1.44-1.39 (m, 2H); ^{13}C NMR (150 MHz, CDCl_3) ppm 168.9, 145.2, 138.3, 137.6, 117.1, 115.2, 114.8, 39.4, 33.3, 32.1, 31.7, 29.0, 26.1; HRMS (ESI): Exact mass calcd for $\text{C}_{13}\text{H}_{21}\text{NNaO}$ [M+Na] $^+$ 230.1521, found 230.1531.

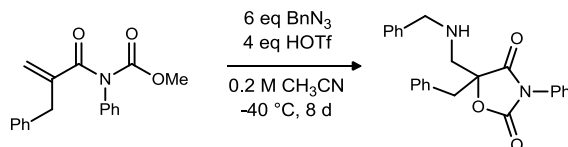


Methyl hex-5-enyl(2-methylenehex-5-enoyl)carbamate (222). Diisopropylamine (37.3 μL , 265 μmol) was dissolved in THF (0.8 mL) and cooled to -78 °C in a dry ice/acetone bath. *n*Butyllithium (2.56 M in hexanes, 99.0 μL , 253 μmol) was added. After 2 m, the reaction was warmed to 0 °C, stirred for 5 m, then recooled to -78 °C. The reaction was allowed to stir for 5 m, then the amide (50.0 mg, 241 μmol) was added via microsyringe. The reaction was stirred for 20 m, then methyl chloroformate (22.3 μL , 289 μmol) was added. The reaction was stirred for 20 m at -78 °C, then allowed to warm to room temperature and stirred for 2.5 h, then quenched with 1 N HCl. The mixture was transferred to a separatory funnel containing diethyl ether and 1 N HCl. The layers were separated, and the aqueous layer was extracted with diethyl ether. The organic layers were combined and washed with satd aq NaHCO_3 . The organic solution was dried, filtered, and concentrated, and the residue was

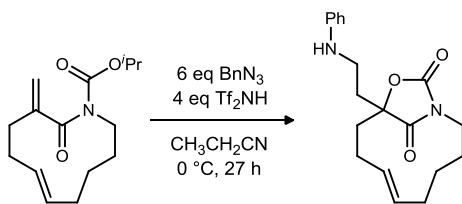
¹²⁷ Smith, B. J.; Sulikowski, G. A., *Angew. Chem. Int. Ed.*, **2010**, *49*, 1599.

¹²⁸ Yip, K.; Zhu, N.; Yang, D., *Org. Lett.*, **2009**, *11*, 1911.

purified via flash column chromatography (0-2% ethyl acetate in hexanes) to give the product as a colorless oil (12.2 mg, 19%) in addition to amide substrate (25.3 mg, 51%). $R_f = 0.31$ (7% EtOAc/hexanes); IR (film) cm^{-1} 3077, 2930, 2858, 1742, 1678, 1639, 1444; $^1\text{H NMR}$ (600 MHz, CDCl_3) δ 5.84 (ddt, $J = 16.9, 10.2, 6.5$ Hz, 1H), 5.79 (ddt, $J = 16.9, 10.2, 6.7$ Hz, 1H), 5.19 (br s, 2H), 5.06 (ddt, $J = 17.2, 1.7, 1.7$ Hz, 1H), 5.00 (ddt, $J = 17.3, 1.7, 1.7$ Hz, 1H), 4.98 (ddt, $J = 10.3, 1.5, 1.5$ Hz, 1H), 4.95 (ddt, $J = 10.2, 2.3, 1.3$ Hz, 1H), 3.75 (s, 3H), 3.69 (dd, $J = 7.5, 7.5$ Hz, 2H), 2.43 (dd, $J = 7.7, 7.7$ Hz, 2H), 2.56 (br ddd, $J = 7.5, 7.5, 7.5$ Hz, 2H), 2.07 (br ddd, $J = 7.2, 7.2, 7.2$ Hz, 2H), 1.62-1.57 (m, 2H), 1.43-1.40 (m, 2H); $^{13}\text{C NMR}$ (150 MHz, CDCl_3) ppm 173.7, 155.5, 146.9, 138.3, 137.6, 115.2, 115.1, 114.7, 53.3, 45.0, 33.3, 32.1, 31.8, 28.1, 26.0; HRMS (ESI): Exact mass calcd for $\text{C}_{15}\text{H}_{23}\text{NNaO}_3$ $[\text{M}+\text{Na}]^+$ 288.1576, found 288.1571.



5-Benzyl-5-((benzylamino)methyl)-3-phenyloxazolidine-2,4-dione (231). The imide (8.9 mg, 30 μmol) was dissolved in acetonitrile (150 μL), and benzyl azide (23 μL , 180 μmol) was added. The reaction mixture was cooled to -40 $^\circ\text{C}$, and triflic acid (11 μL , 120 μmol) was added. After 8 d, the reaction was quenched at -40 $^\circ\text{C}$ with triethylamine (17 μL , 120 μmol). The reaction was concentrated, and the residue was purified via flash column chromatography (10% ethyl acetate in hexanes) to give the product as a colorless oil (6.1 mg, 53%) in addition to imide substrate (3.5 mg, 39%). $R_f = 0.25$ (20% EtOAc/hexanes); IR (film) 3029, 2922, 1816, 1741, 1598, 1498, 1453, 1407 cm^{-1} ; $^1\text{H NMR}$ (600 MHz, CDCl_3) δ 7.38-7.25 (m, 13H), 6.87 (dd, $J = 7.8, 1.3$ Hz, 2H), 3.88 (d, $J = 13.6$ Hz, 1H), 3.85 (d, $J = 13.6$ Hz, 1H), 3.29 (d, $J = 13.4$ Hz, 1H), 3.22 (d, $J = 13.4$ Hz, 1H), 3.18 (s, 2H) [NH not observed]; $^{13}\text{C NMR}$ (150 MHz, CDCl_3) ppm 173.1, 153.9, 139.5, 132.5, 130.6, 130.2, 129.2, 128.9, 128.7, 128.5, 127.9, 127.8, 127.2, 125.9, 90.3, 54.0, 52.4, 39.3; HRMS (ESI): Exact mass calcd for $\text{C}_{24}\text{H}_{23}\text{N}_2\text{O}_3$ $[\text{M}+\text{H}]^+$ 387.1709, found 387.1706.



(E)-10-(2-(phenylamino)ethyl)-11-oxa-1-azabicyclo[8.2.1]tridec-6-ene-12,13-dione (234). The imide (11 mg, 41 μmol) was dissolved in propionitrile (200 μL), and benzyl azide (31 μL , 250 μmol) was added. The solution was cooled to 0 $^\circ\text{C}$ and triflimide (47 mg, 170 μmol) was added as a solution in propionitrile (200 μL). After 27 h, the reaction was quenched with triethylamine (23 μL , 170 μmol) at 0 $^\circ\text{C}$. After 10 m, the mixture was concentrated, and the residue was purified via flash column chromatography (15% ethyl acetate in hexanes) to give the product as a colorless oil (6.3 mg, 46%). $R_f = 0.21$ (20% EtOAc/hexanes); IR (film) 3398, 2925, 2853, 1809, 1730, 1603, 1509, 1448, 1414 cm^{-1} ; $^1\text{H NMR}$ (600 MHz, CDCl_3) δ 7.16 (dd, $J = 8.5, 7.4$ Hz, 2H), 6.71 (t, $J = 7.3$ Hz, 1H), 6.54 (d, $J = 8.5$ Hz, 2H), 5.47 (dddd, $J = 15.2, 10.4, 4.8, 1.5$ Hz, 1H), 5.25 (dddd, $J = 14.9, 11.2, 3.8, 1.4$ Hz, 1H), 3.39 (ddd, $J = 14.0, 5.8, 3.0$ Hz, 1H), 3.33 (ddd, $J = 14.1, 10.6, 2.2$ Hz, 1H), 3.19 (ddd, $J = 7.2, 7.2, 1.8$ Hz, 2H), 2.38-2.30 (m, 1H), 2.22 (dd, $J = 14.5, 3.6$ Hz, 1H), 2.19 (dd, $J = 13.9, 3.8$ Hz, 1H), 2.15 (ddd, $J = 14.6, 7.3, 7.3$ Hz, 1H), 2.09 (ddd, $J = 14.6, 6.4, 6.4$ Hz, 1H), 2.11-2.05 (m, 1H), 2.01-1.97 (m, 1H), 1.85-1.78 (m, 2H), 1.74-1.66 (m, 2H), 1.47-1.41 (m, 1H) [NH not observed]; $^{13}\text{C NMR}$ (150 MHz, CDCl_3) ppm 176.4, 155.8, 147.3, 134.3, 129.3, 128.0, 117.9, 112.8, 86.0, 42.4, 37.9, 37.7, 33.7, 33.4, 28, 26.9, 26.0; HRMS (ESI): Exact mass calcd for $\text{C}_{19}\text{H}_{25}\text{N}_2\text{O}_3$ $[\text{M}+\text{H}]^+$ 329.1865, found 329.1857.

CHAPTER IV

SUPPLEMENTAL INFORMATION

Proton (^1H), carbon (^{13}C), and two-dimensional nuclear magnetic resonance spectra (NMR) were acquired on a Bruker DRX-600 (600 MHz), Bruker DRX-500 (500 MHz), or Bruker DRX-400 (400 MHz) instrument. Fluorine (^{19}F) spectra were recorded using a Bruker DPX-300 (300 MHz). Chemical shifts are measured relative to residual solvent peaks as an internal standard set to 7.26 for CDCl_3 , 2.50 for $\text{DMSO-}d_6$, and 3.31 for $\text{MeOD-}d_4$.

Figure 41. ^{13}C NMR (DMSO- d_6) of 39

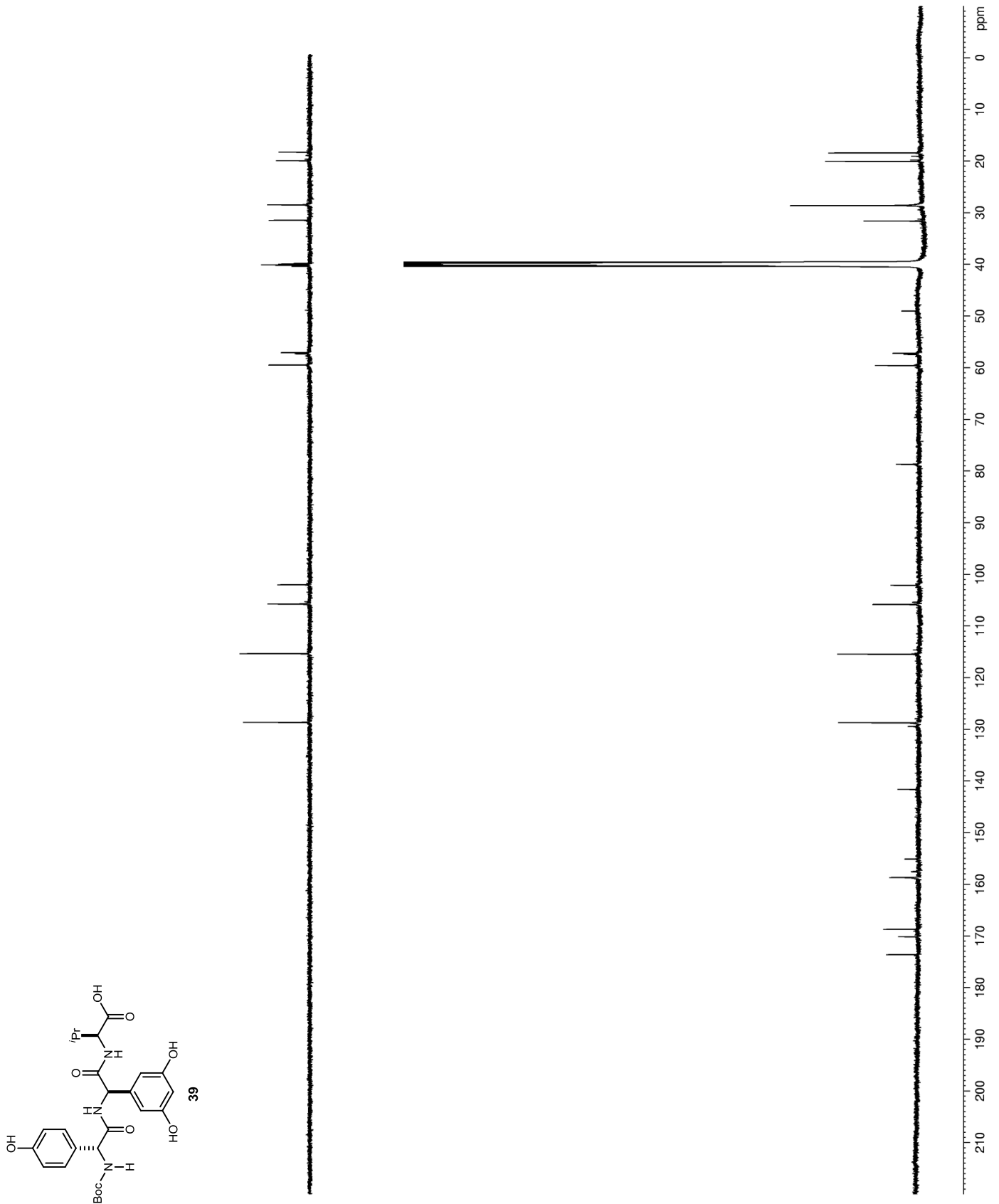


Figure 42. ^1H NMR ($\text{DMSO-}d_6$) of 55

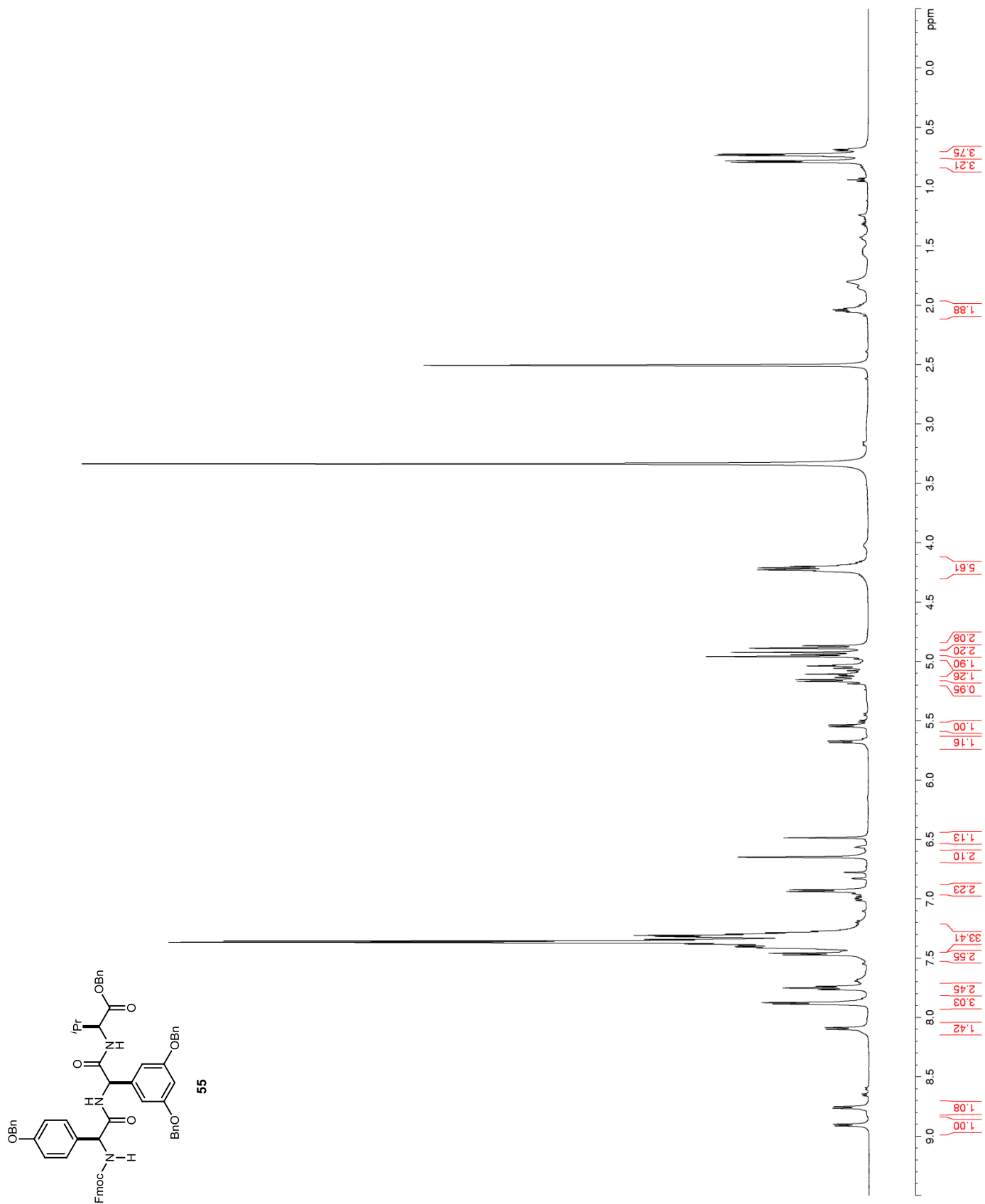


Figure 43. ^{13}C NMR (DMSO- d_6) of 55

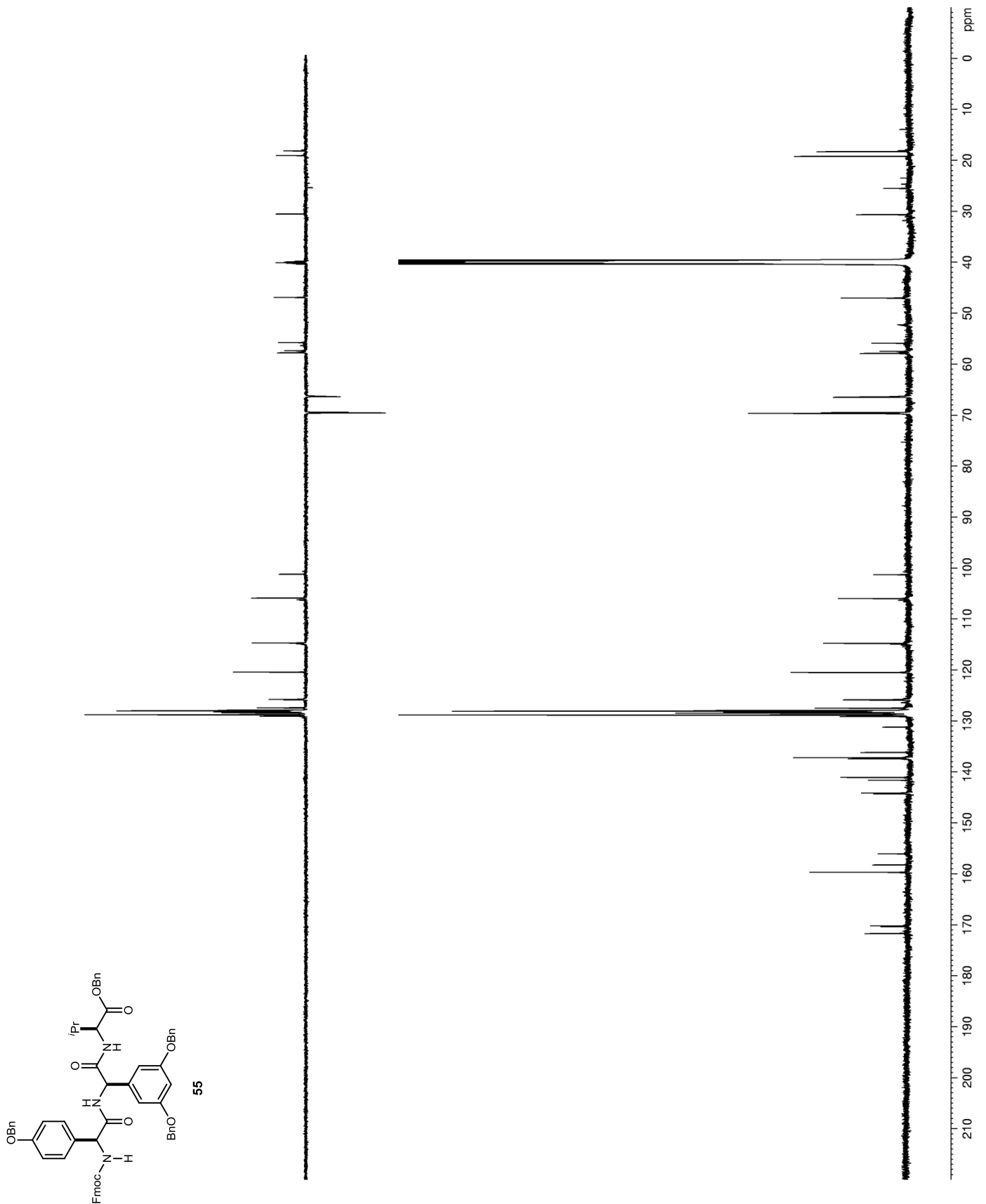


Figure 44. ^1H NMR ($\text{DMSO-}d_6$) of 56

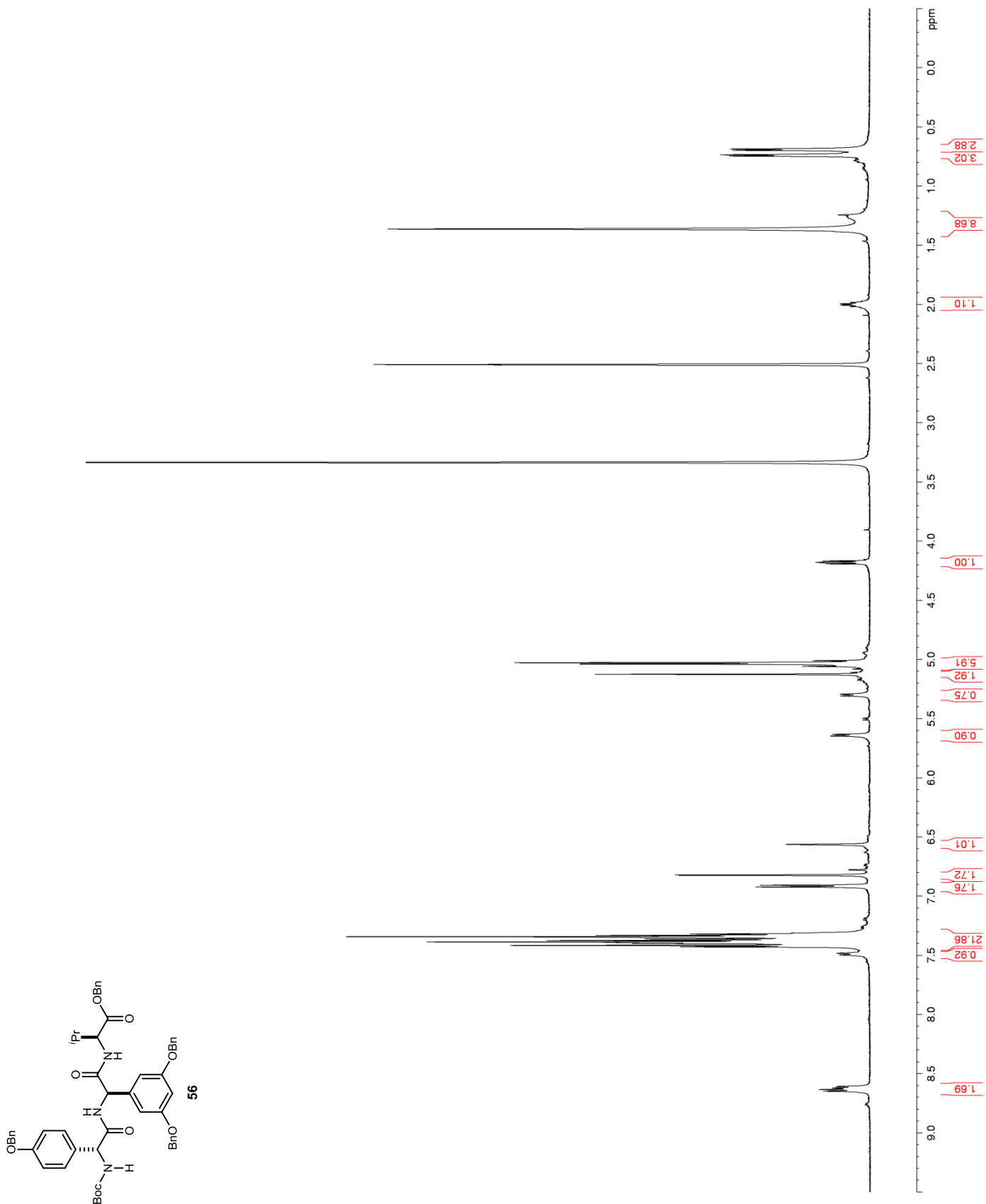


Figure 45. ^{13}C NMR (DMSO- d_6) of 56

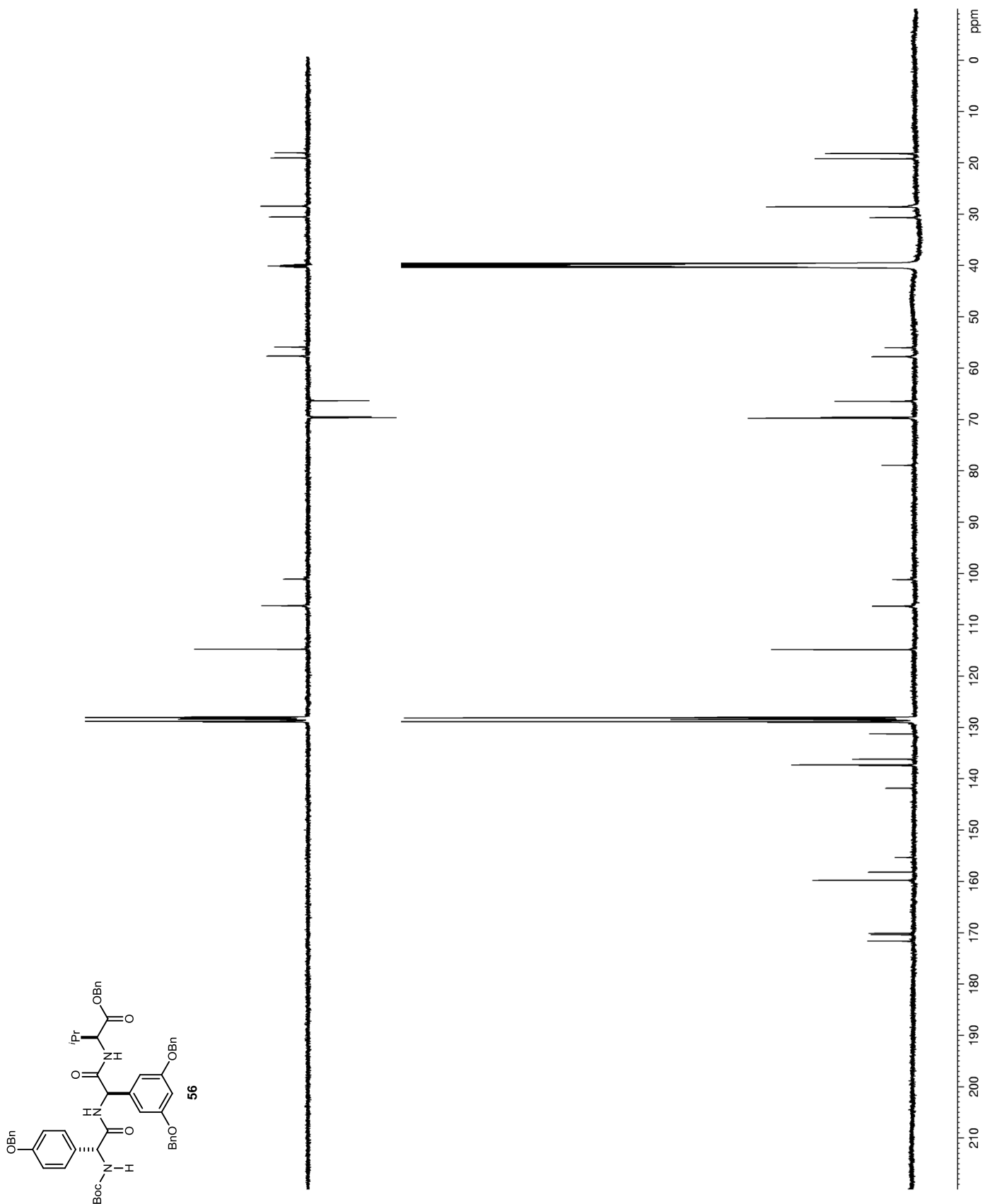


Figure 46. ^1H NMR ($\text{DMSO-}d_6$) of TFA-59

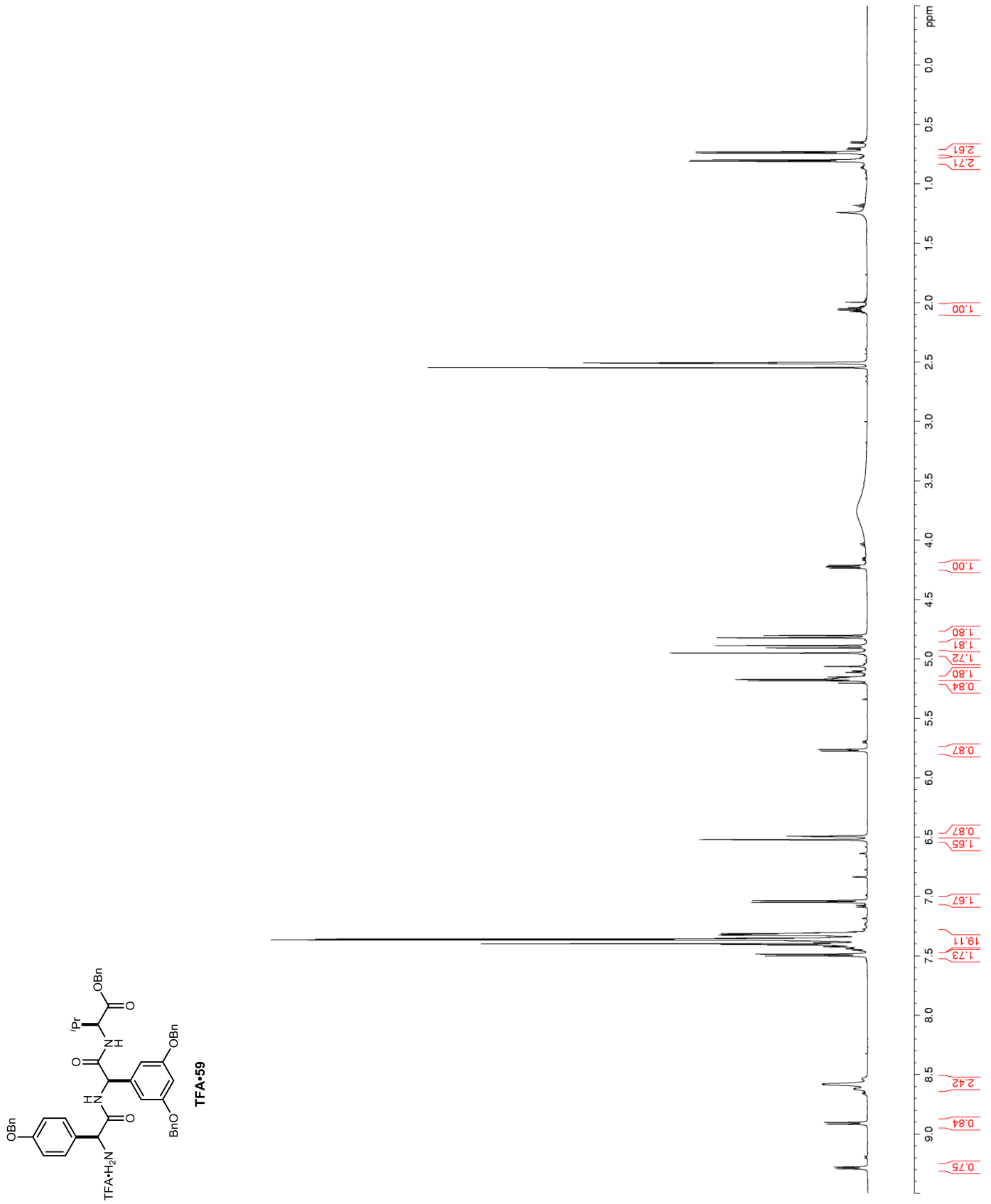


Figure 47. ^{13}C NMR (DMSO- d_6) of TFA•59

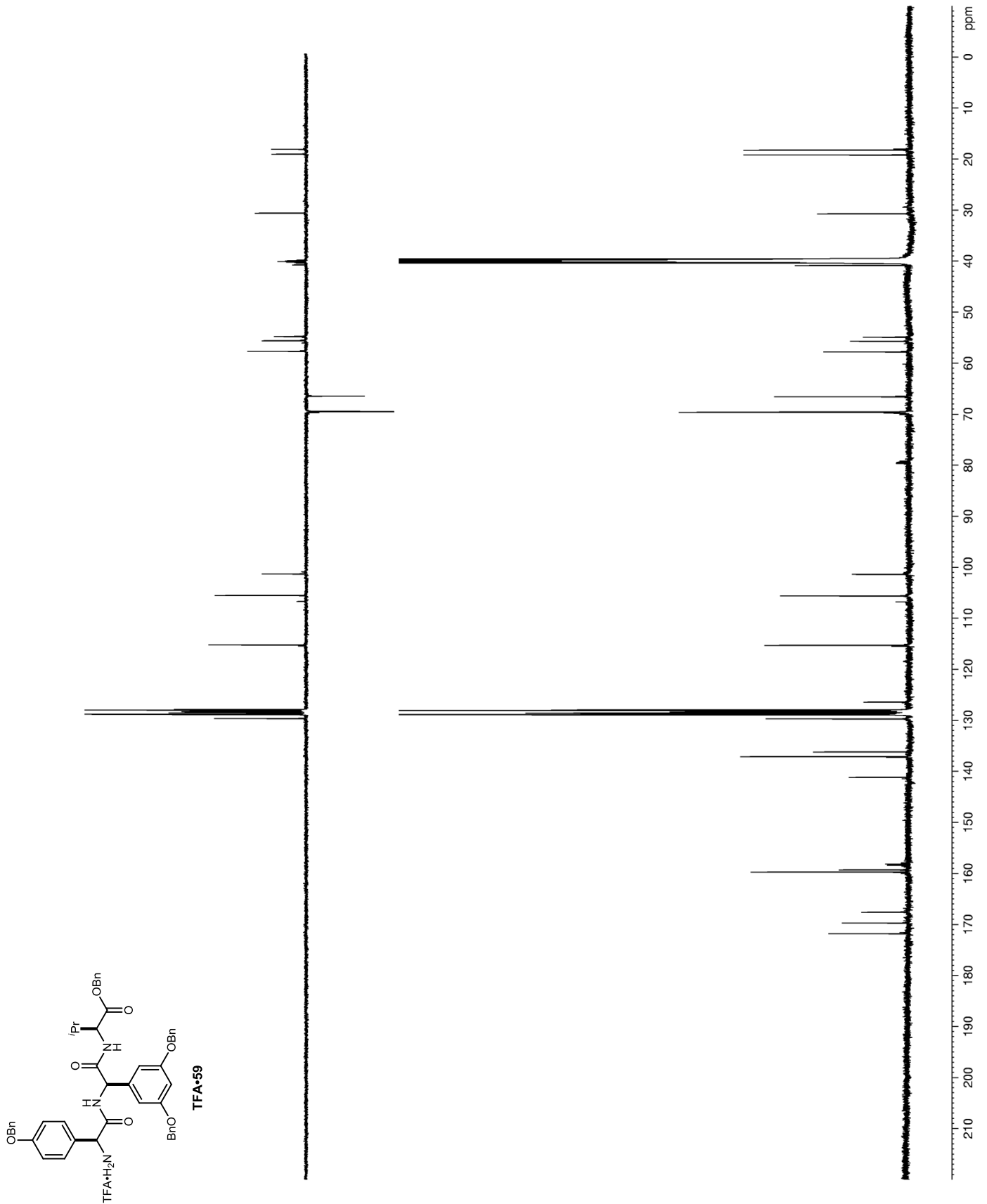


Figure 48. ^{19}F NMR (DMSO- d_6) of TFA·59

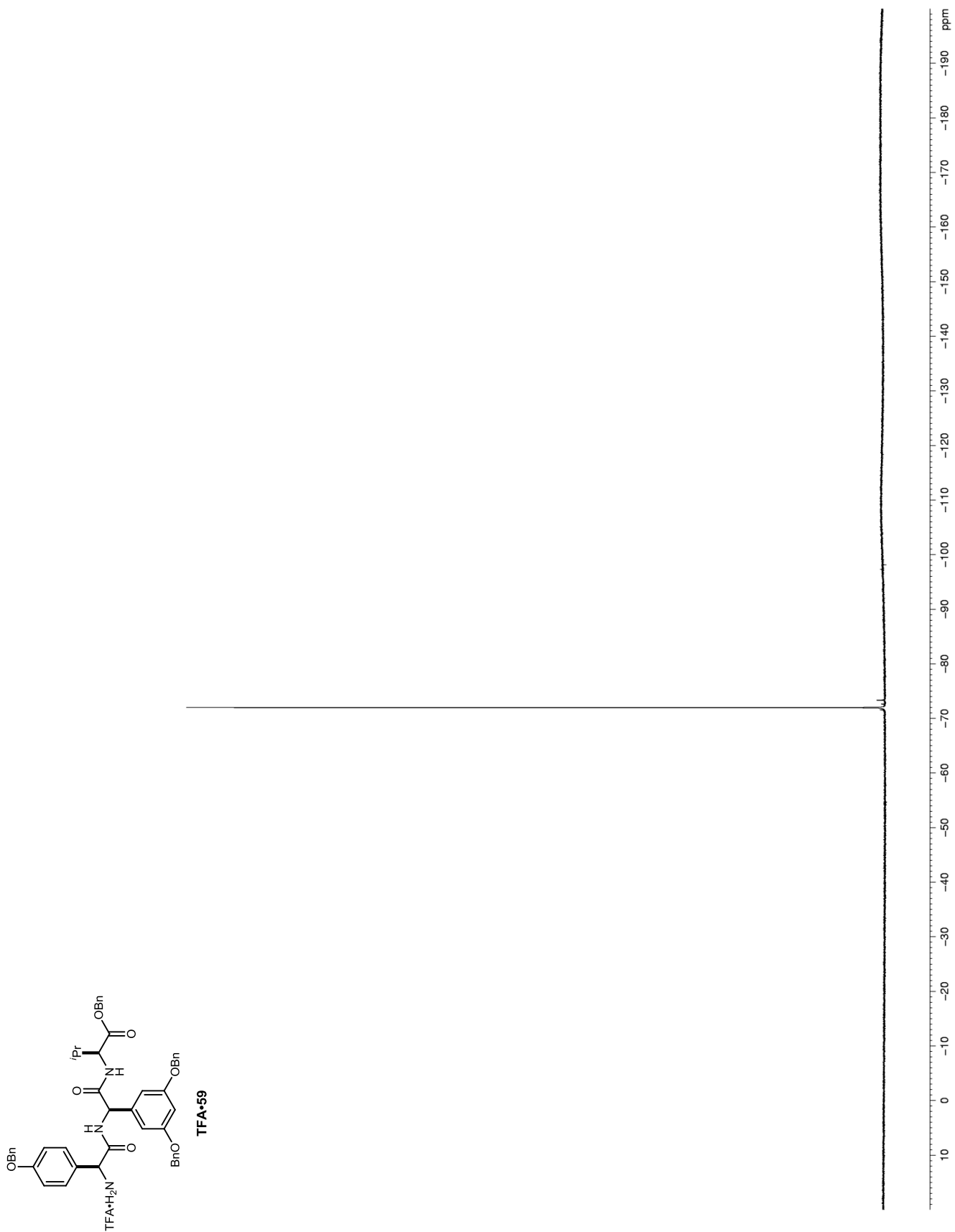


Figure 49. ^1H NMR ($\text{DMSO-}d_6$) of 63

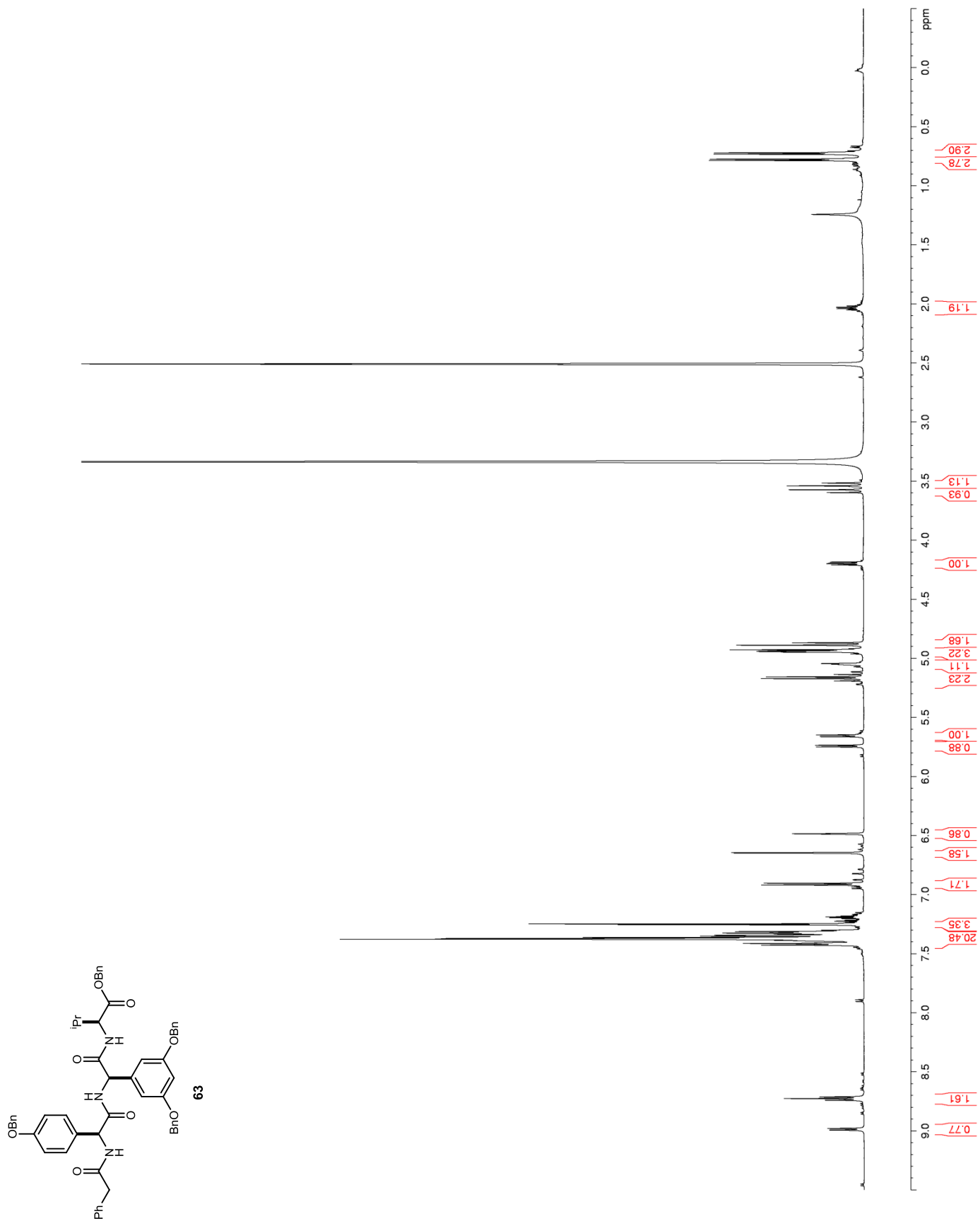


Figure 50. ^{13}C NMR ($\text{DMSO-}d_6$) of 63

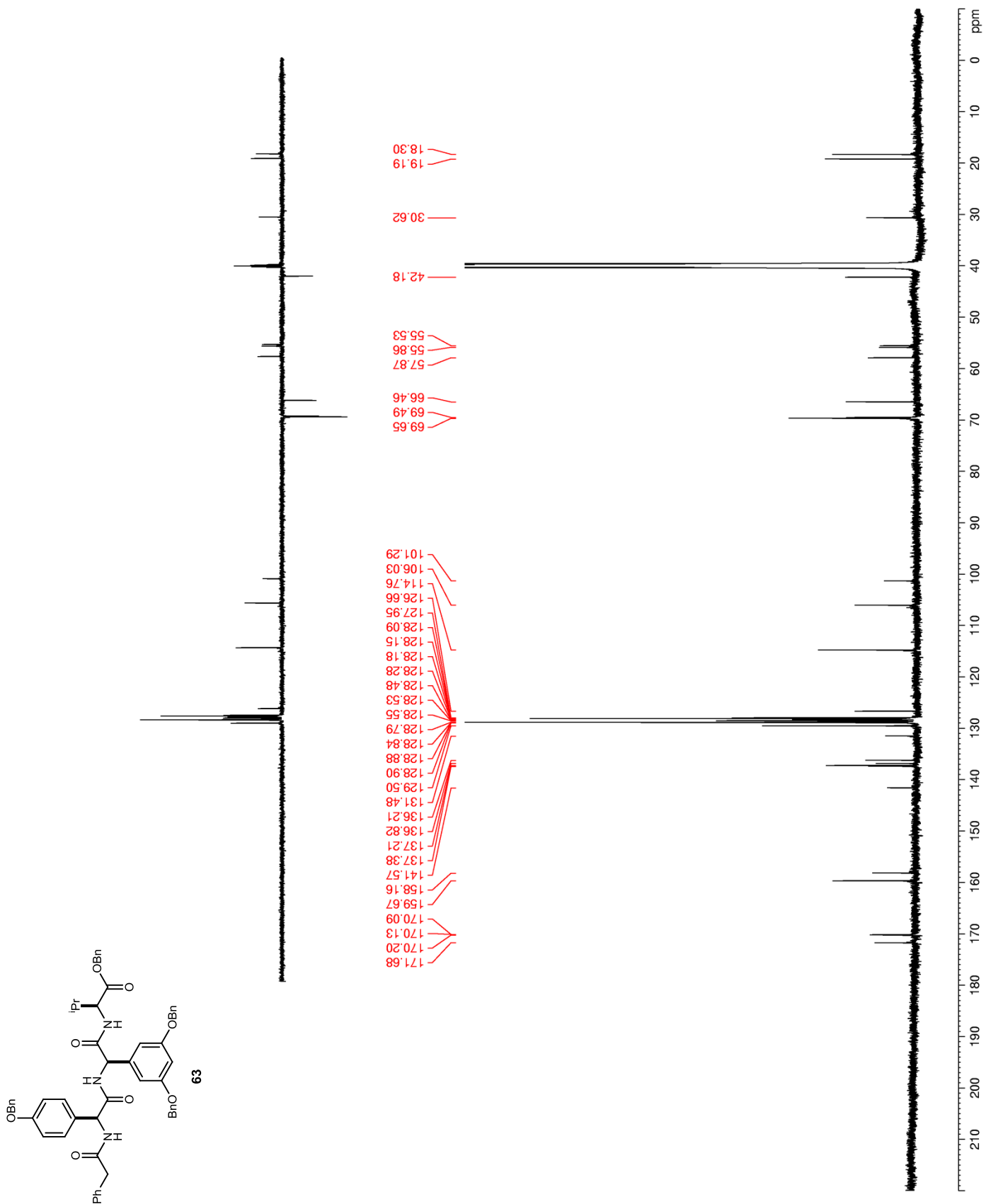


Figure 51. ^1H NMR (CDCl_3) of 65

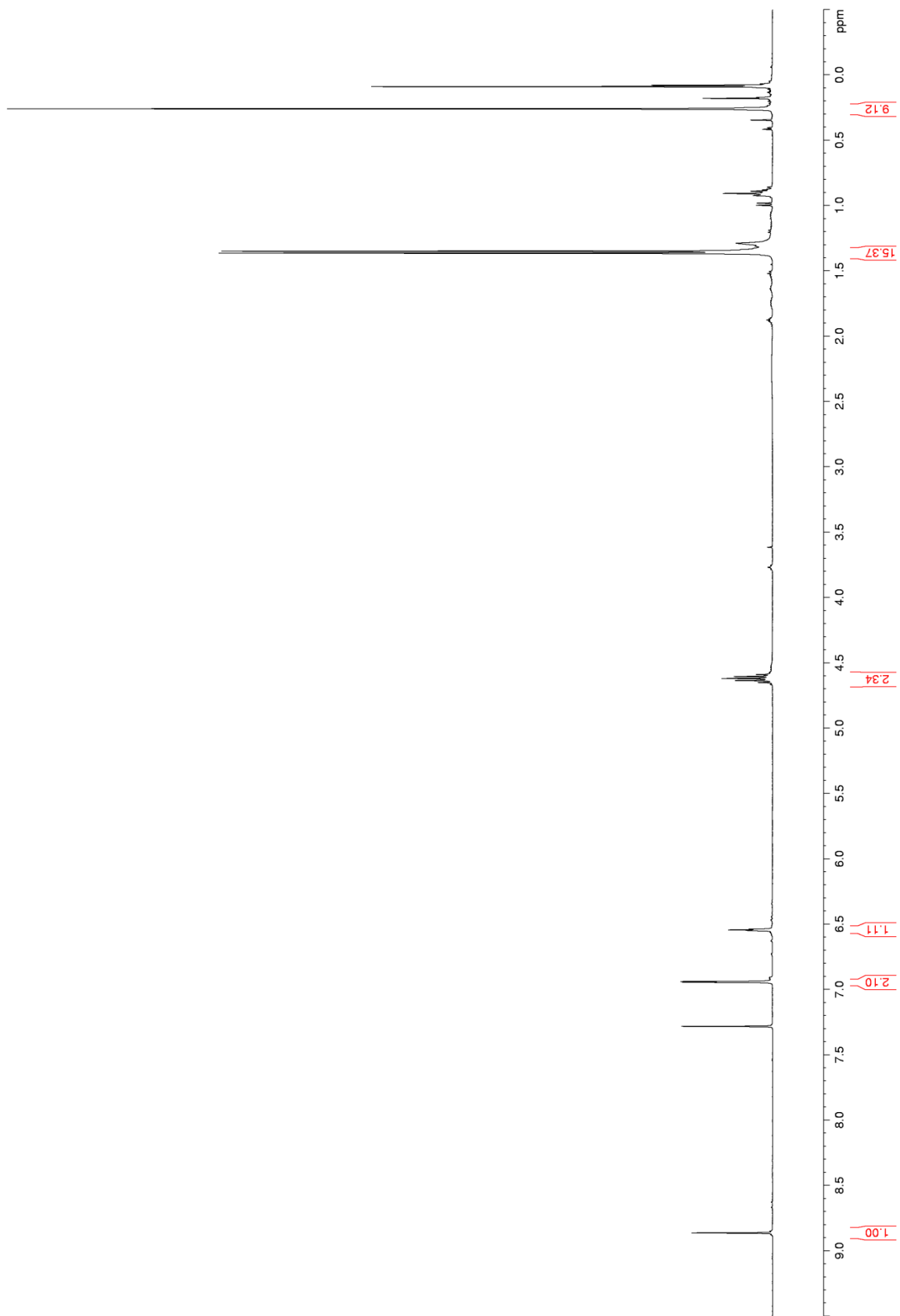
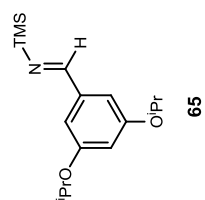


Figure 52. ^1H NMR ($\text{DMSO-}d_6$) of 66

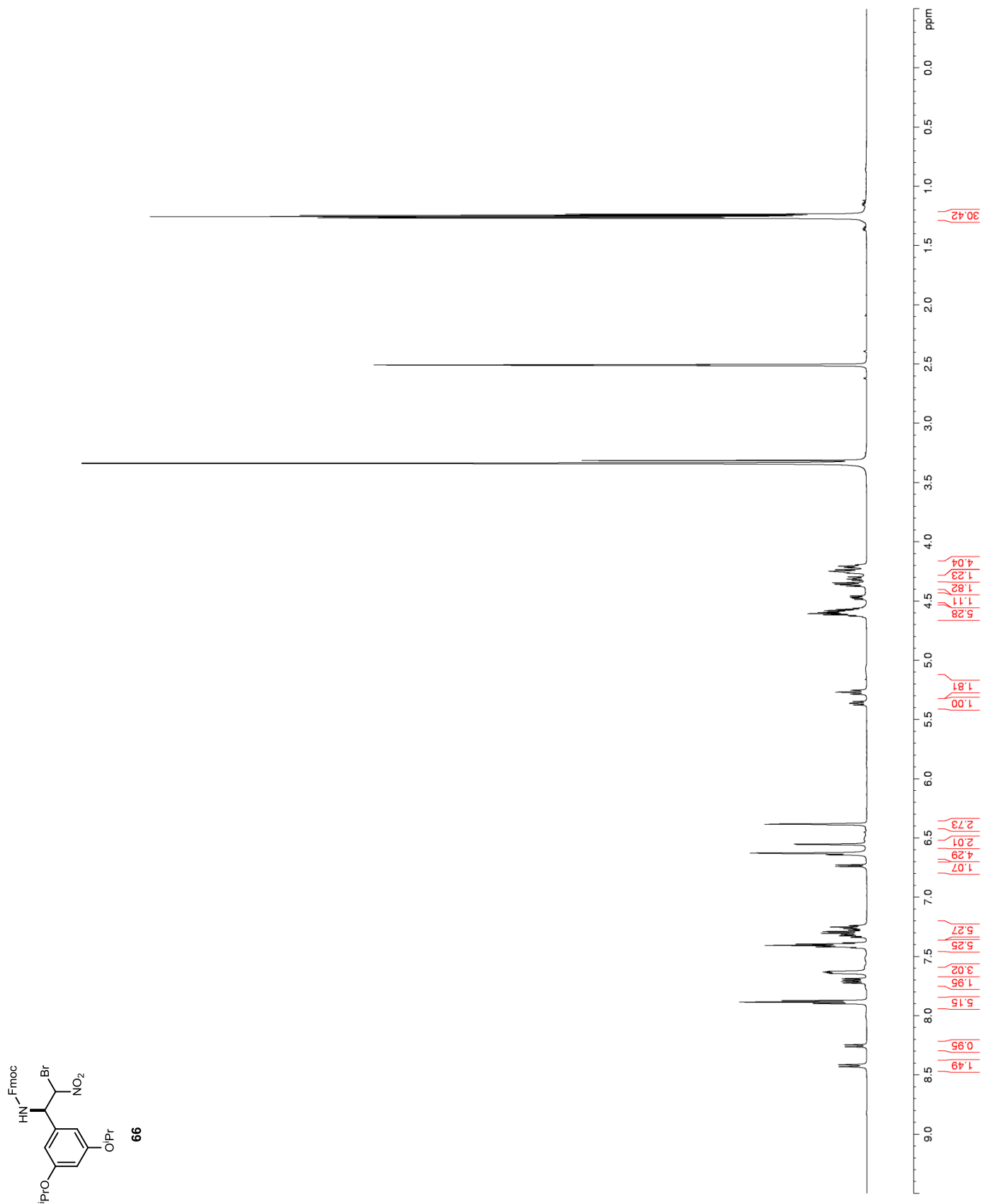


Figure 53. ^{13}C NMR (DMSO- d_6) of 66

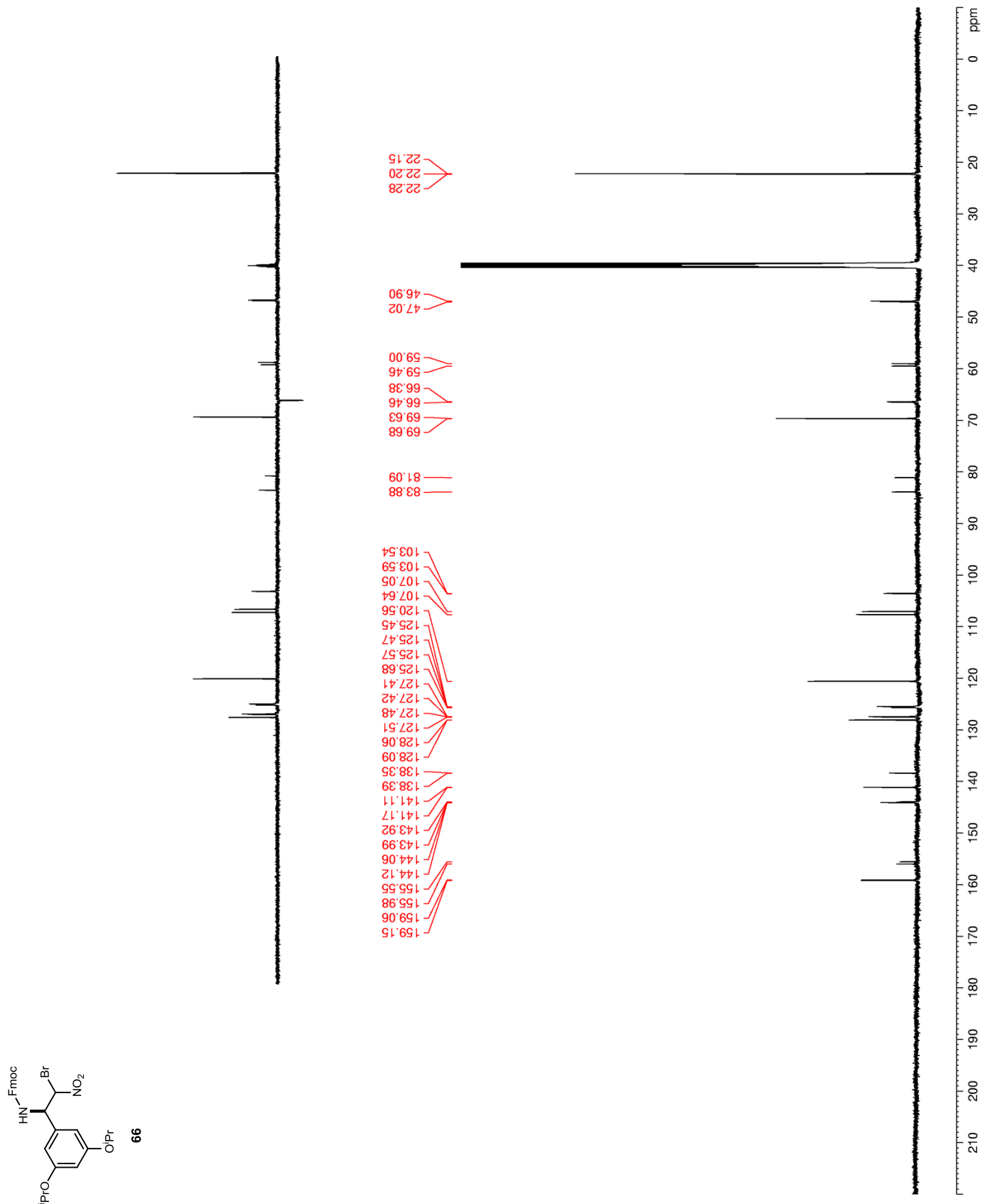


Figure 54. ^1H NMR (CDCl_3) of 68

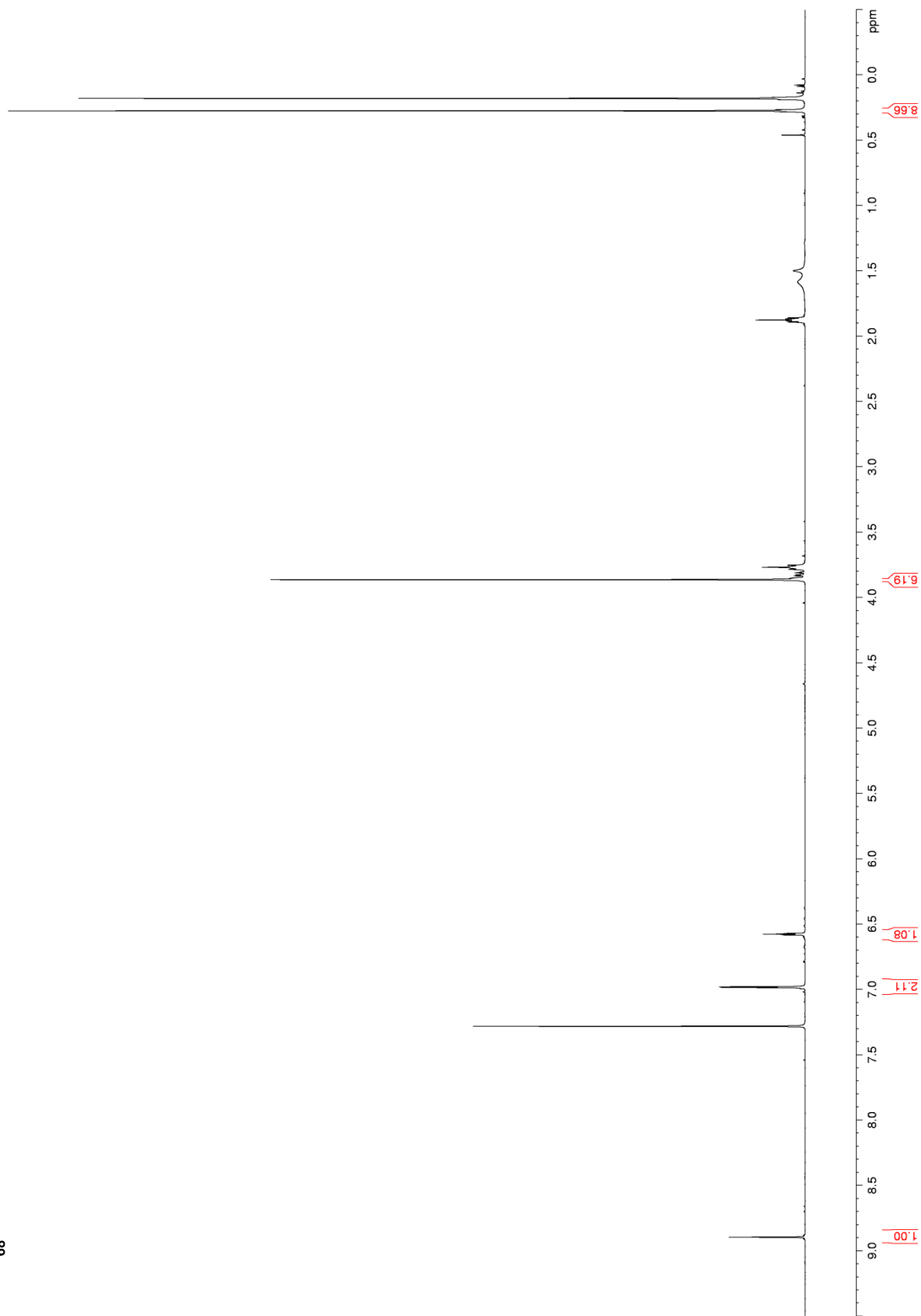
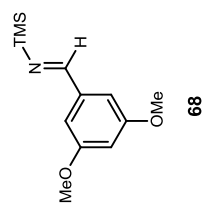


Figure 55. ^1H NMR ($\text{DMSO-}d_6$) of 69

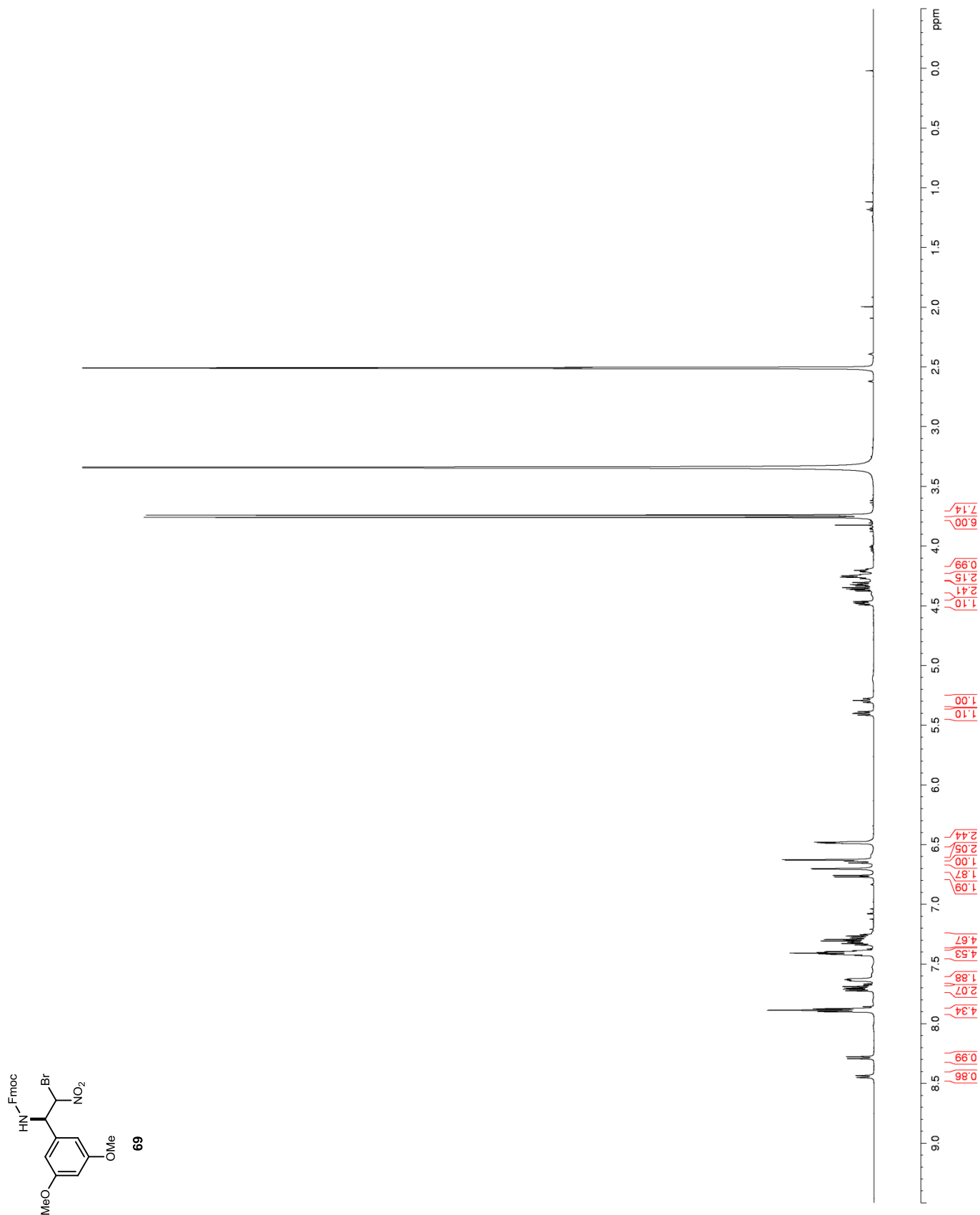


Figure 56. ^{13}C NMR (DMSO- d_6) of 69

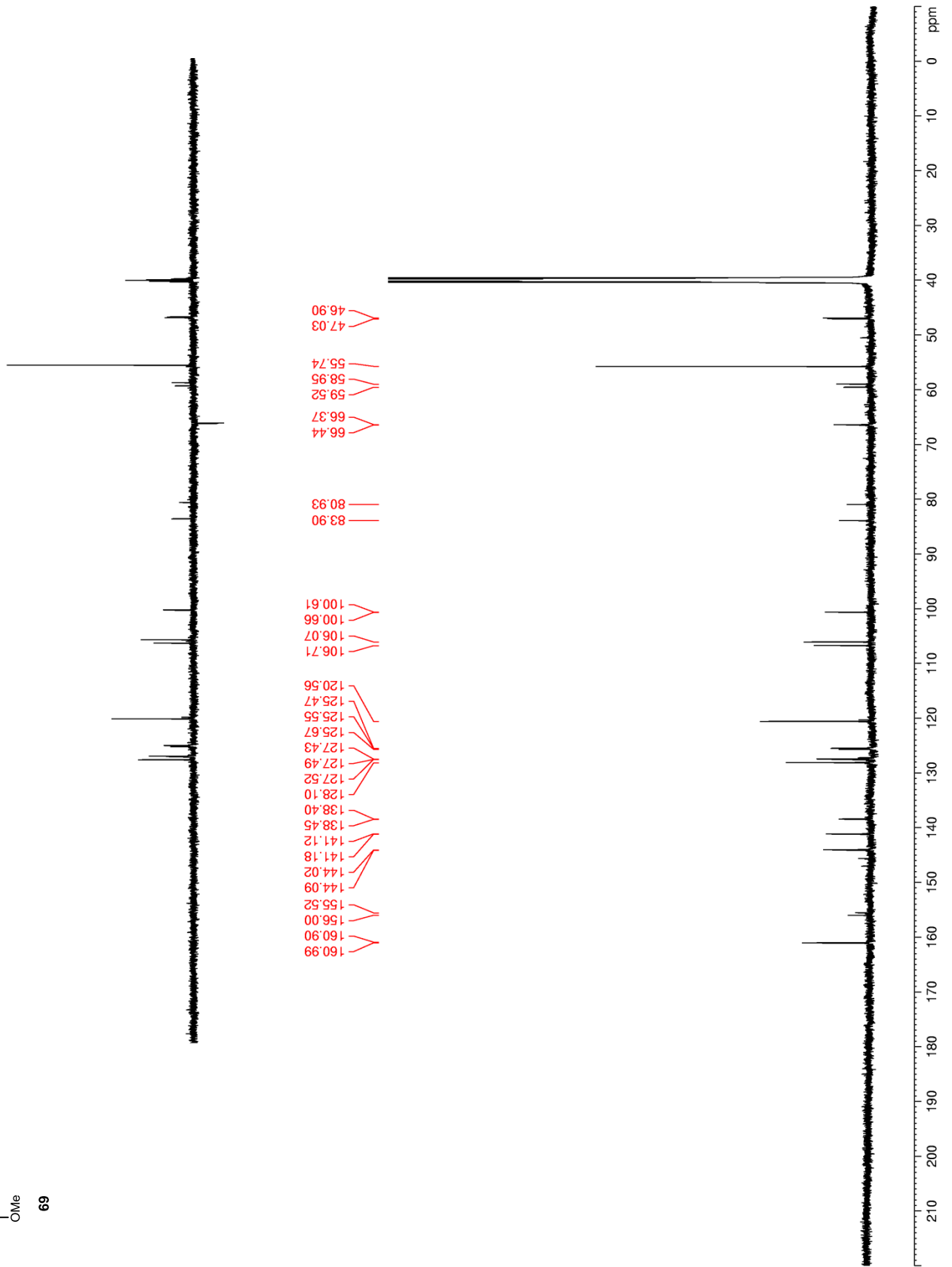
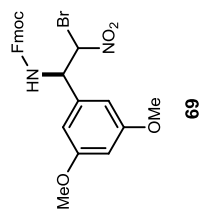


Figure 57. ^1H NMR (DMSO- d_6) of 72

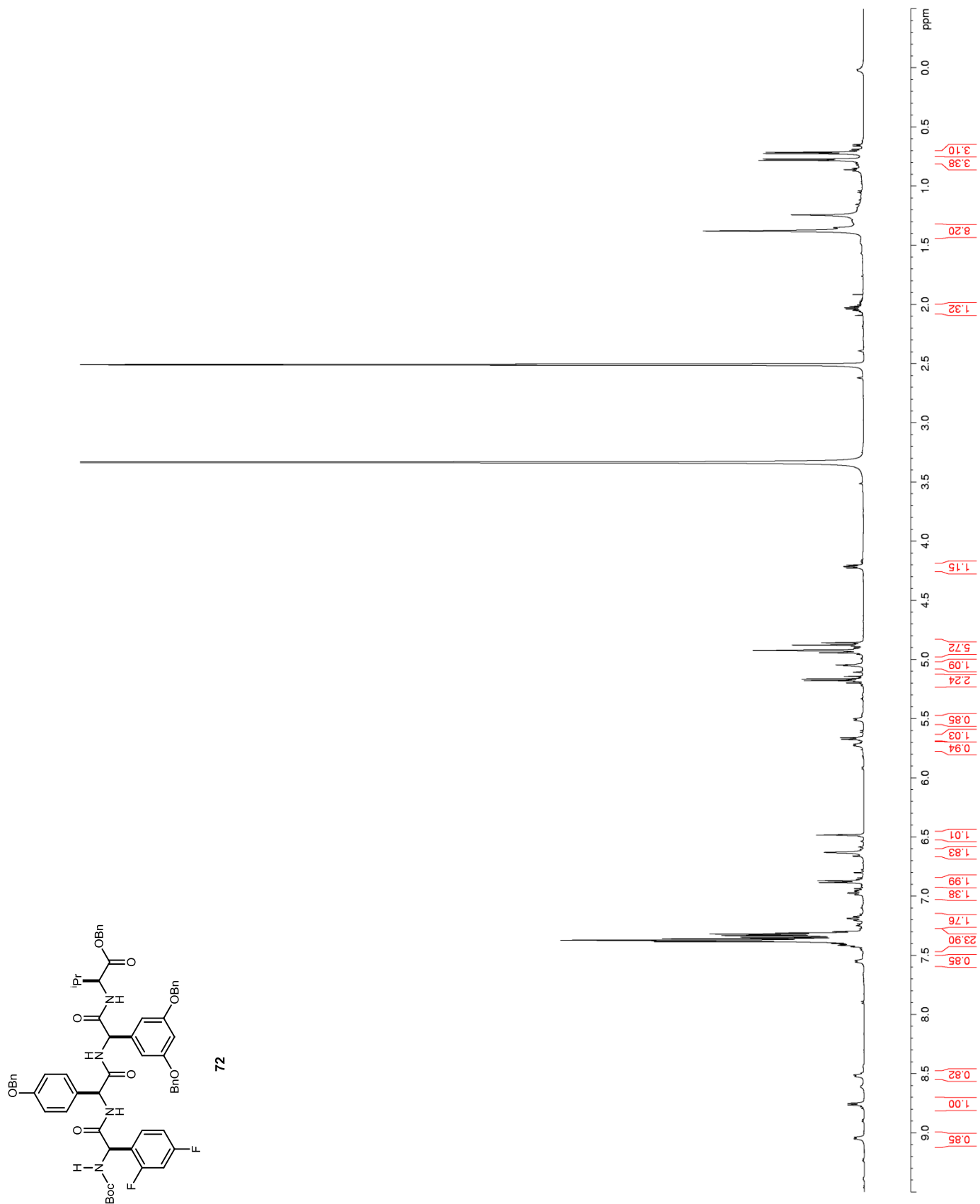


Figure 58. ^{13}C NMR (DMSO- d_6) of 72

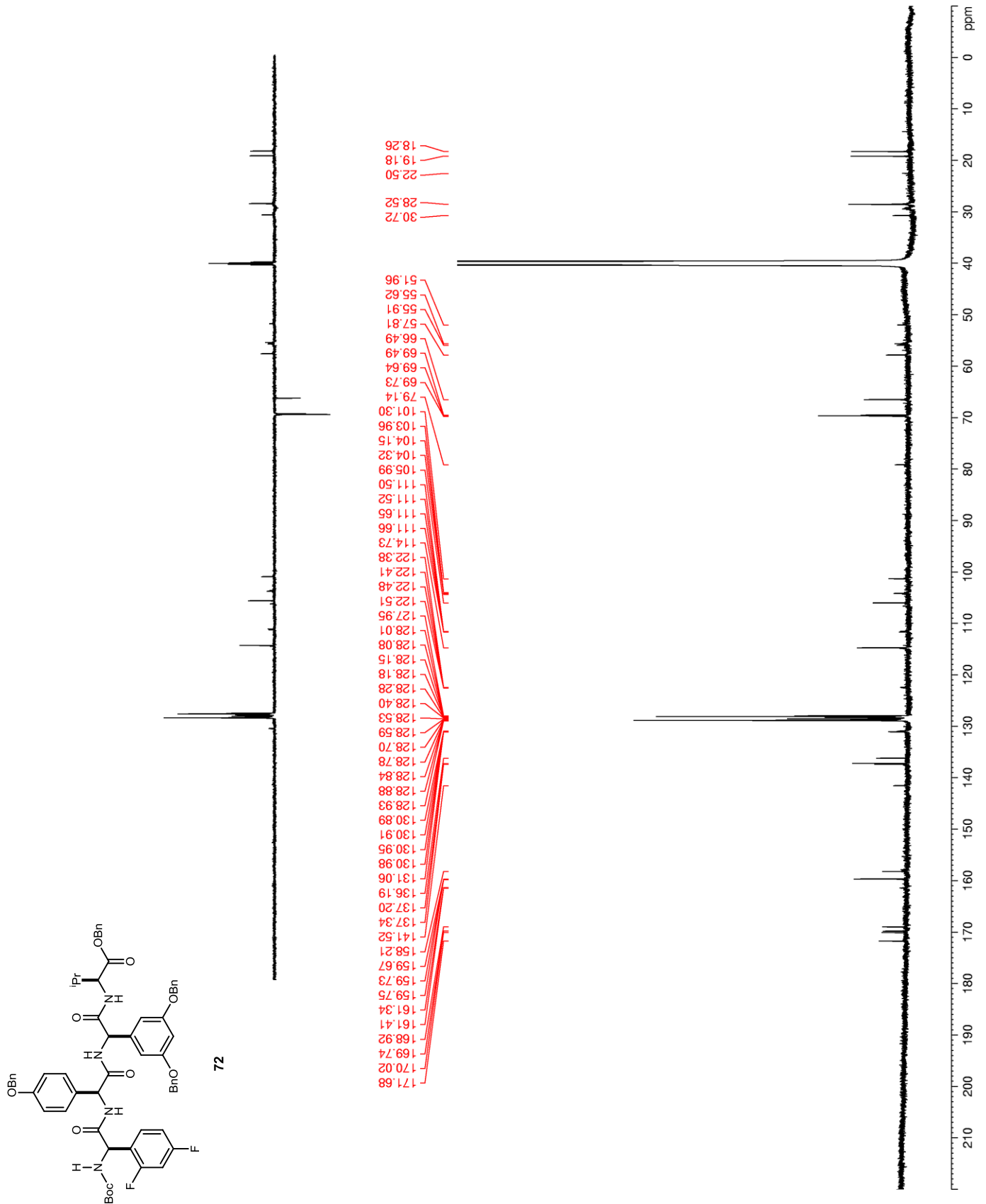


Figure 59. ^{19}F NMR (DMSO- d_6) of 72

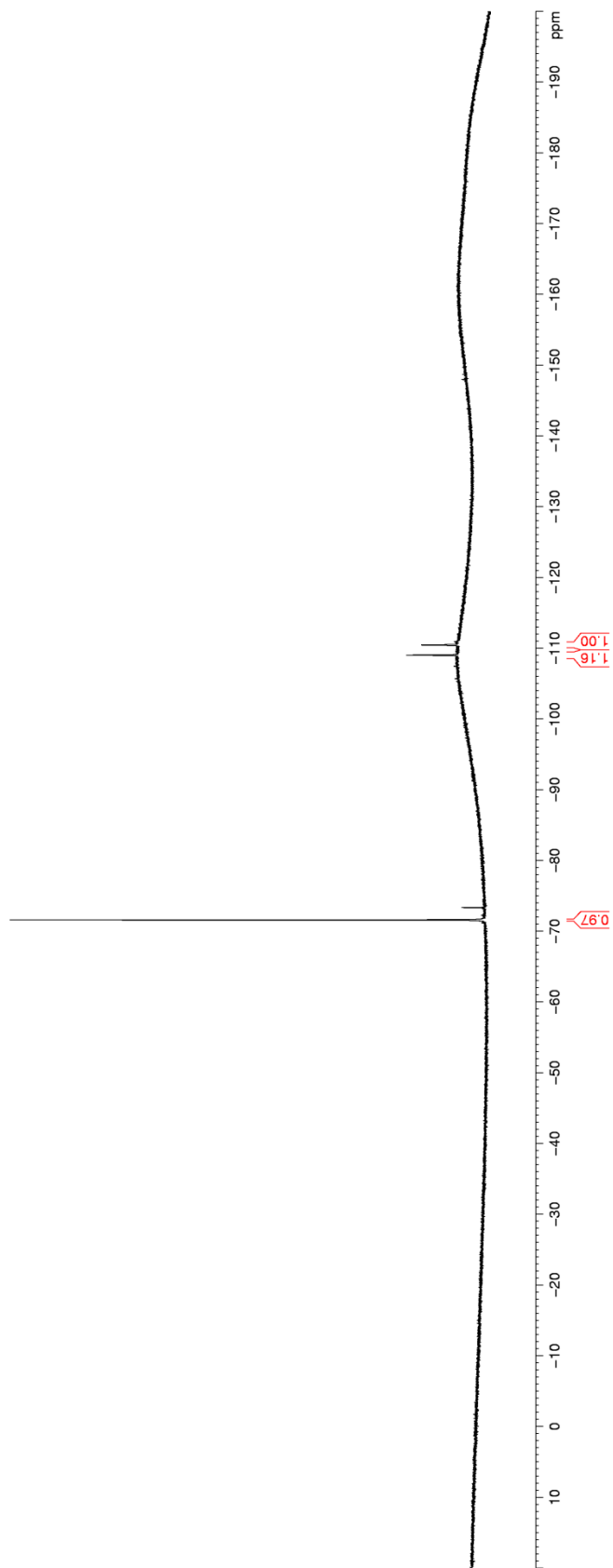
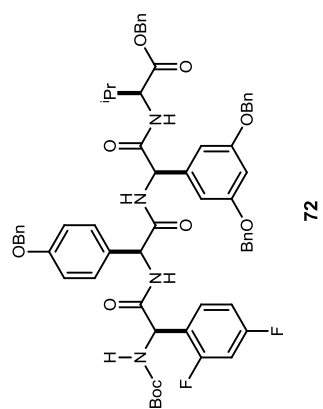


Figure 60. ^1H NMR (DMSO- d_6) of HCl-73

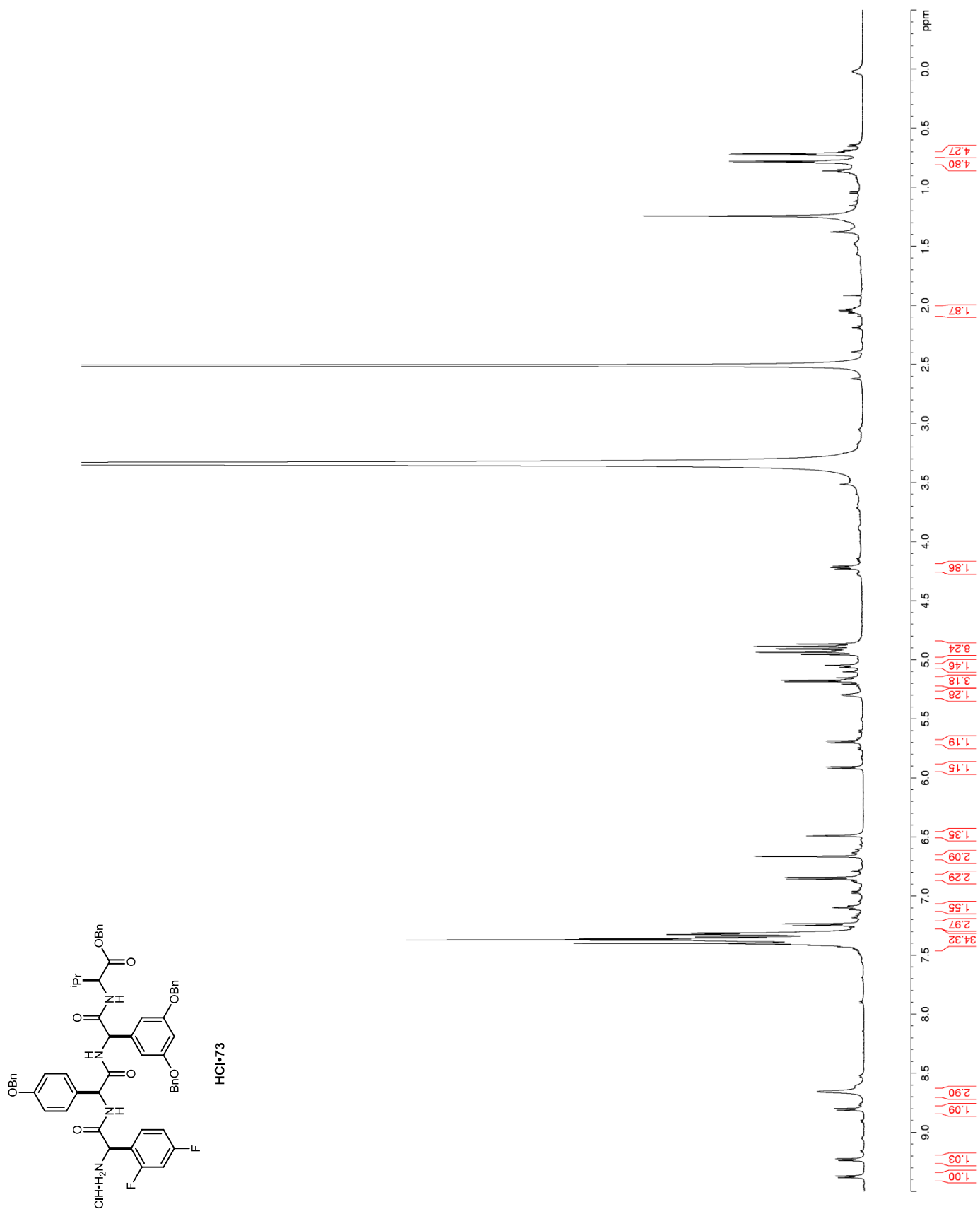


Figure 61. ^{13}C NMR (DMSO- d_6) of HCl·73

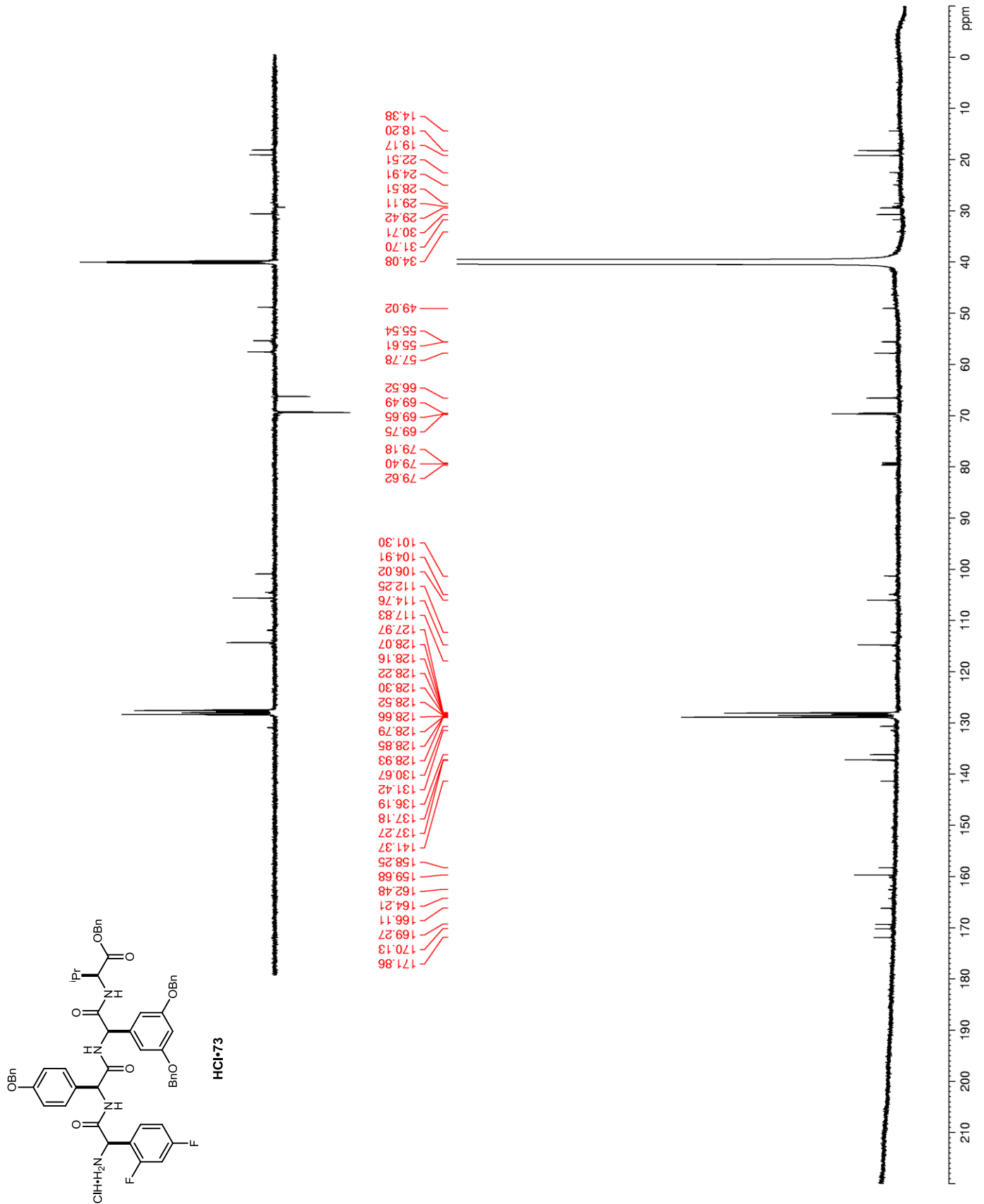


Figure 63. ^1H NMR ($\text{DMSO-}d_6$) of 74

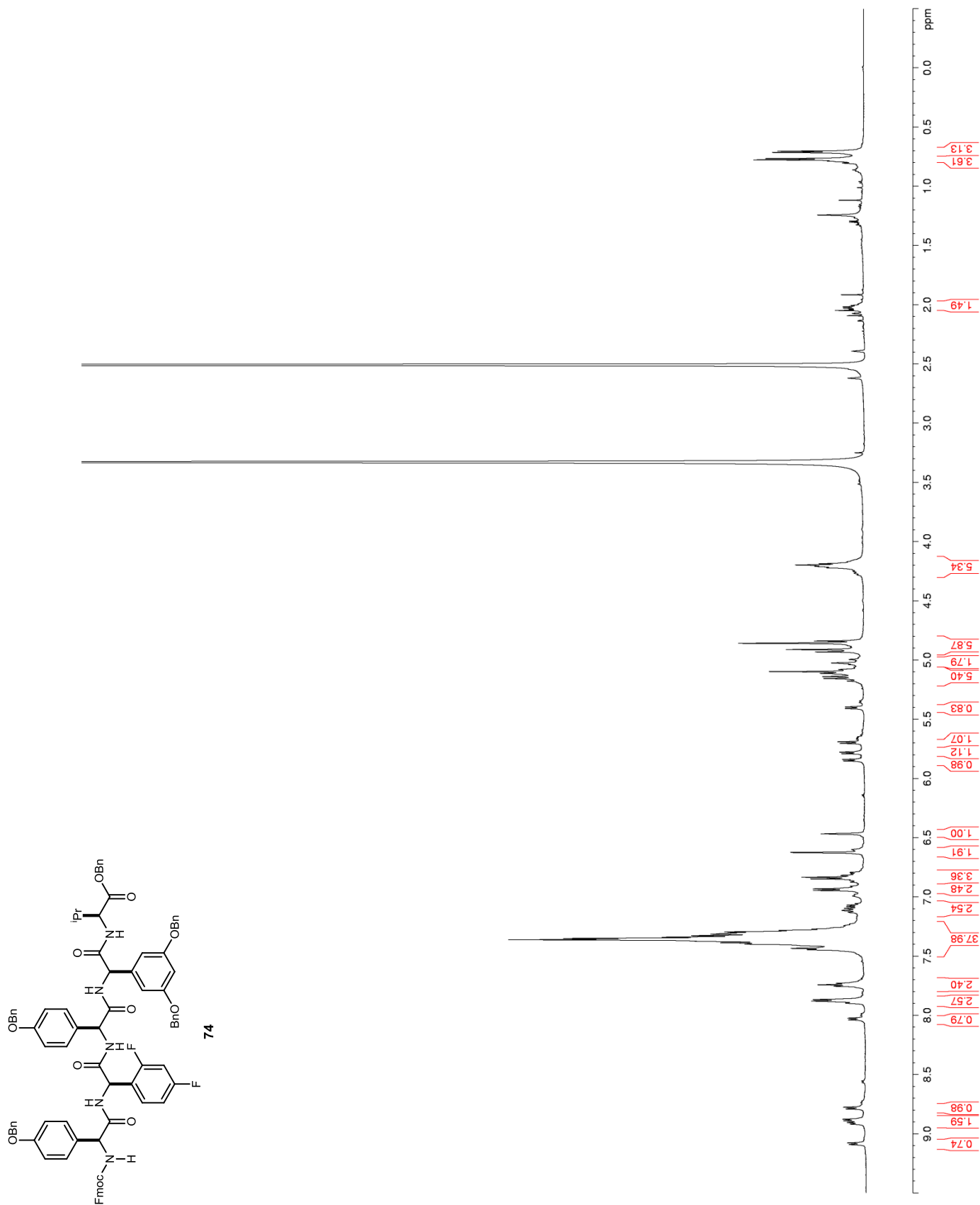


Figure 64. ^{13}C NMR (DMSO- d_6) of 74

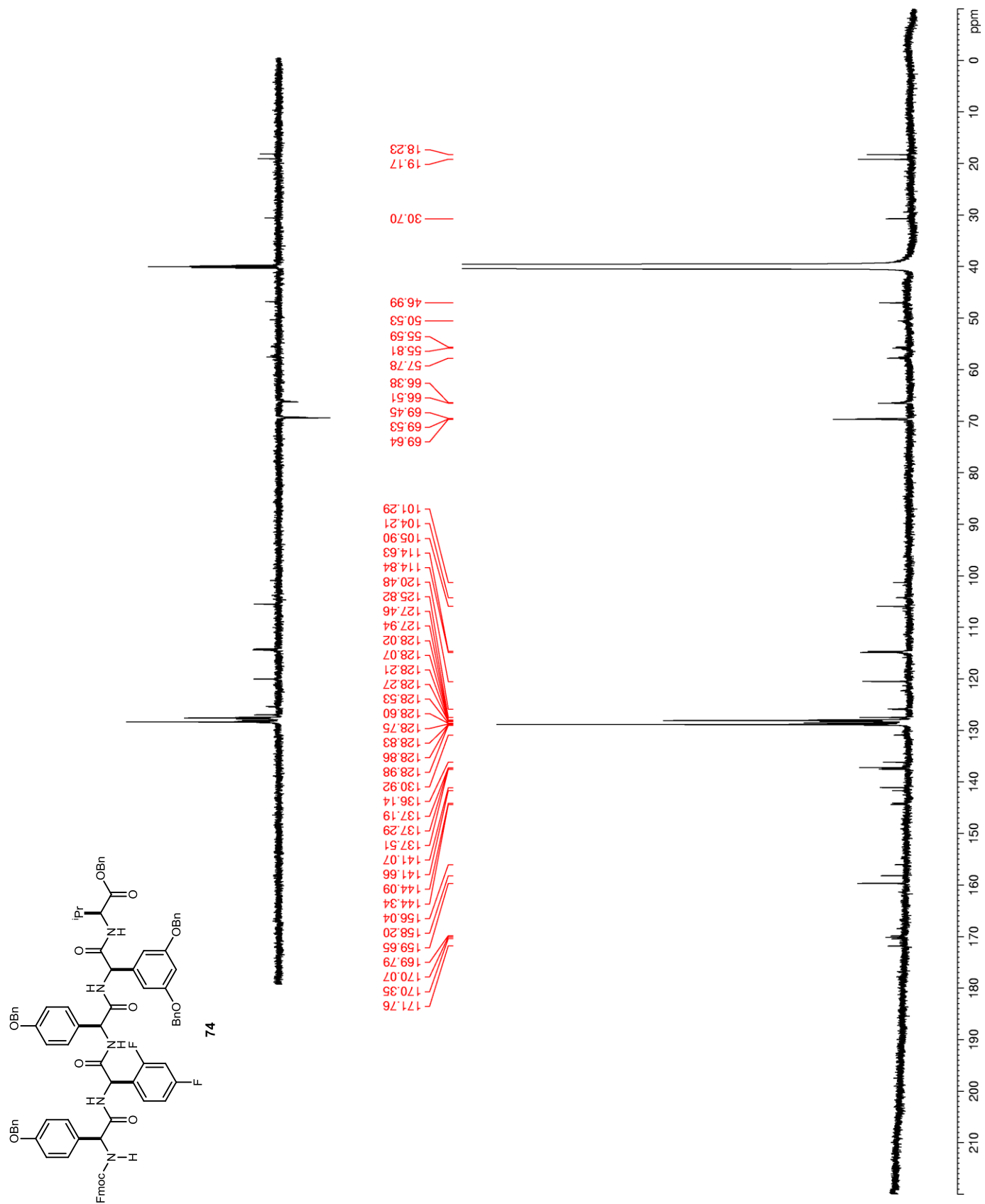


Figure 66. ^1H NMR (DMSO- d_6) of TFA·75

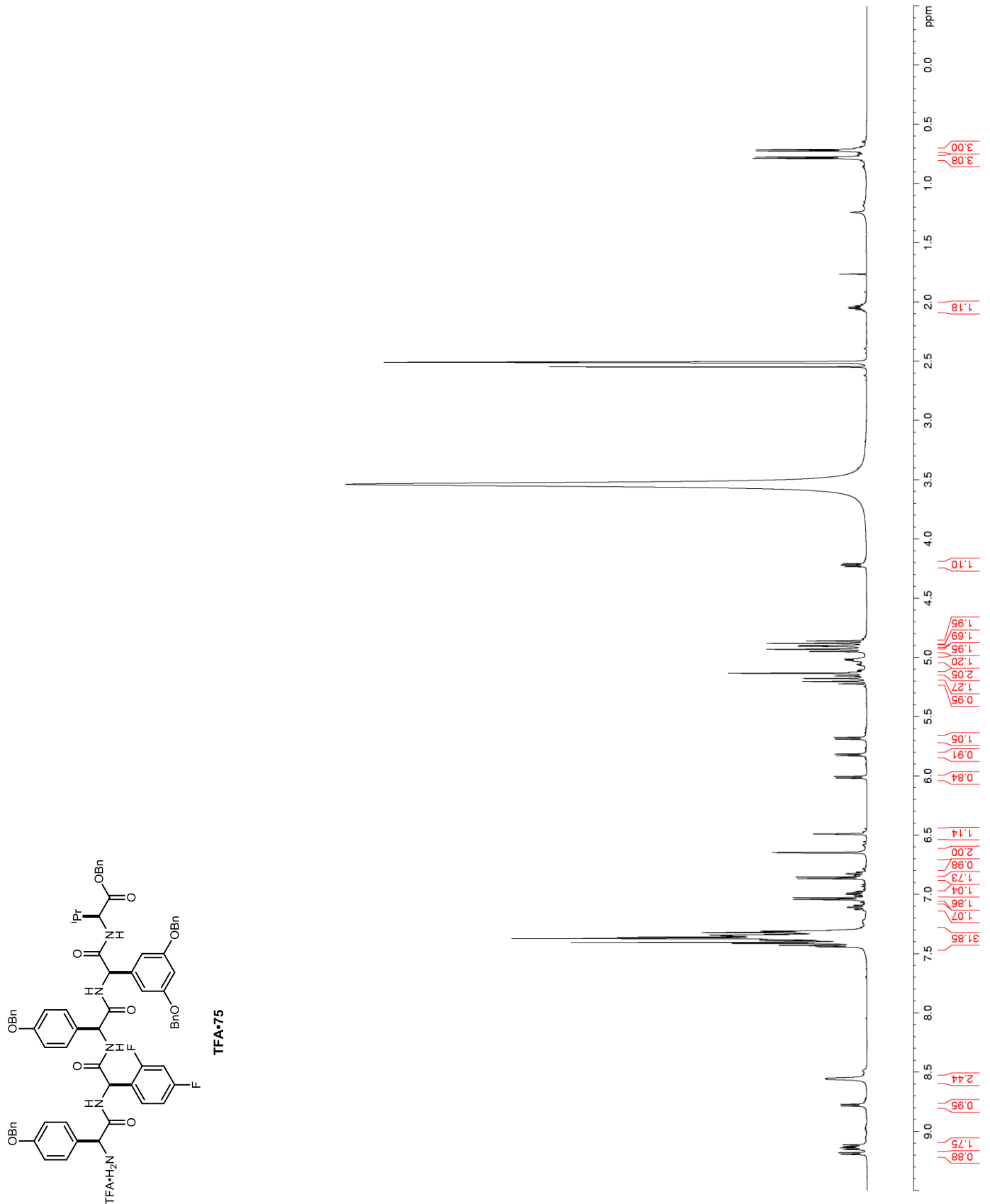


Figure 67. ^{13}C NMR (DMSO- d_6) of TFA·75

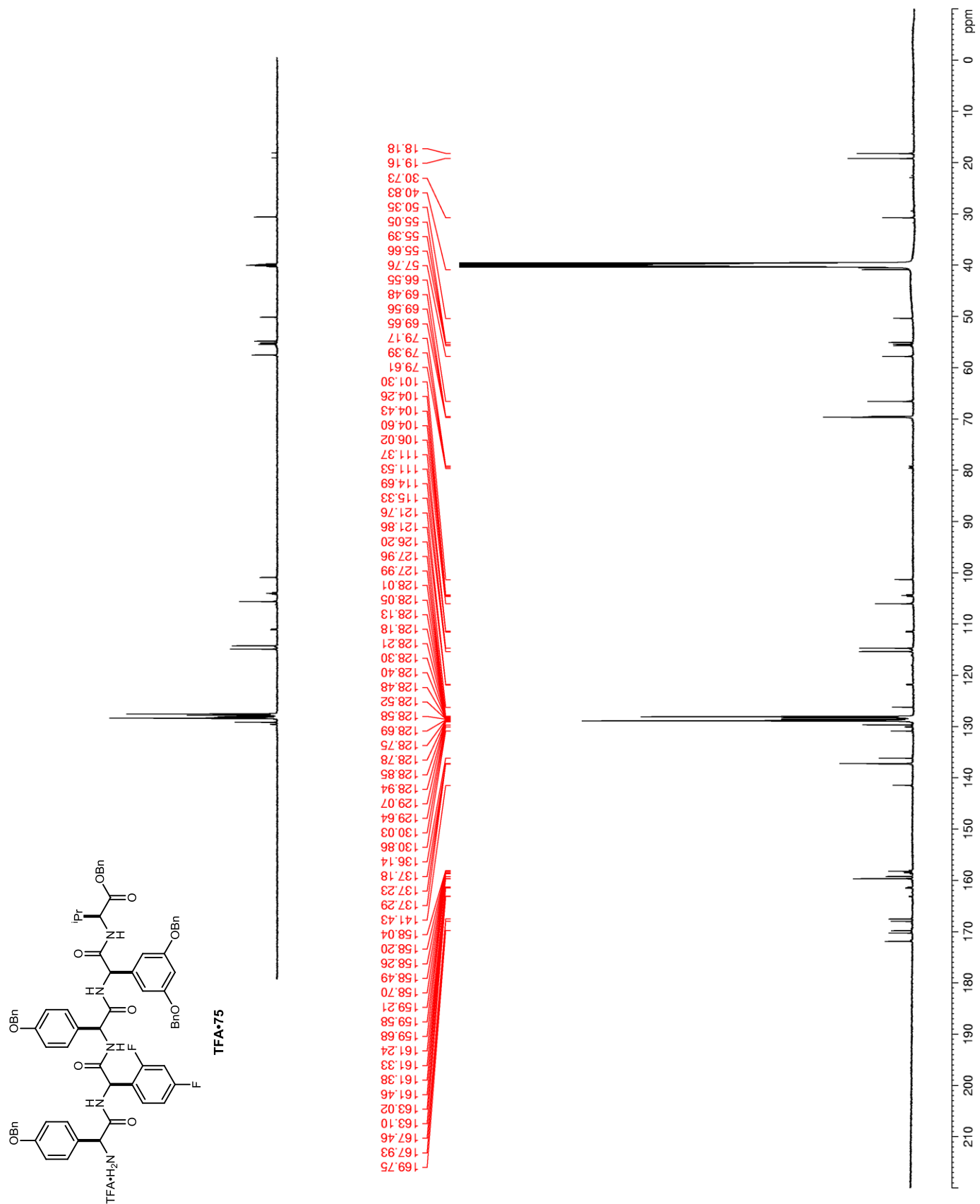


Figure 68. ^{19}F NMR (DMSO- d_6) of TFA·75

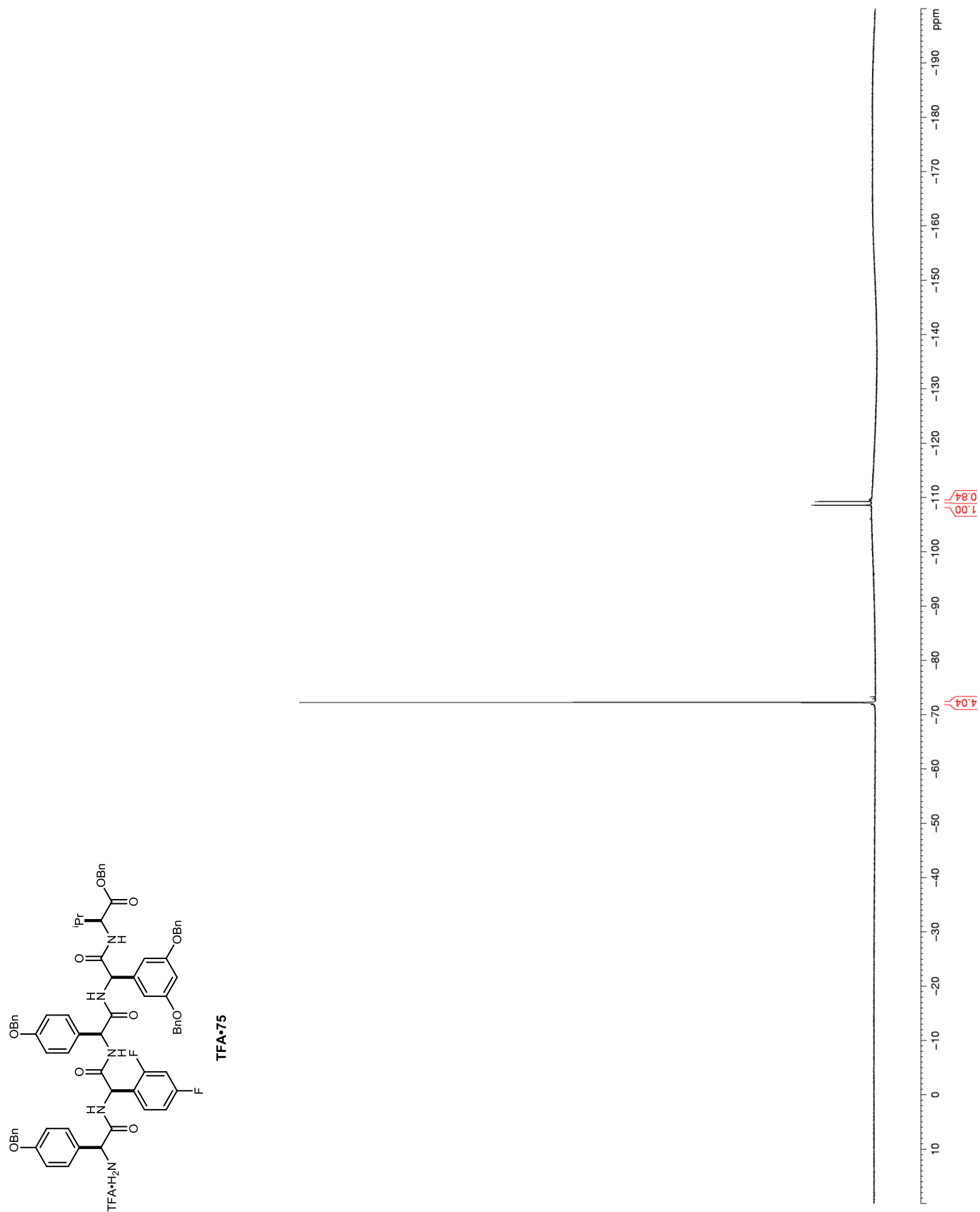


Figure 70. ^{13}C NMR (DMSO- d_6) of 76

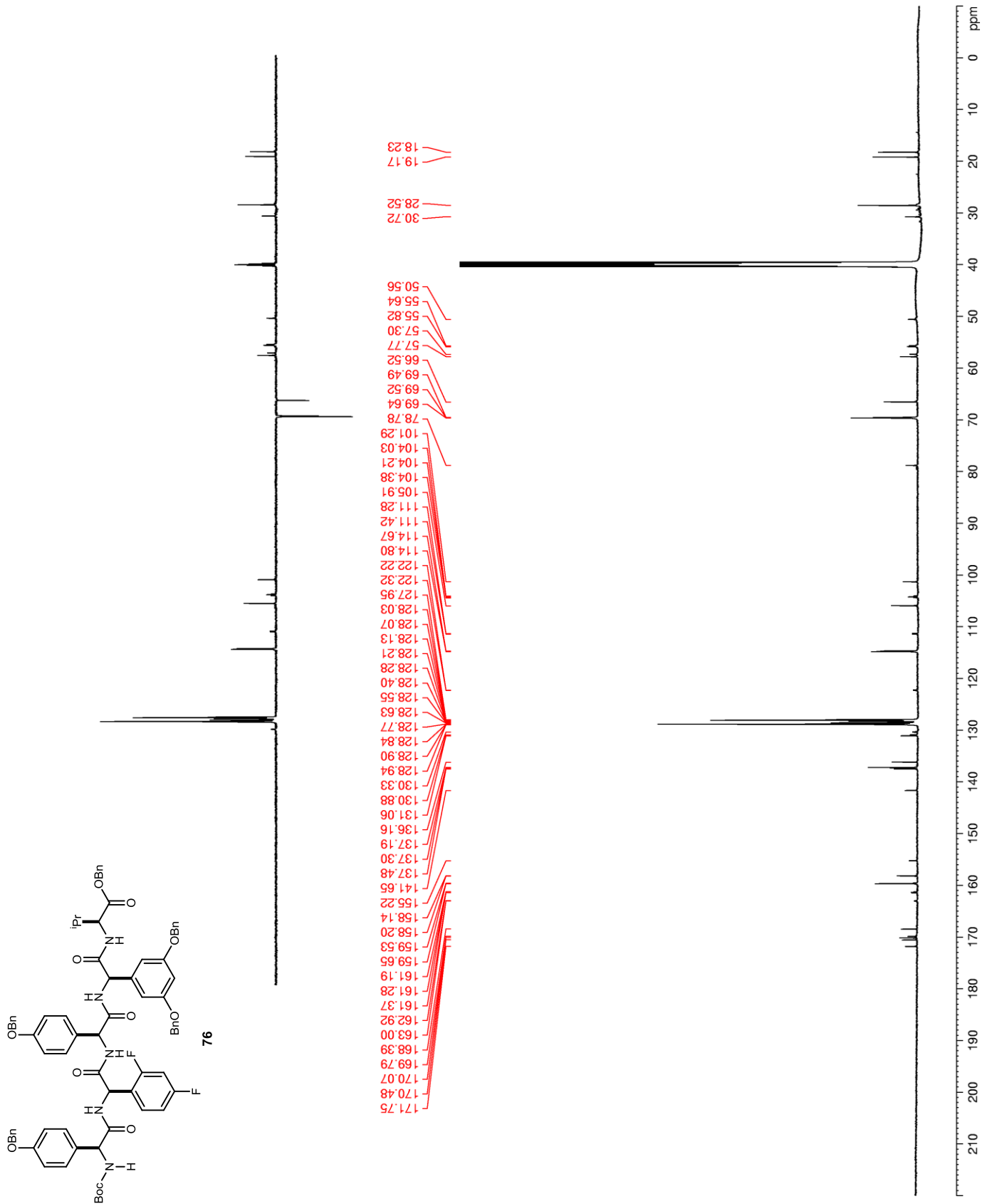


Figure 71. ^{19}F NMR (DMSO- d_6) of 76

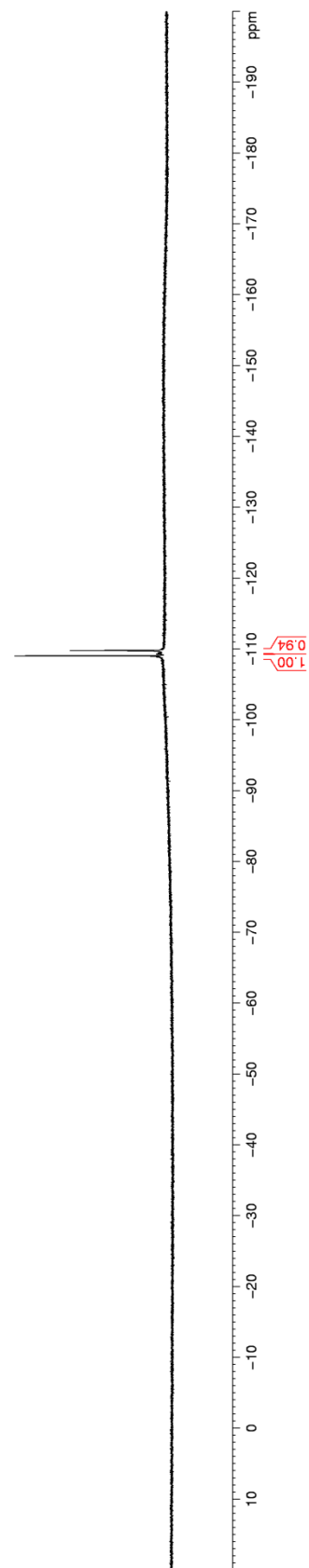
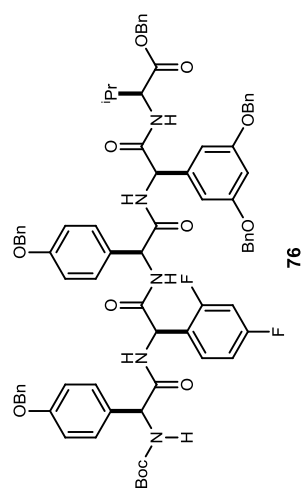


Figure 72. ^1H NMR ($\text{DMSO-}d_6$) of 78

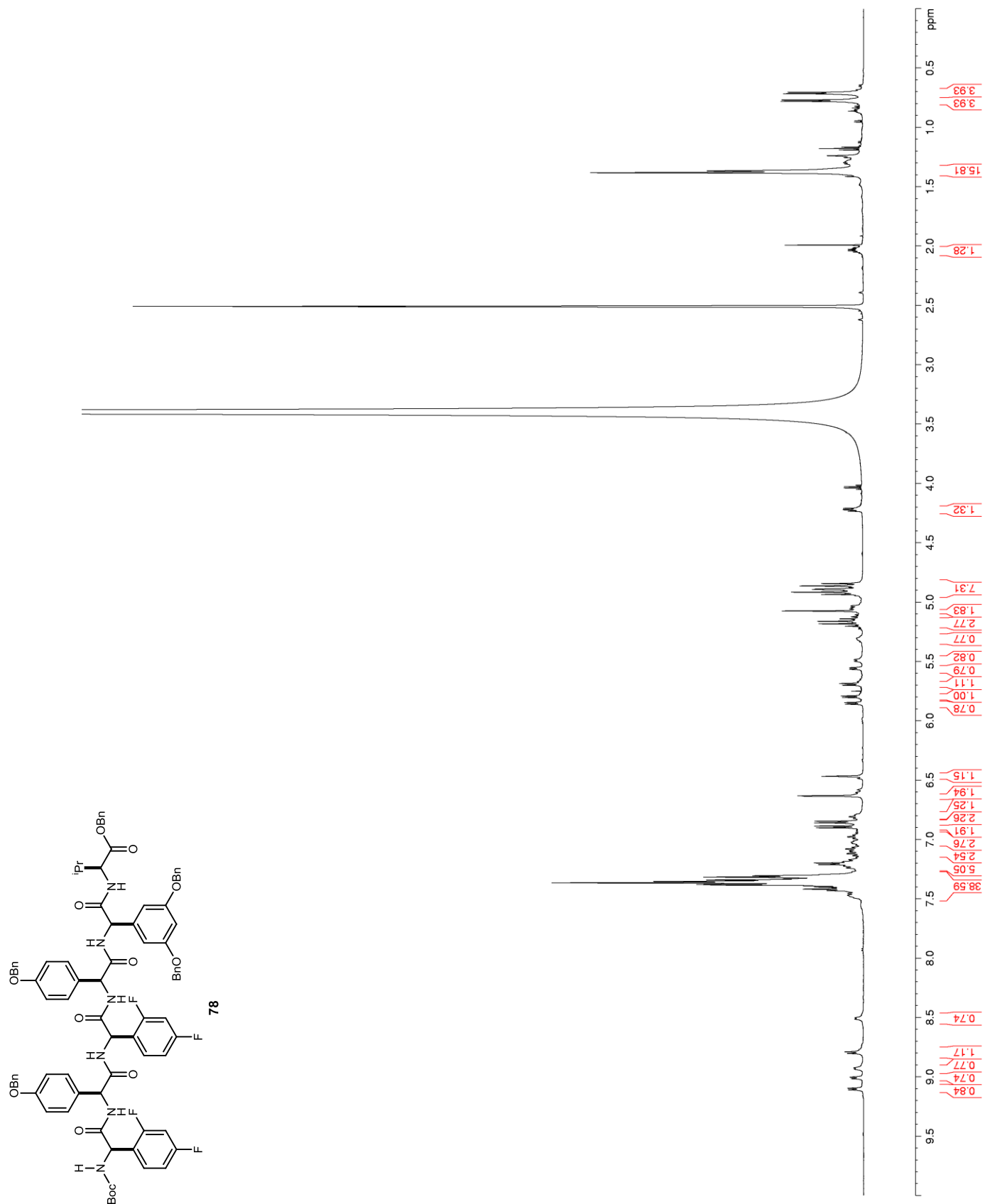


Figure 73. ^{13}C NMR (DMSO- d_6) of 78

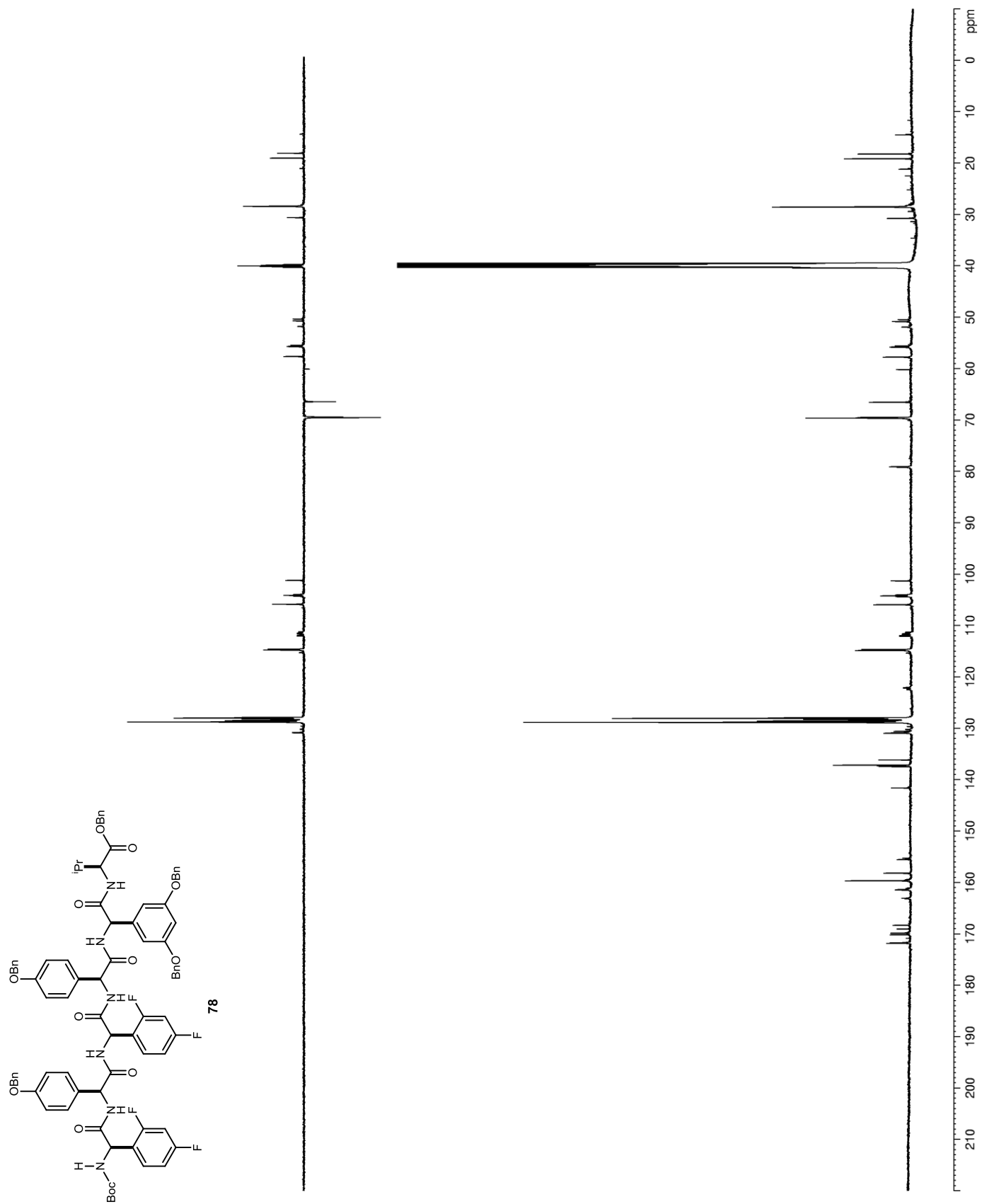


Figure 75. ^1H NMR (DMSO- d_6) of 79

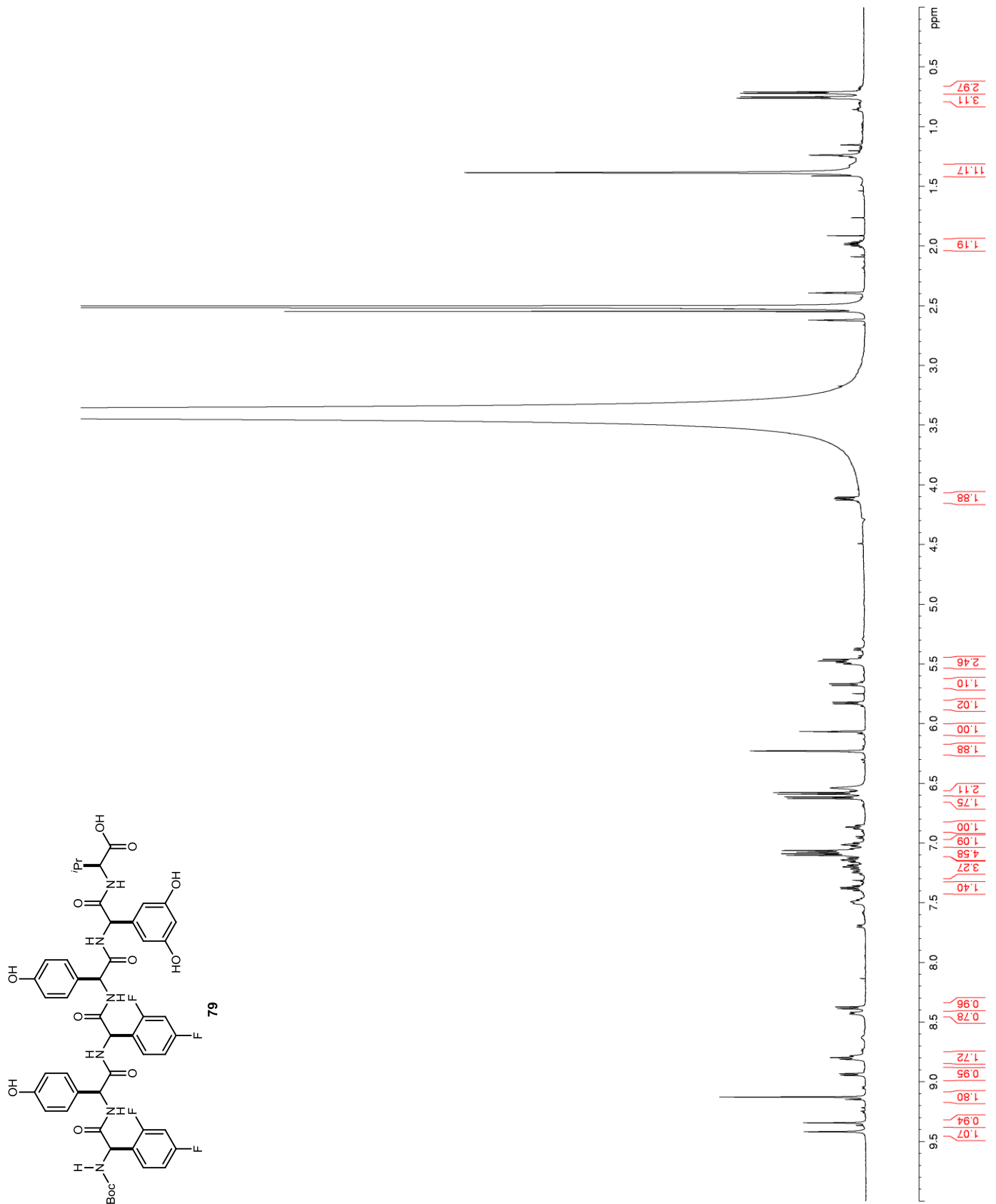


Figure 76. ^{13}C NMR (DMSO- d_6) of 79

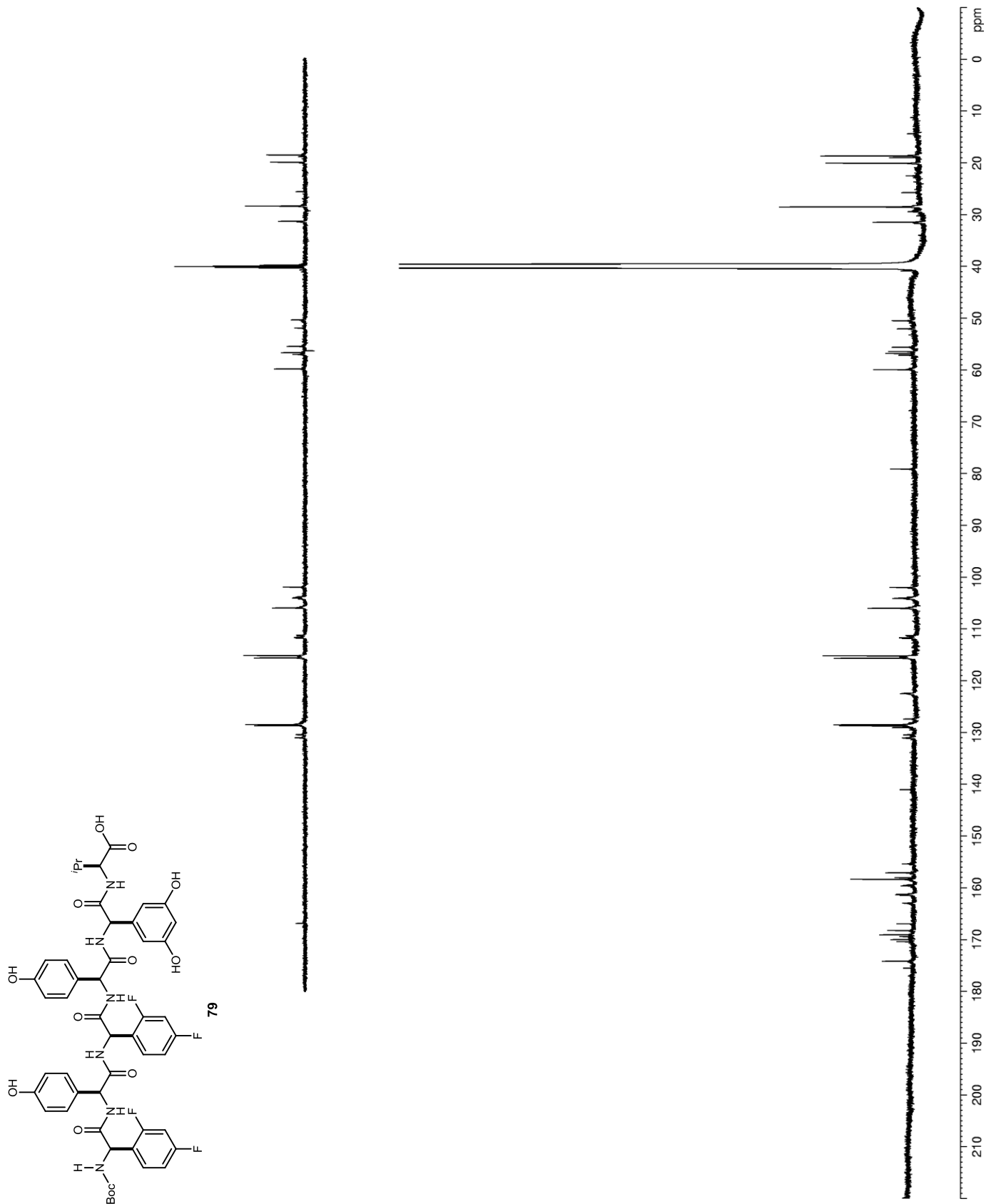


Figure 77. ^{19}F NMR (DMSO- d_6) of 79

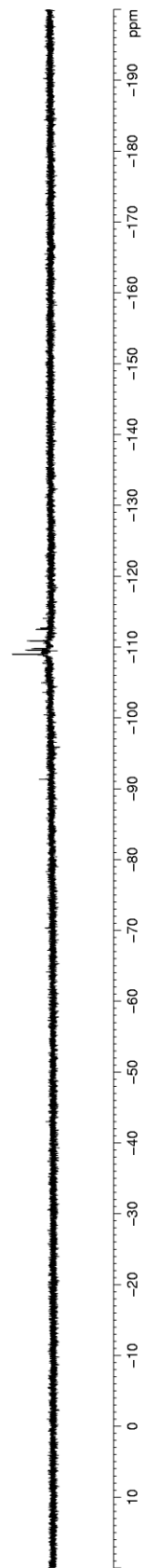
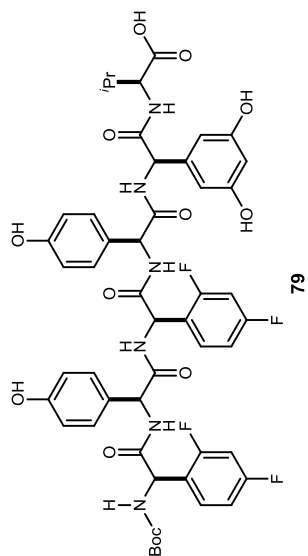


Figure 78. ^1H NMR ($\text{DMSO-}d_6$) of 86

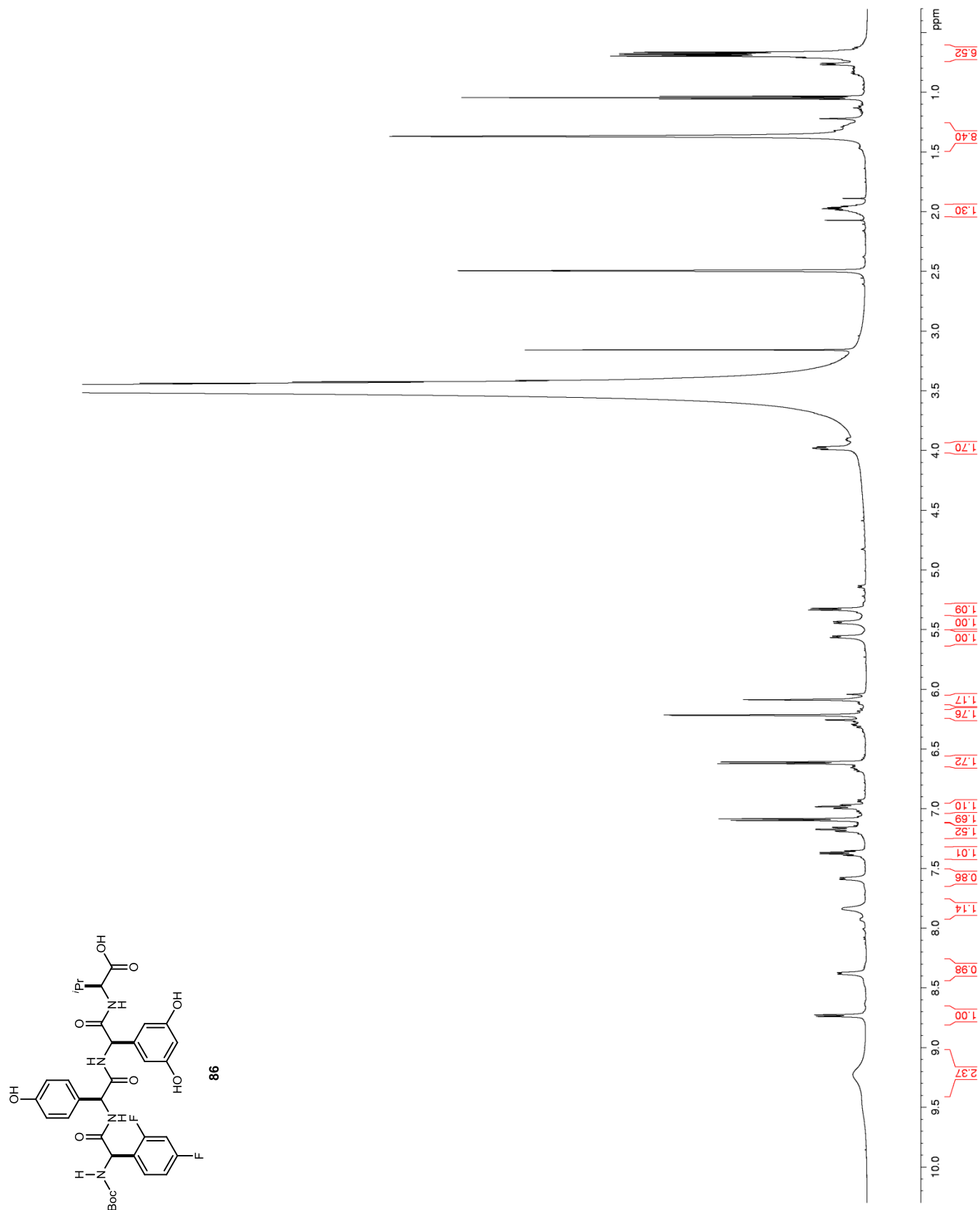


Figure 79. ^{13}C NMR (DMSO- d_6) of 86

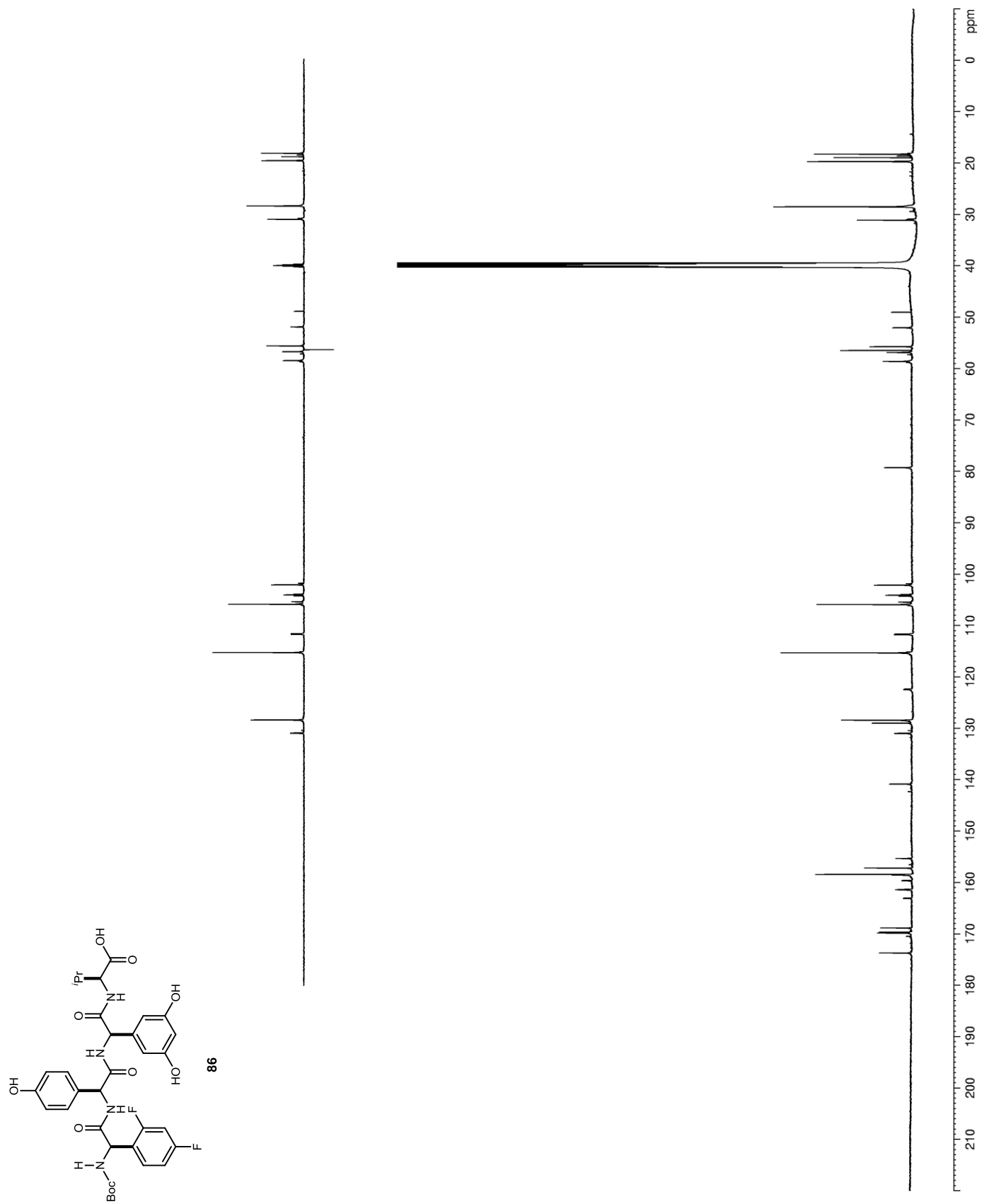
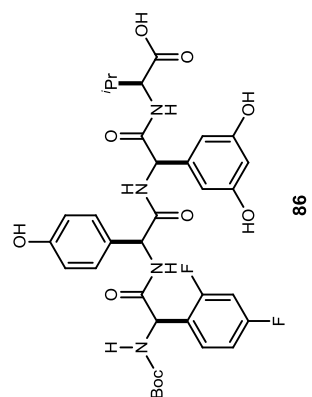


Figure 80. ^{19}F NMR (DMSO- d_6) of 86



86

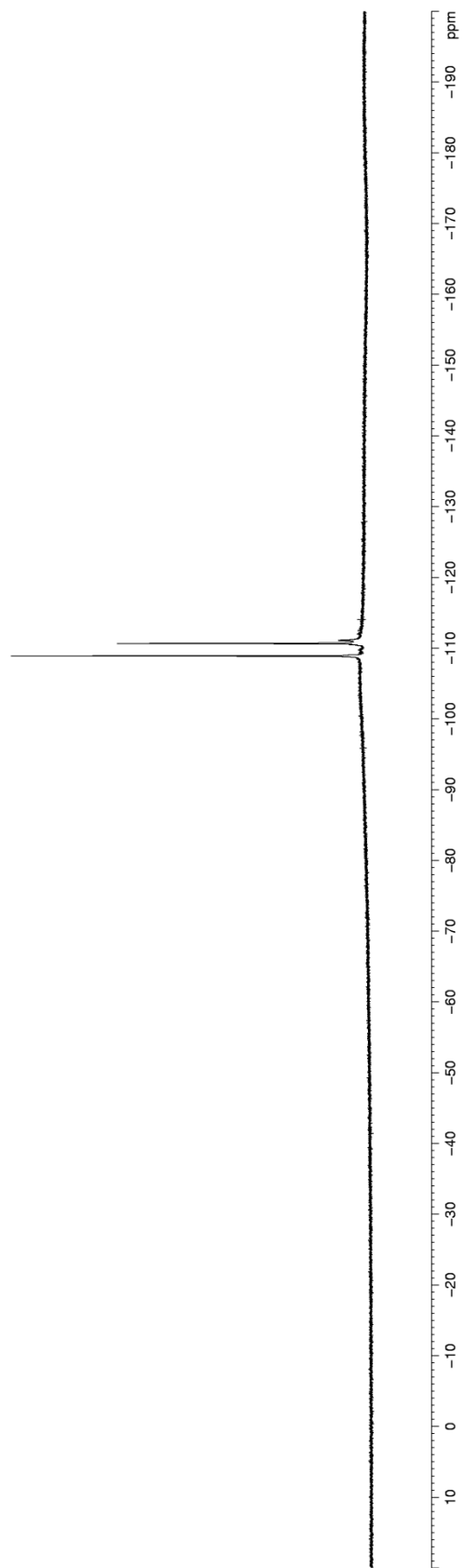


Figure 81. ^1H NMR (CDCl_3) of 149

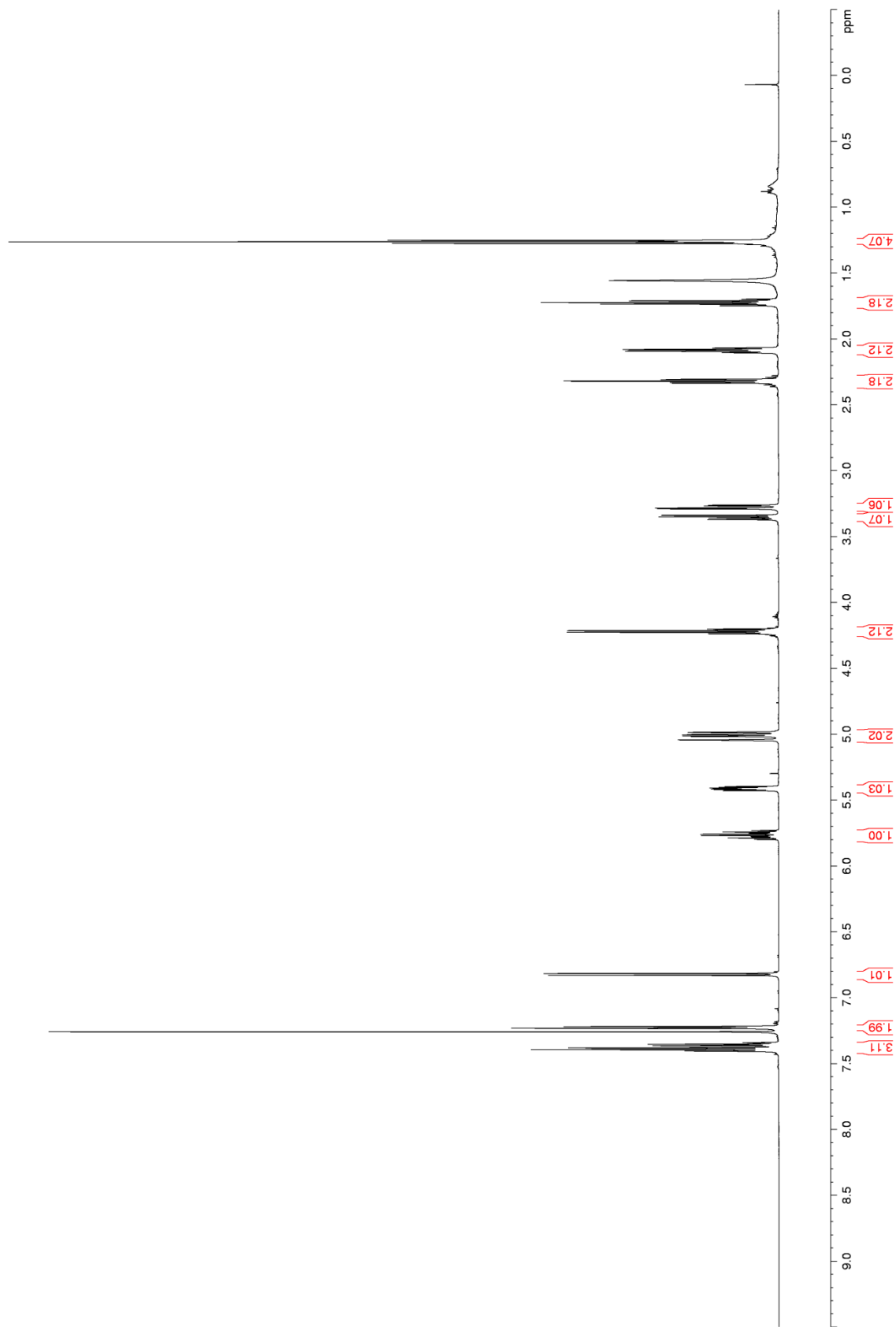
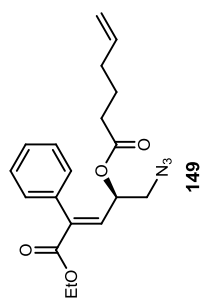


Figure 82. ^{13}C NMR (CDCl_3) of 149

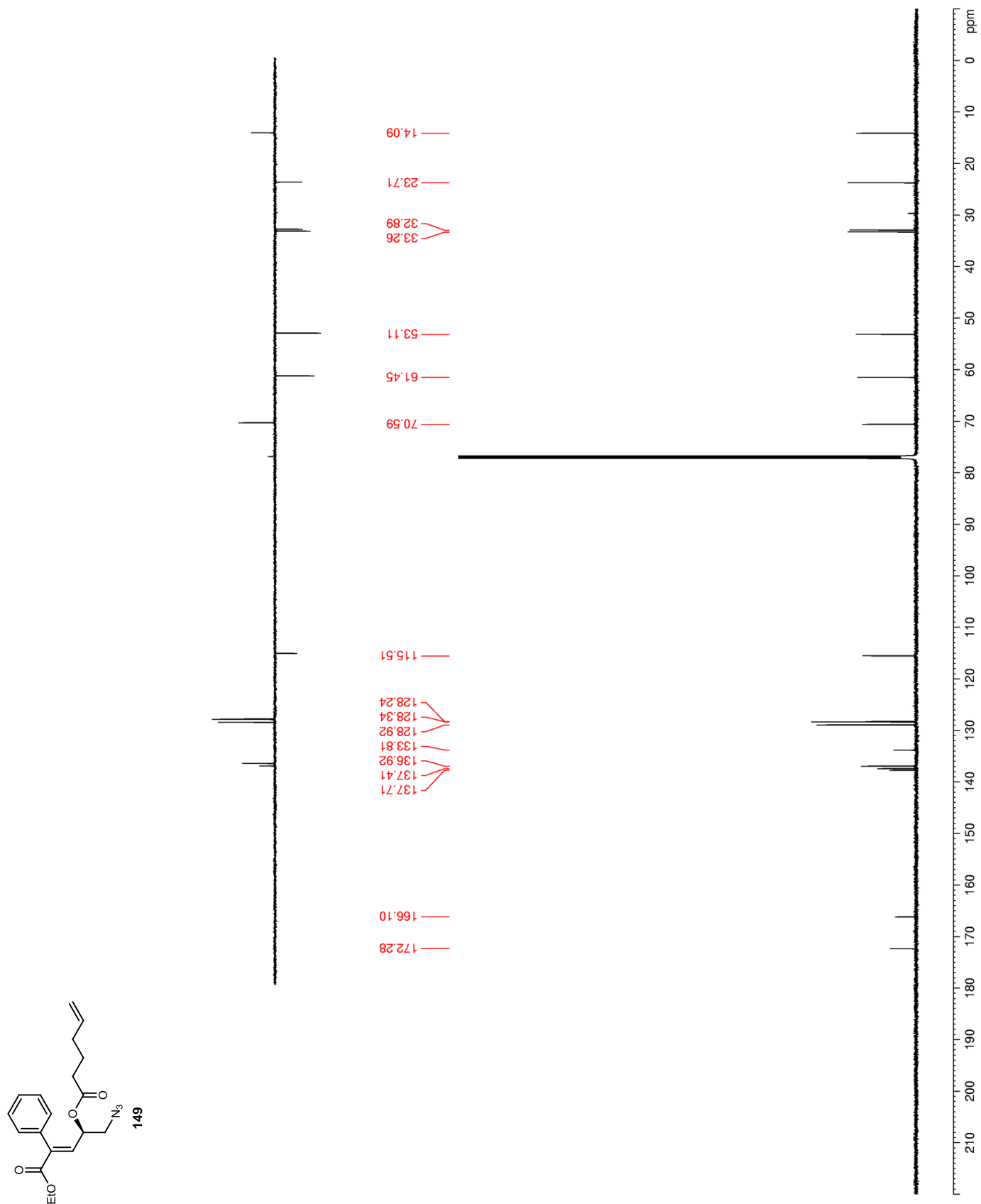


Figure 83. ^{13}C NMR (CDCl_3) of 150

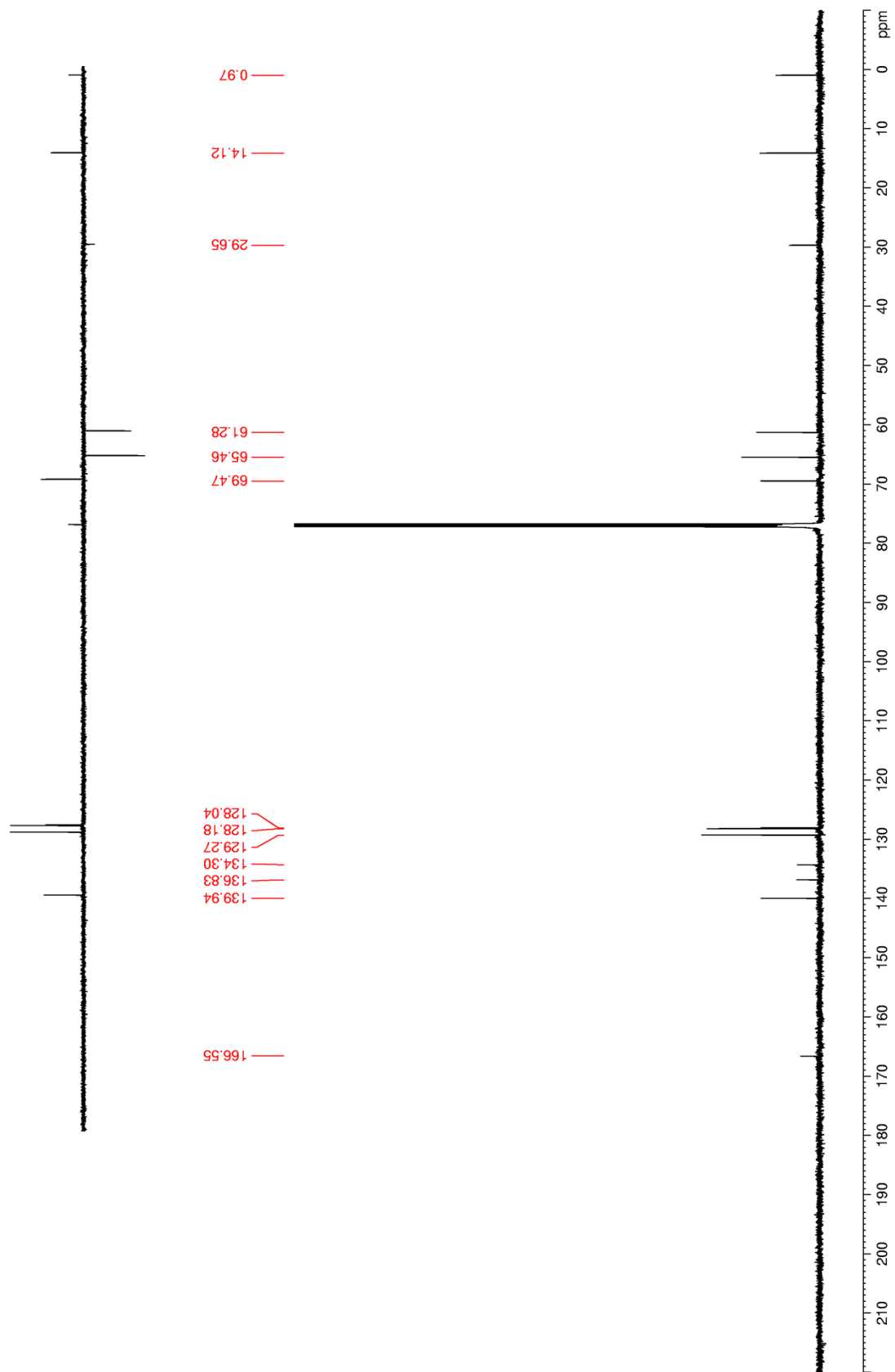
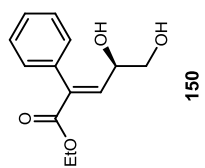


Figure 84. ^1H NMR (CDCl_3) of 150

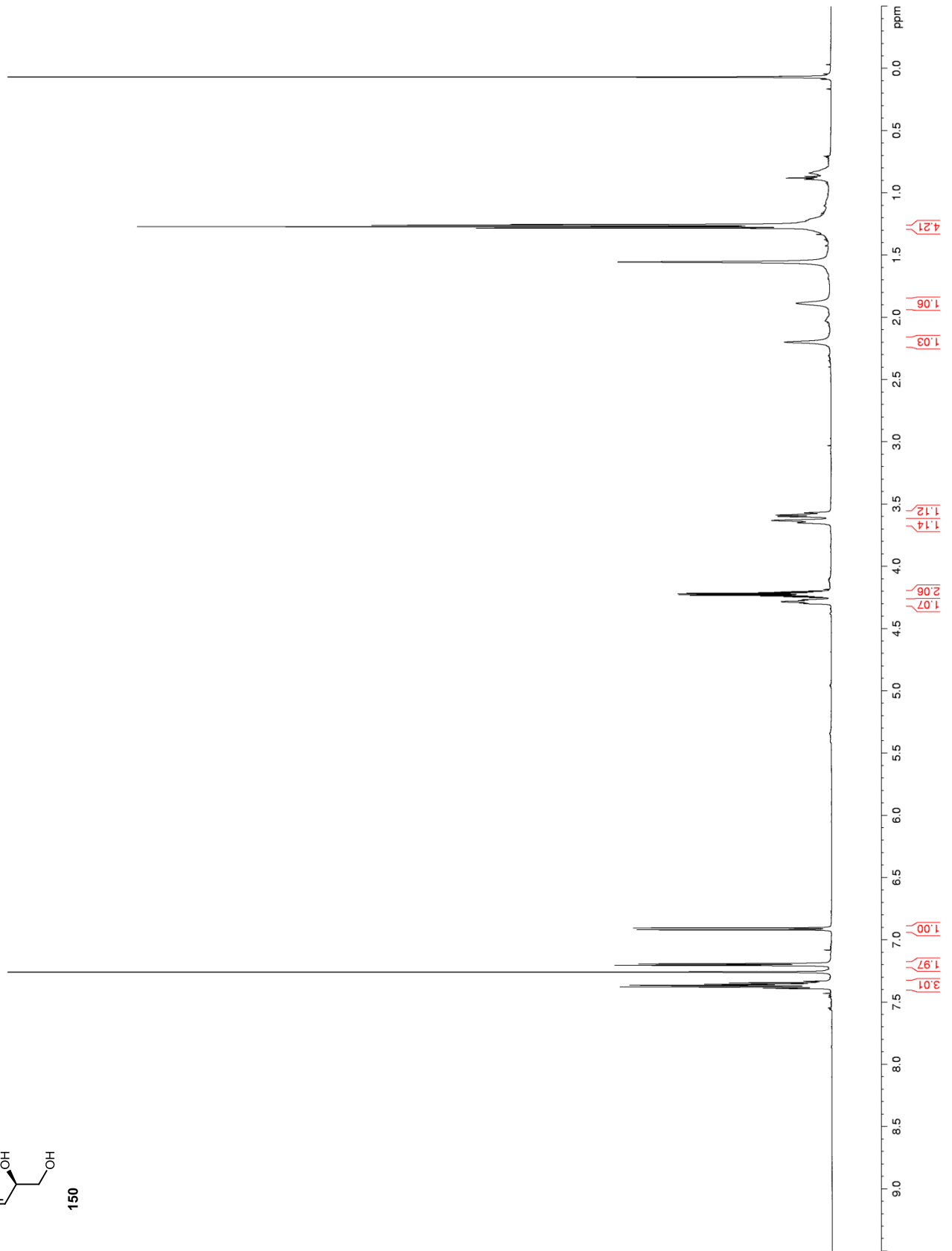
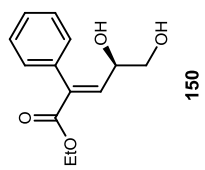
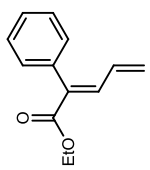


Figure 85. ^1H NMR (CDCl_3) of 151



151

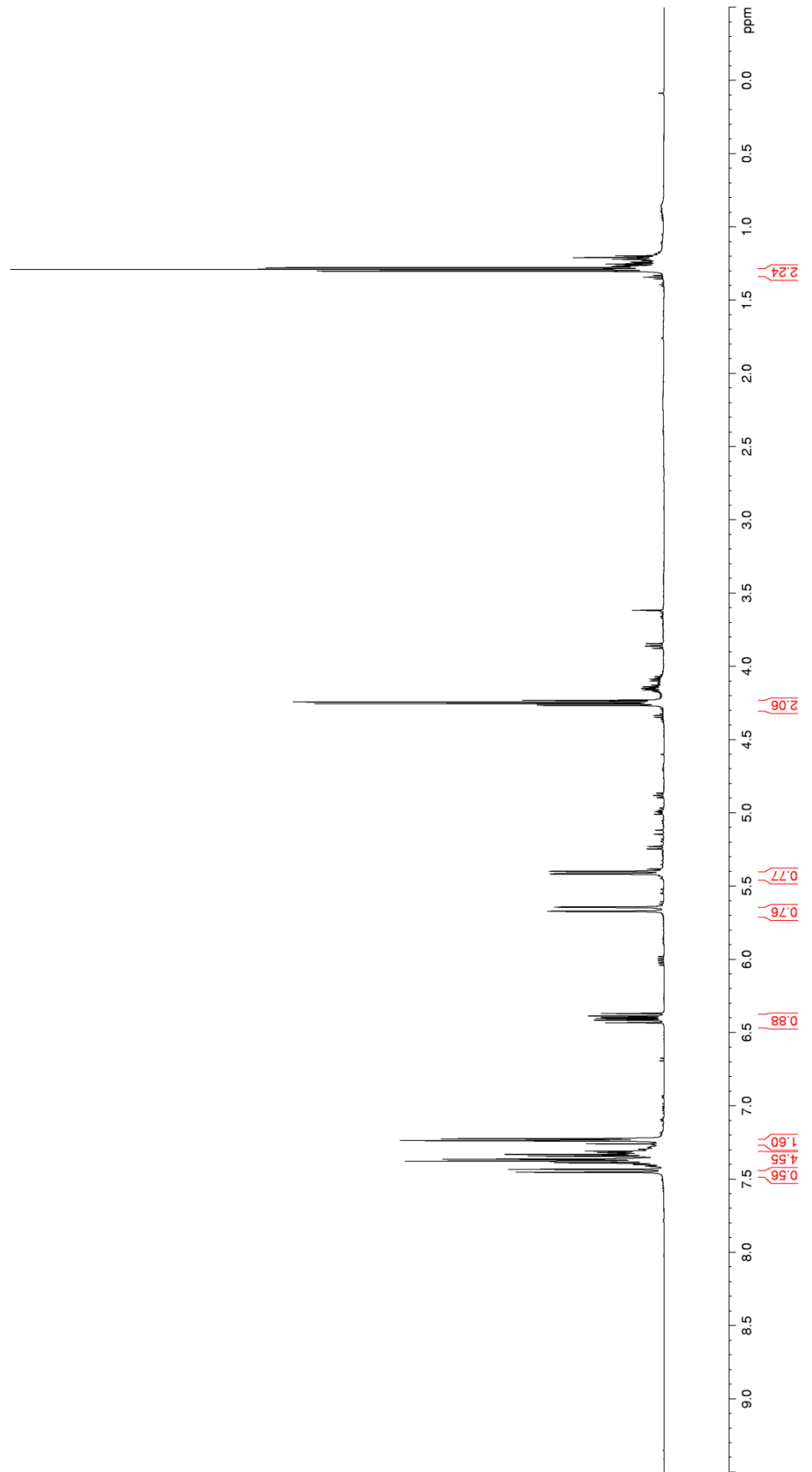


Figure 86. NOESY (CDCl₃) of 151

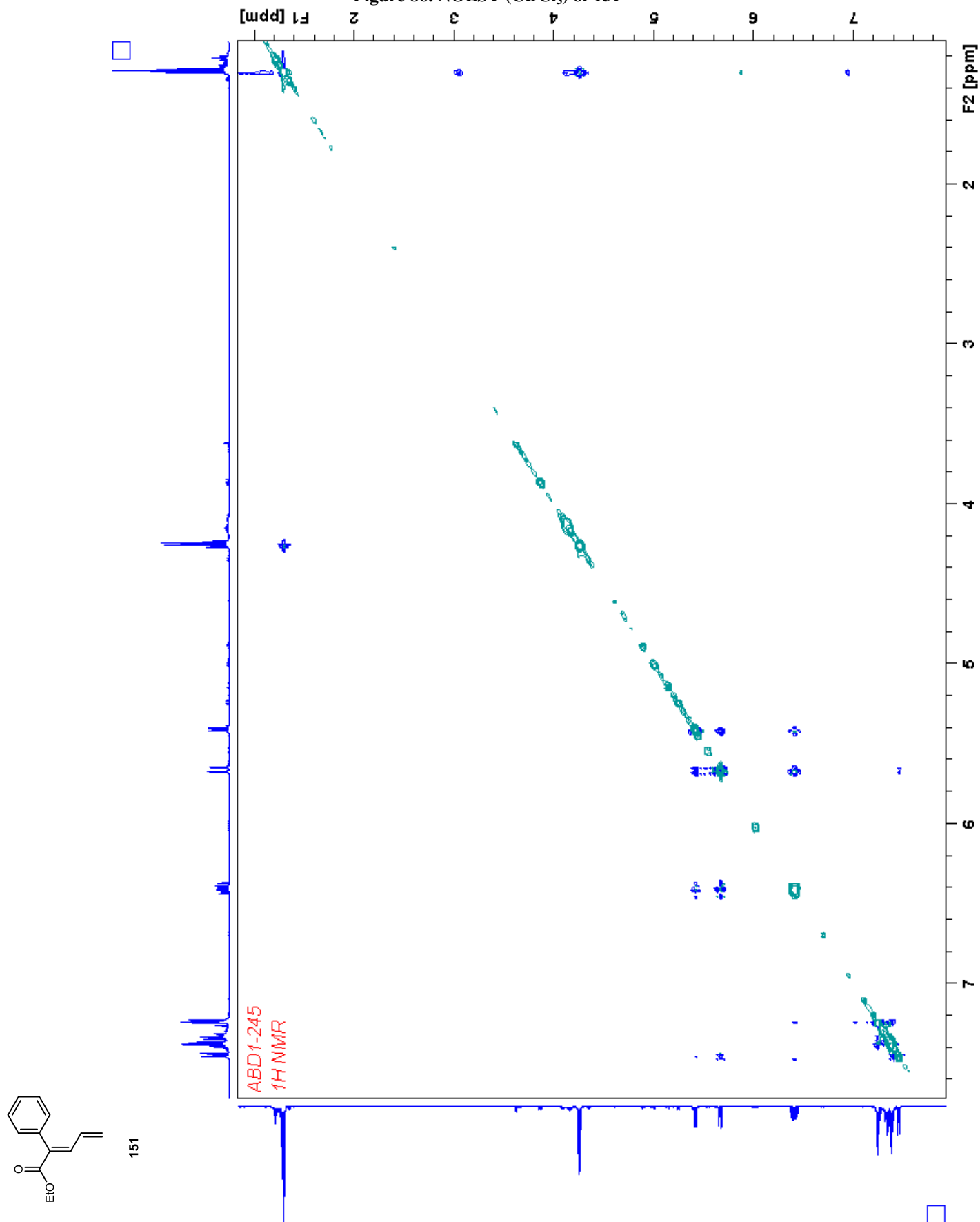


Figure 87. ^1H NMR (CDCl_3) of 155

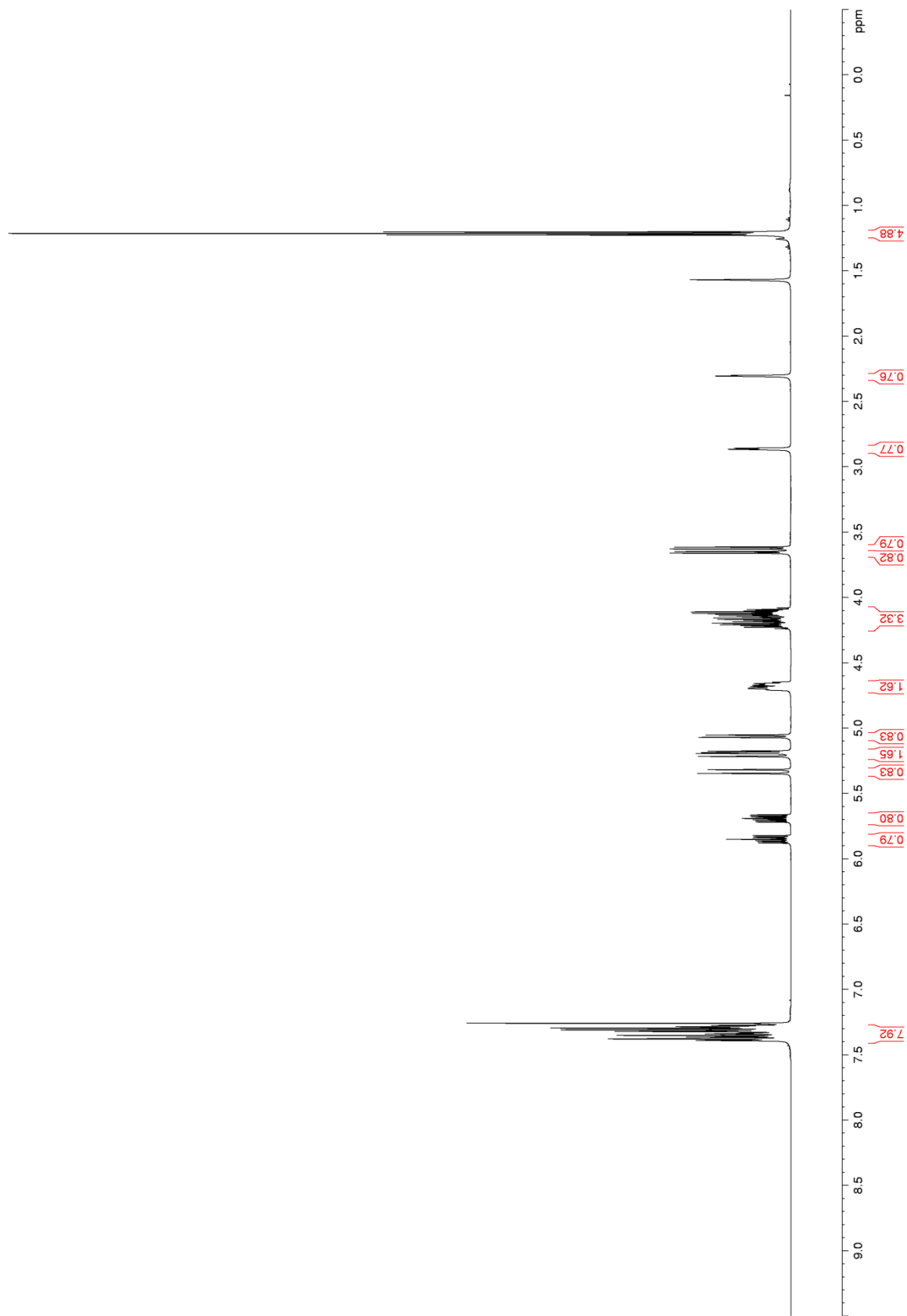
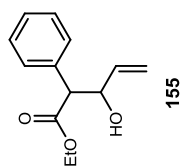


Figure 88. ^{13}C NMR (CDCl_3) of 155

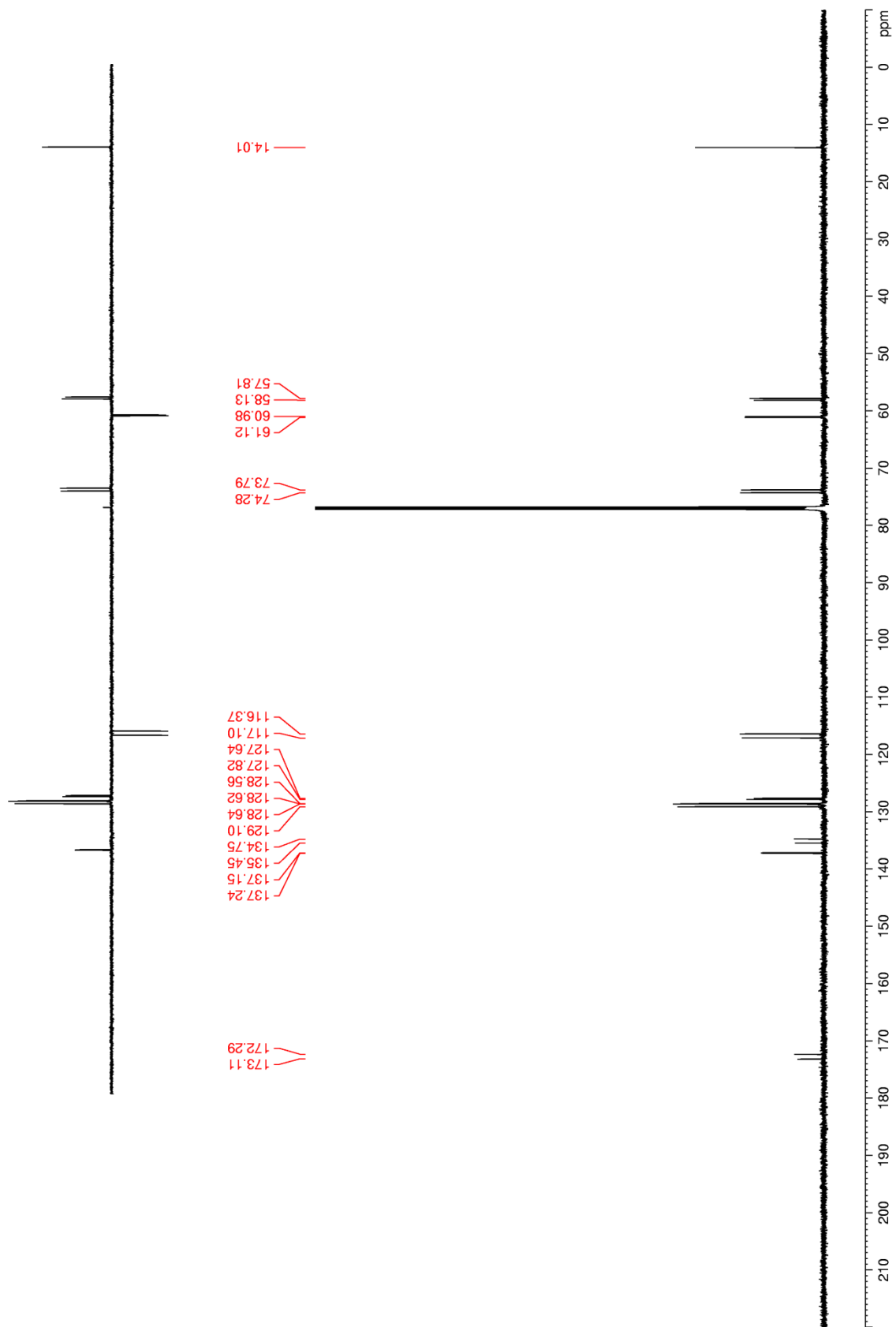
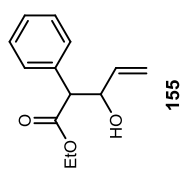


Figure 89. ^1H NMR (CDCl_3) of 156

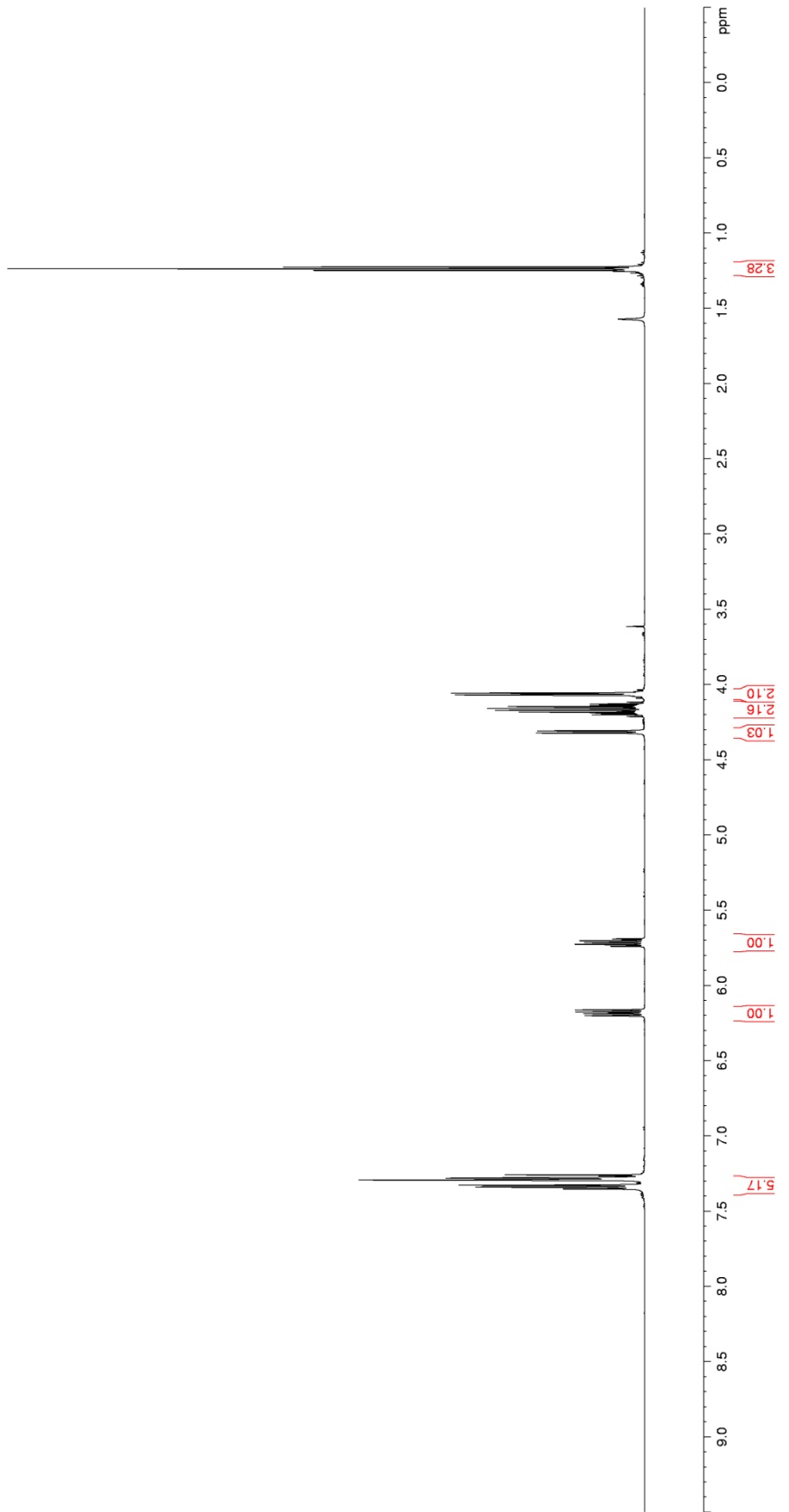
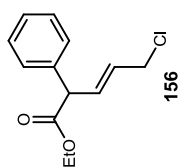


Figure 90. ^{13}C NMR (CDCl_3) of 156

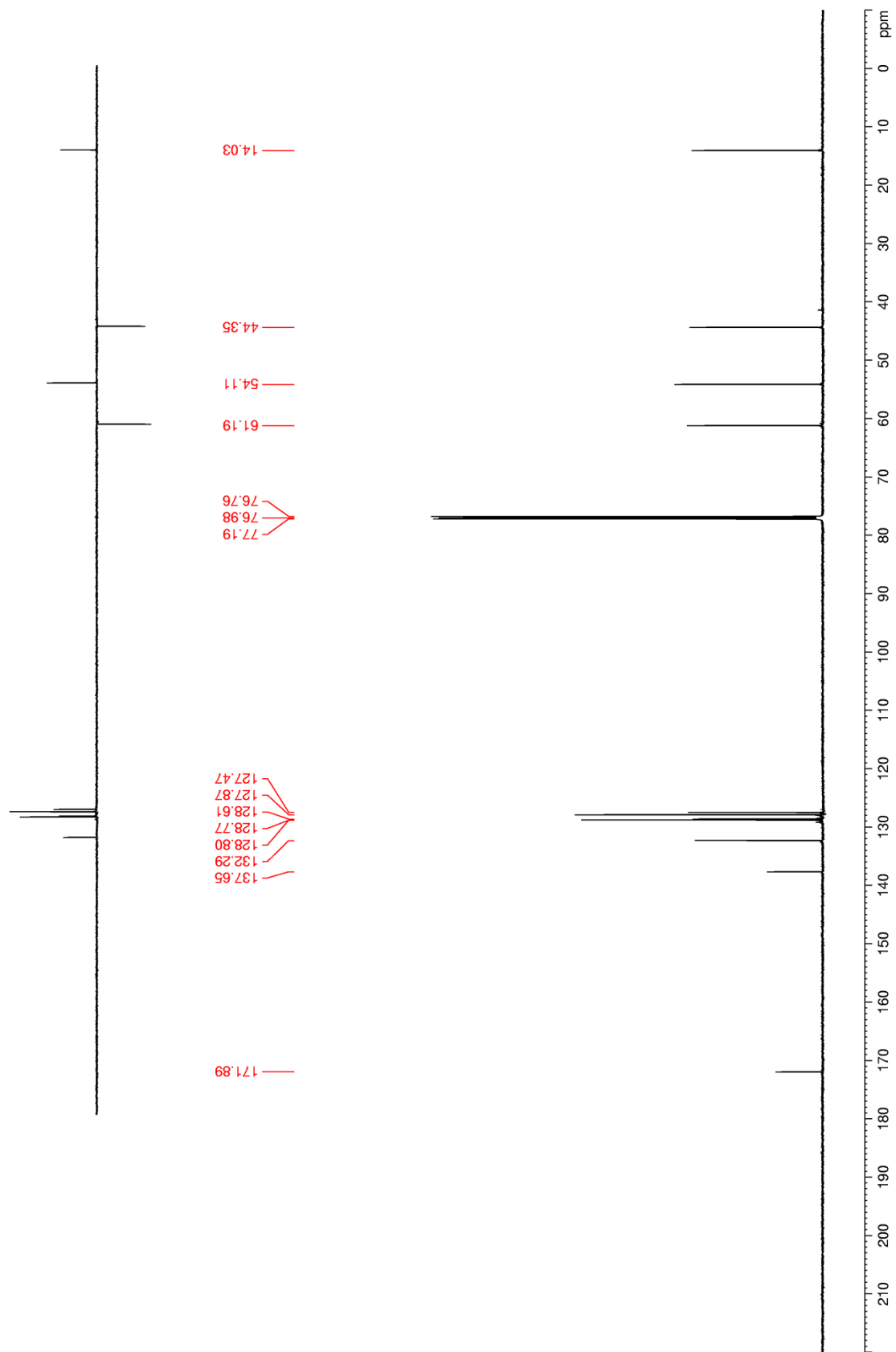
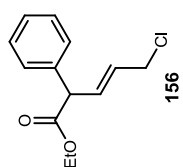


Figure 91. ^1H NMR (CDCl_3) of 157

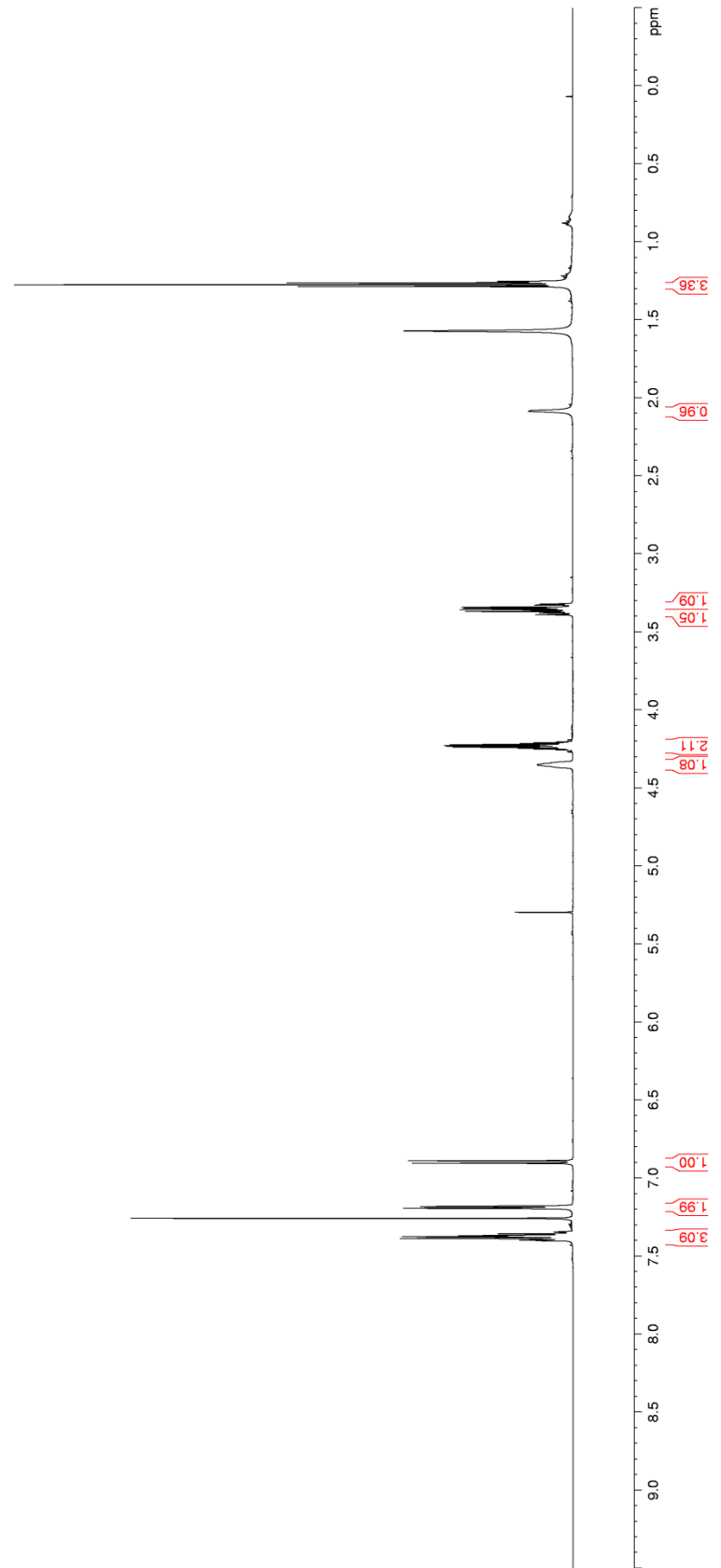
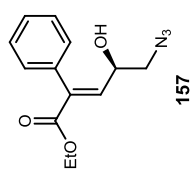


Figure 92. ^{13}C NMR (CDCl_3) of 157

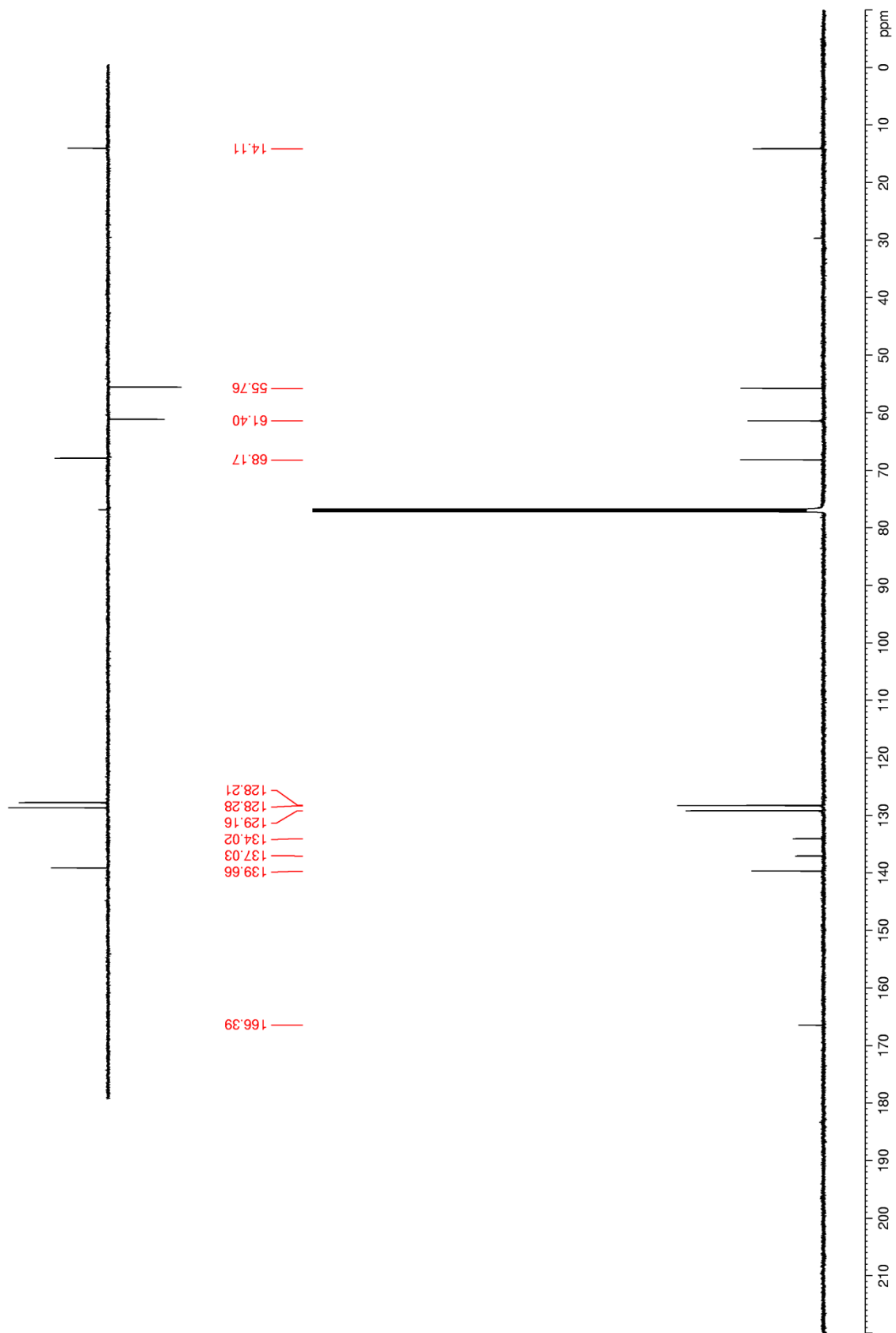
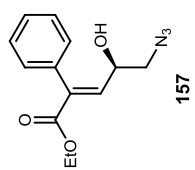


Figure 93. ^1H NMR (CDCl_3) of 159

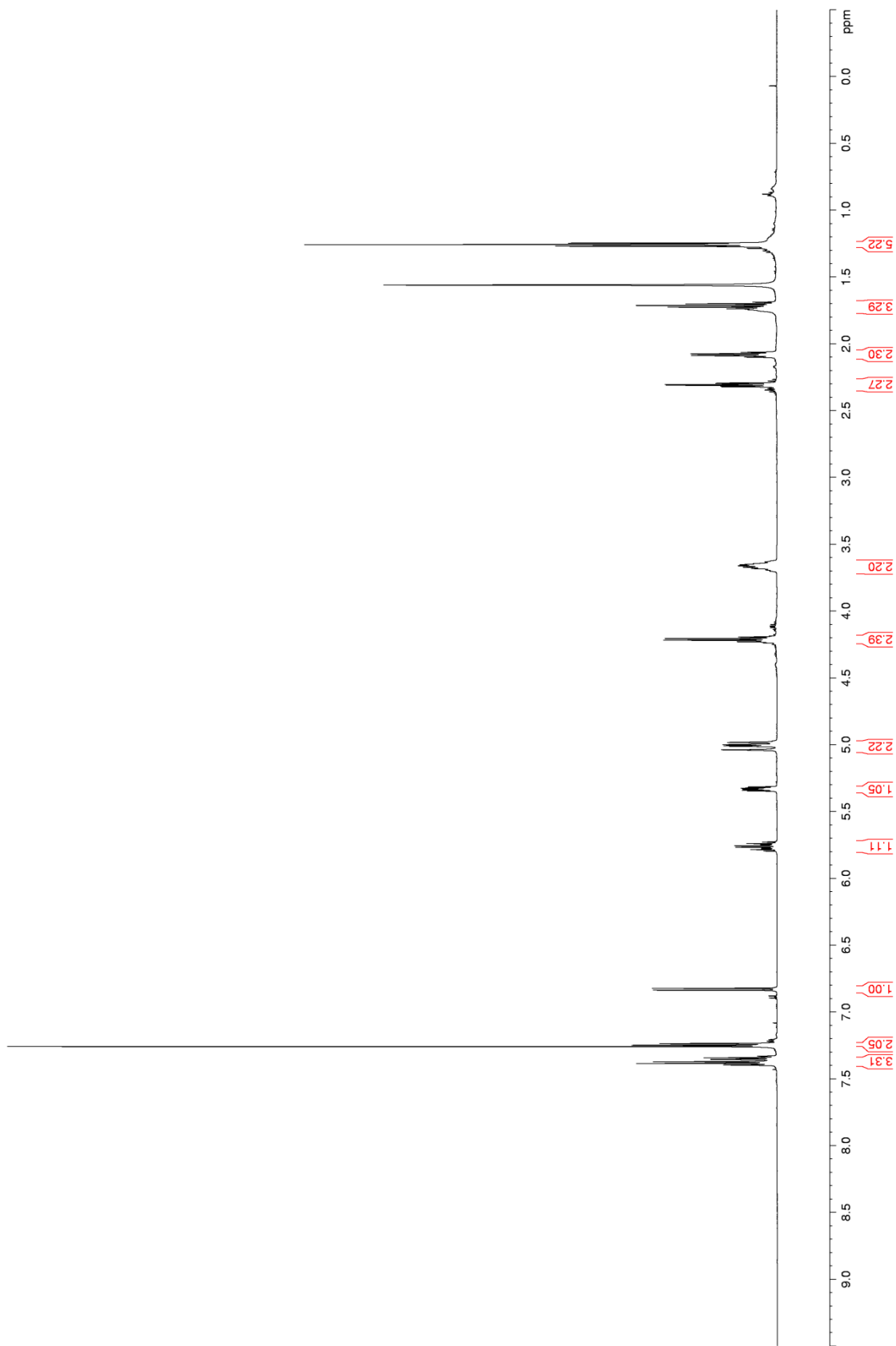
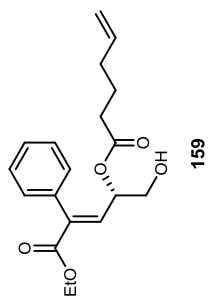


Figure 94. ^{13}C NMR (CDCl_3) of 159

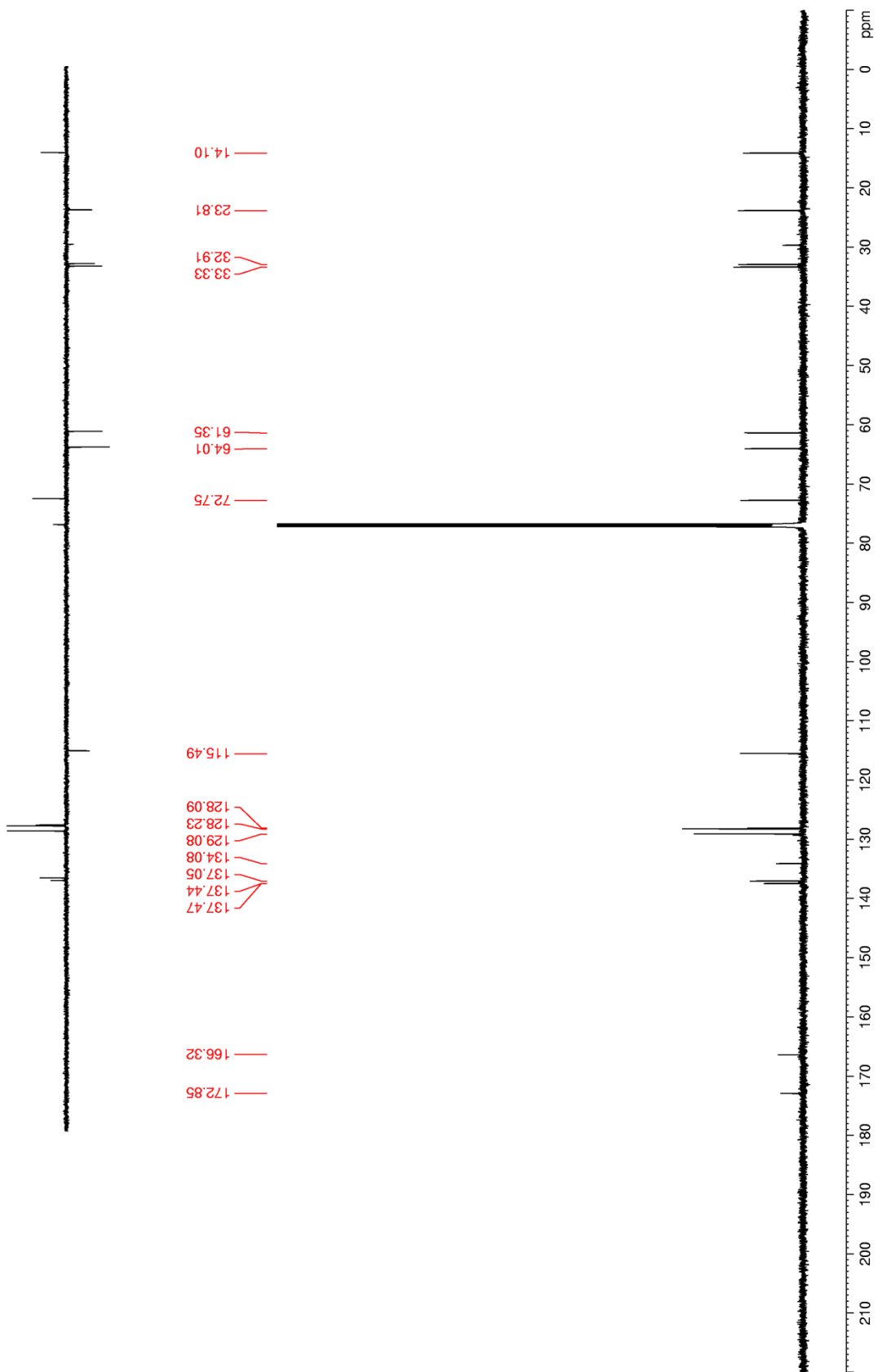
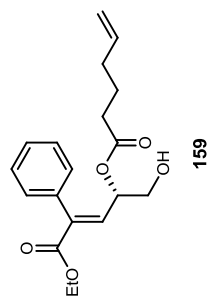


Figure 95. ^1H NMR (CDCl_3) of 160

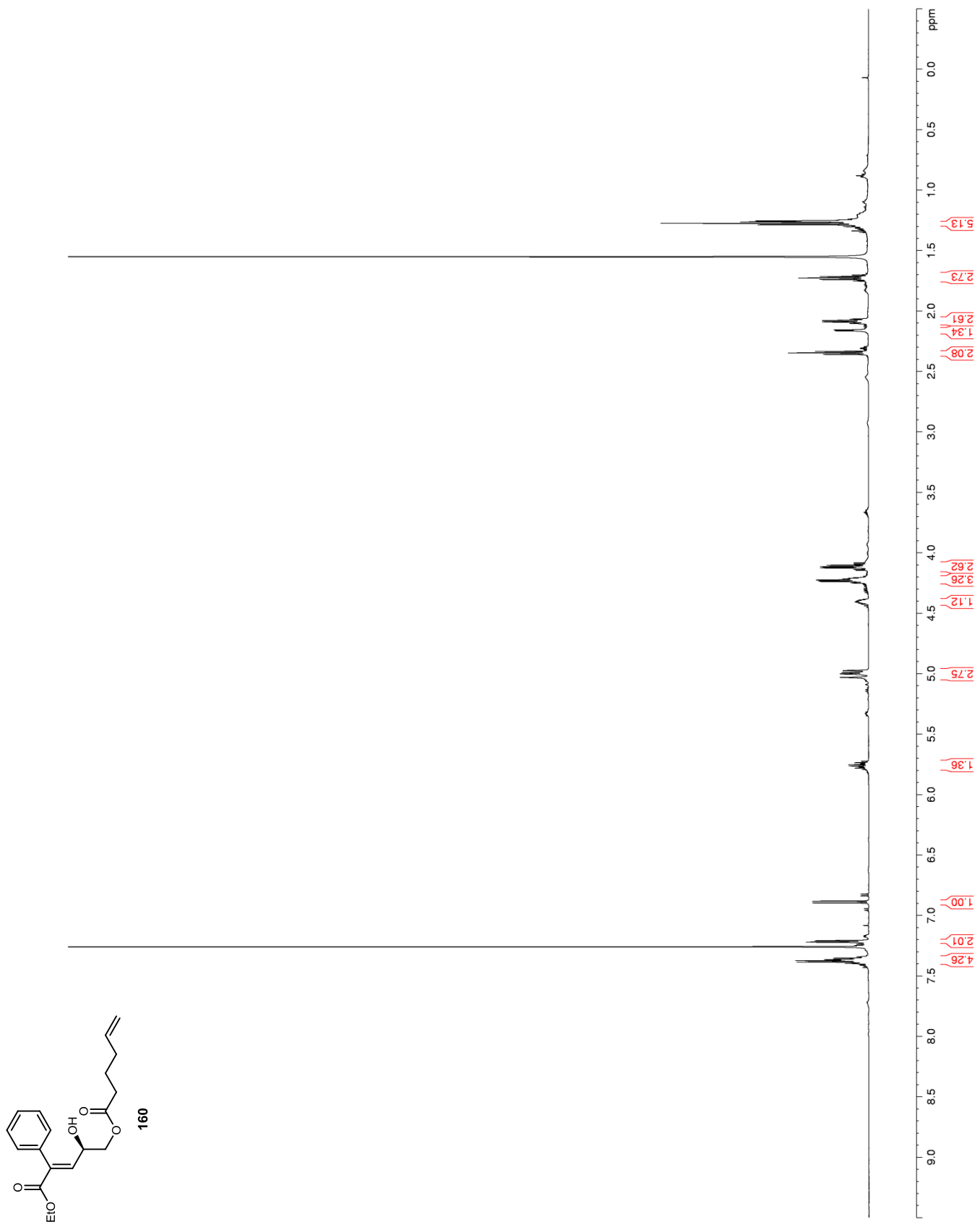


Figure 96. ^{13}C NMR (CDCl_3) of 160

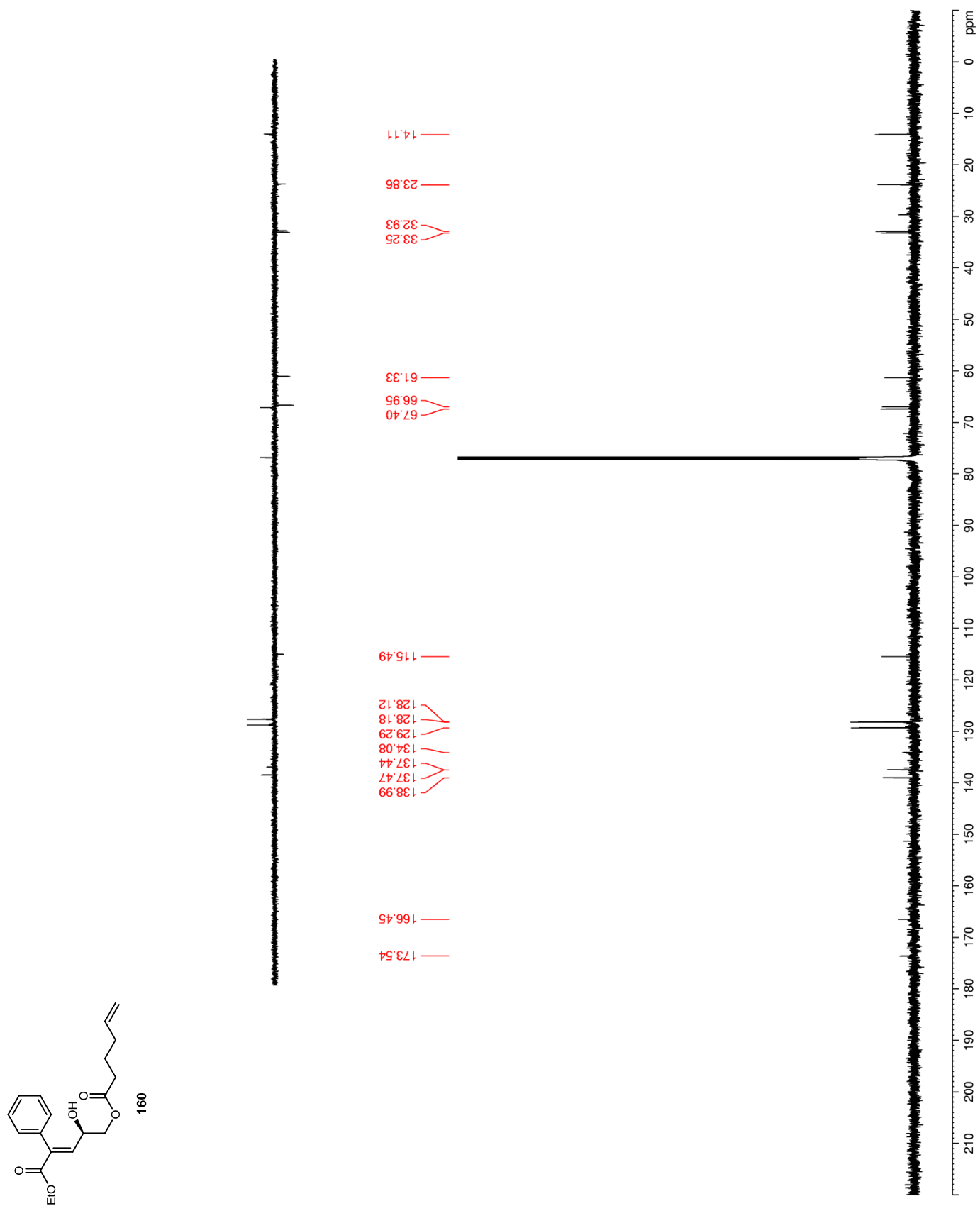


Figure 97. ^1H NMR (CDCl_3) of 161

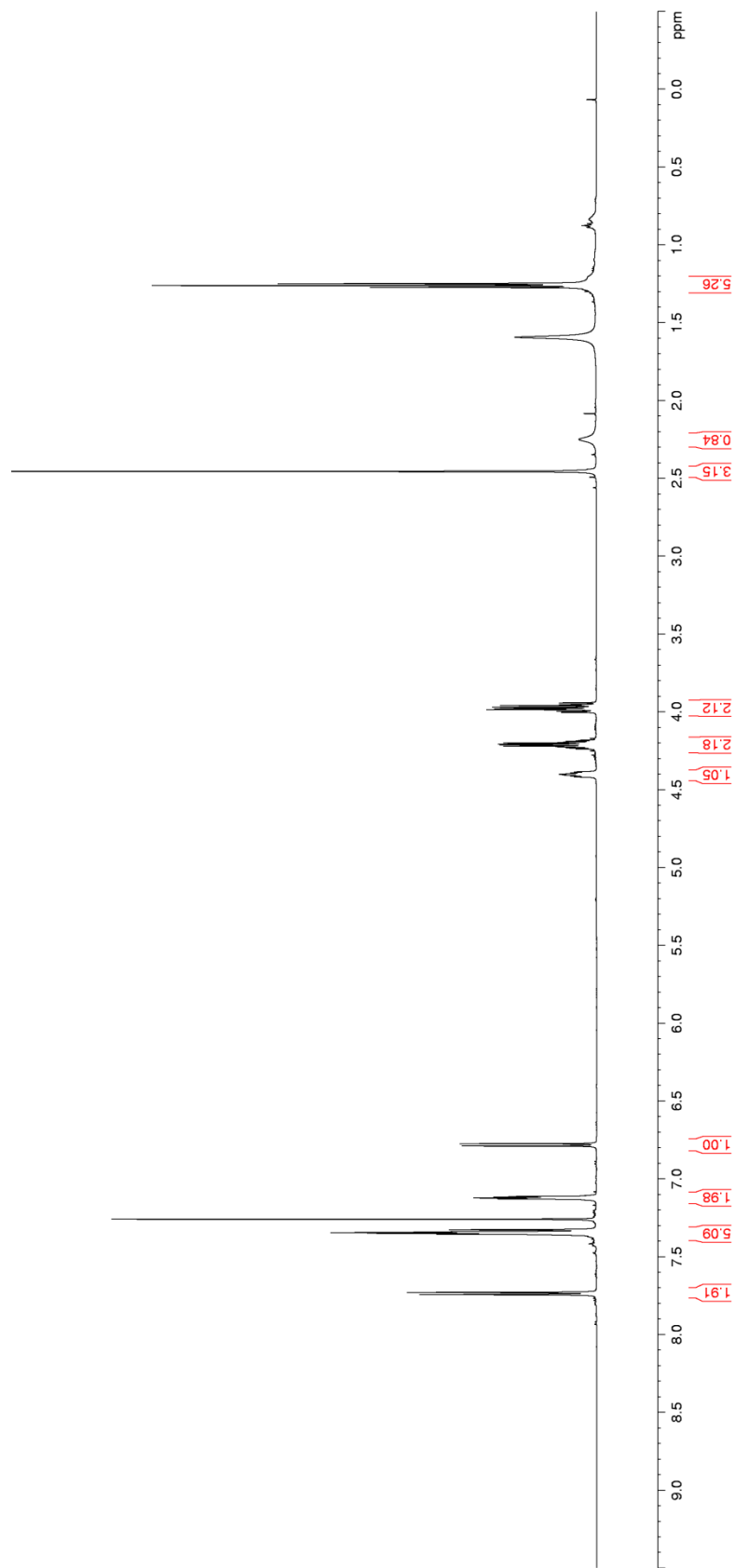
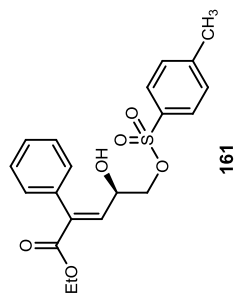


Figure 98. ^{13}C NMR (CDCl_3) of 161

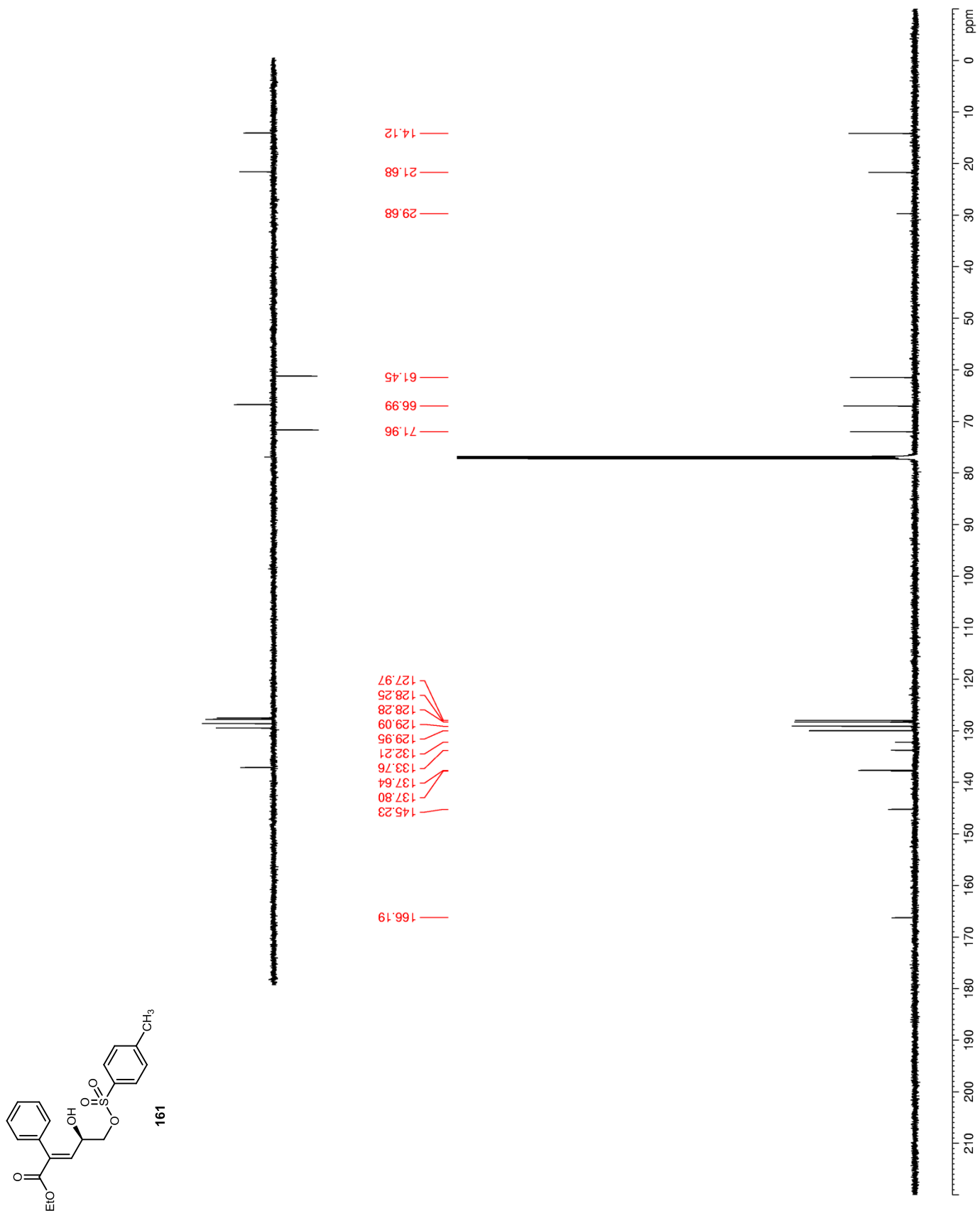


Figure 99. ^1H NMR (CDCl_3) of 163

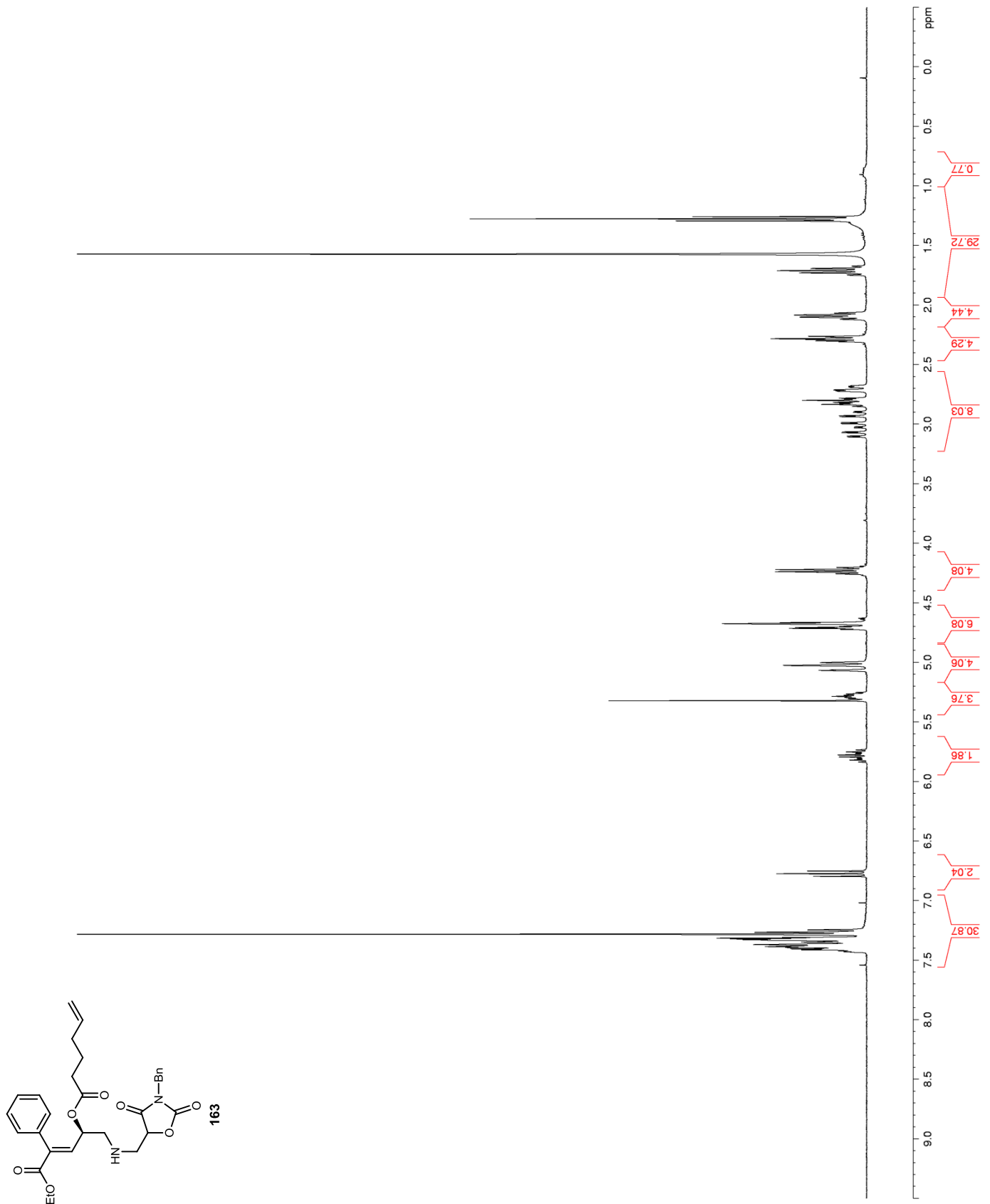


Figure 100. ^{13}C NMR (CDCl_3) of 163

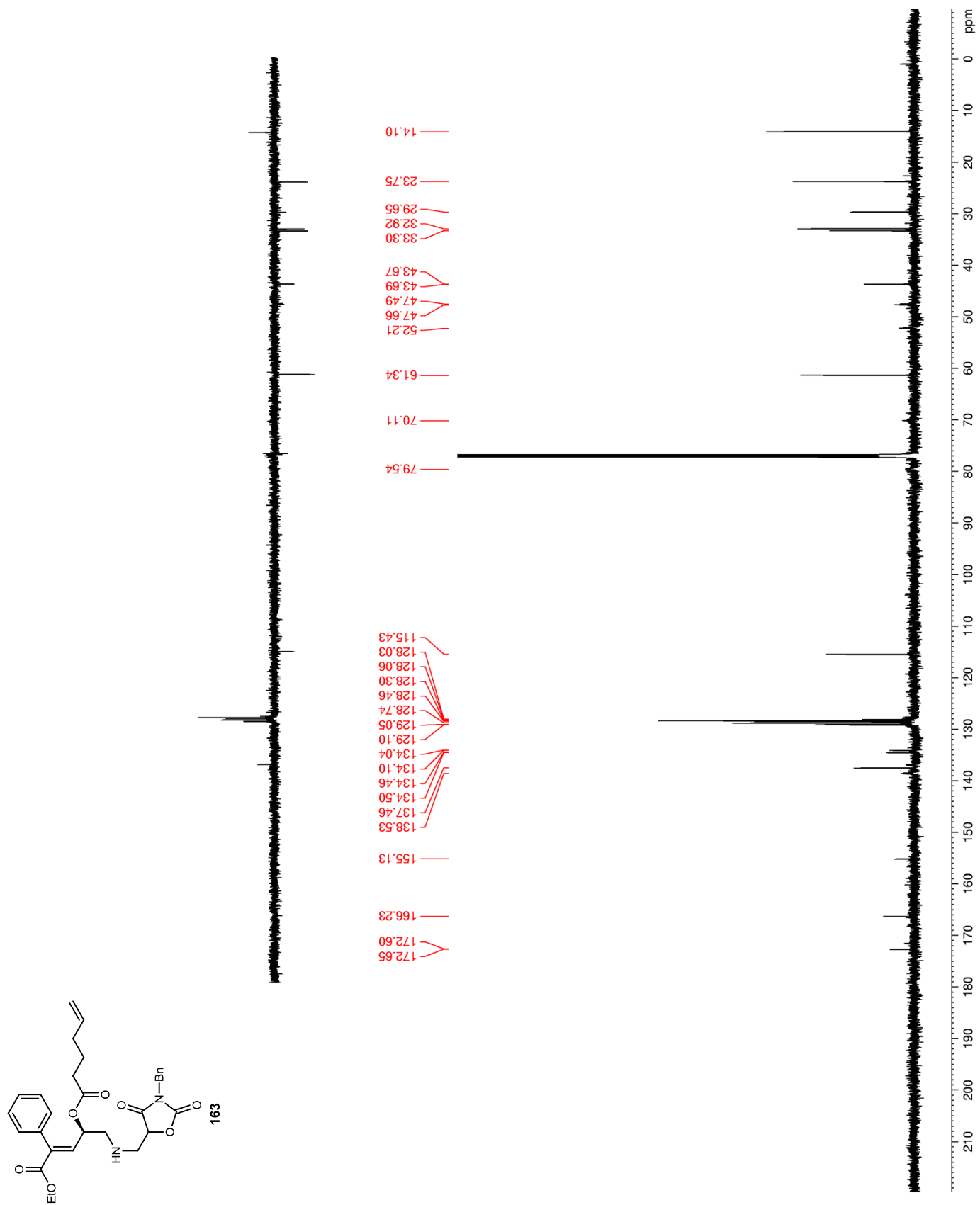
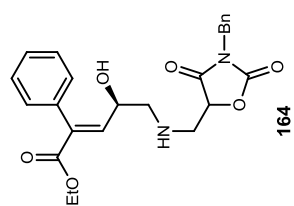


Figure 101. ^1H NMR (CDCl_3) of 164



164

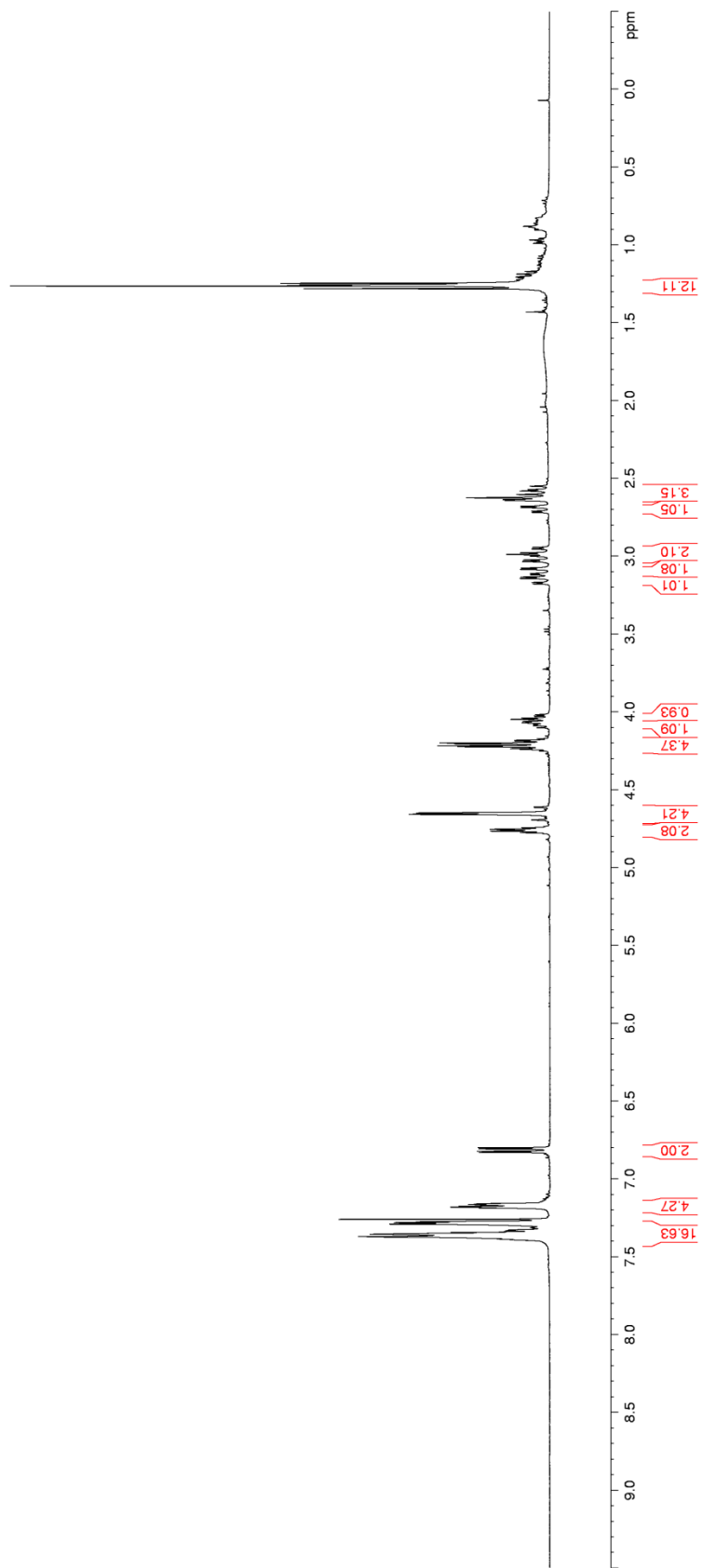


Figure 102. ^{13}C NMR (CDCl_3) of 164

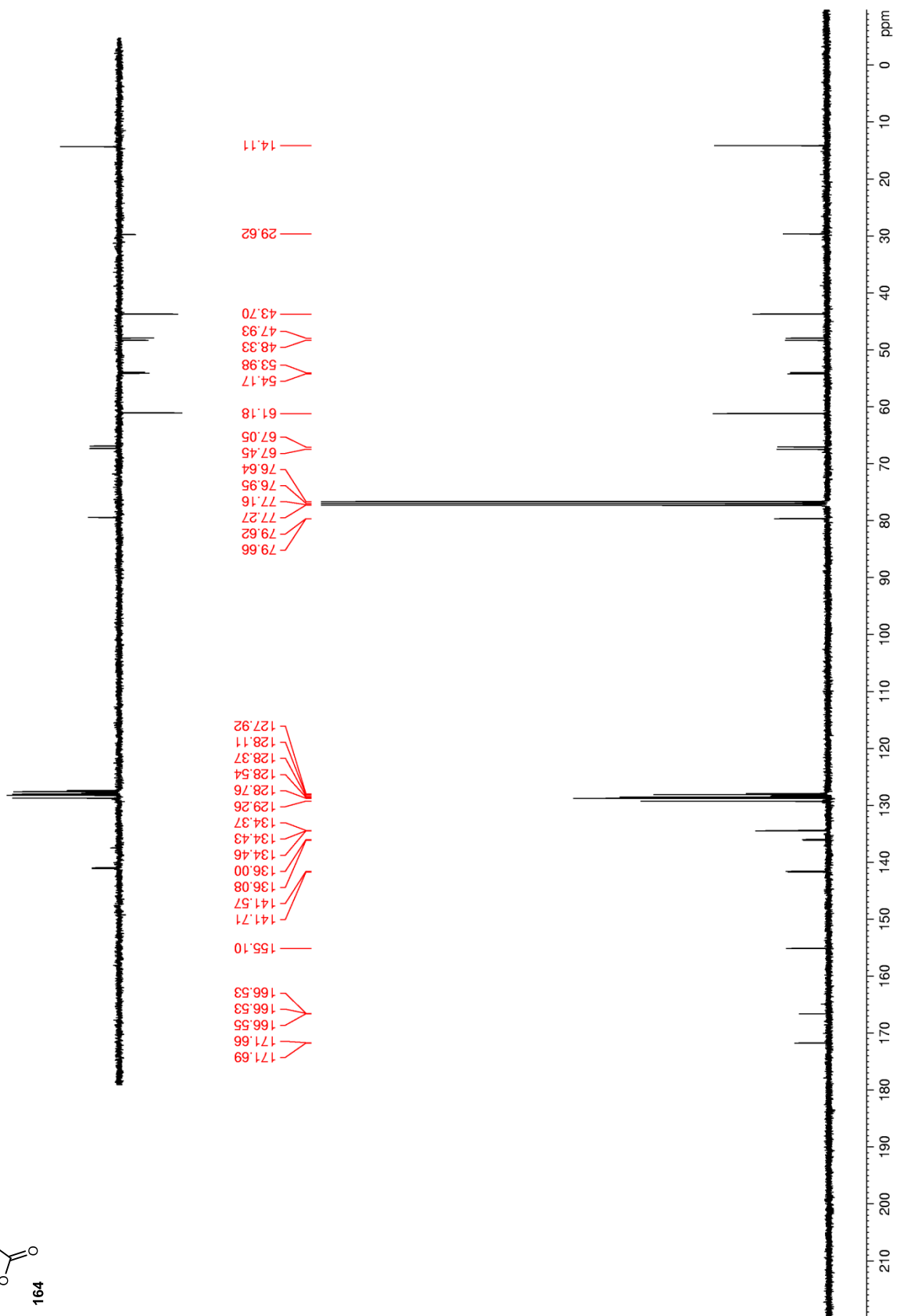
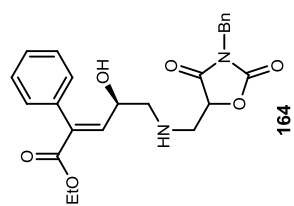


Figure 104. ^{13}C NMR (CDCl_3) of 167

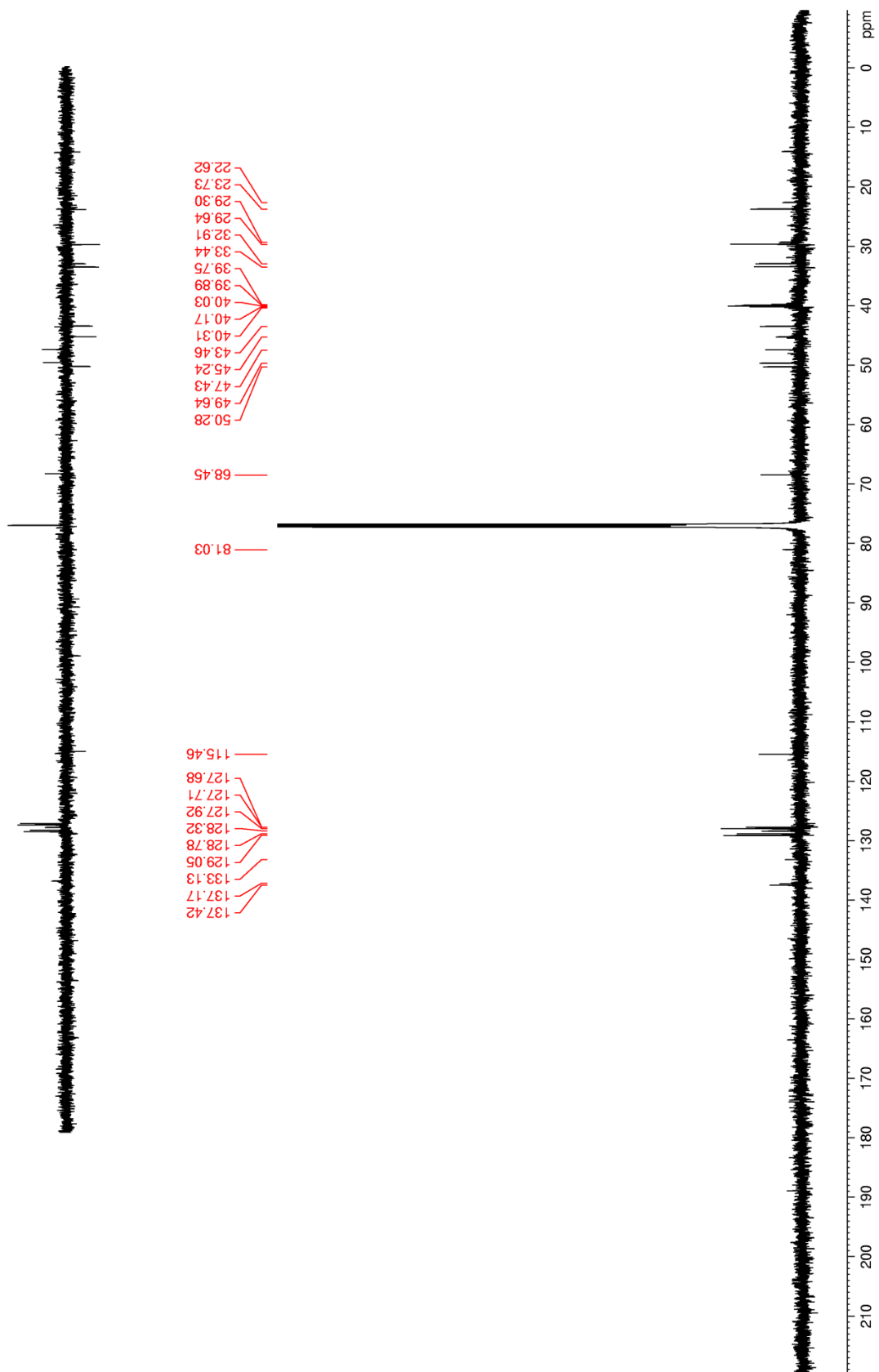
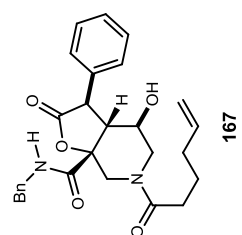


Figure 105. COSY (CDCl₃) of 167

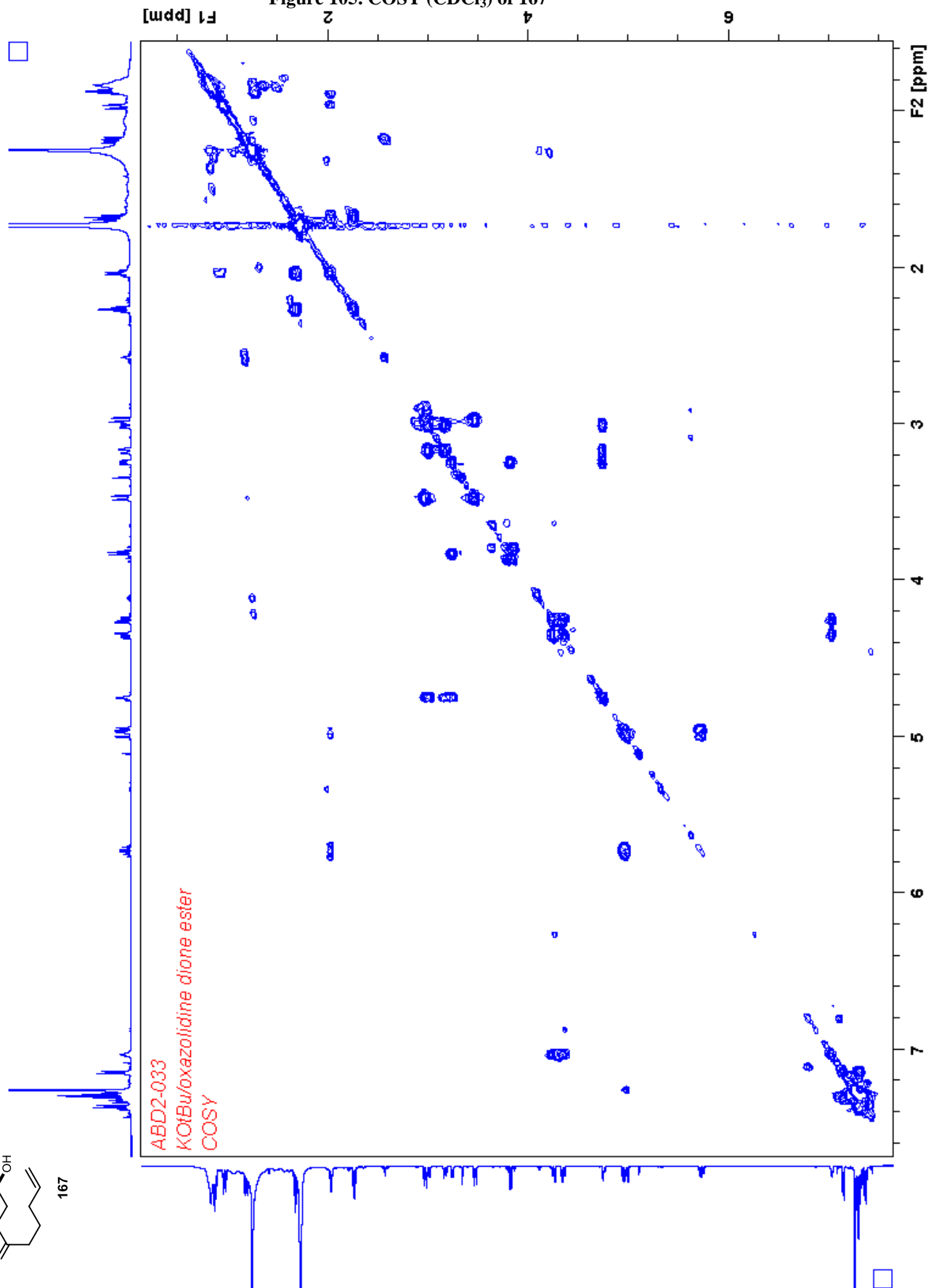
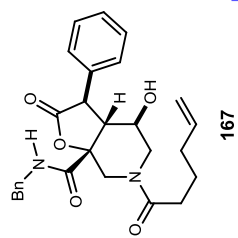


Figure 106. HSQC (CDCl₃) of 167

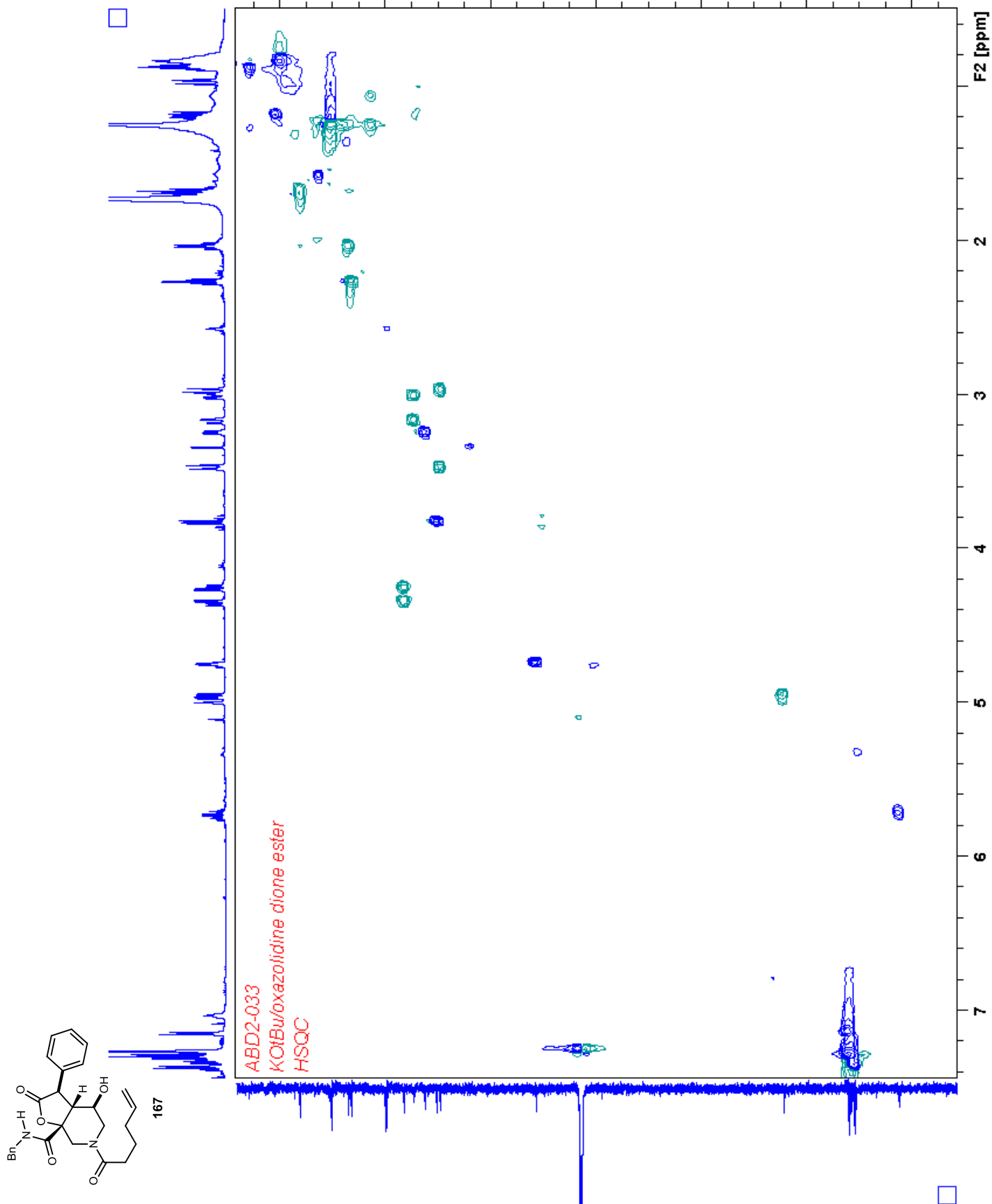


Figure 107. HMBC (CDCl₃) of 167

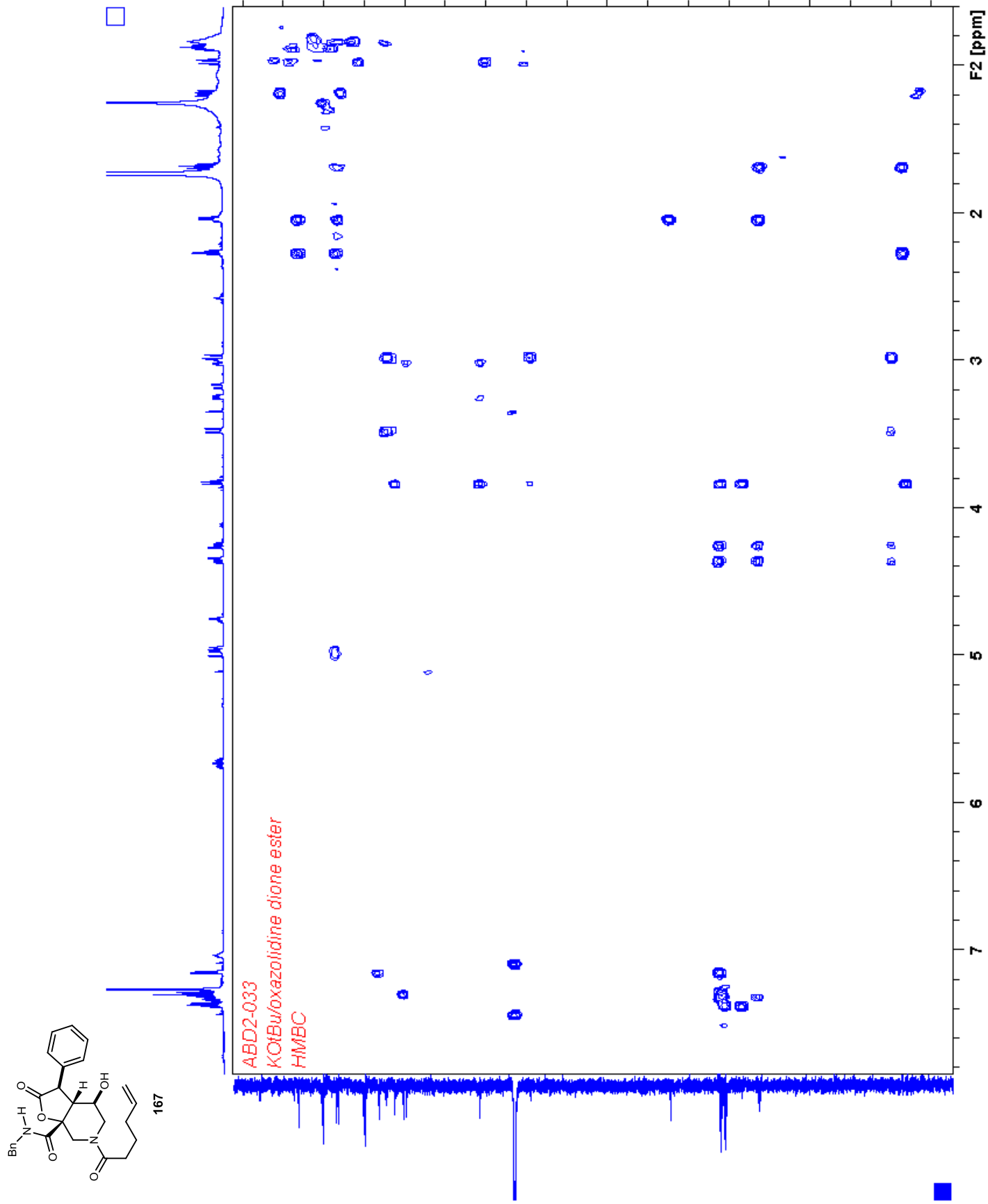


Figure 108. NOESY (CDCl₃) of 167

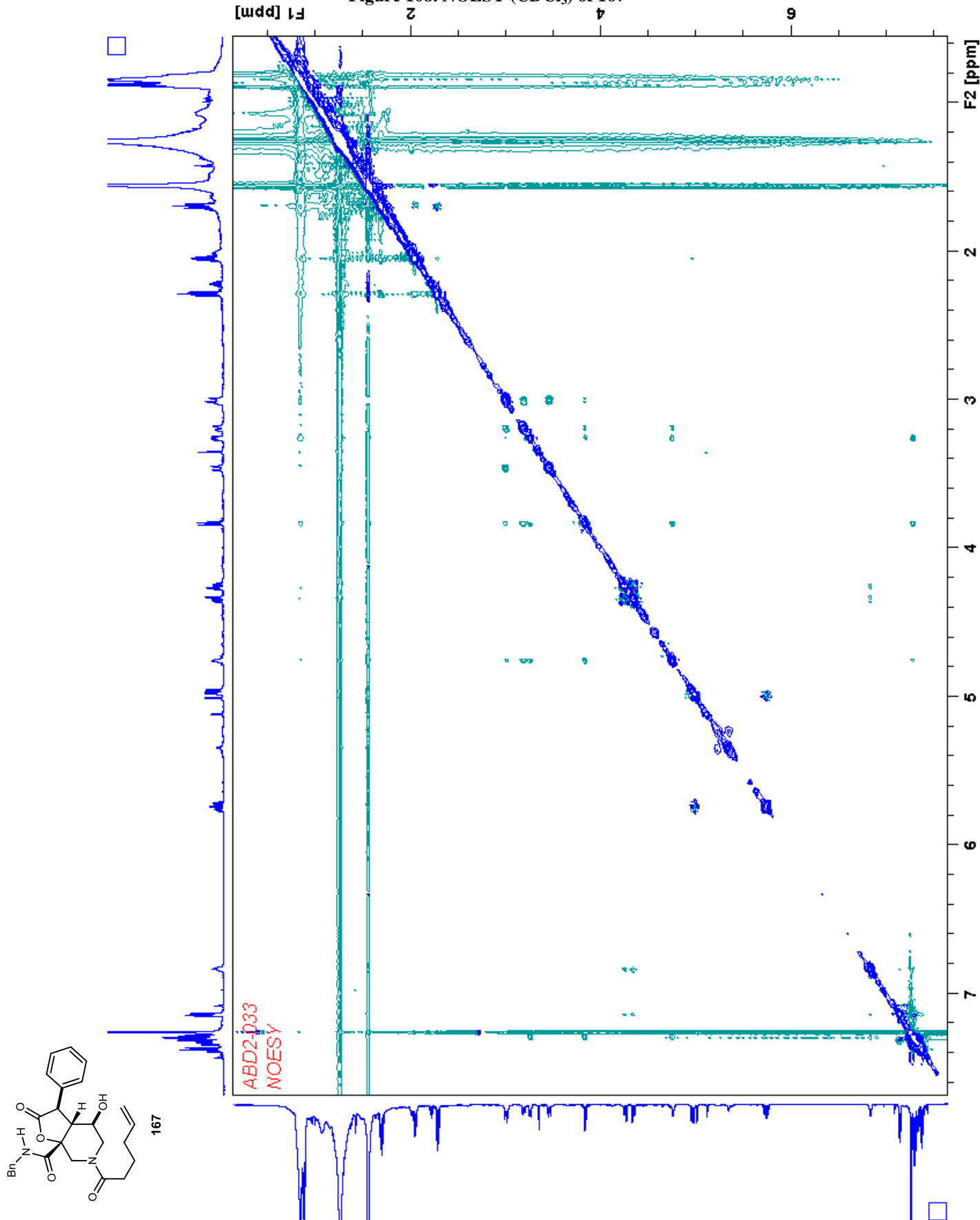


Figure 109. ^1H NMR (CDCl_3) of 176

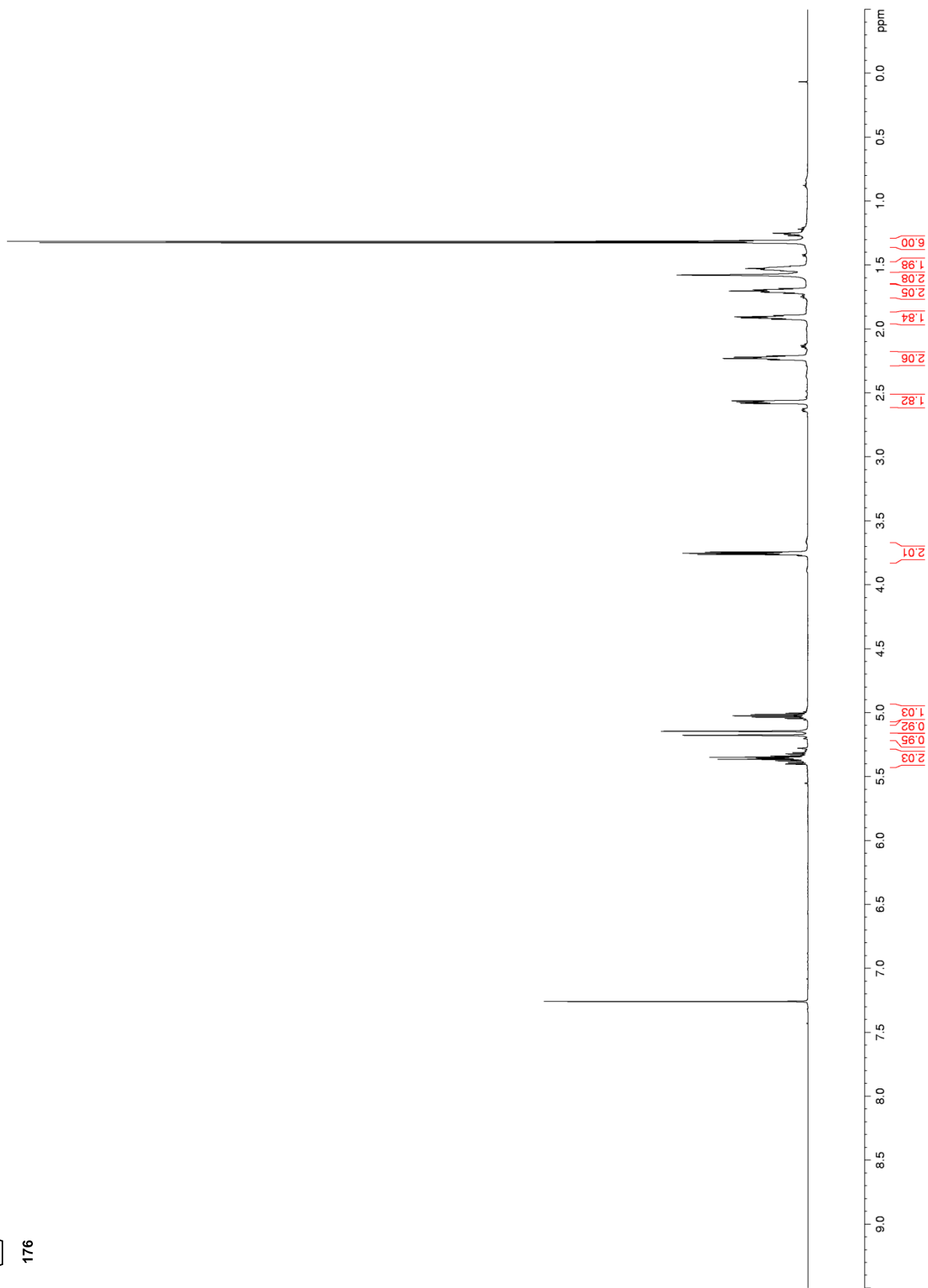
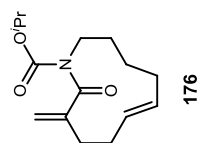


Figure 110. ^{13}C NMR (CDCl_3) of 176

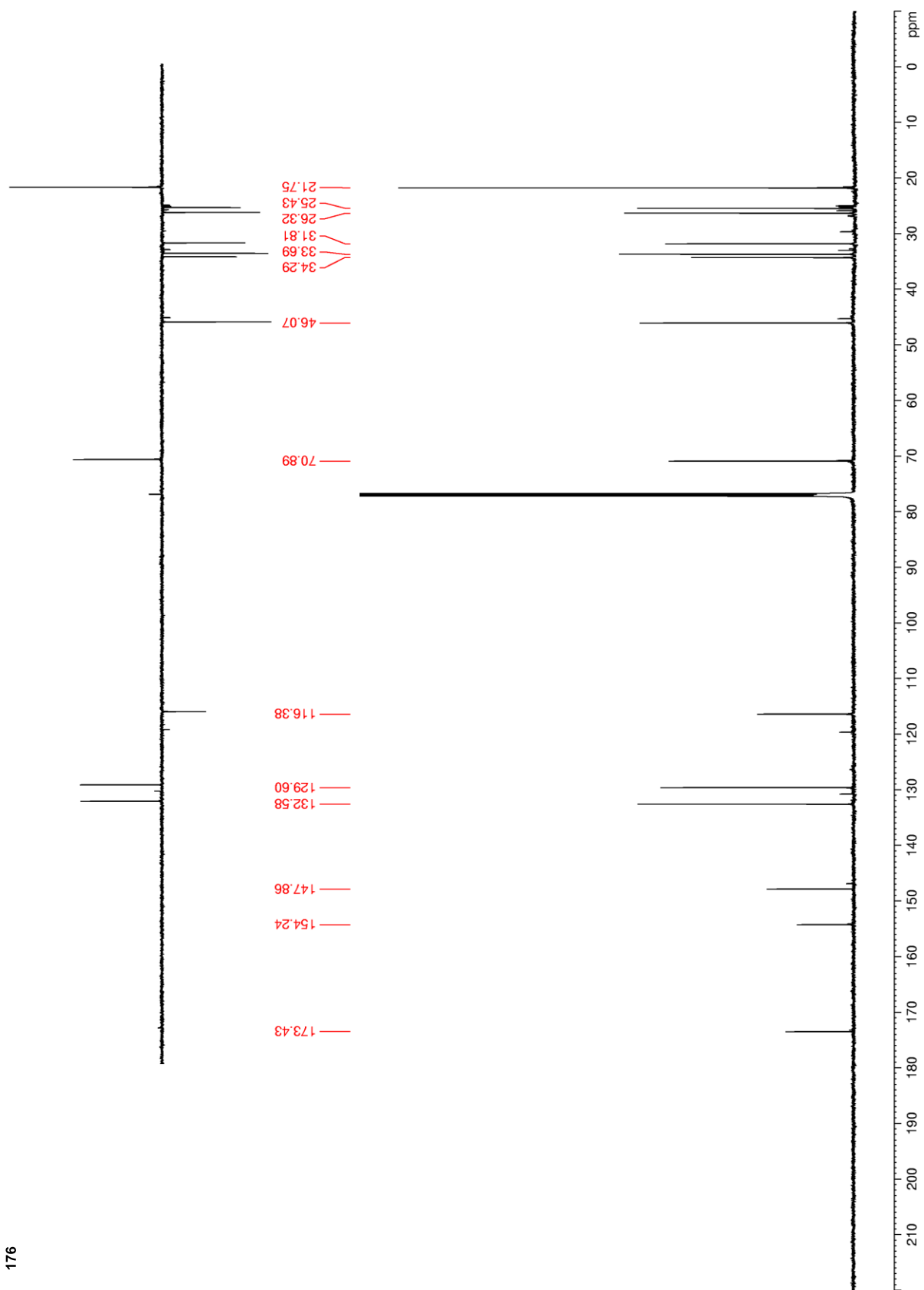
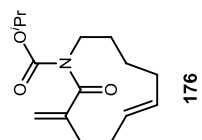


Figure 111. HSQC (CDCl₃) of 176

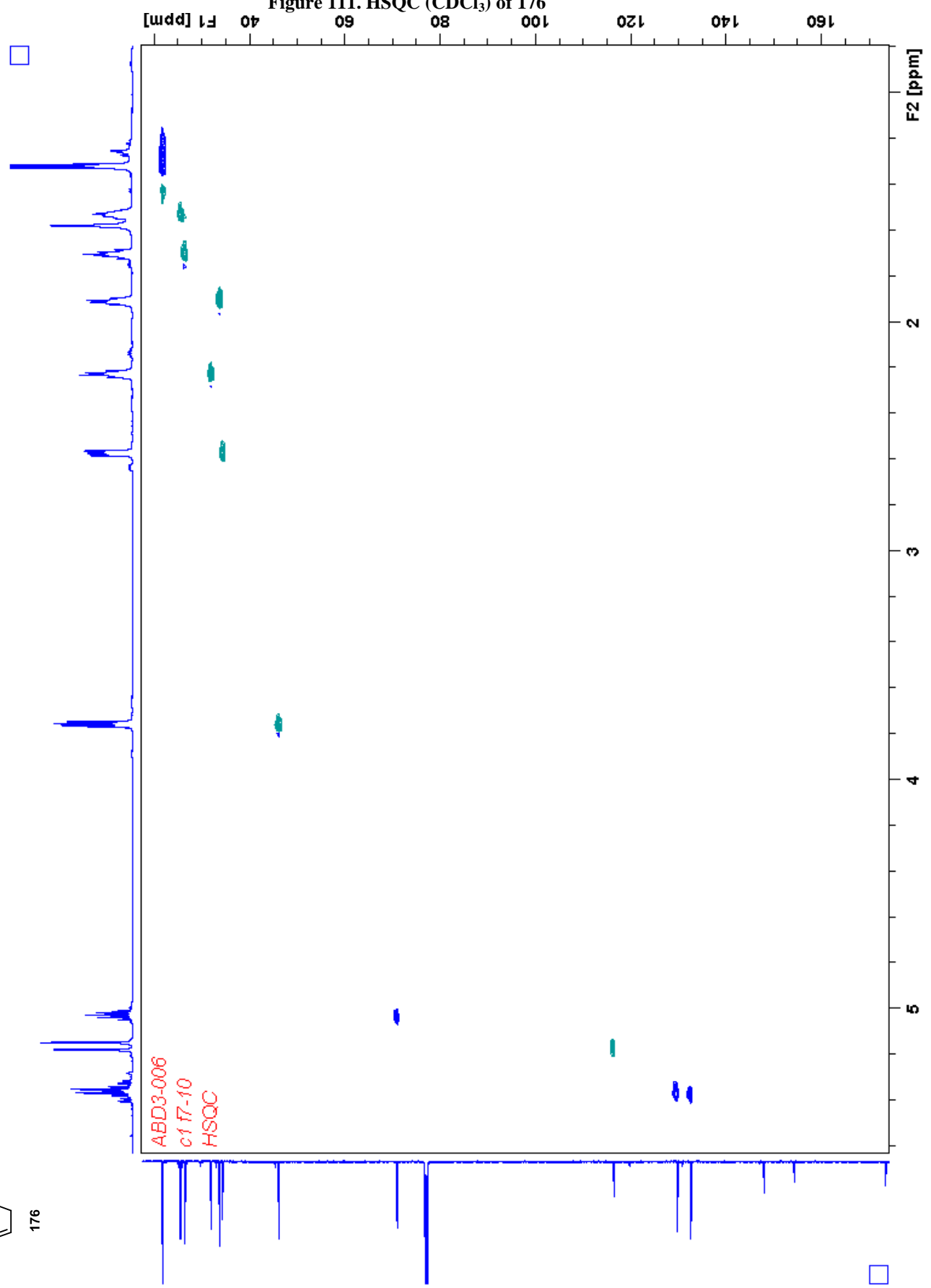
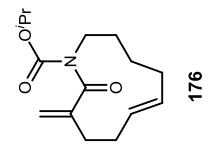


Figure 112. NOESY (CDCl₃) of 176

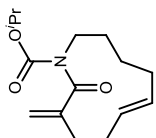
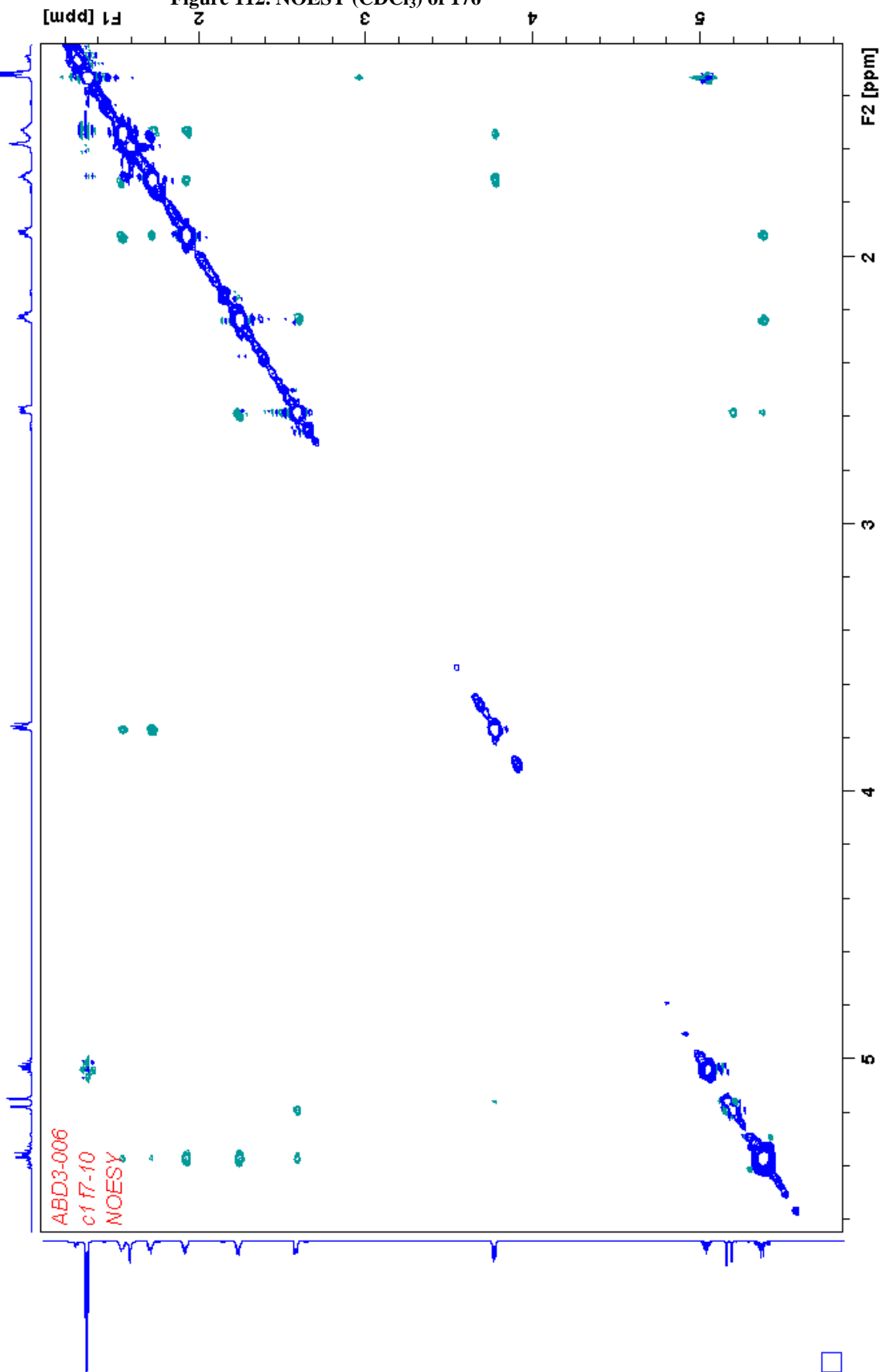


Figure 113. ^1H NMR (CDCl_3) of 186

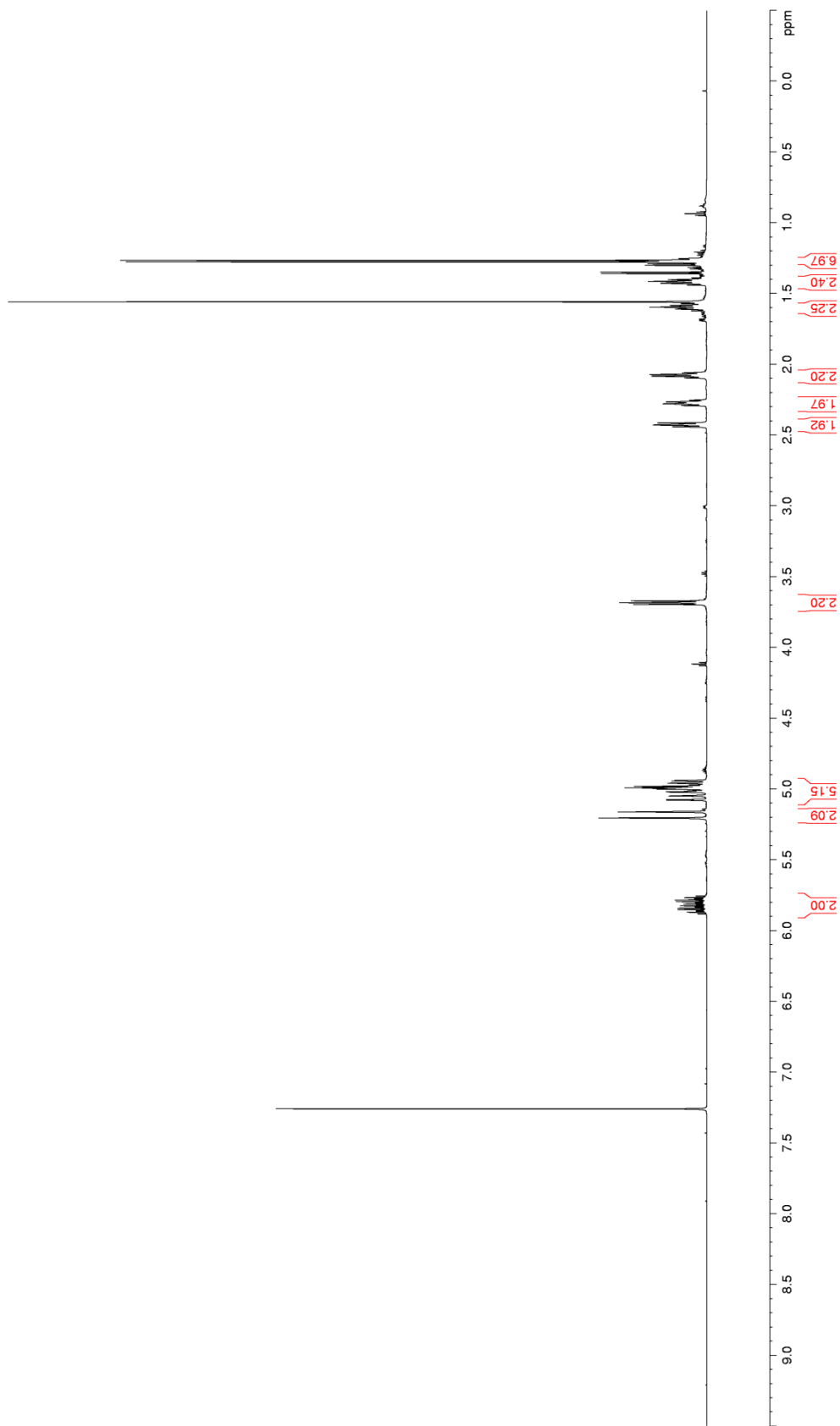
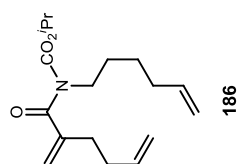


Figure 114. ^{13}C NMR (CDCl_3) of 186

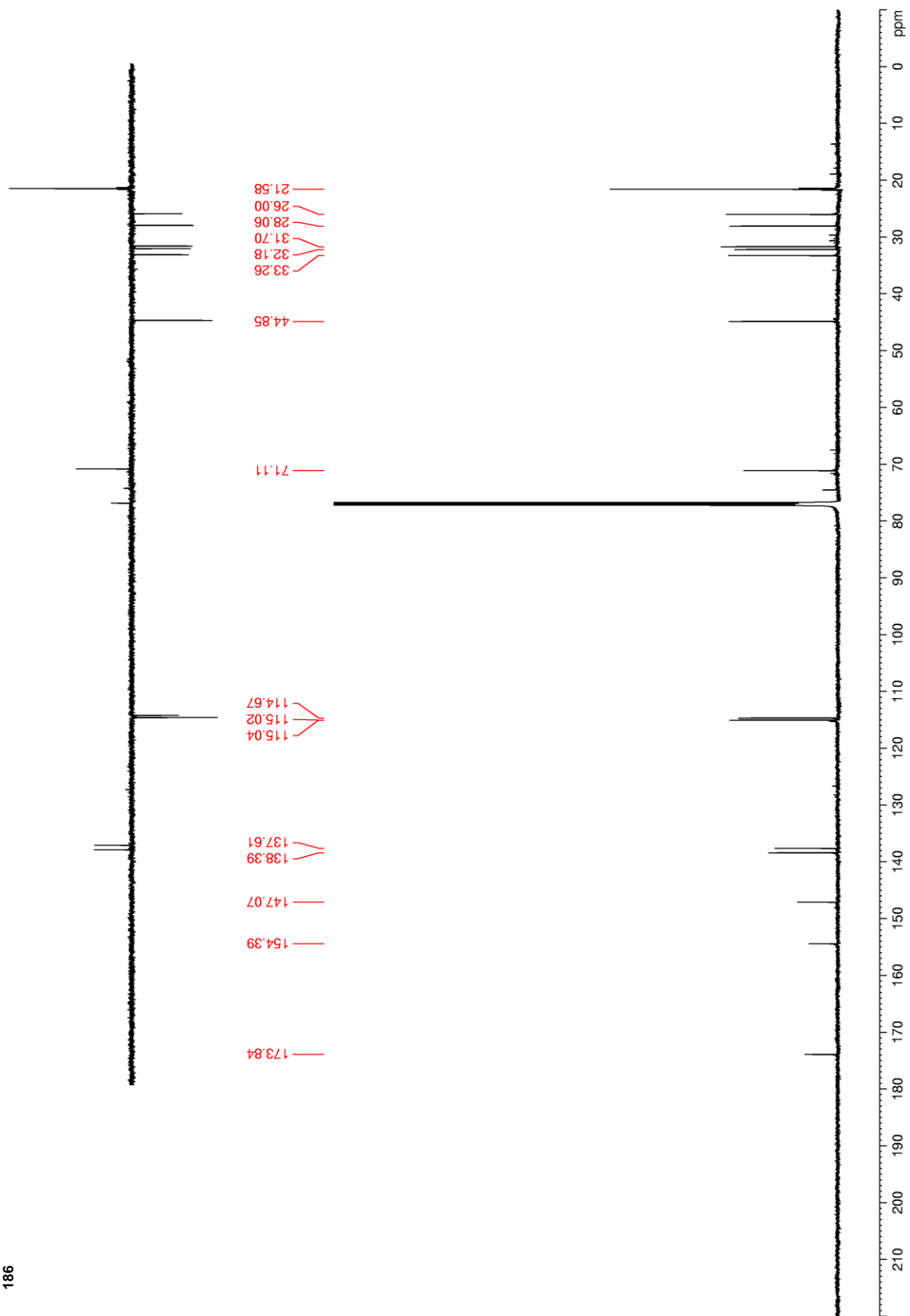
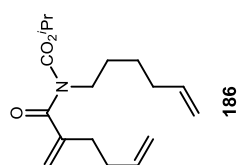


Figure 115. ^1H NMR (CDCl_3) of 197

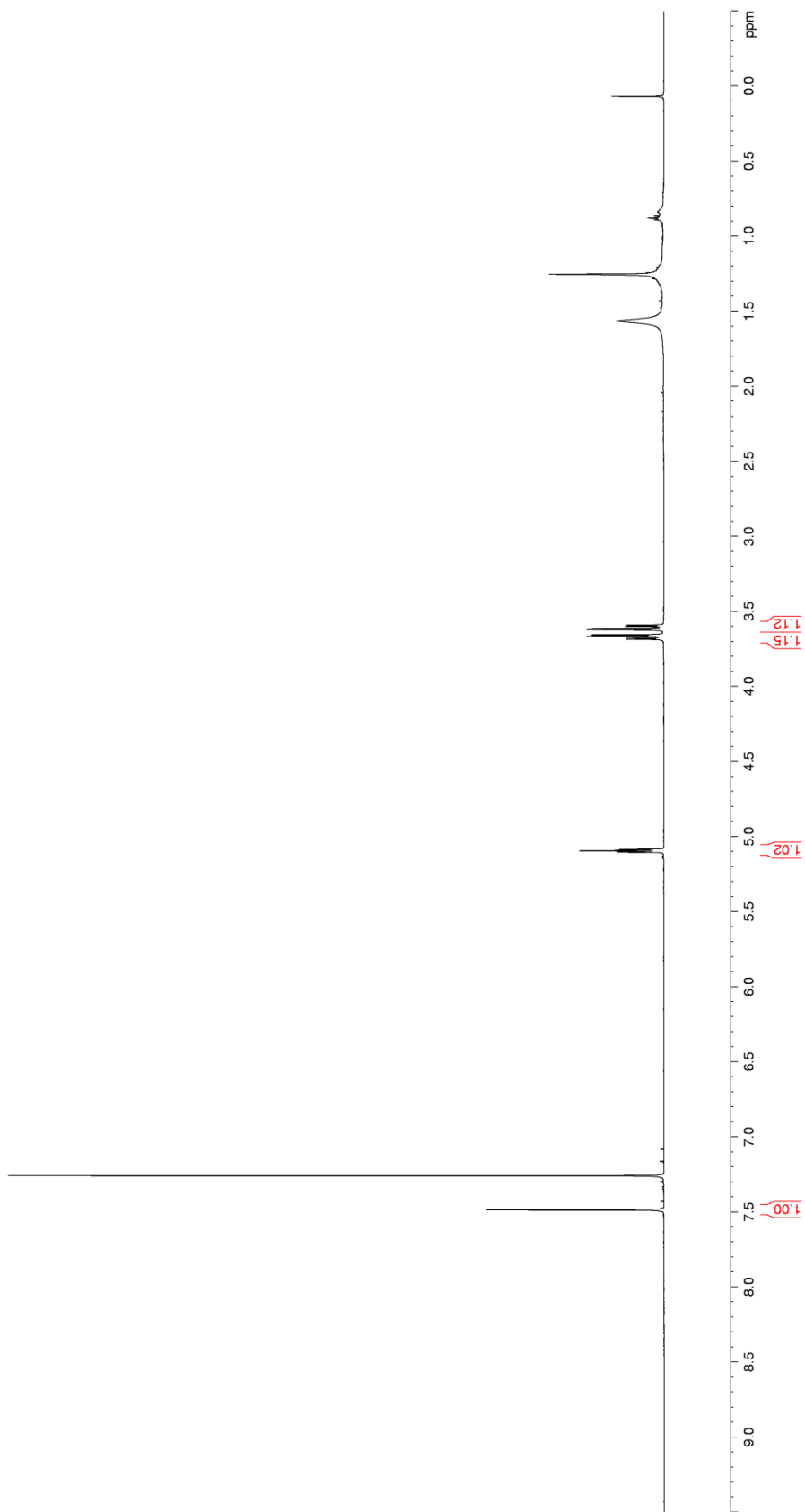
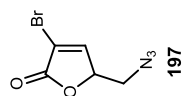


Figure 116. ^{13}C NMR (CDCl_3) of 197

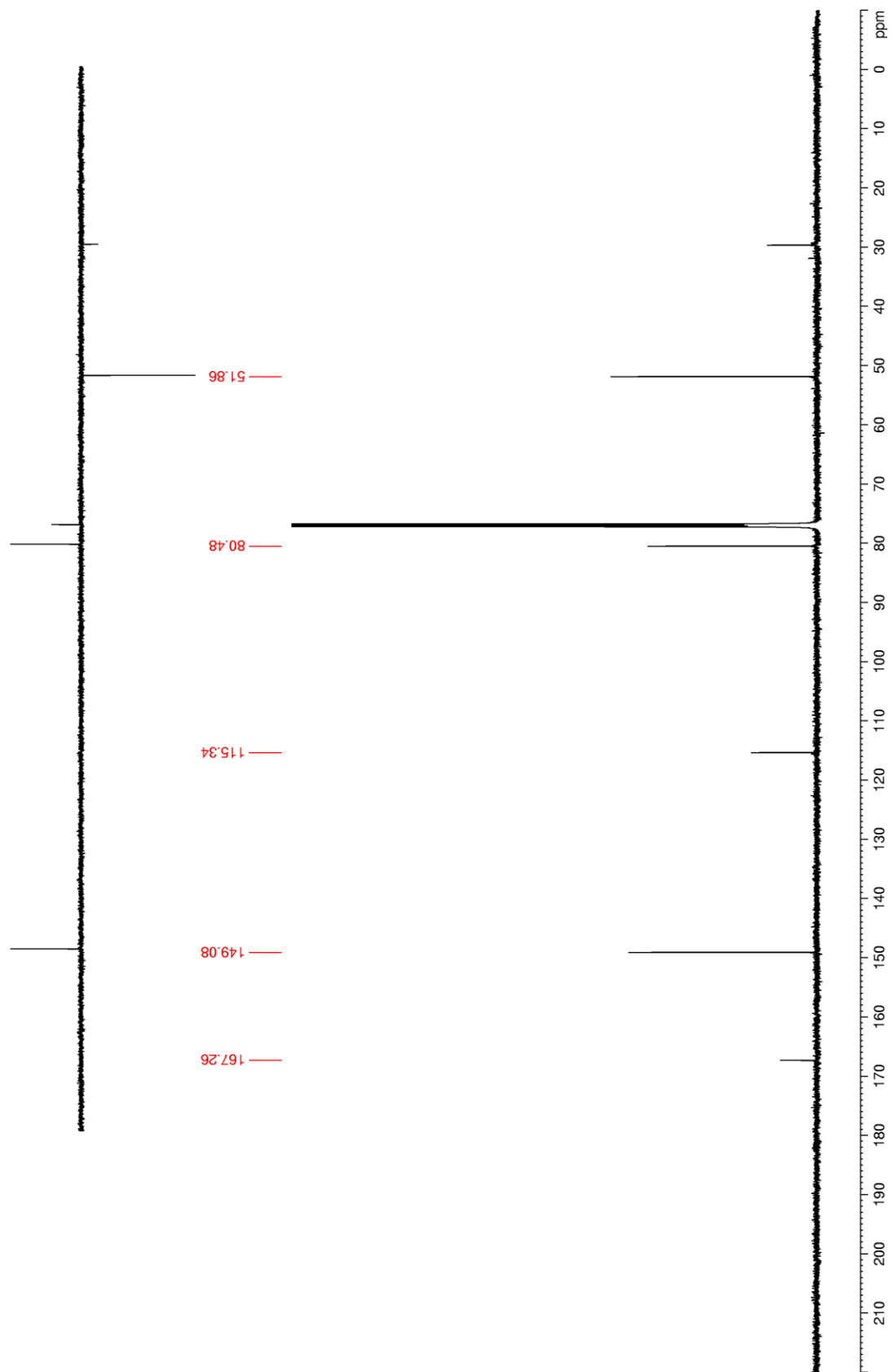
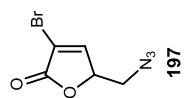


Figure 117. ^1H NMR (CDCl_3) of 204

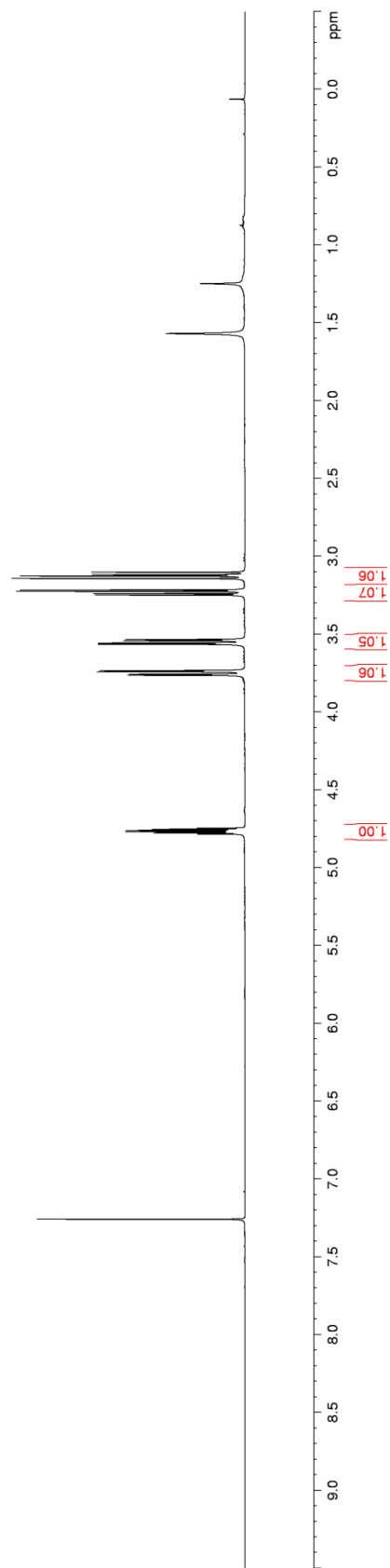
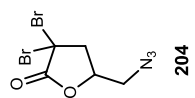


Figure 118. ^{13}C NMR (CDCl_3) of 204

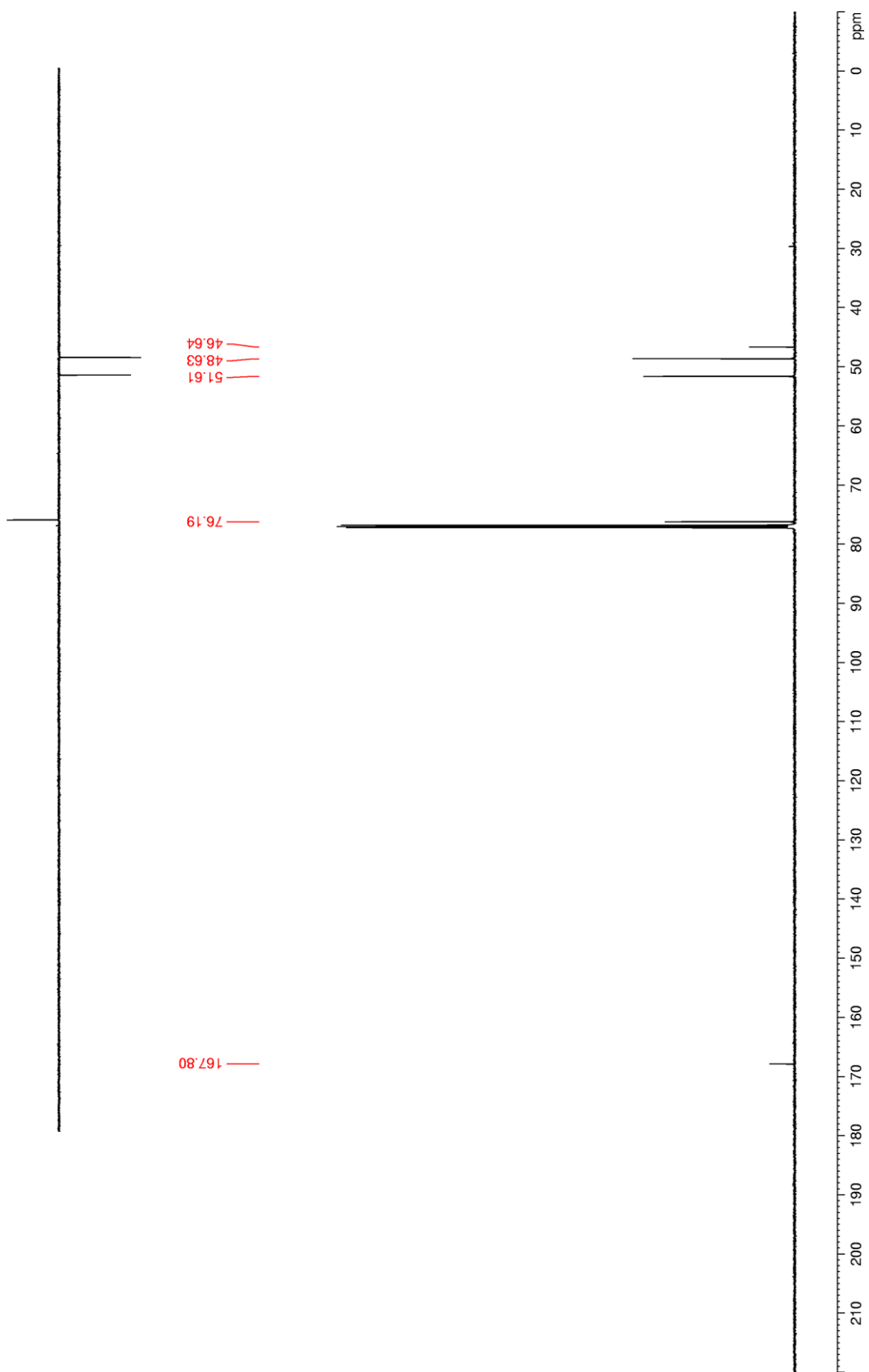
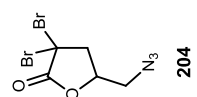


Figure 119. ^1H NMR (CDCl_3) of 205

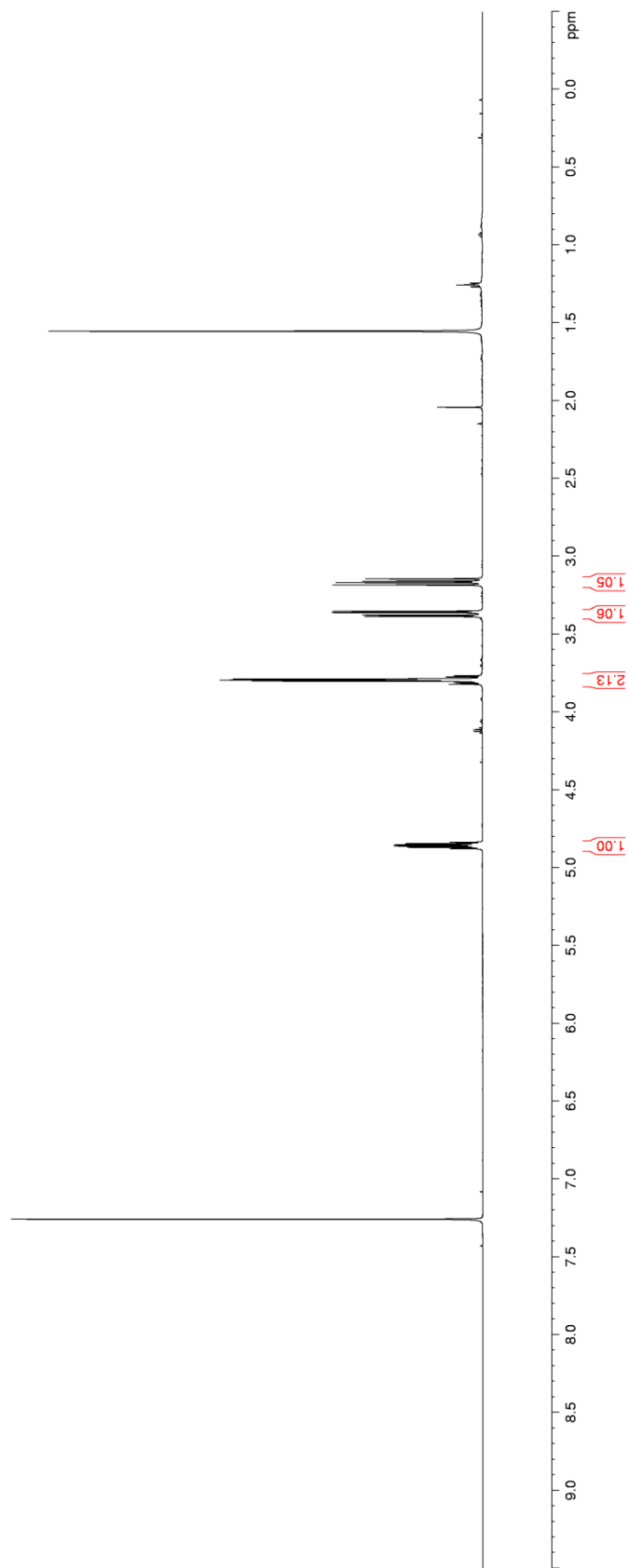
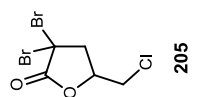


Figure 120. ^{13}C NMR (CDCl_3) of 205

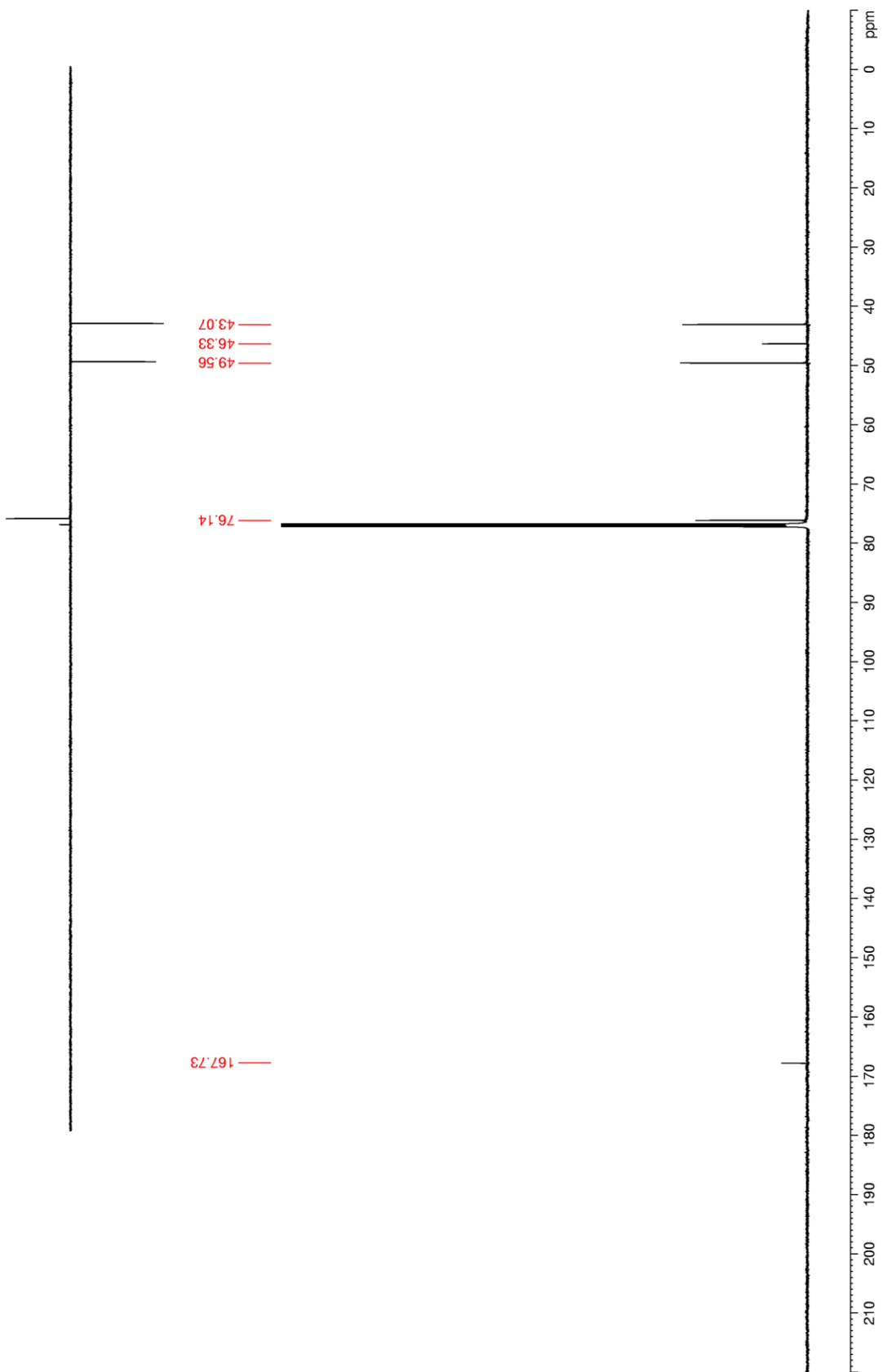
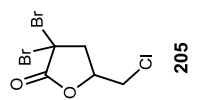


Figure 121. ^1H NMR (CDCl_3) of 206

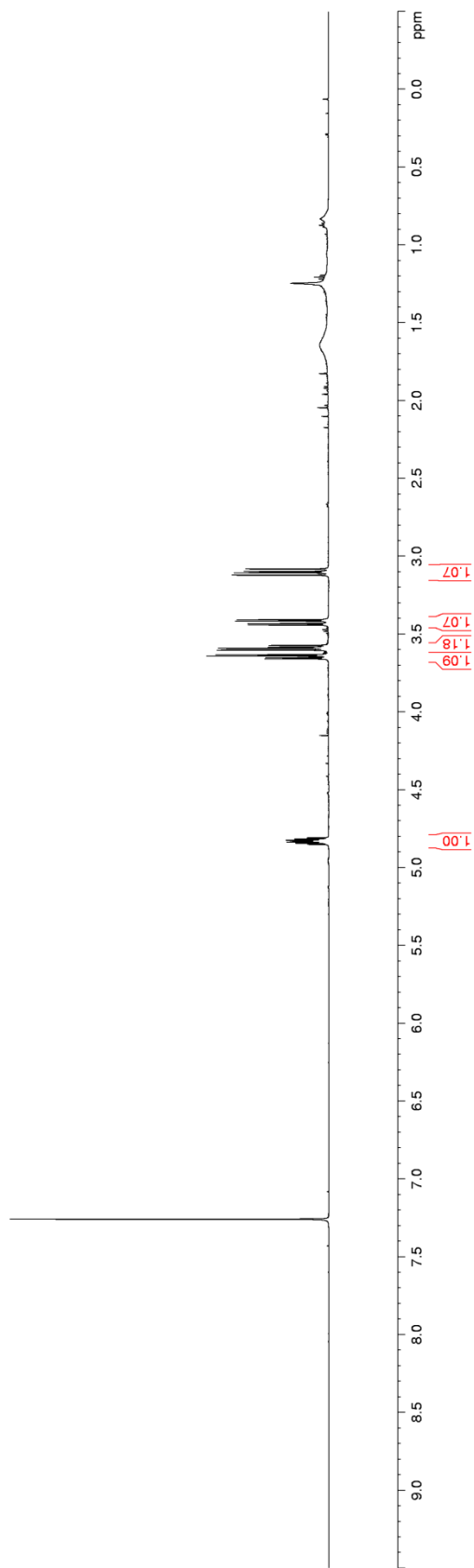
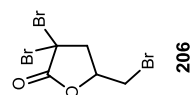


Figure 122. ^{13}C NMR (CDCl_3) of 206

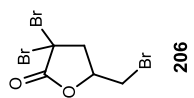
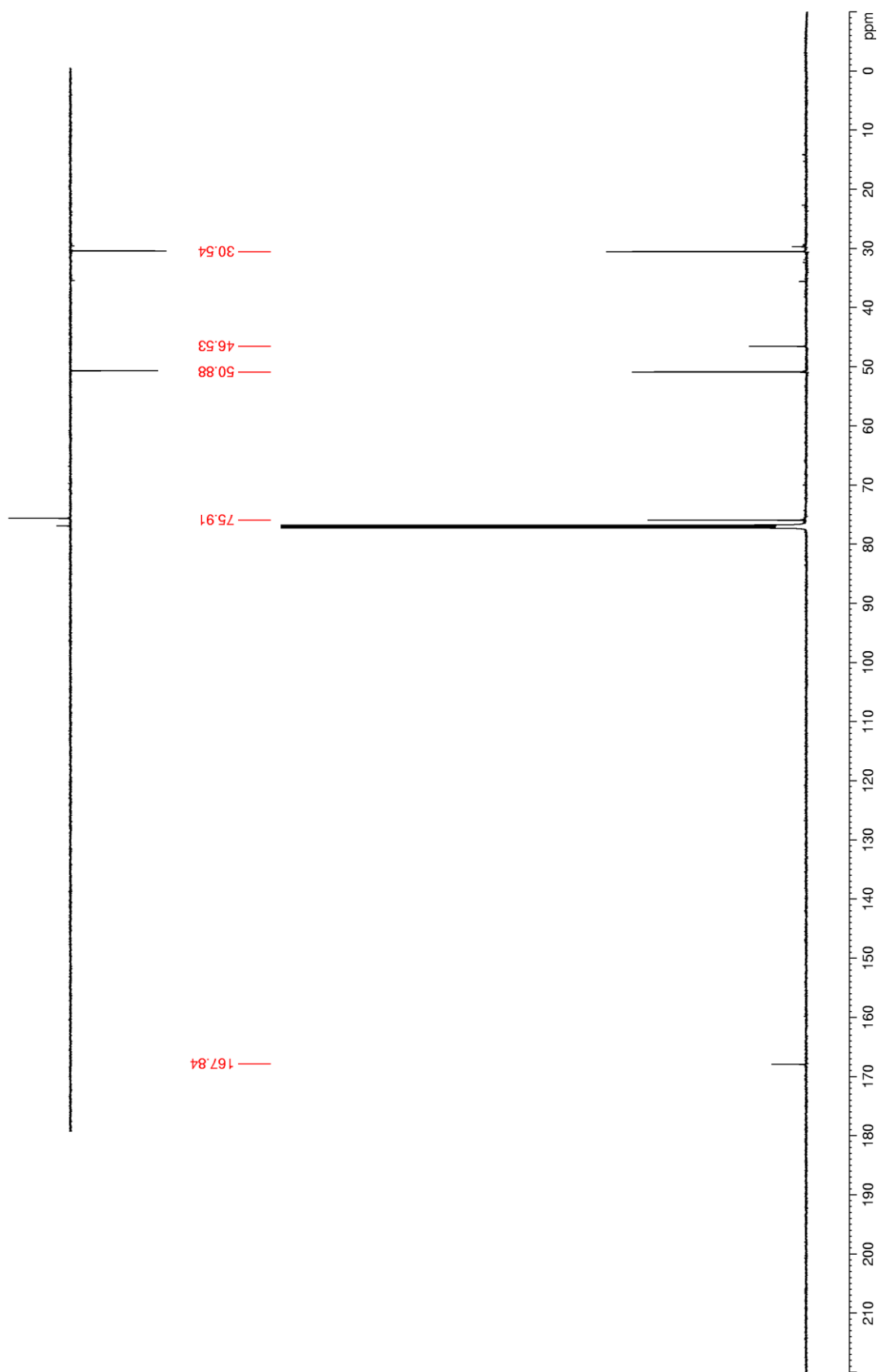
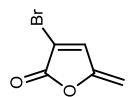


Figure 123. ^1H NMR (CDCl_3) of 212



212

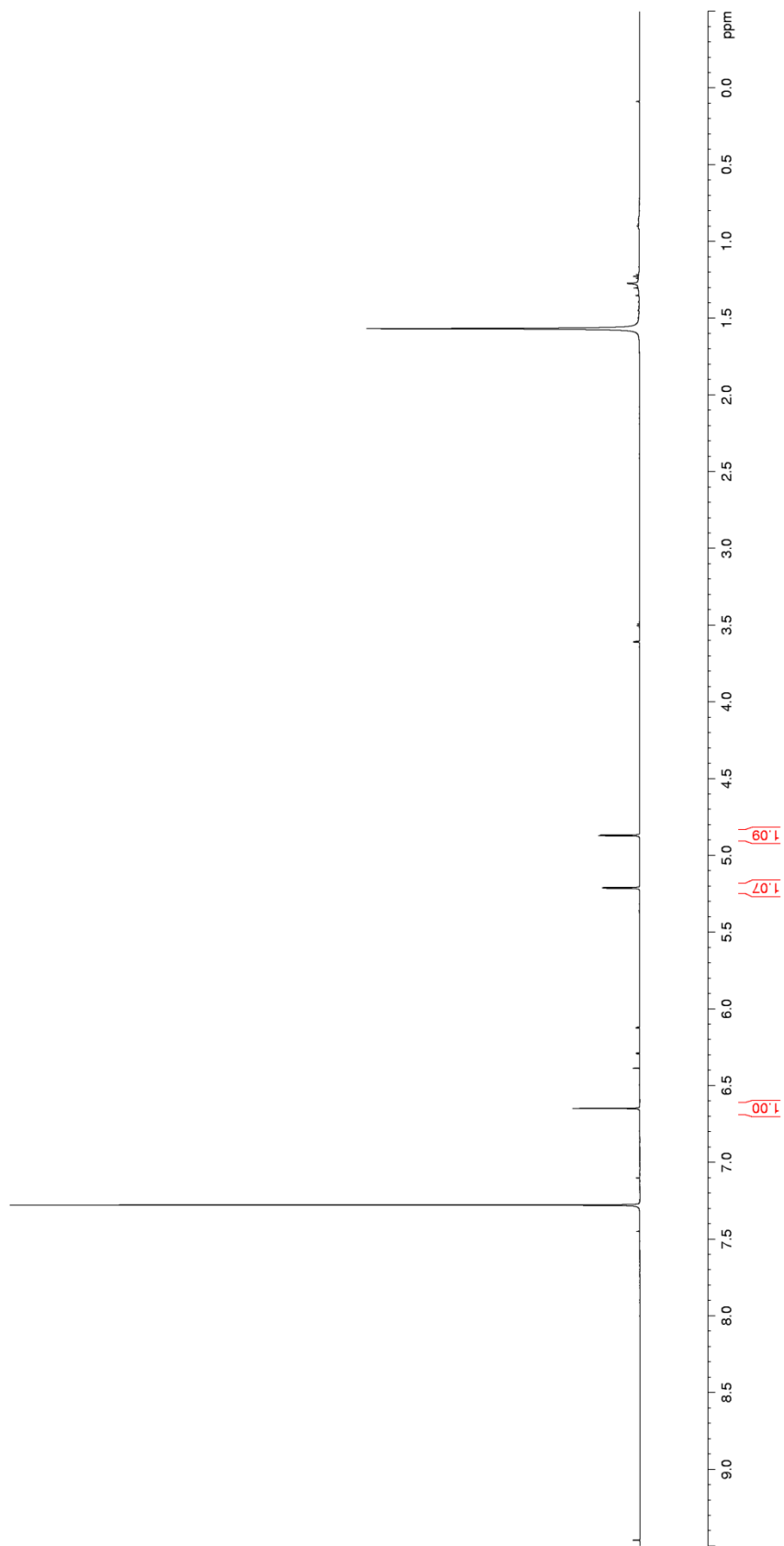
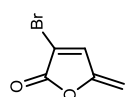


Figure 124. ^{13}C NMR (CDCl_3) of 212



212

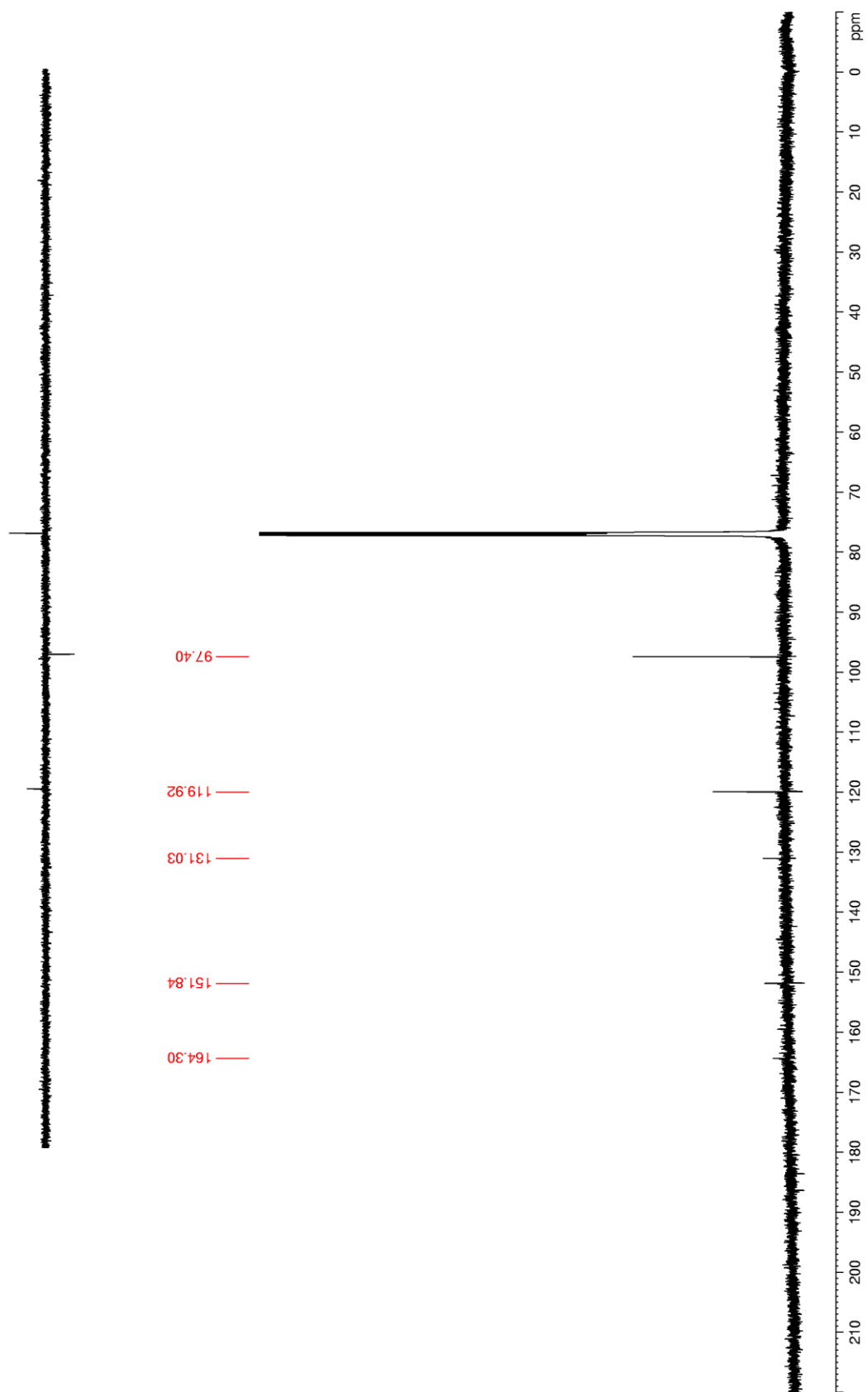


Figure 125. ^1H NMR (CDCl_3) of 214

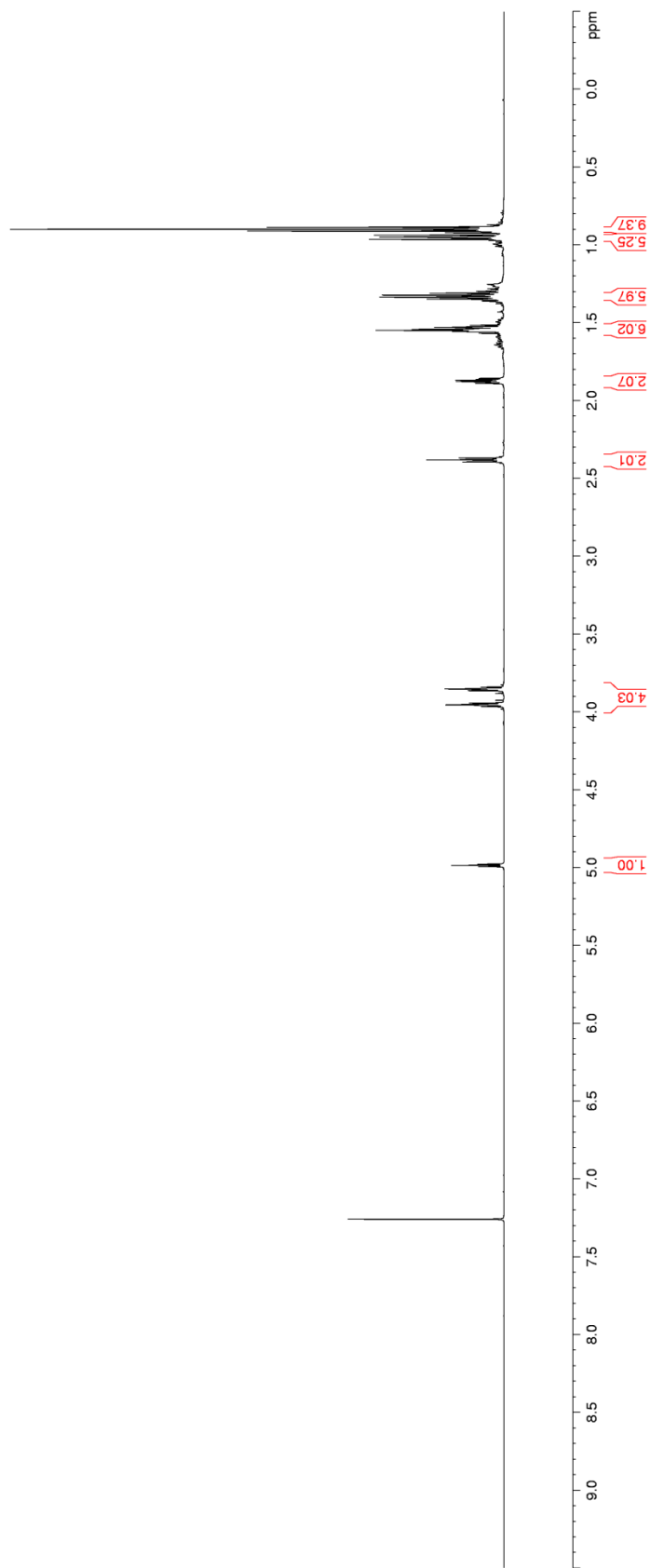
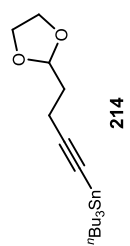


Figure 126. ^{13}C NMR (CDCl_3) of 214

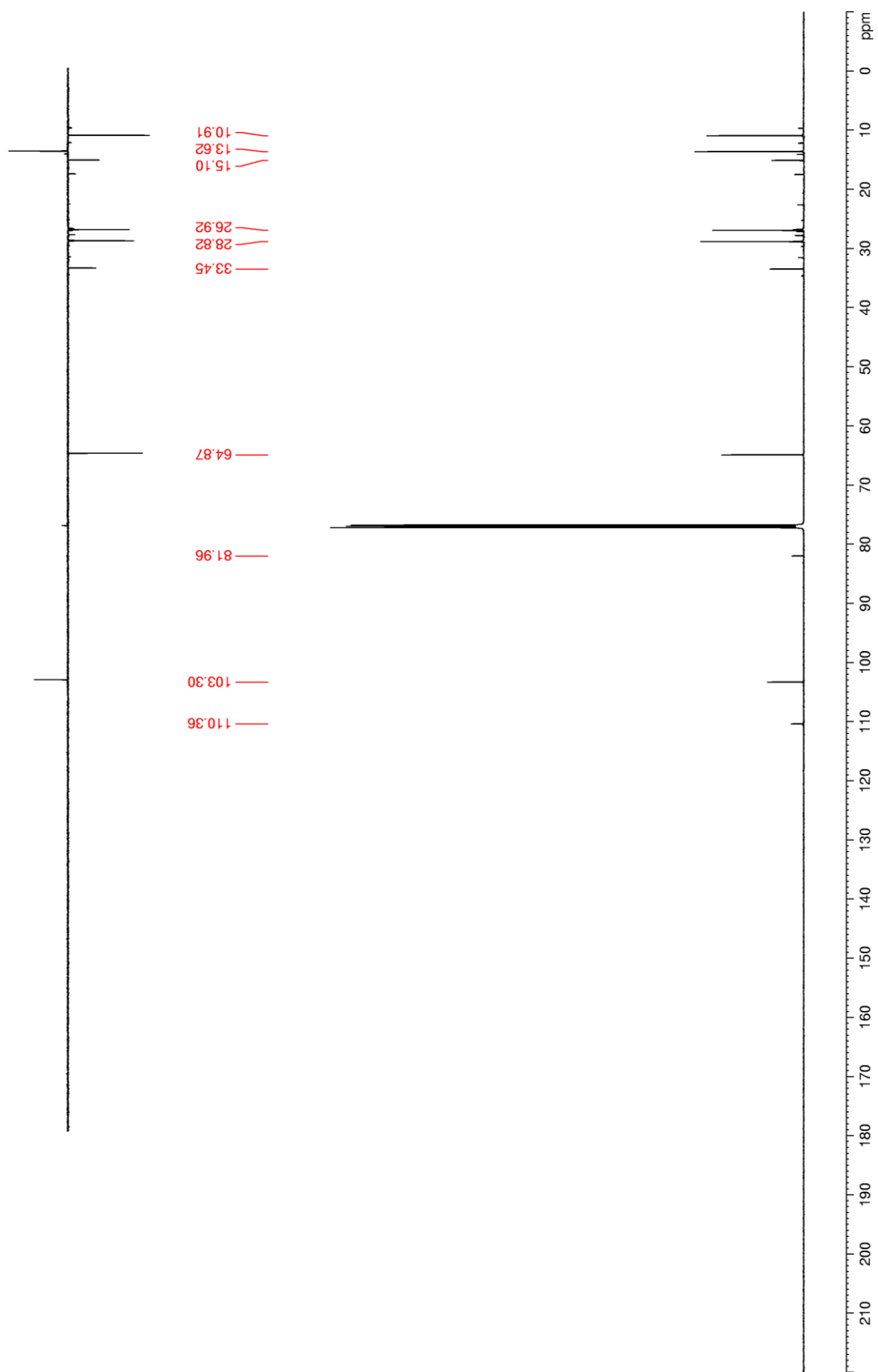
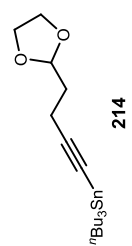


Figure 127. ^1H NMR (CDCl_3) of 216-d1

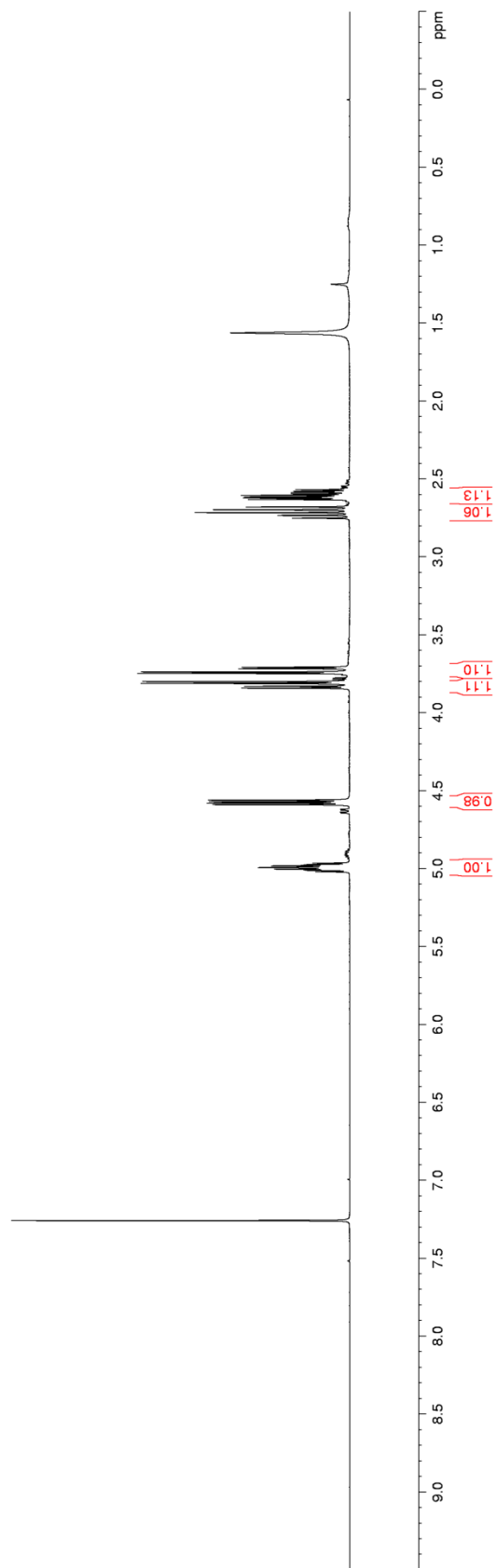
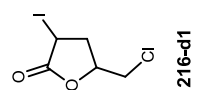


Figure 128. ^{13}C NMR (CDCl_3) of 216-d1

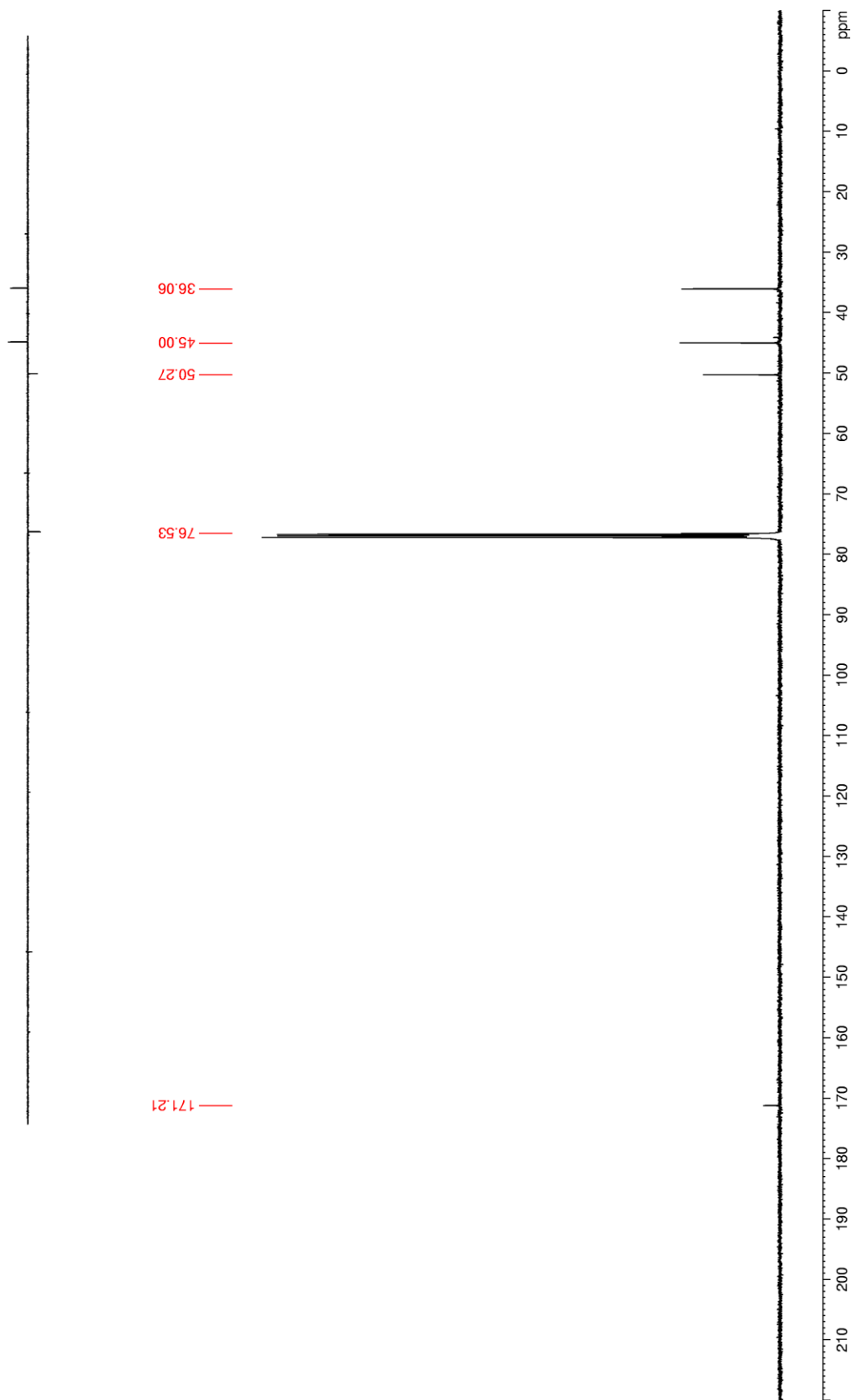
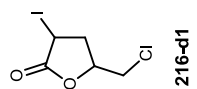


Figure 129. ^1H NMR (CDCl_3) of 216-d2

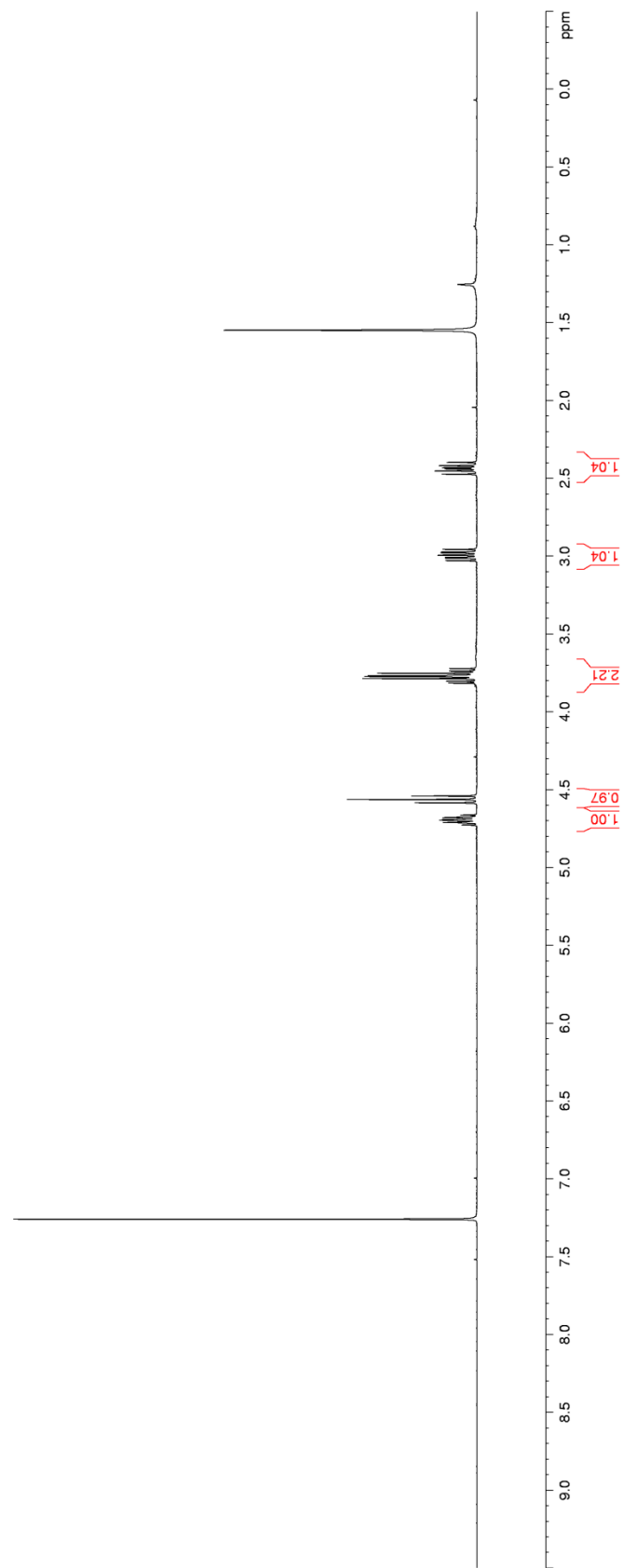
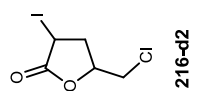


Figure 130. ^{13}C NMR (CDCl_3) of 216-d2

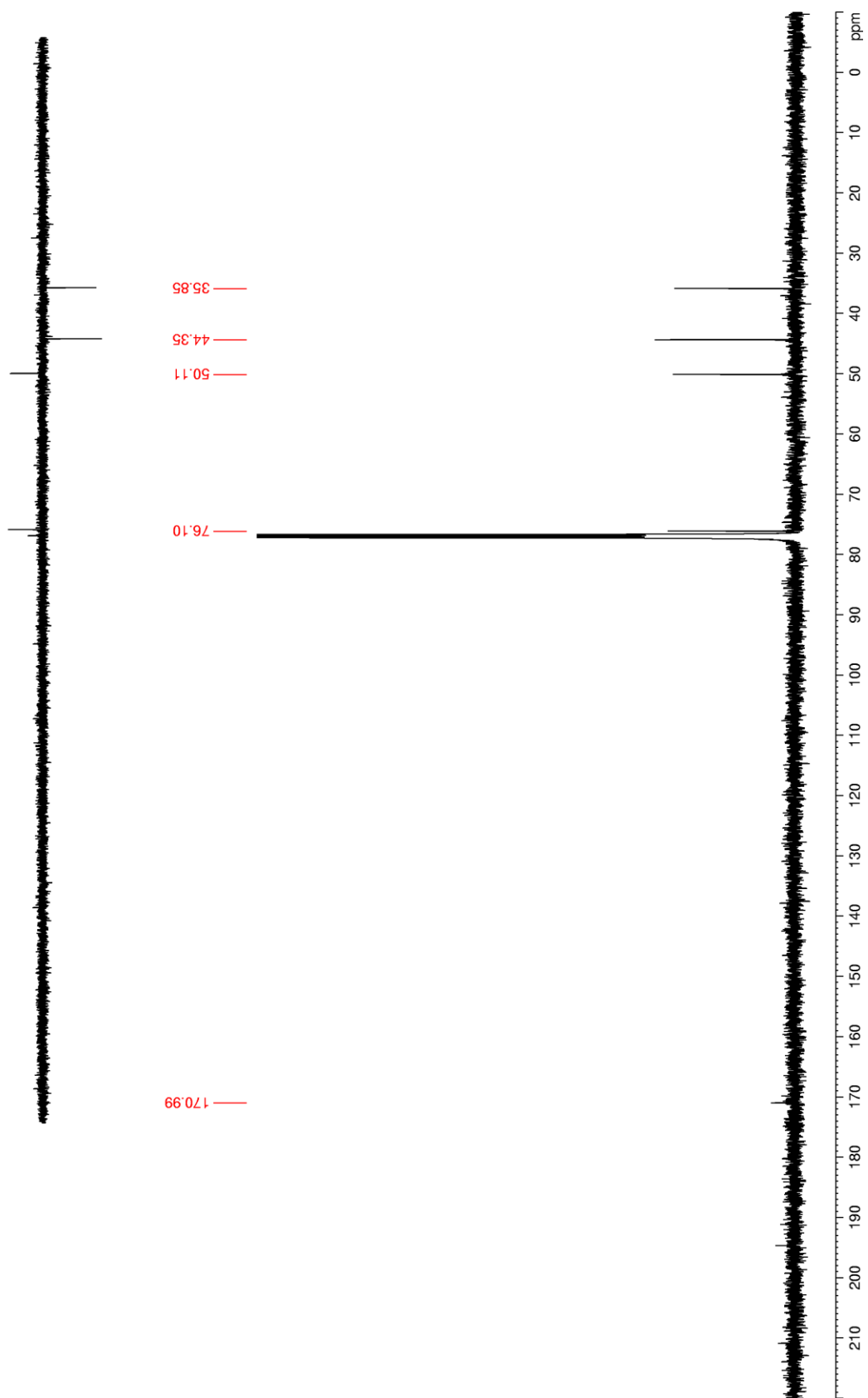
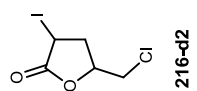


Figure 131. ^1H NMR (CDCl_3) of 220

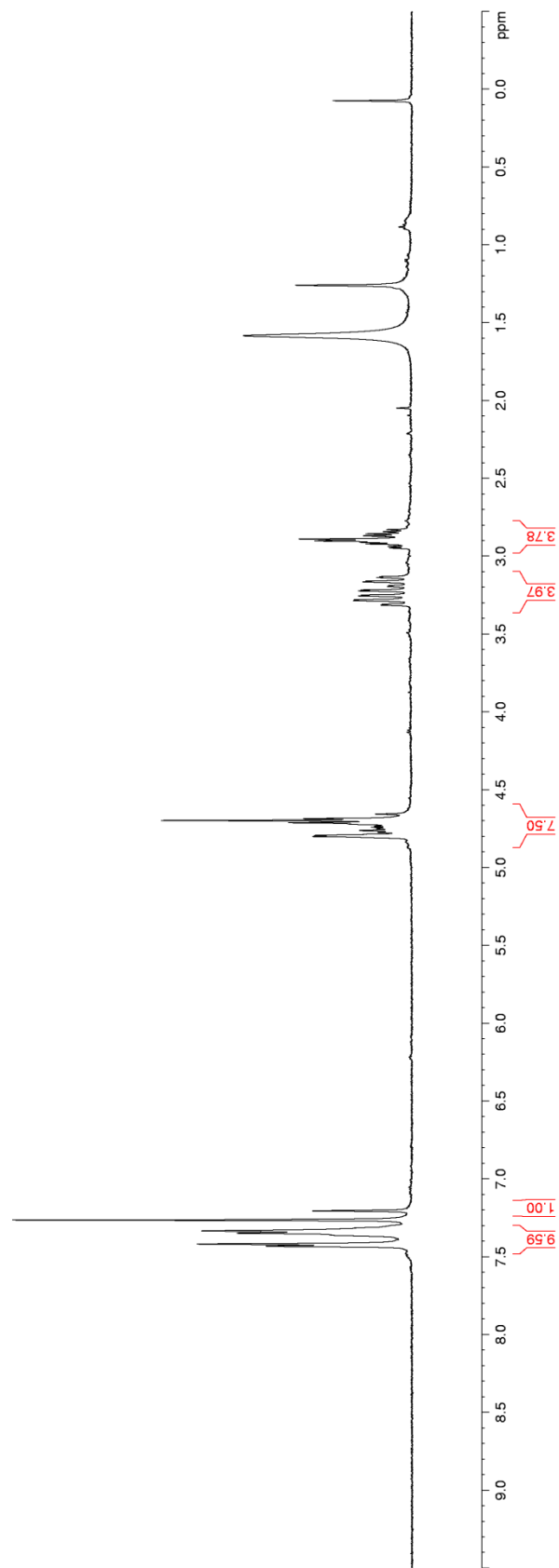
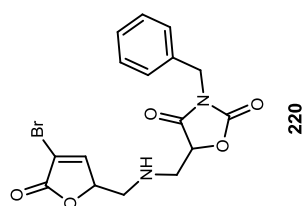


Figure 132. ^{13}C NMR (CDCl_3) of 220

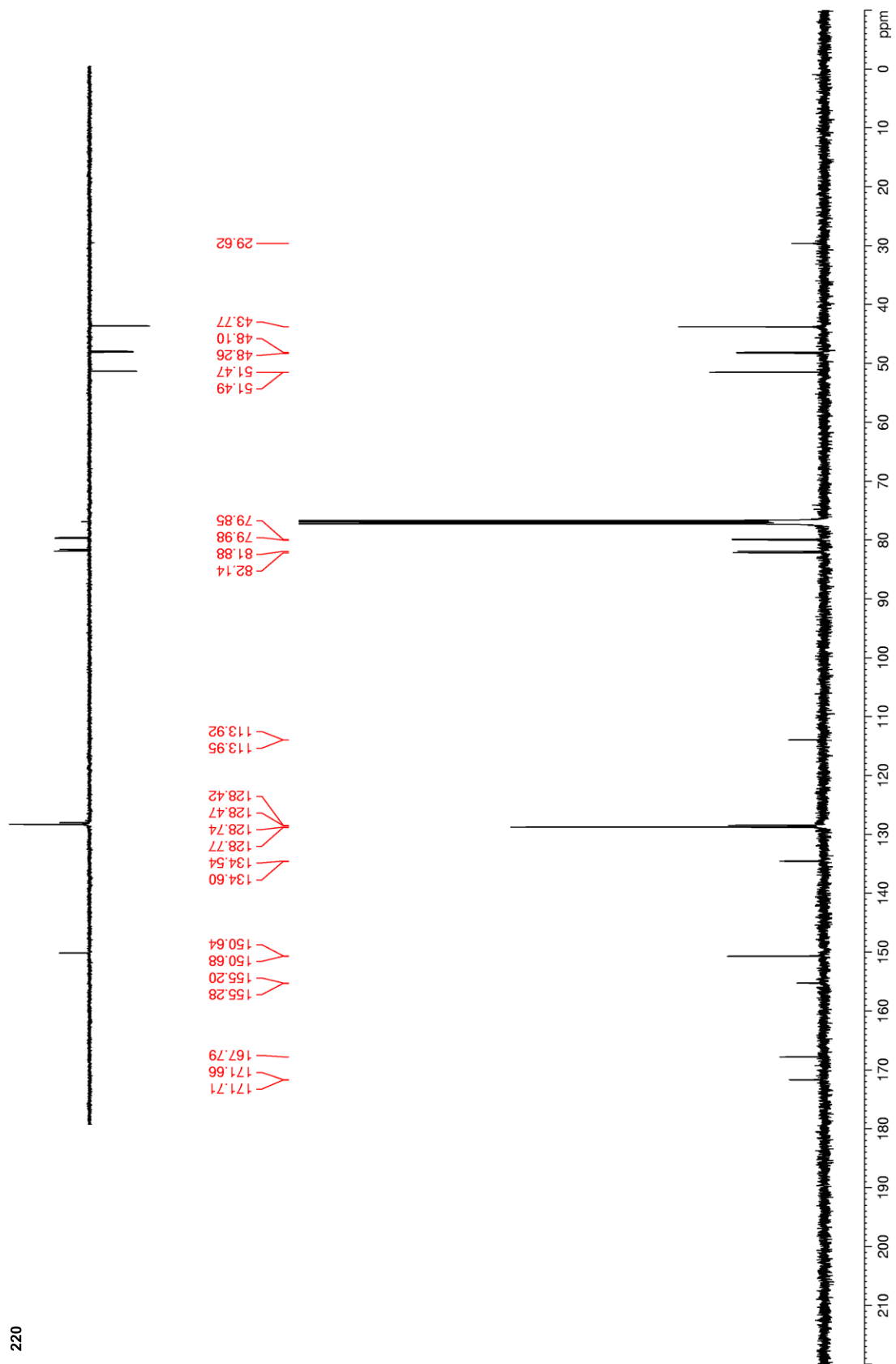
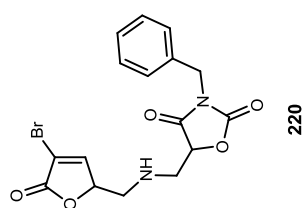


Figure 133. ^1H NMR (CDCl_3) of 221

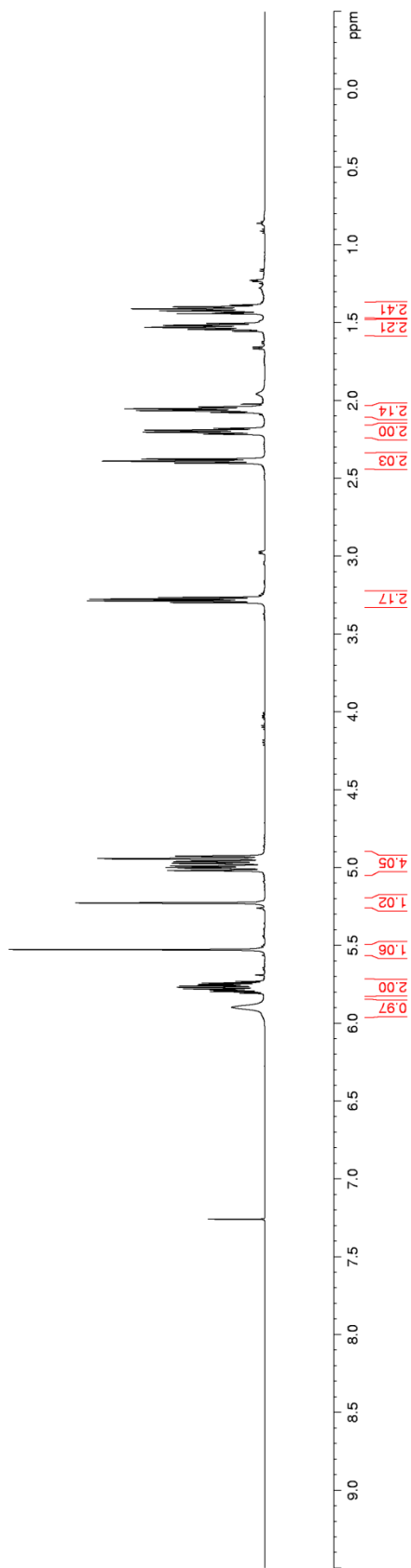
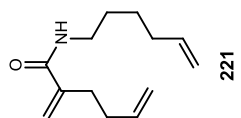


Figure 134. ^{13}C NMR (CDCl_3) of 221

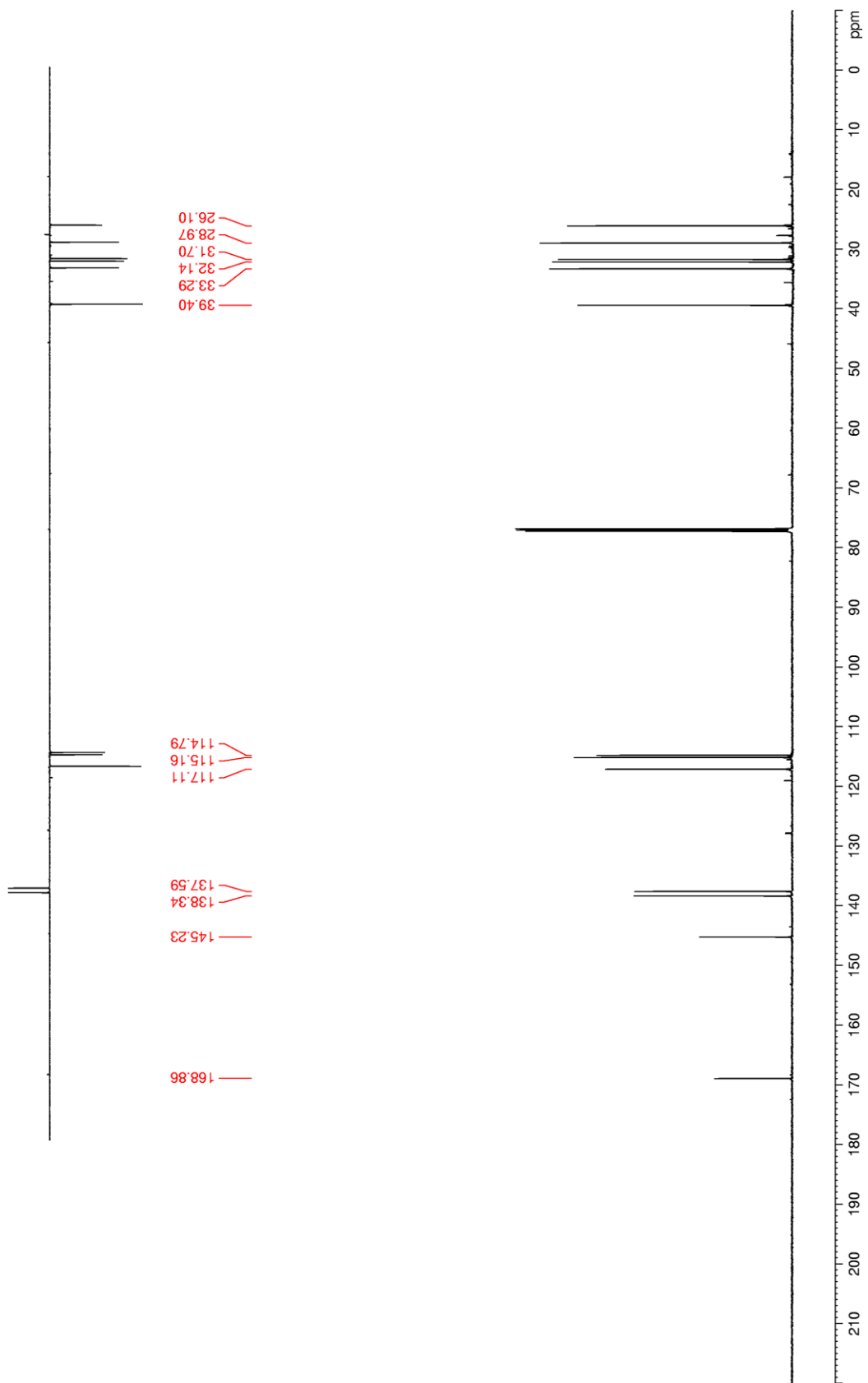
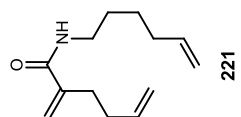


Figure 135. ^1H NMR (CDCl_3) of 222

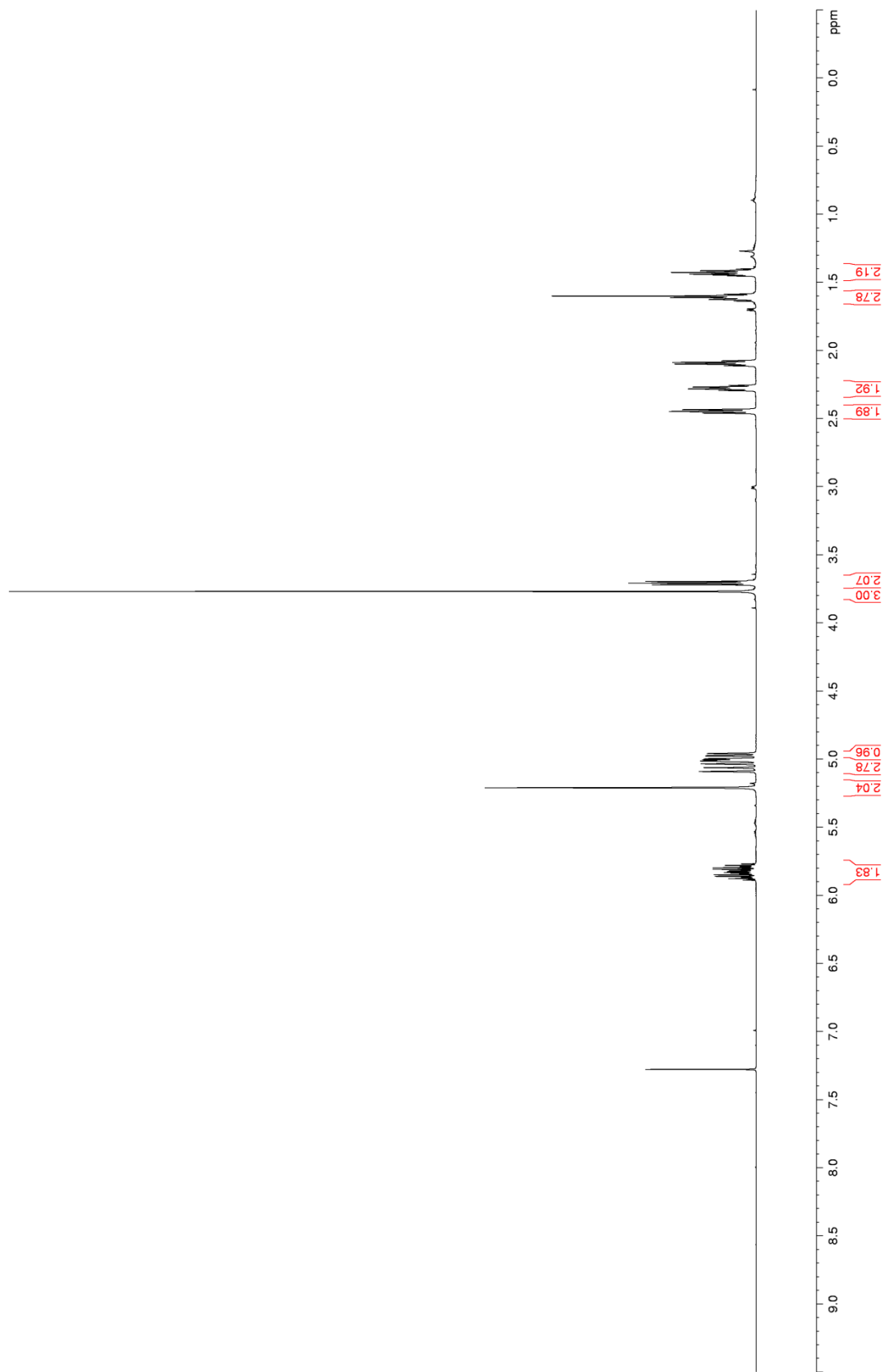
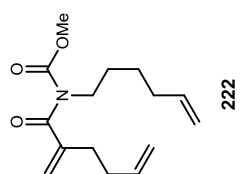


Figure 136. ^{13}C NMR (CDCl_3) of 222

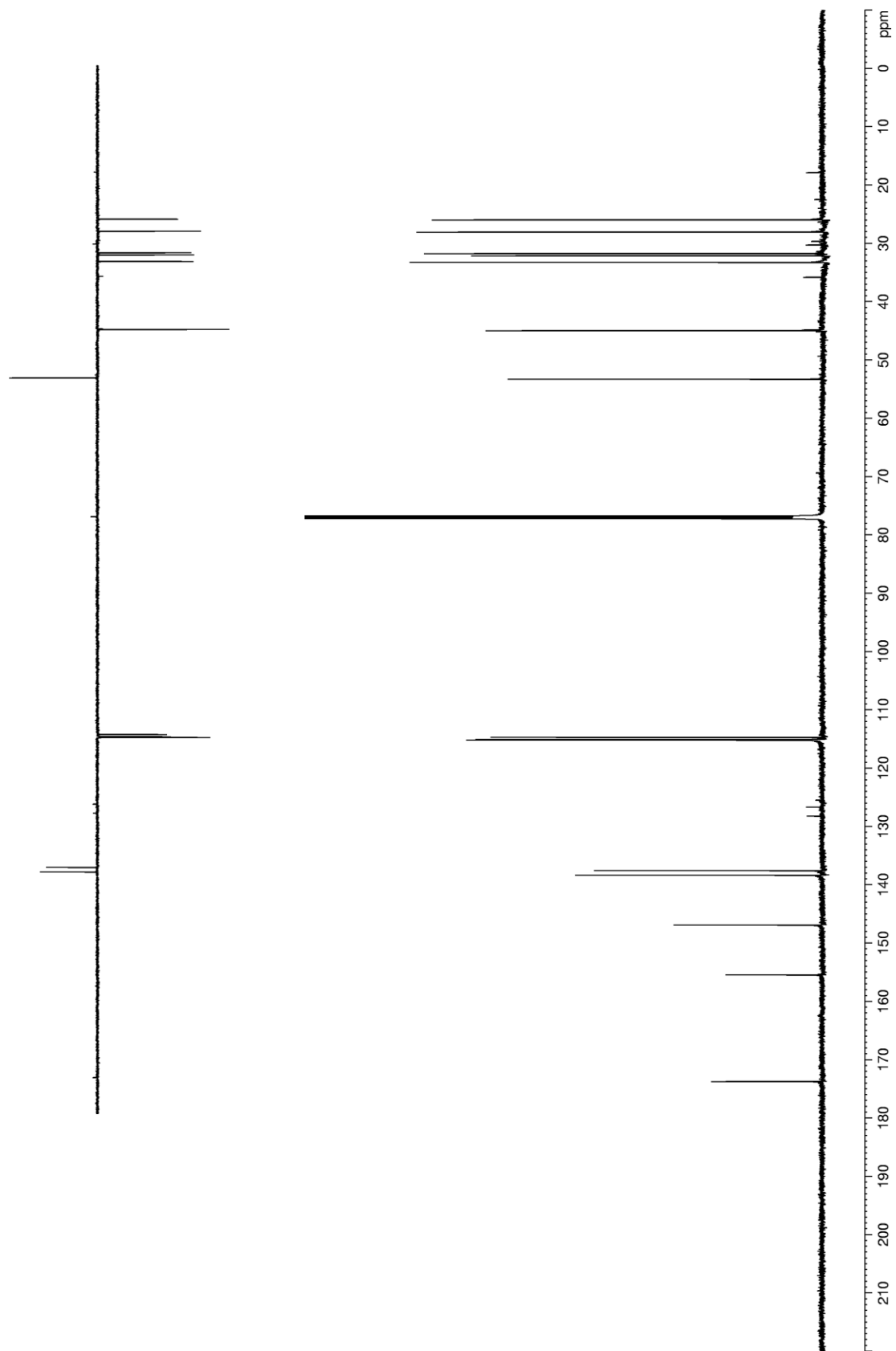
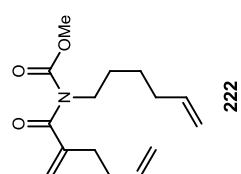


Figure 137. ^1H NMR (CDCl_3) of 223

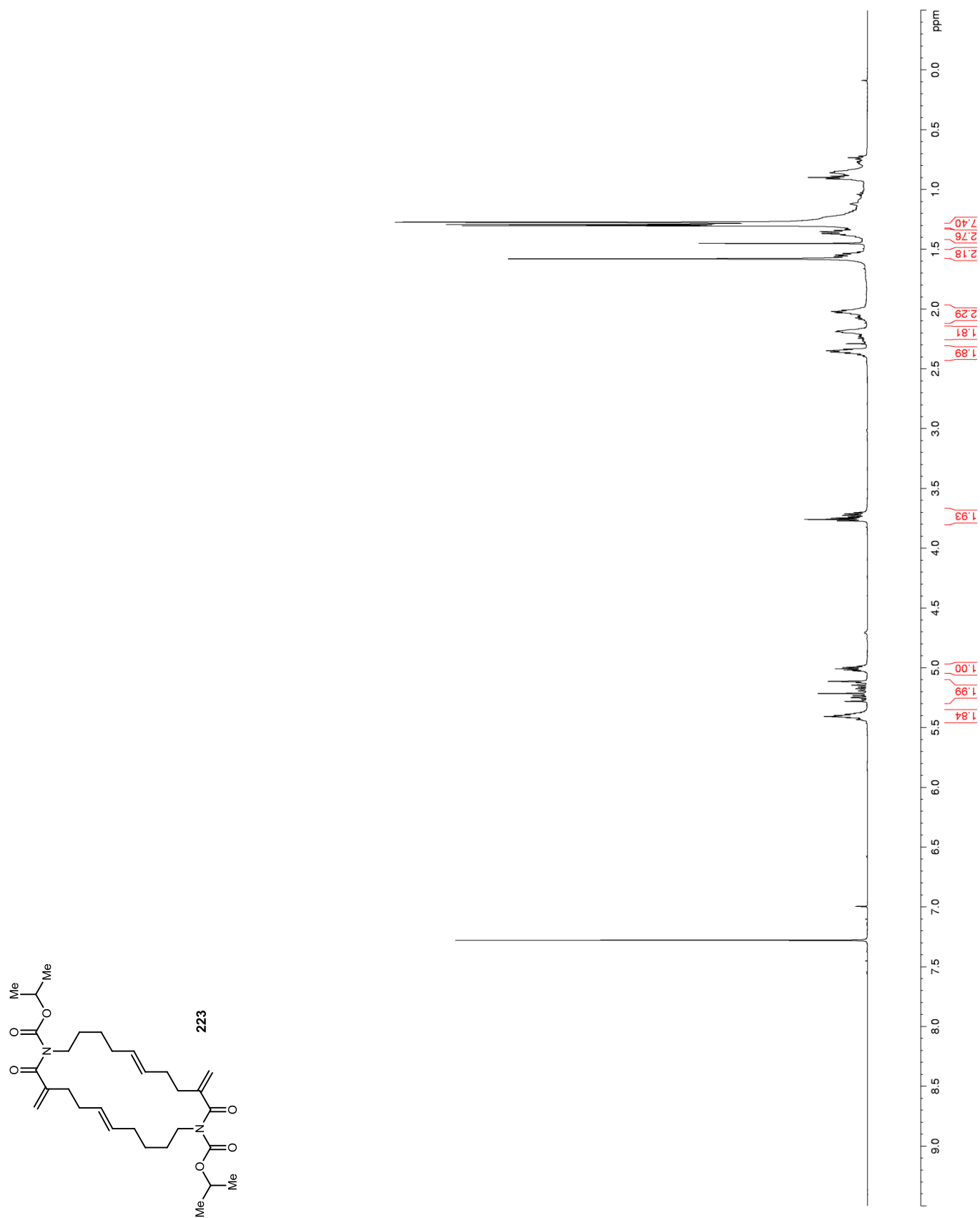


Figure 139. ^1H NMR (CDCl_3) of 231

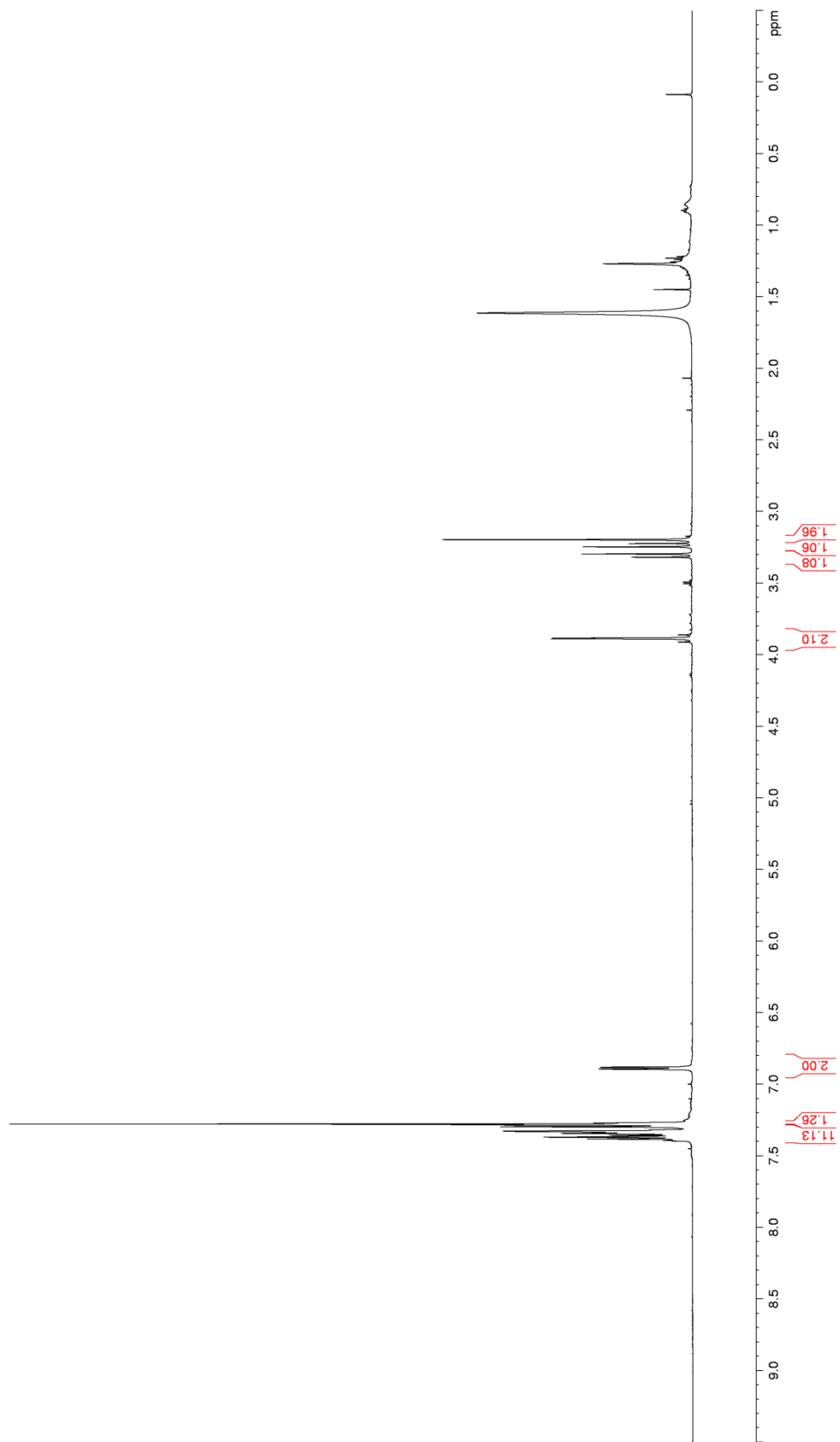
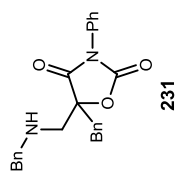


Figure 141. ^1H NMR (CDCl_3) of 234

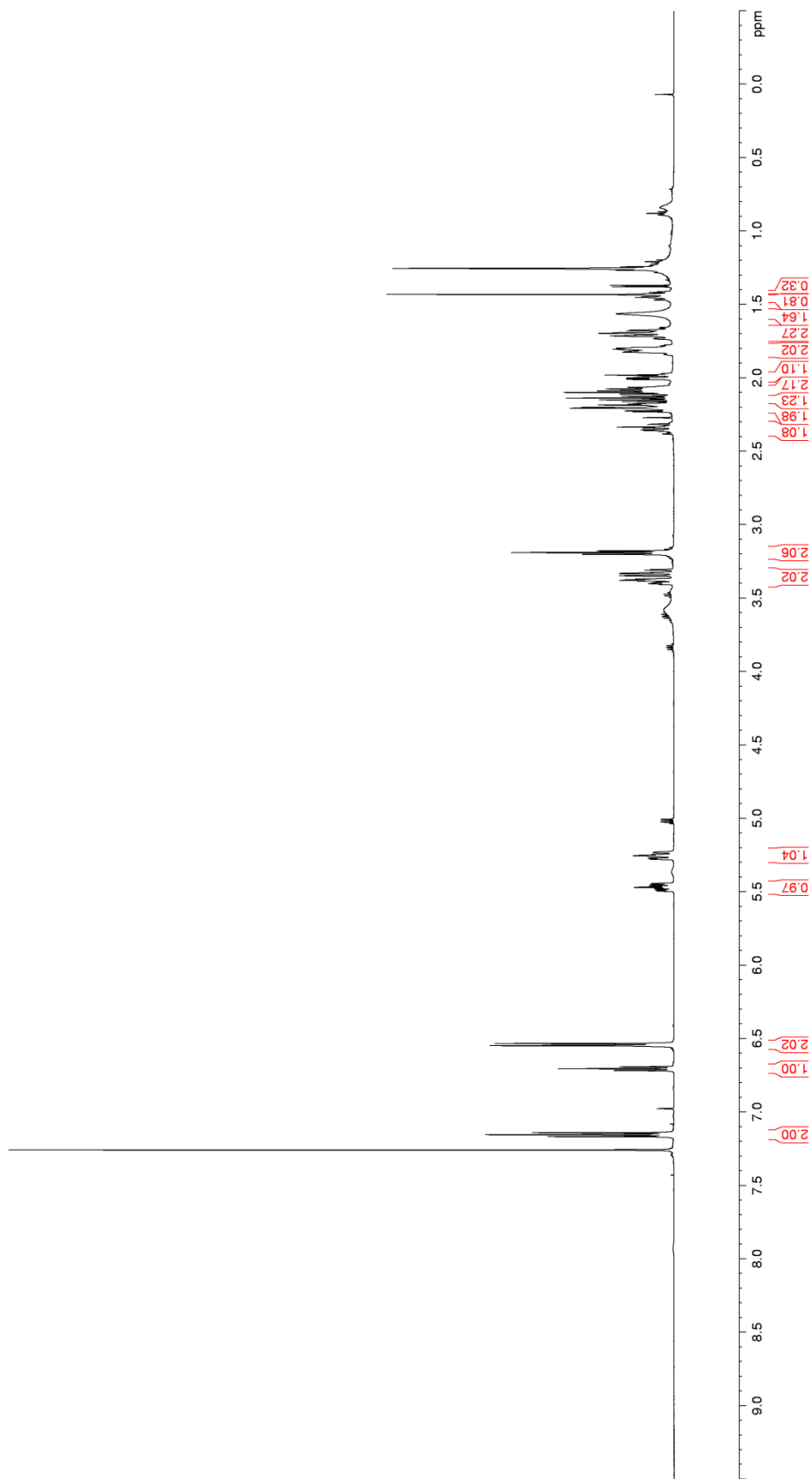
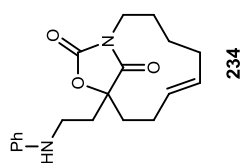


Figure 142. ^{13}C NMR (CDCl_3) of 234

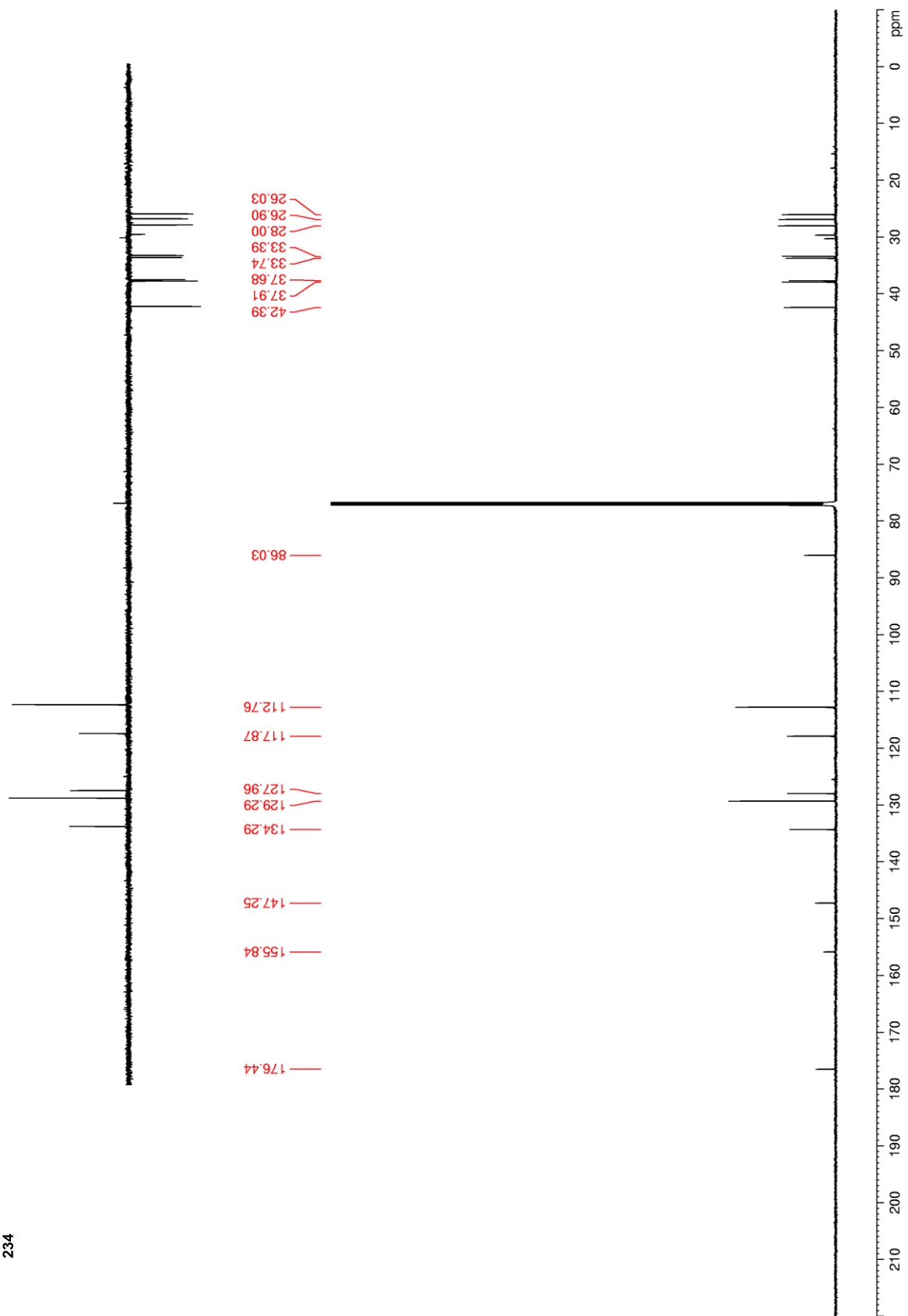
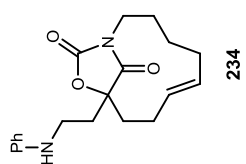


Figure 143. COSY (CDCl₃) of 234

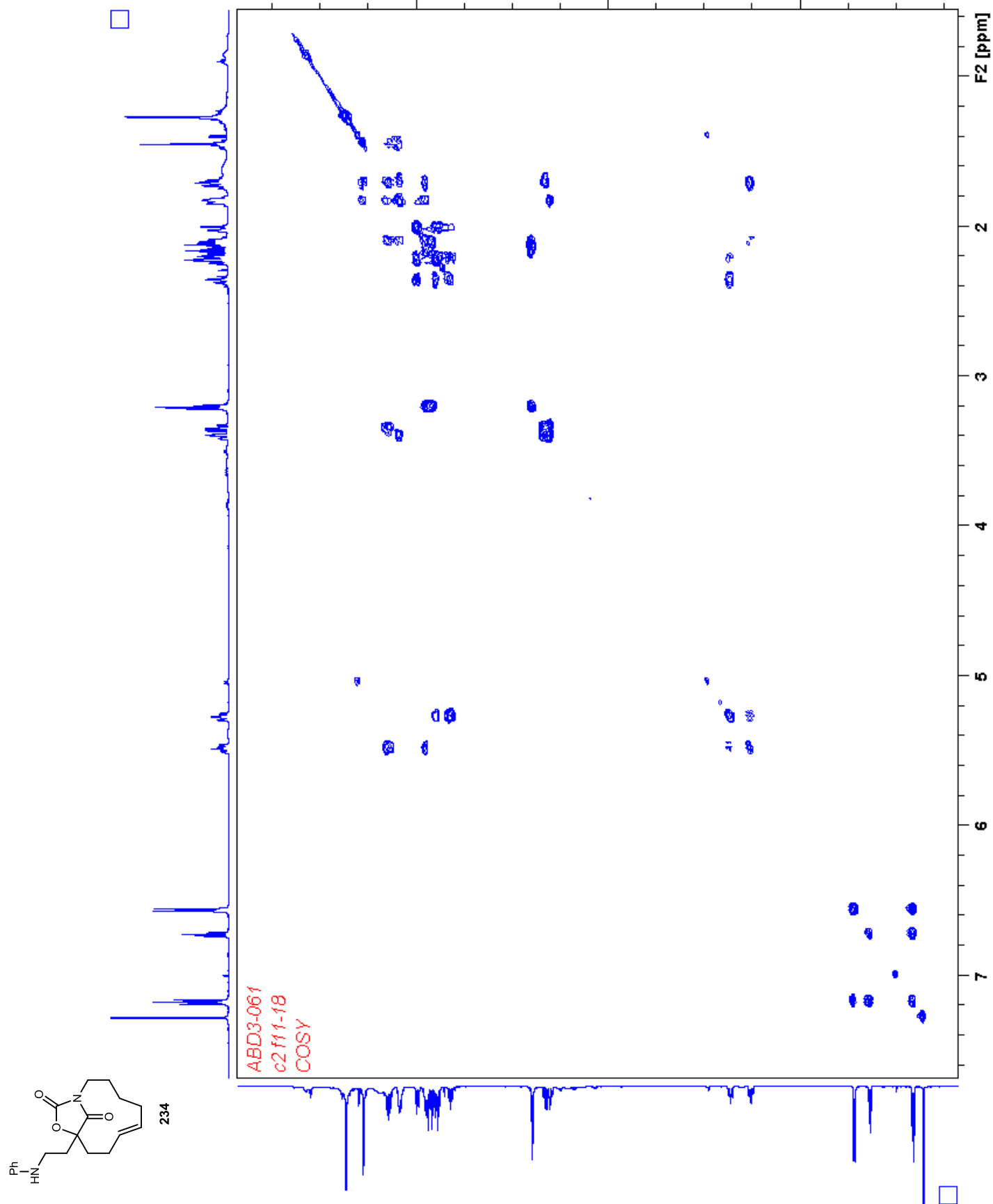


Figure 144. TOCSY (CDCl₃) of 234

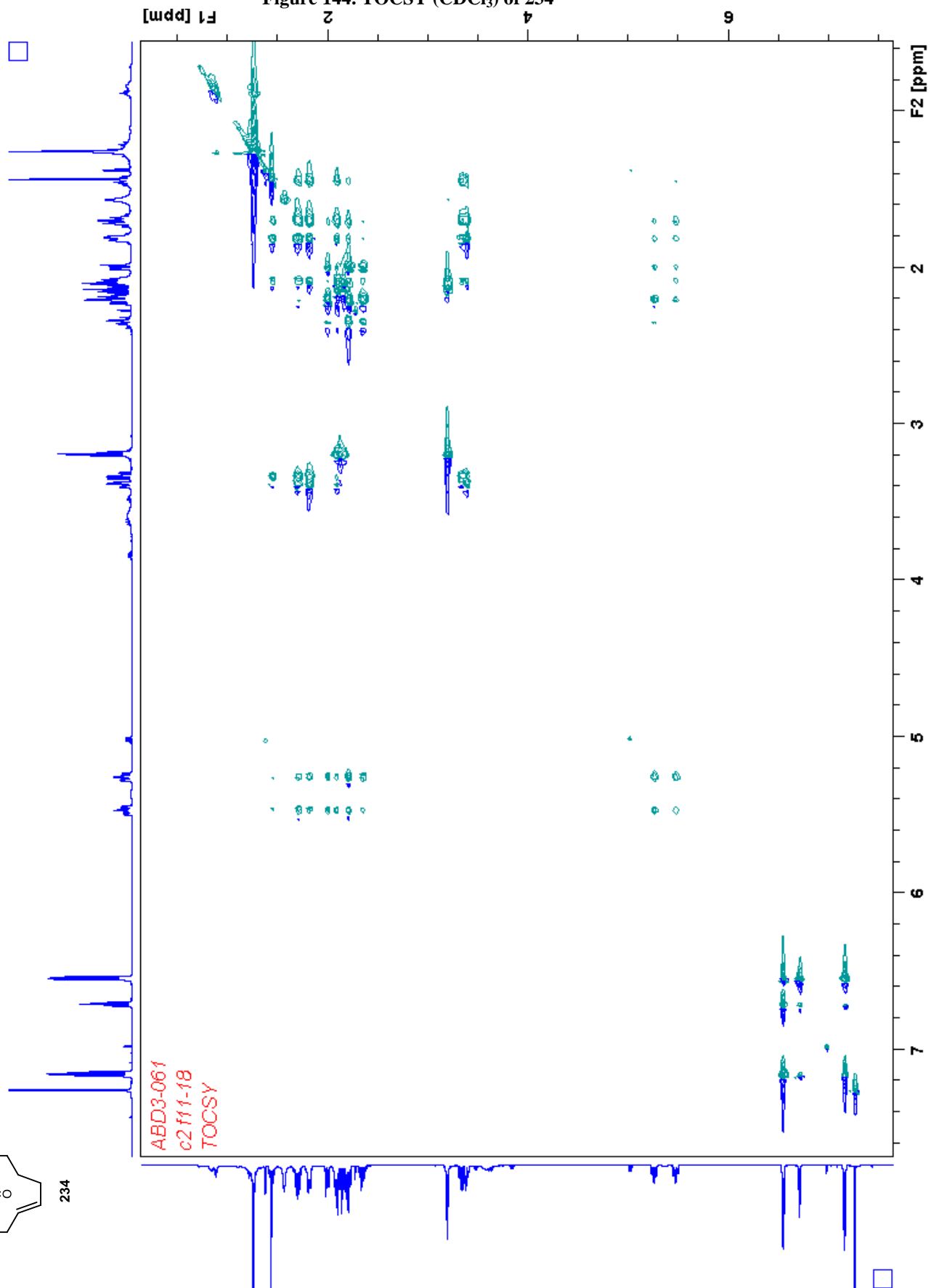
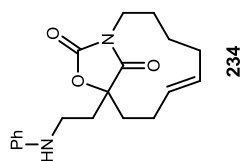


Figure 145. HSQC (CDCl₃) of 234

